DOE/EE-0872

Advanced Combustion Engine Research and Development

VEHICLE TECHNOLOGIES OFFICE

2012

annual progress report

U.S. DEPARTMENT OF ENERGY | Energy Efficiency & Renewable Energy

U.S. Department of Energy
1000 Independence Avenue, S.W.
Washington, D.C. 20585-0121

FY 2012 PROGRESS REPORT FOR ADVANCED COMBUSTION ENGINE RESEARCH AND DEVELOPMENT

Energy Efficiency and Renewable Energy
Vehicle Technologies Office

Approved by Gurpreet Singh

Team Leader, Advanced Combustion Engine R&D
Vehicle Technologies Office

December 2012

DOE-ACE-2012AR

Acknowledgement

We would like to express our sincere appreciation to Alliance Technical Services, Inc. and Oak Ridge National Laboratory for their technical and artistic contributions in preparing and publishing this report.

In addition, we would like to thank all the participants for their contributions to the programs and all the authors who prepared the project abstracts that comprise this report.

Table of Contents

I. INTRODUCTION

I.1 Subprogram Overview and Status

DEVELOPING ADVANCED COMBUSTION ENGINE TECHNOLOGIES

On behalf of the Department of Energy's Vehicle Technologies Office (VTO), we are pleased to introduce the Fiscal Year (FY) 2012 Annual Progress Report for the Advanced Combustion Engine Research and Development (R&D) subprogram. The mission of the VTO is to develop more energy-efficient and environmentally friendly highway transportation technologies that will meet or exceed performance expectations, enable the United States to use significantly less petroleum, and reduce greenhouse gas and other regulated emissions. The Advanced Combustion Engine R&D subprogram supports this mission by removing the critical technical barriers to commercialization of advanced internal combustion engines (ICEs) for passenger and commercial vehicles that meet future federal emissions regulations. Dramatically improving the efficiency of ICEs and enabling their introduction in conventional as well as hybrid electric vehicles is one of the most promising and cost-effective approaches to increasing vehicle fuel economy over the next several decades. Improvements in engine efficiency alone have the potential to increase passenger vehicle fuel economy by 35 to 50 percent, and commercial vehicle fuel economy by 30 percent with a concomitant reduction in greenhouse gas emissions, more specifically, carbon dioxide emissions. These improvements are expected to be even greater when coupled with advanced hybrid electric powertrains.

The following are representative goals of the Advanced Combustion Engine R&D subprogram that can contribute to meeting national energy security, environmental, and economic objectives:

- By 2015, increase the efficiency of ICEs for passenger vehicles resulting in fuel economy improvements of 25 percent for gasoline vehicles and 40 percent for diesel vehicles compared to current gasoline vehicles, and by 2020, achieve fuel economy improvements of 35 percent and 50 percent for gasoline and diesel vehicles, respectively.
- By 2015, increase the efficiency of ICEs for commercial vehicles from 42 percent (2010 baseline) to 50 percent (20 percent improvement) and by 2020, further improve engine efficiency to 55 percent (30 percent improvement) with demonstrations on commercial vehicle platforms.
- By 2015, increase the fuel economy of passenger vehicles by at least 5 percent with thermoelectric generators that convert energy from engine waste heat to electricity.

The passenger and commercial vehicle goals will be met while utilizing advanced fuel formulations that can incorporate a non-petroleum-based blending agent to reduce petroleum dependence and enhance combustion efficiency.

To meet the first two goals, two initiatives launched in 2010 continued in 2012, the SuperTruck and the Advanced Technology Powertrains for Light-Duty Vehicles (ATP-LDVs) to improve the fuel economy of heavy-duty trucks and passenger vehicles, respectively. The funding includes more than $100 million from the American Recovery and Reinvestment Act, and with a private cost share of 50 percent, will support nearly $375 million in total research, development and demonstration projects across the country. The four SuperTruck projects focused on cost-effective measures to improve the efficiency of Class 8 long-haul freight trucks by 50 percent, 20 percent of which will come from improvements to engine efficiency. The ATP-LDV projects supported efforts to increase the fuel economy of passenger vehicles 25 percent using an engine/powertrain-only approach. In 2012, DOE also awarded cost-shared (from 20% to 50%) contracts to four competitively selected teams of suppliers and vehicle manufacturers to develop and demonstrate new innovations to achieve breakthrough engine and powertrain system efficiencies while meeting federal emission standards for passenger and commercial vehicles, including long-haul tractor trailers. These projects address the technical barriers inhibiting wider use of these advanced engine technologies in the mass market.

To meet the third goal, three projects initiated in 2011 continued in 2012 to develop thermoelectric generators with cost-competitive advanced thermoelectric materials that will improve passenger vehicle fuel economy by at least 5 percent in 2015.

This introduction serves to outline the nature, current focus, recent progress, and future directions of the Advanced Combustion Engine R&D subprogram. The research activities of this subprogram are planned in conjunction with U.S.DRIVE (Driving Research and Innovation for Vehicle efficiency and Energy sustainability) and the 21st Century Truck Partnerships and are carried out in collaboration with industry, national laboratories, and universities. Because of the importance of clean fuels and advanced materials in achieving high efficiency and low emissions, R&D activities are closely coordinated with the relevant activities of the Fuels Technology and Materials Technologies subprograms, also within VTO.

CURRENT TECHNICAL FOCUS AREAS AND OBJECTIVES

The Advanced Combustion Engine R&D subprogram focuses on developing advanced ICE technologies for all highway transportation vehicles. Fuel efficiency improvement is the overarching focus of this activity, but resolving the interdependent emissions challenges is a critical integrated requirement. The reduction of engine-out emissions is critical to managing the extra cost of exhaust aftertreatment devices that can be a barrier to market acceptance. Accordingly, research has been emphasizing advanced low-temperature combustion (LTC) modes including homogeneous charge compression ignition (HCCI), pre-mixed charge compression ignition (PCCI), reactivity controlled compression ignition (RCCI), and lean-burn gasoline which will increase efficiency beyond current state-of-the-art engines and reduce engine-out emissions of nitrogen oxides (NOx) and particulate matter (PM) to near-zero levels. In parallel, research on emission control systems is underway to increase their efficiency and durability for overall emissions compliance at an acceptable cost and with reduced dependence on precious metals. Projects to stretch engine efficiency via innovative combustion methods and thermal energy recovery (such as compound cycles) are in progress as well. In response to the challenges of realizing and implementing higher efficiency engines, the Advanced Combustion Engine R&D subprogram is working toward achieving the following objectives:

- Further the fundamental understanding of advanced combustion processes which simultaneously exhibit high efficiency and low emissions. This will be used in the development of more efficient, cleaner engines which will operate predominately in LTC modes. These technology advances are expected to reduce the size and complexity of emission control hardware and minimize potential fuel efficiency penalties. A fuel-neutral approach is also being taken, with research addressing gasoline- and diesel-based advanced engines, including renewable fuels. The effects of fuel properties on combustion are addressed in the Fuel & Lubricant Technologies subprogram. Improve the effectiveness, efficiency, and durability of engine emission control devices as well as reduce their dependence on precious metals to enable increased penetration of advanced combustion engines in the light-duty market and maintain and/or expand application to heavy-duty vehicles.
- Extend robust engine operation and efficiency through the development and implementation of high-speed predictive models for improvements in combustion control and thermal management.
- Further the development of approaches to producing useful work from engine waste heat such as through incorporation of bottoming cycles.Advanced engine technologies such as turbo-machinery, flexible valve systems, advanced combustion systems, and fuel system components to achieve a reduction in parasitic losses and other losses to the environment to maximize engine efficiency.
- Develop key enabling technologies for advanced engines such as sensors and control systems, diagnostics for engine development, and components for thermal energy recovery.

- Improve the integration of advanced engine/emissions technologies with hybrid-electric systems for improved efficiency with lowest possible emissions.
- Identify that any potential health hazards associated with the use of new vehicle technologies being developed by VTO will not have adverse impacts on human health through exposure to toxic particles, gases, and other compounds generated by these new technologies.
- Develop thermoelectric generators that convert energy in the engine exhaust directly to electricity.
- Develop thermoelectrics and other solid state systems that provide cooling/heating to maintain vehicle occupant comfort. This technology is particularly important for hybrid-electric and all-electric vehicles that have insufficient or no engine heat for occupant heating.

The Advanced Combustion Engine R&D subprogram maintains close communication with industry through a number of working groups and teams, and utilizes these networks for setting goals, adjusting priorities of research, and tracking progress. Examples of the cooperative groups are the Advanced Combustion and Emission Control Tech Team of the U.S,DRIVE Partnership and the Engine Systems Team of the 21st Century Truck. Focused efforts are carried out in the Advanced Combustion Memorandum of Understanding (which includes auto manufacturers, engine companies, fuel suppliers, national laboratories, and universities) and the CLEERS (Cross-Cut Lean Exhaust Emission Reduction Simulation) activity for the Advanced Engine Cross-Cut Team.

TECHNOLOGY STATUS AND KEY BARRIERS

Significant advances in combustion, emission controls, fuel injection, turbo-machinery, and other advanced engine technologies continue to increase the thermal efficiency of ICEs with simultaneous reductions in emissions. With these advances, gasoline and diesel engines continue to be attractive engine options for conventional and hybrid-electric vehicles. These engines offer outstanding drivability, fuel economy, and reliability; they can readily use natural gas and biofuels such as ethanol and biodiesel, and can be integrated with hybrid and plug-in hybrid electric vehicle powertrains.

The majority of the U.S. light-duty vehicle fleet is powered by spark-ignition (SI) gasoline engines. Substantial progress in gasoline engine efficiency in recent years has been the result of advances in engine technologies including direct fuel injection, flexible valve systems, improved combustion chamber design, and reduced mechanical friction.

While all gasoline engines sold in the U.S. operate with stoichiometric combustion (needed for emission control by highly cost-effective three-way catalysts), other areas in the world with less stringent emissions regulations are seeing the introduction of higher efficiency lean-burn gasoline engines. Although these engines are characterized by higher efficiencies at part load, they will require more costly lean-NOx emission controls to meet more stringent U.S. emissions regulations. In addition, the direct injection technology utilized for most advanced gasoline engines produces particulate emissions that although smaller in mass than the diesel engine still represent significant emissions in terms of particulate number counts. Advances in lean-gasoline emission controls are critical for meeting U.S. regulations and ultimately the introduction of this efficiency technology in the U.S. market.

Attaining the high efficiency potential of lean-burn gasoline technology will require better understanding of the dynamics of fuel-air mixture preparation and other enabling technologies. Consistently creating combustible mixtures near the spark plug and away from walls in an overall lean environment is a challenge requiring improved understanding of fuel-air mixture preparation and modeling tools that embody the information. A comprehensive understanding of intake air flows and fuel sprays, as well as their interaction with chamber/piston geometry over a wide operating range is needed.

Generating appropriate turbulence for enhancement of flame speed is a further complexity requiring attention. The wide range of potential intake systems, piston geometries, and injector designs makes the optimization of lean-burn systems dependent on the development of improved simulation tools. Furthermore, reliable ignition and combustion of lean (dilute) fuel-air mixtures remains a challenge. Lean and possibly boosted conditions require a more robust, high-energy ignition system that, along with proper mixture control, is needed to reduce combustion variability. Several new ignition systems have been proposed (high-energy plugs, plasma, corona, laser, etc.) and need to be investigated.

Diesel engines are also well-suited for light-duty vehicle applications, delivering fuel economy considerably higher than comparable SI engines. Key developments in combustion and emission controls, plus low-sulfur fuel have enabled manufacturers to achieve the necessary emissions levels and introduce additional diesel-powered models to the U.S. market. DOE research contributed to all of these areas. Diesels in passenger cars have limited market penetration in the U.S. primarily due to the cost of the added components to reduce emissions and diesel fuel price. Hence reducing the cost of emission compliance continues to be addressed.

The heavy-duty diesel is the primary engine for commercial vehicles because of its high efficiency and outstanding durability. However, the implementation of increasingly stringent heavy-duty engine emission standards over the last decade held efficiency gains to a modest level. Current heavy-duty diesel engines have efficiencies in the 42-43% range. With stability in NOx and PM regulations in 2010, further gains in efficiency are now seen as achievable. Continued aggressive R&D to improve boosting, thermal management, and the reduction and/or recovery of rejected thermal energy are expected to enable efficiencies to reach 55%. Heavy-duty vehicles using diesel engines have significant potential to employ advanced combustion regimes and a wide range of waste heat recovery technologies that will improve engine efficiency and reduce fuel consumption.

Emissions of NOx (and PM) are a significant challenge for all lean-burn technologies including conventional and advanced diesel combustion strategies, both light-and heavy-duty, as well as lean-burn gasoline. Numerous technologies are being investigated to reduce vehicle NOx emissions while minimizing the fuel penalty associated with operating these devices. These technologies include advanced combustion strategies which make use of high levels of dilution to reduce in-cylinder NOx formation as well as post-combustion emissions control devices.

In early 2007, the U.S. Environmental Protection Agency (EPA) finalized the guidance document for using urea selective catalytic reduction (urea-SCR) technology for NOx control in light-duty and heavy-duty diesel vehicles and engines. This guidance allows for the introduction of SCR technology in Tier 2 light-duty vehicles, heavy-duty engines, and in other future diesel engine applications in the U.S. Strategies to supply the urea-water solution (given the name “diesel exhaust fluid”) for vehicles have been developed and are being implemented. Using urea-SCR, light-duty manufacturers have been able to meet Tier 2, Bin 5 which is the “gold standard” at which diesel vehicle sales do not have to be offset by sales of lower emission vehicles. Most heavy-duty diesel vehicle manufacturers are adopting urea-SCR since it has a broader temperature range of effectiveness than competing means of NOx reduction and allows the engine/emission control system to achieve higher fuel efficiency. Although urea-SCR is a relatively mature catalyst technology, more support research is needed to aid formulation optimization and minimize degradation effects such as hydrocarbon fouling.

Another technology being used to control NOx levels in diesel engines and potentially lean-burn gasoline engines is lean-NOx traps (LNTs), which are also referred to as NOx adsorbers. For example, the 2011 Volkswagen Jetta using an LNT in conjunction with exhaust gas recirculation (EGR), a diesel oxidation catalyst (DOC) and diesel particulate filter (DPF) has been certified to Tier 2, Bin 5 and California Low Emissions Vehicle (LEV)-II. Although LNTs have been commercialized for light-duty diesels, further advancement of the technology is needed to expand market penetration of light-duty

diesels and to enable use of LNTs in lean gasoline engine passenger car vehicles. A primary limitation to further adoption of current light-duty diesels is cost. Complex engine and EGR systems and the larger catalyst volumes associated with LNTs and DPFs result in higher overall costs in comparison to conventional gasoline vehicle systems. LNTs are particularly cost-sensitive because they require substantial quantities of platinum group metals, and the cost of these materials is high and volatile due to limited sources that are primarily mined in foreign countries. Improvements in the temperature range of operation for LNTs are also desired to reduce cost and enable success in the lean gasoline engine application. Both LNTs and DPFs result in extra fuel use, or a "fuel penalty", as they require fueling changes in the engine for regeneration processes. Aggressive research has substantially decreased the combined fuel penalty for both devices to approximately four percent of total fuel flow; further reduction would be beneficial. While LNTs have a larger impact on fuel consumption than urea-SCR, light-duty vehicle manufacturers appear to prefer LNTs since overall fuel efficiency is less of a concern and urea replenishment is more of a challenge for light-duty customers as compared to heavy-duty vehicle users. Another improvement being pursued for LNT technology is to pair them with SCR catalysts. The advantage is that the SCR catalyst uses the NH_3 produced by the LNT so no urea is needed. Formulation and system geometries are being researched to reduce the overall precious metal content of LNT+SCR systems which reduces cost and makes the systems more feasible for light-duty vehicles.

A highly attractive solution to reducing vehicle emissions is to alter the combustion process such that engine-out emissions are at levels which remove or reduce the requirements for auxiliary devices while maintaining or improving engine efficiency. This is the concept behind advanced combustion processes such as HCCI, PCCI and other modes of LTC, which exhibit high efficiency with significant reductions in NOx and PM emissions. Note that emissions of hydrocarbons (HCs) and carbon monoxide (CO) are often higher and require additional controls which are often a challenge with the low exhaust temperature characteristic of these combustion modes. Significant progress continues for these advanced combustion systems, and the operational range continues to be expanded to better cover the speed/load combinations consistent with light-duty and heavy-duty drive cycles. The major R&D challenges include fuel mixing, intake air conditioning, combustion timing control, and expansion of the operational range. To meet these challenges, there has been significant R&D on allowing independent control of the intake/exhaust valves relative to piston motion and on improvements in air-handling and engine controls. Many of these technologies are transitioning to the vehicle market.

High dilution operation through advanced EGR has been a major contributor to meeting the 2010 EPA heavy-duty engine emission standards and is also applicable to light-duty diesel and gasoline engines. There are numerous advantages of advanced EGR compared to urea-SCR and LNT packages including lower vehicle weight, less maintenance, and lower operating cost. The disadvantages relative to post-combustion emission controls include increased heat rejection load on the engine and the potential for increased fuel consumption due to more frequent DPF active regeneration.

Complex and precise engine and emission controls require sophisticated feedback systems employing new types of sensors. A major advancement in this area for light-duty engines has been the introduction of in-cylinder pressure sensors integrated into the glow plug. Start-of-combustion sensors (other than the aforementioned pressure sensor) have been identified as a need, and several development projects have been completed. Sensors are also beneficial for the emission control system. NOx and PM sensors are under development and require additional advances to be cost-effective, accurate, and reliable. Upcoming regulations with increased requirements for on-board diagnostics will also challenge manufacturers trying to bring advanced fuel efficient solutions to market. The role of sensors and catalyst diagnostic approaches will be a key element of emission control research in the next few years.

Waste heat recovery approaches (e.g., bottoming cycles) are being implemented in heavy-duty diesel vehicles and explored for light-duty diesel and gasoline applications. Experiments have shown that waste heat recovery has the potential to improve vehicle fuel economy by as much as 10%.

Another form of waste heat recovery is a thermoelectric generator. In current gasoline production passenger vehicles, roughly over 70% of the fuel energy is lost as waste heat from an engine operating at full power. About 35 to 40 percent is lost in the exhaust gases and another 30 to 35 percent is lost to the engine coolant. Thermoelectric generators can directly convert energy in the engine's exhaust to electricity for operating auxiliary loads and accessories, thereby improving the vehicle's fuel economy. Vehicular thermoelectric generators are on a path to commercialization; several manufacturers intend to introduce thermoelectric generators in their cars later this decade in Europe and North America. Use of thermoelectric devices for vehicle occupant comfort heating or cooling is also being pursued as a more fuel efficient alternative to the conventional mobile air conditioning systems that use refrigerants. It is estimated that thermoelectrics can maintain single occupant comfort conditioning with about one-sixth of the energy used by conventional systems that cool the entire driver and passenger cabin. In addition, conventional systems use the refrigerant gas R-134a, which has a warming potential that is 1,300 times that of carbon dioxide, the primary greenhouse gas. U.S. cars inadvertently release amounts of R-134a that is equivalent to about 41 million metric tons of carbon dioxide from compressor seal leakage and frontal vehicle collisions. Europe is already proscribing use of R-134a for vehicles.

FUTURE DIRECTIONS

Internal combustion engines have a maximum theoretical fuel conversion efficiency that is considerably higher than the mid-40% peak values seen today. The primary limiting factors to approaching these theoretical limits of conversion efficiency start with the high irreversibility in traditional premixed or diffusion flames, but more practically the limits are imposed by heat losses during combustion/expansion, structural limits that constrain peak cylinder pressures, untapped exhaust energy, and mechanical friction. Emphasis must be placed on enabling the engine to operate near peak efficiency over a real-world driving cycle to improve vehicle fuel economy. For SI engines this means reducing the throttling losses with technologies such as lean-burn, high dilution, and variable geometry. Exhaust losses are being addressed by analysis and development of compound compression and expansion cycles achieved by valve timing, use of turbine expanders, regenerative heat recovery, and application of thermoelectric generators. Employing such cycles and devices has been shown to have the potential to increase heavy-duty engine efficiency to as high as 55%, and light-duty vehicle fuel economy by 35% to 50%.

Analyses of how "advanced combustion regimes" might impact the irreversibility losses have indicated a few directions to moderate reductions of this loss mechanism, but maximizing conversion of availability (or available energy) to work will require compound cycles or similar measures of exhaust energy utilization. The engine hardware changes needed to execute these advanced combustion regimes include variable fuel injection geometries, turbo- and super-charging to produce very high manifold pressures, compound compression and expansion cycles, variable compression ratio, and improved sensors and control methods. Larger reductions in combustion irreversibility will require a substantial departure from today's processes but are being examined as a long-range strategy.

Most of the basic barriers to high engine efficiency hold true for both gasoline- and diesel-based engines. Recognizing the dominance of gasoline-type SI engines in the U.S., VTO has increased emphasis on their improvement. Gasoline-based engines, including E85 flexible-fuel, can be made at least 20-25% more efficient through direct injection, boosting/downsizing, and lean-burn. Real-world fuel savings might be even higher by focusing attention on the road-load operating points.

Hydrogen engine efficiencies of roughly 45% have been demonstrated based on single-cylinder engine data. The underlying reasons for these impressive levels suggest a case study for applicability to other fuels.

Meeting anticipated future emission standards will be challenging for high efficiency diesel and lean-burn gasoline engines. To address this issue, research on innovative emission control strategies will be pursued through national laboratory and university projects designed to reduce cost and increase performance and durability of NOx reduction and PM oxidation systems. Project areas include development of low-cost base metal catalysts (to replace expensive platinum group metals), lighter and more compact multifunctional components, new control strategies to lessen impact on fuel consumption, and improved sensors and on-board diagnostics for meeting upcoming regulations. Furthermore, simulations of the catalyst technologies are being developed to enable industry to perform more cost-effective system integration during vehicle development. As advanced combustion approaches evolve and engine-out emissions become cleaner, the requirements of emission controls are expected to change as well.

The majority of lean-NOx emission controls development has been focused on diesel engines. With the potential introduction of high efficiency lean-gasoline engines, these technologies will require further research and development as well as emission controls for managing HC/CO emissions. Engine-out PM emissions from lean-gasoline engines, although lower in mass than the diesel engine, are also a concern and may require new processes due to differences in particle size and morphology.

Enabling technologies being developed will address fuel systems, sensors, engine control systems, and other engine technologies. Fuel systems R&D focuses on injector controls and fuel spray development. Engine control systems R&D focuses on developing engine controls and sensors that are precise and flexible for enabling improved efficiency and emission reduction in advanced combustion engines. This also includes a better understanding of stochastic and deterministic in-cylinder processes which limit the speed/load range of many advanced combustion strategies. Control system technologies will facilitate adjustments to parameters such as intake air temperature, fuel injection timing, injection rate, variable valve timing, and EGR to allow advanced combustion engines to operate over a wider range of engine speed/load conditions. Engine technologies development will be undertaken to achieve the best combination that enables advanced combustion engines to meet maximum fuel economy and performance requirements. These include variable compression ratio, variable valve timing, variable boost, advanced sensors and ignition systems, and exhaust emission control devices (to control hydrocarbon emissions at idle-type conditions) in an integrated system. Upcoming EPA onboard diagnostic requirements will be addressed through research on advanced sensors, improved understanding of emission control aging, and development of models that are integral to the diagnostic method. Work in developing enabling technologies for more efficient, emission-compliant engine/powertrain systems will continue to be pursued.

The Solid State Energy Conversion activity will continue on developing advanced thermoelectric generators for converting energy from engine waste heat directly into useful electrical energy for operating vehicle auxiliary loads and accessories to improve the vehicle's fuel economy. Achieving the vehicle-based performance goals requires reduction in the cost of thermoelectric materials, scaling them up into practical devices, reduction in the manufacturing cost of vehicular thermoelectric generators at the production scale for the vehicle market, and making them durable enough for vehicle applications. The cost-shared projects initiated in 2011 with three competitively selected teams will continue in the design and development of cost competitive manufacture of thermoelectric generators for selected passenger vehicle platforms. In addition, the concept of a zonal, dispersed thermoelectric cooling system will continue to be pursued to provide occupant comfort cooling at a greater than 70 percent reduction in power requirements.

The remainder of this report highlights progress achieved during FY 2012 under the Advanced Combustion Engine R&D subprogram. The following 71 abstracts of industry, university, and national laboratory projects provide an overview of the exciting work being conducted to tackle tough technical challenges associated with R&D of higher efficiency, advanced ICEs for light-duty, medium-duty, and heavy-duty vehicles. We are encouraged by the technical progress realized under this dynamic subprogram in FY 2012, but we also remain cognizant of the significant technical hurdles that lay ahead, especially those to further improve efficiency while meeting the light-duty EPA Tier 2 emission standards and the heavy-duty engine standards for the full useful life of the vehicles.

I.2 Project Highlights

The following projects highlight progress made in the Advanced Combustion Engine R&D subprogram during FY 2012.

COMBUSTION AND EMISSION CONTROL

A. Combustion Research

The objective of these projects is to identify how to achieve more efficient combustion with reduced emissions from advanced technology engines.

- Sandia National Laboratories (SNL) is developing the physical understanding to guide engine combustion research and the modeling tools to refine the design of optimal, clean, high-efficiency combustion engines. In the past year they: (1) measured the evolution of in-cylinder mixture distributions for four different swirl ratios and three different injection pressures; (2) demonstrated that engine-out emissions are strongly correlated with the formation of over-lean mixture in the pre-combustion mixture formation process for all operating conditions; (3) identified shortcomings in the modeling of the initial mixture formation process and areas for focusing future efforts; (4) established the dominance of kinetics in determining the engine-out emissions when injection is excessively retarded; and (5) examined the potential of photo-fragmentation with subsequent C_2 laser-induced fluorescence as a diagnostic for in-cylinder detection of C_2H_2. (Miles, SNL)

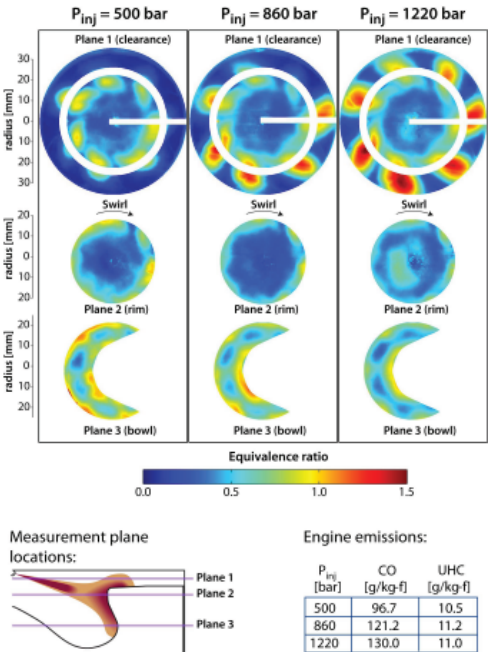

Equivalence ratio distributions measured at 5° bTDC at three different injection pressures. SOI = 23.3° bTDC; 10% O_2 ; swirl ratio = 2.2, 1,500 RPM; 3 bar gross indicated mean effective pressure (gIMEP). (Miles, SNL)

- SNL is developing a fundamental understanding of how in-cylinder controls can improve efficiency and reduce pollutant emissions of advanced LTC technologies. In the past year they: (1) completed a 38-page review article describing a new conceptual model for PPCI LTC which was accepted for publication in the journal Progress in Energy and Combustion Science; (2) implemented a new injection system in the heavy-duty optical engine that allows precise fuel delivery (~1-2 mg) of multiple injections with close spacing (~100 microseconds) with less than 1% shot-to-shot variation, which enables investigation of new research areas; (3) demonstrated up to 62% engine-out soot reduction using new fuel injection system with close-coupled post-injections having combustion phasing favorable for fuel-efficiency across a wide range of EGR, and provided initial in-cylinder observations that suggest post-injection targeting into the main-soot cloud is important for creating interaction; and (4) model predictions show how heat transfer LTC strategies achieve higher efficiency by nearly halving heat transfer, largely by reducing in-cylinder combustion temperatures and by locating combustion away from in-cylinder surfaces. (Musculus, SNL)

- SNL is leading a multi-institution, international, research effort on engine spray combustion called the Engine Combustion Network (ECN), facilitating improvement of engine combustion modeling and accelerating the development of cleaner, more efficient engines. In the past year they: (1) generated a comprehensive spray combustion dataset working collaboratively with eight different experimental institutions from around the world; organized and led an ECN workshop with over 140 participants, where 16 multiple modeling groups submitted results for a side-by-side comparison to this experimental data thereby defining the state of current research and pointing to needed future directions; (2) developed new diagnostic techniques that have quantified and standardized key metrics of spray development, such as liquid length, ignition delay, and lift-off length; and (3) performed high-speed microscopy to reveal the spray liquid structure as it transitions from low temperature and pressure to engine-relevant conditions. (Pickett, SNL)
- Argonne National Laboratory (ANL) is developing physics-based computational fluid dynamics (CFD) models necessary for predictive simulations of the internal combustion engine. In the past year they: (1) demonstrated grid-convergence on diesel spray and engine simulations; (2) demonstrated that detailed chemistry based combustion models are grid-convergent and hence more reliable than simplified combustion models; and (3) developed and validated a 106 species-based reduced reaction model for n-dodecane as surrogate for diesel fuel. This mechanism is being used by industry and academia extensively through the ECN initiated by Sandia National Laboratories. (Som, ANL)
- ANL is studying the mechanisms of spray atomization by making detailed, quantitative measurements in the near-nozzle region of sprays from light-duty diesel injectors. In the past year they made precision measurements of the fuel density in three dimensions, and discovered significant asymmetries as well as differences between the nominally identical injectors. The measurements are being used by computational modelers to improve spray models, this will speed the development of efficient, clean-burning engines. (Powell, ANL)
- ANL is collaborating with combustion researchers within DOE's Office of Science Basic Energy Science and Energy Efficiency Renewable Energy Vehicle Technologies programs to develop and validate predictive chemical kinetic models for a range of transportation-relevant fuels. In the past year they: (1) designed and fabricated new experimental hardware to improve gas conditions in the twin-piston machine's reaction chamber (e.g., minimized fluid dynamic motion and dead volume, tighter sealing at high and low pressures, greater thermal uniformity); (2) validated reduced-order model calculations of the rapid compression machine using experimental chemical thermometry techniques employing cyclochexene; (3) developed guidelines through bench-top experiments for the successful implementation and utilization of aerosol fueling methodologies which facilitate the use of involatile, diesel-relevant components and blends in rapid compression machine experiments; and (4) acquired autoignition data for a 4-component gasoline surrogate at stoichiometric conditions in 21% oxygen diluted with argon at 30 bar with temperatures from 690 to 870 K. (Ciatti, ANL)
- Lawrence Livermore National Laboratory (LLNL) is developing chemical kinetic models for conventional and next-generation transportation fuels that need to be developed so that engine simulation tools can predict fuel effects. In the past year they: (1) validated an approach to formulate gasoline surrogate fuels and a predictive chemical kinetic model for a gasoline surrogate fuel; (2) developed chemical kinetic model for a larger aromatic, a major chemical class in diesel fuel; (3) developed a model for 3-methylheptane, an iso-alkane, that includes low temperature chemistry and determined the effect of branching of iso-alkanes on ignition under engine conditions; (4) developed reduced chemical kinetic model for diesel for the ECN; and (5) developed a functional group method for alkyl-cyclohexanes that greatly reduces the size of the chemical kinetic mechanism. (Pitz, LLNL)

- LLNL is working on the development and application of computationally efficient and accurate simulation tools for prediction of engine combustion. In the past year they: (1) completed wide-ranging validation study of advanced engine combustion in the LLNL multi-zone model implemented in the Converge™ software package (Convergent Science, Inc.-licensed LLNL multi-zone model in October 2010); (2) implemented and validated latest high performance chemical kinetics solvers in Converge™ and OpenFOAM® CFD packages; (3) developed and validated a stand-alone multi-reactor chemical kinetics engine model for simulating multiple HCCI and PCCI engine cycles; (4) validated Converge™ multi-zone solver for direct injection PCCI using the including the latest LLNL chemical kinetics solver; and (5) promoted widespread industry application of LLNL multi-zone model through partnership with Convergent Science, Inc. (Flowers, LLNL)

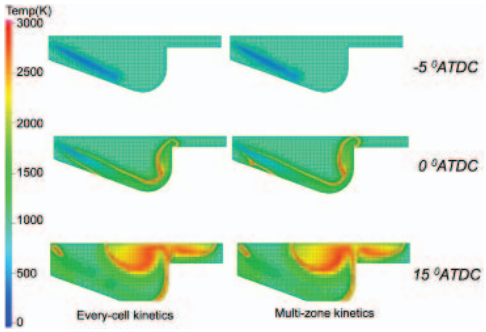

Comparison of spatial temperature evolution during combustion for every-cell kinetics versus multi-zone kinetics for direct injected diesel case (2.4-L/cylinder engine). Figure shows a two-dimensional axisymmetric slice through the center of the injection axis. (Flowers, LLNL)

- LLNL is developing improved solvers for advanced combustion engine simulation. In the past year they: (1) created a new thermochemistry library that is faster than other open source libraries: three times faster than Cantera, and ten times faster than OpenFOAM®; (2) developed a chemistry solver based on adaptive preconditioning that reduces the computational time to integrate large mechanisms by orders of magnitude; (3) reduced computation time for the ignition delay of the 7,200 species 2-methylalkane mechanism from one day using traditional solvers (e.g. those found in Kiva3V, OpenFOAM® and Converge 1.4) to 30 seconds with this project's new solver; (4) implemented and validated the new chemistry solver in the multidimensional CFD software packages Converge and OpenFOAM®; and (5) reduced computation time for the chemistry portion of the Converge™-multizone CFD simulation using the nearly 900 species iso-octane mechanism by an additional factor of 50 beyond the 6-fold speedup achieved through the LLNL multizone model (total speedup 300-fold). (McNenly, LLNL)
- Los Alamos National Laboratory (LANL) is developing code and algorithms for the advancement of speed, accuracy, robustness, and range of applicability of the KIVA combustion modeling software to higher-order spatial accuracy with a minimal computational effort. In the past year they: (1) developed h-adaptive and hp-adaptive predictor-corrector split (PCS) using Petrov-Galerkin finite element methods for all for flow regimes, from incompressible to high-speed compressible and a two-dimensional overset grid method for moving and immersed actuated parts such as valves for robust grid movement; (2) developed two-dimensional (2-D) overset grid method for moving and immersed actuated parts such as valves for robust grid movement. They began developing three-dimensional (3-D) overset grid method; (3) developed nearly automatic grid generation using only hexahedral elements with Cubit grid generator; (4) incorporated KIVA multi-component particle/spray injection algorithm into the PCS solver; (5) incorporated KIVA chemistry package into the PCS solver; (6) incorporated KIVA splash, break-up, collide and wall-film models into the PCS solver; and (7) began researching LES turbulence modeling for wall-bounded flows. (Carrington, LANL)

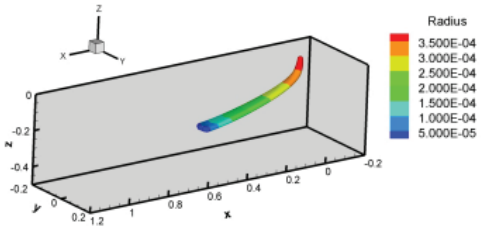

Injection and spray modeling test case for PCS FEM. Diesel spray modeling, droplet breakup and agglomeration showing complete evaporation. (Carrington, LANL)

- SNL is combining unique state-of-the-art simulation capability based on the large-eddy simulation (LES) technique with Advanced Engine Combustion R&D activities to maximize benefits of high-performance massively-parallel computing for advanced engine combustion research. During the past year, they: (1) performed detailed analysis of high-pressure injection processes using LES and real-fluid thermodynamics and compared LES with ECN experimental target data; (2) revealed that the envelope of mixture conditions varies from compressed liquid to supercritical state; at these conditions, the classical view of jet atomization and spray as an appropriate model is questionable; (3) established for the first time that a distinct gas-liquid interface does not exist for a wide range of diesel-relevant injection conditions. Instead lack of inter-molecular forces promotes diffusion over atomization; and (4) developed the theoretical basis to explain why classical spray theory does not apply at certain pressure-temperature regimes associated with direct injection in diesel engines. (Oefelein, SNL)
- Oak Ridge National Laboratory (ORNL) is supporting DOE and industry partnerships in assessment of state-of-the-art and longer-term advanced engine and combustion technologies for future goal setting. They ported CFD packages and additional components to run on ORNL high-performance computing resources (including Titan), and 3.1 Mhr of computational time have been allocated for current tasks, and demonstrated a novel approach for simulating cycle-to-cycle combustion variations through multiple, parallel simulations. (Edwards, ORNL)
- SNL is providing the fundamental understanding (science-base) required to overcome the technical barriers to the development of practical HCCI and HCCI-like engines by industry. In the past year they: (1) determined the effects of all main operating parameters on thermal efficiency, including Tin, fueling rate, engine speed, fuel-type, fueling strategy, and intake pressure; (2) demonstrated gross indicated thermal efficiencies of 47–48% for loads from 8 to 16 bar indicated mean effective pressure, gross for our current engine configuration (compression ratio = 14:1); (3) evaluated the effects of increasing the ethanol content of gasoline from 0 → 10 → 20% (E0, E10 and E20) on engine performance; (4) significantly improved temperature-map imaging resolution, signal/noise, and method of post-processing to remove laser-sheet schlieren effects; and (5) Provided data and analysis to support chemical-kinetic, computational fluid dynamics, and other modeling of HCCI at LLNL, the University of Michigan, and General Motors. (Dec, SNL)
- The University of Michigan (UM) is exploring new high-pressure lean-burn combustion that can enable future gasoline engines with 20-40% improved fuel economy and determining the fuel economy benefits of engines and engine cycles designed to utilize advanced combustion modes. In the past year: (1) a phenomenological quasi-dimensional model of spark-assisted HCCI has been developed for eventual use for system level simulations of engine control strategies and vehicle fuel economy improvement; (2) to assist in the development of the auto-ignition correlation, an engine data analysis tool has been developed; (3) the effects of fuel stratification in a small bore diesel engine using gasoline have been determined for high (19:1) and low (14:1) compression ratios; (4) experiments on spark-assisted compression ignition in the fully flexible valve actuation engine were carried out to quantify the effect of composition and charge temperature at time of spark; and (5) studies with a microwave-assisted spark plug were carried out in a constant-volume chamber aimed at characterizing mixture composition, turbulence, and pressure effects using Schlieren imaging. (Woolridge, UM)
- The University of Wisconsin is developing high efficiency internal combustion engines with goals of improved fuel economy by 20-40% in light-duty and 55% BTE in heavy-duty engines. In the past year: (1) optimum spray and combustion chamber design recommendations made for improved efficiency of heavy-duty and light-duty diesel engines. Gross thermal indicated efficiencies of ~60% in heavy-duty and ~50% in light-duty engines demonstrated; (2) improved thermal efficiency over stock manufacturer light-duty engine achieved without the need for NOx and particulate

matter after-treatment using gasoline compression ignition and dual-fuel RCCI combustion; (3) validated combustion and realistic fuel vaporization submodels developed for biofuels and gasoline/diesel surrogates for engine optimization and concept evaluation; and (4) formulated methodology for efficient engine system transient control strategies appropriate for engine speed/load mode transitions. This project is complete. (Reitz, University of Wisconsin)

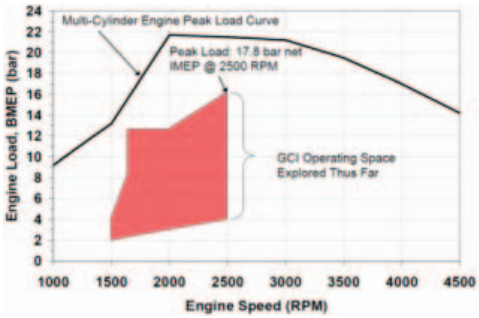

Gasoline direct injection compression ignition operation range for light-duty engine. (Reitz, University of Wisconsin)

- Michigan State University (MSU) is demonstrating an SI and HCCI dual-mode combustion engine for a blend of gasoline and E85 (85% ethanol and 15% gasoline) for the best fuel economy. In the past year: (1) a test bench of the electrical variable valve timing (EVVT) system was designed and fabricated and the model-based EVVT control strategy was developed and validated on the test bench and also on the optical engine; (2) the engine hardware-in-the-loop simulation model was further improved, including new physics-based charge mixing model and updated calibrations based upon optical engine test data; (3) the target four-cylinder metal engine was modified to fit the two-lift valvetrain and electrical cam phasing system. The engine piston was also redesigned to achieve desired compression for HCCI combustion; and (4) the prototype metal engine and the Opal-RT prototype controller were integrated and installed in the MSU dynamometer and the engine is ready for baseline mapping and future tests. (Zhu, Michigan State University)
- SNL is conducting acetylene seeding experiments in an automotive HCCI engine to identify ignition-enhancement effects of potential products of negative valve overlap (NVO) reformation. In the past year they documented significant piston wetting, pool fires, and rich combustion associated with late injection of NVO fuel, performed seeding experiment using a refined protocol to suppress extraneous influences while quantifying the distinct chemical enhancement of HCCI combustion by acetylene, documented the results of the seeding experiments in a journal article, and reproduced several significant trends of seeding experiments using a detailed iso-octane reaction mechanism with CHEMKIN's 0-D Closed Internal Combustion Engine Simulator. (Steeper, SNL)
- ORNL is expanding robust HCCI operation with advanced valve and fuel control technologies. In the past year they: (1) upgraded the air handling system of the ORNL single-cylinder with hydraulic valve actuation to allow boosted operation with external EGR; (2) expanded HCCI load range up to 650 kPa net indicated mean effective pressure ($IMEP_{net}$) with indicated thermal efficiency of greater than 40%: (3) operated newly installed laboratory air handling system to an intake manifold pressure of 190 kPa_a with external EGR of up to 30%; and (4) characterized the independent effect of boost, external EGR, and NVO duration on HCCI. This project is concluded. (Szybist, ORNL)
- ORNL is investigating potential near-term technologies for expanding the usable speed-load range and to evaluate the potential benefits and limitations of engine technologies for achieving high efficiency clean combustion in a light-duty diesel engine. In the past year they developed an RCCI map suitable for use in vehicle system drive cycle simulations, demonstrated greater than 15% improvement in modeled fuel economy with multi-mode RCCI operation as compared to a 2009 port fuel injected gasoline baseline meting the 2012 technical target, and evaluated the HC and CO reduction effectiveness of multiple DOCs with RCCI. (Curran, ORNL)
- ANL is quantifying the influence of low-cetane fuel ignition properties to achieve clean, high-efficiency combustion, optimize the advanced controls available to create a combustion system

that retains diesel-like efficiency while reducing NOx and other criteria pollutants compared to conventional diesel, and demonstrate the use of combustion imaging techniques to aid in determining the operational boundaries of gasoline compression ignition operation. In the past year they: (1) attained a 20% fuel economy improvement using LTC in a conventional powertrain vehicle over a similar port fuel injected vehicle; a 13% improvement versus a gasoline direct injection vehicle; (2) achieved over 40% brake thermal efficiency (BTE) operating from 8 to 20 bar brake mean effective pressure (BMEP) with below 0.4 g/kW-hr NOx, with some points under 0.2 g/kW-hr NOx; and (3) achieved 26% brake thermal efficiency with under 0.1 g/kW-hr NOx at 2 bar BMEP by using uncooled EGR to enable proper ignition propensity. (Ciatti, ANL)

- ORNL is analyzing and defining specific advanced pathways to improve the energy conversion efficiency of internal combustion engines from nominally 40% to as high as 60%, with emphasis on opportunities afforded by new approaches to combustion. In the past year they: (1) continued in-cylinder fuel reforming experiments with the modified Ecotec variable valve actuated engine to measure reactions of different fuels with hot exhaust; (2) initiated collaborative discussions with the National Technical University of Athens to develop an improved mechanism for ethanol in-cylinder reforming; (3) continued collaboration with the Gas Technology Institute (GTI) and Cummins on EGR-based catalytic thermochemical recuperation; (4) continued informal discussions on thermochemical recuperation and in-cylinder reforming with Southwest Research Institute® and Volvo; and (5) issued patent for a novel 6-stroke engine concept that uses water injection for in-cylinder waste heat recovery. (Daw, ORNL)

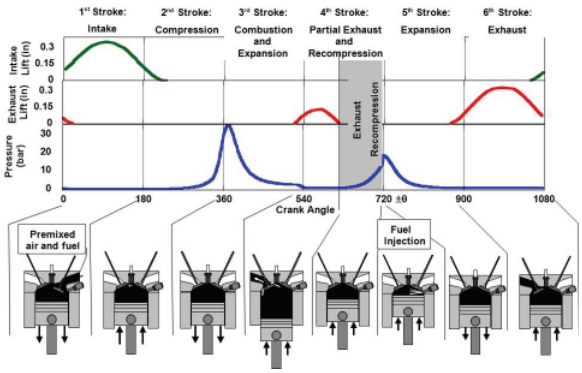

Profile for the experimental 6-stroke cycle on the ORNL modified Ecotec VVA engine. Fuels are injected during exhaust recompression to study in-cylinder, non-catalytic reforming. (Daw, ORNL)

- SNL is designing a free-piston engine suitable for hybrid vehicle applications. In the past year progress included: (1) permanent magnet arrays assembled and incorporated into piston bodies; (2) compressed helium gas injection starting system tested to show capability to bring pistons to desired operating compression ratio in one stroke with good piston synchronization; (3) modeling and experiments with piston pulsing showed deficiency in bounce chamber vent manifolds. Vent manifolds re-designed, fabricated and demonstrated with improved performance; (4) modeling and experiments with piston pulsing showed deficiency in bounce chamber high pressure gas delivery heads. Heads, manifolds and valve plates re-designed, fabricated and demonstrated with improved performance; (5) high pressure nitrogen system assembled to replace air compressor system to extend pressure and flow rate capability for motoring mode; and (6) short duration (~1.5 second) motoring demonstrated with good piston synchronization. Barriers to continuous motoring identified and engineering solutions developed and in-progress to address them. (Johnson, SNL)
- ORNL is quantifying the fuel economy benefit and emissions impact of variable compression ratio engine technology to a modern direct-injection gasoline engine. During the past year, the engine was built, and is now being prepared for dynamometer testing. (Domingo, ORNL)
- ANL is identifying state-of-the-art engine and vehicle technologies currently in production to quantify the benefits of the state-of-the-art vehicle technologies currently in production, optimize vehicle performance using advanced vehicle level modeling and accelerate the development of high efficiency internal combustion engines for light-duty vehicle applications, while meeting the future emission standards, using numerical simulations. In the past year they obtained two new vehicles

and supplied vehicle data sets for the BMW 530i, Toyota Prius and Toyota Auris to the vehicle systems group for the U.S.DRIVE goal setting exercise. (McConnell, ANL)

- ORNL is improving diesel engine-catalyst system efficiency through better combustion uniformity, engine calibrations and catalyst control. In the past year they developed an EGR probe capable of quantifying transient engine EGR uniformity, applied the EGR probe for development of EGR mixer design consistent with achieving next-generation engine efficiencies, and initiated further EGR probe improvements. (Partridge, ORNL)

B. Emission Control R&D

The following project highlights summarize the advancements made in emission control technologies to both reduce exhaust emissions and reduce the energy needed for emission control system operation.

- ORNL continued to co-lead the Cross-Cut Lean Exhaust Emission Reduction Simulation (CLEERS) Planning Committee and facilitation of the SCR, LNT, and DPF Focus group telecoms with strong domestic and international participation. In the past year they: (1) Initiated Focus group telecoms with strong domestic and international participation. In the past year they: (1) initiated expansion of the database and information repository for experimental engine exhaust and aftertreatment measurements and simulation algorithms and modeling tools; (2) coordinated further refinement of LNT and SCR catalyst characterization protocols; (3) provided regular update reports to DOE Advanced Combustion Engine Crosscut Team; (4) organized the 2012 CLEERS workshop at University of Michigan, Dearborn on April 30-May 2, 2012; (5) maintained CLEERS website (www.cleers.org) including functionalities, security, and data to facilitate web meetings and serve focus group interactions; (6) increased utilization of models and kinetic parameters produced by CLEERS projects in full system simulations of alternative advanced powertrain options; and (7) worked with the U.S.DRIVE Advanced Combustion and Emissions Control Low-temperature Task Force to promote awareness of emerging aftertreatment barriers associated with low temperature exhaust from advanced engines. (Daw, ORNL)
- ORNL is collaborating with SNL and PNNL to produce kinetic information for LNT and urea-SCR aftertreatment devices, both as individual and system integrated components as part of the CLEERS project. In the past year they: (1) initiated flow reactor characterization of a new commercial CLEERS LNT reference catalyst used in the lean gasoline direct injection-equipped BMW 120i sedan; (2) collaborated with Gamma Technologies to develop and share kinetic parameter estimates for the new CLEERS BMW reference catalyst; (3) developed a global kinetic model that predicts N_2O and NH_3 formation in LNTs over a wide range of reductant composition, temperature, and regeneration period; (4) in collaboration with ORNL's Center for Nanophase Materials Sciences and Chonbuk National University, characterized novel catalysts with enhanced low-temperature oxidation activity; (5) continued collaborative kinetic measurements and analysis of LNT and SCR catalysts with ICT Prague, Chalmers University of Technology, and Politecnico di Milano; and (6) with PNNL, continued developing global kinetics for a commercial Cu-zeolite SCR catalyst and evaluating the impact of hydrothermal aging on the catalyst function. (Daw, ORNL)
- PNNL is developing improved modeling capabilities for SCR and DPFs through fundamental experiments. In the past year they: (1) obtained kinetic parameters for small-pore zeolite-based Cu SCR catalysts; (2) determined an optimum K loading for overall and best high temperature performance for K-based LNT catalysts; (3) developed and validated a Cu SCR model considering a single NH_3 storage site, based on Cross-Cut Lean Exhaust Emission Reduction Simulation (CLEERS) SCR transient protocol data from ORNL; (4) began development of a new SCR model with two NH_3 storage sites in order to better reproduce effects observed in experimental data;

and (5) proposed an improved unit collector model for prediction of number efficiency in exhaust particulate filters. (Muntean, PNNL)

- PNNL is identifying approaches to significantly improve the high temperature performance and stability of the catalytic NOx reduction technologies. In the past year: (1) model catalysts were prepared at PNNL based on materials described in the open literature; (2) detailed studies of the sensitivity to high temperatures (required for desulfation) of these model catalysts were performed this year; (3) specific new results on the mechanisms of Pt stabilization by the novel support material, $MgAl_2O_4$, were obtained; (4) based on prior literature reports, several synthesis efforts were carried out at PNNL to prepare model CHA-based catalysts; and (5) catalysts were characterized before and after incorporation of Cu by X-ray diffraction, electron paramagnetic resonance and temperature programmed reduction. Baseline reactivity measurements were performed on these catalysts in preparation for mechanistic studies of high- and low-temperature performance loss. (Peden, PNNL)

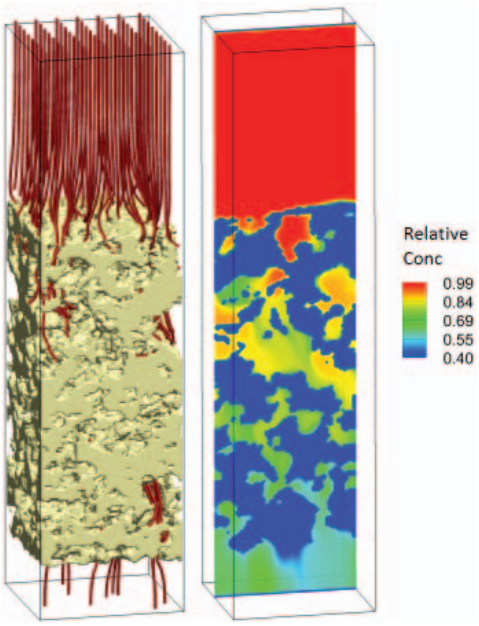

Eulerian-Eulerian Filter Simulation of a Cordierite DPF (Muntean, PNNL)

- PNNL is developing and demonstrating mixed metal oxide-based catalysts as a low-cost replacement for platinum for controlling NOx emissions. In the past year they: (1) identified mixed metal oxide catalyst compositions and forms that show high activity for NO oxidation, and may serve as a suitable replacement for platinum-based catalysts for exhaust gas treatment; (2) demonstrated that the ceria support both decreased the required temperature for formation and increased the quantity of labile oxygen needed for NO oxidation; (3) showed that mixed metal oxide catalysts produced using a simple incipient wetness method compared favorably to those prepared by co-precipitation; and (4) established density function theory methods to help investigate interactions between reactants and potentially active sites. (Pederson, PNNL)
- PNNL is developing a fundamental understanding of the integration of SCR and DPF technologies for on-road heavy-duty vehicle application. In the past year they: (1) developed an understanding of the primary reaction driver(s) in the SCR filter system; (2) developed an understanding of strategies that can be employed for facilitating improved passive soot oxidation in the system in the presence of the SCR process; and (3) developed the ability to accurately predict how changes in active species concentrations will affect system performance. (Rappe, PNNL)
- ORNL is assessing and characterizing catalytic emission control technologies for the reduction of NOx from lean-gasoline engines and identifying strategies for cost reduction of emission controls for lean-gasoline engines. In the past year they: (1) determined the effect of lean-rich timing on a commercial LNT as it impacts lean NOx reduction as well as NH_3 and N_2O production; (2) evaluated a series of catalyst formulations and demonstrated impact of platinum grade metal (PGM) content on NH_3 production as a function of temperature and air/fuel ratio; (3) demonstrated high NOx conversion with a three-way catalyst/selective catalytic reduction passive SCR setup under lean/rich cyclic operation on a flow reactor: (4) characterized the control of a representative lean gasoline engine vehicle (European BMW 120i) and installed that engine with a custom controller in an engine dynamometer laboratory to establish a research platform for on-engine studies. (Toops, ORNL)

- ORNL and Cummins are exploring NOx control and measurement technology for heavy-duty diesel engines. In the past year they: (1) advanced understanding of NH_3 utilization and its influencing parameters; (2) developed and participated in collaboration which developed a kinetic model of distributed SCR performance based on SpaciMS measurements; (3) modeled the spatially distributed intra-SCR performance measured previously in this project; and (4) identified N_2O formation pathways in lean-NOx trap catalysts. (Partridge, ORNL)
- The University of Houston is identifying the NOx reduction mechanisms operative in LNTs and in situ SCR catalysts, and using this knowledge to design optimized LNT-SCR systems in terms of catalyst architecture and operating strategies. In the past year they did the following: (1) application of crystallite-scale LNT model to simulate spatially resolved capillary inlet mass spectrometer SpaciMS experiments for LNT monolith; (2) modeling of the dual component SCR catalyst containing Fe- and Cu-exchanged zeolite to determine the optimal loading and architecture of the two catalysts; and (3) development of a dual layer LNT/SCR model to elucidate the experimental findings and to identify optimal dual layer compositions and operating conditions. (Harold, University of Houston)
- The University of Connecticut is developing three-dimensional composite nanostructures for lean-NOx emission control devices. In the past year they: (1) fabricated and characterized the PGM and BaO loaded 3-D composite nanowire/rod array (such as ZnO/(La,Sr)CoO_3(LSCO) and TiO_2/(La,Sr)MnO_3(LSMO), etc.) on monolith substrates; (2) investigated the (hydro-)thermal and mechanical stability, CO and NO oxidation performance, S-poisoning resistance, as well as NOx storage and reduction performance of the 3-D composite nanostructures; (3) demonstrated ultra-high materials usage efficiency of 3-D composite nano-array catalysts in both PGM and metal oxides, excellent thermal and mechanical robustness, as well as tunable catalytic performance, showing their good potential to be used as the next-generation automotive catalysts: and (4) developed the reliable surface catalytic phase diagrams of perovskite (such as $LaMnO_3$) surfaces through the first principle thermodynamics and KMC simulations. (Gao, University of Connecticut)
- PNNL and CRADA partner Ford are developing an understanding of the deactivation mechanisms of the urea-SCR catalyst used in diesel aftertreatment systems. In the past year they: (1) completed studies of the differing effects of SO_2 to SO_3, including identification of the mechanism of poisoning by SO_3; (2) characterized the nature and distribution of phosphorus deposits observed on engine-aged urea SCR catalysts; (3) performed studies aimed at an understanding of unusual hydrothermal aging of zeolite-based urea SCR catalysts observed at Ford; (4) Investigated the physicochemical properties of model zeolite materials with respect to hydrothermal aging; and (5) evaluated the effects of physicochemical properties of model zeolite materials on the adsorption and desorption of ethanol. This project is completed. (Peden, PNNL)
- ORNL is developing non-destructive, non-invasive neutron imaging technique and implement it to improve understanding of regeneration behavior in DPFs through comprehensive, quantitative device analysis. In the past year they: (1) improved visualization tools to enable identification of particulate from DPF walls; (2) identified particulate depth as a function of length, radius, and particulate loading: and (3) built portable spray chamber with high pressure fluid delivery system for diesel injectors. (Toops, ORNL)
- ANL is developing advanced diesel particulate filtration systems. In the past year: (1) the effects of exhaust emission components were evaluated on soot oxidation; (2) detailed DPF filtration/regeneration processes were characterized; (3) an optimized filter design was proposed in consideration of correlations between pore geometry and size; and (4) a numerical code was developed to predict flow dynamics in a filter with potential to calculation of soot loading profiles. (Lee, ANL)

- ANL is characterizing particulates from a LTC engine. In the past year they (1) revealed that aggregate particles smaller than 10 nm, which were found to be abundant in the LTC engine emissions, are not solid carbon particles; (2) demonstrated that LTC soot particles are much smaller in both primary and aggregate particle sizes than those from conventional diesel engines; (3) showed that soot oxidation is insignificant during the LTC process by examination of nanostructures as well as morphology; and (4) found that biodiesel soot appears to be much smaller in both primary and aggregate sizes than does ultra-low sulfur diesel fuel soot, which results in the reduced total soot mass. (Lee, ANL)

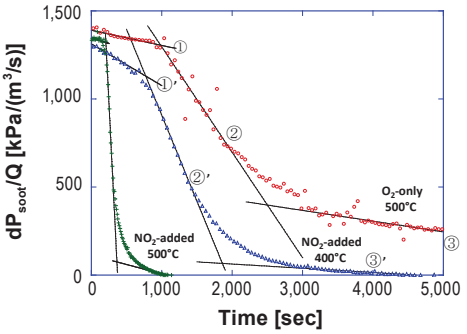

②′ End of 2nd linear (1,700 s)

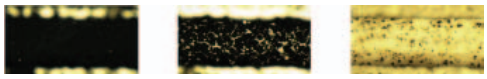

Pressure drop traces during regeneration process under three different inlet gas conditions and visualized images for regeneration with 1,000 ppm NO_2-added emissions at 400°C. (Lee, ANL)

- PNNL is characterizing exhaust particulates from advanced combustion engines such as spark ignition direct injection (SIDI) using readily available fuel blends and using insight gained and prior experience with diesel aftertreatment to jump-start development of optimum aftertreatment technologies. In the past year a second campaign of cooperative experiments was carried out at the University of Wisconsin ERC; several SIDI experiments conducted during the first campaign with ethanol-free gasoline were repeated to confirm consistency with previous results; and new experiments were also carried out at a number of operating points using E20 and E85 ethanol blends. In addition to SIDI, a smaller number of experiments were also carried out with gasoline direct-injection (GDI) compression ignition and RCCI test engines. (Stewart, PNNL)
- Michigan Technological University developing experimentally validated DOC, DPF and SCR models with real-time internal state estimation strategies that support future onboard diagnostics, advanced control system, and system optimization objectives for DOC-DPF-SCR aftertreatment systems that minimize the energy penalty of meeting emission regulations. In the past year: (1) a high-fidelity one-dimensional (1-D) catalyzed particulate filter model was enhanced for calibration of engine data that is being used for reduced order model/state estimation; (2) a lumped catalyzed particulate filter model for reduced order model/state estimation was developed and calibrated; (3) completed development and calibration of the DOC high-fidelity and the reduced order estimator models to engine data; (4) completed development and calibration of the SCR high-fidelity model to the reactor data; and (5) completed development and calibration of the SCR high-fidelity and the reduced order estimator models to engine data. (Johnson, Michigan Technological University)
- The Health Effects Institute is conducting the Advanced Collaborative Emissions Study to characterize the emissions and assess the safety of advanced heavy-duty diesel engine and aftertreatment systems and fuels designed to meet the 2007 and 2010 emissions standards for PM and NOx. In the past year preliminary results of the first two engines tested at Southwest Research Institute® indicated that the intended emissions reductions are met. Daily analysis of exposure atmospheres indicates that the 2007-compliant engine system continues to operate reliably and has consistently provided the targeted exposure concentrations. There were no exposure-related differences in mortality or clinically-evident morbidity in rats after 12 or 24 months (preliminary findings) of exposure. Similarly as observed after 3 months of exposure, the histologic findings at 12 months showed a small increase in the extent of the tissue changes in the respiratory tract, but the severity of the changes remained mostly minimal and effects were observed only at the highest exposure level. (Greenbaum, Health Effects Institute)

C. High Efficiency Engine Technologies

The objective of these projects is to research and develop technologies for more efficient clean engine/powertrain systems to improve passenger and commercial vehicle fuel economy.

- Cummins Inc. is engaged in developing and demonstrating advanced diesel engine technologies to significantly improve the engine thermal efficiency up to 55% and will demonstrate tractor-trailer vehicles with 68% or greater freight efficiency improvement over a 24-hour cycle. In the past year they demonstrated the interim milestone of 50% or greater BTE with a combination of hardware demonstration and simulation of optimized components. (Koeberlein, Cummins)
- Detroit Diesel Corporation is demonstrating a 50% total increase in vehicle freight efficiency measured in ton-miles per gallon, with at least 20% improvement through the development of a heavy-duty diesel engine. In the past year they demonstrated 46.2% engine brake thermal efficiency in the laboratory on the SuperTruck demonstration engine, meeting the year-2 project targets. Development continued on the core engine, with the best results to date being an engine brake thermal efficiency of 46.8%. The waste heat recovery system design was completed. (Sisken, Detroit Diesel Corporation)
- Navistar is demonstrating engine BTE improvements which contribute 20 percent (of the total 50 percent required) improvement in the freight efficiency of a combination tractor-trailer as a part of the DOE SuperTruck Project. In the past year they: (1) Demonstrated an engine combustion strategy leading to a BTE improvement from 42 to 45 percent by extending peak cylinder pressure capability (190→220 bar) and using higher injection pressure (2,200→2,900 bar); and (2) Demonstrated heat recovery using electrical turbo-compounding with advance air system to further increase the BTE to 46.5 percent. (Oehlerking, Navistar)
- Volvo Powertrain North America is identifying concepts and technologies that have potential to achieve 55% BTE on a heavy-duty diesel engine as defined in the SuperTruck project. In the past year they: (1) validated two skeletal-size n-heptane and n-dodecane chemical mechanisms under ECN conditions; (2) achieved up to 2% fuel economy improvement in alternative fuel tests (high derived cetane number/low aromatics fuels) at heavy-duty engine cruise-like point; (3) attained up to 7% BTE improvement in PCCI engine tests; (4) partially premixed combustion tests with 70 octane number demonstrated a wide operating range; and (5) identified a concept capable of 55% BTE. (Amar, Volvo Powertrain North America)

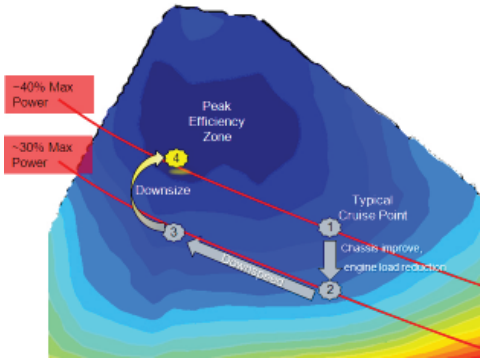

Total system optimization in speed-load range including ORC system integration. (Amar, Volvo)

- Delphi will develop, implement and demonstrate fuel consumption reduction technologies using a new LTC process; gasoline direct injection compression ignition. In the past year: (1) the reduced parasitic loss engine was installed in Phase 1 Vehicle 1 and testing was started; (2) final debug and test preparation was completed on Vehicle 1; (3) a full powertrain calibration was completed for Phase 1 Vehicle 2 using an engine dynamometer engine and the demonstration vehicle. The dynamometer results were integrated into the baseline vehicle calibration; and (4) vehicle fuel economy and emissions tests were performed. (Confer, Delphi Automotive Systems LLC)
- Ford will demonstrate 25% fuel economy improvement in a mid-sized sedan using a downsized, advanced gasoline turbocharged direct injection engine with no or limited degradation in vehicle level metrics. In the past year the team progressed the project through the Combustion System

Development, Single-Cylinder Build and Test, and Engine Design/Procure/Build tasks with material accomplishments. In addition to the prime combustion system completed in Budget Period 1, the team completed a combustion system iteration option which may be employed during the multi-cylinder engine dynamometer evaluation phase. (Wagner, Ford Motor Company)

- General Motors will demonstrate 25% vehicle fuel economy improvement through lean-gasoline combustion while achieving Tier 2 Bin 2 emissions. In the past year they: (1) designed, procured and assembled the second generation, lean downsize boost gasoline combustion engines that incorporates multiple fuel injection authority and high-energy ignition; (2) developed the lean aftertreatment system hardware configuration and calibration to provide comprehensive NOx reduction under all thermal operating conditions; (3) refined the torque-based engine controls architecture and calibration to provide precise EGR control for optimized transitions between lean and stoichiometric operation; (4) achieved the FY 2012 technical target of a lean aftertreatment system capable of emissions within 200% of Tier 2 Bin 2 without particulate mitigations; and (5) approached the FY 2012 technical target of City Federal Test Procedure and Highway fuel economy improvement at 9%, with projections to achieve target with the new lean downsize boost engine. (Smith, General Motors Company)
- Chrysler aims to demonstrate 25% improvement in combined Federal Test Procedure City and Highway fuel economy for the Chrysler minivan. In the past year: (1) the diesel micro pilot engine shows impressive brake specific fuel consumption (BSFC) results at high loads (40% BTE) but difficult to control due to sensitivities to EGR rate, injection events, temperature and humidity; (2) the triple-plug engine demonstrated good fuel efficiency (39% BTE). Significant testing completed with dual-fuel system using port fuel injection ethanol; (3) conducted drive cycle fuel economy testing with new thermal management system installed on surrogate vehicle. Demonstrated 3.0% increase in unadjusted fuel economy due to rapid warm-up; and (4) models for electric system, air conditioning system, engine, vehicle, driver, torque converter and transmission thermal, torque converter mechanical and transmission and differential mechanical completed in the vehicle energy simulator and the vehicle energy model. (Reese, Chrysler Group LLC)
- Cummins is demonstrating 40% fuel economy improvement over a baseline gasoline V-8 pickup truck and Tier 2 Bin 2 tailpipe emissions compliance. In the past year they: (1) completed design and analysis of an all-new engine including all elements required to meet Tier 2 Bin 2 tailpipe emissions (dual-loop EGR and variable swirl control) while meeting a weight target of less than 65 kg/ltr of displacement; (2) procured required hardware to build the new engine and have ready for test in December 2012; (3) demonstrated engine-out emissions of less than 0.4 g/mi NOx, using steady-state operating conditions to approximate the drive cycle without loss of fuel economy; (4) demonstrated mule vehicle with ZF 8-speed automatic transmission and operable direct ammonia delivery system from Amminex. (Ruth, Cummins, Inc.)

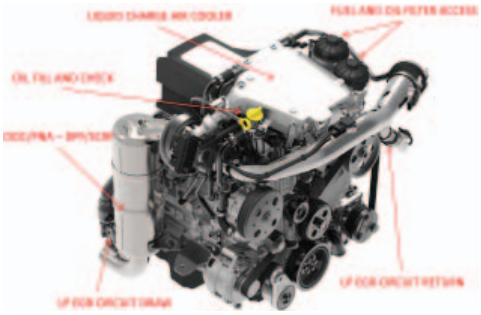

New Cummins Engine Design (Ruth, Cummins)

- Robert Bosch LLC is demonstrating improved fuel economy by 30% with minimum performance penalties. In the past year they: (1) completed vehicle simulations showing greater than 25% fuel economy improvement over the baseline vehicle; (2) completed prototype II engine design and engine management system configuration: (3) demonstrated transient performance of the target combustion modes with closed-loop control via cylinder pressure sensing techniques; (4) initiated demonstration vehicle integration. (Yilmaz, Robert Bosch)

- Filter Sensing Technologies, Inc. is designing, developing, and validating radio frequency (RF) sensors for accurate real-time measurements of DPF loading with low-pressure drop substrates. In the past year they: (1) completed RF model development and generated database of material dielectric properties over a range of frequencies and temperatures for typical DPF systems; (2) validated models with experiments and applied results to guide prototype development; and (3) down-selected final prototype designs and initiated testing to optimize performance. (Sappok, Filter Sensing Technologies, Inc.)
- General Motors is applying high energy ignition and boosting/mixing technology to increase fuel economy in spark ignition gasoline engines by increasing EGR dilution capability. In the past year they: (1) constructed one-dimensional engine simulation models with conventional low-pressure loop and direct EGR; (2) evaluated the vehicle simulation model of a current mid-size GM vehicle to determine the operating points for the subject engine configurations in order to generate fuel economy projections; (3) completed baseline engine testing to establish the fuel consumption and performance baseline; and (4) completed design to package the low-pressure loop EGR system defined through simulation in the engine compartment of a current GM mid-size vehicle. (Keating, General Motors)
- Eaton is demonstrating fuel economy improvement through Rankine cycle waste heat recovery systems utilizing a roots expander in heavy-duty diesel applications. In the past year they: (1) completed baseline engine calibration and experimental data collection of EGR, injection timing, air/fuel ratio sweeps and exhaust restriction sensitivity on performance; (2) validated one-dimensional simulation against experimental data predicting the enthalpy availability; (3) completed analytical investigation to predict the roots-based Rankine cycle performance; (4) achieved analytically, a 5% fuel economy improvement; and (5) developed Roots expander concept design based on simulation and analytical results. (Subramanian, Eaton)
- MAHLE Powertrain is demonstrating breakthrough thermal efficiency of 45% on a light-duty gasoline engine platform while demonstrating potential to meet U.S. emissions regulations. In the past year they: (1) Developed single-cylinder optical and corresponding single-cylinder thermodynamic engines as tools to study and optimize Turbulent Jet Ignition (TJI) hardware, utilizing production engine platforms and incorporating TJI; (2) Initiated 3-D analysis of TJI concept by providing detailed boundary condition parameters synthesized from previous experiments and 1-D analysis; and (3) Optimized design of experiments to methodically examine engine performance as a function of TJI hardware variations and to correlate experimental data with 3-D analysis results. (Blaxill, MAHLE Powertrain)

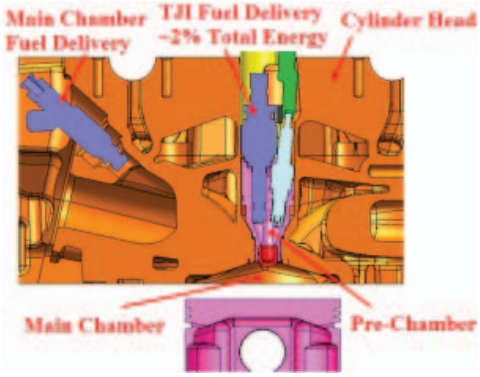

Spark Ignition Engine Incorporating MAHLE Powertrain's Turbulent Jet Ignition. (Blaxill, MAHLE Powertrain)

- Ford is focusing on complete and optimal system solutions to address boost system challenges, such as efficiency degradation and compressor surge, etc., in diesel combustion/emission control system development, and to enable commercialization of advanced diesel combustion technologies, such as HCCI/LTC. In the past year: (1) an IHI production turbo was selected as the donor turbo based on the variable geometry turbocharger packaging size in which the advanced mixed flow turbine can be fit; (2) a production 3.2-L I-5 diesel engine was selected as base engine. The advanced turbocharger based on the IHI donor turbocharger was design, analyzed and fabricated. The advanced turbo assembly was flow bench tested at supplier's facility; (3) the advanced turbocharger assembly was equipped with an "active casing treatment" to extend flow capacity of the

compressor; (4) the advanced compressor design has demonstrated 2-4% brake BSFC improvement on steady-state conditions at part load, even though the advanced turbo was designed for 30% increase in flow capacity over the donor turbo; and (5) the base Puma I-5 engine was calibrated for Tier 2, Bin 8 tailpipe emissions. Efforts were made to meet Tier 2, Bin 5 tailpipe emissions with the base IHI donor turbocharger. Using the same engine setup and calibration, except the turbocharger change, the newly developed advanced turbocharger demonstrated 3.3% fuel economy improvement over the donor turbocharger. This project is complete. (Sun, Ford)

- LANL is developing a prototype NOx sensor based on mixed-potential technology using a $La_{1-x}Sr_xO_{3-\delta}$ (LSC) sensing electrode and a prototype NH_3 sensor based on mixed-potential technology using an Au sensing electrode. In the past year they: (1) qualitatively reproduced NOx sensitivity and selectivity of a LANL bulk sensor in a commercially manufacturable device; (2) demonstrated ±5 ppm NH_3 sensitivity in a Pt/ytrria-stabilized zirconia/Au mixed potential sensor; and (3) Demonstrated ±5 ppm NOx sensitivity in a Pt/YSZ/LSC mixed potential sensor. (Mukundan, Los Alamos National Laboratory).

SOLID STATE ENERGY CONVERSION

Several projects are being pursued to capture waste heat from advanced combustion engines in both light- and heavy-duty vehicles using thermoelectrics (TEs). Following are highlights of the development of these technologies during FY 2012.

- Gentherm Inc. is developing a high-efficiency TE waste energy recovery system for passenger vehicle applications. In the past year vehicle platform/powertrain selections have been made by BMW and Ford after extensive fuel efficiency improvement performance trade-off analysis. BMW will use a BMW X5 30i with a 4-cylinder gasoline engine. Ford will use a Ford Explorer with 2-L EcoBoost I-4. An initial thermoelectric generator (TEG) architecture design concept has been finalized which addresses issues associated with previous TEG designs. TE material improvement has begun with the construction of the "holistic performance model" for skutterudite TE material. Early tests of oxidation/sublimation suppression coating systems indicate potential for success. (Crane, Gentherm)
- General Motors is identifying distributed cooling and heating strategies that can efficiently augment or replace a vehicle's central heating, ventilation and air conditioning system by delivering localized cooling/heating of key human body segments that strongly influence an occupant's perceived thermal comfort. In the past year: (1) Team selection criteria lead to a 2012 eAssist Buick LaCrosse for final demonstration; (2) All phases of testing benefit from UC Berkeley thermal manikin evaluation, providing detailed localized comfort measurement with an absence of psychological influence; (3) The team has finalized the design and test for the Volt coolant TE heat exchanger; (4) Volt test data showed the new coolant TE heater with coefficient of performance (COP) = 1 for extremely low temperature (large ΔT) and achieved COP > 2.3 depending on ΔT; and (5) The developed thermoelectric devices for the Lacrosse are being examined and plan to be modified and retrofitted into Volt demonstration vehicle. (Bozeman, General Motors)
- General Motors is developing cost-competitive advanced TEGs for direct conversion of vehicle waste heat into useful electrical power. In the past year they: (1) Assessed skutterudite material and module performance; (2) Identified parasitic thermal and electrical losses associated with diffusion barriers, thermal interfaces, and electrical interconnects; (3) Achieved a projected 10% heat conversion efficiency for skutterudite TE modules in laboratory tests; (4) Selected a full-size light-duty truck as the project target vehicle; (5) Completed the gap analysis that supports establishing the technology development requirements for the overall TEG system and supports the program objective to improve FE in light-duty vehicles by 5%; (6) Determined that over 1 kW of TEG power

will be needed to improve FE by 5% based on vehicle performance data, vehicle simulations, and system modeling; and (7) Developed improved modeling tools for a combined system model incorporating an exhaust gas temperature model based on combustion power, the TEG model based on our earlier work on the previous TEG project, and a unified model of the vehicle high voltage electrical power bus. (Meisner, General Motors)

The Chevrolet Suburban target vehicle used for our previous TEG development project. The lower panel shows the underside view of the vehicle. (Meisner, General Motors)

- GMZ Energy is developing a robust TEG system that will provide at least 5% fuel efficiency improvement for a light-duty vehicle platform. In the past year they: (1) Fabricated bismuth telluride devices with 4.3% efficiency between 80°C to 200°C and half-Heusler devices with 4.3% efficiency between 200°C to 450°C; (2) Designed TEG systems that can produce up to 500 W electricity; and (3) Demonstrated up to 4% fuel economy improvement with simulated TEG power output of 480 W. (D'Angelo, GMZ Energy)
- Ohio State University is developing high-efficiency high figure of merit (zT) thermoelectric materials (PbSe and Mg_2Sn) that contain no rare or precious elements, and are non-toxic. In the past year they: synthesized pure Mg_2Sn and doped it with Ag, Cu, Zn and Indium (In) as a reference impurity. Thermomagnetic and galvanomagnetic measurement show that Ag-doped samples are p-type with a maximum power factor of 18μ $Wcm^{-1}K^{-2}$, a maximum figure of merit (zT) of 0.25 at 540 K and a high effective mass of 0.9 m_o. A new type of nano Ag paste was developed to eliminate sintering pressure. Mechanical chips were used for device attachment. It produces excellent bonding quality (~25 MPa die-shear strength and free of large voids). (Heremans, Ohio State University)
- Purdue University is enabling the broad adoption of TE waste heat recovery systems, or TEGs, at a scale commensurate with the global vehicle manufacturing enterprise. In the past year they: (1) identified materials for high temperature thermoelectric; (2) developed solution-phase method to synthesize chalcogenide nanowires with thermoelectric performance better than the state of the art; and (3) explored complex metal sulfides as potential candidates to replace tellurides and antimonides for mid temperature range thermoelectric application. (Xu, Purdue University)
- Stanford is performing systems-level modeling and full device-scale characterization, with the ultimate goal of constructing a complete architecture for optimizing a TEG system for recovering waste heat from automobile combustion. In the past year they reported the first in situ degradation data under thermal cycling for ZT and its component properties for commercial modules – along with infrared imaging – to assess the role of interfaces in the reliability of thermoelectrics. The reduction in electrical conductivity with thermal cycling was found to be the primary degradation mechanism. (Goodson, Stanford)
- Stony Brook University successfully obtained single-phase higher manganese silicide using melt-spinning and successfully demonstrated thermal spray of silicide materials. In the past year, the thermal, electrical conductivity and Seebeck coefficient of the sprayed Mg_2Si have been characterized. Results show: (1) Both vacuum plasma spray thermal spray method and atmospheric plasma spray with internal power injection can reduce thermal conductivity, likely due to enhanced phonon scattering; (2) Atmospheric plasma spray with internal power injection achieved good electrical conductivity; (3) Vacuum plasma spray with proper power level setting and substrate

temperature control achieved similar Seebeck coefficient compared with either hot press or spark plasma sintering. (Zuo, Stony Brook University)

- Texas A&M is synthesizing inorganic nanowires and quantum wires of both $CoSb_3$ and InSb, and organic conducting polymer thin films, and assembling them into inorganic-organic hybrid TE cells with sizes ranging from a few mm^2 to a few cm^2, using conjugated linker molecules to tether the nanowires to each other or to conducting polymer thin films. In the past year they: (1) Accomplished the large-scale synthesis of both unfunctionalized and conjugated organic molecule functionalized Zn_3P_2 nanowire powder using self-catalysis; (2) Evaluated the thermoelectric performance of pellets obtained by hot pressing Zn_3P_2 nanowire powders; (3) Evaluated the thermoelectric performance of poly(3,4-ethylenedioxythiophene) films of various thicknesses; and (4) Accomplished the small-scale synthesis of phase-pure $CoSb_3$ nanowires (i.e., devoid of any contaminant $CoSb_2$ and CoSb phases) and phase-pure InSb nanowires (i.e., devoid of any indium oxide contaminant). (Vaddiraju, Texas A&M)
- The University of California, Los Angeles is developing novel materials and interfaces for improved thermomechanical reliability of TE vehicle exhaust waste heat harvesting devices. In the past year they found that, to minimize open pores, metal particles have to be of nanometer size. They synthesized Cu nanoparticles by using a direct and economic approach where a copper salt (copper sulfate, $CuSO_4$) is dissolved in water and Cu^{2+} ions are reduced to metallic Cu nanoparticles using a strong reducing agent. Sintered pellets of pure Cu and a series of Cu-ZrW_2O_8 compositions with up to 50 wt% (74 vol%) oxide have been prepared. They also successfully developed a numerical model for the mechanical characteristics of capillary confined liquid elements and experimentally confirmed its validity. (Ju, University of California, Los Angeles)
- The University of California, Santa Cruz, is developing novel TE materials based on abundant and non-toxic Zintl phase magnesium silicide alloys and optimizing the TE power factor and figure of merit by band engineering and electron filtering. In the past year they: (1) Developed an understanding of electron scattering in Mg_2Si nanocomposites; (2) Optimized $Mg_2Si_{0.4}Sn_{0.6}$ with and without embedded nanoparticle scattering at different electron concentrations and temperatures; (3) Low temperature synthesis and SPS of n-type $Mg_{2-x}Yb_xSi$ with embedded Yb_3Si_5 nanoparticles; and (4) Low temperature synthesis and SPS of n-type $Mg_2Si_{1-x}Sn_x$ with embedded Si and Mg_2Si nanoparticles. (Shakouri, University of California, Santa Cruz)
- Virginia Tech is fabricating and characterizing new TE materials growth with techniques capable of producing large quantities of efficient, yet non-toxic and inexpensive elements capable of long-term operation at high temperatures over thousands of thermal cycles. In the past year they designed, fabricated, and tested heat exchangers that use impinging jets that provide excellent heat transfer with limited pressure drop penalty. They found that the heat exchangers with impinging liquid jets provide temperatures 10-20°C lower than for geometries tested with standard guided flow. On the exhaust side, we explored a variety of pin-fin configurations and found that simple pin-fins with length <15% of the channel height can increase heat transfer rates by a factor of two on the exhaust-side heat exchanger, while limiting pressure drop to <2 psi. In order to fully examine the heat exchangers and to verify their computational models for thermal management and power output, they created a scaled-down test rig that includes the hot gas flow, a coolant loop, both heat exchangers, and thermoelectric elements all integrated in an exhaust system. (Huxtable, Virginia Tech)
- The University of Texas at Austin is increasing the zT of abundant silicide materials to a level competitive with the state of the art found in materials containing much more scarce and expensive elements, and enhancing the thermal management system performance for silicide TE devices installed in a diesel engine. In the past year they; (1) developed a scalable method of synthesizing Mg_2Si-Mg_2Sn-Mg_2Ge ternary solid solutions; (2) Developed a matrix encapsulation

method to successfully generate HMS – Cu_3Si nanocomposites. Fully embedded nanostructures between 2-20 nm and larger Cu_3Si lamellae 100 nm to 20 µm in size are observed by microscopy. Preliminary thermal analysis suggests thermal conductivity is reduced.; (3) A finite difference model for thermal performance of a heat exchanger and TE device model has been created and optimized for steady-state operation. They have been combined for a full-scale model; and (4) A flat plate-straight fin heat exchanger was built and tested for thermal performance under various loading on a 6.7-liter Cummins diesel engine. Surrogate materials with similar materials properties and resistance to heat flow as TE materials were used. (Shi, University of Texas at Austin)

I.3 Honors and Special Recognitions/Patents

HONORS AND SPECIAL RECOGNITIONS

1. Invited Paper/Presentation "Quantitative Mixture Preparation Studies in Late-Injection Diesel Combustion Systems using Toluene LIF," Miles PC, Petersen BR, Sahoo D. *Paper presented at 10th International Symposium on Combustion Diagnostics*, May 22-23, 2012, Baden-Baden, Germany. (Paul Miles, SNL).

2. Invited Presentation "Quantitative Measurements of Flow and Scalar Fields Supporting Predictive Simulation for Engine Design," *CALSTART Leadership Circle, June 12, 2012, Livermore, CA*. (Paul Miles, SNL).

3. Invited Seminar "Physical Fluid Dynamics in Reciprocating Engines," Miles PC. Royal Institute of Technology, March 1, 2012, Stockholm, Sweden. (Paul Miles, SNL).

4. ILASS Americas William Robert Marshall Award, 2012 (for best paper judged to be the most significant contribution to the ILASS 23rd Annual Conference on Liquid Atomization and Spray Systems. (Joseph Oefelein, SNL).

5. Invited Lecture: Bill Partridge, Jae-Soon Choi, "Understanding Ammonia Formation and Utilization & Sulfation of Lean NOx Trap Catalysts via Intra-Reactor Spatiotemporal Diagnostics," IFP (French Institute of Petroleum) Énergies nouvelles (IFPEN), Lyon, France, September 7, 2012. (Bill Partridge, ORNL)

6. SAE John Johnson award for outstanding research in diesel engines, as the lead author of SAE paper 2011-01-0686. Lyle Pickett, Julien Manin, Mark Musculus, Dennis Siebers, Caroline Genzale, and Cherian Idicheria. (Lyle Pickett, SNL)

7. Invited Lecture: Jon Yoo, Jim E. Parks, Vitaly Prikhodko , William P. Partridge, Sam Geckler. "An Absorption Spectroscopy Probe for Diagnosing EGR Spatial Uniformity & Cylinder-Resolved Exhaust Transients," Crosscut Workshop on Lean Emissions Reduction Simulation (CLEERS) Teleconference (intra- and international attendance via teleconference) Oak Ridge National Laboratory, June 19, 2012. (Bill Partridge, ORNL)

8. ILASS Marshall award for best 2011 technical paper. Rainer Dahms, Joe Oefelein, Lyle Pickett. (Lyle Pickett, SNL)

9. Ra, Y., Loeper, P., Reitz, R.D., Krieger, R.B., Foster, D.E., Durrett, R.P., Gopalakrishnan, V., Plazas, A., Peterson, R., and Szymkowicz, P., "Study of high speed gasoline DICI engine operation in the LTC regime," SAE Paper 2011-01-1182, named SAE Horning Award winner for 2011. (Rolf Reitz, University of Wisconsin)

10. Charles K. Westbrook, Invited Plenary Lecture, The International Conference on Modeling and Diagnostics for Advanced Engine Systems (COMODIA), 2012, Fukuoka, Japan.

11. Charles K. Westbrook (LLNL), President of the Combustion Institute, 2008-2012.

12. Invited Keynote: Thermo- and Fluid Dynamic Processes in Direct-Injection Engines (THIESEL), Valencia, Spain, September 2012. (John Dec, SNL).

13. Reitz, R.D., 2012 DOE Vehicle Technologies R&D Award. (Rolf Reitz, University of Wisconsin)

14. Outstanding Innovation Award – 2011 Distinguished Licensing Award. Awarded by Los Alamos National Laboratory Technology Transfer Division, August 9th, 2012.

15. K.T. Liao, Z. Ren, Z.H. Zhang, P.-X. Gao, Free standing Cu-Sn alloying via low temperature solution process, CMOC symposium 2012, Storrs, CT, April. 11, 2012. (Best student oral presentation award, Gao, University of Connecticut)

16. Z. Ren, Y.B. Guo, G. Wrobel, P.-X. Gao, Hierarchical Koosh Ball Nanoarchitectures: Towards Multifunctional and Three Dimensional Integration of Nanoscale Building Blocks, CMOC symposium 2012, Storrs, CT, April 11, 2012. (Best student poster award, Gao, University of Connecticut)

INVENTION AND PATENT DISCLOSURES

1. Patent application number 61664012, "Thermoelectric Power Generation System Using Gradient Heat Exchanger", Y. Zhang, June 25, 2012. (D'Angelo, GMZ Energy)

2. Szybist, J.P. and Conklin, J.C., "Highly Efficient 6-Stroke Engine Cycle with Water Injection," U.S. Patent No. 8,291,872, issued October 23, 2012. (Daw, ORNL)

3. Dec, J. E., Yang, Y., and Dronniou, N. "A Method for Operating Homogeneous Charge Compression Ignition Engines Using Conventional Gasoline," Application Number 13/230,320. (Dec, SNL)

4. P.-X. Gao, Y.B. Guo, Z.Ren, Z.H. Zhang, "Metal oxide nanorod arrays on monolithic substrates", US non-provisional patent filed, PCT filed, 2012. (Gao, University of Connecticut)

5. P.-X. Gao, Z.H. Zhang, "Temperature-programmed-reduction Fabrication Method for Tubular Structure Devices", US provisional patent filed, 2012. (Gao, University of Connecticut)

6. P.-X. Gao, Y.B. Guo, and Z. Ren, "Ultra-efficient, robust and well-defined nano-array based monolithic catalysts," Invention Disclosure 12-079, University of Connecticut, 2012. (Gao, University of Connecticut)

7. United States Patent US 8256220: "Exhaust Gas Bypass Control for Thermoelectric Generator" issued 4 September 2012. (Meisner, General Motors)

8. United States Patent US 82286424: "Thermoelectric Generator System and Method of Control," issued 16 October 2012. (Meisner, General Motors)

9. J.E. Parks, W.P. Partridge "Oxygen Concentration Sensors and Methods of Rapidly Measuring the Concentration of Oxygen in Fluids," United States Patent, Patent No. US 8,248,612 B2, Date of Patent August 21, 2012. (Parks, ORNL)

10. R. Maggie Connatser, William P. Partridge, James E. Parks, II, "On-Engine Ammonia Detection Using Evanescent Fields," 9/6/2011. ID-2694 , Patent Pending; USPTO Serial Number 61/654,321; Filed June 1, 2012. (Parks, ORNL)

11. Bill Partridge, Jim Parks, Jon Yoo, "EGR Probe based on MIR Spectroscopy using Modulated LEDs and a Single-Port-Access Optical Probe," ID-2759, Patent Pending; USPTO Serial Number 61/657,205; Filed June 8, 2012. (Parks, ORNL)

12. D. Hornback, K. Laboe, G. Black, "Automotive Engine Coolant Heating System with Integrated EGR Cooler", patent application submitted for Chrysler IDR#708870US1, Dickstein Shapiro LLP. (Ron Reese, Chrysler)

13. R. Wakeman, "Pendulum Absorber Snubber", patent application submitted for Chrysler IDR# 708946, Dickstein Shapiro LLP. (Ron Reese, Chrysler)

14. C. Brunstetter, J. Jaye, G. Tallarek, J. Adams, "Battery Trickle Charge Algorithm with Current Feedback", patent application submitted for Chrysler IDR# 709111, Dickstein Shapiro LLP. (Ron Reese, Chrysler)

15. Bromberg, L., Sappok, A., Koert, Parker, R., and Wong, V., "Microwave Sensing for Determination of Loading of Filters," U.S. Patent # 7679374, 2010. (Sappok, Filter Sensing Technologies, Inc.)

16. Submitted "Using AIS Throttle to Reduce TipOut EGR Overshoot in LPEGR System", ID No 83228949, DOE Case No S-130,540 – 03/08/2012. (Wagner, Ford)

17. Submitted "Cooled EGR Operation Under Enrichment Conditions To Circulate Rich Exhaust For Fuel Economy Improvement", ID No 83228424, DOE Case No S-130,541 – 03/08/2012. (Wagner, Ford)

18. Pending US Patent: "Combustion Control with External Exhaust Gas Recirculation (EGR) Dilution" (Yilmaz, Robert Bosch)

I.4 Future Project Directions

COMBUSTION RESEARCH

The focus in FY 2013 for combustion and related in-cylinder processes will continue to be on advancing the fundamental understanding of combustion processes in support of achieving efficiency and emissions goals. This will be accomplished through modeling of combustion, in-cylinder observation using optical and other imaging techniques, and parametric studies of engine operating conditions.

- Argonne National Laboratory (ANL) is studying the mechanisms of spray atomization by making detailed, quantitative measurements in the near-nozzle region of sprays from light-duty diesel injectors. In the coming year they plan to: (1) In collaboration with the ECN, the multi-hole "Spray B" injectors will be studied, and compared with the previous measurements of the simpler single-hole nozzles; (2) Fabricate the hardware necessary to study ECN GDI injectors, and begin a campaign to study their operation; (3) Spray measurements will be done in conjunction with Argonne's Engine and Emissions Research group; and (4) Further studies of cavitation will be done to improve the community's understanding of this phenomenon and its impact on fuel/air mixing. (Powell, ANL)
- SNL is developing the physical understanding to guide development of modeling tools to refine the design of optimal, clean, high-efficiency combustion systems. In the coming year they will: (1) Examine the impact of 'stepped-lip' piston bowl geometries on the mixture preparation process and compare with conventional bowl geometries; (2) Investigate the potential for multiple injection strategies to reduce emissions of HC and CO through prevention of over-penetration; (3) Identify fundamental factors impacting pilot combustion that prevent combustion noise control techniques used with conventional diesel combustion from being applied to low-temperature combustion; and (4) Evaluate the sources of asymmetry in fuel distributions, including the in-cylinder flow and asymmetrical features of the head and piston top on the mixture preparation, combustion, and emissions formation processes. (Miles, SNL)
- SNL will continue developing fundamental understanding of how in-cylinder controls can improve efficiency and reduce pollutant emissions of advanced LTC technologies. In the coming year they plan to start building a design-level conceptual-model understanding of multiple injection processes, determine how combustion design affects heat transfer and efficiency, and build understanding of in-cylinder LTC soot and poly-cyclic aromatic hydrocarbons. (Musculus, SNL)
- SNL is leading a multi-institution, international, research effort on engine spray combustion called the ECN, facilitating improvement of engine combustion modeling and accelerating the development of cleaner, more efficient engines. In the coming year they plan to develop spray and combustion datasets for gasoline direct-injection systems, characterize multi-hole sprays compared to axial-hole sprays, and quantify soot and soot precursor formation processes at target conditions. (Pickett, SNL)
- ORNL will continue investigating potential near-term technologies for expanding the usable speed-load range and to evaluate the potential benefits and limitations of these technologies for achieving HECC in a light-duty diesel engine. In the coming year they plan to: evaluate the potential of increasing combustion efficiency through combustion optimization and engine hardware design (i.e. combustion chamber geometry), evaluate transient RCCI performance including controls and stability concerns, evaluate aftertreatment performance (including effect on particulate matter, PM) over the over light-duty operating range, and investigate the mitigation of noise from advanced combustion. (Curran, ORNL)
- SNL is combining unique state-of-the-art simulation capability based on the LES technique with Advanced Engine Combustion R&D activities to maximize benefits of high-performance

massively-parallel computing for advanced engine combustion research. In the coming year, SNL plans to extend development of models and corresponding benchmark simulations aimed at understanding high-Reynolds-number, direct-injection processes for both diesel and GDI engine applications over a wide range of pressures and temperatures, and establish a hierarchy of high-fidelity LES benchmark simulations of in-cylinder flows with emphasis on key optical engine experiments (HCCI, diesel, GDI). (Oefelein, SNL)

- LLNL will continue working on the development and application of computationally efficient and accurate simulation tools for prediction of engine combustion. In the coming year they plan to: (1) Validate and develop combustion simulation capabilities that will enable the prediction of performance and emissions in the development of new vehicle powertrain technologies; (2) Conduct detailed analysis of HCCI and direct-injection engine experiments and conduct analysis of clean and efficient diesel engines that use stoichiometric and LTC modes; (3) Develop numerically efficient and physically accurate models for fuel sprays and flame propagation that can be utilized within engine design simulation codes; (4) Develop fully-parallelized multi-dimensional CFD-chemistry solvers for analysis of non-homogeneous engine combustion; and (5) Distribute advanced combustion models to U.S. industrial and academic partners. (Flowers, LLNL)
- SNL will continue providing the fundamental understanding (science-base) required to overcome the technical barriers to the development of practical HCCI and HCCI-like engines by industry. In the coming year, they will: (1) Explore further increases in the thermal efficiency of boosted HCCI by raising the compression ratio (or expansion-ratio only using a Miller-cycle cam); (2) Determine the performance potential of various realistic gasoline-like fuels; (3) Work with Cummins Engine Co. to modify the cylinder head of our research engine to accommodate a spark plug for studies of spark-assisted HCCI; (4) Investigate the potential for obtaining boundary-layer profiles at the piston-top surface from T-map images simultaneously with Twall and heat-flux data; (5) Continue to collaborate with LLNL on improving chemical-kinetic mechanisms of single components and a gasoline-surrogate mixture; and (6) Continue collaborations with General Motors and the University of Michigan on modeling of thermal stratification in HCCI engines and discussions and modeling of boosted HCCI. (Dec, SNL)
- SNL is conducting acetylene seeding experiments in the automotive HCCI engine to identify ignition-enhancement effects of potential products of NVO reformation. In the coming year they plan to: (1) Employ two methods of gas sampling to speciate the products of NVO reactions (a unique 6-stroke engine cycle implemented at ORNL, and a cylinder-dump mechanism mounted in Sandia's automotive HCCI engine; (2) Apply the tunable-diode-laser absorption diagnostic developed previously to characterize in-cylinder acetylene formation during NVO fueling. Extend the diagnostic to measure other species (e.g., H_2O, CO_2, C_2H_2) to clarify the extent of NVO reformation reactions; and (3) Apply KIVA, CHEMKIN, and GT Power models of our optical engine to build a coherent understanding of NVO fueling and its effect on main combustion. (Steeper, SNL)
- ORNL is supporting DOE and industry partnerships in assessment of state-of-the-art and longer-term advanced engine and combustion technologies for future goal setting. In the coming year they plan to: (1) Demonstrate potential of high-performance computing to provide unprecedented new information on the development of combustion instabilities for advanced combustion engines; (2) Development and validation of high-fidelity, multi-processor simulation tool to accelerate design and optimization of fuel-injector design for direct-injection gasoline applications; and (3) Initiate development of a new open-source engine code optimized for massively parallel systems based upon OpenFOAM® and existing sub-models. (Edwards, ORNL)
- LANL is developing code and algorithms for the advancement of speed, accuracy, robustness, and range of applicability of the KIVA combustion modeling software to higher-order spatial accuracy

with a minimal computational effort. In the coming year they plan to: (1) Continue developing the hp-adaptive finite-element method for multispecies flows in all flow regimes; (2) Continue developing 3-D robust overset grid method for immersed actuated parts such as valves. Merge overset grid method into hp-adaptive FEM framework; (3) Continue developing the parallel solution method for the hp-adaptive PCS algorithm; (4) Continue developing more appropriate turbulence models for more predictive modeling; (5) Verify and validate combustion and spray models, and the local Arbitrary Lagrangian-Eulerian in 3-D; and (6) Investigate other spray modeling methods for more predictive modeling capability. (Carrington, LANL)

- LLNL is developing chemical kinetic models for conventional and next-generation transportation fuels need to be developed so that engine simulation tools can predict fuel effects. During the coming year, LLNL intends to: (1) Continue to develop detailed chemical kinetic models for larger alkyl aromatics; (2) Develop an improved 2-component surrogate mechanism for diesel to be used for multidimensional CFD simulations; (3) Develop more accurate surrogate kinetics models for gasoline fueled HCCI including ethanol or exhaust gas recirculation; (4) Determine the role of C=C double bonds in the ignition behavior of C10 straight-chain hydrocarbons; and (5) Develop improved chemical kinetic models for methyl cyclohexane and a preliminary detailed model for n-butyl cyclohexane. (Pitz, LLNL)
- SNL will continue designing a free-piston engine suitable for hybrid vehicle applications. Future planned activities include: (1) Motor the engine continuously for tens of seconds to minutes at a time to assess piston synchronization, thermal response, and compression ratio control; (2) Perform combustion experiments and measure indicated thermal efficiency and emissions at various compression ratios and equivalence ratios with hydrogen and, resources permitting, natural gas; (3) Characterize a new design for the pistons intended to reduce frictional losses and improve overall efficiency; and (4) Based on experimental results and modeling predictions, assess the overall engine design and performance with respect to the target fuel-to-electricity conversion efficiency of 50% at 30 kW output. (Johnson, SNL)
- ANL is developing physics-based CFD models necessary for predictive simulations of the internal combustion engine. In the next year they plan to: (1) Implement and validate high fidelity LES-based turbulence models. Demonstrate grid-convergence on LES studies; (2) Further development of the KH-ACT model by dynamically coupling nozzle flow and spray simulations; and (3) Develop and validate a two-component surrogate (n-dodecane and m-xylene) mechanism for diesel fuel. (Som, ANL)
- ORNL is analyzing and defining specific advanced pathways to improve the energy conversion efficiency of internal combustion engines from nominally 40% to as high as 60%, with emphasis on opportunities afforded by new approaches to combustion. In the coming year they plan to: (1) Continue in-cylinder water injection and reforming experiments with the modified Ecotec engine and an expanded range of fuels and reaction chemistry analysis; (2) Continue GTI-Cummins collaboration on EGR-based catalytic thermochemical recuperation; (3) Develop improved kinetics model for in-cylinder fuel reforming; and (4) Continue SNL massively-parallel large eddy simulation solver experiment construction and shakedown as budget and priorities permit. (Daw, ORNL)
- ANL will continue to quantify the influence of low-cetane fuel ignition properties to achieve clean, high-efficiency combustion. They will evaluate additional fuel properties (Research Octane Number, viscosity and volatility) using fuels provided by BP and the DOE Fuels for Advanced Combustion Engines program for gasoline, analyze the PM coming from LTC and studying the formation/oxidation process to relate PM to engine operating conditions, and conduct additional engine performance tests for Autonomie simulations to support LTC development as applied to vehicles. (Ciatti, ANL)

- ANL is collaborating with combustion researchers within DOE's Office of Science Basic Energy Science and Energy Efficiency Renewable Energy Vehicle Technologies programs to develop and validate predictive chemical kinetic models for a range of transportation-relevant fuels. In the coming year they plan to: (1) Develop, refine and validate additional reduced-order, physics-based models for RCM processes in order to improve fundamental understanding, as well as reduce uncertainties in chemical kinetic modeling. Develop additional metrics for mechanism validation, including rate of heat release; (2) Acquire additional data for baseline research-grade gasoline, and blends of 4- and 5-component gasoline surrogates. Identify deficiencies in detailed chemical kinetic models, and work to improve these; (3) Acquire data for blends of iso-octane + various cetane enhancers, and gasoline + cetane enhancers relevant to a range of low-temperature combustion concepts; develop/validate chemical kinetic models for these; (4) Develop and validate a control-oriented model capable of predicting autoignition timing over wide range of conditions, including various fuel reactivities applicable to advanced combustion concepts. (Ciatti, ANL)
- ORNL is improving diesel engine-catalyst system efficiency through better combustion uniformity, engine calibrations and catalyst control. In the coming year they plan to apply EGR probe at the Cummins Technical Center to development of advanced-intake architectures consistent with achieving next-generation engine efficiencies, improve EGR probe to achieve Cooperative Research and Development Agreement goals, and identify and develop diagnostics for addressing efficiency barriers. (Partridge, ORNL)
- ANL is identifying state-of-the-art engine and vehicle technologies currently in production to quantify the benefits of the state-of-the-art vehicle technologies currently in production, optimize vehicle performance using advanced vehicle level modeling, and accelerate the development of high efficiency internal combustion engines for light-duty vehicle applications, while meeting the future emission standards, using numerical simulations. In the coming year they plan to evaluate new technologies such as the Nissan Micra (1.4 liter turbocharged direct injected engine) and another vehicle to be identified, analyze the new emerging technologies and how they are used, and conduct analysis on the new and emerging technologies to determine their maximum fuel saving potential. (McConnell, ANL)
- ORNL is developing non-destructive, non-invasive neutron imaging technique and implement it to improve understanding of regeneration behavior in DPFs through comprehensive, quantitative device analysis. In the coming year they plan to incorporate ash-laden and catalyzed samples into the DPF study and move to fluid dynamic study within fuel injectors. (Toops, ORNL)
- ANL is characterizing particulate characteristics from a low-temperature combustion engine. In the coming year they plan to: (1) Evaluate the effects of engine operating parameters, such as injection timing, air-fuel ratio and engine load, on morphology, nanostructures of SIDI soot emissions by using a transmission electron microscope; (2) Assess nanoparticles from SIDI engines with alcohol-blended fuels, in comparison with particles from gasoline combustion; and (3) Evaluate thermo-physico-chemical properties of SIDI soot by using a thermogravimetric analyzer, a Raman microscope, and a transmission electron microscope. (Lee, ANL)
- LLNL is developing improved solvers for advanced combustion engine simulation. In the coming year they plan to: (1) Continue efforts to distribute the project's new solvers and libraries to industrial and academic partners, and to the multidimensional CFD software packages they use; (2) Improve the fluid transport calculation for a large number of reacting species and other simulation bottlenecks that occur now that the chemistry solver is substantially faster; (3) Investigate new nonlinear solvers and stiff integration strategies that would enable fewer timesteps to solution, accelerating the chemistry calculation for all mechanism sizes; (4) Explore a more robust error theory for reduced order models used in combustion to ensure that physical accuracy is maintained in a rigorous manner; and (5) Develop algorithms based on the new

chemistry solver for graphical processing units, which are widely available low-cost, energy efficient, highly-parallel computing architectures. (McNenly, LLNL)

- UM will continue exploring new high-pressure lean-burn combustion that can enable future gasoline engines with 20-40% improved fuel economy and determining the fuel economy benefits of engines and engine cycles designed to utilize advanced combustion modes. In the coming year, they plan to: (1) Expand thermodynamic and system analyses of mixed combustion modes in a representative turbocharged engine system to include realistic combustion constraints, different compression ratios, and if time, hybridization. Assess the potential benefit of lean/dilute burn, high pressure engine operation under optimal engine-vehicle drive train scenarios; (2) Bring together experimental work on spark-assisted compression ignition with recently completed models to provide new insight. Perform additional experiments as necessary; (3) Assess the validity of the flamelet-based combustion submodels in mixed-mode combustion under high-pressure, lean-burn conditions. Conduct parametric studies to identify sensitivities of key control variables; (4) Investigate effects of varying turbulent intensities, transient phenomena, and expanded operating range using newly configured optically accessible DI engine; and (5) Explore opportunities for improved engine efficiency through chemistry and properties of novel fuels and fuel blends. Carry out engine experiments with fuels characterized in RCM and RCF studies. (Woolridge, UM)
- MSU will continue demonstrating an SI and HCCI dual-mode combustion engine for a blend of gasoline and E85 (85% ethanol and 15% gasoline) for the best fuel economy. They plan to complete HCCI closed-loop combustion control dynamometer tests, along with the determination of the HCCI operational range, and develop the final test plan and complete the final performance and emission tests. (Zhu, MSU)

EMISSION CONTROL R&D

In FY 2013, work will continue on LNTs and urea-SCR to reduce NOx emissions. The focus of activities will be on making these devices more efficient, more durable, and less costly. For PM control, the focus will be on more efficient methods of filter regeneration to reduce impact on engine fuel consumption.

- PNNL is developing improved modeling capabilities for SCR and DPFs through fundamental experiments. In the coming year they plan to: (1) Continue detailed kinetic and mechanistic studies for NO reduction over the state-of-the-art small-pore zeolite-based Cu SCR catalysts; (2) Continue fundamental studies of novel high-temperature LNT formulations; (3) Characterize current production and advanced DPF substrates through advanced image and statistical analysis of high resolution computed tomography data and extend these studies to include DPFs coated with SCR catalysts for integrated DPF/SCR systems; and (4) Develop and validate SCR aging models based on CLEERS transient protocol data. (Muntean, PNNL)
- PNNL is identifying approaches to significantly improve the high temperature performance and stability of the catalytic NOx reduction technologies. In the coming year: Studies aimed at determining performance limitations, sulfur sensitivity and desulfation behavior of candidate alternative support and NOx storage materials that provide improved high-temperature performance will continue. An overall goal of the work will continue to be to develop a deeper understanding of the mechanisms of NOx storage and reduction activity, and performance degradation of materials that have been reported to show good NSR performance at temperatures considerably higher than BaO/alumina-based materials. As have the initial studies to be described here, these fundamental studies will be carried out in conjunction with baseline performance and stability experiments on fully formulated catalysts provided by Johnson Matthey. (Peden, PNNL)

- ORNL is assessing and characterizing catalytic emission control technologies for the reduction of NOx from lean-gasoline engines and identifying strategies for cost reduction of emission controls for lean-gasoline engines. In the coming year they plan to: (1) Continue evaluation of three-way catalyst formulations for NH_3 generation, especially ones that have NOx storage component included; (2) Conduct studies on the lean gasoline engine research platform to understand real exhaust effects on processes observed in flow reactor studies (with simulated exhaust mixtures); and (3) Determine catalytic NH_3 production viability under rich engine operation for SCR reactions. (Toops, ORNL)
- ORNL will continue improving diesel engine-catalyst system efficiency through better combustion uniformity, engine calibrations and catalyst control. In the coming year they will quantify spatiotemporal performance of a commercial Cummins SCR catalyst under degreened and field aged conditions. (Partridge, ORNL)
- ORNL will continue to co-lead the CLEERS planning committee, the LNT Focus Group and support the DPF and SCR Focus Groups as needed. They will also provide standard reference LNT materials, data, and kinetic modeling results for focus group evaluation, maintain and expand the CLEERS website, continue providing regular update reports to the DOE Advanced Combustion Engine Cross-Cut team, will organize and conduct the 2013 CLEERS workshop in the spring of 2013, and implement an updated CLEERS industry survey in 2013. (Daw, ORNL)
- ORNL is collaborating with SNL and PNNL to produce kinetic information for LNT and urea-SCR aftertreatment devices, both as individual and system integrated components as part of the CLEERS project. In the coming year they plan to: (1) Continue evaluation of the BMW LNT catalyst kinetic parameters and distribute results on the CLEERS website; (2) Refine the set of kinetic and aging parameters for the commercial small-pore Cu-zeolite SCR catalyst under joint investigation by ORNL and PNNL; (3) Continue identification of rate-determining steps, key surface species, and associated catalyst sites in SCR zeolite catalysts through flow reactor and surface spectroscopy experiments; (4) Extend the available laboratory characterization data for LNT and SCR catalysts to include temperatures down to 150°C; (5) Utilize above results to improve models for simulating LNT and SCR NOx reduction performance under both laboratory and vehicle drive cycle conditions; (6) Continue investigations of novel low-temperature oxidation catalysts; and (7) Develop modeling and lab characterization approaches for passive sorbers. (Daw, ORNL)
- ANL is characterizing the oxidation behavior of diesel PM emissions in terms of heat release and oxidation rate. In the coming year they plan to characterize the physical and chemical properties of gasoline direct injection engine particulates, design and fabricate a bench-scaled gasoline particulate filter system, evaluate filtration and regeneration characteristics in a gasoline particulate filter with different filter materials, and perform numerical modeling for soot loading in filtration. (Lee, ANL)
- PNNL will continue developing a fundamental understanding of the integration of SCR and DPF technologies for on-road heavy-duty vehicle application. In the coming year they plan to: (1) Pursue investigating alternative DPF substrates for inclusion in the technology, including possibly silicon carbide, aluminum titanite, and others. Consider quick screening studies for comparison to cordierite wash coating results; (2) Continue to interrogate passive soot oxidation feasibility in the integrated device, including continued parametric investigations interrogating the effect of NO_2:NOx ratio, SCR catalyst loading, NH_3:NOx ratio; and (3) Continue model development activities. (Rappe, PNNL)
- PNNL is characterizing exhaust particulates from advanced combustion engines such as SIDI using readily available fuel blends and using insight gained and prior experience with diesel aftertreatment to jump-start development of optimum aftertreatment technologies. In the coming year they plan to: (1) Employ micro-scale modeling to explore other possible approaches to achieve

high filtration efficiency in high temperature exhaust; (2) Use improved unit collector models to explore tradeoffs between parameters such as number efficiency, backpressure, and unit volume in SIDI applications; (3) Conduct experiments to evaluate candidate filter technologies for SIDI; and (4) Apply advanced particulate characterization to subsequent generations of engines – leaner operation, higher fuel efficiency. (Stewart, PNNL)

- PNNL is developing and demonstrating mixed metal oxide-based catalysts as a low-cost replacement for platinum for controlling NOx emissions. In the coming year they plan to optimize mixed metal oxide catalyst compositions and forms for NO oxidation, to enable the noble metal content of DOC and LNT catalysts to be reduced or eliminated, and perform a detailed characterization of mixed metal oxide catalysts using state-of-the-art analytical and computational techniques to develop a thorough understanding the nature of active centers on those catalysts. (Pederson, PNNL)
- The University of Houston will continue to identify the NOx reduction mechanisms operative in LNTs and in situ SCR catalysts, and to use this knowledge to design optimized LNT-SCR systems in terms of catalyst architecture and operating strategies. They will complete experiments on the LNT/SCR sequential and double-layer configurations, and to make further upgrades in the kinetic and reactor models of these systems. (Harold, University of Houston)
- The University of Connecticut will continue developing three-dimensional composite nanostructures for lean-NOx emission control devices. They plan to: (1) Further optimize and quantitatively characterize the PGM and BaO-loaded 3-D composite nano-array based on metal oxides (e.g., ZnO, and TiO_2) and perovskite (e.g., LSMO, LSCO); (2) Further investigate, understand and improve the PGM and metal oxide materials utilization and catalytic conversion efficiencies of 3-D composite nano-array catalysts; (3) Further evaluate the composite nano-array catalysts on high temperature hydrothermal stability; and (4) Further evaluate the catalytic performance of 3-D composite nanowires/nanorods arrays on CO and NO oxidations, S-resistance and NSR performance. (Gao, University of Connecticut)
- Michigan Technological University will continue to develop experimentally validated DOC, DPF and SCR models with real-time internal state estimation strategies that support future onboard diagnostics, advanced control system, and system optimization objectives for DOC-DPF-SCR aftertreatment systems that minimize the energy penalty of meeting emission regulations. In the coming year: (1) HC impact on SCR performance will be tested on the bench reactor at ORNL - HC effect model will be built and calibrated from this; (2) Similar estimation strategies to those for the SCR and DOC will be implemented for a catalyzed particulate filter along with evaluation of sensor combinations for on-board diagnostics; (3) Passive oxidation testing and the mass retained and concentration sensors study will be performed; (4) Perform engine tests to experimentally characterize PM loading maldistribution in the catalyzed particulate filter and its dependency on regeneration parameters; (5) High-fidelity catalyzed particulate filter model will be used to determine optimum PM kinetics from active regeneration and passive oxidation data; (6) Transient testing with a Cummins 2010 6.7-L ISB engine SCR system to determine model response as compared to experimental data including NOx, and NH_3 sensor data; and (7) ISB SCR testing to determine NH_3 maldistribution as a function of temperature and space velocity. (Johnson, Michigan Technological University)
- The Health Effects Institute is conducting the Advanced Collaborative Emissions Study to characterize the emissions and assess the safety of advanced heavy-duty diesel engine and aftertreatment systems and fuels designed to meet the 2007 and 2010 emissions standards for PM and NOx. In the coming year they will decide whether to commission further analyses in Phase 3B to fill in gaps due to termination of the Sun and Veranth studies, complete the ancillary studies, complete Phase 2 testing and Phase 3B exposures. (Greenbaum, Health Effects Institute)

HIGH EFFICIENCY ENGINE TECHNOLOGIES

The objective of these projects is to increase engine and vehicle efficiency of both light- and heavy-duty vehicles using advanced technology engines and advanced drivetrains. The following describe what is planned for completion in FY 2013.

- Cummins Inc. is engaged in developing and demonstrating advanced diesel engine technologies to significantly improve the engine thermal efficiency up to 55% and will demonstrate tractor-trailer vehicles with 68% or greater freight efficiency improvement. In the coming year they plan to complete the 50% freight efficiency vehicle demonstration testing, analysis and targeted testing of technologies for achievement of a 55% BTE engine, and complete the build of the 68% 24-hour freight efficiency demonstration vehicle. (Koeberlaein, Cummins)
- Detroit Diesel Corporation is demonstrating a 50% total increase in vehicle freight efficiency measured in ton-miles per gallon, with at least 20% improvement through the development of a heavy-duty diesel engine. In the coming year they plan to demonstrate 50% engine brake thermal efficiency via improvements in the base engine to reach 48% thermal efficiency and an additional 2% increase in thermal efficiency via the waste heat recovery system; build and test the final engine system in the SuperTruck vehicle to demonstrate the improvements in the vehicle as part of the 50% vehicle freight efficiency improvement; and analytically demonstrate the pathway to reach 55% engine brake thermal efficiency. (Sisken, Detroit Diesel Corporation)
- Navistar is demonstrating engine BTE improvements which contribute 20 percent (of the total 50 percent required) improvement in the freight efficiency of a combination tractor-trailer as a part of the DOE SuperTruck Project. In the coming year a pathway to 55 percent BTE is being demonstrated with a dual-fuel engine using a fuel reactivity controlled compression ignition strategy. (Oehlerking, Navistar)
- Volvo Powertrain North America is identifying concepts and technologies that have potential to achieve 55% BTE on a heavy-duty diesel engine as defined in the SuperTruck project. In the coming year they plan to complete a working transported PDF combustion CFD model that works together with a moving mesh. With that in place they will start the validation work with engine test data. They will also verify assumptions behind the 55% BTE concept. (Amar, Volvo Powertrain North America)
- Ford will demonstrate 25% fuel economy improvement in a mid-sized sedan using a downsized, advanced gasoline turbocharged direct injection engine with no or limited degradation in vehicle level metrics. In the coming year: (1) Demonstration vehicle and components available to start build and instrument; (2) Vehicle build, instrumented, and development work started; and (3) Aftertreatment system development indicates capability to meet intermediate metrics supporting emissions objectives. (Wagner, Ford Motor Company)
- General Motors will demonstrate 25% vehicle fuel economy improvement through lean gasoline combustion while achieving Tier 2 Bin 2 emissions. In the coming year, they plan to: (1) Expand the torque-based controls to support boosted operation; (2) Optimize the combustion system to allow extended lean stratified operation under boosted conditions with optimization of the fuel injection and ignition parameters; (3) Refine the lean aftertreatment system hardware to incorporate the optimum elements of the active and passive technologies which will yield lowest initial and operational costs; (4) Install the optimized lean downsize boost engine and final refined lean aftertreatment hardware; (5) Integrate the 12-volt stop/start and advanced thermal management systems hardware and functionality; (6) Calibrate the 2nd generation lean downsize boost engine and 4th generation lean aftertreatment system to provide optimal fuel economy, emissions compliance and seamless drivability. (Smith, General Motors Company)

- Chrysler aims to demonstrate 25% improvement in combined Federal Test Procedure City and Highway fuel economy for the Chrysler minivan. In the coming year they plan to: (1) Complete final design, procurement, build and demonstration of targeted improvements for Alpha 2 engine; (2) Complete thermal management system, third iteration of vehicle crank pendulum, integrated controlled charge algorithm and install with engine into vehicle; (3) Complete control strategies to enable engine calibration, drivability and fuel economy improvements for implemented technologies including twin turbo, cooled EGR, secondary air and multi-fuel; (4) Continue diesel micro pilot combustion learning through continued engine testing and simulation efforts at ANL; and (5) Complete implementation of the vehicle energy model. (Reese, Chrysler Group LLC)
- Robert Bosch LLC is improving fuel economy by 30% with minimum performance penalties. In the coming year they plan to evaluate fuel economy and emission benefits of target combustion modes on the prototype II engine at transient dynamometer, integrate the prototype II engine into a demonstration vehicle, enabling full SI capability, and complete control strategies for multi-mode combustion, ready for engine management system integration. (Yilmaz, Robert Bosch)
- Cummins is demonstrating 40% fuel economy improvement over a baseline gasoline V-8 pickup truck and Tier 2 Bin 2 tailpipe emissions compliance. In the coming year they plan to: (1) Develop new engine hardware to meet the intermediate goal of Tier 2 Bin 2 emission levels; (2) Integrate the new engine into existing mule vehicle; (3) Develop control technology to include the passive NOx adsorber operation to the intended application; and (4) Develop control technology for the optimization of the direct ammonia delivery system with SCR on filter as well as under-floor SCR. (Ruth, Cummins Inc.)
- Filter Sensing Technologies, Inc. is designing, developing, and validating RF sensors for accurate real-time measurements of DPF loading with low-pressure drop substrates. In the coming year they plan to develop and calibrate RF prototype sensors with reference DPF configuration, evaluate sensor baseline performance and identify/quantify error sources, determine sensor accuracy for various operating conditions and DPF configurations, and develop specifications and designs for pre-production sensor. (Sappok, Filter Sensing Technologies, Inc.)
- General Motors is applying high energy ignition and boosting/mixing technology to increase fuel economy in spark ignition gasoline engines by increasing EGR dilution capability. In the coming year they plan to: (1) Update and test a GM 2.0-L turbocharged engine updated with the low pressure loop EGR system defined through simulation and packaging studies. The base engine will be updated with increased compression ratio and a novel high energy, extended duration ignition system; (2) Design an updated 2.0-L turbocharged base engine to facilitate efficient operation with increased compression ratio and direct EGR; (3) Investigate novel boosting/mixing arrangements. (Keating, General Motors)
- Eaton is demonstrating fuel economy improvement through Rankine cycle waste heat recovery systems utilizing a roots expander in heavy-duty diesel applications. In the coming year they plan to: (1) Prototype and evaluate the roots expander first level concept for performance in an ethanol organic Rankine cycle (ORC) system; (2) Iterate the roots expander designs based on performance feedback to maximize effectiveness and durability; (3) Design a robust roots expander for integration into a heavy-duty diesel engine ORC system; (4) Prototype and validate the performance of final roots expander design in an ethanol-based ORC system; (5) Design and build a heavy-duty diesel engine Rankine cycle system with integrated roots expander; and (6) Demonstrate roots-based Rankine cycle system on a heavy-duty diesel engine. (Subramanian, Eaton)
- MAHLE Powertrain is demonstrating breakthrough thermal efficiency of 45% on a light-duty gasoline engine platform while demonstrating potential to meet U.S. emissions regulations. In the coming year they plan to: (1) Complete single-cylinder optical engine build and installation, and

acquire high speed imaging and speciation data; (2) Complete single-cylinder thermodynamic engine build and installation, and acquire data to evaluate TJI hardware variation effects on engine performance; (3) Correlate 3-D analysis results with experimental data from both optical and thermodynamic engines. (Blaxill, MAHLE Powertrain)

- Delphi will develop, implement and demonstrate fuel consumption reduction technologies using a new LTC process: gasoline direct injection compression ignition (GDCI). In the coming year they plan to test Phase 2 technologies on multi-cylinder engines, map GDCI operation on performance dynamometer, develop GDCI engine control systems, continue single-cylinder engine tests and detailed FIRE and KIVA simulations to refine the combustion process and component designs, and build the Phase 2 vehicle. (Confer, Delphi Automotive Systems LLC)
- Los Alamos National Laboratory is developing a prototype NOx sensor based on mixed-potential technology using a $La_{1-x}Sr_xO_{3-\delta}$ sensing electrode and a prototype NH_3 sensor based on mixed-potential technology using an Au sensing electrode. In the coming year they plan to: (1) Evaluate sensing technology under dynamometer conditions at end user site; (2) Analyze the impact of interference gases on NOx sensor performance; and (3) Conduct long-term durability studies including thermal cycling. (Mukundan, Los Alamos National Laboratory)
- ORNL is quantifying the fuel economy benefit and emissions impact of variable compression ratio (VCR) engine technology to a modern direct-injection gasoline engine. In the coming year they plan to: (1) Conduct demonstration testing of VCR engine including measurements of the engine performance, VCR actuator mechanism response time and fuel consumption at Automotive Specialists in Concord, North Carolina; (2) Conduct a post test inspection of key engine components by Automotive Specialist and reassemble engine for delivery to ORNL; and (3) Install the engine at ORNL dynamometer test facility and conduct experiments to investigate the effect of VCR on engine efficiency at the maximum brake torque spark timing over the engine map with a VCR research engine. Engine experiments will combine parametric sweeps of spark timing, compression ratio, and cam phasing to determine the optimal efficiency at each engine speed/load operating condition. Emissions from the engine will also be measured before and after a three-way catalyst. (Domingo, ORNL)

SOLID STATE ENERGY CONVERSION

Research will continue in FY 2013 on TEs for converting waste heat from advanced combustion engines directly to electricity. Research will focus on development of practical systems that are suitable for future production.

- Gentherm Inc. is developing a high-efficiency TE waste energy recovery system for passenger vehicle applications. In the coming year they will conduct further modeling; conduct component, cartridge, and multi-cartridge-level testing for both performance and durability; complete vehicle and TEG system requirements; conduct further work on oxidation/sublimation suppression coating, and scale up TE material and cartridge fabrication methods (Crane, Gentherm)
- General Motors is identifying distributed cooling and heating strategies that can efficiently augment or replace a vehicle's central heating, ventilation and air conditioning system by delivering localized cooling/heating of key human body segments that strongly influence an occupant's perceived thermal comfort. In the coming year they will focus on commercial design of new comfort components and estimating efficiency improvements for the integrated system and, test and evaluate the distributed heating, ventilation and air conditioning system in vehicle and calculate efficiency improvements of the distributed system. (Bozeman, General Motors)
- General Motors will continue development of a cost-effective TEG that is fully integrated into a GM production light-duty vehicle. They plan to select TE materials for prototype TE modules,

establish design targets for TEG components, establish design targets for TEG subsystem, and fabricate and test TE modules for the TEG prototype. (Meisner, General Motors)

- GMZ Energy Inc. will continue development of TEGs using significantly improved nanostructured bulk TE materials that they have developed and an innovative two-stage cascade design. They plan to build reliable TE modules with >4.5% efficiency, design and build robust heat exchangers with >50% thermal efficiency, and build and test TEGs in selected vehicle platforms and achieve maximum fuel economy improvement with minimum cost. (D'Angelo, GMZ Energy Inc.)
- Ohio State University is developing high-efficiency high zT TE materials (PbSe and Mg_2Sn) that contain no rare or precious elements, and are non-toxic. In the coming year they will focus their effort on the following two tasks. (a) The thermal and electrical properties of nano-Ag sintered bonding layer between TE element and heat exchanger will be characterized. The goal is to develop a bond layer with an electrical contact resistance $<10^{-5}\Omega cm^2$ and a thermal contact resistance $<10^{-3}$ $KW^{-1}cm^2$. (b) Thermomechanical reliability of nano-Ag sintered bonding layer will be tested. The goal is to fulfill the integration and packaging of TE devices with an overall performance that is not degraded by more than 20% over the theoretical performance of the material, with a 10-year lifetime, and the capability to withstand 106 thermal cycles from 773 K to 300 K. (Heremans, Ohio State University)
- Purdue University is enabling the broad adoption of TE waste heat recovery systems, or TEGs, at a scale commensurate with the global vehicle manufacturing enterprise. In the coming year they plan to: understand the interaction between the filling metal atoms and the parent skutterudite material; evaluate the impacts of nanostructure size, surface roughness, and composition modulation on TE figure of merit, analyze other material systems and conduct research in the scalable synthesis of nanowire heterostructures to further decouple electron and phonon transport; refine the heat exchanger design with the use of multiple types of TE materials; and explore the possibility of developing other nanostructures for TE application. (Xu, Purdue University)
- Stanford is performing systems-level modeling and full device-scale characterization, with the ultimate goal of constructing a complete architecture for optimizing a TEG system for recovering waste heat from automobile combustion. During FY 2013 they will utilize this novel infrared thermometry experimental setup to perform measurements of TE materials and nanostructured interfaces under high temperature operating conditions. This experimental setup will also be used to conduct thermal cycling of the materials and interfaces with in situ measurements of thermoelectric properties and contact resistances. Candidate nanostructured thermal interface materials will be explored that are synthesized via metal electrodeposition through removable templates, such as vertically-aligned metal nanowires. (Goodson, Stanford)
- Stony Brook University successfully obtained single-phase higher manganese silicide using melt-spinning and successfully demonstrated thermal spray of silicide materials. In the coming year: (1) More APS runs of Mg_2Si with internal power injection are being conducted to verify the repeatability of the spray method on Mg_2Si TE material. The thermal, electrical conductivity as well as Seebeck coefficient will be characterized as well; (2) Annealling of the VPS samples (21 kW, with substrate temperature control) will be done to enhance the microstructure by reduce the boundary layers; (3) Thicker filled skutterudite samples will be sprayed and annealed to form the correct TE phase; (4) Iron disilicide (Fe_2Si) will be sprayed to make the three-dimensional TE module to demonstrate the manufacturing process with thermal spray and laser cutting using an actual TE material; and (5) Thermal sprayed TE properties modeling using effective medium theory, percolation theory and Millman's theorem will be investigated to gain better understanding of thermal sprayed material properties. (Zuo, Stony Brook University)
- Texas A&M is synthesizing of inorganic nanowires and quantum wires of both $CoSb_3$ and InSb, and organic conducting polymer thin films, and assembling them into inorganic-organic hybrid TE

cells with sizes ranging from a few mm^2 to a few cm^2, using conjugated linker molecules to tether the nanowires to each other or to conducting polymer thin films. In the coming year they plan to mass produce $CoSb_3$ and InSb nanowire powders. (Vaddiraju, Texas A&M)

- The University of California, Los Angeles is developing novel materials and interfaces for improved thermomechanical reliability of TE vehicle exhaust waste heat harvesting devices. In the coming year: measurements of the thermal and electrical conductivities of the nanocomposites are currently under way. Efforts to improve the processing conditions and starting materials will also continue. They are also planning to carry out hot pressing experiments in which the Cu-ZrW_2O_8 composite will be bonded directly to Mg_2Si TE elements. Design, fabrication, and experimental characterization of flexible interfaces and oxidation-mitigation structures will also be carried out. (Ju, University of California, Los Angeles)
- The University of California, Santa Cruz, is developing novel TE materials based on abundant and non-toxic Zintl phase magnesium silicide alloys and optimizing the TE power factor and figure of merit by band engineering and electron filtering. In the coming year they plan to perform low temperature synthesis and SPS of p-type Mg2Si with embedded nanoparticles, and conduct characterization and transport modeling. (Shakouri, University of California, Santa Cruz)
- Virginia Tech is fabricating and characterizing new TE materials growth with techniques capable of producing large quantities of efficient, yet non-toxic and inexpensive elements capable of long-term operation at high temperatures over thousands of thermal cycles. In the upcoming year they will work to improve their p-type Mg-Silicide material and to optimize the sintering temperature and time of the ZnO system in order to maximize ZT. For their established Mg-Silicide materials, we are subjecting the materials and interfaces to long-term thermal cycling and reliability studies. On the thermal management and heat exchanger side, they will use their experimentally verified computational fluid dynamics models to design improved second-generation heat sinks, and use their laboratory test rig to quantitatively examine the performance of each component on the overall thermoelectric generator system. (Huxtable, Virginia Tech)
- The University of Texas at Austin is increasing the ZT of abundant silicide materials to a level competitive with the state of the art found in materials containing much more scarce and expensive elements, and enhancing the thermal management system performance for silicide TE devices installed in a diesel engine. In the coming year they plan to further increase the ZT of both p-type HMS and n-type Mg_2Si-Mg_2Sn-Mg_2Ge ternary solid solutions, and use them to fabricate TE devices for engine testing. (Shi, University of Texas at Austin)

II. COMBUSTION RESEARCH

II.1 Fuel Injection and Spray Research Using X-Ray Diagnostics

Christopher F. Powell (Primary Contact),
Alan Kastengren, Jin Wang
Argonne National Laboratory
9700 S Cass Ave
Argonne, IL 60439

DOE Technology Development Manager:
Gurpreet Singh

Overall Objectives

- Study the mechanisms of spray atomization by making detailed, quantitative measurements in the near-nozzle region of sprays from light-duty diesel injectors.
- Perform these measurements under conditions as close as possible to those of modern engines.
- Utilize the results of our unique measurements in order to advance the state of the art in spray modeling.
- Provide industrial partners in the spray and engine community with access to a unique and powerful spray diagnostic.

Fiscal Year (FY) 2012 Objectives

- Perform measurements of fuel density, needle life, and nozzle geometry using the hardware and conditions of the Engine Combustion Network's (ECN's) Spray A condition. Share this data with computational modelers for validation and improvement of engine modeling.
- Explore the use of X-rays diagnostics for other advanced combustion applications, such as chemical kinetics, cavitation, and injector flows.

FY 2012 Accomplishments

- In collaboration with Sandia's ECN, we completed measurements of the four single-hole ECN injectors. We made precision measurements of the fuel density in three dimensions, and discovered significant asymmetries as well as differences between the nominally identical injectors. The measurements are being used by computational modelers to improve spray models, this will speed the development of efficient, clean-burning engines.
- Several new pieces of equipment were completed in 2012. These include a new fuel system for gasoline direct injection (GDI) injectors which are capable of delivering fuel up to 200 bar, and operating GDI injectors from a range of manufacturers. We also fabricated a new spray chamber which can be used to study both diesel and GDI sprays. This chamber is flexible enough to accommodate a very broad range of spray umbrella angles, eliminating the need to build a costly spray chamber for every injector. These two devices significantly expand our capabilities for studying modern fuel injection hardware.
- We performed time-dependent measurements of the boundary layer density inside an operating shock tube. This characterized the performance of this new device so that it can be used for studying combustion kinetics, an area of significant uncertainty in engine modeling.
- In order to improve the fundamental knowledge of sprays, we conducted the first-ever quantitative measurements of cavitation density. These measurements allowed us to determine the exact density distribution inside a cavitating fuel flow. These measurements are being compared to cavitation simulations in collaboration with some of the world's leading cavitation modelers.
- We conducted the world's first measurements of gas bubbles inside an operating production diesel injector. These measurements revealed cavitation occurring inside the orifice for certain nozzle geometries. They also revealed gas bubbles being drawn into the injector at the end of injection. Under engine conditions, the bubbles will cause fuel to be pushed out of the injector when the exhaust valves open, resulting in unburned hydrocarbon or particulate matter emissions.

Future Directions

- In collaboration with ECN, the multi-hole "Spray B" injectors will be studied, and compared with the previous measurements of the simpler single-hole nozzles. The geometry and fuel distribution from these multi-hole nozzles will be measured using X-ray diagnostics, and made available to our experimental and modeling partners in the ECN.
- ECN is beginning a program studying GDI injection. We will fabricate the hardware necessary to study these injectors, and begin a campaign to study their operation. The results will be shared with

our ECN partners with the goal of improving the understanding of GDI combustion.

- Spray measurements will be done in conjunction with Argonne's Engine and Emissions Research group. These will measure the fuel/air mixing from compression ignition and gas-fueled engines, providing these research programs with the data that is needed for high-fidelity modeling.
- Further studies of cavitation will be done to improve the community's understanding of this phenomenon and its impact on fuel/air mixing. Sandia National Laboratories has expressed interest in collaboration on this topic.

Introduction

Fuel injection systems are one of the most important components in the design of combustion engines with high efficiency and low emissions. A detailed understanding of the fuel injection process and the mechanisms of spray atomization can lead to better engine design. The limitations of visible light diagnostics in the near-nozzle region of the spray have led us to develop X-ray diagnostics for the study of fuel sprays. X-rays are highly penetrative, and measurements are not complicated by the effects of scattering. The technique is non-intrusive, quantitative, highly time-resolved, and allows us to make detailed measurements of the spray, even in the densely-packed region very near the nozzle.

Approach

This project studies the sprays from commercially available fuel injectors. Our approach is to make detailed measurements of the sprays from these injectors using X-ray absorption. This will allow us to map the fuel distribution in these sprays, extending the existing knowledge into the near-nozzle region. The X-ray measurements are performed at the Advanced Photon Source at Argonne National Laboratory. A schematic of the experimental setup is shown in Figure 1; detailed descriptions of the experimental methods are given in [1] and [2]. The technique is straightforward; it is similar to absorption methods commonly used in optical analysis. However, X-ray radiography has a significant advantage over optical techniques in the measurement of sprays: because the measurement is not complicated by the effects of scattering, there is a simple relation between the measured X-ray intensity and the mass of fuel in the path of the X-ray beam. This allows direct determination of the mass of fuel at any position in the spray as a function of time. It is the goal of our

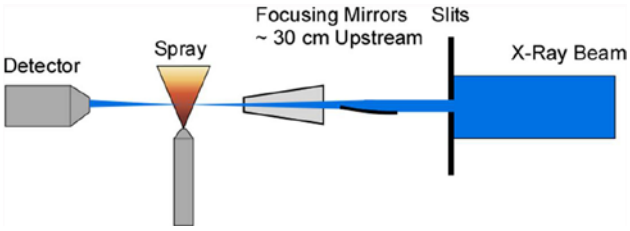

FIGURE 1. Schematic of the Experimental Setup

work to use X-ray radiography to measure sprays from commercial fuel injectors at different injection pressures, different ambient pressures, and using different nozzle geometries. This will enable us to quantify how each of these variables affects the structure of the spray. We will collaborate with industrial partners including engine and fuel injection system manufacturers so that they will have access to these diagnostics for improvement of their products. We will also collaborate with spray modelers to incorporate this previously unknown information about the spray formation region into new models. This will lead to an increased understanding of the mechanisms of spray atomization and will facilitate the development of fuel injection systems designed to improve efficiency and reduce pollutants.

In addition to measurements of sprays, we will explore other applications of X-ray diagnostics for combustion research. This includes X-ray imaging of the internal components of fuel injectors while they are in operation. This diagnostic is useful for injector manufacturers who are trying to develop and optimize injector designs. We are also exploring studies of cavitation in order to improve the fundamental understanding of this phenomenon and its role in spray atomization. Recent measurements have also evaluated the use of X-rays as a diagnostic for shock tubes, enabling better measurements of combustion kinetics to improve engine modeling.

Results

Much of our experimental work this year focused on measurements performed as part of the ECN. This collaboration is led by Sandia National Laboratories, who has defined a specific set of operating conditions and procured a set of shared identical hardware. We have used Argonne's unique X-ray diagnostics to study the "Spray A" operating conditions. Last year we completed X-ray imaging of the internal geometry and needle motion of the Spray A injectors. This year we completed measurements of the fuel density distribution, and shared these results with the ECN computational modelers. The data is now being used for validation of injector and spray models, including models that incorporate the eccentric

needle motion when calculating fuel flow. At the ECN2 Workshop in September, Argonne's data was used for validation by at least six different spray modeling groups (Figure 2). These data are being actively used to improve spray models and simplify the development of efficient, clean-burning engines.

Shock tubes are a common tool for generating the high temperature and pressure needed for studies of combustion chemistry. In 2012, we used X-ray absorption to probe the gas flowfield inside a miniature shock tube built by Argonne's Chemistry division. These measurements demonstrated that X-ray absorption provides a useful diagnostic of the gas density in the shock tube before and during the firing cycle of the tube (Figure 3). These data provide a valuable measure of the shock tube's performance, and have been used to validate the predictions of temperature and pressure inside the device which are critical for kinetics measurements. These measurements also demonstrated that commercial polycrystalline diamond windows can be used as X-ray transparent windows even under high temperature conditions. While more research is needed regarding the performance of these windows, these results demonstrate a path to performing X-ray radiography under more challenging environments than have been previously possible.

Cavitation is an important problem in high pressure fuel injection systems, such as those found in modern direct injection diesel engines. Cavitation - where fuel in the injector vaporizes due to sudden changes in pressure - can cause mechanical damage to injector components and affect fuel/air mixing and thus pollutant formation. State-

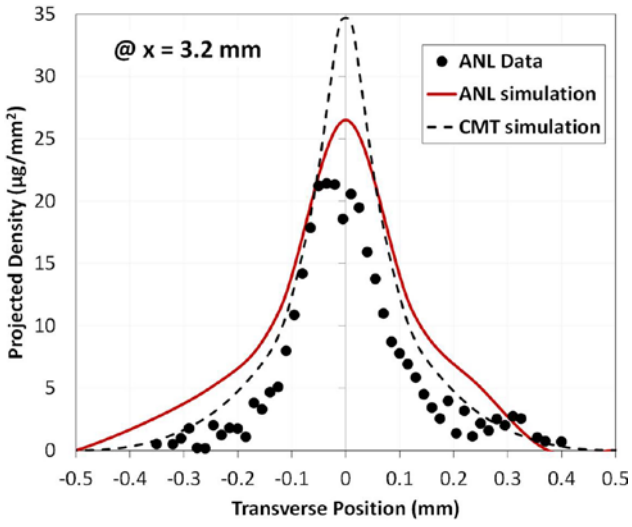

FIGURE 2. Comparison of Argonne X-ray measurements of the fuel distribution with simulations from Som (Argonne) and Pastor (Universidad Politécnica de Valencia). Preliminary simulation results courtesy of S. Som and J. Pastor.

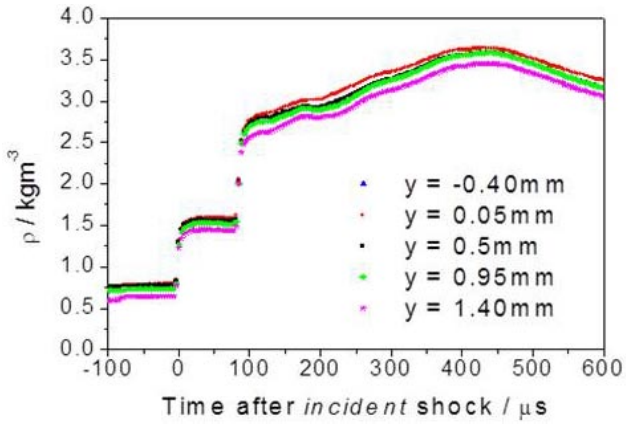

FIGURE 3. Plot of the gas density inside a shock tube versus time. The plot shows the density increases upon the arrival of the incident and reflected shocks. This direct measurement of the gas density has been used to validate the predictions of temperature and pressure in the device, enabling its use for accurate measurements of combustion chemistry.

of-art computer models for cavitation are now being incorporated into engine modeling software to account for these factors. However, there is little information available on the accuracy of these models because cavitation is very difficult to measure experimentally. This year we have adapted X-ray radiography methods to obtain precise and accurate measurements of cavitation in a transparent nozzle. In collaboration with researchers from the University of Massachusetts Amherst [3] and utilizing the Fusion computing facility at Argonne, we have also developed high resolution computer simulations of cavitation under similar conditions to the X-ray experiments. The experiments reveal phenomena which are not fully captured by the models (Figure 4), and these discoveries will feed back into the development of better and more accurate engine modeling software, as well as a broader understanding of this complex physical phenomenon.

High speed imaging of injector operation was developed at Argonne in order to study the motion of steel components inside the injector, such as the valve lift. Due to improvements in our imaging technique, this year we were able to image the motion of gas bubbles inside production injectors for the first time. The bubbles we observed came from two sources. First, when fuel was flowing out of the injector, cavitation was visible in some nozzles. This represents the first ever observation of cavitation in steel injector nozzles. Second, at the end of injection, bubbles were drawn into the injector sac through the nozzle holes (Figure 5). The presence of these bubbles inside the injector will likely have an impact on emissions, since the bubbles will expand when the exhaust valves open and drive any remaining fuel out of the injector into a cold combustion chamber.

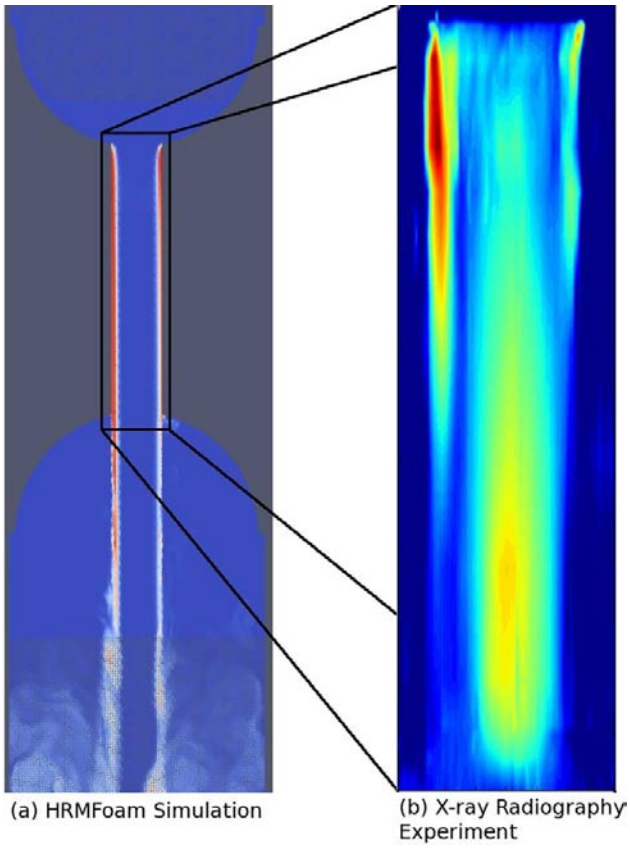

FIGURE 4. X-ray radiography measurements of cavitation (right) can now be directly compared to state-of-art numerical models (left) used in engine simulation software.

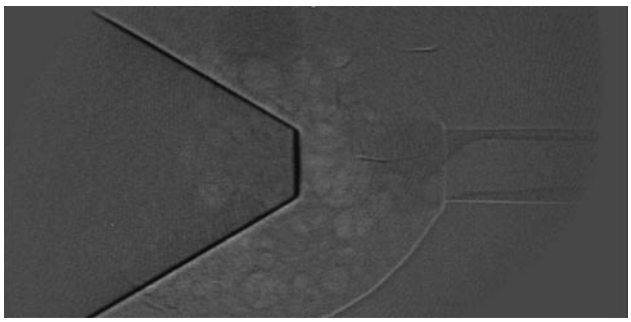

FIGURE 5. X-ray image through a steel injector nozzle showing bubbles that were drawn into the sac at the end of injection. The presence of these bubbles is likely to have an impact on emissions.

We are analyzing these results based on several injector parameters and will publish the results next year.

Conclusions

- The X-ray measurements can be used to help understand the mixing of fuel and air in the engine, and its impact on engine emissions and performance. Such measurements are not possible using other imaging techniques, and represent a powerful data set for validating computational models of fuel flow.
- The time-dependent mass measurements provide unique information to spray modelers, and allow them to test their models in the spray formation region, something that was impossible previously. This data is crucial for the development of accurate spray models and for the detailed understanding of spray behavior. The quantitative measurements that we have provided may help to elucidate the mechanisms of spray atomization. This could ultimately lead to the design of cleaner, more efficient engines.
- The impact of our work on the engine community is shown by the expanding list of collaborators and by the significant in-kind contributions to our work that are being made by fuel system and engine manufacturers.

References

1. "Time-Resolved Measurements of Supersonic Fuel Sprays using Synchrotron X-rays", C.F. Powell, Y. Yue, R. Poola, and J. Wang, *J. Synchrotron Rad.* 7:356-360 (2000).

2. "Spray Density Measurements Using X-Ray Radiography" A.L. Kastengren, C.F. Powell, *Journal of Automobile Engineering*, Volume 221, Number 6, 2007, pp 653-662.

3. "Application of the Homogeneous Relaxation Model to Simulating Cavitating Flow of a Diesel Fuel", K. Neroorkar, B. Shields, R. Grover, Jr., A. Plazas Torres, D. Schmidt. SAE Technical Paper 2012-01-1269, 2012.

FY 2012 Publications

1. "The 7BM beamline at the APS: a facility for time-resolved fluid dynamics measurements", A. Kastengren, C.F. Powell, D. Arms, E.M. Dufresne, H. Gibson and J. Wang. J. Synchrotron Rad. 19 (2012).

2. "High Pressure Gaseous Injection: A Comprehensive Analysis of Gas Dynamics and Mixing Effects", R. Scarcelli, A.L. Kastengren, C.F. Powell, T. Wallner, N.S. Matthias. American Society of Mechanical Engineers ICEF2012-92137, September 2012.

3. "Image Processing Techniques for Determining Needle Lift in Fuel Injectors", F. Zak Tilocco, Alan L. Kastengren, Christopher F. Powell. American Society of Mechanical Engineers ICEF2012, September 2012.

4. "CFD and X-ray Investigation of the Characteristics of Under-Expanded Gaseous Jets", R. Scarcelli, A.L. Kastengren, C.F. Powell, T. Wallner, N.S. Matthias. COMODIA-2012, Fukuoka, Japan, July 2012.

5. "Time-Resolved X-Ray Radiography of Diesel Injectors from the Engine Combustion Network", A.L. Kastengren1, F.Z. Tilocco, D. Duke, C.F. Powell, Seoksu Moon,

Xusheng Zhang. ICLASS 2012, 12th Triennial International Conference on Liquid Atomization and Spray Systems, Heidelberg, Germany, September 2–6, 2012.

6. "A Study of Gas-Centered Swirl Coaxial Injectors using X-ray Radiography", S.A. Schumaker, A.L. Kastengren, M.D.A. Lightfoot, S.A. Danczyk and C.F. Powell, ICLASS 2012, 12th Triennial International Conference on Liquid Atomization and Spray Systems, Heidelberg, Germany, September 2–6, 2012.

II.2 Low-Temperature Automotive Diesel Combustion

Paul Miles
Sandia National Laboratories
P.O. Box 969
Livermore, CA 94551-0969

DOE Technology Development Manager:
Gurpreet Singh

Subcontractor:
University of Wisconsin Engine Research Center,
Madison, WI

Overall Objectives

- Provide the physical understanding of the in-cylinder combustion processes needed to minimize the fuel consumption and the carbon footprint of automotive diesel engines while maintaining compliance with emissions standards.
- Develop efficient, accurate computational models that enable numerical optimization and design of fuel-efficient, clean engines.
- Provide accurate data obtained under well-controlled and characterized conditions to validate new models and to guide optimization efforts.

Fiscal Year (FY) 2012 Objectives

- Investigate the impact of swirl ratio and injection pressure on mixture preparation and provide quantitative data for model validation.
- Establish ability of current modeling practice to accurately compute flow swirl and injection pressure effects and identify focus areas for improvement of models and simulation practice.
- Examine the factors influencing the optimal injection timing for partially premixed compression ignition (PPCI) combustion modes.
- Develop optical diagnostic techniques to identify hydrocarbon (HC) species characteristic of moderately rich combustion ($1 \lesssim \phi \lesssim 1.5$).

Accomplishments

The accomplishments below target the barriers of 1) lack of fundamental knowledge, and 2) lack of a predictive modeling capability identified in the Vehicle Technologies Program 2011-2015 multi-year program plan:

- Measured the evolution of in-cylinder mixture distributions for four different swirl ratios and three different injection pressures.
- Demonstrated that engine-out emissions are strongly correlated with the formation of over-lean mixture in the pre-combustion mixture formation process for all operating conditions.
- Identified shortcomings in the modeling of the initial mixture formation process and areas for focusing future efforts.
- Established the dominance of kinetics in determining the engine-out emissions when injection is excessively retarded.
- Examined the potential of photo-fragmentation with subsequent C_2 laser-induced fluorescence as a diagnostic for in-cylinder detection of C_2H_2.

Future Directions

- Examine the impact of 'stepped-lip' piston bowl geometries on the mixture preparation process and compare with conventional bowl geometries.
- Investigate the potential for multiple injection strategies to reduce emissions of HC and CO through prevention of over-penetration.
- Identify fundamental factors impacting pilot combustion that prevent combustion noise control techniques used with conventional diesel combustion from being applied to low-temperature combustion (LTC).
- Evaluate the sources of asymmetry in fuel distributions, including the in-cylinder flow and asymmetrical features of the head and piston top on the mixture preparation, combustion, and emissions formation processes.

Introduction

Direct-injection diesel engines have the highest proven brake fuel efficiency of any reciprocating internal combustion engine technology. However, conventional diesel combustion produces elevated emissions of both soot and oxides of nitrogen (NO_x). To address this shortcoming, LTC techniques that prevent the formation of these pollutants within the engine are being developed. These techniques employ high levels of dilution, which can make the creation of an appropriate in-cylinder fuel-air mixture challenging. Dilution and lower

temperatures also markedly slow the reaction kinetics. The combination of poor mixture formation and slower chemistry can result in a loss of efficiency, high levels of HC and CO emissions, and excessive combustion noise. A major focus of this work is to understand the main causes of combustion inefficiency and high emissions, through examination of both the in-cylinder mixture preparation process and oxidation kinetics.

This year, the project has focused on developing an understanding of how variations in the level of flow swirl and injection pressure, two variables that design and calibration engineers can easily vary, impact the mixture preparation process. The mixture distributions formed are subsequently correlated with both the in-cylinder distributions of HC and CO measured later in the cycle, and with engine-out emissions levels, to identify the sources of these emissions and potential mitigation strategies. Multi-dimensional computer simulations of the mixture formation process are also performed, to assess the ability of current engine models to accurately predict and optimize this process and to identify areas where further model development is needed to permit truly predictive engine simulations.

Approach

The research approach involves carefully coordinated experimental, modeling, and simulation efforts. Detailed measurements of in-cylinder flows, fuel and pollutant spatial distributions, and other thermo-chemical properties are made in an optical engine facility based on a General Motors 1.9-liter automotive diesel engine. Close geometric and thermodynamic correspondence between the optical engine and the production engine allow the combustion and engine-out emissions behavior of a traditional, all-metal test engine to be closely matched. These measurements are closely coordinated and compared with the predictions of numerical simulations.

The experimental and numerical efforts are mutually complementary. Detailed measurements of the in-cylinder variables permit the evaluation and refinement of the models used in the computer simulations, while the simulation results can be used to obtain a more detailed understanding of the in-cylinder flow and combustion physics—a process that is difficult if only limited measurements are available. Jointly, these efforts address the principal goals of this project: development of the physical understanding to guide and the simulation tools to refine the design of optimal, clean, high-efficiency combustion systems.

Results

The mixture preparation process is characterized by acquiring quantitative measurements of the in-cylinder mixture equivalence ratio distribution at crank angles between the start-of-injection (SOI) and the start of rapid, high-temperature heat release. Figure 1 illustrates the geometry of the optically accessible engine and the experimental set-up used. A horizontal laser sheet is passed through windows in the cylinder liner, and illuminates a plane within the combustion chamber. Fluorescent emissions are collected through the optical piston, and imaged onto a charge-coupled device camera. The images acquired are distorted by the curved surfaces of the transparent piston; however, a corrective transformation is derived from calibration targets and is employed to obtain distortion-free images. By referencing the images against similar images obtained in a uniform fuel-air mixture, accounting for the temperature dependence of the photophysical properties of the tracer molecule, the fluorescence images can be transformed into quantitative images of fuel-air equivalence ratio.

Figure 2 illustrates how increasing injection pressure impacts the mixture formation process when the injection timing is fixed at 23.3° before top-dead center (bTDC). The equivalence ratio distributions shown were acquired at 5° bTDC, just before ignition—as defined by the onset of high-temperature heat release. Measurements were made in three planes, located as shown in the lower-left portion of the figure. The white regions in the upper, clearance volume plane and in the lower, bowl plane represent areas where the laser sheet was blocked by

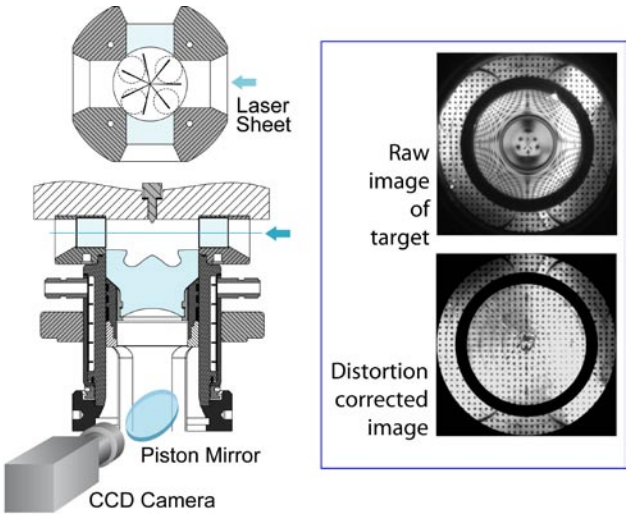

CCD - charge-coupled device

FIGURE 1. Illustration of the experimental configuration employed for fuel-tracer laser-induced fluorescence measurements and example of the distortion correction applied to the images.

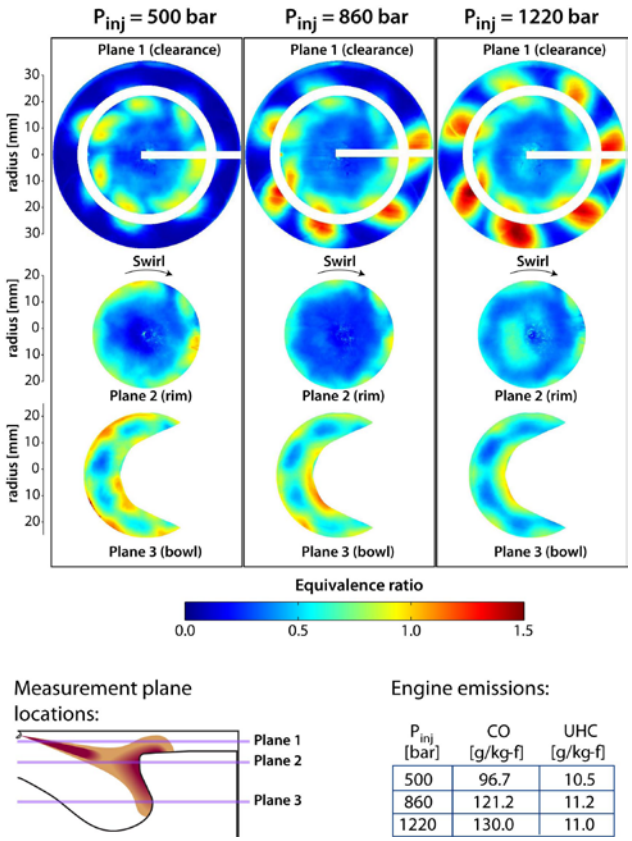

FIGURE 2. Equivalence ratio distributions measured at 5° bTDC at three different injection pressures. SOI = 23.3° bTDC; 10% O_2 ; swirl ratio = 2.2, 1,500 RPM; 3 bar gross indicated mean effective pressure (gIMEP).

the injector tip or the central bowl protrusion, or where optical distortion was too severe to correct.

Increased injection pressure clearly leads to increased penetration into the squish volume in the outer portion of the clearance plane. At the higher injection pressures the fuel has penetrated to the edges of the field of view, and is near or contacting the cylinder walls. Upon ignition, volume expansion within the bowl will almost certainly drive some of this mixture into the top ring-land crevice, where it will later contribute to HC and CO emissions. Surprisingly, richer mixtures are observed within the heads of the jets as injection pressure is increased. This is in part due to the fixed injection timing, which causes the fuel jets to strike the piston higher on the bowl rim at higher injection pressures. However, the injection timing selected provides optimal fuel efficiency at the 860 bar injection pressure. Notice further that, at the higher injection pressures, there is a significant amount of over-lean mixture ($\phi \lesssim 0.6$) within the squish volume between the fuel jets, as well as in the central region of the clearance volume and the bowl rim plane. This lean mixture can be expected to burn poorly and also lead to HC and CO emissions. Likewise, higher injection pressure leads to more over-lean mixture within the bowl, while only very limited regions of over-rich mixture are seen at the lowest pressure. Overall, the mixture formation process is clearly superior with the lower injection pressure.

The measured engine-out emissions, shown in the lower-right portion of Figure 2, support these observations. CO emissions rise rapidly with increasing injection pressure. HC emissions, however, increase as the pressure is increased from 500 to 860 bar but level off or decrease slightly with further increases. The likely reason for this behavior can be seen in the bowl rim plane when P_{inj}=1,220 bar. At this high injection pressure, the fuel jets have penetrated deep into the bowl, traversed the bowl floor, and are rising up and enriching the mixture in the central portion of the bowl rim plane.

The effect of this enrichment on the oxidation process can be understood from the simulation results presented in Figure 3. These results show the expected yield of HC and CO associated with each equivalence ratio, as predicted by homogeneous reactor simulations employing detailed chemical kinetic mechanisms. Notice that for a SOI of 23.3° bTDC and earlier, HC emissions are dominated by mixtures with $\phi \lesssim 0.3$, while CO emissions are dominated by richer mixtures, $0.3 \lesssim \phi \lesssim 0.5$, say. Mixture enrichment in the bowl rim plane by the heads of the high pressure fuel jets reduces the amount of very lean mixture which dominates HC

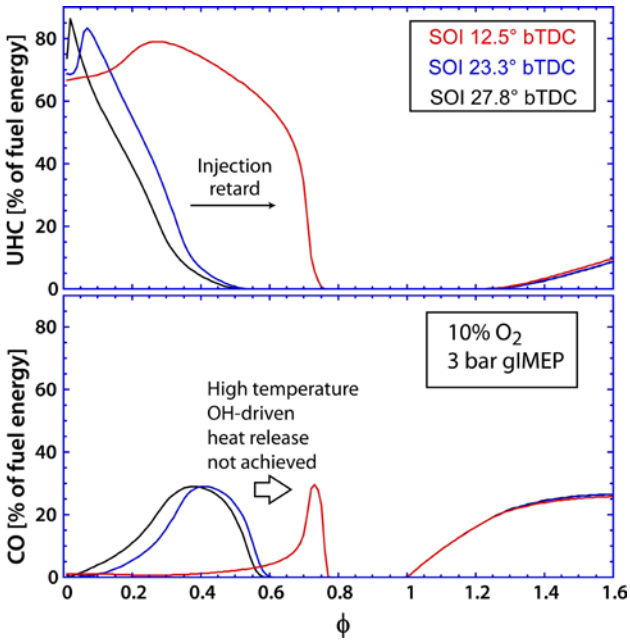

UHC - unburned hydrocarbon

FIGURE 3. Yield of HC and CO predicted by homogenous reactor simulations in a 10% O_2 charge. The pressure was constrained to match the experiments.

emissions, but increases the amount of slightly richer mixture leading to CO emissions.

Figure 3 also illustrates the impact of injection timing on the oxidation kinetics. Notably, even with modestly retarded injection timings of 12.5° bTDC, the yield of HC is impacted dramatically. For mixtures with $\phi \lesssim 0.7$, the slower oxidation kinetics delays the onset of the high temperature ignition processes into the expansion stroke, where charge cooling can prevent its occurrence. Hence HC emissions increase significantly, while for many equivalence ratios CO emissions can decrease—the progress of combustion is so severely inhibited that CO does not form. Consequently, as ignition is retarded, we anticipate that HC emissions will increase more rapidly than CO—behavior that is commonly observed in engine tests.

Equivalence ratio distributions at the start of high temperature heat release measured for the same injection timings shown in Figure 3 are shown in Figure 4. Several clear trends can be observed as the injection timing is retarded:

1. Less fuel enters the squish volume, the fuel is further from the bore wall, and peak equivalence ratios are lower.
2. Less over-lean mixture is found between the heads of the jets.
3. Less very-lean mixture ($\phi \lesssim 0.3$) is found in the upper-central regions of the cylinder.
4. Richer mixtures are found in the bowl, but peak equivalence ratios are low enough that little soot formation is expected.

Overall, from a mixture preparation viewpoint, retarded injection is preferred. Nevertheless, due to the highly negative impact of retarding SOI on HC oxidation seen in Figure 3, HC emissions nearly double as SOI is retarded from 23.3 to 12.5° bTDC.

Finally, to further the development of a predictive simulation capability, we have compared numerical simulations of the mixture preparation process to the experimental measurements. In general, with grid resolutions typical of current practice (~1 mm^3), the fuel jet penetration is significantly under-predicted for all injection pressures and swirl ratios, and the deflection of the jet by the swirling flow is over-predicted. These differences develop early in the mixture preparation process, regardless of the magnitude of the swirl ratio. As shown in Figure 5, less than 1° after the end-of-injection, the tangential deflection of the fuel jets is considerably greater in the simulation results, even within approximately 15 mm of the nozzle. Surprisingly, despite the lower penetration, the breadth of the fuel jets is also under-predicted. This indicates that the current modeling of both the air entrained into the fuel jets and the subsequent turbulent diffusion of the mixture requires improvement.

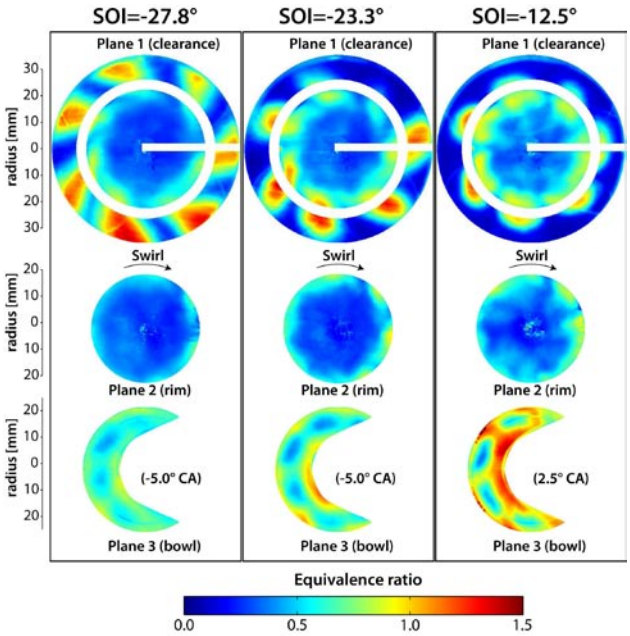

Engine emissions:

SOI [° bTDC]	CO [g/kg-f]	UHC [g/kg-f]
27.8	177.9	18.5
23.3	121.2	11.2
12.5	103.4	21.1

FIGURE 4. Equivalence ratio distributions measured at ignition for three different injection timings. P_{inj} = 800 bar; swirl ratio = 2.2; 10% O_2; 1,500 RPM; 3 bar gIMEP.

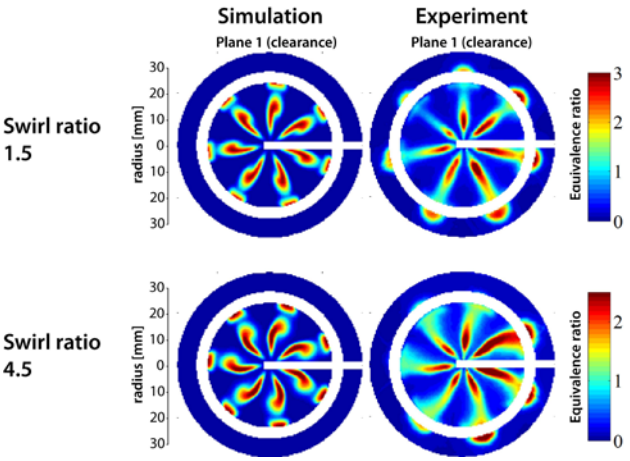

FIGURE 5. Comparison of simulated and measured equivalence ratio distributions in the clearance volume, for both low and high swirl ratios.

Conclusions

Quantitative measurements of the in-cylinder fuel-air equivalence ratio distributions, coupled with numerical simulations, have provided considerable insight into the mixture formation process and the sources of HC and CO emissions, over a range of flow swirl ratios, injection pressures, and injection timings. The ability of current multi-dimensional models to predict these distributions has also been investigated. Examples of conclusions reached from this work are:

- Increased injection pressure, at the light-load operating condition investigated, is generally detrimental. Mixture distributions formed have both more over-lean and more over-rich regions and there is a greater potential for fuel to enter the top ring-land crevice.
- As injection is retarded toward top-dead center in PPCI combustion systems, the mixture distributions improve. There is less potential for crevice unburned HC, and less over-lean mixture throughout the combustion chamber with little penalty in the form of over-rich regions. Nevertheless, emissions and efficiency deteriorate due to the adverse impact of retarded timing on reaction kinetics.
- Current models and/or modeling practice must be improved in order to accurately predict the initial mixture preparation process. Fuel jet penetration and diffusion (spreading) are both under-predicted, and the sensitivity of the fuel-air distribution to flow swirl is excessive.

FY 2012 Selected Publications/Presentations

1. "A Computational Investigation of the Effects of Swirl Ratio and Injection Pressure on Wall Heat Transfer in a Light-Duty Engine," Perini F, Dempsey A, Reitz RD, Sahoo D, Petersen BR, Miles PC. *Submitted to the 2013 SAE World Congress, Offer No.: 13PFL-0745.*

2. "In-Cylinder Flow," Borée J, Miles PC. Submitted to *Encyclopedia of Automotive Engineering.*

3. "Atmospheric Pressure Acetylene Detection by UV Photo-fragmentation and Induced C2 Emission," Miles PC, Li B, Li Z, and Aldén, M. *In press: Applied Spectroscopy.*

4. "Conceptual Models for Low-Load, Single-Injection, EGR-Diluted, Partially Premixed Low-Temperature DI Diesel Combustion," Musculus MPB, Miles PC, and Pickett LM. *In press: Prog. in Energy Combust Sci.*

5. "Review of Equivalence Ratio Measurements in a Light-Duty Diesel Engine Operating in a Light-Load Partially Premixed Regime," Petersen BR, Sahoo D, Miles PC. *Paper presented at THIESEL 2012: Thermo- and Fluid Dynamic Processes in Direct Injection Engines*, Sept. 11–14, 2012, Valencia, Spain.

6. "Characterization of Reactivity Controlled Compression Ignition (RCCI) Using Premixed Hydrated Ethanol and Direct Injection Diesel in Heavy-Duty and Light-Duty Engines," Dempsey AB, Walker NR, Splitter D, Wissink M, Reitz RD. *Paper presented at THIESEL 2012: Thermo- and Fluid Dynamic Processes in Direct Injection Engines*, Sept. 11–14, 2012, Valencia, Spain.

7. Impact of Injection Timing on the Mixture Preparation and Chemical Kinetics of Early-Injection (PCI), Low-Temperature Combustion," Miles PC, Petersen BR, Sahoo D. *Paper presented at Eighth International Conference on Modeling and Diagnostics for Advanced Engine Systems - COMODIA-2012*, July 23-26, 2012, Fukuoka, Japan.

8. "The Impact of Swirl Ratio and Injection Pressure on Fuel-Air Mixing in a Light-Duty Diesel Engine," Sahoo D, Petersen BR, Miles PC. *Paper presented at 2012 ASME Spring Meeting, Paper ICES2012-81234.*

9. "Equivalence Ratio Distributions in a Light-Duty Diesel Engine Operating under Partially-Premixed Conditions," Petersen BR, Miles PC, Sahoo D. *Presented at the 2012 SAE World Congress, SAE Technical Paper 2012-01-0692, SAE Intl. J. of Engines 5:2:526-537, 2012.*

10. "Comparison of Quantitative In-Cylinder Equivalence Ratio Measurements with CFD Predictions for a Light Duty Low Temperature Combustion Diesel Engine," Dempsey AB, Wang B-L, Reitz RD, Petersen BR, Sahoo D, Miles PC. *Presented at the 2012 SAE World Congress, SAE Technical Paper 2012-01-0143, SAE Intl. J. of Engines 5:2:162-184, 2012.*

11. "Further Validation of the Generalized RNG Turbulence Model in a Backward Step Flow and Model Assessment in a HSDI Diesel Engine," Wang B-L, Bergin MJ, Petersen BR, Miles PC, Reitz RD, Han Z. *Presented at the 2012 SAE World Congress, SAE Technical Paper SAE 2012-01-0140.*

Special Recognitions

1. Invited Paper/Presentation "Quantitative Mixture Preparation Studies in Late-Injection Diesel Combustion Systems using Toluene LIF," Miles PC, Petersen BR, Sahoo D. *Paper presented at 10th International Symposium on Combustion Diagnostics*, May 22-23, 2012, Baden-Baden, Germany.

2. Invited Presentation "Quantitative Measurements of Flow and Scalar Fields Supporting Predictive Simulation for Engine Design," *CALSTART Leadership Circle, June 12, 2012, Livermore, CA.*

3. Invited Seminar "Physical Fluid Dynamics in Reciprocating Engines," Miles PC. *Royal Institute of Technology, March 1, 2012, Stockholm, Sweden.*

II.3 Heavy-Duty Low-Temperature and Diesel Combustion & Heavy-Duty Combustion Modeling

Mark P.B. Musculus
Combustion Research Facility
Sandia National Laboratories
P.O. Box 969, MS9053
Livermore, CA 94551-0969

DOE Technology Development Manager:
Gurpreet Singh

Overall Objectives

This project includes diesel combustion research at Sandia National Laboratories (SNL) and combustion modeling at the University of Wisconsin (UW). The overall objectives are:

- Develop fundamental understanding of how in-cylinder controls can improve efficiency and reduce pollutant emissions of advanced low-temperature combustion (LTC) technologies.
- Quantify the effects of fuel injection, mixing, and combustion processes on thermodynamic losses and pollutant emission formation.
- Improve computer modeling capabilities to accurately simulate these processes.

Fiscal Year (FY) 2012 Objectives

- Consolidate observations spanning years of optical and computational research in partially premixed compression ignition (PPCI) LTC into a coherent conceptual model (SNL).
- Implement and demonstrate new high precision fuel system for multiple injections in optical engine (SNL).
- Explore close-coupled post injections for mitigating particulate matter (PM) emissions and improving fuel efficiency (SNL).
- Compare the multi-mode model predictions to experimental data and identify directions for improving thermal efficiency (UW).

Accomplishments

- Completed a 38-page review article describing a new conceptual model for PPCI LTC which was accepted for publication in the journal Progress in Energy and Combustion Science.
- Implemented a new injection system in the heavy-duty optical engine that allows precise fuel delivery (~1-2 mg) of multiple injections with close spacing (~100 microseconds) with less than 1% shot-to-shot variation, which enables investigation of new research areas.
- Demonstrated up to 62% engine-out soot reduction using new fuel injection system with close-coupled post-injections having combustion phasing favorable for fuel-efficiency across a wide range of exhaust gas recirculation (EGR), and provided initial in-cylinder observations that suggest post-injection targeting into the main-soot cloud is important for creating interaction.
- Model predictions show how heat transfer LTC strategies achieve higher efficiency by nearly halving heat transfer, largely by reducing in-cylinder combustion temperatures and by locating combustion away from in-cylinder surfaces.

Future Directions

- Start building a design-level conceptual-model understanding of multiple injection processes:
  - Explore fuel-injection schedules using multiple pilot, post, and split injections that are currently deployed by industry.
  - Identify mechanisms and critical requirements (injector rate-shaping, dwell, duration, etc.) to achieve emissions and efficiency improvements across wide parameter space.
- Determine how combustion design affects heat transfer and efficiency:
  - Measure spatial and temporal evolution of heat transfer across range of combustion modes; correlate to progression of in-cylinder combustion processes.
- Build understanding of in-cylinder LTC soot and poly-cyclic aromatic hydrocarbons (PAHs):
  - Use multiple laser wavelengths and high-temporal-resolution imaging/spectroscopy to track PAH growth and conversion to soot.

Introduction

Over the past decade, LTC strategies for compression-ignition engines have shown promise for reducing engine-out emissions of nitrogen oxides (NOx) and particulate matter (PM) while maintaining or even improving fuel efficiency. Initially, these strategies were explored as a means to achieve stringent emissions targets without exhaust aftertreatment. In recent years, practical experience with exhaust aftertreatment systems has proven them effective, but interest in LTC remains for improving efficiency and for reducing the aftertreatment burden, especially at low-load conditions. One common way to achieve LTC is to dilute the intake stream with EGR, and one broad category of EGR-diluted LTC is PPCI. Compared to conventional diesel combustion, PPCI uses either advanced or retarded direct fuel injection to provide more time for fuel-air mixing prior to ignition.

The general in-cylinder spray, mixing, combustion, and pollutant-formation processes of conventional diesel combustion are relatively well understood, thanks in large part to insight gained from numerous laser-based imaging diagnostic studies in optical engines. The widely-used conceptual model for conventional diesel combustion [1] was formulated from optical diagnostic data, and has served as a useful foundation of understanding. Until recently, a comparable conceptual model framework did not exist for PPCI LTC strategies. In this report, a new conceptual model is proposed for PPCI LTC. The new model is based on optical diagnostic data from both heavy- and light-duty optical engines, as well as from other optical spray and combustion chambers.

Approach

This project uses an optically-accessible, heavy-duty, direct-injection diesel engine (Figure 1). A large window in the piston crown provides primary imaging access to the piston bowl, and other windows at the cylinder wall provide cross-optical access for laser diagnostics. For many of the experiments that provide data for the new conceptual model, the engine uses a Cummins XPI heavy-duty common rail injector, which is capable of multiple injections at rail pressures up to 2,200 bar. For the post-injection studies (not part of the new conceptual model), a Delphi DFI-1.5 light-duty injector and support system capable of precise delivery of small closely spaced injections was installed in the engine.

Various laser-imaging diagnostics probed the in-cylinder spray, mixing, combustion, and pollutant formation processes under PPCI LTC conditions. Figure 1 shows a generic imaging setup, with two cameras to acquire simultaneous images from separate techniques. As described in the results section and in [2], various

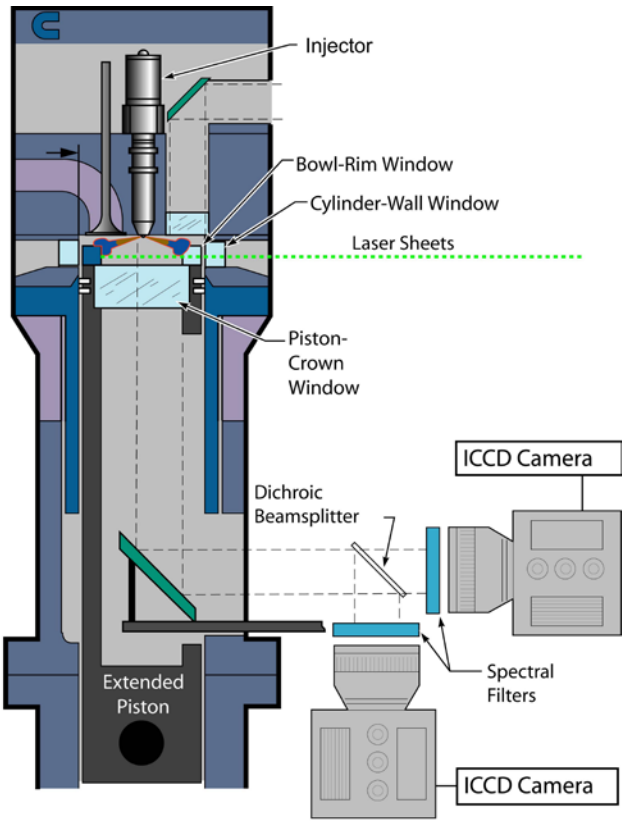

ICCD - intensified charged-coupled device

FIGURE 1. Schematic diagram of the optically accessible direct injection diesel engine and optical setup.

pairings of diagnostics were employed. To image the liquid-fuel spray, elastic Mie-scattering of 532-nm laser light was captured by a gated, intensified charge-coupled device camera. Vapor-fuel penetration was visualized by planar laser-induced fluorescence (PLIF) of diesel fuel components using an ultraviolet (UV) laser source. To probe the first-stage ignition processes, as well as to detect unburned fuel, PLIF of formaldehyde (H_2CO), a combustion intermediate, was employed. The same technique can also capture PLIF of PAHs, which are soot precursor species, and laser-induced incandescence of soot itself. The second-stage ignition and concomitant completion of combustion was revealed by PLIF of the hydroxyl radical (OH), a combustion intermediate that is formed when the combustion of fuel is complete (or nearly complete) in regions of intermediate stoichiometry. Additional diagnostic details are available in [2] and in references citied within.

Results

Presented here is a brief summary of a few key elements of the PPCI LTC conceptual model. For a more complete description, see [2].

A series of images showing the initial liquid- and vapor-fuel penetration for an early-injection PPCI LTC condition are assembled in Figure 2. One of the eight fuel-jets, the horizontal jet penetrating from left to right, is fully illuminated by the 30-mm wide laser sheets, the edges of which are delimited by the horizontal dashed lines. Corresponding illustrations of a fuel jet from the PPCI LTC conceptual model are shown to the right of each image.

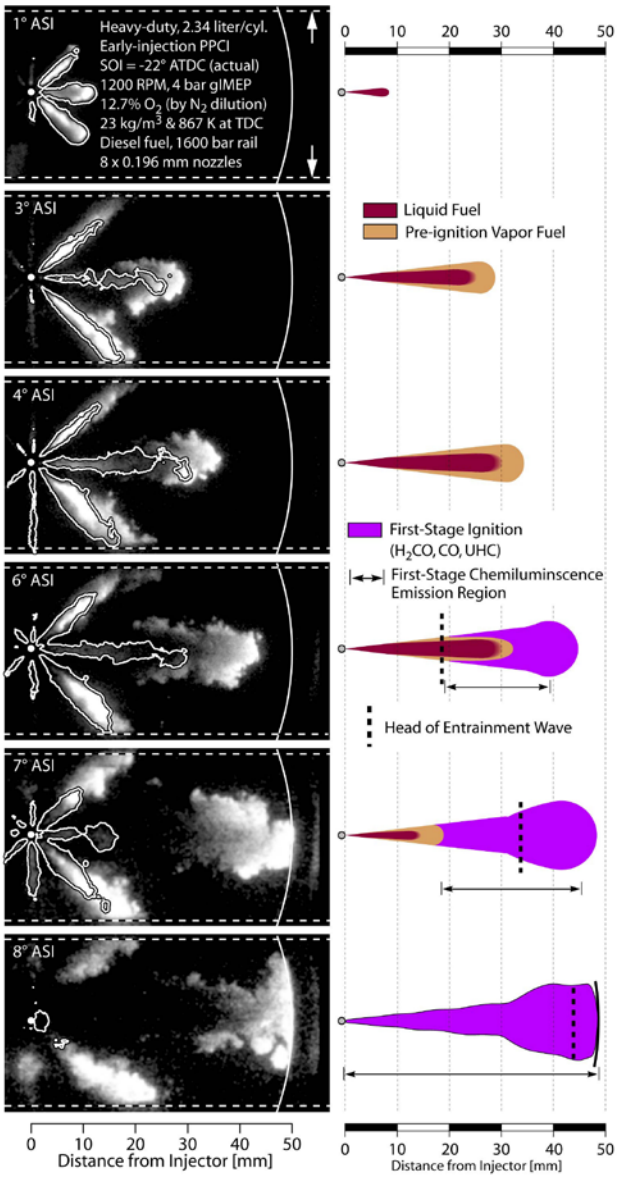

FIGURE 2. Left: Fuel fluorescence from both liquid and vapor diesel fuel (grayscale, significant attenuation) and Mie-scattered light from liquid-fuel only (contours) observed for an early-injection PPCI operating condition in a heavy-duty engine [3]. The curved white line is the piston bowl-wall (49-mm radius), and the laser sheet (dashed lines) propagates from right to left along the axis of the jet penetrating to the right. Right: Corresponding illustrations from the conceptual model for PPCI LTC.

The grayscale images show diesel-fuel PLIF, and the overlaid contours show the liquid-fuel boundary. The grayscale images are primarily from vapor fuel, but they must be interpreted with care. Diesel fuel absorbs ultraviolet light very strongly, so the laser intensity is rapidly attenuated as it passes through the fuel. As a result, fuel on the left side of the images is often not illuminated by the laser light, especially for the later images. Hence, the intensity of the fluorescence emission does not indicate fuel concentration. Instead, the grayscale images only indicate the spatial and temporal evolution of the leading edge (right side) of the penetrating fuel jet.

The early evolution of the PPCI jet in Figure 2 is similar to a conventional diesel jet (not shown). Liquid fuel (contours in left column, dark brown in right column) and vapor fuel (grayscale/light brown) penetrate together until near 3° after the start of injection (ASI), after which the vapor penetrates beyond the liquid [3]. For early-injection LTC conditions into lower-temperature, less dense ambient gases, the jet penetrates somewhat faster, and the liquid length (35 mm or more) is typically longer than for conventional conditions (~25 mm). After the injection-rate peaks, the deceleration of the liquid fuel exiting the nozzle increases local entrainment of ambient gases near the nozzle. Jet simulations show that the region of increased entrainment propagates downstream in a wave at twice the jet penetration rate. The head of the entrainment wave, which initiates at the peak injection rate near 5° ASI, is indicated by a vertical dotted line. As the injection rate ramps down and ends, the entrainment wave propagates downstream, temporarily increasing entrainment in its wake. After the head of the entrainment wave passes the liquid length at 7° ASI, increased mixing helps to vaporize the downstream portions of the fuel jet. As a result, the instantaneous liquid length rapidly shortens, and fuel is fully vaporized within 1° after the end of injection (no liquid contours or dark brown in bottom row of Figure 2). The bottom of the right column in Figure 2 also shows first-stage ignition (violet), which is discussed in detail in the following paragraph.

The left column in Figure 3 shows simultaneous PLIF images of formaldehyde (false-colored red) and OH (green) [4]. Formaldehyde is first detected at 7° ASI, during the first-stage (cool-flame) ignition event. The formaldehyde first appears throughout much of the downstream jet, and then extends upstream to fill the whole jet, as depicted by the fully violet jet at 8° ASI. (The corresponding image to the left does not show formaldehyde closer to the injector because of the angle of the horizontal laser sheet relative to the jet axis, but other sheet orientations and elevations confirm formaldehyde near the injector.) OH (green) first

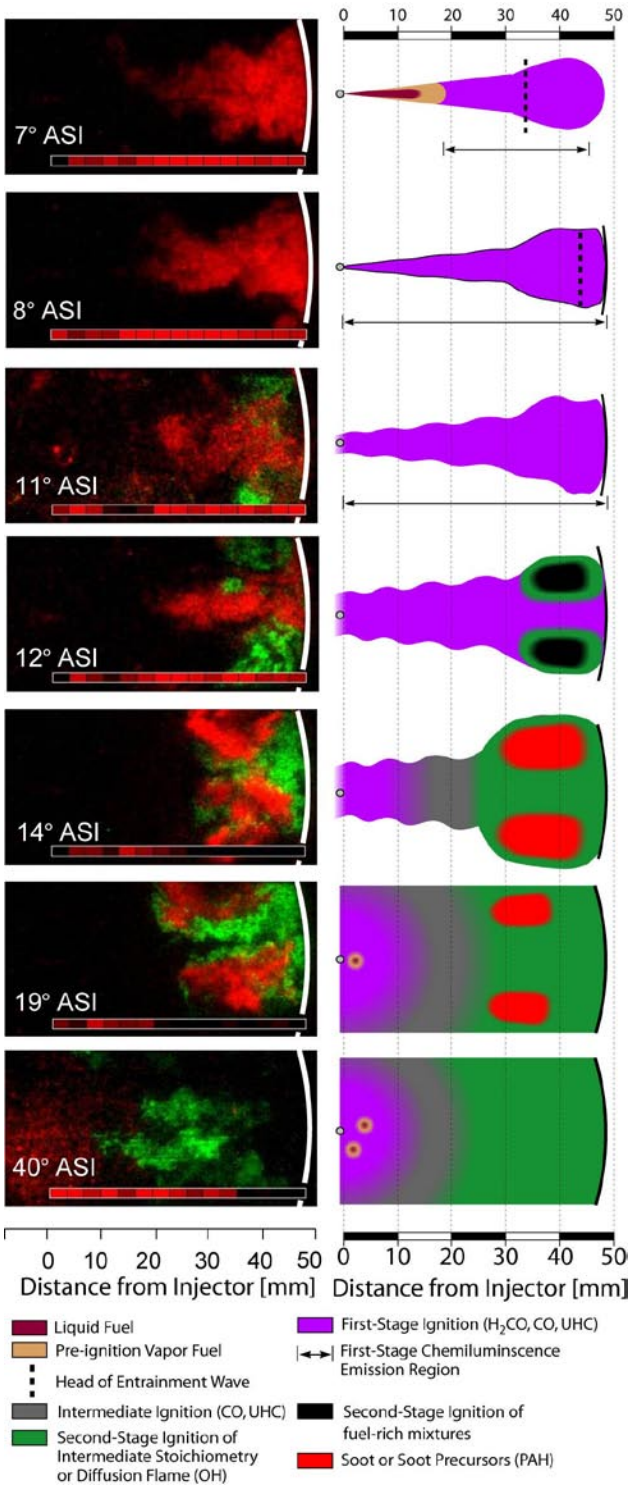

FIGURE 3. Left: Combined single-shot formaldehyde PLIF and PAH PLIF/soot laser-induced incandescence (red) and OH PLIF (green) for a late-injection LTC condition in a heavy-duty engine [4]. Red in the colorbar indicates a strong signature of formaldehyde in the fluorescence spectrum. Right: Corresponding illustrations from the conceptual model for PPCI LTC.

appears in the downstream jet, near the piston bowl-wall. Embedded within the OH field in the downstream jet are rich pockets (black), which later form soot and soot precursors (bright red in both images and illustrations).

Late in the combustion even, most of the soot and its precursors are consumed, but formaldehyde remains late in the cycle, near the injector (bottom row in Figure 3). Additional fuel-concentration measurements (not shown here) indicate that the fuel mixtures near the injector are too fuel-lean to achieve complete combustion in the time available before cylinder expansion. This incomplete combustion contributes to unburned fuel emissions. Although not measured directly, carbon monoxide (CO) is predicted by chemical kinetics simulations to be co-located with the formaldehyde, and also to exist in an intermediate-ignition region (grey in illustrations) between the formaldehyde and OH. Finally, late in the cycle, liquid droplets can dribble from the injector holes and/or sac volume (not shown). They may create locally fuel-rich regions and can contribute modestly to unburned hydrocarbon and CO emissions.

These and other details are incorporated in the conceptual model for heavy-duty PPCI LTC, key features of which (center column) are contrasted to conventional diesel combustion (left column) in Figure 4. Figure 4 also shows key illustrations for the light-duty perspective of the PPCI LTC model (right column). Figure 4 shows that in the conventional diesel conceptual model, insufficiently mixed fuel generates soot and smoke (red), and a hot flame (green) forms nitrogen oxides (NOx), a smog precursor. By contrast, EGR and modified fuel injection in PPCI LTC engines for both heavy- and light-duty delays fuel ignition until after the end of fuel injection, so that the fuel is better mixed with air and much less soot is formed. The data also show that incomplete combustion (purple/gray) arises from over-mixed regions, which provides guidance for optimization to reduce CO and unburned hydrocarbon emissions for LTC. Spray/swirl and spray/bowl interactions are also important for the light-duty engine, affecting fuel mixing and pollutant formation, as described in detail in [2].

In addition to the PPCI LTC conceptual model development, a new fuel injection system was also implemented in the engine to allow studies of engine-out soot reduction by post injections that are closely coupled to the main injection to yield combustion phasing of the post injections that is favorable for fuel efficiency. Figure 5 shows an initial comparison of engine-out soot emissions for load sweeps with a single injection (closed symbols) and a constant main plus a series of post injections of increasing duration (open symbols) at an LTC condition with 12.6% intake oxygen. Similar trends were also observed at 15%, 18%, and 21% intake oxygen. While many previous studies have shown soot reductions

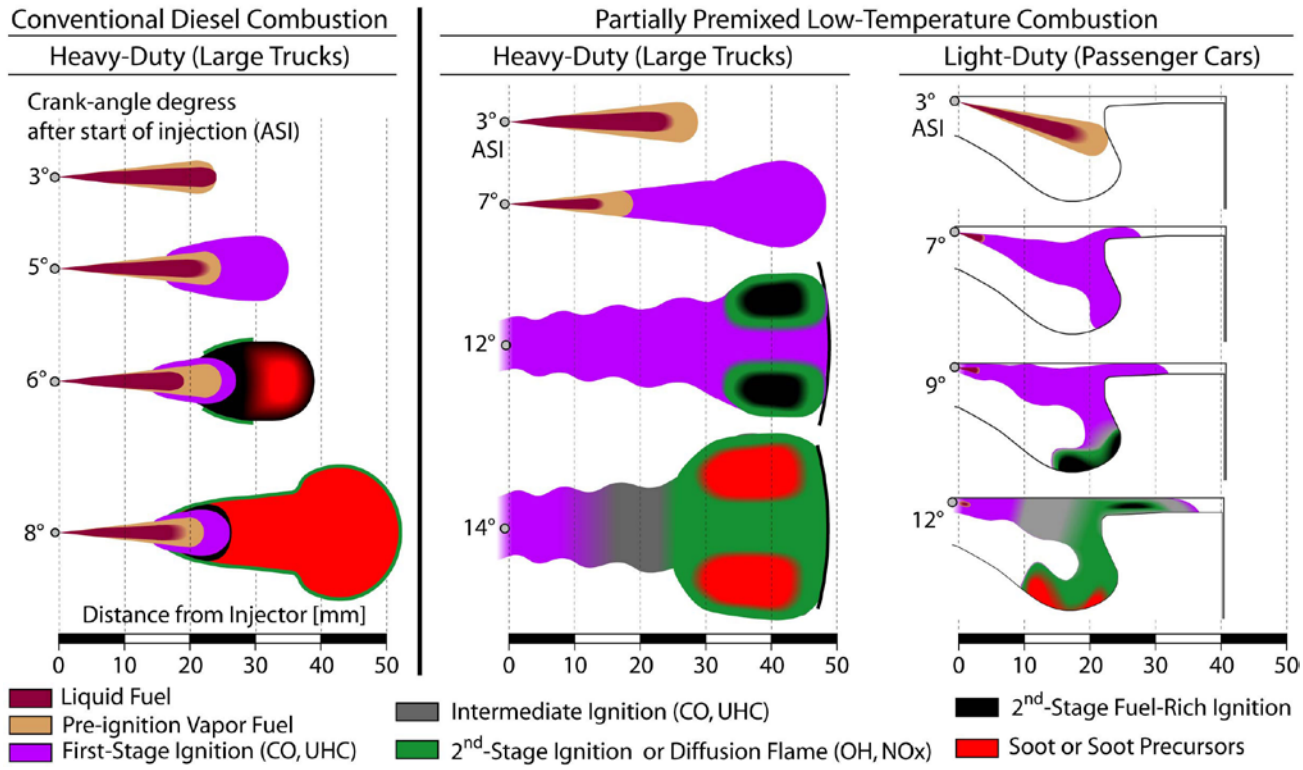

FIGURE 4. PPCI LTC conceptual model features for conventional heavy-duty diesel combustion (left) and partially-premixed low-temperature diesel combustion for heavy-duty trucks (middle) or light-duty passenger cars (right).

with post injections, the data in Figure 5 are significant because they show a clear decrease in engine-out soot when the main injection is held constant, and a post injection is added. Compared to the usual constant-load perspective, where the main injection duration decreases along with the addition of a post injection, the constant-main-injection configuration of Figure 5 unambiguously shows that the post injection must interact with the main injection to reduce soot. Initial optical studies of the post-injection interaction (not shown here) suggest that the targeting and penetration of the post injection into the residual main-injection soot is important for achieving soot reduction, but many confounding factors preclude a clear conclusion. Future plans for more optical data from multiple optical diagnostics, similar to the approach employed to inform the conceptual models, will help to clarify the in-cylinder mechanisms of soot reduction by post injections in future experiments.

Finally, computer-model simulations at the University of Wisconsin show that efficiency improvements achieved with dual-fuel reactivity-controlled compression ignition (RCCI) are largely due to reductions in heat transfer. Figure 6 shows comparisons of heat-transfer predictions for conventional and RCCI combustion. The lower peak temperature of RCCI,

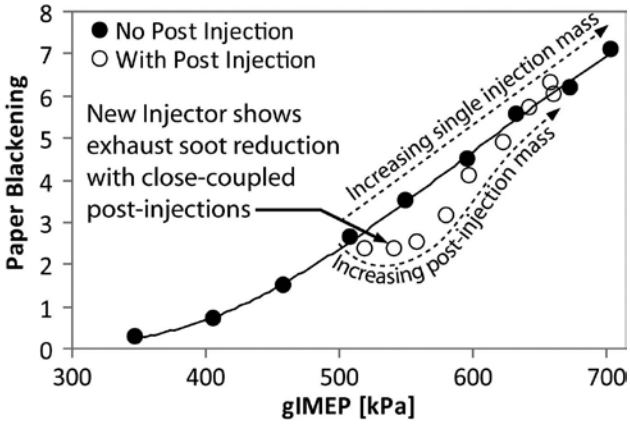

FIGURE 5. Engine out-soot emissions at 12.6% intake oxygen with conventional diesel fuel injection timing for a load sweep with single injections (filled symbols) or increasing duration of post injection with a constant main injection (open symbols).

achieved by fuel-lean combustion and EGR, helps to reduce heat transfer, as well as the more centralized location of combustion, which occurs farther from the walls than in conventional diesel combustion.

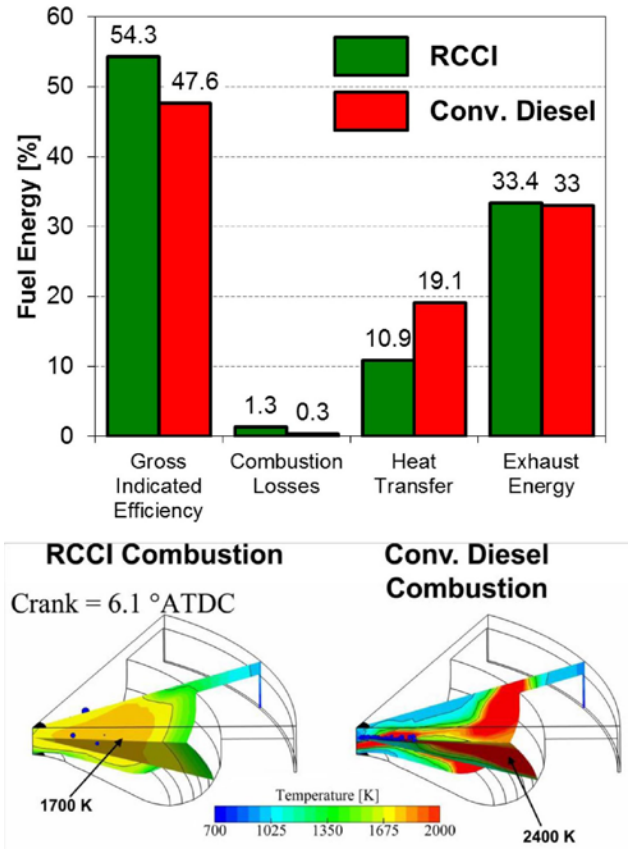

FIGURE 6. Top: Energy budget for conventional diesel (red) and RCCI (green), showing difference in losses. Bottom: Snapshot of computer-predicted temperature distributions for RCCI and conventional diesel combustion.

Conclusions

The recent research efforts described in this report provide improved understanding of in-cylinder LTC mixing and combustion processes required by industry to build cleaner, more efficient, heavy-duty engines. Specific conclusions include:

- Results from multiple optical and laser diagnostic studies of partially premixed compression ignition LTC have been distilled into a conceptual model for both heavy- and light-duty engines.
- A newly implemented fuel injector and delivery system provides repeatable, precise, close-coupled multiple injections.
- Close-coupled post injections show unambiguous interaction of the post injection with the main injection soot, both using engine-out measurements and optical imaging.
- Computer models predict that much of the fuel-efficiency benefit of RCCI is due to reduction of heat transfer, achieved by creating fuel-lean mixtures and EGR dilution, as well as by location combustion away from cylinder surfaces.

References

1. Dec JE. A conceptual model of D.I. diesel combustion based on laser-sheet imaging. SAE Paper 970873 SAE Trans. 1997; 106(3):1319-1348.

2. Musculus MPB, Miles PC, Pickett LM. Conceptual models for partially premixed low-temperature diesel combustion. Progress in Energy and Combustion Science 2012 (in press).

3. Singh SS, Reitz RD, Musculus MP, Lachaux T. Validation of engine combustion models against detailed in-cylinder optical diagnostics data for a heavy-duty compression-ignition engine. Int. J. Engine Res. 2007; 8(1):97-126.

4. Genzale CL, Reitz RD, Musculus MPB. Effects of piston bowl geometry on mixture development and late-injection low-temperature combustion in a heavy-duty diesel engine. SAE Paper 2008-01-1330 SAE International Journal of Engines 2008; 1(1):913-937.

FY 2012 Publications/Presentations

1. "Conceptual models for low-load, single-injection, EGR-diluted, partially premixed low-temperature DI diesel combustion," M.P.B. Musculus, P.C. Miles, and L.M. Pickett, Progress in Energy and Combustion Science, in press, November 2012.

2. "Chemiluminescence and fuel PLIF imaging of reactivity controlled compression ignition (RCCI) combustion," S.L. Kokjohn, R.D. Reitz, and M.P.B. Musculus, ILASS Americas, May 2011.

3. "Experimental facilities and measurements – fundamentals," M.P.B. Musculus, L.M. Pickett, and S.A. Kaiser, book chapter in Encyclopedia of Automotive Engineering, submitted Sept. 2011.

4. "Laser diagnostics of soot precursors in a heavy-duty diesel engine at low-temperature combustion conditions," M.K. Bobba and M.P.B. Musculus, Combustion and Flame 159(2) 832-843, 2012.

5. "The influence of large-scale structures on entrainment in a decelerating transient turbulent jet revealed by large eddy simulation," B. Hu, M.P.B. Musculus, and J.C. Oefelein, Physics of Fluids 24(4) 045106, 2012.

6. "Investigation of fuel reactivity stratification for controlling PCI heat-release rates using high-speed chemiluminescence imaging and fuel tracer fluorescence," S.L. Kokjohn, D.A. Splitter, M.P.B. Musculus, and R.D. Reitz, SAE paper 2012-01-0375, SAE Int. J. of Engines 5:248-269, 2012.

7. "Fuel reactivity controlled compression ignition (RCCI): a pathway to controlled high-efficiency clean combustion," S.L. Kokjohn, R.M. Hanson, D.A. Splitter, R.D. Reitz, International Journal of Engine Research 12(3) 209-226, June 2011.

8. "Investigation of the roles of flame propagation, turbulent mixing, and volumetric heat release in conventional and low temperature diesel combustion," S.L. Kokjohn and R.D. Reitz, ASME J. Eng. Gas Turbines Power, October 2011.

9. "Modeling charge preparation and combustion in diesel fuel, ethanol, and dual fuel PCCI engines," S.L. Kokjohn, D.A. Splitter, R.M. Hanson, R.D. Reitz, V. Manente, and B. Johansson, Atomization and Sprays 21(2), 107-119, 2011.

II.4 Spray Combustion Cross-Cut Engine Research

Lyle M. Pickett
Sandia National Laboratories
P.O. Box 969, MS 9053
Livermore, CA 94551-9053

DOE Technology Development Manager:
Gurpreet Singh

Overall Objectives

Facilitate improvement of engine spray combustion modeling, accelerating the development of cleaner, more efficient engines.

Fiscal Year (FY) 2012 Objectives

- Lead a multi-institution, international, research effort on engine spray combustion called the Engine Combustion Network (ECN).
- Develop spray combustion datasets with quantified spray mixing, evaporation, ignition, and lift-off length characteristics for computational fluid dynamics (CFD) model evaluation and improvement.
- Evaluate the effect of engine-relevant pressures and temperatures on the near-field liquid structure of fuel sprays.

Accomplishments

- Generated a comprehensive spray combustion dataset working collaboratively with eight different experimental institutions from around the world. Organized and led an ECN workshop with over 140 participants, where 16 multiple modeling groups submitted results for a side-by-side comparison to this experimental data thereby defining the state of current research and pointing to needed future directions.
- Developed new diagnostic techniques that have quantified and standardized key metrics of spray development, such as liquid length, ignition delay, and lift-off length.
- Performed high-speed microscopy to reveal the spray liquid structure as it transitions from low temperature and pressure to engine-relevant conditions.

Future Directions

- Develop spray and combustion datasets for gasoline direct-injection systems.
- Characterize multi-hole sprays compared to axial-hole sprays.
- Quantify soot and soot precursor formation processes at target conditions.

Introduction

All future high-efficiency engines will have fuel directly sprayed into the engine cylinder. Engine developers agree that a major barrier to the rapid development and design of these high-efficiency, clean engines is the lack of accurate fuel spray CFD models. The spray injection process largely determines the fuel-air mixture processes in the engine, which subsequently drives combustion and emissions. More predictive spray combustion models will enable rapid design and optimization of future high-efficiency engines, providing more affordable vehicles and also saving fuel.

Approach

To address this barrier, we have established a multi-institution collaboration, called the ECN, to both improve spray understanding and develop predictive spray models. By providing highly leveraged, quantitative datasets (made available online [1]) CFD models may be evaluated more critically and in a manner that has not happened to date. Productive CFD evaluation requires new experimental data for the spray and the relevant boundary conditions, but it also includes a working methodology to evaluate the capabilities of current modeling practices. This year we organized ECN experimental and modeling activities through frequent web conference exchanges, culminating with the second ECN workshop. 104 participants from over 20 different countries attended the workshop, and 40 more accessed the live presentations via webcast. Eight institutions contributed experimental data and 16 different groups offered CFD simulations at these same operating conditions. Organizers gathered experimental and modeling results prior to the workshop to allow a side-by-side comparison and expert review of the current state of the art for diagnostics and engine modeling for specific aspects of spray and combustion modeling.

Experimentally, we have focused on providing new quantitative diagnostics that also offer benefits toward standardization when implemented in different facilities. These diagnostics include measurement of the nozzle internal geometry, near-field liquid distribution, spray penetration and evaporation, ignition, lift-off length, and so forth. Figure 1 shows a diagnostic developed to quantify the liquid-phase penetration and shape of liquid droplets or ligaments. Past experiments using Mie-scatter from the liquid displayed inconsistencies because of dependencies upon the lighting or imaging arrangement [2]. The improved diagnostic shown in the figure utilizes light from a light-emitting diode prepared with a diffuser/lens arrangement as back lighting. This diffused back-illumination (DBI) arrangement seeks to avoid misinterpretation because of schlieren effects that would happen if the light were completely collimated, but at the same time, provide a reference light intensity that quantifies the scattering/extinction caused by liquid [3]. Each light pulse from the light-emitting diode is only 50 ns in duration, to permit temporal isolation of the spray, and a burst of pulses are synchronized with a high-speed camera operating at frequencies greater than 100,000 frames/s. This versatile instrument permits time-resolved, and more quantitative, imaging of the spray development and vaporization. This same experimental setup was implemented by five different experimental institutions/facilities at the same target conditions.

High-speed microscopy was also implemented using the same DBI imaging setup shown in Figure 1 while replacing the 50-mm lens with a with a long-distance microscope lens configured for a magnification of 4× and 4.7 µm/pixel. This system was implemented to reveal the spray liquid structure at various conditions.

Results

The high-speed diffused back-illumination system was implemented at the Spray A conditions of the ECN. The time-averaged optical depth or extinction τ is presented in a two-dimensional map at the top of Figure 2, while the bottom shows profiles measured on the axis of the spray using DBI or laser extinction. These plots show that extinction by liquid extends to about 10-11 mm downstream, providing a measurement of the maximum liquid penetration length. The spray also appears symmetric, unlike Mie-scatter imaging, which shows biases towards the lighting direction. However, the DBI imaging also shows some measured extinction downstream of 10 to 11 mm while this does not occur with HeNe laser illumination with a larger collection angle. These results indicate that vaporized fuel and temperature gradients create intense beam steering that should not be confused with liquid extinction. Adequate collection angle is required to avoid this artifact. At the same time the current DBI implementation tracks the steep decline in liquid extinction occurring near the liquid length, and is consistent with the laser setup. This consistency and quantification could not be achieved in the past using different Mie-scatter approaches. Various institutions have now implemented this same experimental setup at Spray A conditions permitting a more relevant comparison of results.

Figure 3 shows observations of the liquid spray structure when the imaging system was changed to long-distance microscopy and the ambient pressure and temperature reduced to 5 bar and 440 K. Microscopic features (labeled in the figure), such as fuel ligament or droplet breakup can be observed during the transients, particularly at the end of injection when the injection pressure drops, decreasing the turbulence and slowing

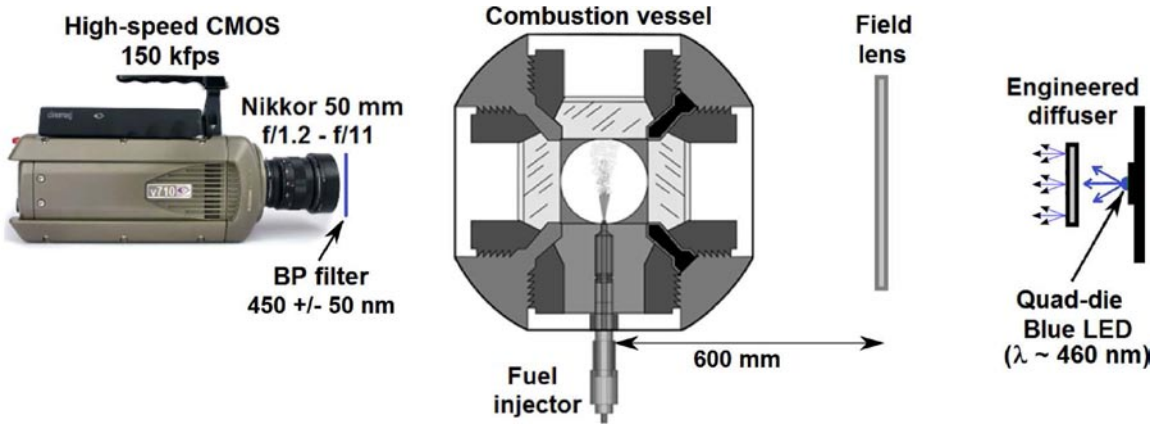

CMOS - complementary metal oxide semiconductor; BP - bandpass filter; LED - light-emitting diode

FIGURE 1. Schematic of the diffused back-illumination high-speed imaging arrangement around the spray combustion vessel.

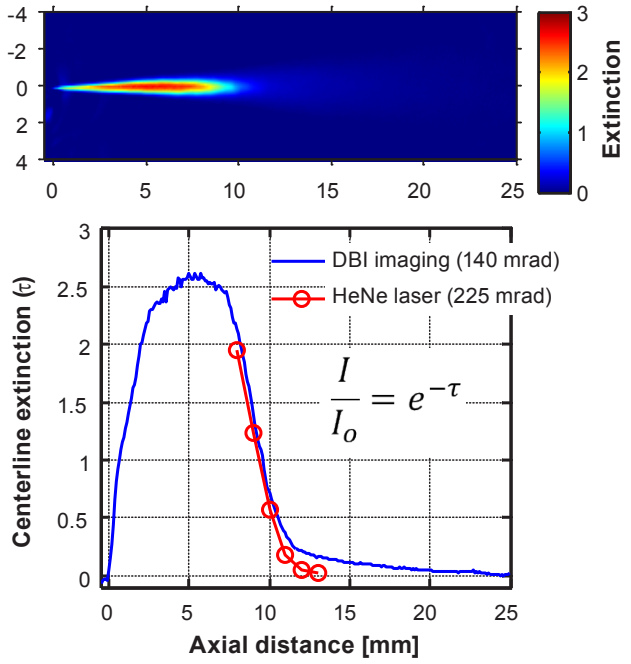

FIGURE 2. Two-dimensional extinction map obtained with the DBI technique (top) together with the extinction profile measured on spray axis (bottom plot). "Spray A" condition. Ambient: 900 K, 60 bar (22.8 kg/m3), 0% O2. Injection: 0.090 mm nozzle, 150 MPa, n-dodecane, 363 K.

down the spray. The slower flow at the end of injection produces liquid structures that are larger than that during the main injection at high pressure, while the thermo-physical ambient and fuel conditions are the same. Thus, analysis of the structure at the end of injection ultimately provides insights as to the impact of thermodynamic conditions on fluid properties and spray mixing, much like designed experiments for isolated droplets, for example. For conditions relevant to diesel sprays (gas temperature exceeding 800 K), microscopic imaging information like that given in Figure 3 is nonexistent in the literature. Considering the importance of fuel and ambient gas properties on the breakup, development and mixing processes, investigation at high pressure and temperature is needed. Direct observations of the liquid structure can provide fundamental information to modelers enabling more accurate predictions of spray development.

Images of the spray structure at high pressure conditions are markedly different, as shown in Figure 4 (also see the movies available as supplementary material [4]). The low ambient temperature condition (T = 440 K) at the right clearly shows droplets and ligaments, similar to that observed in Figure 3 at lower ambient pressure. The high temperature and pressure condition at the left (Spray A) shows structures at the end of injection that appear diffuse or blurry, and the high-speed image sequence shows no evidence of fuel structures held

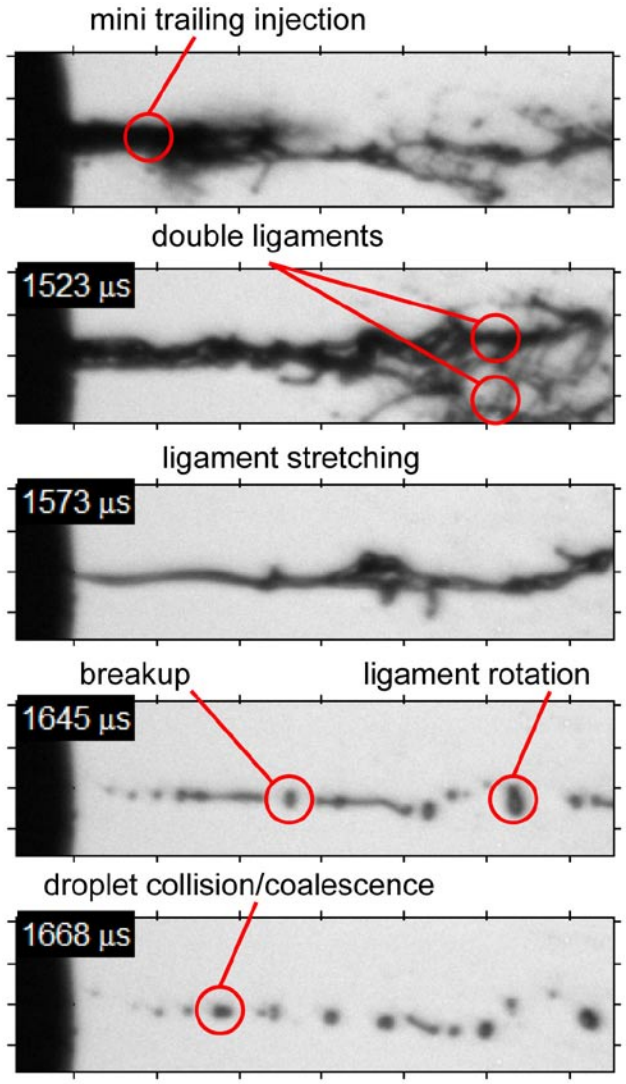

FIGURE 3. Time sequence at the end of injection showing droplet and ligament dynamics at low temperature (440 K) and pressure (5 bar). All other conditions are "Spray A."

together by surface tension forces. One issue is that under such high temperature and pressure conditions, the quality of the images is affected by beam-steering, as discussed earlier. However, a detailed analysis of the image sharpness shows that droplets and ligaments of the size observed at 440 K would be visible at 900 K.

While it is possible that very small droplets are now formed at Spray A conditions that are below our imaging resolution, we must also consider the possibility that forces that cause droplets and ligaments, i.e. surface tension, are greatly diminished or even non-existent for some high temperature and pressure conditions. A detailed thermodynamic analysis has been performed at these same conditions in collaborative research with Joe Oefelein and Rainer Dahms of Sandia National

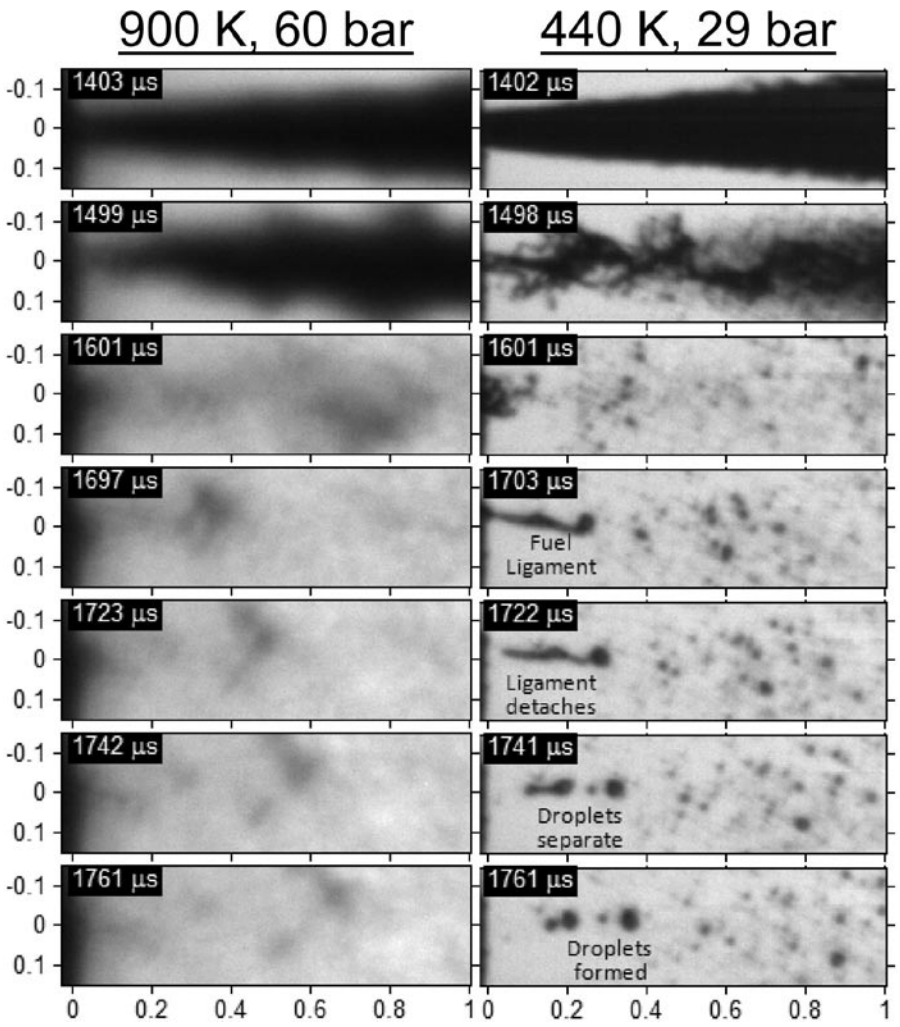

FIGURE 4. Microscopic imaging of liquid structure at 900 K (left) and 440 K (right) conditions. All other conditions are "Spray A."

Laboratories [4], supporting the idea of diminishing surface tension forces to the point where the liquid-ambient interface breaks down and diffusion processes dominate. Under these circumstances, there can be a continuous phase transition from compressed-liquid to a supercritical gaseous state [4] and it would be inappropriate to treat the spray with atomization and breakup processes as traditionally performed.

Emphasizing the need to provide quantitative datasets for model validation that include combustion aspects, we show the lift-off length measured in different facilities as a function of ambient temperature in Figure 5. Note that these facilities have different operation strategies and each has undergone significant work to characterize the ambient and fuel temperature boundary conditions to ensure performance at the specified conditions as necessary for participation in the ECN. Results show consistency in the measured lift-off length, which justifies the merging and leveraging

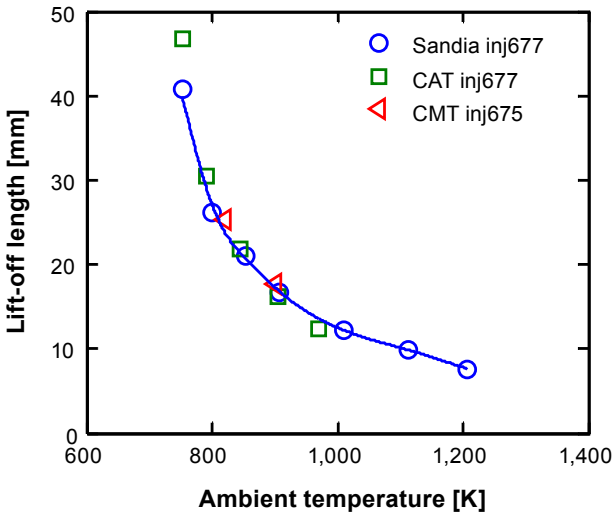

FIGURE 5. Measured lift-off length at three different institutions at Spray A conditions with variation in ambient temperature.

of datasets. In contrast, modeling results submitted to date do not show the same consistency with respect to experimental results or in comparison to each other. The best simulations produce residual errors, when considering the mean variance over all temperatures, of approximately 20%, which is far higher than the experimental variance.

Conclusions

Research this year has shown significant advances with respect to modeling and experimental coordination as a part of the ECN. Progress has been made in the quantification and standardization of diagnostics for the nozzle internal geometry, near-field liquid distribution, spray penetration and evaporation, ignition, and lift-off length. Advances highlighting the liquid distribution and structure were shown above but much more information about other diagnostics and modeling effort may be found on the ECN website. Modeling approaches to date have more variance than that found experimentally, suggesting the need to further improve their predictive capability. Collectively, this project provides unique information needed for the development of high-fidelity CFD models that will be used to optimize future engine designs.

References

1. Engine Combustion Network, http://www.sandia.gov/ECN.

2. Pickett, L.M., Genzale, C.L., Manin, J., Malbec, L.-M., and Hermant, L., "Measurement Uncertainty of Liquid Penetration in Evaporating Diesel Sprays," ILASS 2011-111, 2011

3. Manin, J., Bardi, M., and Pickett, L.M., "Evaluation of the liquid length via diffused back-illumination imaging in vaporizing diesel sprays," COMODIA, 2012.

4. Dahms, R., Oefelein, J.C., Pickett, L.M., and Manin, J., "Understanding High-Pressure Gas-Liquid Interface Phenomena in Diesel Engines," Proc. Combust. Inst. 2012.

FY 2012 Publications

1. Aizawa, T., Nishigai, H., Kondo, K., Yamaguchi, T., Nerva, J.-G., Genzale, C.L., Kook, S., and Pickett, L.M., "Transmission Electron Microscopy of Soot Particles Directly Sampled in Diesel Spray Flame - A Comparison between US#2 and Biodiesel Soot," SAE Int. J. Fuels Lubr. 5:665-673, 2012.

2. Bajaj, C., Abraham, J., and Pickett, L.M., "Vaporization Effects on Transient Diesel Spray Structure," Atomization and Sprays 21:411-426, 2011.

3. Dahms, R., Oefelein, J.C., Pickett, L.M., and Manin, J., "Understanding High-Pressure Gas-Liquid Interface Phenomena in Diesel Engines," Proc. Combust. Inst. 2012.

4. Kook, S. and Pickett, L.M., "Liquid Length and Vapor Penetration of Conventional, Fischer-Tropsch, Coal-Derived, and Surrogate Fuel Sprays at High-Temperature and High-Pressure Ambient Conditions," Fuel 93:539-548, 2012.

5. Kook, S. and Pickett, L.M., "Soot Volume Fraction and Morphology of Conventional, Fischer-Tropsch, Coal-Derived, and Surrogate Fuel at Diesel Conditions," SAE Int. J. Fuels Lubr. 5:647-664, 2012.

6. Lillo, P.M., Pickett, L.M., Kook, S., Persson, H., and Andersson, Ö., "Diesel Spray Ignition Detection and Spatial/Temporal Correction," SAE Int. J. of Engines 5:1330-1346, 2012.

7. Manin, J., Bardi, M., Pickett, L.M., Dahms, R., and Oefelein, J.C., "Development and mixing of diesel sprays at the microscopic level from low to high temperature and pressure conditions," THIESEL, 2012.

8. Manin, J., Bardi, M., and Pickett, L.M., "Evaluation of the liquid length via diffused back-illumination imaging in vaporizing diesel sprays," COMODIA, 2012.

9. Nerva, J.-G., Genzale, C.L., Kook, S., Garcia-Oliver, J.M., and Pickett, L.M., "Fundamental Spray and Combustion Measurements of Soy Methyl-Ester Biodiesel," Int. J. Engine Research, doi:10.1177/1468087412456688, 2012.

Special Awards and Recognition

1. SAE John Johnson award for outstanding research in diesel engines, as the lead author of SAE paper 2011-01-0686. Lyle Pickett, Julien Manin, Mark Musculus, Dennis Siebers, Caroline Genzale, and Cherian Idicheria.

2. ILASS Marshall award for best 2011 technical paper. Rainer Dahms, Joe Oefelein, Lyle Pickett.

II.5 High-Efficiency Clean Combustion in Light-Duty Multi-Cylinder Diesel Engines

Scott J. Curran (Primary Contact),
Robert M. Wagner, Vitaly Y. Prikhodko,
James E. Parks, and Zhiming Gao
Oak Ridge National Laboratory (ORNL)
2360 Cherahala Blvd
Knoxville, TN 37830

DOE Technology Development Manager:
Gurpreet Singh

Overall Objectives

- Develop and evaluate the potential of high-efficiency clean combustion (HECC) strategies with production viable hardware and aftertreatment on multi-cylinder engines.
- Expand the HECC operational range for conditions consistent real-world drive cycles as other operational modes consistent with down-sizing and hybrid electric vehicle (HEV)/plug-in hybrid electric vehicle (PHEV) operation.
- Improve the fundamental thermodynamic understanding of efficiency opportunities and challenges of HECC.
- Characterize the controls challenges including transient operation and fundamental instability mechanisms which may limit the operational range of potential of HECC. This includes the development of low-order models for prediction and avoidance of abnormal combustion events.
- Understand the interdependent emissions and efficiency challenges including integration of exhaust aftertreatments for HECC and multi-mode operation.
- Support demonstration of DOE and U.S. DRIVE efficiency and emissions milestones for light-duty diesel engines.

Fiscal Year (FY) 2012 Objectives

- Develop a reactivity-controlled compression ignition (RCCI) combustion map on a multi-cylinder engine suitable for light-duty drive cycle simulations. The map will be developed to maximize efficiency with lowest possible emissions with production viable hardware and biofuels as necessary.
- Demonstrate improve modeled fuel economy of 15% for passenger vehicles solely from improvements in powertrain efficiency relative to a 2009 port fuel injection (PFI) gasoline baseline. The 2009 PFI gasoline baseline to be modeled using a representative engine map to ensure an accurate comparison.
- Quantify the effectiveness of diesel oxidation catalyst metal loadings on hydrocarbon (HC) and carbon monoxide (CO) destruction with RCCI for steady state as well as mode switching.
- Characterize the potential of a HC trap for storage of RCCI HC for transient operation.

Accomplishments

- Developed an RCCI map suitable for use in vehicle system drive cycle simulations.
- Demonstrated greater than 15% improvement in modeled fuel economy with multi-mode RCCI operation as compared to a 2009 PFI gasoline baseline meeting the 2012 technical target.
- Evaluated the HC and CO reduction effectiveness of multiple diesel oxidation catalysts (DOCs) with RCCI.

Future Directions

- Evaluate the potential of increasing combustion efficiency through combustion optimization and engine hardware design (i.e. combustion chamber geometry).
- Evaluate transient RCCI performance including controls and stability concerns.
- Evaluate aftertreatment performance (including effect on particulate matter, PM) over the light-duty operating range. Data will also be used with vehicle model to simulate emissions performance over the light-duty drive cycle to determine aftertreatment needs for meeting Tier 2 Bin 5 and Tier 2 Bin 2 emission limits.
- Investigate the mitigation of noise from advanced combustion.
- 2013 DOE Vehicle Technologies milestones:
  - Develop RCCI aftertreatment effectiveness map with maximized efficiency with lowest possible emissions suitable for drive cycle simulations (third quarter).
  - Demonstrate 20% increase in fuel economy over 2009 PFI gasoline vehicle in vehicle simulation solely from improved powertrain efficiency (fourth quarter).

Introduction

Advanced combustion concepts have shown promise in achieving high thermal efficiencies with ultra-low oxides of nitrogen (NOx) and PM emissions. RCCI makes use of in-cylinder blending of two fuels with differing reactivity for improved control of the combustion process. Previous research and development at ORNL has demonstrated successful implementation of RCCI on a light-duty multi-cylinder engine over a wide range of operating conditions with a focus on identifying the translational effects of going from a combustion concept to a multi-cylinder engine with production viable hardware. It is difficult to draw conclusions on drive cycle fuel economy and emissions performance for combustion strategies in the development stage which only have demonstrated a limited number of steady-state operating points. The objective of this activity is first develop and then use an experimental RCCI engine map in vehicle systems simulations to model fuel economy and emissions over a variety of drive cycles. Within this activity, the interdependency of fuel economy and emissions performance including the performance of exhaust aftertreatments is investigated for advanced combustion.

Approach

A 4-cylinder GM 1.9-L diesel engine installed at ORNL was modified to include a PFI system using conventional gasoline injectors and pistons that were designed for RCCI operation as shown in Figure 1. A flexible microprocessor-based control system allowed for control over both fueling systems and complete authority over engine operating parameters. Experimental steady-state RCCI operating points on the modified RCCI engine using an in-house methodology for RCCI combustion were used to develop a speed/load map consistent with a light-duty drive cycle with sufficient detail to support vehicle simulations. The engine map was developed using a certification grade gasoline and a 20% biodiesel blend. The potential fuel economy of RCCI operation was evaluated using vehicle systems simulations with experimental steady-state engine maps compared to a representative 2009 gasoline PFI engine as baseline for comparison. The simulations used a multi-mode RCCI/diesel operating strategy where the engine would operate in RCCI mode whenever possible but at the highest and lowest engine operating points, the engine would switch to diesel mode as shown in Figure 2. All simulations were carried out in Autonomie using a 1,580 kg passenger vehicle (mid-size sedan i.e. Chevrolet Malibu) over numerous U.S. federal light-duty drive cycles. RCCI fuel

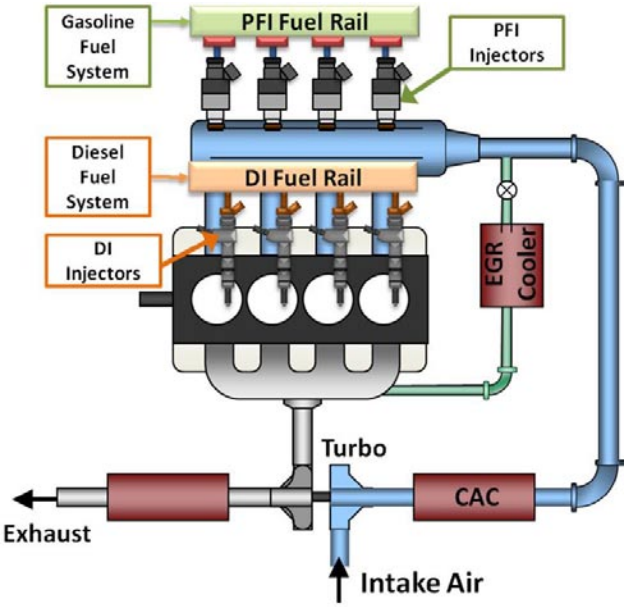

FIGURE 1. ORNL Multi-Cylinder RCCI Engine

economy simulation results were compared to the same vehicle powered by 4.0-L 2009 PFI gasoline engine over multiple drive cycles Engine-out drive cycle emissions were compared to conventional diesel combustion (CDC) and observations regarding relative gasoline and diesel tank sizes needed for the various drive cycles are also summarized.

To further evaluate the potential emissions performance of RCCI operation, several DOCs with different precious metal loadings were evaluated for effectiveness to control HC and CO emissions from RCCI operating on gasoline and diesel fuel. Each catalyst was evaluated in a steady-state engine operation with temperatures ranging from 160 to 260°C. The performance of the DOCs was evaluated during multi-mode engine operation by switching from diesel combustion at higher exhaust temperature to RCCI combustion mode at lower temperature. To further investigate multi-mode engine operation, two DOCs were evaluated in-line with a zeolite-based HC trap.

Results

Multi-mode RCCI/CDC operation was shown through vehicle system simulations using experimental engine data to have the potential to offer greater than 15% fuel economy improvement over a 2009 gasoline PFI baseline over all hot drive cycles examined (no warm-up portion) as shown in Figure 3. The peak efficiency from the RCCI operating map was found to be within the region that is relevant to the federal light-duty drive cycles, unlike conventional diesel combustion whose

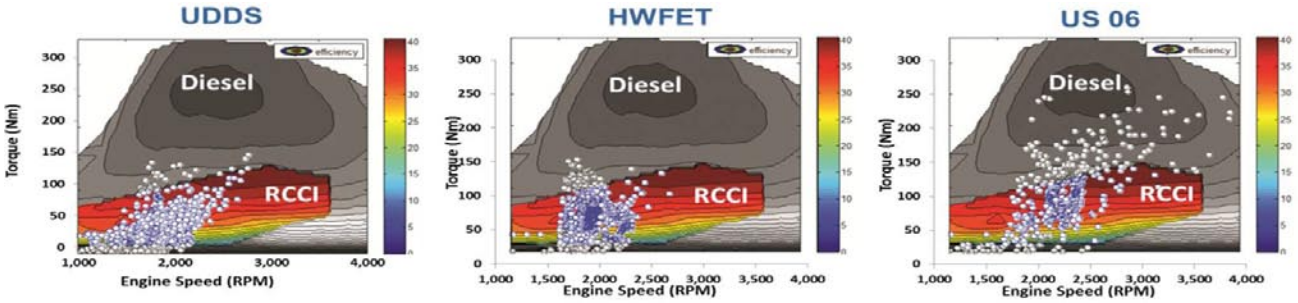

UDDS - urban dynamometer driving cycle; HWFET - highway fuel economy test

FIGURE 2. RCCI Coverage of Various Drive Cycles with Engine Speed and Load Points Overlain

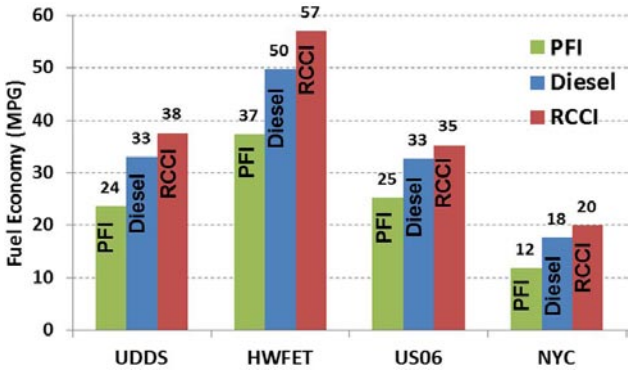

FIGURE 3. Drive Cycle Fuel Economy for PFI, CDC and Multi-Mode RCCI Operation

peak efficiency is well outside the drive cycle. However, the current range of the experimental RCCI engine map does not allow full coverage of many light-duty drive cycles. RCCI fuel economy improvements were observed despite lack of complete drive cycle coverage. The results here showed that how much of an effect that multi-mode operation can have on engine-out NOx emissions depending on the amount of the drive cycle coverage that RCCI operation can allow. Fuel usage over the drive cycles showed that nearly equal amounts of gasoline and diesel fuel would most likely be needed to be carried onboard for RCCI multi-mode operation. During RCCI only operation fuel usage was found to be between 57% and 69% gasoline.

Modeled drive cycle emissions results showed between a 17% and 21% reduction in NOx with multi-mode RCCI as compared to diesel only operation on both city and highway driving cycles. However, HC and CO emissions increased with RCCI on the order of 2 to 3 times compared to CDC. The increased HC and CO emissions along with reduced exhaust temperatures will be a challenge for exhaust aftertreatments. The combination of high CO and HC emissions with low exhaust temperatures will be a significant challenge due to the limited effectiveness of current oxidation catalysts at low temperatures.

To help better understand the emissions challenges, the performance of two commercially available DOCs with different precious metal loadings and Pt:Pd ratios were characterized and compared to a model DOC containing Pt only. Each catalyst was evaluated for CO/HC oxidation activity and light-off temperatures with RCCI exhaust containing both unburned and partially burned hydrocarbons from two fuels. For the DOC, HC oxidation was found to be limited by CO oxidation as expected. Exhaust from fuel-efficient RCCI combustion has lower temperature and higher CO and HC and at exhaust temperatures below light-off, very low CO and HC oxidation efficiencies for DOCs occur and are extenuated by the higher CO/HC levels as shown in Figure 4.

Conclusions

Advanced combustion techniques such as RCCI can increase engine efficiency and lower NOx and PM emissions. This activity has shown the importance of taking a comprehensive engine systems approach to help meet Vehicle Technologies Program goals and milestones.

- Multi-mode RCCI operation can allow greater than a 15% improvement in modeled fuel economy as compared to a 2009 PFI gasoline baseline.
- In-cylinder blending of two fuels with different fuel reactivity (octane/cetane) allows increased control over combustion compared to single fuel advanced combustion techniques.
- Increased HC/CO emissions will be a challenge and will require progress in low temperature aftertreatment.

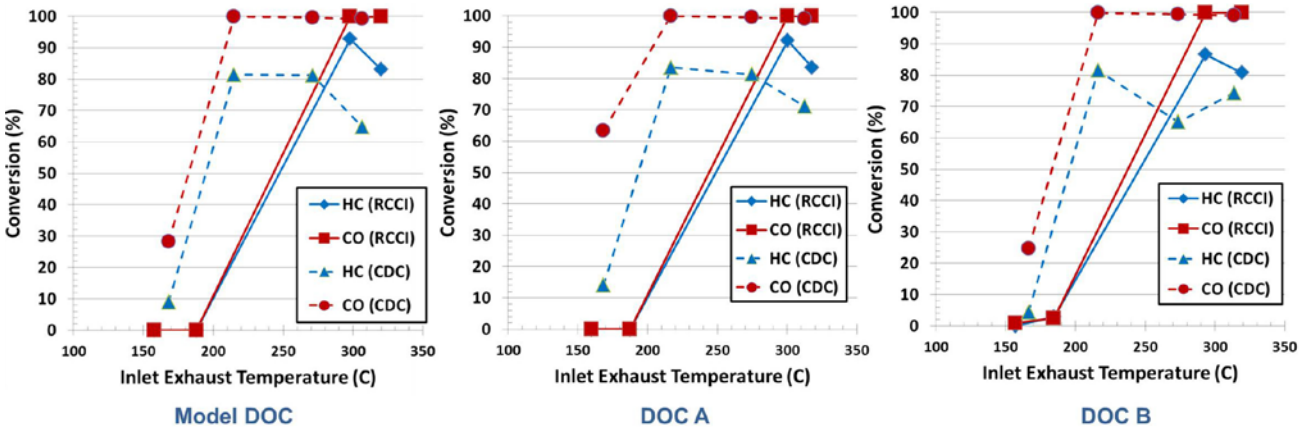

FIGURE 4. DOC Effectiveness Dependent on Exhaust Temperature and Engine Condition

FY 2012 Publications/Presentations

1. Curran, S.J., Hanson, R.M., and Wagner, R.M., "Reactivity controlled compression ignition (RCCI) combustion on a multi-cylinder light-duty diesel engine", International Journal of Engine Research (2012).

2. Hanson, R.M., Curran, S.J., Reitz, R., and Wagner, "Piston optimization for RCCI in Light-Duty Multi-Cylinder Engine," SAE Paper 2012-01-0380 (2012).

3. Curran, S.J., Hanson, R.M., and Wagner, R.M., "Effect of E85 on RCCI Performance and Emissions on a Multi-Cylinder Light-Duty Diesel Engine". SAE 2012-01-0376 (2012).

4. Curran, S.J., Szybist, J.P., and Wagner, R.M., "Reactivity Controlled Compression Ignition Performance with Renewable Fuels", ICEF2012-92192, Proceedings of the ASME 2012 Internal Combustion Engine Division Fall Technical Conference, ICEF2012, September 23–26 (2012).

5. Prikhodko, V.Y., Pihl, J.A., Lewis, S.A., and Parks, J.E., "Hydrocarbon Fouling of SCR during PCCI combustion", SAE Technical Paper Series 2012-01-1080 (2012).

6. Prikhodko, V.Y., Pihl, J.A., Lewis, S.A., and Parks, J.E., "Effect of Hydrocarbon Emissions from PCCI-Type Combustion on the Performance of Selective Catalytic Reduction Catalysts", Journal of Engineering for Gas Turbines and Power 134, pp. 082804-1 (2012).

7. Prikhodko, V.Y., Curran, S.J., Barone, T.L., Lewis, S.A., Storey, J.M., Cho, K., Wagner, R.M., and Parks J.E., "Diesel Oxidation Catalyst Control of Hydrocarbon Aerosols from Reactivity Controlled Compression Ignition Combustion", Proceedings of the ASME 2011 International Mechanical Engineering Congress and Exposition, November 11–17, 2011, Denver, CO, Paper IMECE2011-64147 (2011).

8. Parks, J.E., Prikhodko, V.Y., Lewis, S.A., and Pihl, J.A., "Hydrocarbon fouling of SCR during Premixed Charge Compression Ignition (PCCI) combustion", 2011 Directions in Engine-Efficiency and Emissions Research Conference (DEER), October 3–6, 2011 (2011).

9. Parks, J.E., Prikhodko, V.Y., Pihl, J.A., and Lewis, S.A., "Addressing Emission Challenges from Advanced Combustion Strategies", SAE 2011 Light Duty Diesel Emissions Control Symposium, November 2–3, 2011, Ann Arbor, MI (2011). [invited]

10. Parks, J.E., Prikhodko, V.Y., Pihl, J.A., and Lewis, S.A., "Hydrocarbon fouling of SCR during Premixed Charge Compression Ignition (PCCI) combustion", CTI Exhaust Systems Conference, January 24–25, 2012, Stuttgart, Germany (2012). [invited]

11. Curran S.J., Hanson, R.M., Barone, T.L., Storey, J.M., Wagner, R.M, "Range-extension and multi-cylinder performance of RCCI Combustion, Presentation, Advanced Engine Combustion Working Group Meeting (Livermore, CA; February 2012).

12. Curran S.J., Szybist, J.P., Barone, T.L., Storey, J.M., Wagner, R.M, "Recent Advancements in Multi-Cylinder RCCI Combustion", Presentation, Advanced Engine Combustion Working Group Meeting (Southfield, MI; June 2012).

13. Curran S.J., Prikhodko, V.Y., Parks, J.E., and Wagner, R.M., "High Efficiency Clean Combustion in Multi-Cylinder Light-Duty Engines", Presentation, 2012 DOE Hydrogen Program and Vehicle Technologies Merit Review (Washington, D.C.; May 2012).

14. Curran, S.J., Gao, Z., and Wagner, R.M., "DOE ACE JOULE Milestones: RCCI Mapping and RCCI Fuel Economy Estimates", Presentation, September 2012 ACEC Tech Team Meeting, (September 13, 2012, Southfield, MI).

15. Curran, S.J., Wagner, R.M., Hanson, R.M., and Szybist, J.P., "Reactivity Controlled Compression Ignition Combustion in a Multi-Cylinder Light-Duty Diesel Engine", SAE Powertrain Fuels and Lubricants Meeting, (Malmo Sweden, September, 2012). [invited]

16. Curran, S.J., "The role of renewable fuels in enabling high efficiency internal combustion engines", Sustainable Technology through Advanced Interdisciplinary Research (STAIR) Seminar Series at the University of Tennessee, (September 11, 2012, Knoxville, TN). [invited]

17. Curran S.J., Szybist, J.P., and Wagner, R.M., "Reactivity Controlled Compression Ignition Performance with Renewable Fuels", ASME 2012 Internal Combustion Engine Division Fall Technical Conference, ICEF2012, (September 23–26, 2012, Vancouver, BC, Canada).

18. Prikhodko, V.Y., Curran, S.J., Parks, J.E., and Wagner, R.M., "Effectiveness of a DOC to control CO/HC emissions from RCCI combustion", Poster, 2012 U.S. DOE Directions in Engine-Efficiency and Emissions Research Conference, (October 15–19, 2012, Dearborn, MI).

19. Curran, S.J., Gao, Z., and Wagner, R.M., "Light-Duty Reactivity Controlled Compression Ignition Drive Cycle Fuel Economy and Emissions Estimates", Poster, 2012 U.S. DOE Directions in Engine-Efficiency and Emissions Research Conference, (October 15–19, 2012, Dearborn, MI).

20. Curran, S.J., Wagner, R.M., and Gao, Z., "Background on RCCI and B20 RCCI Results With Both Gasoline and Ethanol Blends ", Presentation, 2012 National Biodiesel Board Biodiesel Technical Workshop, (October 30-31, 2012, Kansas City, MO. [invited]

II.6 Large Eddy Simulation Applied to Advanced Engine Combustion Research

Joseph C. Oefelein (Primary Contact),
Rainer N. Dahms
Sandia National Laboratories
7011 East Avenue, Mail Stop 9051
Livermore, CA 94551-0969

DOE Technology Development Manager:
Gurpreet Singh

Overall Objectives

- Combine unique state-of-the-art simulation capability based on the large eddy simulation (LES) technique with Advanced Engine Combustion R&D activities.
- Perform companion simulations that directly complement optical engine and supporting experiments being conducted at the Combustion Research Facility and elsewhere.
- Maximize benefits of high-performance massively-parallel computing for advanced engine combustion research using DOE leadership computer platforms.

Fiscal Year (FY) 2012 Objectives

- Perform detailed large eddy simulation (LES) of direct injection processes with emphasis on Engine Combustion Network (ECN) www.sandia.gov/ecn experiments.
- Focus on the Spray H (n-heptane) and Spray A (n-dodecane) cases.
- Establish basic theory and corresponding model base for treatment of high-pressure injection processes at supercritical pressures typical of diesel engines.

Accomplishments

- Performed detailed analysis of high-pressure injection processes using LES and real-fluid thermodynamics and compared LES with ECN experimental target data.
- Revealed that the envelope of mixture conditions varies from compressed liquid to supercritical state. At these conditions, the classical view of jet atomization and spray as an appropriate model is questionable.
- Established for the first time that a distinct gas-liquid interface does not exist for a wide range of diesel-relevant injection conditions. Instead lack of inter-molecular forces promotes diffusion over atomization.
- Developed the theoretical basis to explain why classical spray theory does not apply at certain pressure-temperature regimes associated with direct injection in diesel engines.

Future Directions

- Extend development of models and corresponding benchmark simulations aimed at understanding high-Reynolds-number, direct-injection processes for both diesel and gasoline direct injection (GDI) engine applications over a wide range of pressures and temperatures.
- Establish a hierarchy of high-fidelity LES benchmark simulations of in-cylinder flows with emphasis on key optical engine experiments (HCCI, diesel, GDI).

Introduction

We have performed a detailed analysis of high-pressure phenomena and its potential effects on the fundamental physics of fuel injection in diesel engines. We focus on conditions when cylinder pressures exceed the thermodynamic critical pressure of the injected fuel and describe the major differences that occur in the jet dynamics compared to that described by classical spray theory. Calculations were performed by rigorously treating the experimental operating conditions and relevant thermo-physical gas-liquid mixture properties. Results were further processed using linear gradient theory, which facilitates calculations of detailed vapor-liquid interfacial structures, and compared the results with the high-speed imaging data. Analysis of the data reveals that fuel enters the chamber as a compressed liquid and is heated at supercritical pressure. Further analysis suggests that, at certain conditions studied here, the classical view of spray atomization as an appropriate model is questionable. Instead, non-ideal real-fluid behavior must be taken into account using a multicomponent formulation that applies to arbitrary hydrocarbon mixtures at supercritical conditions.

Approach

A modified 32-term Benedict-Webb-Rubin equation of state was combined with non-linear mixing rules to obtain the real-fluid behavior of an arbitrary hydrocarbon mixture at all pressures. From this equation of state, homogeneous fluid properties like the compressibility factor, enthalpy, entropy, heat capacities, and fugacity coefficients can be obtained. This method was then applied to calculate vapor-liquid equilibrium temperature and mixture composition conditions for two investigated chamber pressures: 60 bar (the ECN Spray A case) and 30 bar, respectively. The envelope of all possible equilibrium conditions is shown in Figure 1. Likewise, adiabatic mixing temperatures are defined assuming negligible heat of vaporization effects, which results in a linear enthalpy distribution in mixture fraction space. Then, the equation of state is applied to calculate the temperature for each composition determined by the mixture fraction in order to match the prescribed linear enthalpy distribution. The calculated adiabatic mixing temperatures for the two defined experiments are also shown in Figure 1 and are compared with prior vapor equilibrium conditions. Even if a thermodynamic equilibrium and a distinct two-phase interface exists, its vapor mixes with the ambient gas. This mixing process is modeled using the adiabatic real-fluid mixing envelope. Then, the representative vapor-liquid interface state is found at the intersection point of corresponding mixing and vapor equilibrium temperatures. Such representative interface states for the two investigated experiments, denoted as "High-Temperature Interface" (1) and "Low-Temperature Interface" (2), are also shown in Figure 1. The temperatures across the interface are assumed to be constant, which is consistent with vapor-liquid equilibrium theory. This analysis is then combined with Linear Gradient Theory to provide the detailed interface density profile and the value of surface tension.

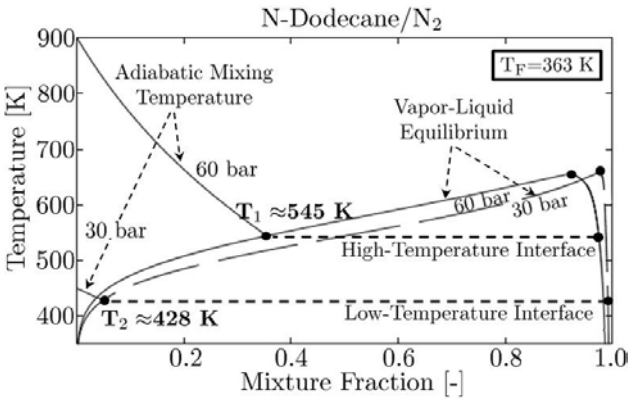

FIGURE 1. Representative vapor liquid interface states from vapor-liquid equilibrium conditions and adiabatic mixing temperatures.

Gradient Theory provides a widely accepted methodology to calculate detailed interface structures between gases and liquids. It presents a thermo-mechanical model of continuous fluid media and converts statistical mechanics of inhomogeneous fluids into non-linear boundary value problems. At equilibrium, as applied here, the model has been shown to be equivalent to mean-field molecular theories of capillarity. The solid foundations of this theory were established by van der Walls in 1894 and reformulated later by Cahn and Hilliard in 1958. Over past decades, Gradient Theory has been successfully applied to a wide variety of fluids: hydrocarbons and their mixtures, polar compounds and their mixtures, polymer and polymer melts, vapor-liquid and liquid-liquid interfaces. Recently, Gradient Theory has even been successfully compared to Monte Carlo molecular simulations of vapor-liquid and liquid-liquid interfaces. There, it proved successful in capturing both surface tension and details of subcritical vapor-liquid molecular interfacial structures. Linear Gradient Theory has been derived from Gradient Theory by assuming a linearized minimization function of the Helmholtz free energy density distribution across the vapor-liquid interface for the calculation of the interfacial density profiles. Linear Gradient Theory has proven successful in calculating binary and multicomponent interface states. Under the conditions here, it is also valid due to the dominant effect of the heavy-weight dense fuel component over the light weight ambient gas.

Results

The reconstructed interface profiles are shown in Figure 2. From these profiles, vapor-liquid interfacial thicknesses have been computed. Such length scales become meaningful once compared to the local mean free pathway, also shown in Figure 2. Fluid particles equilibrate over distances comparable to molecular length scales represented by such mean free pathways. As the mean free pathway at the low-temperature interface is larger than the interface thickness, the temperature of the vapor equilibrates with the temperature of the liquid (TV=TL) and their interfacial processes are governed by molecular dynamics, thereby justifying the applied vapor-liquid equilibrium assumptions. This interface exhibits surface tension forces, supports evaporation and heat of vaporization phenomena, and is therefore expected to lead to the classical spray phenomena as two-phase theory applies. Such heat of vaporization effects have been neglected in the computation of the interface state by assuming an adiabatic mixing temperature. Therefore, the actual interface temperature is lower than the one predicted in this simulation. However, this neglected cooling effect shifts this interface even more into the classical two-

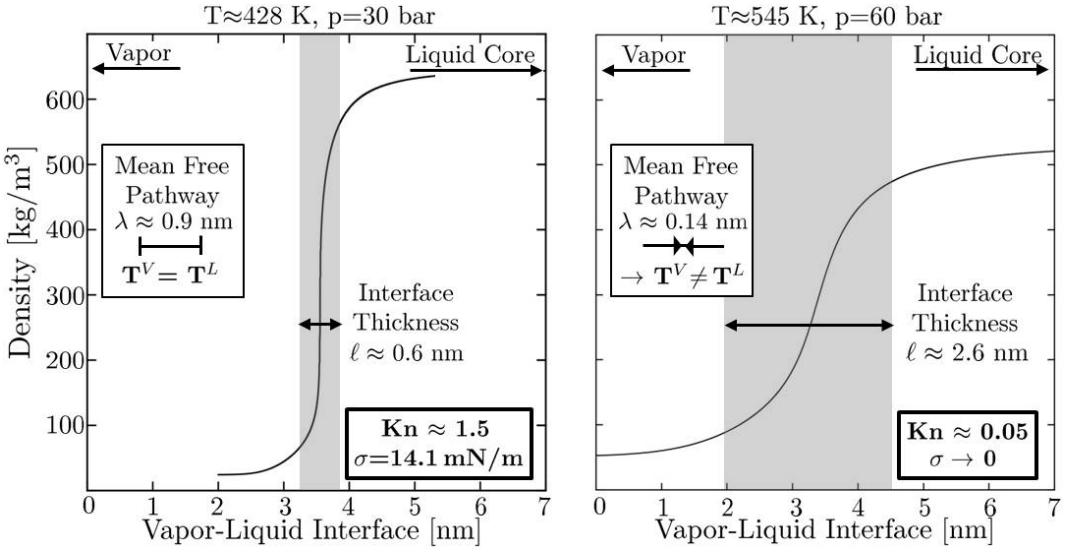

FIGURE 2. Linear Gradient Theory analysis of representative interface states.

phase regime, which validates the conclusion being made here. At the high-temperature interface, however, the situation is reversed. The mean free pathway has become more than an order of magnitude shorter than the interface thickness. Then, vapor-liquid interfacial processes are not governed by molecular dynamics anymore as this interface enters the continuum regime. Under the conditions here, the heat flux across the interface becomes linearly related to the temperature gradient. As the ambient gas temperature is substantially higher than the liquid temperature, the temperature equilibrium assumption between vapor and liquid also breaks down (TV≠TL). Vapor-liquid equilibrium assumptions and classical two-phase theory do not apply. The calculated vapor-liquid equilibrium value of surface tension forces is therefore meaningless. This continuous interface exhibits diminished surface tension forces. Such interfaces cannot support evaporation or heat of vaporization phenomena. This validates the applied adiabatic mixing temperature assumption to calculate the state of the high-temperature interface. These two distinctively different two-phase interfacial phenomena are classified using a Knudsen-number criterion, which relates the thickness of the vapor-liquid interfacial layer to the local mean free pathway. Knudsen numbers less than Kn<0.1 characterize interfaces which will enter the continuum regime governed by the Navier-Stokes equations. Knudsen numbers greater than Kn>0.1 characterize non-continuum flows. As shown in Figure 2, this criterion confirms for the low-temperature interface state (Kn≈1.5>0.1) that classical two-phase theory applies, while the same criterion for the high-temperature interface shows (Kn≈0.05<0.1), that continuum assumptions including the definition of the mixture fraction become valid across the interface. The distinct effect of pressure on the local mean free pathway and therefore on the dynamics of internal vapor-liquid interface processes is shown in Figure 3. The presented analysis shows that the mean free pathway decreases substantially with increasing pressure. It also shows that the high-temperature interface is characterized by a higher concentration of large-size fuel components.

Informed by this analysis, a liquid injection regime diagram can be defined that quantifies the conditions under which surface tension forces diminish in multicomponent mixtures. Based on the Knudsen-number criterion (and the mixture saturation limit criterion from the thermodynamic mixture state regime diagram), regimes of classical sprays and diffusion dominated mixing due to diminished vapor-liquid interfaces are shown in Figure 4. It presents the regime diagram for n-dodecane injected as a liquid at

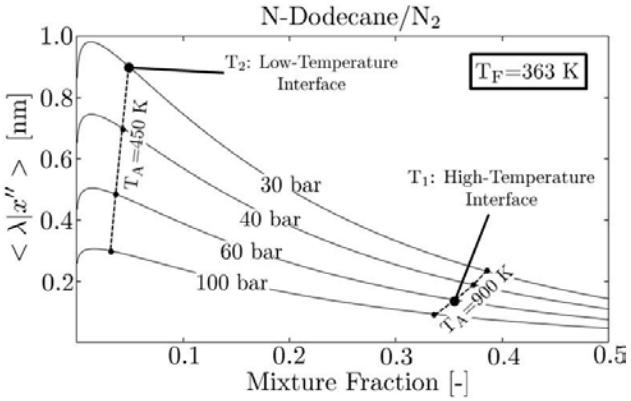

FIGURE 3. Local mean free pathway, conditioned on the location of the vapor-liquid interface, as a function of pressure.

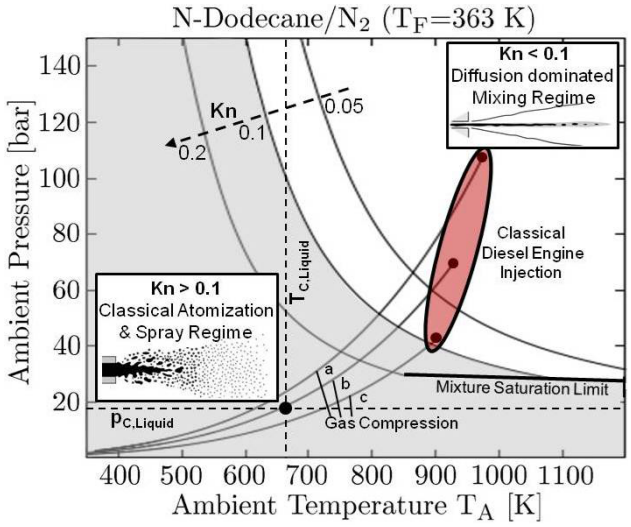

FIGURE 4. Liquid injection regime diagram to quantify the conditions when classical sprays transition into diffusion dominated jets.

a temperature of TF=363 K into gaseous nitrogen at varying ambient pressures and temperatures. Isolines of different Knudsen-number values are shown which span a reasonable range of uncertain vapor-liquid interface conditions. Across this range, the variation in Knudsen-numbers is not substantial enough to predict the actual interface behavior. Three ambient gas pressure-temperature lines, which span a range of conditions during different diesel engine compression cycles, are also presented. These compression lines show representative diesel engine conditions for turbocharged (a), medium load (b), and light load (c) operations, and result from varying in-cylinder conditions at the time of intake valve closure. These conditions read p=2.5 bar, T=363 K (a), p=1.6 bar, T=343 K (b), and p=1 bar, T=335 K (c), respectively. Then, classical diesel engine fuel injection conditions are found at full-compression pressure-temperature states (highlighted in red in Figure 4). The cylinder pressures at such times of full engine compression exceed the mixture saturation limit for all considered cases. Their gas compression pathways cross the range of uncertain vapor-liquid interface conditions. However, only under representative full compression light load operation, classical fuel injection actually takes place at such conditions, which are regarded as uncertain. In general, however, the liquid injection regime diagram suggests that classical spray phenomena may not occur, contrary to conventional wisdom, under typical diesel engine injection conditions. Instead, the fuel is injected as a continuous liquid jet with diminished surface tension forces. Then, interfacial convection-diffusion layers develop between the injected liquid and the ambient gas. Such layers are largely affected by non-ideal thermal and transport processes and cannot support evaporation phenomena or the formation of liquid ligaments or droplets. Some experimental validation of this theory has already been provided (see Ref. 1). In agreement with the predictions of this theory, classical spray phenomena have been shown to persist under the low-temperature chamber conditions while a more diffusive mixture preparation process without the formation of liquid ligaments or drops has been observed under the high-temperature chamber conditions.

Conclusions

Past works have suggested that two extremes exist with regard to liquid injection in high-pressure systems. At lower pressures, the classical situation exists where a well-defined interface separates the injected liquid from ambient gases due to the presence of surface tension. Under these conditions, surface tension forces form a discontinuous non-continuum interface that promotes primary atomization, secondary breakup, and the resultant spray phenomena that has been the well recognized and widely assumed. At high-pressure conditions, however, the situation can become quite different. Under these conditions, a distinct gas-liquid interface may not exist. Effects of surface tension become diminished and the lack of these inter-molecular forces minimizes or eliminates the formation of drops and promotes diffusion dominated mixing processes prior to atomization. Here, we have presented some of the first evidence that diffusion dominated mixing, not atomization, occurs at certain diesel engine conditions. In addition, we have developed a theoretical analysis that explains why and quantifies the change in the interfacial dynamics that leads to the transition between the classical non-continuum "jump" conditions associated with two-phase flows and the continuous gas-liquid interfacial diffusion layers. To frame the observations described above, we performed both LES to understanding aspects related to the state of the local mixture and have corroborated our findings through experimental observations. Experimental imaging of injection processes suggests that drop formation occurs at low ambient temperature, but diffusion dominated mixing occurs without apparent formation of fuel drops at engine-relevant high ambient temperature conditions. To explain this transition, we extended our real-fluid model to account for multicomponent vapor-liquid equilibrium, the presence of surface tension, and the interface states for two investigated conditions. Using this framework, linear gradient theory was then applied to reconstruct the detailed interface structure. The high temperature interface showed a substantially reduced surface tension and a wider interface thickness compared to the low-temperature interface. An applied Knudsen-number criterion then revealed a major finding. Contrary

to conventional wisdom, gas-liquid interfacial diffusion layers develop not necessarily because of vanishing surface tension forces, but because of broadening vapor-liquid interfaces. These interfaces become so thick that they enter the continuum length scale regime. Thus, independent of any residual surface tension forces that might be present, the Navier-Stokes equations apply across the high-temperature vapor-liquid interface if the viscous stress term is modified appropriately. Similarly, continuum based diffusion laws apply across the vapor-liquid interface, producing a continuous phase transition. Similar conditions are anticipated for more complex and realistic multicomponent diesel fuels since their critical properties are comparable to those of n-dodecane. Future work will build on these observations to develop a clear understanding of the transitional nature of interfacial multiphase flow dynamics as a function of pressure.

FY 2012 Publications/Presentations

1. R.N. Dahms, J. Manin, L.M. Pickett, and J.C. Oefelein. Understanding high-pressure gas-liquid interface phenomena in diesel engines. Proceedings of the Combustion Institute, 34, 2013. In Press.

2. Lacaze and J.C. Oefelein. A tabulated chemistry model for non-premixed combustion at high-pressure supercritical conditions. Flow, Turbulence and Combustion, 2012. In Press.

3. Manin, M. Bardi, L.M. Pickett, R.N. Dahms, and J.C. Oefelein. Development and mixing of diesel sprays at the microscopic level from low to high temperature and pressure conditions. Proceedings of the 7th THIESEL Conference on Thermo- and Fluid-Dynamic Processes in Direct Injection Engines, September 11–14, 2012. Valencia, Spain.

4. J.C. Oefelein, R.N. Dahms, G. Lacaze, J.L. Manin, and L.M. Pickett. Effects of pressure on the fundamental physics of fuel injection in diesel engines. Proceedings of the 12th International Conference on Liquid Atomization and Spray Systems, September 2–6 2012. Heidelberg, Germany.

5. B.T. Helenbrook and J.C. Oefelein. Reduced order drag modeling of liquid drops. Proceedings of the 24th Annual Conference on Liquid Atomization and Spray Systems, May 20–23 2012. San Antonio, Texas.

6. J.C. Oefelein, R.N. Dahms, and G. Lacaze. Detailed modeling and simulation of high-pressure fuel injection processes in diesel engines. SAE International Journal of Engines, 5(3):1–10, 2012.

7. R. Knaus, J. Oefelein, and C. Pantano. On the relationship between the statistics of the resolved and true rate of dissipation of mixture fraction. Flow, Turbulence and Combustion, 89(1):37–71, 2012.

8. G. Lacaze and J.C. Oefelein. A non-premixed combustion model based on flame structure analysis at supercritical pressures. Combustion and Flame, 159:2087–2103, 2012.

9. B. Hu, M.P. Musculus, and J.C. Oefelein. The influence of large-scale structures on entrainment in a decelerating transient turbulent jet revealed by large eddy simulation. Physics of Fluids, 24:1–17, 2012.

10. G. Lacaze and J.C. Oefelein. A model for non-premixed combustion at high pressure supercritical conditions based on flame structure analysis. Proceedings of the 2011 Australian Combustion Symposium, November 29 – December 1 2011. University of Newcastle, Australia.

11. A.M. Kempf, B.J. Geurts, and J.C. Oefelein. Error analysis of large eddy simulation of the turbulent non-premixed Sydney bluff-body flame. Combustion and Flame, 158:2408–2419, 2011.

12. R.N. Dahms, L.M. Pickett, and J.C. Oefelein. Understanding diesel engine fuel injection phenomena using a real-fluid thermodynamic mixture property model. Proceedings of the 2011 Fall Meeting of the Western States Section of the Combustion Institute, October 16–18 2011. Riverside, California.

13. R. Mari, G. Lacaze, and J.C. Oefelein. Supercritical flows – A numerical study. Technical report, Institut Sup´erieur de l' A´eronautique et de I'Espace, Toulouse, France, September 2011.

14. G. Lacaze and J.C. Oefelein. A tabulated chemistry model for non-premixed combustion at high-pressure supercritical conditions. Proceedings of the Seventh Mediterranean Combustion Symposium, September 11–15 2011. Sardinia, Italy.

15. J.C. Oefelein and R. Sankaran. High-fidelity large eddy simulation of combustion for propulsion and power. Proceedings of the SciDAC 2011 Meeting, July 10–14, 2011. Denver, Colorado. http://press.mcs.anl.gov/scidac2011/.

Special Recognitions & Awards/Patents Issued

1. ILASS Americas William Robert Marshall Award, 2012 (for best paper judged to be the most significant contribution to the ILASS 23rd Annual Conference on Liquid Atomization and Spray Systems.

II.7 Computationally Efficient Modeling of High Efficiency Clean Combustion Engines

Daniel L. Flowers (Primary Contact), Salvador Aceves, Nick Killingsworth, Matt McNenly, Geoff Oxberry, Tom Piggott, Russell Whitesides, Randy Hessel (University of Wisconsin), Robert Dibble (University of California, Berkeley), J.Y. Chen (University of California, Berkeley)

Lawrence Livermore National Laboratory (LLNL)
P.O. Box 808, L-792
Livermore, CA 94551

DOE Technology Development Manager:
Gurpreet Singh

Subcontractors:
University of Wisconsin, Madison, WI
University of California, Berkeley, CA

Overall Objectives

- Enhance understanding of clean and efficient engine operation through detailed numerical modeling.
- Gain fundamental and practical insight into high efficiency clean combustion (HECC) regimes through numerical simulations and experiments.
- Develop and apply numerical tools to simulate HECC by combining multidimensional fluid mechanics with chemical kinetics.
- Reduce computational expense for HECC simulations.
- Democratize high fidelity engine simulation by bringing computational tools to the desktop computer for use by engine designers and researchers.

Fiscal Year (FY) 2012 Objectives

- Validate advanced engine combustion simulations using LLNL multi-zone implemented in Convergent Science, Inc.'s (CSI) Converge™ software.
- Implement and validate the latest LLNL-developed detailed chemical kinetic solvers in multi-dimensional computational fluid dynamics (CFD) engine simulation software for homogeneous charge compression ignition (HCCI) and premixed charge compression ignition (PCCI) simulations.
- Develop multi-reactor kinetics model usable for fast multi-cycle simulation of HCCI engine combustion.

Accomplishments

- Completed wide-ranging validation study of advanced engine combustion in the LLNL multi-zone model implemented in the Converge™ software package (CSI-licensed LLNL multi-zone model in October 2010).
- Implemented and validated latest high performance chemical kinetics solvers in Converge™ and OpenFOAM® CFD packages.
- Developed and validated a stand-alone multi-reactor chemical kinetics engine model for simulating multiple HCCI and PCCI engine cycles.
- Validated Converge™ multi-zone solver for direct injection PCCI including the latest LLNL chemical kinetics solver.
- Promoted widespread industry application of LLNL multi-zone model through partnership with CSI.

Future Directions

- Validate and develop combustion simulation capabilities that will enable the prediction of performance and emissions in the development of new vehicle powertrain technologies.
- Conduct detailed analysis of HCCI and direct-injection engine experiments and conduct analysis of clean and efficient diesel engines that use stoichiometric and low temperature combustion modes.
- Develop numerically efficient and physically accurate models for fuel sprays and flame propagation that can be utilized within engine design simulation codes.
- Develop fully-parallelized multi-dimensional CFD-chemistry solvers for analysis of non-homogeneous engine combustion.
- Distribute advanced combustion models to U.S. industrial and academic partners.

Introduction

This project focuses on the development and application of computationally efficient and accurate simulation tools for prediction of engine combustion. Simulation of combustion aids in development of new high-efficiency and low-emission engines by allowing detailed characterization of in-cylinder engine processes that are difficult to measure directly. Simulation also allows exploratory investigations of new concepts, such as new combustion chamber geometry, allowing valuable and limited experimental resources to be focused on the most promising strategies.

Combustion simulation is computationally demanding because it combines three-dimensional turbulent fluid flow with highly exothermic chemical reactions proceeding at rates that span several orders of magnitude. As such, simulation of an internal combustion engine cycle with chemistry and fluid flow typically requires access to large-scale computing resources. One major motivation of this research is to use physical and mathematical methods to reduce computational expense of combustion simulation with minimal loss of accuracy. These computationally efficient tools are applied to understand the fundamental physical processes occurring in engines operating with high efficiency clean combustion strategies.

Approach

We use high-fidelity simulations to predict internal combustion engine operation, seeking to maximize computational performance by taking advantage of physical discretization strategies, numerical methods, and new computer architectures. Thermo-kinetic chemistry and fluid mechanics that occurs in engine combustion (diesel, spark ignition, HCCI, etc.) is challenging to simulate because of the large gradients present and the wide range of time-scales over which processes occur, from femtoseconds to milliseconds. We developed a multi-zone solver that significantly reduces the computational burden of chemistry simulation combined with computational fluid mechanics with little loss in accuracy. The multi-zone model solves chemistry in a non-geometric thermo-chemical phase-space, significantly reducing the number of chemistry calculations needed to calculate an engine cycle relative to the standard geometric discretization.

Multi-zone chemistry modeling allows for higher fidelity of combustion simulation through a more effective use of available computational resources. Combining multi-zone modeling with parallel CFD gives increased fidelity to the fluid mechanics part of combustion simulation along with the chemistry. However, chemistry simulation for complex fuels still can be computationally expensive. Previously, work in numerical methods for chemical kinetic solvers was conducted as a subcomponent of this project. In FY 2012 a separate project dedicated to advanced chemical kinetic solvers was established [1]. The preconditioned solvers developed in that project directly support multi-dimensional combustion simulation. This development of high efficiency solvers for parallel CFD and multi-zone chemistry provides a higher degree of physical resolution of engine processes using computational resources available to engine designers.

Results

This year's effort has been focused on continued development and application of computational tools to effectively simulate advanced high-efficiency engine combustion strategies. The multi-zone combustion model has been demonstrated to be accurate and effective for predicting HCCI and PCCI combustion using practical, engineering levels of resolution for the fluid mechanics with detailed chemical kinetic mechanisms [3-4]. The standard approach to solving chemical kinetics in computational fluid mechanics codes is to solve chemistry in every cell of the CFD grid, resulting in a requirement to solve from tens of thousands to several million chemical reactors. With detailed chemistry for realistic fuels, solving chemistry in every cell requires unreasonably long computational times, from days to weeks for a single engine cycle simulation for even modestly sized mechanisms with hundreds of species.

The multi-zone model only solves the fluid mechanics using the typical geometric discretization, the combustion chemical kinetics are resolved with a chemical coordinate and temperature discretization. The multi-zone model reduces the number of reactors that need to be solved to typically a few hundred, giving significant reduction in computational time. The multi-zone model part of the simulation has been implemented on parallel computing platforms and is coupled with CFD codes like OpenFOAM® [5] and Converge™ [6] that are able to process engine fluid flows on parallel computers.

In October 2010, CSI, a Madison, Wisconsin-based engine CFD software maker, licensed the LLNL multi-zone combustion model for implementation in their Converge™ software package. Converge™ is widely used by engine researchers and designers in the U.S. auto and engine industry, and this license agreement has allowed LLNL combustion models to be accessible within a commercial software package. LLNL collaborated with CSI to evaluate the accuracy and computational performance of the Converge™ multi-zone compared to Converge™ using every-cell chemistry [7]. One case studied is direct injected diesel combustion in a 2.4-L

per cylinder heavy-duty diesel engine. Figure 1 shows a comparison of the pressure within the combustion chamber predicted by Converge™ using every-cell chemistry and the LLNL multi-zone model. The multi-zone kinetics model gives very similar pressure prediction to the every-cell kinetic chemistry approach.

Comparison of the evolution of the spatial distribution of temperature on a two-dimensional plane within the combustion chamber (Figure 2) shows very similar results for the multi-zone kinetics model and the every-cell kinetics. Further comparisons highlighting the accuracy and performance of the LLNL multi-zone model in Converge™ are featured in the recent joint CSI-LLNL publication [7]. Figure 3 shows the comparison of chemistry simulation time for every-cell kinetics versus the multi-zone model. The multi-zone reduces the simulation time from 16 hours to less than 2 hours. For this case, the Converge™ multi-zone gives physically consistent predictions with an order of magnitude reduction in computational time.

Figures 4-6 show another example of multi-zone based combustion simulation, comparison of experiments to Converge™/LLNL multi-zone simulations for a low-load early direct injection PCCI engine. This case involves direct injection of iso-octane fuel at 80 degrees before top-dead center (TDC) from an 8-hole injector. Symmetry allows for simulation of a 45-degree sector of the combustion chamber. The mixture is overall very lean with a fuel-air equivalence ratio of 0.12. This operating point represents a low load or idle operating condition. The engine is the Sandia 1-L/cylinder HCCI research engine, and the experimental data is reported in a paper by Dec et al. [8]. This operating point was selected because it is extremely challenging to simulate marginal or partial burn conditions without detailed chemical kinetics. Figure 4 shows the distribution of the mass fraction of fuel (iC_8H_{18}) within the combustion chamber prior to start of ignition. Figure 4 shows that fuel is

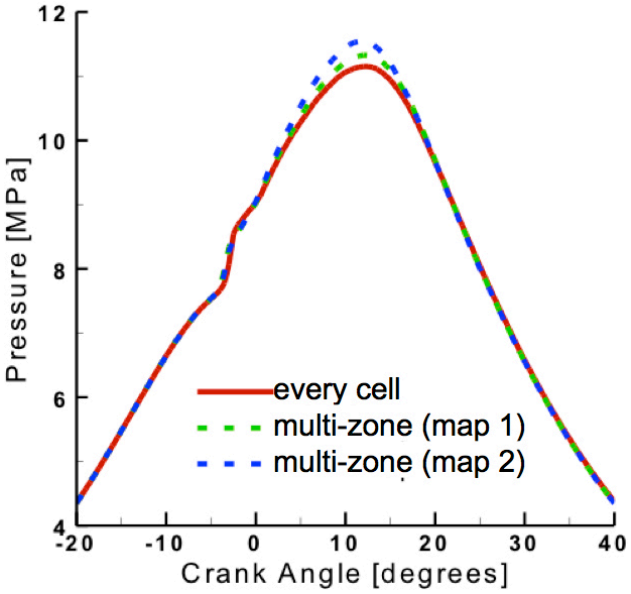

FIGURE 1. Pressure versus crank angle for direct injected diesel case (2.4-L/cylinder engine), comparing every-cell kinetics to the multi-zone kinetics model. Two different remapping strategies are shown. Remap 1 strategy, based on Babajimopoulos et al. [2] is found to give better prediction.

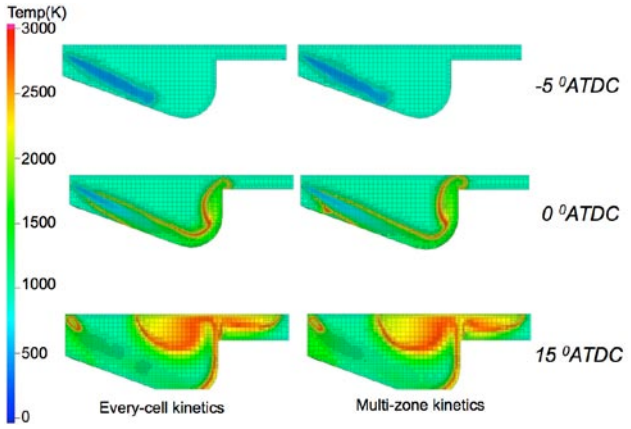

FIGURE 2. Comparison of spatial temperature evolution during combustion for every-cell kinetics versus multi-zone kinetics for direct injected diesel case (2.4-L/cylinder engine). Figure shows a two-dimensional axisymmetric slice through the center of the injection axis.

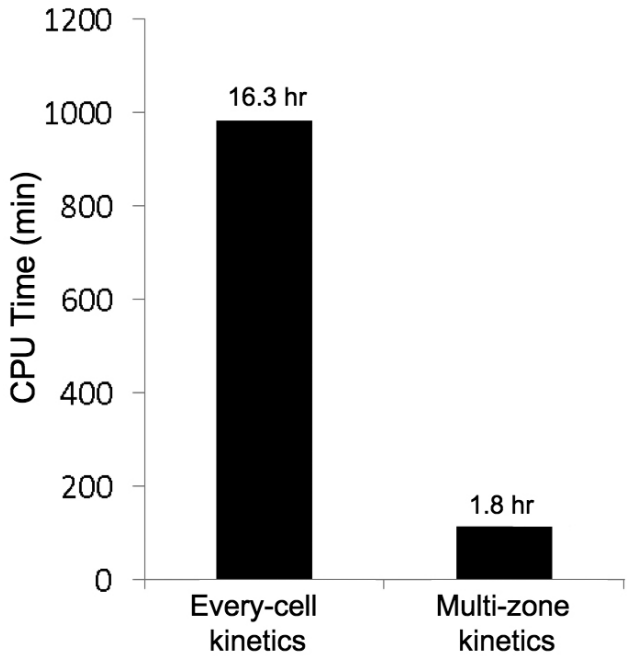

FIGURE 3. Chemistry simulation time comparison for every-cell kinetics versus the multi-zone kinetics model for direct injected diesel case (2.4-L/cylinder engine).

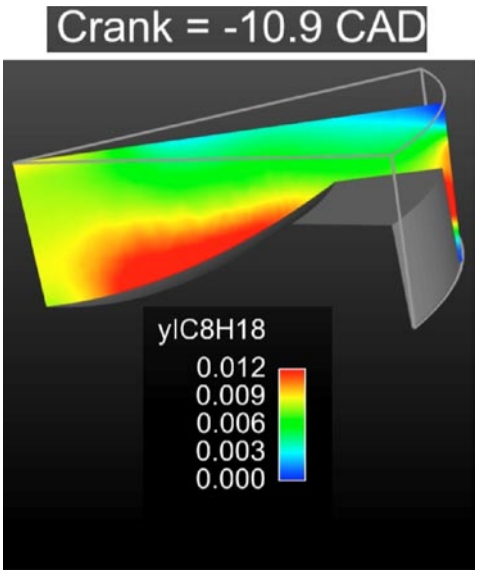

FIGURE 4. Fuel distribution in the combustion chamber before ignition for early direct injection iso-octane PCCI case (1.0-L/cylinder engine). Figure shows a two-dimensional axisymmetric slice through the center of the injection axis.

mostly concentrated in the center of the combustion chamber and in the crevice.

Figure 5 shows the spatial distribution of mass fractions of fuel (iC_8H_{18}), carbon monoxide (CO), carbon dioxide (CO_2), hydroxyl radicals (OH) and temperature at 22 degrees after TDC. This point is representative of the state of the combustion chamber just after heat release is complete, illustrating the important features of the combustion and emissions processes. Fuel is consumed throughout the combustion chamber except in the crevice region. Carbon monoxide is formed throughout the combustion chamber, but is consumed only in the very center of the combustion chamber, where carbon dioxide is formed. Hydroxyl radicals can only be observed in the center of the combustion chamber where temperatures are highest. Regions of higher fuel concentration result in higher temperatures when they burn. Fuel is first converted from intermediate products to carbon monoxide. Conversion of carbon monoxide to carbon dioxide requires temperatures to reach at least 1,500 K to get sufficient hydroxyl radical production. Temperatures are sufficiently high for full conversion of carbon monoxide to carbon dioxide only in the center of the chamber where fuel concentration before combustion is highest. The fuel in the crevice region does not react due to the low temperatures, and high surface area to volume ratio of the ring crevice.

Figure 6(a) shows very good agreement between the simulated pressure for this case compared to the experimental measurement. Figure 6(b) shows comparison of simulation predicted emissions of total hydrocarbons, carbon monoxide, and carbon dioxide compared to experiment. The excellent agreement on emissions suggests that the model captures the bulk quenching and crevice quenching effects that result in carbon monoxide and hydrocarbon emissions.

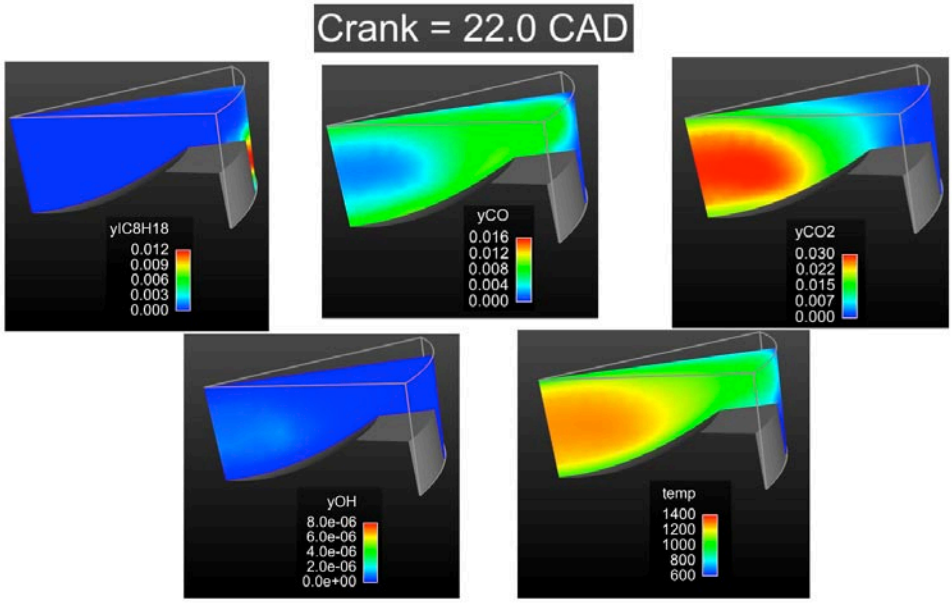

FIGURE 5. Species and temperature distribution in the combustion chamber after heat release for early direct injection isooctane PCCI case (1.0-L/cylinder engine). Figure shows two-dimensional axisymmetric slices through the center of the injection axis.

The simulation results for Figures 4-6 utilize the LLNL adaptively preconditioned solver developed by McNenly as part of the complementary project (II.A.38). This results in significant additional simulation speedup on top of the multi-zone model speedup reported in Figure 3. For HCCI simulations of the Sandia Dec engine using an 857 species isooctane mechanism, every cell simulations of the engine cycle require about 70 hours, with 60 hours of that being chemistry simulation. Using the multi-zone model and the traditional dense chemistry solver approach, the total simulation time is reduced to 15.5 hours, with 5.5 hours required for chemistry. Using the multi-zone model with the LLNL adaptively preconditioned solver, the total simulation time is 10.2 hours with 0.2 hours required for chemistry. The combination of the LLNL multi-zone model and the LLNL adaptively preconditioned solver give 300-fold speedup relative to traditional approaches.

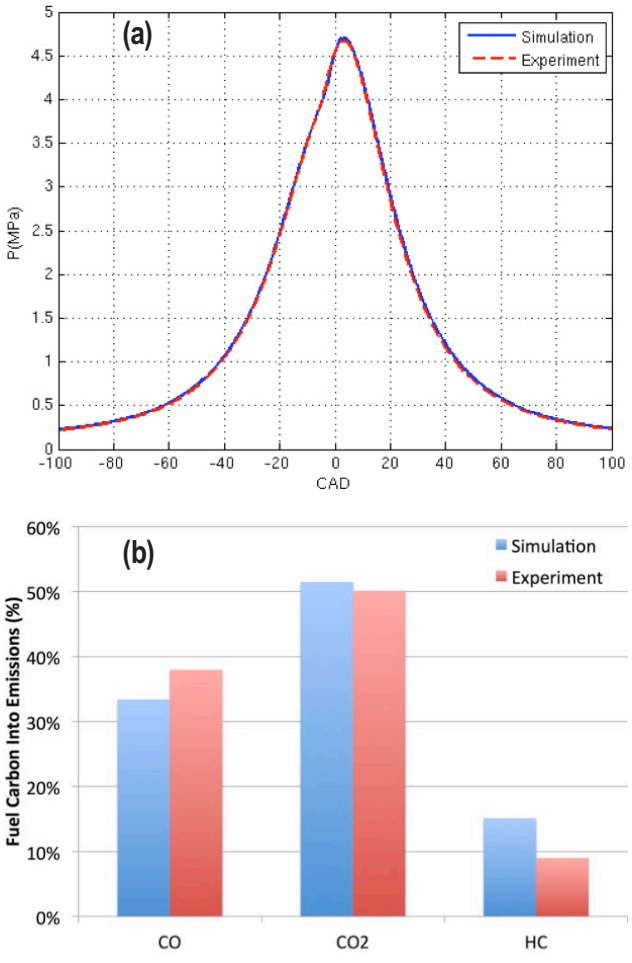

FIGURE 6. Pressure versus crank angle (a) and emissions (b) comparing simulation to experiment for an early direct injection iso-octane PCCI case (1.0-L/cylinder engine).

The results presented exemplify the kind of simulation capabilities developed in this project for advanced engine combustion processes. Another major activity is improving the multi-zone modeling approach through more robust zone discretization schemes and remapping approaches. We have developed a flexible and reliable model testing and development platform by connecting the multi-zone kinetics model to the OpenFOAM® [6] multi-dimensional physics simulation package. Other work includes development of a multi-reactor model that runs fast enough to be used within engine cycle simulation packages [9]. This model uses a motored CFD simulation to estimate a representative spatial distribution of heat transfer within the combustion chamber. The combustion chamber is discretized with twenty to forty chemical reactors, and a cycle simulation can be conducted in less than a minute when using a block preconditioned solver [10]. This approach allows for simulating cycle-to-cycle interactions in HCCI and PCCI engines.

Conclusions

We have made significant advances developing high performance computing tools for simulation of advanced engine combustion:

- Converge™ with the LLNL multi-zone kinetics solver tested for direct injected diesel combustion. Demonstrated an order of magnitude speedup with multi-zone with results very consistent with chemical kinetics in every cell.
- Implemented LLNL's adaptively preconditioned kinetic solver in Converge™ along with the multi-zone combustion model. Achieved 300-fold speedup over traditional every cell dense kinetic solver approach for 857 species isooctane chemistry.
- Validated early direct injection PCCI compared to Sandia experiment. Achieved very good prediction of in-cylinder pressure and emissions compared to experiments.
- Developed fast-running kinetic based model that captures burn duration, emissions, and cycle-to-cycle interactions for prediction of PCCI and HCCI engine operation.

In the next year we will apply these high performance simulation tools to investigating fundamental characteristics of advanced engine combustion regimes. We will continue to distribute our latest models and solvers to support the simulation efforts of our U.S. industry partners.

References

1. McNenly, M.J., Improved solvers for advanced engine combustion simulation," II.A.38 in Advanced Combustion Engine Research and Development 2012 Annual Progress Report, U.S. Department of Energy, 2012.

2. Babajimopoulos, A., Assanis, D.N., Flowers, D.L., Aceves, S.M. and Hessel, R.P., "A fully coupled computational fluid dynamics and multi-zone model with detailed chemical kinetics for the simulation of premixed charge compression ignition engines," International Journal Engine Research, Volume 6, Issue 5, pages 497-512, 2005.

3. Hessel, R., Babajimopoulos, A., Foster, D., Aceves, S., Davisson, M, Espinosa-Loza, F.J., Flowers, D.L., Pitz, W., Dec, J., Sjoberg, M., " Modeling Iso-octane HCCI using CFD with Multi-Zone Detailed Chemistry; Comparison to Detailed Speciation Data over a Range of Lean Equivalence Ratios, 2008-01-0047.

4. Flowers, D.L., Aceves, S.M., Babajimopoulos, A., "Effect of Charge Non-uniformity on Heat Release and Emissions in PCCI Engine Combustion," SAE Paper 2006-01-1363.

5. http://www.openfoam.org/

6. http://convergecfd.com/products/converge/

7. Raju, M., Wang, M., Dai, M., Piggott, W.T., Flowers, D.L., "Acceleration of Detailed Chemical Kinetics Using Multi-zone Modeling for CFD in Internal Combustion Engine Simulations," SAE Paper 2012-01-0135.

8. Dec, J. and Sjöberg, M., "A Parametric Study of HCCI Combustion - the Sources of Emissions at Low Loads and the Effects of GDI Fuel Injection," SAE Technical Paper 2003-01-0752, 2003.

9. Kodavasal, J., McNenly, M.J., Babajimopoulos, A., Aceves, S.M., Assanis, D.N., Havstad, M.A., and Flowers, D.L., "An Accelerated Multi-zone for Engine Cycle Simulation (AMECS) of HCCI combustion," in review, 2012.

10. McNenly, M.J., Havstad, M.A., Aceves, S.M., and Pitz, W.J., 2010, Integration Strategies for Efficient Multizone Chemical Kinetics Models: SAE 2010 World Congress & Exhibition, Detroit, MI, SAE Paper No. 2010-01-0576.

FY 2012 Publications/Presentations

1. Kodavasal, J., McNenly, M.J., Babajimopoulos, A., Aceves, S.M., Assanis, D.N., Havstad, M.A., and Flowers, D.L., "An Accelerated Multi-zone for Engine Cycle Simulation (AMECS) of HCCI combustion," in review, 2012.

2. Flowers, D.L., "Simulation of High Efficiency Clean Combustion Engines and Detailed Chemical Kinetic Mechanisms Development," 18th Directions in Engine-Efficiency and Emissions Research (DEER) Conference, Dearborn, Michigan, October 15–19, 2012.

3. Whitesides, R.A., McNenly, M.J., Piggott III, W.T., Hessel, R.P., Flowers, D.L. and Aceves, S. M., "Advances in Multi-dimensional Modeling of Clean & Efficient Engine Concepts," AEC/HCCI Working Group Meeting June 19, 2012, Detroit, MI.

4. Hsieh, H., Sanz-Argent, J., Petitpas, G., Havstad, M., Flowers, D., "Sensitivity analysis of large system of chemical kinetic parameters for engine combustion simulation," ASME V&V Symposium, Las Vegas, NV, May 2–4, 2012.

5. Bedoya, I. et al., "A sequential Chemical Kinetics-CFD-Chemical Kinetics methodology to predict HCCI combustion and main emissions," SAE Paper 2012-01-1119.

6. Raju, M.P. et al.,"Acceleration of Detailed Chemical Kinetics Using Multi-zone Modeling for CFD in Internal Combustion Engine Simulations," SAE Paper 2012-01-0135.

7. Hessel, R.P., Flowers, D.L, Aceves, S.M., "Crevice and Blowby Model Development and Application," International Multidimensional Engine Modeling Meeting, April 2012, Detroit, Mi.

8. Kodavasal, J., "A Methodology to Capture Thermal Stratification in a Multi-zone HCCI Combustion Model," AEC/HCCI Working Group Meeting, Feb 2012.

9. McNenly, M.J. and Whitesides, R.A. "Improving Improving Combustion Software for Modeling Detailed Chemical Kinetics," AEC/HCCI Working Group Meeting, Feb 2012.

II.8 HCCI and Stratified-Charge CI Engine Combustion Research

John E. Dec
Sandia National Laboratories
MS 9053, P.O. Box 969
Livermore, CA 94551-0969

DOE Technology Development Manager:
Gurpreet Singh

Overall Objectives

Provide the fundamental understanding (science-base) required to overcome the technical barriers to the development of practical homogeneous charge compression ignition (HCCI) and HCCI-like engines by industry.

Fiscal Year (FY) 2012 Objectives

- Conduct a systematic investigation to determine how key engine operating parameters affect the thermal efficiency of boosted HCCI.
- Determine the highest thermal efficiency attainable with our current engine configuration.
- Initiate an investigation of the effects of expected variations in ethanol content of pump gasoline on HCCI/SCCI efficiency and high-load capability.
- Investigate the changes in thermal stratification (TS) with operating conditions, including speed, intake temperature (T_{in}), wall temperature (T_{wall}), and swirl.
- Support chemical-kinetic mechanism development at Lawrence Livermore National Laboratory (LLNL), and modeling of thermal stratification at the University of Michigan and General Motors.

Accomplishments

- Determined the effects of all main operating parameters on thermal efficiency, including T_{in}, fueling rate, engine speed, fuel-type, fueling strategy, and intake pressure (P_{in}).
  - Combined optimal values of operating parameters to obtain the highest efficiency for the current engine configuration and fuels.
- Demonstrated gross indicated thermal efficiencies of 47–48% for loads from 8 to 16 bar gross indicated mean effective pressure ($IMEP_g$) for our current engine configuration (compression ratio = 14:1).
- Showed that increasing the ethanol content of gasoline from 0 ⇨ 10 ⇨ 20% (E0, E10, E20) allowed the maximum load to be increased from 16.3 ⇨ 18.1 ⇨ 20.0 bar IMEPg, respectively.
- Significantly improved temperature-map (T-map) imaging resolution, signal/noise, and method of post-processing to remove laser-sheet schlieren effects.
- Quantified variations in TS over range of engine speeds, T_{in}, T_{wall}, and swirl.
  - Conducted a probability density function analysis of the TS at various conditions.
  - Initiated analysis of cold-pocket size and location.
- Provided data and analysis to support chemical-kinetic, computational fluid dynamics, and other modeling of HCCI at LLNL, the University of Michigan, and General Motors.

Future Directions

- Explore further increases in the thermal efficiency of boosted HCCI by raising the compression ratio (or expansion-ratio only using a Miller-cycle cam).
- Determine the performance potential of various realistic gasoline-like fuels:
  - Complete investigation of the effects of the ethanol content of gasoline (E0, E10, E20).
  - Expand study to include premium gasoline and E100, as compared to E0, E10, or E20.
- Work with Cummins Engine Co. to modify the cylinder head of our research engine to accommodate a spark plug for studies of spark-assisted HCCI.
- Investigate the potential for obtaining boundary-layer profiles at the piston-top surface from T-map images simultaneously with T_{wall} and heat-flux data.
- Continue to collaborate with LLNL on improving chemical-kinetic mechanisms of single components and a gasoline-surrogate mixture.
- Continue collaborations with General Motors and the University of Michigan on modeling of thermal stratification in HCCI engines and discussions and modeling of boosted HCCI.

Introduction

Improving the efficiency of internal combustion engines is critical for meeting global needs to reduce petroleum consumption and CO_2 emissions. HCCI engines have a strong potential for contributing to these goals since they have high thermal efficiencies, ultra-low oxides of nitrogen (NO_X) and particulate emissions, and with intake-pressure boost, can achieve loads comparable to diesel engines, as will be shown. Additionally, HCCI provides a means for producing high-efficiency engines operating on gasoline, thus complementing diesel engines, which use middle distillates, for better utilization of crude oil supplies.

The work on this project during FY 2012 has contributed to overcoming three key technical barriers to the practical implementation of HCCI combustion in production engines: 1) increasing efficiency, 2) extending operation to higher loads, and 3) providing an improved understanding of in-cylinder processes. First, a systematic investigation of the effects of key engine operating parameters on thermal efficiency allowed high efficiencies to be achieved over a wide range of loads. Second, a study of the effects of adding 10 or 20% ethanol to a petroleum-based gasoline led to an additional increase in efficiency and a significant increase in the high-load limit of HCCI. Finally, laser-imaging thermometry has been applied to understand how naturally occurring thermal stratification varies with changes in operating conditions.

Approach

Studies were conducted in our dual-engine HCCI laboratory using a combination of experiments in both the optically accessible and all-metal HCCI single-cylinder research engines (displacement = 0.98 liters). This facility allows operation over a wide range of conditions, and it can provide precise control of operating parameters such as combustion phasing, injection timing, intake temperature, intake pressure, engine speed, and mass flow rates of supplied fuel and air. The facility also allows the use of cooled exhaust gas recirculation (EGR). For the current studies, both engines were fitted with compression ratio = 14:1 pistons. Additionally, the laboratory is equipped with a full emissions bench (hydrocarbons [HCs], CO, CO_2, O_2, NO_X, and smoke).

Investigations of the effects of engine operating parameters on thermal efficiency and the effects of the ethanol content of gasoline on HCCI performance were conducted in the all-metal engine. For the efficiency study, several key parameters were systematically varied while holding the other key parameters constant to the extent possible. This allowed either the optimal value of each parameter or the tradeoffs between various parameters to be clearly determined. Combining the best settings for these parameters, within the various constraints, provided high-efficiency operation over a range of loads. To understand the effects of the ethanol content of gasoline on HCCI performance, a conventional petroleum-based gasoline (E0) was compared to E10 and E20, which were obtained by blending pure ethanol with the conventional E0 gasoline. This approach eliminates variations in performance due to change in the composition of the base fuel, but does increase the anti-knock index from 87 for E0 up to the range of a mid-grade pump gasoline (anti-knock index = 89) for E20, assuming linear blending.

Laser-sheet imaging studies of the effects of operating conditions on thermal stratification were conducted in the optically accessible engine using a special optical configuration that allows simultaneous viewing of both the near-wall and bulk-gas regions of the charge. For these experiments, the laser sheet was oriented vertically as it passed through windows in the upper part of the cylinder wall. Images were acquired from the side through a third cylinder-wall window, which also acts a diverging lens to allow viewing out to the cylinder walls. Thus, images can be obtained showing a representative cross-section of the bulk gas as well as the near-wall regions along the firedeck, piston top, and cylinder walls. Temperature images were derived from planar laser-induced fluorescence images of toluene, based on an in situ calibration. The toluene was introduced as a tracer in the fuel, and it was selected over other potential tracers because it allows noise from background fluorescence to be removed with spectral filtering.

Results

To realize the full potential of boosted HCCI it is important to understand how the operating parameters affect thermal efficiency, how they can be adjusted to optimize efficiency, and the trade-offs involved. Accordingly, a systematic study was conducted on the effects of key operating parameters, including: ringing intensity, T_{in}, engine speed, fuel type, fueling rate, fueling strategy, and P_{in}. In this work, the ringing intensity is used as a measure of the onset knock rather than the maximum pressure rise rate (PRR_{max}) because the allowable PRR_{max} varies with boost and engine speed, whereas the ringing intensity accounts for changes in these parameters [1].

Figure 1 shows the effect of variations in T_{in} on the gross indicated thermal efficiency (T-E) at an intake pressure of 2.0 bar, which is near the center of the range of boost levels investigated [2-4]. As shown by the solid and dashed black lines, when combustion phasing is

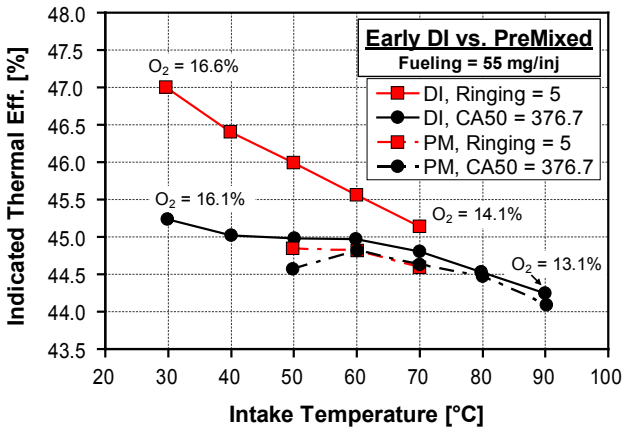

FIGURE 1. The effect of changes in T_{in} on thermal efficiency for fully premixed (PM) and early-DI fueling, for both constant CA50 = 376.7°CA and for constant ringing = 5 MW/m^2. Intake-O_2 molar percentages are shown for the endpoints of the two DI sweeps, indicating changes in the amount of EGR.

held constant (constant 50% burn point [crank angle 50, CA50]), reducing T_{in} from 90 to 30°C increases the T-E from about 44.2 to 45.2%, and the change is nearly identical for either premixed (PM) or early direct-injection (DI) fueling. Note that data were not acquired with premixed fueling for T_{in} < 50°C because of fuel condensation in the intake system. Since changes in T-E caused by changes in CA50 have been eliminated, the increase in T-E for these data occurs because heat-transfer losses are lower and the charge-gas $\gamma = c_p/c_v$ is higher with reduced T_{in}. Thus, the efficiency of HCCI engines can be increased by using the lowest practical intake temperature, depending on the fueling technique.

Figure 1 also shows that for early-DI fueling (*i.e.* 60°CA after top-dead center [TDC] intake), an even greater efficiency improvement can be obtained with reduced T_{in} if CA50 is advanced up to the ringing-intensity limit of 5 MW/m^2, as shown by the solid red line. Note that further advancing CA50 causes ringing >5 MW/m^2, resulting in engine knock, which significantly increases heat transfer losses with a commensurate drop in thermal efficiency [4]. Measurements in the optically accessible engine show that the reason CA50 can be advanced for early-DI fueling is that incomplete fuel/charge-gas mixing produces a partially stratified mixture [4]. For P_{in} = 2 bar, gasoline autoignition rates vary with the local equivalence ratio [3,4], so this non-uniform mixture autoignites sequentially from the richest regions to the leanest, significantly reducing the heat release rate (HRR), and therefore PRR_{max} and ringing intensity, for a given CA50. For premixed fueling, the constant CA50 data are already at the ringing limit of 5 MW/m^2, so the constant CA50 and ringing = 5 data are nearly identical.

The effects of engine speed and fuel-type (E0 vs. E10) on the T-E were also investigated. Engine speed was systematically varied, and at each speed, the highest efficiency was determined, as described in Ref. [4]. The results showed that the highest efficiencies were obtain in the range of 1,200 to 1,300 rpm (not shown). Since speed had little effect in this range, 1,200 rpm was selected to be consistent with previous studies. Adding 10% ethanol to the base gasoline reduced the amount of EGR required to control autoignition timing at boosted conditions. Less EGR increases the γ of the charge gas, resulting in a modest but consistent increase in T-E (not shown) [4]. It also increases the high load limit as discussed later.

The effects of fueling rate and fueling strategy on thermal efficiency for E10 with P_{in} = 2.4 bar are shown in Figure 2. For all data points, CA50 is retarded by the minimum amount necessary to reach a ringing of 5 MW/m^2, thus keeping efficiencies as high as possible while preventing knock. The premixed-fueling curve shows the typical trend of changes in efficiency with load ($IMEP_g$). Thermal efficiencies are highest for the lowest loads shown, and they decrease with increasing load because CA50 must be more retarded to prevent knock. The highest load shown is at knock/stability limit. At this point, an additional increase in fueling would cause knock, but further CA50 retard results in unstable combustion or misfire. At loads lower than the lowest load shown, stable operation can be obtained, but the charge becomes so dilute that combustion efficiencies drop significantly, resulting in high CO emissions and reduced T-E [5]. Therefore, it is preferable to reduce the load by reducing the boost pressure while maintaining a fuel/charge-mass ratio no lower than that of the lowest loads shown in Figure 2.

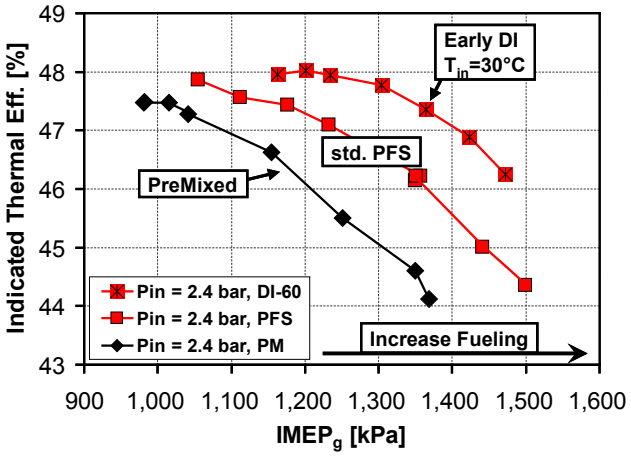

FIGURE 2. Thermal efficiency as a function of load for three fueling strategies: 1) fully premixed, T_{in} = 60°C, 2) standard PFS (91% premixed and 9% late-DI, T_{in} = 60°C), and 3) early-DI fueling (60° after TDC intake) with T_{in} = 30°C.

The other two curves in Figure 2 show the increase in T-E and/or load that can be achieved using two different methods of partial fuel stratification (PFS) to reduce the HRR. The standard method for producing PFS is to premix 80–95% of the fuel, and then to directly inject the remainder 45–60°CA before TDC compression, using T_{in} = 60°C to prevent condensation of the premixed fuel [3,4]. For the conditions shown in Figure 2, standard PFS reduces the HRR to allow CA50 to be advanced sufficiently for the T-E to be increased from about 44 to 46% at the maximum premixed load. Dropping T_{in} to 30°C and using 100% early-DI fueling further increases the T-E to about 47% for this same load. Alternatively, for the same T-E, the maximum load can be increased by about 10% over the premixed high-load limit using standard PFS.

Using these PFS fueling strategies and/or optimizing other parameters for high T-E gave significant improvements in T-E over a range of loads, compared to our original high-load boosted results [2]. As shown in Figure 3, thermal efficiencies of 47–48% were reached from 8 to 13.5 bar $IMEP_g$ with E0, and from 9.5 to 16 bar $IMEP_g$ with E10, compared to T-Es of only 43–44% for our original results. The data in Figure 3 also show that for P_{in} above about 2 bar, intake pressure has little effect on the indicated T-E that can be achieved. However, as shown by the three points at the far left of the plot, the maximum T-E that could be achieved drops progressively as P_{in} is reduced below 2 bar, falling to 43% at P_{in} = 1.0 bar. This is mainly a result of the increased intake temperatures required when the autoignition enhancement with boost is reduced. With a higher T_{in}, T-E suffers because of higher heat transfer losses and a reduced γ.

Figure 4 shows the effects of PFS and the ethanol content of the gasoline on the maximum load that can be reached as a function of intake boost. The black line shows the results for premixed conventional gasoline (E0) from Ref. [2]. One of the factors limiting the load for E0 at $P_{in} \geq 2.6$ bar is that so much EGR is required to compensate for the autoignition enhancement with boost, that the amount of air available for combustion becomes limited. Adding ethanol reduces this autoignition enhancement with boost, reducing the EGR required and leaving more air available for combustion. As a result, the maximum load can be increased from 16.3 bar $IMEP_g$ for E0, to 18.1 bar for E10, to 20.0 bar for E20, the latter being very close to the high-load load limit of a turbocharged diesel engine with the same 155 bar cylinder-head pressure limit as this HCCI engine. Also shown in Figure 4, applying PFS increases the maximum load attainable for E0 and E10 at intermediate values of P_{in} that are high enough for the fuel autoignition rate to be sensitive to variation in the local equivalence ratio (ϕ-sensitive) [3], but still low enough for sufficient air to be available.

For premixed HCCI, the peak HRR, and therefore the knocking propensity, is controlled by the amount of naturally occurring TS. Similar to the description of the effects of PFS above, TS causes a sequential autoignition from hottest region to coldest, reducing the HRR considerably compared to a truly homogeneous charge. Understanding the in-cylinder distribution of the TS and how it changes with operating conditions is important for control algorithms and for developing methods of adjusting the TS to extend the operating

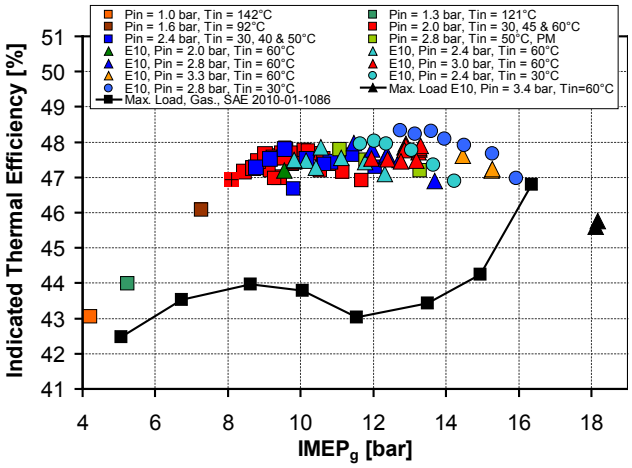

FIGURE 3. Thermal efficiency as a function of load ($IMEP_g$) for selected high efficiency points for both E0 and E10. Also shown are efficiencies for the maximum loads achieved with E0 for various P_{in}, from Ref. [2], and the efficiencies for the highest load points with E10 (see Figure 4). Ringing ≤ 5 MW/m^2, and NO_x and soot emissions are more than a factor of 10 below U.S. 2010 standards for all boosted data points.

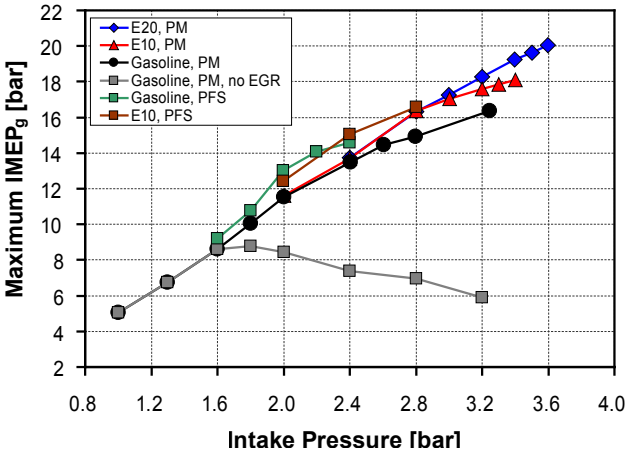

FIGURE 4. Maximum $IMEP_g$ attainable as a function of P_{in} for premixed (PM) fueling with E0, E10, and E20, and with standard PFS for E0 and E10. Ringing ≤5 MW/m^2, and NO_x and soot emissions are more than a factor of 10 below U.S. 2010 standards for all boosted data points.

range. Using an improved optical setup and image post-processing technique, quantitative T-map images were acquired to investigate the effects of several parameters on the TS, including: engine speed, T_{in}, T_{wall}, and swirl. Figure 5 shows an example of the results for changes in engine speed from 600 to 1,500 rpm. Our previous work has shown that the TS arises mainly from turbulent structures of colder gas extending from the firedeck and piston top into the bulk gas [6]. Figure 5a shows that the probability of these cold structures occurring decreases significantly as the engine speed is increased from 600 to 1,500 rpm. Similarly, a more quantitative measure of the TS, the standard deviation of the temperature fluctuations (Std-Dev T'), in Figure 5b shows a consistent trend of decreasing TS with increased speed. The higher TS at low speeds shows that the increased time for turbulent convection at lower speeds dominates over the potential for higher turbulence with increased gas velocities at higher speeds.

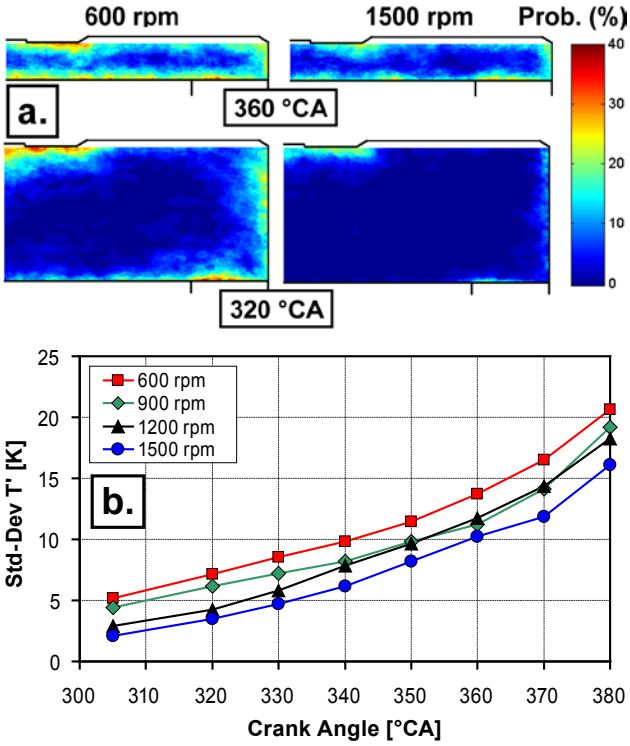

FIGURE 5. Effects of engine speed on the thermal stratification: a) images showing the probability of finding turbulent structures of colder gas at 600 and 1,500 rpm, and b) changes in the amount of thermal stratification through the compression stroke as measured by the standard deviation of the temperature fluctuations (Std-Dev T') for 600, 900, 1,200, and 1,500 rpm.

Conclusions

The studies described in this report significantly advance the understanding of HCCI with respect to three DOE, Office of Vehicle Technologies technical goals: 1) increased thermal efficiency, 2) extending the high-load limit of low-temperature HCCI and partially stratified HCCI-like combustion, while maintaining ultra-low NO_X and particulate emissions, and 3) developing an improved understanding of the in-cylinder processes related to thermal stratification.

- A systematic study of the key operating parameters affecting the T-E of boosted HCCI engines produced the following results:
  - T-E can be improved by using the lowest practical intake temperature.
  - The highest T-Es occurred for engine speeds of 1,200–1,300 rpm.
  - CA50 should be retarded sufficiently to prevent engine knock, which can increase heat transfer losses and reduce T-E.
  - However, CA50 should be retarded by only the minimum amount required to control knock, since retarding CA50 reduces the effective expansion ratio which reduces the T-E.
  - The effect of fueling rate on T-E involves a trade-off between obtaining good combustion efficiency and minimizing the CA50 retard required to prevent knock. For a given P_{in}, a lower fueling rate requires less CA50 retard to prevent knock, but if the fueling rate is too low, combustion efficiency suffers. In general, the highest T-E is obtained for the lowest fueling rate that still gives a combustion efficiency above about 97%.
- For intake pressures where the fuel autoignition is ϕ-sensitive, both standard and early-DI PFS significantly reduce HRRs, so less CA50 retard is required to prevent knock, which increases the T-E. Alternatively, for the same CA50, fueling can be increased, extending operation to high loads.
- Through adjustment of various operating parameters, T-Es of 47–48% were reached from 8 to 13.5 bar $IMEP_g$ with E0, and from 9.5 to 16 bar $IMEP_g$ with E10.
- Adding ethanol reduces the EGR requirement with boost leaving more air available for combustion. This allowed the maximum load to be increased from 16.3 bar $IMEP_g$ for E0, to 18.1 bar for E10, or to 20.0 bar for E20, showing that HCCI can achieve loads similar to a turbocharged diesel engine.
- Thermal imaging data acquired over a range of operating conditions showed that TS increases with decreased speed, increased T_{in}, decreased T_{wall}, and increased swirl.

References

1. Eng, J.A., "Characterization of Pressure Waves in HCCI Combustion," SAE Paper 2002-01-2859, 2002.

2. Dec, J.E. and Yang, Y., "Boosted HCCI for High Power without Engine knock and with Ultra-Low NOx Emissions – using Conventional Gasoline," *SAE Int. J. Engines*, **3**(1): 750-767, SAE paper 2010-01-1086, 2010.

3. Dec, J.E., Yang, Y., and Dronniou, N., "Boosted HCCI – Controlling Pressure-Rise Rates for Performance Improvements using Partial Fuel Stratification with Conventional Gasoline," *SAE Int. J. Engines*, **4**(1): 1169-1189, SAE paper 2011-01-0897, 2011.

4. Dec, J.E., Yang, Y., and Dronniou, N., "Improving Efficiency and using E10 for Higher Loads in Boosted HCCI Engines," SAE paper 2012-01-1107, SAE World Congress, April 2012.

5. Dec, J.E. and Sjöberg, M., "A Parametric Study of HCCI Combustion – the Sources of Emissions at Low Loads and the Effects of GDI Fuel Injection," *SAE Transactions*, **112**(3), pp. 1119-1141, SAE paper 2003-01-0752, 2003.

6. Dronniou, N. and Dec, J.E., "Investigating the Development of Thermal Stratification from the Near-Wall Regions to the Bulk-Gas in an HCCI Engine with Planar Imaging Thermometry," SAE paper 2012-01-1111, SAE World Congress, April 2012.

FY 2012 Publications/Presentations

1. Dec, J.E., "The Importance of Intermediate-Temperature Reactions in HCCI and HCCI-like Engines," Multi-Agency Coordinating Committee for Combustion Research (MACCCR) – 5th Annual Fuels Review, Sandia National Labs, Sept. 17–20, 2012.

2. Dec, J.E. "Increasing the Load Range and Efficiency of HCCI using Fuel Stratification," Thermo- and Fluid Dynamic Processes in Direct-Injection Engines (THIESEL), Valencia, Spain, Sept 11–14, 2012.

3. Dec, J.E., Yang, Y., and Dronniou, N., "Improving Efficiency and using E10 for Higher Loads in Boosted HCCI Engines," SAE paper 2012-01-1107, SAE World Congress, April 2012.

4. Dronniou, N. and Dec, J.E., "Investigating the Development of Thermal Stratification from the Near-Wall Regions to the Bulk-Gas in an HCCI Engine with Planar Imaging Thermometry," SAE paper 2012-01-1111, SAE World Congress, April 2012.

5. Yang, Y., Dec. J.E., Dronniou, N. and Canella, W., "Boosted HCCI Combustion Using Low-Octane Gasoline with Fully Premixed and Partially Stratified Charges," SAE paper 2012-01-1120, SAE World Congress, April 2012.

6. Mehl, M., Pitz, W. J., Sarathy, S. M., Yang, Y., and Dec, J.E., "Detailed Kinetic Modeling of Conventional Gasoline at Highly Boosted Conditions and the Associated Intermediate Temperature Heat Release," SAE paper 2012-01-1109, SAE World Congress, April 2012.

7. Krisman, A., Hawkes, E.R., Kook, S., Sjöberg, M., and Dec, J.E., "On the Potential of Ethanol Fuel Stratification to Extend the High-Load limit in Stratified-Charge Compression-Ignition Engines," Fuel, **99**:45-54, 2012.

8. Dronniou, N., Dec, J.E., and Yang, Y. "Investigating the Influence of Engine Operating Conditions on the Development of Thermal Stratification in a HCCI Engine with Planar Imaging Thermometry," DOE Advanced Engine Combustion Working Group Meeting, February 2012.

9. Yang, Y., Dec, J.E., Dronniou, N., and Cannella, W., "Boosted HCCI Combustion Using Low-Octane Gasoline with Fully Premixed and Partially Stratified Charges," DOE Advanced Engine Combustion Working Group Meeting, February 2012.

10. Dec, J.E., Yang, Y., and Dronniou, N., "Improving Efficiency and Load Range of Boosted HCCI using Partial Fuel Stratification with Conventional Gasoline," DEER 2011 – 17th Directions in Engine-Efficiency and Emissions Research Conference, October 2011.

11. Sjöberg, M. and Dec, J.E., "Smoothing HCCI Heat Release with Vaporization-Cooling-Induced Thermal Stratification using Ethanol," *SAE Int. J. Fuels & Lubricants*, **5**(1):7-27, SAE paper 2011-01-1760, 2011.

12. Dec, J.E., Yang, Y., and Dronniou, N., "Boosted HCCI – Controlling Pressure-Rise Rates for Performance Improvements using Partial Fuel Stratification with Conventional Gasoline," *SAE Int. J. Engines*, **4**(1): 1169-1189, SAE paper 2011-01-0897, 2011.

13. Yang, Y., Dec, J.E., Dronniou, N., Sjöberg, M., and Cannella, W.J., "Partial Fuel Stratification to Control HCCI Heat Release Rates: Fuel Composition and Other Factors Affecting Pre-Ignition Reactions of Two-Stage Ignition Fuels," *SAE Int. J. Engines*, **4**(1): 1903-1920, SAE paper 2011-01-1359, 2011.

14. Snyder, J.A., Dronniou, N., Dec, J.E., and Hanson, R.K., "PLIF Measurements of Thermal Stratification in an HCCI Engine under Fired Operation," *SAE Int. J. Engines*, **4**(1): 1669-1688, SAE paper 2011-01-1291, 2011.

Special Recognitions & Awards/Patents Issued

1. U.S. Patent Application Filed: Dec, J.E., Yang, Y., and Dronniou, N. "A Method for Operating Homogeneous Charge Compression Ignition Engines Using Conventional Gasoline," Application Number 13/230,320.

2. Invited Keynote: Thermo- and Fluid Dynamic Processes in Direct-Injection Engines (THIESEL), Valencia, Spain, September 2012.

II.9 Automotive HCCI Combustion Research

Richard Steeper
Sandia National Laboratories
MS 9053
P.O. Box 969
Livermore, CA 94551-0969

DOE Technology Development Manager:
Gurpreet Singh

Overall Objectives

- Perform fundamental engine research addressing technical barriers to the achievement of DOE efficiency and emissions goals for automotive gasoline engines.
- Develop and apply advanced diagnostics in an optically accessible homogeneous charge compression ignition (HCCI) engine to enhance our knowledge of fundamental in-cylinder processes.
- Advance the capabilities of engine simulation and analysis tools by validating with research engine data.
- Disseminate knowledge gained from experiments through collaborative interaction with industry, academic, and national lab partners.

Fiscal Year (FY) 2012 Objectives

- Conduct ongoing research on fueling during negative valve overlap (NVO) as a means of enhanced control of HCCI combustion.
- Characterize in-cylinder processes including fuel injection, wall wetting, and combustion during NVO-fueled operation via direct imaging.
- Refine seeding experiments to better measure the fundamental chemical effects of NVO fueling on HCCI combustion.
- Utilize a CHEMKIN piston/cylinder reactor simulation to understand the reactions responsible for chemical effects measured in experiments.

Accomplishments

- Documented significant piston wetting, pool fires, and rich combustion associated with late injection of NVO fuel.
- Performed seeding experiment using a refined protocol to suppress extraneous influences while quantifying the distinct chemical enhancement of HCCI combustion by acetylene. Documented the results of the seeding experiments in a journal article.
- Reproduced several significant trends of seeding experiments using a detailed iso-octane reaction mechanism with CHEMKIN's 0-D Closed Internal Combustion Engine Simulator.

Future Directions

- Employ two methods of gas sampling to speciate the products of NVO reactions: (1) a unique 6-stroke engine cycle implemented at Oak Ridge National Laboratory, and (2) a cylinder-dump mechanism mounted in Sandia's automotive HCCI engine.
- Apply the tunable-diode-laser absorption diagnostic developed previously to characterize in-cylinder acetylene formation during NVO fueling. Extend the diagnostic to measure other species (e.g., H_2O, CO_2, C_2H_2) to clarify the extent of NVO reformation reactions.
- Apply KIVA, CHEMKIN, and GT Power models of our optical engine to build a coherent understanding of NVO fueling and its effect on main combustion.

Introduction

Challenges to the implementation of gasoline HCCI combustion — including phasing control, operating-range extension, and emissions control — all can benefit from advanced charge-preparation strategies. Alternative strategies such as retarded injection and variable valve timing can be used to modify local charge composition and temperatures, thereby controlling ignition phasing, rate of heat release, combustion efficiency, and engine-out emissions. A current focus of our research is understanding the NVO strategy for HCCI combustion. Partial fueling during the NVO period can affect main combustion both thermally (NVO reactions elevate residual gas temperature) and chemically (NVO reformation reactions produce species that are carried over to main combustion), and understanding these effects is necessary in order to take full advantage of the strategy. Knowledge gained in this project supports DOE's goal of developing advanced energy-efficient, low-emission engine technologies.

Approach

Multiple optical diagnostics are applied in our gasoline HCCI engine to quantify in-cylinder processes. Direct imaging allows assessment of fuel injection; laser-induced fluorescence imaging quantifies composition and temperature distributions; laser-absorption produces time-resolved species concentration histories; and chemiluminescence imaging characterizes ignition and combustion processes. Development of new diagnostics as well as computational fluid dynamics/combustion models is facilitated through continuing collaborations with university and national lab partners. Regularly scheduled technical exchanges with manufacturers, national labs, and academia leverage the knowledge gained in the research project.

Results

FY 2012 experiments have focused on NVO fueling as a means of controlling HCCI combustion under low-load, split-fueled operation. Using a high-speed camera in the optical engine, we have imaged fuel injection, ignition, and combustion processes during NVO fueling for a range of operating conditions. Intense laser-diode-array illumination enabled capture of spray impingement and fuel film formation that occurs when injecting fuel near top-dead center of NVO. Under these operating conditions, combustion luminosity imaging reveals bright flames associated with localized rich combustion. In contrast, there is no persistent piston wetting associated with early NVO injection, and the observed ignition and combustion for these conditions are spatially uniform and similar in appearance to typical HCCI combustion. The observed rich combustion observed for late NVO fuel injection supports a hypothesis that acetylene could be produced during late NVO fueling, and motivates our interest in isolating its effects via seeding experiments.

In the seeding experiments, we are able isolate chemical effects of specific reformed species by mixing candidate species one-at-a-time in the intake air stream. At the same time, we remove the influence of (other) reformed species by eliminating fuel injection during NVO, while compensating for lost thermal energy by increasing intake air temperature. The observable for these experiments is any change in heat release during main compression or expansion correlated with the presence of acetylene.

The seeding experiment protocol was modified this year to suppress the extraneous influence of combustion phasing on our measurements. Since engine heat release is very sensitive to phasing, allowing combustion phasing to vary while comparing heat release data can introduce non-linear trends. Instead, we adjusted intake air temperature to achieve the same CA50 phasing (crank angle at which 50% of the burn is achieved) for all experiments. In addition, total chemical energy was held constant by adjusting fuel mass to compensate for varying acetylene seed mass. The result is a less dramatic change in heat release observed as seed mass is increased, but an increased confidence that we are measuring the fundamental effects of acetylene.

Figure 1 compares experiment results from low-load HCCI experiments at several seed concentrations of acetylene. For the reference case (*unseeded*), 11 mg of iso-octane are direct-injected during intake (no other fuel or seed added). The remaining cases represent increasing addition of acetylene seed, with iso-octane reduced in each case to hold constant the total chemical energy added. Conceptually, this approximates NVO-fueled operation in which a varying fraction of NVO fuel is reformed to acetylene and is carried over from NVO to main ignition. The effect of acetylene on main combustion is clear in Figure 1: it increases peak heat release rate and advances its location. While distinct from the unseeded case, the seeded curves are all similar, with no clear trend associated with increasing seed concentration.

Figure 2 presents an alternative quantification of acetylene's effect on main combustion. As mentioned above, intake temperature was adjusted to achieve target CA50 phasing, and Figure 2a presents mass-averaged charge temperatures at intake valve closing for each seeding case. Two different load conditions are plotted, but both reveal the same steady drop in required intake temperature as seed mass is increased. This represents an operating advantage: the presence of acetylene allows a cooler intake temperature while maintaining the same main combustion phasing.

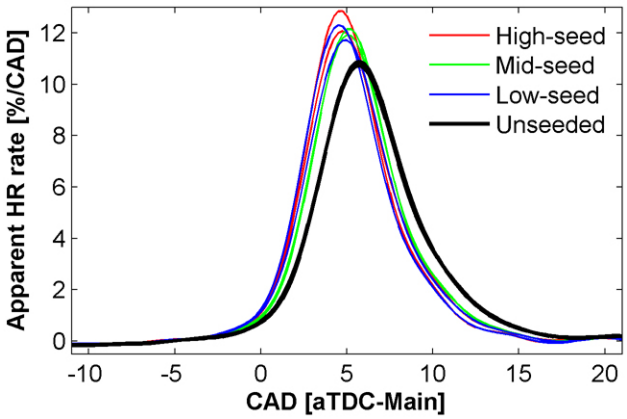

HR - heat release; CAD - crank angle degrees

FIGURE 1. Apparent heat release rate during main combustion for unseeded and seeded operation. Two typical curves shown for each seeding level: Unseeded: 0 ppm; Low seed: 680 ppm; Mid seed: 1,500 ppm; High seed: 2,250 ppm. Engine operation at a speed of 1,200 rpm and indicated mean effective pressure of 2.5 bar.

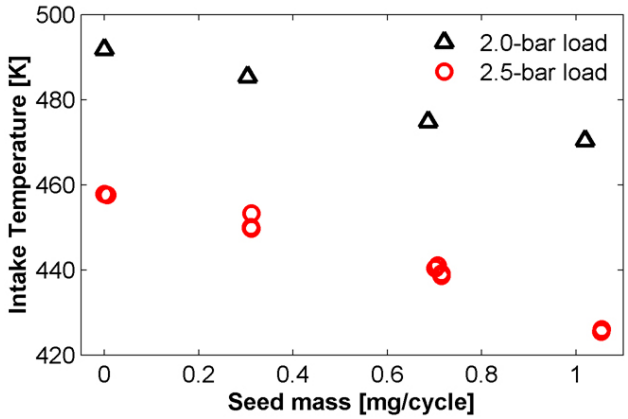

FIGURE 2a. Estimated mass-averaged charge temperatures at intake valve closing for seeding experiments at load conditions of 2.0 bar and 2.5 bar. The data fall at four seed-mass-per-cycle values that correspond to the four ppm values provided in Figure 1 caption.

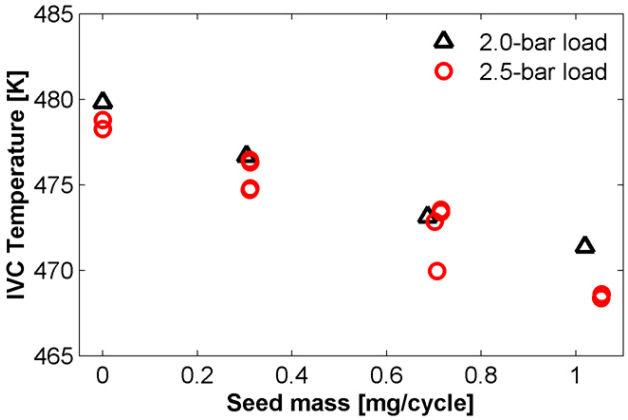

FIGURE 2b. Estimated mass-averaged charge temperatures at intake valve closing for the same experiments as in Figure 2a.

Figure 2b plots temperatures at intake valve closing following mixing of intake air and hot NVO products. Here the two load conditions are nearly superimposed, but again, both reveal a beneficial decrease in required temperature as acetylene mass increases. Future experiments will attempt to quantify the production of acetylene during actual NVO-fueled operation, but the current work establishes that relatively small concentrations of acetylene produced in this way could chemically affect main combustion phasing. In fact, manfacturer interest in the topic arises from the potential for using the technique to gain cycle-by-cycle authority over HCCI phasing.

Explaining the chemical effects of NVO fueling on main combustion requires an understanding of NVO reaction chemistry. To this end, we have employed CHEMKIN's 0-D Closed Internal Combustion Engine Simulator, most recently applying it to the acetylene

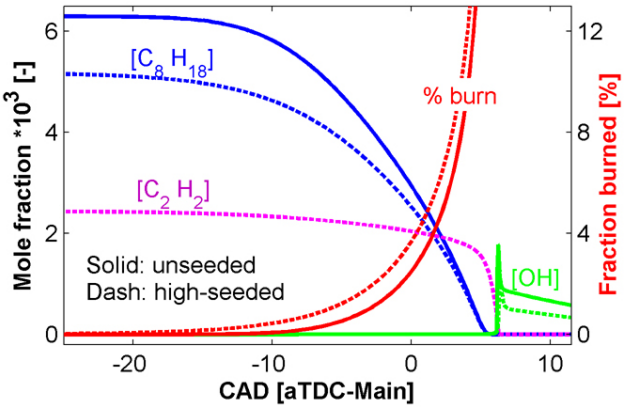

FIGURE 3. Selected species concentration profiles and mass fraction burn profiles predicted by CHEMKIN simulation of the seeding experiments.

seeding experiments described above. Although absolute temperatures predicted with the tool are off by a few tens of degrees centigrade, the simulation captures the same monotonic decrease in charge temperatures required to achieve target combustion phasing in our experiments.

CHEMKIN-predicted mole fraction histories for the acetylene experiments are shown in Figure 3, comparing unseeded and seeded simulations. Initial fuel (iso-octane) concentration for the high-seed case is lower than the unseeded case to compensate for the chemical energy of the added seed, but otherwise the profiles are similar. The acetylene profile, on the other hand, is distinct in showing a gradual decline until close to peak heat release (the latter marked by an abrupt increase in OH concentration). As an indicator of overall reaction progress, the fraction burned curves shown in the graph predict advanced heat release for the seeded case in agreement with the experimental enhancement of main combustion due to the presence of acetylene. These results increase confidence in our modeling of NVO reaction chemistry.

Conclusions

- Optical imaging in the automotive HCCI engine has documented wall wetting, fuel films, and pool fires associated with late NVO fueling. In contrast, early NVO fuel injection shows little piston wetting and relatively homogeneous combustion. This indicates that NVO reactions proceed in very different environments depending on injection timing.
- Seeding experiments in which combustion phasing has been held constant have quantified the enhancement of HCCI combustion due to part-per-thousand concentrations of acetylene. The results support the hypothesis that reactive species such as acetylene formed during NVO reactions and carried

over to main compression could chemically enhance HCCI combustion.

- Chemical kinetics simulations of the seeding experiments successfully predicted the observed combustion enhancement due to acetylene. This provides some confidence that the simulation can enhance our understanding of the relevant chemistry as well as suggest other active species that could contribute to the observed trends.

FY 2012 Publications/Presentations

1. Steeper, R.R., "Automotive HCCI Combustion Research," DOE/OFCVT Advanced Combustion Technologies FY11 Annual Report, 2011.

2. Puranam, S.V. and Steeper, R.R., "The Effect of Acetylene on Iso-octane Combustion in an HCCI Engine with NVO," *SAE Int. J. Engines* **5**(4), 2012, doi:10.4271/2012-01-1574.

3. Steeper, R.R., "Advanced Combustion Research for Enabling High-Efficiency, Clean Engines for Future Fuels," GM/Sandia Calibration Workshop, Detroit, Feb. 23, 2012.

4. Steeper, R.R., "Automotive HCCI Engine Research," DOE Vehicle Technologies Annual Merit Review, Washington, DC, May 15, 2012.

5. Steeper, R.R., "Acetylene Seeding Experiments in a Gasoline HCCI-NVO Engine," DOE Advanced Engine Combustion Working Group Meeting, USCAR, Detroit, June 19, 2012.

6. Steeper, R.R., "The Effect of Acetylene on Iso-octane Combustion in an HCCI Engine with NVO," SAE International PF&L Meeting, Malmo, Sweden, Sept. 18, 2012.

II.10 Engine Efficiency Fundamentals – Accelerating Predictive Simulation of Internal Combustion Engines with High Performance Computing

K. Dean Edwards (Primary Contact),
C. Stuart Daw, Charles E.A. Finney,
Sreekanth Pannala, Miroslav K. Stoyanov,
Robert M. Wagner, Clayton G. Webster
Oak Ridge National Laboratory (ORNL)
National Transportation Research Center
2360 Cherahala Blvd
Knoxville, TN 37932

DOE Technology Development Manager:
Gurpreet Singh

Overall Objectives

- Develop and make use of predictive simulation tools for accelerated combustion development, design, calibration, and control through use of high-performance computing (HPC) resources. This effort makes use of special HPC resources at ORNL in collaboration with industry stakeholders. Current partnerships include Ford and General Motors.
- Support industry and DOE through the combination of ORNL expertise in internal combustion engine research and high performance computing expertise.

Fiscal Year (FY) 2012 Objectives

- Establish resources and simulation tools for use with ORNL HPC resources to support internal combustion engine modeling.
- Develop a novel approach for investigating cycle-to-cycle combustion variability which uses multiple, parallel combustion simulations with cycle feedback of key parameters to replace time-prohibitive, serial combustion simulations.

Accomplishments

- Computational fluid dynamics (CFD) packages and additional components have been ported to run on ORNL HPC resources (including Titan), and 3.1 Mhr of computational time have been allocated for current tasks.
- Demonstrated a novel approach for simulating cycle-to-cycle combustion variations through multiple, parallel simulations.

Future Directions

- Demonstrate potential of HPC to provide unprecedented new information on the development of combustion instabilities for advanced combustion engines.
- Development and validation of high-fidelity, multi-processor simulation tool to accelerate design and optimization of fuel-injector design for direct-injection gasoline applications.
- Initiate development of a new open-source engine code optimized for massively parallel systems based upon OpenFOAM® and existing sub-models.

Introduction

This project supports rapid advancements in engine design, optimization, and control required to meet new Corporate Average Fuel Economy standards and emissions regulations through the development of advanced simulation tools and novel techniques to best utilize HPC resources. This effort couples ORNL's leadership role in HPC with experimental and modeling expertise with engine and emissions-control technologies. Specific project tasks evolve to support the needs of industry and DOE. Two tasks are currently supported:

- **Task 1:** Use of highly parallelized engine simulations to understand the stochastic and deterministic processes which drive cycle-to-cycle variability in dilute combustion systems. Collaborative effort with Ford Motor Company and Convergent Science, Inc.
- **Task 2:** Use of detailed CFD simulations to understand and optimize the design of direct-injection gasoline fuel injectors for improved engine efficiency. Collaborative effort with General Motors.

Approach

The aim of this project is to develop and apply innovative approaches which use HPC resources for simulation of engine systems to address specific issues of interest to industry and DOE. The specific issues addressed and approaches applied for the two current tasks are described below.

Task 1

Dilute combustion provides a potential pathway to simultaneous efficiency and emissions improvements in light-duty engines. However, at sufficiently high dilution levels, the flame front becomes unstable resulting in complex cycle-to-cycle combustion variability forcing the adoption of wide safety margins and failure to achieve the full potential benefits of charge dilution. There is growing interest in the use of computational simulations to understand the physics and chemistry behind the combustion stability limit to facilitate control of the instabilities allowing operation at the 'edge of stability.' A major challenge is that many of the associated dynamical features are very subtle and/or infrequent requiring simulation of hundreds or thousands of sequential engine cycles in order to observe the important unstable events with any statistical significance. Complex CFD simulations with full chemical kinetic modeling can require days of computational time for a single cycle making serial simulation of thousands of cycles time-prohibitive. In this task, we address these computational challenges by replacing simulations of many successive engine cycles with multiple, concurrent, single-cycle simulations to generate meta-models through adaptive sparse grid sampling and then utilizing the resulting meta-models for further studies of combustion instability.

Task 2

Multi-hole injectors utilized by spark-ignited direct-injection engines offer the flexibility of manufacturing the nozzle holes at various orientations to engineer a variety of spray patterns. The challenge is to determine the optimal design to maximize efficiency and emissions benefits for a given application. Detailed analytical tools, such as CFD, can provide a cost-effective approach to reduce the number of potential injector concepts for a given combustion system. In this task, we are working with General Motors to develop and validate a high-fidelity, multi-processor simulation tool to accelerate design and optimization of fuel injector hole patterns for direct-injection gasoline applications. Our approach involves the use of an optimization routine (such as a genetic algorithm) to coordinate parallel fuel-spray and combustion simulations with different injector geometries to hasten convergence on an optimal design.

Results

Initial efforts for FY 2012 were focused on assembling the required tools and resources. Through collaboration with Convergent Science, Inc., Converge™ CFD software has been licensed and ported for use on the ORNL HPC resources including Titan (formerly known as Jaguar) for use in Task 1. OpenFOAM® and various submodels have also been ported to ORNL HPC resources for use in Task 2. Applications for time on the ORNL HPC resources were submitted and awarded 3.1 Mhr split equally between the two tasks. Additional results specific to Task 1 are discussed in the following.

Task 1

Figure 1 compares our concurrent simulation strategy with traditional serial simulation. The key difference is the substitution of single-cycle engine simulations for long, multi-cycle simulations. Each single-cycle simulation starts with different values of model parameters and/or initial conditions. The resulting responses are then analyzed to find the parameters having the most significant impact on combustion stability. These parameters are then further explored to refine knowledge of their impact on combustion. By intelligently sampling the parameter space through an adaptive sparse grid approach, it is possible to construct a meta-model of the engine behavior which is computationally trivial compared to the detailed CFD simulations but provides the same statistical response to the key input and feedback parameters.

Initial development and demonstration of our approach has been performed using a simplified engine combustion model that is computationally inexpensive but still has the correct global dynamics. Once our adaptive, concurrent simulation strategy has been fully demonstrated with the simple combustion model, we plan to repeat the meta-model-building procedure with highly detailed CFD combustion models ran on massively parallel computers. The ultimate objective is to create and use refined meta-models to more intensively explore the combustion instability hyperspace (see Figure 2).

Early results suggest that our approach is capable of accurately capturing much of the complex dynamics of the simple engine model with the resulting meta-model. Figure 3 shows a statistical comparison of multiple-cycle simulation results for the two models using consistent values for the input parameters at two nominal equivalence ratios (φ_0 = 0.8 and 0.7) where the predicted cycle-to-cycle variability is quite different. The statistical method used in this figure, symbolization, partitions the global combustion heat release into eight equiprobable regions (symbols), with each value on the horizontal axis representing a unique sequence of successive symbols. The vertical axis reflects the relative frequency of occurrence for each sequence.

In Figure 3, the relatively flat histogram on the left (for φ_0 = 0.8) represents expected random variations about the equiprobable value of 1/64 consistent with relatively small, noisy combustion variations around a fixed point. At increased dilution (φ_0 = 0.7), the

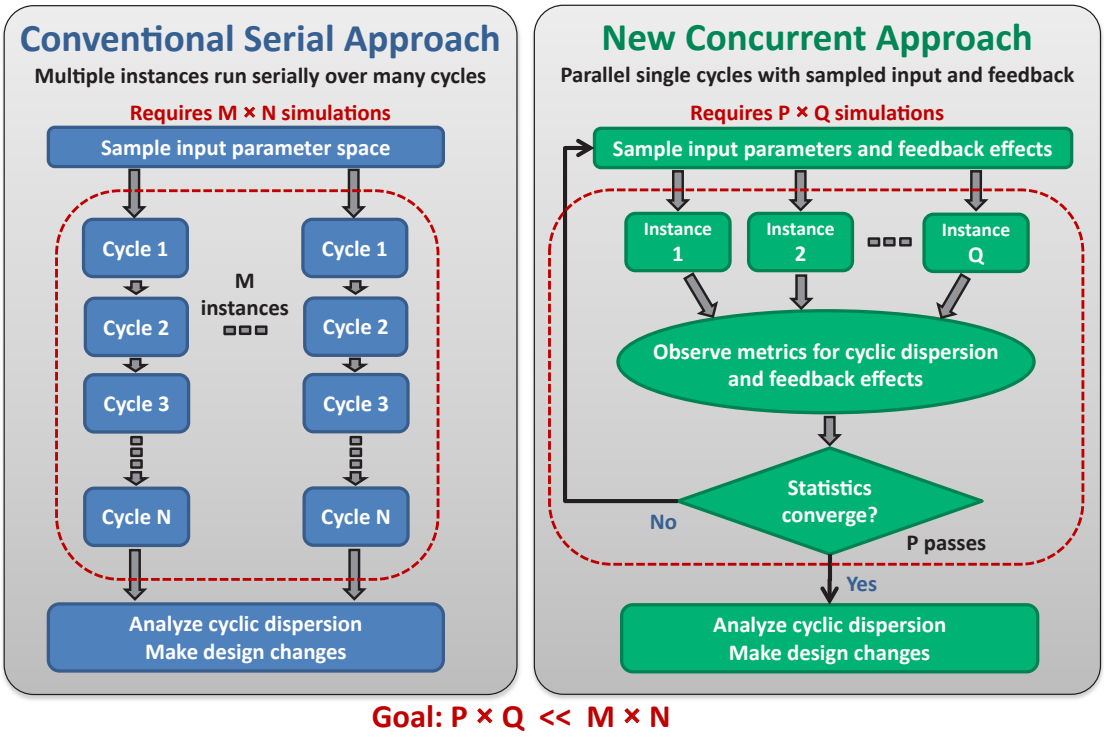

FIGURE 1. The concurrent modeling strategy replaces serial combustion simulations over many engine cycles with multiple single-cycle simulations.

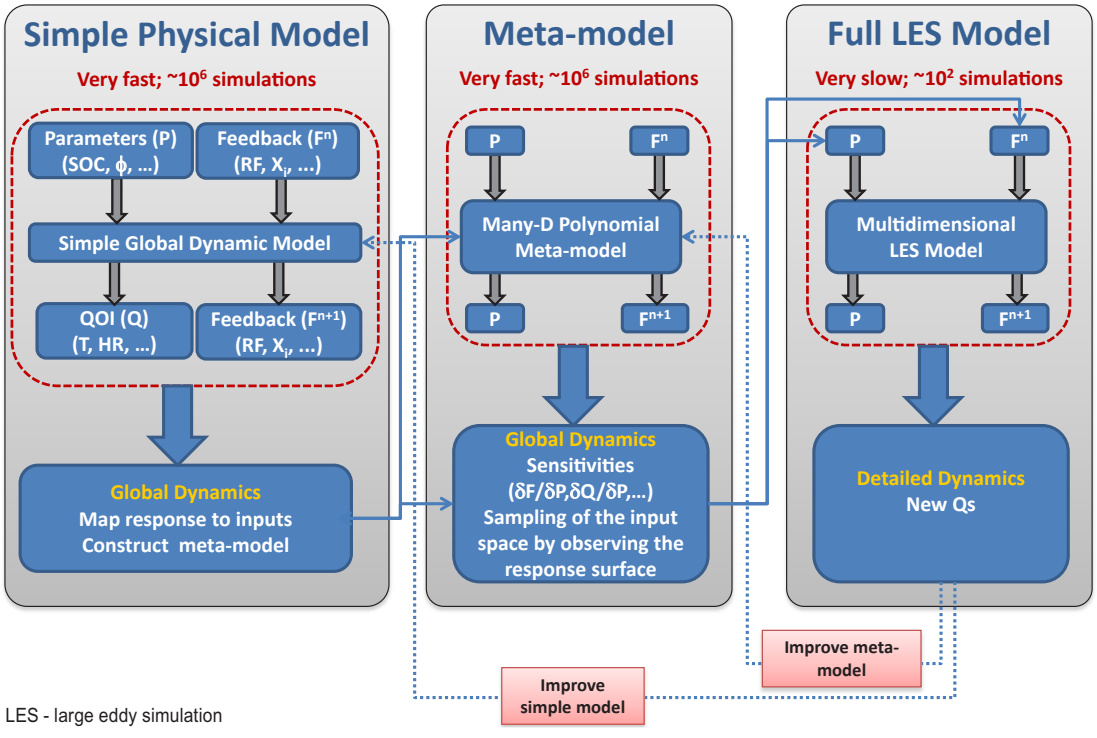

FIGURE 2. The initial meta-models will be refined using simulations with more highly detailed physical models. Exploration of the detailed physical model response surface will be guided by the initial meta-models and make further use of concurrent adaptive simulation.

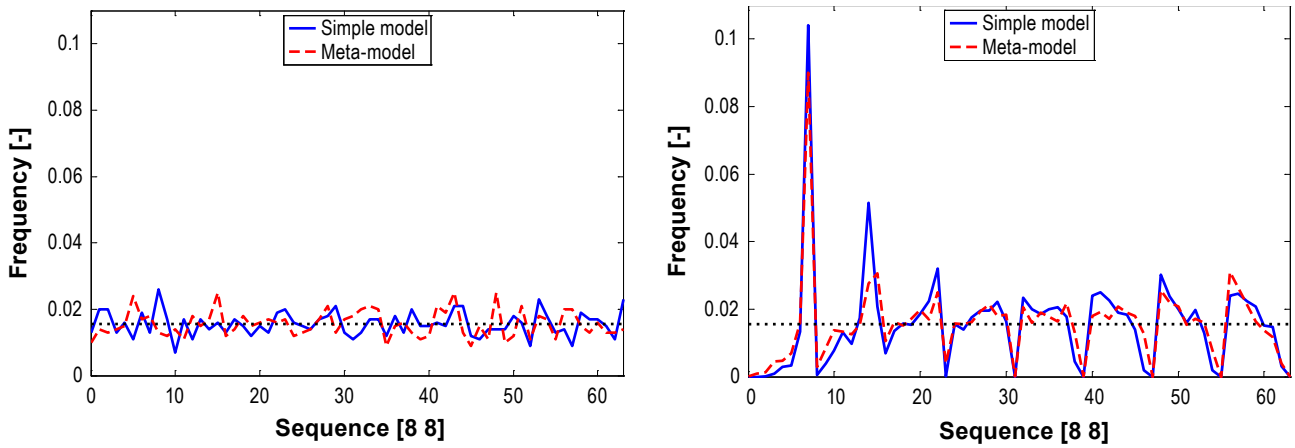

FIGURE 3. Symbol-sequence histograms comparing simple and meta-model dynamics for equivalence ratio of 0.8 (left), dominated by stochastic variations, and 0.7 (right), dominated by deterministic effects.

sharp peaks for certain sequences reflect deterministic feedback effects from residual gas which lead to large combustion oscillations. The ability of the meta-model to capture both the stochastic and deterministic cycle-to-cycle variations is crucial.

Conclusions

Increasing industry interest in utilizing HPC resources to hasten design advancements in internal combustion engines has led to collaborative efforts with industry stakeholders in two important areas: understanding and controlling cycle-to-cycle variability in dilute combustion and optimization of spark-ignited direct-injection fuel injector design. Early progress on these tasks is on track and showing great promise.

FY 2012 Publications/Presentations

1. CEA Finney, MK Stoyanov, S Pannala, CS Daw, RM Wagner, KD Edwards, CG Webster, JB Green (2012). Application of high-performance computing for simulating the unstable dynamics of dilute, spark-ignited combustion. Proceedings of the 2012 International Conference on Theory and Applications of Nonlinear Dynamics (ICAND). 26–30 August 2012; Seattle, WA, USA.

2. RM Wagner, S Pannala (2012). High-performance computing: Accelerating the development of high-efficiency engines. 2012 Global Powertrain Congress. 25 October 2012; Troy, MI, USA.

Special Recognitions

This project has received recognition in several external publications:

1. High Performance Computing at Oak Ridge National Laboratory. 2012 DEER Newsletter.

2. High Performance Computing key enabler for accelerating development of high efficiency engines. Green Car Congress. November 5, 2012. http://www.greencarcongress.com/2012/11/hpc-20121105.html

3. A New Era in Automotive Engine Development Driven by HPC. Digital Manufacturing Report (owned by hpcwire.com). October 25, 2012. http://www.digitalmanufacturingreport.com/dmr/2012-10-25/a_new_era_in_automotive_engine_development_driven_by_hpc.html

II.11 KIVA Development

David B. Carrington
Los Alamos National Laboratory
P.O. Box 1663
Los Alamos, NM 87545

DOE Technology Development Manager:
Gurpreet Singh

Subcontractors:
- Dr. Juan Heinrich, University of New Mexico, Albuquerque, NM
- Dr. Xiuling Wang, Purdue University, Calumet, Hammond, IN
- Dr. Darrell W. Pepper, University of Nevada, Las Vegas. Las Vegas, NV

Overall Objectives

- Develop algorithms and software for the advancement of speed, accuracy, robustness, and range of applicability of the KIVA internal engine combustion modeling – to be more predictive. This to be accomplished by employing higher-order spatially accurate methods for reactive turbulent flow, and spray injection, combined with robust and accurate actuated parts simulation and more appropriate turbulence modeling.
- To provide a KIVA software that is easier to maintain and is easier to add models to than the current KIVA. To reduce code development costs into the future via more modern code architecture.

Fiscal Year (FY) 2012 Objectives

- Continue developing code and algorithms for the advancement of speed, accuracy, robustness, and range of applicability of the KIVA combustion modeling software to higher-order spatial accuracy with a minimal computational effort.
- Finish developing underlying discretization to an *hp*-adaptive predictor-corrector split (PCS) using a Petrov-Galerkin (P-G) finite element method (FEM) for all flow regimes.
- Implement KIVA Spray and Chemistry in the *hp*-adapitve PCS FEM solver.
- Develop two-dimensional (2-D) overset grid method for moving and immersed actuated parts such as valves for robust grid movement.

Accomplishments

- Developed the *hp*-adaptive PCS using P-G FEM for all for flow regimes, from incompressible to high-speed compressible. Partially verified the *hp*-adaptive (FEM) framework and PCS solver.
- Developed 2-D overset grid method for moving and immersed actuated parts such as valves for robust grid movement. We have begun developing three-dimensional (3-D) overset grid method.
- Developed nearly automatic grid generation using only hexahedral elements with Cubit grid generator. Continue extending this capability in Cubit.
- Incorporated KIVA multi-component particle/spray injection algorithm into the PCS solver.
- Incorporated KIVA chemistry package into the PCS solver.
- Incorporated KIVA splash, break-up, collide and wall-film models into the PCS solver.
- Began researching large eddy simulation (LES) turbulence modeling for wall-bounded flows.

Future Directions

- Continue developing the *hp*-adaptive FEM for multispecies flows in all flow regimes. Continue implementing this method to perform modeling of internal combustion engines, other engines, and general combustion.
  - Continue developing comprehensive comparative results to benchmark problems and to commercial software as part of the verification and validation of the algorithms.
- Continue developing 3-D robust overset grid method for immersed actuated parts such as valves. Merge overset grid method into *hp*-adaptive FEM framework.
- Continue developing the parallel solution method for the *hp*-adaptive PCS algorithm. Parallel structure to be supplied by MPICH (the portable implementation of message passing interface, MPI) and/or OpenMP paradigms for newest computer architectures.
- Continue developing more appropriate turbulence models for more predictive modeling.
- Verify and validate combustion and spray models, and the local Arbitrary Lagrangian-Eulerian (ALE) in 3-D.
- Investigate other spray modeling methods for more predictive modeling capability.

Introduction

Los Alamos National Laboratory and its collaborators are facilitating engine modeling by improving accuracy of the modeling, and improving the robustness of software. We also continue to improve the physical modeling methods. We are developing and implementing new mathematical algorithms, those which represent the physics within an engine. We provide software that others may use directly or that they may alter with various models e.g., sophisticated chemical kinetics, different turbulent closure methods or other fuel injection and spray systems.

Approach

Development of computational fluid dynamics (CFD) models and algorithms relies on basic conservation laws and various mathematical and thermodynamic concepts and statements including calculus of variations. The process encompasses a great many requirements including:

1. Knowledge of turbulence and turbulent modeling for multiphase/multispecies fluid dynamics.
2. Knowledge of combustion dynamics, modeling, and spray methods.
3. Skill at developing, implementing numerical methods for multi-physics CFD on complex domains.
4. Careful validation and verification of the developed code and algorithms.

Results

When considering developing algorithms and the significant effort involved to produce reliable software for solving the physics of multi-species reactive flow, it is often better to have algorithms which are more accurate at a given resolution and provide for higher resolution and accuracy only where and when it is required. We began developing a new KIVA engine/combustion code with this idea in mind [1]. This new construction is a Galerkin FEM approach that utilizes conservative momentum, species, and energy transport. Our system uses a P-G and coupled pressure stabilization [2].

A projection method is combined with higher order polynomial approximation for model dependent physical variables (*p*-adaptive) along with grid enrichment (locally higher grid resolution – *h*-adaptive). Overset grids are used for actuated and immersed moving parts to provide more accurate and robust solutions in the next generation of KIVA. The scheme is particularly effective for complex domains, such as engines.

The *hp*-adaptive FEM is at a minimum 2nd order accurate in space and 3rd order for advection terms, but becomes higher order where required as prescribed by the adaptive procedures [2]. The *hp*-adaptive method employs hierarchical basis functions, constructed on the fly as determined by a stress-error measure [3].

The *h*-adaptive method, along with a conservative P-G upwinding technique, accurately captures shocks. Figure 1 shows viscous supersonic Mach 2.25 occurring over an 18^{o} compression ramp. The recirculation zone shown in Figure 1a is an affect of the adverse pressure gradient developing in the boundary layer at the incline and is in agreement with the experimental data. The velocity compares to experimental data as shown in Figure 2 [4]. Differences seen are related to the k-ω turbulence closure model; other models can capture the boundary layer more precisely but are more costly and can be less generic. The data only shows absolute speed, and not direction. Taking this in account, the velocity for the k-ω model is actually closer to the actual data than indicated in the Figure 2b and 2c.

Figure 3 shows both 2-D and 3-D subsonic/transonic flow over a NACA 0012 airfoil that too agrees with known solutions and data. This system incorporates a method for the measurement of the error in the discretization, and adjusts the spatial accuracy to minimize the error or bring it under some specified amount while minimizing the total number of nodes or elements in the domain.

Using the FEM method with the spray models provides a more accurate representation of the droplets interaction with the conveying fluid and with walls than the original finite volume method of KIVA. Because the FEM method allows for a continuous representation of phase-space, grid-scale accuracy can be applied everywhere. Problems with coarse grids influencing the spray are only related to the solution accuracy -- the spatial representation of the spray model is therefore convergent. The KIVA multi-component spray model, a method based the algorithm developed by Dukowicz [5] and expanded by Torres, et al. [6] for break-up, agglomeration, and surface films, is being installed in the *hp*-FEM PCS solver.

In Figure 5, diesel is shown injected into a duct having developed flow and inlet speed of 25 m/s (Mach 0.061) with inlet Reynolds number of ~1,204,000. The droplet radius is changing as a function of convective heat and mass transfer, evaporating the droplets. Heat conduction within the droplet, collisions and agglomeration occurs as the droplets are transported. Each parcel can have around 500 droplets (for 3-D) with mean behavior. The number of parcels/droplets is determined by the flow rate and injector size and if often

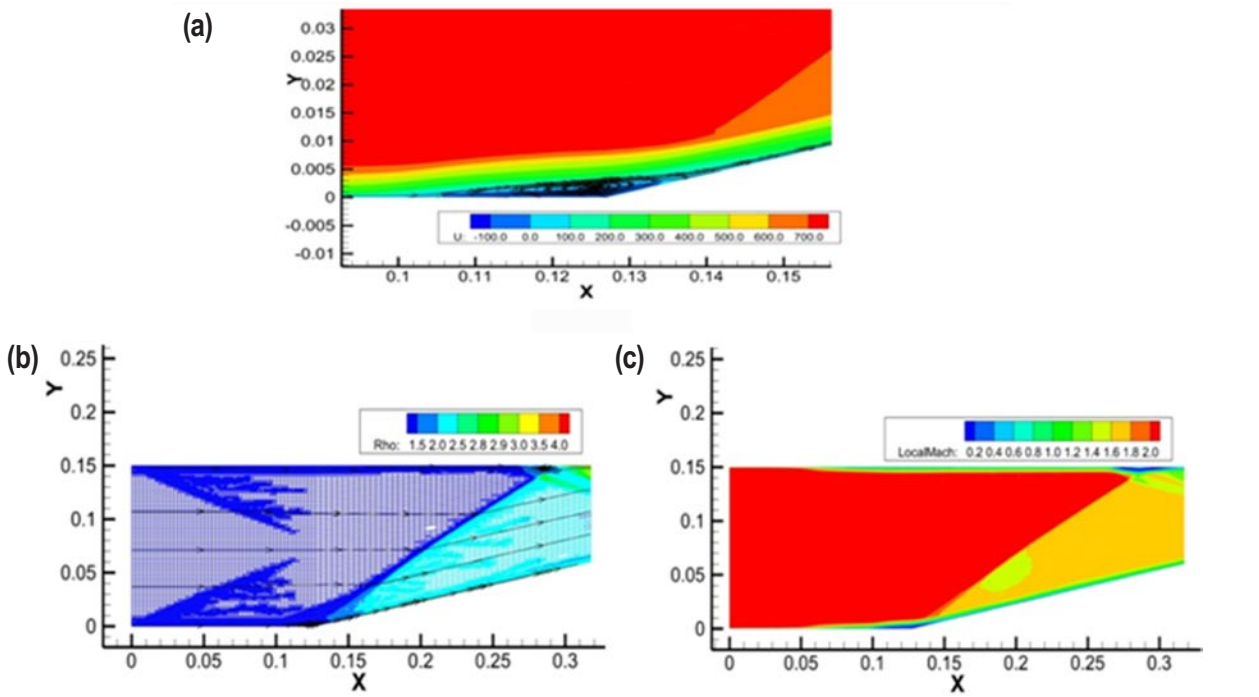

FIGURE 1. Mach 2.25 steady-state flow properties for 2-D supersonic viscous flow through a 18° compression ramp: a) recirculation, shock separation (distance in meters), b) density, c) local mach number.

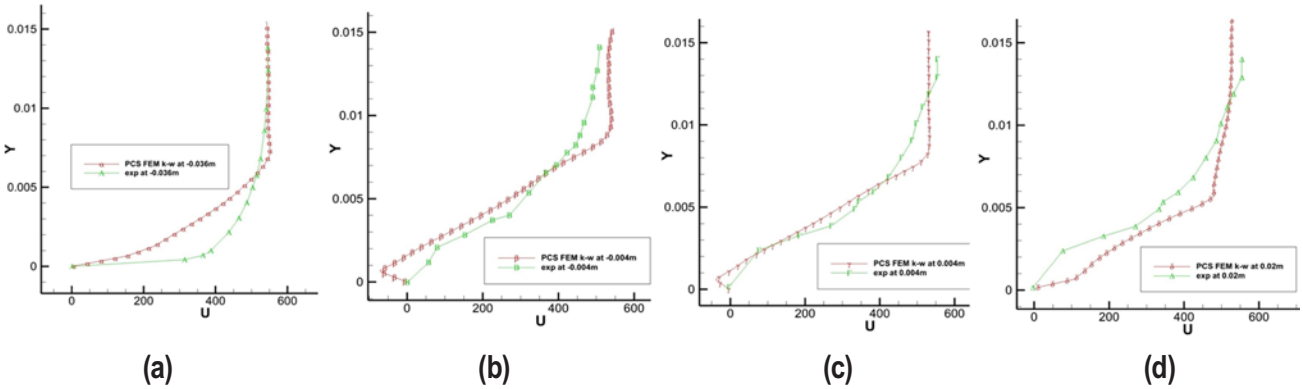

FIGURE 2. U (mean velocity) in bottom boundary layer using k-w 2-equation model. Comparison to data at various locations: upstream(-) and downstream(+) of the ramp a) -0.032 m, b) -0.004 m, c) +0.004 m, and d) +0.02 m.

in the neighborhood of 4,000 parcels for about 200,000 droplets being represented.

In 2012, we completed the 2-D local ALE method as shown in Figure 6 with its 2nd order error convergence property. The local ALE scheme uses overset grids for immersed parts described by their boundaries which overlays the fluid grid. The moving parts within the fluid are not taken into account during the grid generation process. Hence, ports and cylinder portions of the grid are continuously represented. Because of this feature, the system allows computer-aided design to grid in nearly a single step, providing nearly automatic grid generation.

The ALE system adjusts the grid locally as the parts move through the fluid, and maintains 2nd order spatial accuracy while never allowing the grid to tangle or producing an element that cannot be integrated accurately [7]. Since the fluid is represented continuously, fluxing of material through the grid as it is moves is not required. This need to flux through the grid is just one portion of the error when the usual ALE method is employed with finite volumes. Here the fluid solver remains Eulerian and the moving grid portions are no longer entwined with fluid solution. The extensible 2-D constructions are now facilitating development 3-D capability.

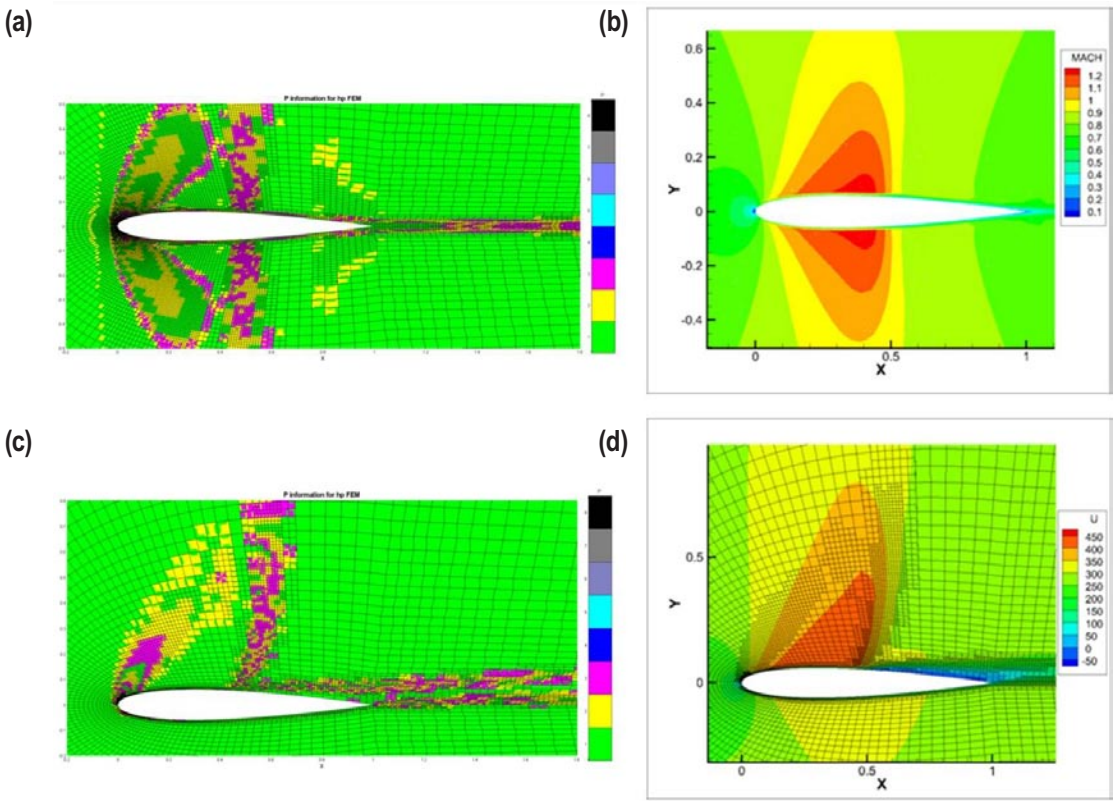

FIGURE 3. Transonic flow over an NACA 0012 airfoil using *hp*-adaptive PCS FEM: a) hp grid with colors showing order of approximation, b) Mach numbers, c) at 4° angle of attack (AOA), hp grid with colors showing order of approximation, d) at 4° AOA, U component of velocity.

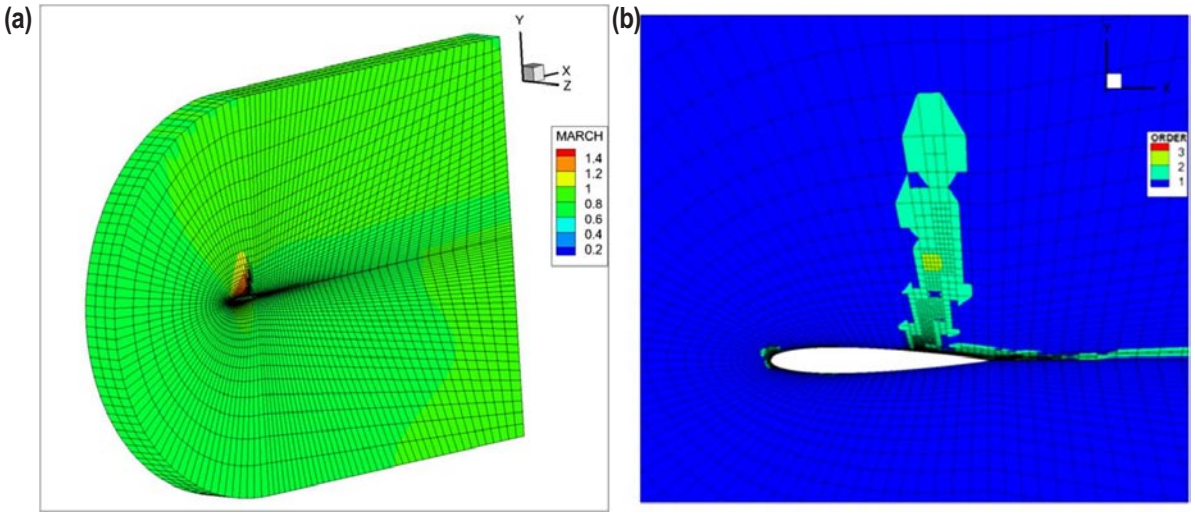

FIGURE 4. Transonic flow over a 3-D NACA 0012 airfoil at 4° AOA using hp-adaptive PCS FEM: a) Mach numbers, b) hp grid with colors showing order of approximation.

Error for this formulation against an analytic solution for flow between two separating plates, is a fraction of a percent, nearly exact. The method has a little better than 2nd order spatial convergence as shown in Figure 6a. In Figure 6b, a 2-D piston is shown with fluid intake through a port. The solution is performed for incompressible flow to facilitate development and validation.

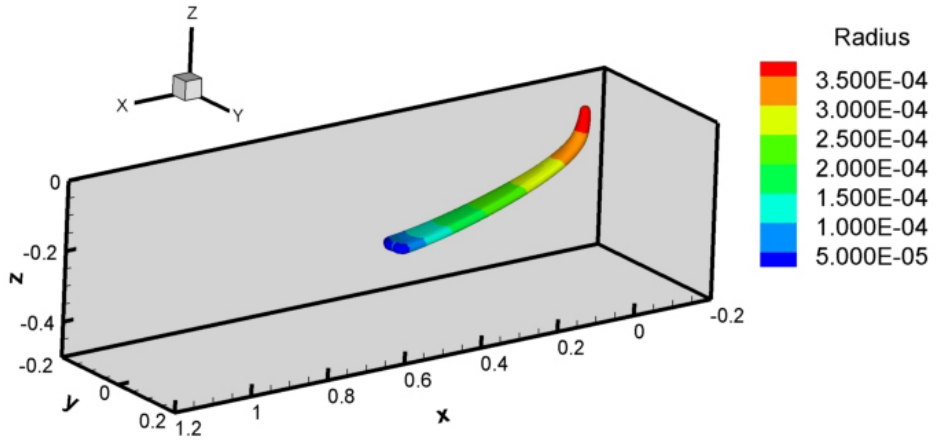

FIGURE 5. Injection and spray modeling test case for PCS FEM. Diesel spray modeling, droplet breakup and agglomeration showing complete evaporation.

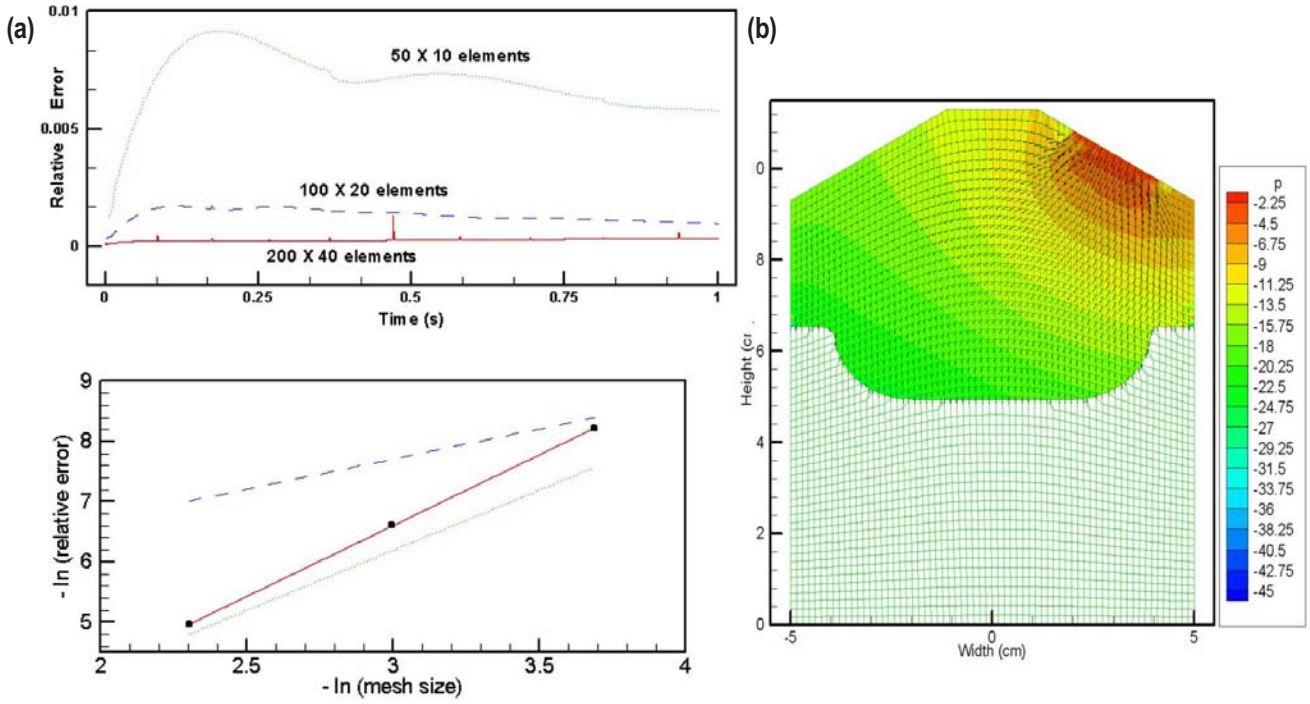

FIGURE 6. a) Convergence rate for analytic expanding channel benchmark. The blue squares are the calculated average errors; the slope of the solid line is 2.25, b) Simulation showing pressure and velocity vectors of a 2-D engine with ports.

Use of Cubit [http://cubit.sandia.gov/] for engine grid generation is being investigated. Once the commands (technology) are implemented in script, the grid generation process is automatic. This work supports our effort to produce hexahedral grid generation that is essentially automatic. Because the FEM grid is designed for use with the overset grid scheme, it is much easier to produce a grid nearly automatically than it is for the current KIVA-4 unstructured grid code that utilizes a grid snapping system. The developers of Cubit, in particular, one of their partners, CSIMSOFT Inc. is working to support KIVA-4 grid output in Cubit, based on the LANL file converter, Cubit2KIVA. We also are supporting the Gambit grid generator in the software.

Conclusions

In FY 2102, we continue to advance the accuracy, robustness, and range of applicability internal combustion engine modeling algorithms and coding for

engine simulation. We have performed the following to advance the state of the art:

1. Development of an *hp*-adaptive PCS FEM for all for flow regimes, with some compressible flow verification and validation.
2. Development of new method for immersed moving parts, extending the 2-D method to 3-D.
3. Incorporating the KIVA spray model into the *hp*-adaptive PCS FEM solver.
4. Incorporated the KIVA reactive chemistry model into PCS FEM solver.
5. Work on parallel solution process with the *hp*-adaptive FEM continues.

References

1. Carrington, D.B., (2011) "A Fractional step hp-adaptive finite element method for turbulent reactive flow," Los Alamos National Laboratory Report, LA-UR-11-00466.

2. Carrington, DB., Wang, X. and Pepper, D. W. (2012), A predictor-corrector split projection method for turbulent reactive flow, accepted Journal of Computational Thermal Sciences, Begell House, Inc.

3. Wang, X., Carrington, D.B., Pepper, D.W., An adaptive FEM model for unsteady turbulent convective flow over a backward-facing step, Journal of Computational Thermal Sciences, Begell House Inc. (2009).

4. Vallet, I., Reynolds-stress modeling of M=2.25 shock-wave/turbulent boundary-layer interaction, Int. J. Numer. Meth. Fluids, vol. 56, Wiley, p. 525-555 (2008).

5. Dukowicz, J.K., A particle-fluid numerical method for liquid sprays, JCP, Academic Press, vol. 35, no. 2, p. 229-253 (1980).

6. Torres, D.J., O'Rourke, P.J., Amsden, A.A., A discrete multicomponent fuel model, Atomization and Sprays vol.13, iss.2-3, p.131-172, (2003) .

7. Carrington, D.B., Munzo, D.A., Heinrich, J.C (2012), A local ALE for flow calculations in physical domains containing moving interfaces, submitted to Advances in Computational Fluid Dynamics, Hindawi.

FY 2012 Publications/Presentations

1. Carrington, D.B., Wang, X. and Pepper, D.W. (2012), A predictor-corrector split projection method for turbulent reactive flow, submitted to Journal of Computational Thermal Sciences, Begell House, Inc.

2. Carrington, D.B., Munzo, D.A., Heinrich, J.C (2012), "A local ALE for flow calculations in physical domains containing moving interfaces," submitted to Advances in Computational Fluid Dynamics, Hindawi.

3. Carrington, D.B., "A Fractional step *hp*-adaptive finite element method for turbulent reactive flow," Los Alamos National Laboratory Report, LA-UR-11-00466, 2011.

4. Carrington, D.B., Wang, X., Pepper, D.W., "An h-Adaptive Finite Element Method for Turbulent Heat Transfer," Computer Modeling in Engineering & Sciences, Tech Science Press, vol. 61, no 1, pp. 23-44, 2010.

5. Carrington, D.B., Wang, X. Pepper, D.W., "An h-Adaptive Finite Element Method for Turbulent Heat Transfer," *International Conference on Computational and Experimental Engineering and Sciences*, Las Vegas, NV, March 23, LA-UR 10-01692, 2010.

6. Wang, X, Carrington, D.B., Pepper, D.W., "An Adaptive FEM Model for Unsteady Turbulent Convective Flow Over a Backward-Facing Step," Journal of Computational Thermal Sciences, Begell House Inc., vol. 1, no. 2, pp. 121-135, 2009.

Special Recognitions & Awards/Patents Issued

1. Outstanding Innovation Award – 2011 Distinguished Licensing Award. Awarded by Los Alamos National Laboratory Technology Transfer Division, August 9th, 2012.

II.12 Chemical Kinetic Models for HCCI and Diesel Combustion

William J. Pitz (Primary Contact),
Charles K. Westbrook, Marco Mehl,
S. Mani Sarathy
Lawrence Livermore National Laboratory (LLNL)
P.O. Box 808, L-372
Livermore, CA 94551

DOE Technology Development Manager:
Gurpreet Singh

Overall Objectives

- Develop detailed chemical kinetic models for fuel components used in surrogate fuels for compression ignition (CI), homogeneous charge compression ignition (HCCI) and reactivity controlled combustion ignition (RCCI) engines.
- Combine component models into surrogate fuel models to represent real fuels. Use them to model low-temperature combustion strategies in HCCI, RCCI, and CI engines that lead to low emissions and high efficiency.

Fiscal Year (FY) 2012 Objectives

- Develop a chemical kinetic model for a larger alkyl aromatic.
- Develop more accurate surrogate kinetics models for gasoline.
- Develop a reduced surrogate mechanism for diesel to be used for multidimensional computational fluid dynamics (CFD) simulations.
- Develop a functional group method to represent cycloalkanes in diesel fuel.
- Validate and improve 2- and 3-methyl alkanes mechanisms with new data from shock tubes and jet-stirred reactors.

Accomplishments

- Validated an approach to formulate gasoline surrogate fuels and a predictive chemical kinetic model for a gasoline surrogate fuel.
- Developed chemical kinetic model for a larger aromatic, a major chemical class in diesel fuel.
- Developed a model for 3-methylheptane, an iso-alkane, that includes low-temperature chemistry. Determined the effect of branching of iso-alkanes on ignition under engine conditions.
- Developed a reduced chemical kinetic model for diesel for the Engine Combustion Network.
- Developed a functional group method for alkyl-cyclohexanes that greatly reduces the size of the chemical kinetic mechanism.

Future Directions

- Continue to develop detailed chemical kinetic models for larger alkyl aromatics.
- Develop an improved 2-component surrogate mechanism for diesel to be used for multidimensional CFD simulations.
- Develop more accurate surrogate kinetics models for gasoline fueled HCCI including ethanol or exhaust gas recirculation.
- Determine the role of C=C double bonds in the ignition behavior of C10 straight-chain hydrocarbons.
- Develop improved chemical kinetic models for methyl cyclohexane and a preliminary detailed model for n-butyl cyclohexane.

Introduction

Predictive engine simulation models are needed to make rapid progress towards DOE's goals of increasing combustion engine efficiency and reducing pollutant emissions. These engine simulation models require chemical kinetic submodels to allow the prediction of the effect of fuel composition on engine performance and emissions. Thus chemical kinetic submodels for conventional and next-generation transportation fuels need to be developed to fulfill these requirements.

Approach

Gasoline and diesel fuels consist of complex mixtures of hundreds of different components. These components can be grouped into chemical classes including n-alkanes, iso-alkanes, cycloalkanes, alkenes, oxygenates, and aromatics. Since chemical kinetic models cannot be developed for hundreds of components, specific components need to be identified to represent each of these chemical classes. Then detailed chemical kinetic models for these selected components can be developed. These component models are subsequently merged together to produce a "surrogate" fuel model for gasoline, diesel, and next-generation transportation fuels.

This approach can create realistic surrogates for gasoline or diesel fuels that reproduce experimental behavior of the practical real fuels that they represent. Detailed kinetic models for surrogate fuels can then be simplified as needed for inclusion in multidimensional CFD models or used in full detail for purely kinetic modeling.

Results

We have developed a new approach for formulating surrogates for gasoline fuels [1]. This approach matches the reactivity of the gasoline fuel in the negative temperature coefficient (NTC) regime which is essential for predicting the low and intermediate temperature heat release for gasoline fuels in HCCI engines. We have recently validated this approach in fundamental combustion devices by comparing a gasoline surrogate model and the actual gasoline surrogate to a real gasoline fuel [2,3]. The comparisons were done in a rapid compression machine and shock tube which simulate conditions in an internal combustion engine. In Figure 1, a comparison of the predicted ignition delay times using the gasoline surrogate model are made to the experimentally measured ignition delay times in a rapid compression machine and a shock tube [2]. This and other validations show that the approach we use to formulate a surrogate and its associated chemical kinetic surrogate model provides an accurate description of the real gasoline fuel.

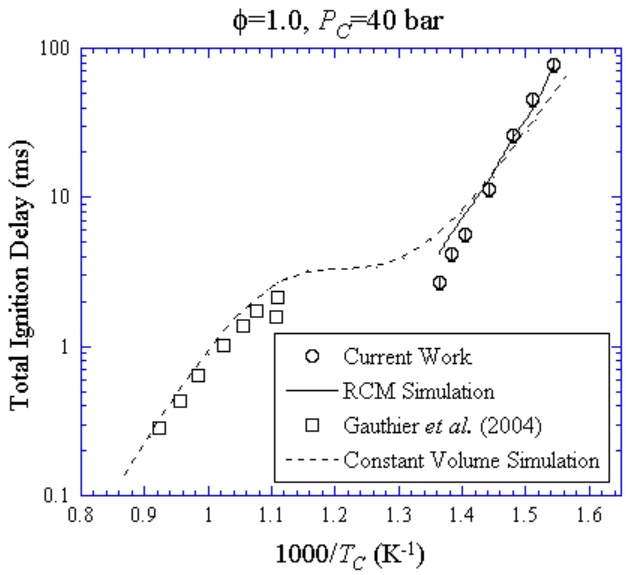

FIGURE 1. Comparison of ignition delays times for the detailed chemical kinetic surrogate model and a real gasoline for stoichiometric fuel/air mixtures at 40 bar in a shock tube [10] and in an RCM [2]. The constant volume simulation (dashed line) corresponds to the shock tube measurements (squares) and the rapid compression machine simulation (solid line) corresponds to the rapid compression machine measurements (circles).

Iso-alkanes are present in diesel fuel in large concentrations [4] and are a chemical class that needs to be represented in a diesel surrogate model to correctly predict ignition properties. During FY 2012, we extended a model for 3-methyl heptane to include low-temperature chemistry important for ignition in diesel and HCCI engines. We then validated our model under conditions in a high-pressure jet stirred reactor [5] and a shock tube [6]. The comparisons in these devices were performed at elevated pressures and covered a wide temperature regime including the NTC regime. Figure 2 shows a comparison of simulated and measured species concentrations from low to high temperature in a jet stirred reactor at 10 atm with a stoichiometric mixture of 3-methylheptane. Figure 3 shows simulated ignition delay times using LLNL models for four different alkane isomers, including 3-methylheptane, compared with experimental measurements in a high-pressure shock tube. The agreement between the model and experiments is reasonable. For the ignition comparison, the simulations and experiments show that ignition of iso-alkanes is dependent on both the position and on the number of the methyl branches. Specifically, ignition is inhibited by adding more methyl branches to the carbon chain and by shifting of the methyl branch from the second (2mhp) to the third (3mhp) position.

In FY 2012, we expanded our capability to model larger alkyl-aromatics and developed chemical kinetic models for n-propyl – and n-butyl – benzene. These alkyl aromatics are of the carbon size range important for diesel fuels. In collaboration with Dr. Curran's group at the National University of Ireland Galway, we validated our models in a shock tube and rapid compression machine that simulated conditions in internal combustion engines. Because alkyl-benzenes are mixed with other components in real fuels, we also validated our model

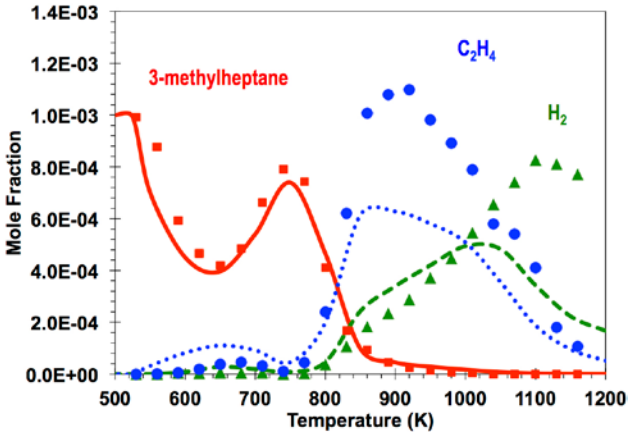

FIGURE 2. Simulated (curves) and experimental species profiles (symbols) for a stoichiometric mixture of 3-methylheptane in a jet stirred reactor at 10 atm and a residence time of 0.7 sec [5].

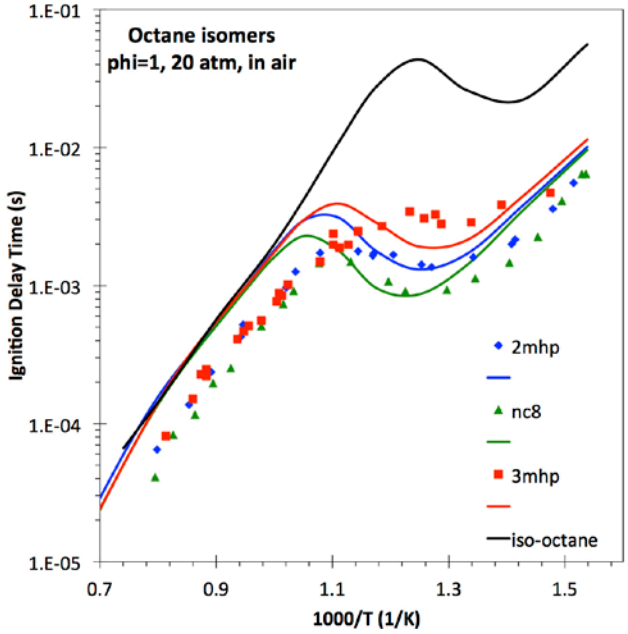

FIGURE 3. Comparison of simulated (curves) and measured (symbols) ignition delay times for four C8 alkanes in a shock tube and a rapid compression machine [6]. The pressure is 20 atm and the fuel/air mixtures are stoichiometric. (nc8 is n-octane, 2mhp is 2-methylheptane and 3mhp is 3-methylheptane. There are no experimental data for iso-octane available at these conditions).

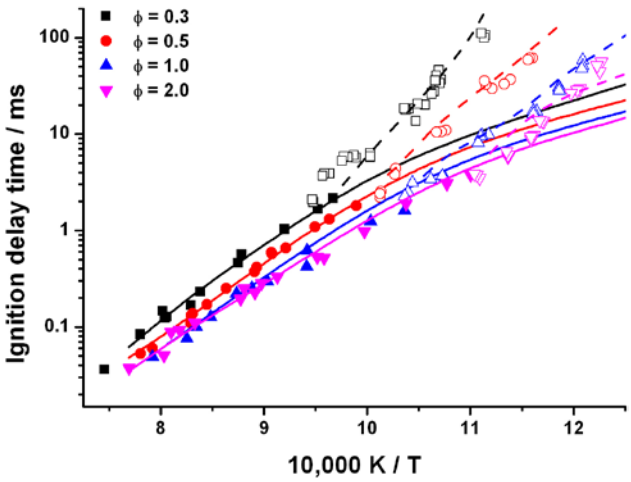

FIGURE 4. The ignition of n-propylbenzene in a shock tube at 30 atm over a range of equivalence ratios. The shock tube simulations correspond to solid lines and the measurements to filled symbols. The RCM simulations correspond to dashed lines and the measurements to open symbols.

for a mixture of n-propylbenzene with n-heptane [7]. For pure n-propylbenzene, the results using the model under typical engine conditions are shown in Figure 4 and compared to ignition delay times measured in a shock tube at 30 atm. The agreement with the experimental data is excellent across a wide range of temperatures and equivalence ratios. Our goal for FY 2013 is to expand our capabilities further into the diesel range of aromatic compounds.

Chemical kinetic models for real fuels need to be reduced in size to allow their use in CFD engine simulation codes. In FY 2010, we developed a new approach called the functional group approach that greatly reduces the size of a chemical kinetic fuel mechanism and its accompanying computational requirements. In FY 2010-11, we applied this method to the case of n-alkanes and iso-alkanes which allowed the reduction of the mechanisms by factors of about 30 in number of species, which greatly reduces the computer resources required to run them in CFD models. In FY 2012, we developed a functional group approach for cyclohexanes with an n-alkyl group attached to the ring. These cycloalkanes are typical of the type present in diesel fuel. We used this functional group approach to simulate the ignition behavior of n-butyl cyclohexane. We compared these preliminary results to ignition times experimentally measured by University of Ireland Galway in a shock tube over a wide range of temperatures and equivalence ratios at 30 atm. The comparison of the simulations and experiments was reasonable, but simulated ignition delay times were a factor of 2-3 too long, so that some model improvements need to be made.

We also developed a reduced model for surrogate diesel fuel in collaboration with Dr. Som at Argonne National Laboratory and Prof. Lu at University of Connecticut. We assisted in the development a reduced mechanism for n-dodecane and in the simulation of the ignition and stabilization of a diesel spray in a constant volume combustion chamber [8]. N-dodecane was selected as a target diesel surrogate compound by the Engine Combustion Network [9], a collaboration of international researchers in engine combustion. In the reduced mechanism, the number of species was reduced by a factor of 27 compared to the detailed mechanism, which greatly minimized the computational resources needed to run the model in an engine simulation code. Figure 5 shows a comparison of results from the LLNL detailed chemical kinetic model and the reduced mechanism. It shows that the reduced model well reproduces ignition delay times computed by the detailed mechanism over a wide range of temperature and pressure important for diesel combustion.

Conclusions

- We have extended our detailed kinetic modeling capabilities to the higher molecular-weight alkylated aromatics of n-propyl- and n-butyl-benzene, which are important compounds for diesel fuel.

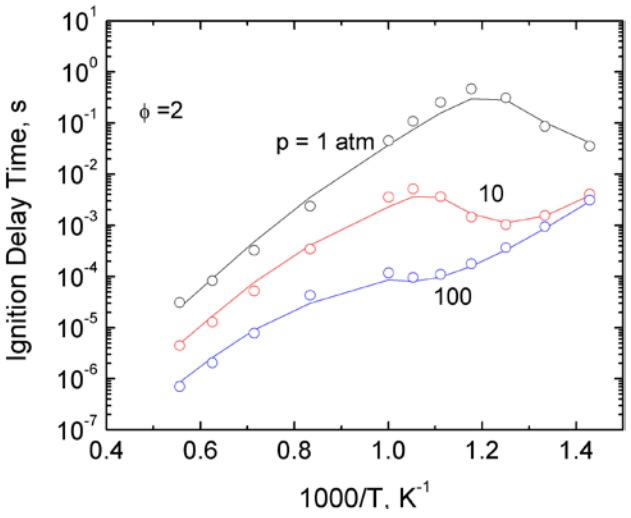

FIGURE 5. Comparison of ignition delay times computed with the reduced mechanism (circles) and the detailed mechanism (lines) for n-dodecane. The comparison is for a wide range of temperatures, a fuel-rich equivalence ratio of 2 and pressures of 1, 10, and 100 atm [8].

- We extended our 3-methyl heptane model, a representative compound for iso-alkanes in transportation fuels, to include low-temperature chemistry important for diesel ignition. We validated model by comparison to high pressure ignition data in a shock tube and to measured species profiles in a jet-stirred reactor.
- We have used the LLNL functional group approach to develop a preliminary mechanism for a series of n-alkyl-cyclohexanes that reduces the number of species by about a factor of 30 compared to a conventional detailed mechanism.
- With Argonne National Laboratory and University of Connecticut, we developed a reduced model for n-dodecane to be used as a surrogate for diesel fuel in multidimensional engine codes.

References

1. M. Mehl, J.Y. Chen, W.J. Pitz, S.M. Sarathy and C.K. Westbrook, "An approach for formulating surrogates for gasoline with application towards a reduced surrogate mechanism for CFD engine modeling," *Energy & Fuels* 25, 5215-5223 (2011).

2. G. Kukkadapu, K. Kumar, C.-J. Sung, M. Mehl and W.J. Pitz, "Experimental and surrogate modeling study of gasoline ignition in a rapid compression machine," *Combust. Flame* 159 (10) (2012) 3066-3078.

3. G. Kukkadapu, K. Kumar, C.-J. Sung, M. Mehl and W.J. Pitz, "Autoignition of gasoline and its surrogates in a rapid compression machine," *Proc. Combust. Inst.*, in press (2012).

4. W.J. Pitz and C.J. Mueller, "Recent progress in the development of diesel surrogate fuels," *Prog. Energy Combust.* 37 (3) (2011) 330-350.

5. F. Karsenty, S.M. Sarathy, C. Togbe, C.K. Westbrook, G. Dayma, P. Dagaut, M. Mehl and W.J. Pitz, "Experimental and Kinetic Modeling Study of 3-Methylheptane in a Jet-Stirred Reactor," *Energy & Fuels* 26 (8) (2012) 4680–4689.

6. W. Wang, Z. Li, M.A. Oehlschlaeger, D. Healy, H.J. Curran, S.M. Sarathy, M. Mehl, W.J. Pitz and C.K. Westbrook, "An experimental and modeling study of the autoignition of 3-methylheptane," *Proc. Combust. Inst.* In press, (2012).

7. D. Darcy, M. Mehl, J.M. Simmie, J. Wurmel, W.K. Metcalfe, C.K. Westbrook, W.J. Pitz and H.J. Curran, "An experimental and modeling study of the shock tube ignition of a mixture of n-heptane and n-propylbenzene as a surrogate for a large alkyl benzene," *Proc. Combust. Inst.,* in press, (2012).

8. Z. Luo, S. Som, S.M. Sarathy, M. Plomer, W.J. Pitz, D.E. Longman and T. Lu, "Development and Validation of an n-Dodecane Skeletal Mechanism for Diesel Spray-Combustion Applications," *Combustion Theory and Modelling* (2012), Submitted.

9. "Engine Combustion Network" http://www.sandia.gov/ecn/.

10. B.M. Gauthier, D.F. Davidson and R.K. Hanson, "Shock tube determination of ignition delay times in full-blend and surrogate fuel mixtures," *Combust. Flame* 139 (4) (2004) 300-311.

FY 2012 Publications/Presentations

1. M. Mehl, W.J. Pitz, S.M. Sarathy, C.K. Westbrook, H.J. Curran, "Modeling the combustion of high molecular weight fuels by a functional group approach", Inter. J. Chem. Kinet., 44 (4) (2012) 257-276.

2. M. Mehl, W.J. Pitz, J.E. Dec, Y. Yang, " Detailed Kinetic Modeling of Conventional Gasoline at Highly Boosted Conditions and the Associated Intermediate Temperature Heat Release", Society of Automotive Engineers, Paper SAE 2012-01-1109.

3. W. Wang, Z. Li, M.A. Oehlschlaeger, D. Healy, H.J. Curran, S.M. Sarathy, M. Mehl, W.J. Pitz and C.K. Westbrook, "An experimental and modeling study of the autoignition of 3-methylheptane," Proc. Combust. Inst., doi: 10.1016/j.proci.2012.06.001 (2012).

4. Kukkadapu, G., Kumar, K., Sung, C.-J., Mehl, M. and Pitz, W.J., "Autoignition of Gasoline and Its Surrogates in a Rapid Compression Machine," Proc. Combust. Inst., doi: 10.1016/j.proci.2012.06.135 (2012).

5. Karsenty, F., Sarathy, S.M., Togbe, C., Westbrook, C.K., Dayma, G., Dagaut, P., Mehl, M. and Pitz, W.J., "Experimental and Kinetic Modeling Study of 3-Methylheptane in a Jet-Stirred Reactor," Energy & Fuels 26 (8) (2012) 4680–4689.

6. Darcy, D., Mehl, M., Simmie, J.M., Wurmel, J., Metcalfe, W.K., Westbrook, C.K., Pitz, W.J. and Curran, H.J., "An Experimental and Modeling Study of the Shock Tube Ignition of a Mixture of N-Heptane and N-Propylbenzene as

a Surrogate for a Large Alkyl Benzene," Proc. Combust. Inst. doi: 10.1016/j.proci.2012.06.131 (2012).

7. Kukkadapu, G., Kumar, K., Sung, C.-J., Mehl, M. and Pitz, W.J., "Experimental and Surrogate Modeling Study of Gasoline Ignition in a Rapid Compression Machine," Combust. Flame 159 (10) (2012) 3066-3078.

8. Sarathy, S.M., C. Yeung, C.K. Westbrook, W.J. Pitz, M. Mehl and M.J. Thomson . "An experimental and kinetic modeling study of n-octane and 2-methylheptane in an opposed flow diffusion flame." Combust. Flame: 158 (7): 1277-1287, 2011.

9. S.M. Sarathy, C.K. Westbrook, M. Mehl, W.J. Pitz, C. Togbe, P. Dagaut, H. Wang, M.A. Oehlschlaeger, U. Niemann, K. Seshadri, P.S. Veloo, C. Ji, F. Egolfopoulos and T. Lu, "Comprehensive chemical kinetic modeling of the oxidation of 2-methylalkanes from C7 to C20," Combust. Flame 158 (12) (2011) 2338-2357 (2011).

10. M. Mehl, J.Y. Chen, W.J. Pitz, M.S. Sarathy, and C.K. Westbrook, "An approach for formulating surrogates for gasoline with application towards a reduced surrogate mechanism for CFD engine modeling", Energy & Fuels: 25 (11) 5215-5223, 2011.

11. C.J. Mueller, W.J. Cannella, T.J. Bruno, B. Bunting, H.D. Dettman, J.A. Franz, M.L. Huber, M. Natarajan, W.J. Pitz, M.A. Ratcliff and K. Wright, "Methodology for Formulating Diesel Surrogate Fuels with Accurate Compositional, Ignition-Quality, and Volatility Characteristics," Energy & Fuels 26 (6) (2012) 3284–3303.

12. D. Darcy, C.J. Tobin, K. Yasunaga, J. Simmie, J. Wurmel, S.S. Ahmed, T.X. Niass, C.K. Westbrook, and H.J. Curran, "A High Pressure Shock Tube Study of n-Propylbenzene Oxidation and its Comparison with n-Butylbenzene", Combust. Flame 159, 2219-2232 (2012).

13. McDonald, M.E., Davidson, D.F., Hanson, R.K., Pitz, W.J., Mehl, M., and Westbrook, C.K., "Formulation of an RP-1 pyrolysis surrogate from shock tube measurements of fuel and ethylene time histories", Fuel, doi: 10.1016/j.fuel.2012.10.008 (2012).

14. Westbrook, C.K., "Recent Advances in Autoignition Kinetics of Automotive Fuels", (invited plenary paper) COMODIA 2012, Fukuoka, Japan, July 23-26, 2012.

Special Recognitions & Awards/Patents Issued

1. S. Mani Sarathy, Postdoc Fellowship, Natural Sciences and Engineering Research Council of Canada, 4/2010 to 4/2012.

2. Charles K. Westbrook, President of the Combustion Institute, 2008-2012.

3. Charles K. Westbrook, Invited Plenary Lecture, The International Conference on Modeling and Diagnostics for Advanced Engine Systems (COMODIA), 2012, Fukuoka, Japan.

II.13 Free-Piston Electric Generator (FPEG)

Terry Johnson (Primary Contact) and
Mike Leick
Sandia National Laboratories
P.O. Box 969, MS 9661
Livermore, CA 94551-0969

DOE Technology Development Manager:
Gurpreet Singh

Subcontractor:
Ron Moses, Los Alamos, NM

Overall Objectives

- Study the effects of continuous operation (i.e. gas exchange) on indicated thermal efficiency and emissions of an opposed free-piston linear alternator engine utilizing homogeneous charge compression ignition (HCCI) combustion at high compression ratios (~20-40:1).
- Concept validation of passively synchronizing the opposed free pistons via the linear alternators, providing a low cost and durable design.
- Proof of principle of electronic variable compression ratio control, allowing optimized combustion timing and fuel flexibility, by means of mechanical control of bounce chamber air pressure.
- Provide a research tool to explore the free-piston engine operating envelope across multiple inputs: boost level, equivalence ratio, alternative fuels.

Fiscal Year (FY) 2012 Objectives

- Install magnets on piston assembly and pulse pistons to show stabilizing effect of alternators.
- Initially run the engine under motoring mode only to test capability for continuous piston motion synchronization.
- Perform combustion experiments and measure indicated thermal efficiency at various compression ratios and equivalence ratios with hydrogen.

Accomplishments

- Permanent magnet arrays assembled and incorporated into piston bodies.
- Compressed helium gas injection starting system tested to show capability to bring pistons to desired operating compression ratio in one stroke with good piston synchronization.
- Modeling and experiments with piston pulsing showed deficiency in bounce chamber vent manifolds. Vent manifolds re-designed, fabricated and demonstrated with improved performance.
- Modeling and experiments with piston pulsing showed deficiency in bounce chamber high pressure gas delivery heads. Heads, manifolds and valve plates re-designed, fabricated and demonstrated with improved performance.
- High pressure nitrogen system assembled to replace air compressor system to extend pressure and flow rate capability for motoring mode.
- Short duration (~1.5 second) motoring demonstrated with good piston synchronization. Barriers to continuous motoring identified and engineering solutions developed and in-progress to address them.
- Significant progress toward hydrogen combustion experiments:
  - Hydrogen fuel injectors and flow meter experimentally evaluated and calibrated.
  - Combustion exhaust analyses system assembled and calibrated.
  - Extensive safety analysis performed and approved through the Sandia environmental, safety and health site.
  - Hardware and software controls and safeguards developed for safe operation.
  - Hydrogen supply system hardware currently being installed.
- Modeling development continues to inform and guide design:
  - Thermodynamic model used to re-design bounce chamber vent system, design nitrogen system, and predict motoring performance.
  - Electromagnetic model used to understand effects of friction on piston stability and ways to improve stability. Also used to understand transition from motoring to combustion.

Future Directions

- Motor the engine continuously for tens of seconds to minutes at a time to assess piston synchronization, thermal response, and compression ratio control.
- Perform combustion experiments and measure indicated thermal efficiency and emissions at various

compression ratios and equivalence ratios with hydrogen and, resources permitting, natural gas.
- Characterize a new design for the pistons intended to reduce frictional losses and improve overall efficiency.
- Based on experimental results and modeling predictions, assess the overall engine design and performance with respect to the target fuel-to-electricity conversion efficiency of 50% at 30 kW output.

Introduction

As fuel efficiency of the typical American automobile becomes more important due to hydrocarbon fuel cost and availability issues, powertrain improvements will require smaller output engines combined with hybrid technologies to improve efficiency. In particular, the plug-in hybrid concept will require an electrical generator of approximately 30 kW output. Unfortunately, current crankshaft spark-ignition internal combustion engines with optimized power outputs of 30 kW have thermal efficiencies of less than 32%.

The free-piston generator of this project has a projected fuel-to-electricity conversion efficiency of 50% at 30 kW output. The project has progressed by conducting idealized combustion experiments, designing and procuring the linear alternators required for control and power conversion, and conducting computational fluid dynamics design of the inlet/exhaust processes. The current proof-of-concept engine was designed and fabricated based on this initial work. As it has been experimentally evaluated, the engine design has been improved to enable further evaluation of motoring control and eventually combustion efficiency.

Approach

By investigating the parameters unique to free-piston generators (linear alternator, opposed piston coupling, uniflow port scavenging) as separate entities, each piece can be used at its optimum design point. More importantly, upon assembly of a research prototype for performance demonstration (the goal of this project), understanding of the pieces in the device will allow the proper contribution of each component to the combined performance of the assembly.

Demonstration of the research prototype has been carried out in stages. First, synchronous starting of the opposed pistons was demonstrated followed by synchronous motoring. Modeling has been used to guide design modifications and experimental procedures leading to combustion.

Results

Figure 1 shows the Sandia FPEG research prototype. Bounce chamber cylinders, air injection valves, vent manifolds, and pistons were all obtained and fully assembled in FY 2011 except for the magnets. The permanent magnet arrays for the linear alternator were assembled on backirons and integrated with the pistons early this year. In addition, most of the air injection and bounce chamber vent system was redesigned and replaced this year, as will be described below. Instrumentation and data acquisition systems were also installed in FY 2011 and described in the FY 2011 report.

Following the magnet assembly tests were performed using the compressed helium starting system to drive the pistons to compression ratios in the intended operating range. Figure 2 shows an example He start test. The pistons are driven hard enough to achieve a significant compression ratio and bounce back far enough to actuate the air drive valves. However, in these initial tests the pins attached to the pistons to contact and actuate the valve plate were removed. With no further energy input, the piston motion decays due to friction and electromagnetic drag forces. These initial He start tests showed that the bounce chamber vent system was inadequate to handle the pressure and flow rate required from the air drive system to motor the pistons. Thus, the vent manifolds and downstream plumbing were redesigned and replaced. Figure 1 shows the new manifolds (1) with the inset showing the computer-aided design (CAD) model.

Initial air motoring that consisted of several cycles was achieved soon after the magnets were assembled. However, a number of improvements to the system were

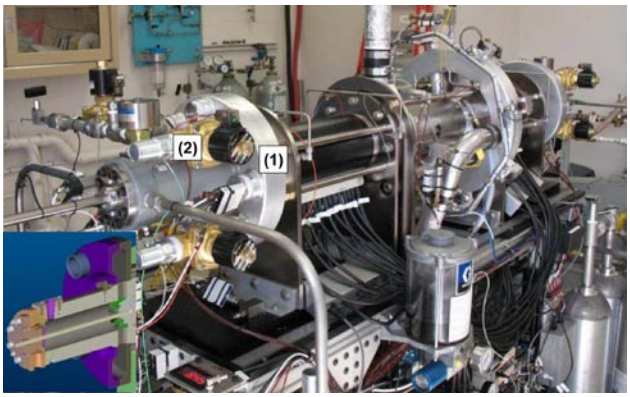

FIGURE 1. Sandia FPEG Research Prototype. Inset shows CAD model of redesigned bounce chamber vent manifold.

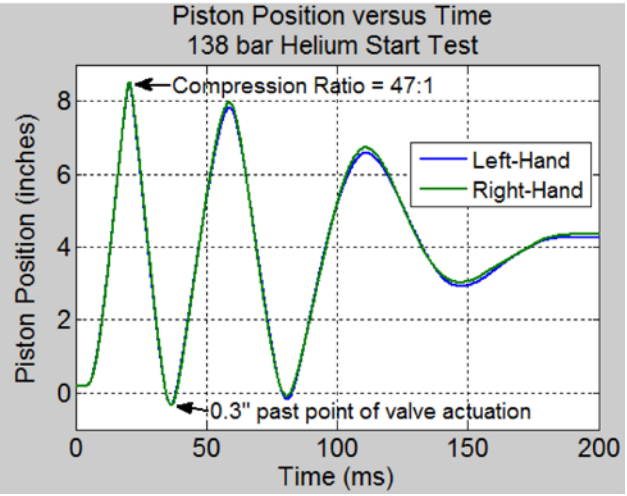

FIGURE 2. Example He start test.

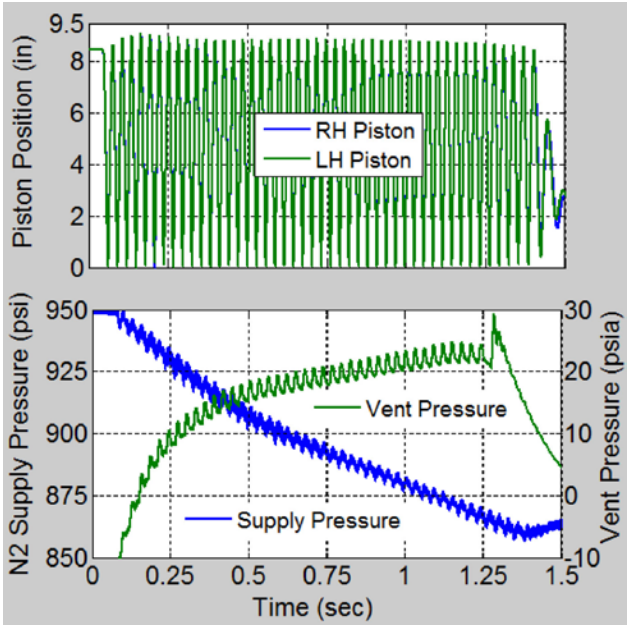

RH - right-hand; LH - left-hand

FIGURE 3. Example air motoring test. Piston position (top) referenced to the combustion chamber centerline. Nitrogen supply pressure and bounce chamber vent pressure (bottom).

required to enable continuous motoring. These included the addition of a high pressure nitrogen supply system to replace the insufficient air compressor and a redesign of the air drive supply plumbing, bounce chamber heads, valve plates, and piston pins. The nitrogen system can supply enough gas to run the system for 10 minutes continuously at our highest expected flow rate. Since our experiments will mostly be short duration (~1 min), 10 or more experiments can be run with each 16-pack of 1A cylinders. The 16-packs are easily swapped out and an extra one is always kept ready. For the bounce chamber heads, several iterations of the valve plate design finally produced plates that would seal robustly and were tough enough for continued actuation. The bounce chamber heads and piston pins were modified to increase the valve actuation travel. It was found through motoring experiments and modeling that allowing for valve actuation earlier in the return stroke and for an extended length would improve the stability of the piston motion. The redesigned bounce chamber heads and piston pins allow for nearly 1" of valve actuation.

The above modifications enabled one of the primary goals for FY 2012; continuous motoring. Figure 3 shows an example of a motoring test performed with the system. For this test, the nitrogen supply pressure was set to 950 psi and the test was initiated with a He start at 2,175 psi. The vent manifold is evacuated at the beginning of the test to facilitate venting the He and transitioning to nitrogen. As the test proceeds, the pressure in the vent manifold (shown in the lower plot of Figure 3) increases toward a steady-state value of ~21 psia. At the same time, the nitrogen supply pressure drops from the initial setpoint of 950 psi to about 860 psi. This drop in supply pressure is due to a slow response from the pressure regulator. The combination of increasing vent pressure and decreasing supply pressure causes the piston travel to decay until the point that the air valves are not actuated and the piston motion dies out, as shown in the top plot of Figure 3. This test, although quite short, demonstrates that continuous synchronous motoring of the pistons is possible. With an adjustment to the regulator control and reduction in the pressure drop through the vent manifold, the system will be motored for significantly longer.

Figure 4 shows the piston synchronization during this test. The piston separation, the difference in left and right piston position with respect to a perfect mirror image, is shown in the top plot. This separation never exceeds 0.25" and shows a beat pattern where the separation grows and shrinks repeatedly. The bottom plot in Figure 5 shows a simulation result that predicts qualitatively similar behavior. Based on the simulation results, the beat pattern is initiated by a difference in friction between the two pistons. However, as the separation grows, the electromagnetic drag on the pistons works to restore synchronous motion. This demonstration of passive synchronization through the linear alternator force is an important result in the development of the FPEG system.

For our motoring tests we measure the current produced in each of the 14 circuits that make up the linear alternator system. With these current measurements we can calculate the raw electrical power produced by the system. We can also calculate the pressure-volume work added to the system by the air drive system. With this information we can then perform energy balance

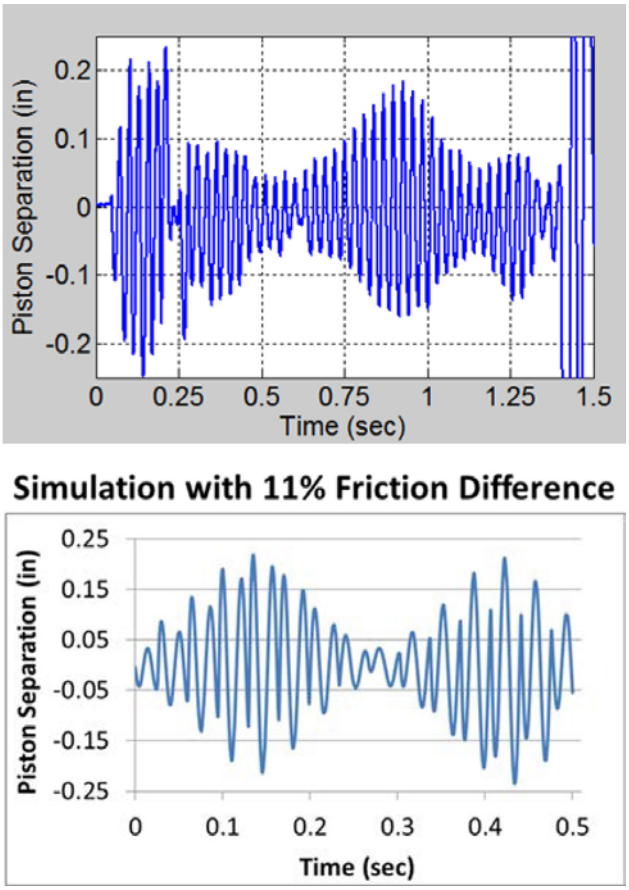

FIGURE 4. Piston separation during motoring showing passive synchronization through linear alternator electromagnetic drag force. Data from research prototype (top) and simulation result (bottom).

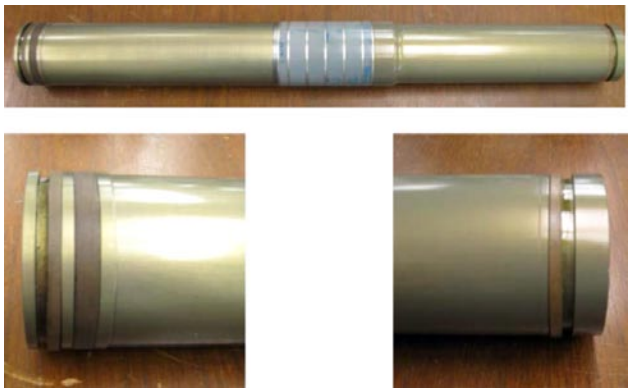

FIGURE 5. Piston compression rings cut in half to test for friction reduction.

calculations to determine the electrical efficiency achieved and energy loss mechanisms. For the example motoring run shown in Figure 3, the average power input from the air drive system was 43 kW. About 46% of that power was converted to electrical power. It is estimated that 16% is lost via heat transfer and gas blow-by in the combustion chamber and 38% is lost to friction between the pistons and the cylinder. With planned modifications to the system these loss terms should be reduced.

Actually, many of the challenges encountered this year in implementing the air drive system were a direct result of piston friction. Piston friction required high air drive pressures and flow rates to keep the pistons motoring. This, in turn, necessitated the nitrogen supply system and the vent system modifications. In addition, high frictional energy dissipation directly reduces the overall efficiency of the FPEG prototype. So, an effort was undertaken to reduce piston friction. The result was a redesign of the pistons to include modified compression rings and rider rings. It was found through experiment and modeling that sliding friction between the compression rings and the cylinder was the dominant factor. This force is proportional to the contact area. Thus, by cutting the ring width in half, friction could be reduced by up to a factor of two. This was confirmed through tests of the current pistons with the compression rings cut in half as shown in Figure 5. The new pistons will be ready for testing early in FY 2013.

Finally, significant progress toward hydrogen combustion experiments has been made this year. The hydrogen fuel injectors and flow meter were experimentally evaluated and calibrated. Figure 6 shows the results of fuel injector testing. It was found that repeatable control over hydrogen mass flow per pulse could be achieved by controlling injector pulsewidth with a stable upstream pressure. Also, injector-to-injector repeatability was found to be quite consistent. In addition, the combustion exhaust analyses system has been assembled and calibrated. An extensive safety analysis was performed for hydrogen combustion experiments and approved through the Sandia environmental, safety and health site. Hardware and software controls and safeguards have been developed for safe operation and the hydrogen supply system hardware is currently being installed. Initial hydrogen combustion experiments are scheduled for late November or early December.

Conclusions

- Synchronous piston start with required compression ratio and valve actuation achieved with He injection system.
- Stable piston motoring with air drive system achieved for short times (~1.5 seconds) demonstrates passive synchronization through linear alternator electromagnetic drag force.
- Barriers to continuous motoring identified and engineering solutions are in progress to address them.

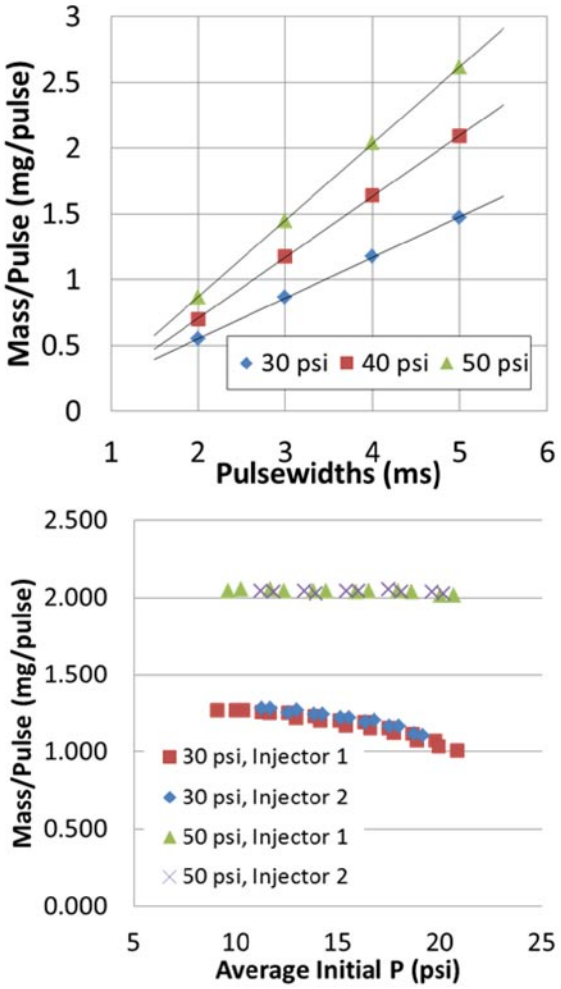

FIGURE 6. Hydrogen fuel injector test results demonstrate precise control capability and injector-to-injector repeatability.

- Modeling has been important to guide design decisions and understand experimental results.
- Preparation for hydrogen combustion experiments has been completed. Experiments will begin in late November or early December 2012.

FY 2012 Publications/Presentations

1. T.A. Johnson and M.T. Leick, "Free-Piston Engine", 2012 DOE Hydrogen and Vehicle Technologies Merit Review (Washington, D.C., May 2012).

II.14 Spray and Combustion Modeling using High-Performance Computing (HPC) Tools

Sibendu Som (Primary Contact),
Douglas E. Longman, Qingluan Xue
Argonne National Laboratory
9700 S Cass Ave
Argonne, IL 60439

DOE Technology Development Manager:
Gurpreet Singh

Overall Objectives

- Development of physics-based spray models which account for in-nozzle flow effects.
- HPC tool development on codes used by the industry for internal combustion engine (ICE) applications.
- Development and validation of reduced chemical-kinetic models for realistic diesel fuel surrogates.
- Development and validation of high-fidelity turbulence models for diesel engine applications.

Fiscal Year (FY) 2012 Objectives

- Develop spray and combustion models, HPC tools and implement in CONVERGE code [1] since this is used extensively by the industry.
- Demonstrate grid-convergence on diesel spray and engine simulations to improve the fidelity of the calculations.
- Implement advanced load-balancing algorithms to improve scaling efficiency on a large number of cores and demonstrate scalability on ~500 processors.
- Develop and validate a reduced chemical kinetic mechanism using n-dodecane as a surrogate for diesel fuel.

Accomplishments

- Lagrangian droplet models are widely used for engine simulations. However many researchers have reported a strong dependency on the grid size. This large grid size dependency makes it difficult for modelers to know ahead of time what cell size to utilize. We have recently demonstrated grid-convergence on diesel spray and engine simulations.
- Typical production type engine simulations in the industry are performed on 16-32 processors. We have performed engine simulations on 512 processors in a scalable fashion. These simulations were performed with a peak cell-count of 34 million cells, which is the largest diesel engine simulation run till-date. This simulation provided unprecedented insights into the combustion process. We have also demonstrated that detailed chemistry based combustion models are grid-convergent and hence more reliable than simplified combustion models.
- We have developed and validated a 106 species-based reduced reaction model for n-dodecane as a surrogate for diesel fuel. This mechanism is being used by industry and academia extensively through the Engine Combustion Network (ECN) led by Sandia National Laboratories.

Future Directions

- Existing HPC simulations have been performed on single-cylinder engines. Future studies will involve simulation of multi-cylinder engines which will require 1,000s of processors.
- Implement and validate high fidelity large eddy simulation (LES)-based turbulence models. Demonstrate grid-convergence on LES studies.
- Further development of KH-ACT model [2] by dynamically coupling nozzle flow and spray simulations.
- Develop and validate a two-component surrogate (n-dodecane and m-xylene) mechanism for diesel fuel.

Introduction

ICE processes are multi-scale and highly coupled in nature and characterized by turbulence, two-phase flows, and complicated spray physics. Furthermore, the complex combustion chemistry of fuel oxidation and emission formation makes engine simulations a computationally daunting task. However, given the cost for performing detailed experiments spanning a wide range of operating conditions and fuels, computational fluid dynamics (CFD) modeling aided by HPC has the potential to result in considerable cost savings. Development of physics-based CFD models are necessary for predictive simulations of the ICE. HPC can play an important role in ICE development by reducing the cost for design and optimization studies. This is largely accomplished by

being able to conduct detailed simulations of complex geometries and moving boundaries with high-fidelity models describing the relevant physical and chemical interactions, and by resolving the relevant temporal and spatial scales. These simulations provide unprecedented physical insights into the complex processes taking place in these engines, thus aiding designers in making judicious choices. The major focus of our research in FY 2012 has been towards the development and validation of robust and predictive models for diesel engine applications aided by HPC tools.

Approach

During the past year, we have focused on improving the fidelity of engine simulations by using higher temporal and spatial resolutions. A key element in our research has been to demonstrate grid-convergence on diesel spray and engine simulations [3]. The following approach has been implemented in CONVERGE code and is critical to achieving grid convergence:

1. Adaptive mesh refinement – Demonstration of grid convergence can only be accomplished if cell sizes below the point of convergence can be simulated. Adaptive mesh refinement allows the use of a very fine grid in the vicinity of the spray while keeping the overall cell count relatively low.
2. Fully implicit momentum coupling – Grid convergence cannot be adequately demonstrated if running with a fine mesh causes numerical instabilities. Previous studies have suffered from such instabilities when the cell size was on the order of the nozzle diameter or smaller. The current methodology utilizes a fully implicit liquid-gas momentum coupling approach to keep the simulations stable in the presence of small cells and high liquid volume fractions
3. Improved liquid-gas coupling – The current methodology utilizes a Taylor series expansion to calculate the gas-phase velocity in the liquid-gas coupling calculations. Use of the Taylor series expansion significantly reduces grid artifacts on the spray over traditional "nearest node" coupling approaches.
4. Temporal and spatial liquid mass distribution – When refining the mesh around a spray, a common error is to keep the total number of injected parcels over the injection duration constant. This can result in the undesirable behavior of ever increasing liquid penetration from successive refinements of the mesh. When the mass in a cell is small compared to the mass of a parcel, the amount of momentum in the liquid is enough to quickly bring the cell's velocity up to the liquid velocity. As a result, there is minimal or no drag on the parcel's drops outside of the core of the spray, resulting in excessive penetration. To remedy this issue, the current approach significantly increases the injected number of parcels as the embed scale is increased. Similar undesirable behavior can occur when a point source injection is used with a fine mesh. In the current approach, the liquid mass is injected within a circle instead of at a point source. The radius of the circle is equal to the nozzle radius.

In order to improve the load-balancing capability in CONVERGE, METIS [4] was chosen to replace the original algorithm. METIS is widely known for its efficiency in partitioning complex geometries and its capabilities to minimize the connectivity and to enforce contiguousness between partitions.

Results

Some critical findings associated with the four different objectives for FY 2012 highlighted before are discussed here. Further details can be obtained from the authors' publications in FY 2012.

Figure 1 plots the cell count on each processor with and without METIS for the 0.5 mm grid resolution case, run on 256 cores i.e., 32 compute nodes. The improvement in load-balancing due to METIS implementation can be observed. For example, the maximum number of CFD cells on a single processor without METIS is 17,136, whereas the minimum value is 0. The corresponding values with METIS are 7,953 and 3,805 respectively. Clearly, the load balance

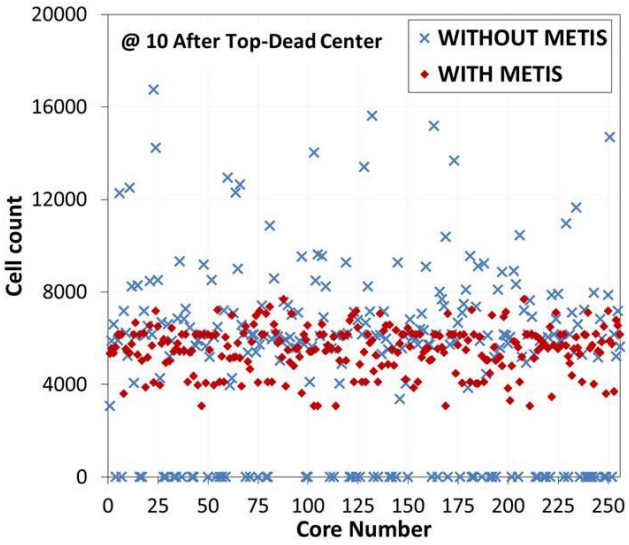

FIGURE 1. Comparison of number of CFD cells on each core with and without METIS implementation for a closed-cycle diesel engine simulation.

improves significantly with METIS, which also improved speedup on high number of cores. This project was done in collaboration with Convergent Science Inc., and Caterpillar Inc.

Figure 2 plots the temperature distributions on a cut-plane for the simplified (CTC) and detailed chemistry-based (SAGE) combustion models for three different grid resolutions (0.5 mm, 0.25 mm, and 0.125 mm) on a cut-plane at 13° crank angle (CA) after top-dead center (ATDC). The temperature distribution for the CTC model is significantly different for the three grid resolutions investigated. The temperature distributions on this cut-plane for the SAGE model seem grid-convergent since the contours for 0.25 mm and 0.125 mm are similar. The results with the SAGE model were also grid-convergent for several other performance and emission parameters of interest. It should be noted that the 0.125 mm simulation was run on 34 million cells which to the best of our knowledge is the largest CFD simulation of a diesel engine.

Figure 3 presents the influence of grid size on the temperature, OH mass fraction, and equivalence ratio contours for the reacting spray cases at an ambient oxygen concentration of 21% similar to the ECN conditions [5]. The flame structure in terms of temperature, OH mass fraction and equivalence ratio is distinctly different between the 1-mm case and the other grid sizes. The flame is observed to propagate further upstream and the flame length is also longer for the 1-mm case. In general, the flame length is seen to decrease with decreasing cell size. The contour plots of 0.25-mm and 0.125-mm cases look quite similar, further demonstrating grid convergence for the combustion spray simulations.

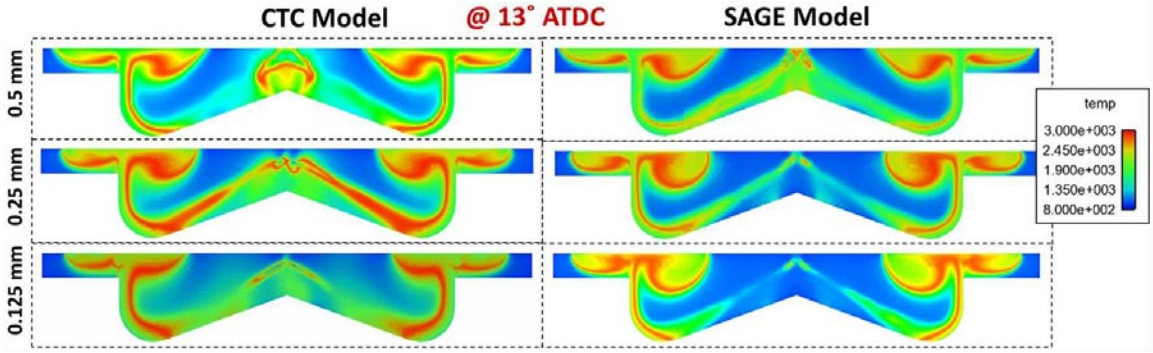

FIGURE 2. Comparison of temperature contours at 13°CA ATDC between simplified (CTC) and detailed chemistry-based (SAGE) combustion models for three different minimum grid sizes for a closed-cycle Caterpillar single-cylinder diesel engine simulation.

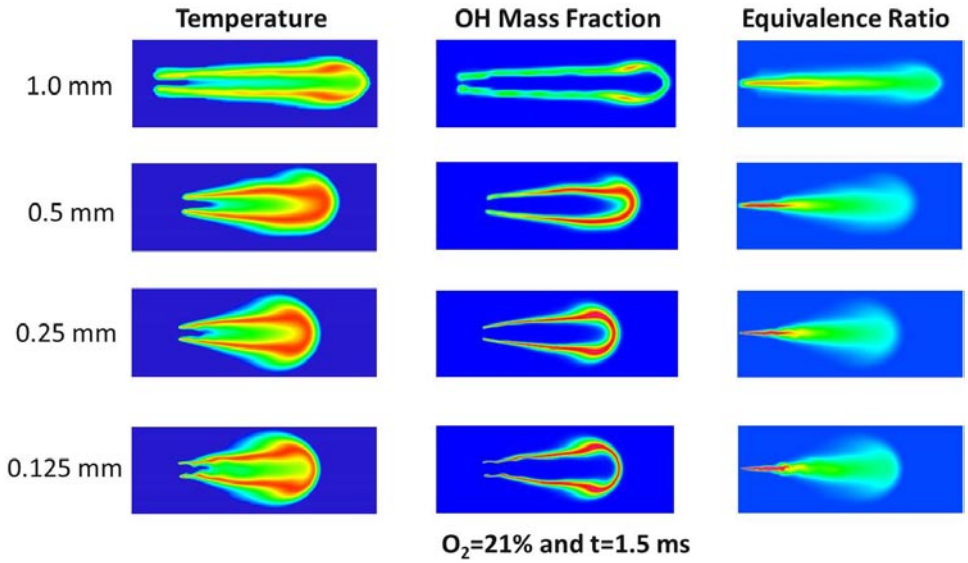

FIGURE 3. Comparison of temperature, OH mass fraction, and equivalence ratio for different minimum cell sizes. The simulations are performed in a constant volume combustion chamber mimicking the ECN experimental conditions [5] for n-heptane fuel.

Figure 4 presents a comparison of the measured [5] and predicted flame lift-off length (LOL) and ignition delay as a function of ambient temperature for a reduced 106 species n-dodecane mechanism developed in collaboration with Lawrence Livermore National Laboratory and University of Connecticut. In general simulations can capture the trend that increasing the ambient temperature results in lowered ignition delays and flame LOL. However, ignition delay is over-predicted under all ambient temperature conditions especially at 900 K and 1,200 K. An increase in ambient temperature results in lowering of flame LOL due to the increased chemical reactivity, which moves the ignition and flame stabilization locations upstream. It is also apparent that the phenomenon controlling ignition delay is different from flame stabilization since a good match in ignition delay does not necessarily result in improved flame LOL prediction.

Conclusions

- Grid-convergence was demonstrated with the current spray models for key parameters of interest in both non-reacting and reacting spray simulations. A cell size of 0.25 mm was observed to produce grid-convergent results and also resulted in reasonable run-times.
- Load-balancing in engine simulations was significantly improved by the implementation of METIS algorithm thus enhancing computational speedup. This also enabled the simulations of a diesel engine with 34 million computational cells.
- Grid convergence was observed on several key engine performance and emission parameters using a detailed chemistry approach. Results with the simplified combustion model were not grid-convergent.
- An n-dodecane reduced reaction mechanism was able to capture key combustion characteristics such as ignition delay and flame LOL.

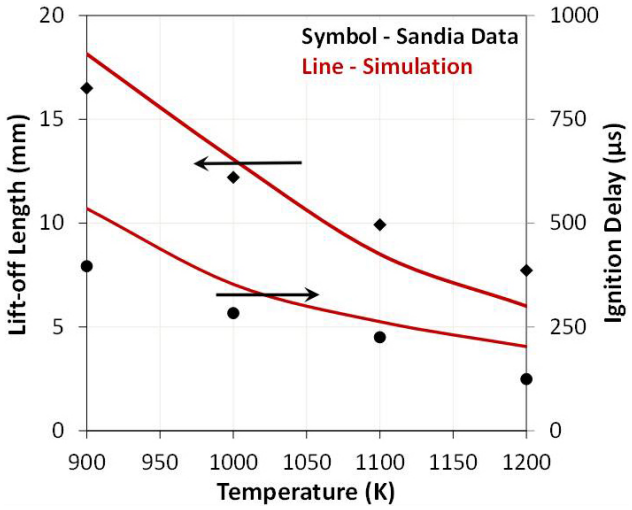

FIGURE 4. Measured [5] and predicted ignition delay and flame LOL, vs. ambient temperature for the n-dodecane reduced mechanism under Engine Combustion Network conditions.

References

1. Richards, K.J., Senecal, P.K., Pomraning, E., CONVERGE (Version 1.4.1) Manual, Convergent Science, Inc., Middleton, WI, 2012.

2. Som, S., Aggarwal, S.K., 2010, "Effects of primary breakup modeling on spray and combustion characteristics of compression ignition engines", Combustion and Flame, Vol. 157, pp.1179-1193.

3. Senecal P.K., Pomraning E., Richards K., Som S., "Grid convergent spray models for internal combustion engine CFD simulations", *Proceedings of the ASME 2012 Internal combustion engine division fall technical conference* (2012) ICEF2012-92043.

4. Karypis G., "METIS – A Software Package for Partitioning Unstructured Graphs, Partitioning Meshes, and Computing Fill-Reducing Orderings of Sparse Matrices Version 5.0" (2011).

5. http://www.sandia.gov/ecn/proceed/proceedECN1.php

Selected FY 2012 Publications

1. S. Som, D.E. Longman, Z. Luo, M. Plomer, T. Lu, P.K. Senecal, E. Pomraning, "Simulating flame lift-off characteristics of diesel and biodiesel fuels using detailed chemical-kinetic mechanisms," *Journal of Energy Resources Technology* 134 (3), 2012.

2. Z. Luo, M. Plomer, T. Lu, S. Som, D.E. Longman, S.M. Sarathy, W.J. Pitz, "Development and Robust validation of a reduced mechanism for biodiesel surrogates for compression ignition engine applications," *Fuel* 99: 143-153, 2012.

3. M. Raju, M. Wang, P.K. Senecal, S. Som, D.E. Longman, "A reduced diesel surrogate mechanism for compression ignition engine applications," ICEF2012-92045, *ASME Internal Combustion Engine Division Fall Technical Conference*, Vancouver, Canada, September, 2012.

4. P.K. Senecal, E. Pomraning, K.J. Richards, S. Som, "Grid-Convergent Spray Models for Internal combustion engine CFD simulations," ICEF2012-92043, *ASME Internal Combustion Engine Division Fall Technical Conference*, Vancouver, Canada, September, 2012.

5. S. Som, P.K. Senecal, E. Pomraning, "Comparison of RANS and LES Turbulence Models against Constant Volume Diesel Experiments," *24th Annual Conference on Liquid atomization and spray systems*, San Antonio, TX, May, 2012.

6. S. Som, D.E. Longman, G. D'Errico, T. Lucchini, "Comparison and standardization of numerical approaches for the prediction of non-reacting and reacting diesel sprays," SAE Paper No. 2012-01-1263, *SAE 2012 World Congress,* Detroit, April, 2012.

7. S. Som, D.E. Longman, Z. Luo, M. Plomer, T. Lu, "Three Dimensional simulations of diesel sprays using n-dodecane as a surrogate," *Eastern States Section of the Combustion Institute Fall Technical Meeting*, Storrs, October 2011.

8. W. Liu, R. Sivaramakrishnan, M.J. Davis, **S. Som**, D.E. Longman, T. Lu, "Development of a reduced biodiesel surrogate model for compression ignition engine modeling," *34th Proceedings of the Combustion Institute*, Poland, 2012. http://dx.doi.org/10.1016/j.proci.2012.05.090

II.15 Stretch Efficiency – Exploiting New Combustion Regimes

Stuart Daw (Primary Contact), Josh A. Pihl, James P. Szybist, Michael J. Lance
Oak Ridge National Laboratory (ORNL)
NTRC Site
2360 Cherahala Blvd.
Knoxville, TN 37932

DOE Technology Development Manager:
Gurpreet Singh

Objectives

- Define and analyze specific advanced pathways to improve the energy conversion efficiency of internal combustion engines from nominally 40% to as high as 60%, with emphasis on opportunities afforded by new approaches to combustion.
- Implement critical measurement and proof of principle experiments for the identified pathways to stretch efficiency.

Accomplishments

- Published peer reviewed article summarizing the thermodynamic effects of fuel type on ideal engine efficiency.
- Continued in-cylinder fuel reforming experiments with the modified Ecotec variable valve actuated (VVA) engine to measure reactions of different fuels with hot exhaust.
- Initiated collaborative discussions with the National Technical University of Athens to develop an improved mechanism for ethanol in-cylinder reforming.
- Continued collaboration with the Gas Technology Institute (GTI) and Cummins on exhaust gas recirculation (EGR)-based catalytic thermochemical recuperation (TCR).
- Continued informal discussions on thermochemical recuperation and in-cylinder reforming with Southwest Research Institute® and Volvo.
- Patent issued for a novel 6-stroke engine concept that uses water injection for in-cylinder waste heat recovery.

Future Directions

- Continue in-cylinder water injection and reforming experiments with the modified Ecotec engine and an expanded range of fuels and reaction chemistry analysis.
- Continue GTI-Cummins collaboration on EGR-based catalytic TCR.
- Develop improved kinetics model for in-cylinder fuel reforming.
- Continue SNL massively-parallel large eddy simulation solver experiment construction and shakedown as budget and priorities permit.

✧ ✧ ✧ ✧ ✧

Introduction

In conventional internal combustion engines, unutilized fuel energy ends up as waste heat. Waste heat cannot be utilized directly by the piston, but it can be converted into forms which can be recycled and used to boost piston output. The goal of this project is to identify and demonstrate strategies that enable waste heat recuperation into forms that can boost the thermodynamic efficiency of single-stage engines. Two potential forms of waste heat recycling, steam generation and TCR, are of interest in this study. In the former, exhaust heat is converted to pressurized steam that generates additional piston work. In the latter, exhaust heat chemically transforms the fuel. Under the proper conditions, the modified fuel can increase piston work, either by releasing more energy or by allowing more dilute combustion.

Approach

Our approach to improving internal combustion engine efficiency is based on developing a better understanding of the exergy losses in current engines and then developing ways to mitigate them. Previous studies of internal combustion engine thermodynamics conducted in collaboration with Professors Jerald Caton (Texas A&M University) and David Foster (University of Wisconsin) identified combustion irreversibility as the largest single contributor to fuel exergy loss. In addition, these studies revealed that thermal exhaust exergy is not directly usable by the piston, unless it is first transformed into a more suitable state. Our current efforts focus on development, analysis, and experimental evaluation of novel concepts that transform and recuperate thermal

exhaust exergy and improve dilute combustion by the addition of syngas. We are guided by combined input from industry, academia, and national labs, such as that summarized in the recently published report from the Colloquium on Transportation Engine Efficiency held in March 2010 at USCAR [1].

In previous years we identified three promising approaches for improving engine efficiency: counterflow preheating of inlet fuel and air with exhaust heat [2]; TCR [3]; and chemical looping combustion [4]. Of these, TCR appears to have the greatest near-term potential, and we have begun focusing on how TCR might be implemented in either in-cylinder or EGR-based versions. We also continued basic thermodynamic analyses of how water injection and variations in fuel properties might be utilized [5,6].

Results

Results from our fundamental thermodynamic analyses of fuel chemistry on engine thermodynamic efficiency have been published in an article in Energy & Fuels [6]. Briefly, we modeled the effects of 23 different fuels on the First and Second Law thermodynamic efficiencies of an adiabatic internal combustion engine. The First Law efficiency was calculated using the lower heating value (LHV), while Second Law efficiency was calculated in terms of exergy, which represents the inherent chemical energy available to perform work. We found that First Law efficiency can deviate by as much as 9% between fuels, while the Second Law efficiency exhibits a much smaller degree of variability. We also found that First and Second Law efficiencies can be nearly the same for some fuels (methane and ethane) but differ substantially for other fuels (hydrogen and ethanol).

Our fuel effects results revealed that the differences in First and Second Law efficiencies are due to differences in the LHV and exergy for a given fuel. In order to clarify First Law efficiency differences between fuels, as well as the differences between LHV and exergy, we introduced a new term, the molar expansion ratio (MER), defined as the ratio of product moles to reactant moles for complete stoichiometric combustion. We found that the MER reflects an important part of the physics behind fuel-specific efficiency differences as well as differences between First and Second Law efficiencies. Our study also revealed how First and Second Law efficiencies are affected by two other fuel-specific thermochemical properties, the ratio of specific heats and extent of dissociation in the reaction products following combustion.

It should be noted that, while the above study clarified important questions about fuel chemistry effects, it was ideal in a number of respects. There are additional layers of modeling complexity that need to be added before these results can be directly applied to real engines. In real engines, the effect of heat transfer can be significant, whereas this study assumed adiabatic conditions. Fuel vaporization effects can also impact in-cylinder temperature and heat transfer. Additionally, real engines do not undergo instantaneous constant volume combustion, but rather have finite combustion duration and ignition kinetics can make a non-ideal combustion phasing or low compression ratios necessary to mitigate engine knock.

This year we continued investigating two different experimental TCR approaches, in-cylinder TCR and EGR-based TCR. To investigate the former approach, we continued measurements of non-catalytic reforming in the ORNL-modified Ecotec engine after fuel is injected into recompressed exhaust gases in the 6-stroke cycle illustrated in Figure 1. Experiments with injection of isooctane, ethanol, and methanol have produced significantly lower exhaust temperatures than what can be accounted for from the latent fuel heats alone (see Figure 2). This implies the presence of a significant level of endothermic reaction for all of these fuels. A detailed analysis of the reaction products and possible kinetic mechanisms was initially confounded by the fact that we were only able to sample the recompression products after they mixed with the stoichiometric combustion exhaust. The engine exhaust manifold has since been modified (Figure 3), so that the recompression products can be analyzed directly without dilution. We expect to compare these measurements in the coming year with predictions from detailed non-catalytic kinetic reforming models such as that proposed by Vourliotakis et al. [8].

To investigate the potential of EGR-based TCR, we continued technical discussions with GTI and Cummins concerning pilot-scale TCR experiments with a Cummins natural gas engine. Previous testing at Cummins indicated that there was rapid deactivation of the GTI reforming catalyst when it was exposed to EGR. Cummins has indicated that resolution of the causes of this deactivation would be necessary in order for them to continue to pursue this version of TCR. Using samples of the catalyst supplied by GTI, we began detailed microscopic and laboratory bench reactor evaluations. An example scanning electron micrograph of the GTI catalyst revealing the basic structure of the washcoat deposited on a metal foil substrate is depicted in Figure 4. So far we have not observed any loss of layer integrity in the GTI catalyst, nor have we seen indications of sulfur (a potential catalyst poison). We have also been unable to replicate the reported catalyst deactivation in the laboratory. As depicted in Figure 5, our experiments with the fresh GTI catalyst show high (and stable)

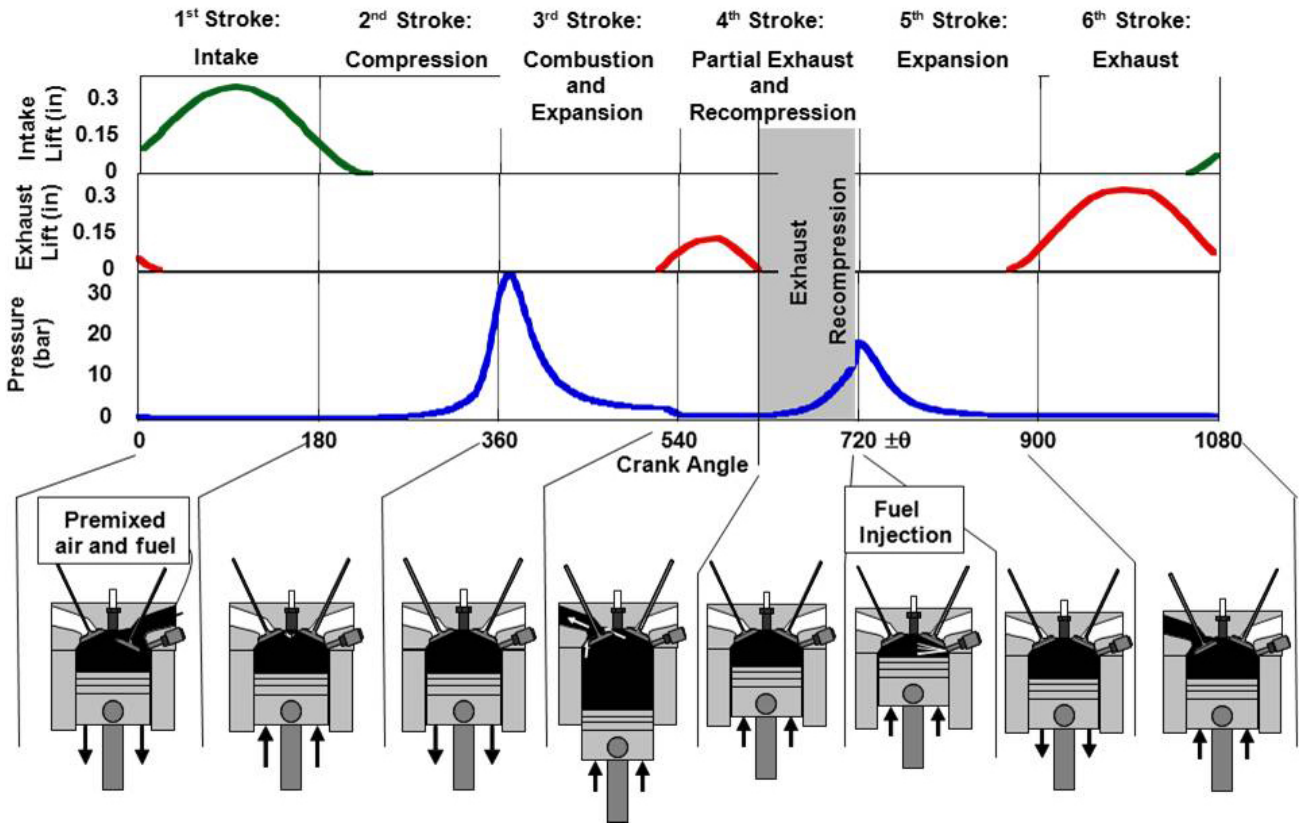

FIGURE 1. Profile for the experimental 6-stroke cycle on the ORNL modified Ecotec VVA engine. Fuels are injected during exhaust recompression to study in-cylinder, non-catalytic reforming.

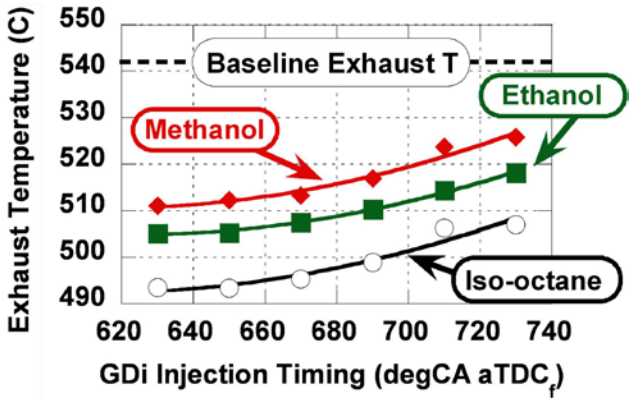

GDi - gasoline direct injection; CA - crank angle; aTDC - after top-dead center

FIGURE 2. Temperature variation in mixed combustion and recompression exhaust upon injection of a constant mass of different fuels over a range of injection timings. Temperature differences reflect fuel-specific differences in endothermic heat adsorption.

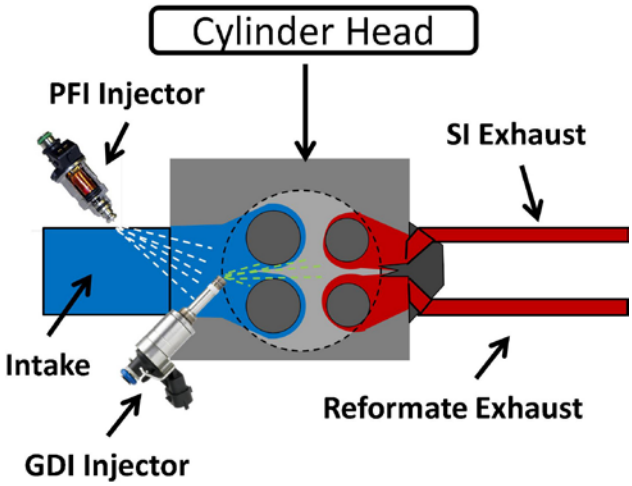

SI - spark ignition

FIGURE 3. Schematic of the modified Ecotec VVA engine exhaust manifold, which separates the combustion exhaust and recompression stroke products.

reforming activity even below the EGR temperatures reportedly used in the Cummins experiments. The catalyst continues to be active in the presence of oxygen as well, implying that it might be used in EGR from lean combustion. Our next experiments will focus on reformer startup and shutdown procedures.

Conclusions

A theoretical study of the thermodynamic effects of fuel stoichiometry has helped clarify engine efficiency

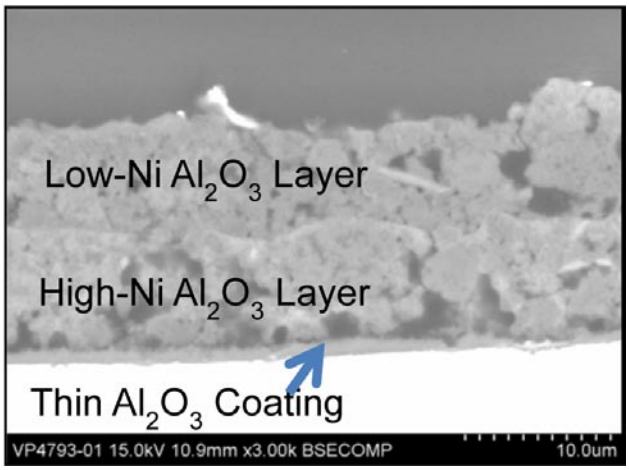

FIGURE 4. Microscopic cross-section of the GTI reforming catalyst washcoat.

differences associated with fuel chemistry. The study revealed that MER for each fuel reflects an important part of the physics behind fuel-specific efficiency differences as well as differences between First and Second Law efficiencies. Our study also revealed how First and Second Law efficiencies are affected by two other fuel-specific thermochemical properties, the ratio of specific heat and extent of dissociation in the reaction products following combustion.

We continue to refine experimental measurements of the chemistry and kinetics of in-cylinder, non-catalytic TCR and EGR-based catalytic TCR. Modifications to the ORNL VVA Ecotec engine exhaust will allow much more precise measurements of the product species and reforming reactions under recompression conditions with different fuels. These measurements are expected to be critical for developing relevant kinetic mechanisms for in-cylinder TCR. We are continuing to attempt to replicate the catalyst deactivation effects in the laboratory that were seen in natural gas engine testing of EGR-TCR.

References

1. C.S. Daw, R.L. Graves, R.M. Wagner, and J.A. Caton, "Report on the Transportation Combustion Engine Efficiency Colloquium Held at USCAR, March 3–4, 2010," ORNL/TM-2010/265, October 2010.

2. C.S. Daw, K. Chakravarthy, J.C. Conklin and R.L. Graves, "Minimizing destruction of thermodynamic availability in hydrogen combustion," International Journal of Hydrogen Energy, 31, (2006), pp 728-736.

3. V.K. Chakravarthy, C.S. Daw, J.A. Pihl, J.C. Conklin, "A Study of the Theoretical Potential of Thermochemical Exhaust Heat Recuperation in Internal Combustion Engines," Energy & Fuels, 2010, 24 (3), pp 1529-1537.

4. V.K. Chakravarthy, C.S. Daw, and J.A. Pihl, "A thermodynamic analysis of alternative approaches to chemical looping combustion," Energy & Fuels, 25 (2011), pp 656–669.

5. J.C. Conklin and J.P. Szybist, "A highly efficient six-stroke internal combustion engine cycle with water injection for in-cylinder exhaust heat recovery," Energy, 35 (2010), pp 1658–1664.

6. James P. Szybist, Kalyana Chakravathy, and C. Stuart Daw, "Analysis of the Impact of Selected Fuel Thermochemical Properties on Internal Combustion Engine Efficiency," Energy and Fuels, 26 (2012), pp 2798-2810.

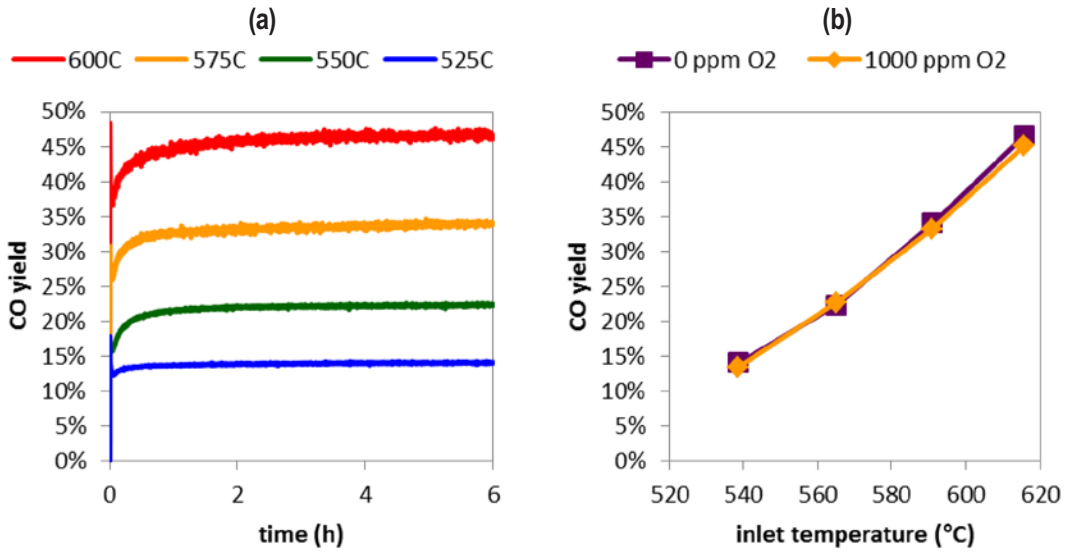

FIGURE 5. Measured CH_4 conversion to CO by the GTI reforming catalyst under lab-simulated EGR at different temperatures (a) and different O_2 concentrations (b). The inlet gas contained 15.7% CH_4, 16.0% H_2O, 8.0% CO_2, and 0 or 1,000 ppm O_2, and the gas space velocity was 3,500 h^{-1}.

7. C. Stuart Daw, Josh A. Pihl, James P. Szybist, Bruce Bunting, Michael Lance, and Robert Wagner, "Stretch Efficiency for Combustion Engines: Exploiting New Combustion Regimes," 2012 DOE OVT Peer Review, May 14–18, 2012, Project ace_15_daw.

8. G. Vourliotakis, G. Skevis, and M.A. Founti, "Detailed kinetic modeling of non-catalytic ethanol reforming for SOFC applications," International Journal of Hydrogen Energy, 34 (2009), pp 7626-7637.

FY 2012 Publications/Presentations

1. James P. Szybist, Kalyana Chakravathy, and C. Stuart Daw, "Analysis of the Impact of Selected Fuel Thermochemical Properties on Internal Combustion Engine Efficiency," Energy and Fuels, 26 (2012), pp 2798-2810.

2. Jim Szybist, Josh Pihl, Stuart Daw, and Bruce Bunting, "Preliminary Measurements of In-Cylinder Fuel Reforming," Presentation at the Spring 2012 AEC/HCCI Working Group Meeting at Sandia National Laboratory (Sandia, CA USA, February 2012).

3. C. Stuart Daw, Josh A. Pihl, James P. Szybist, Bruce Bunting, Michael Lance, and Robert Wagner, "Stretch Efficiency for Combustion Engines: Exploiting New Combustion Regimes," 2012 DOE OVT Peer Review, May 14-18, 2012, Project ace_15_daw.

Special Recognitions & Awards/Patents Issued

1. Szybist, J.P. and Conklin, J.C., "Highly Efficient 6-Stroke Engine Cycle with Water Injection," U.S. Patent No. 8,291,872, issued October 23, 2012.

II.16 Use of Low Cetane Fuel to Enable Low-Temperature Combustion

Stephen Ciatti
Argonne National Laboratory
9700 S. Cass Ave.
Bldg. 362
Argonne, IL 60439

DOE Technology Development Manager:
Gurpreet Singh

Subcontractor:
University of Wisconsin-Madison Engine Research Center, Madison, WI

Overall Objectives

- Optimize the operating conditions to use low cetane fuel to achieve clean, high-efficiency engine operation.
- Demonstrate the use of low-temperature combustion (LTC) as an enabling technology for high efficiency vehicles.

Fiscal Year (FY) 2012 Objectives

- Quantify the engine operating parameters of LTC by using different cetane rating fuels.
- Optimize the engine control parameters (injection strategy, exhaust gas recirculation [EGR], intake temperature) for each fuel to study the effect of Research Octane Number (RON) on engine efficiency and emissions.
- Demonstrate the use of LTC in an Autonomie simulation to validate higher efficiency vehicles.

Accomplishments

- Attained a 20% fuel economy improvement using LTC in a conventional powertrain vehicle over a similar port fuel injected vehicle; a 13% improvement versus a gasoline direct injection vehicle.
- Achieved over 40% brake thermal efficiency operating from 8 to 20 bar brake mean effective pressure (BMEP) with below 0.4 g/kW-hr oxides of nitrogen (NO_x), with some points under 0.2 g/kW-hr NO_x.
- Achieved 26% brake thermal efficiency with under 0.1 g/kW-hr NO_x at 2 bar BMEP by using uncooled EGR to enable proper ignition propensity.

Future Directions

- Evaluate additional fuel properties (RON, viscosity and volatility) using fuels provided by BP and the DOE Fuels for Advanced Combustion Engines program for gasoline.
- Analyze the particulate matter (PM) coming from LTC and studying the formation/oxidation process to relate PM to engine operating conditions.
- Conduct additional engine performance tests for Autonomie simulations to support LTC development as applied to vehicles.

Introduction

Current diesel engines already take advantage of the most important factors for efficiency – no throttling, high compression ratio and low heat rejection. However, diesel combustion creates a significant emissions problem. Mixing or diffusion combustion creates very steep gradients in the combustion chamber because the ignition delay of diesel fuel is extremely short. PM and NO_x are the result of this type of combustion, requiring expensive after-treatment solutions to meet emissions regulations.

The current work seeks to overcome the mixing controlled combustion dilemma by taking advantage of the long ignition delay of gasoline to provide much more premixing of fuel and air before ignition occurs. This premixing allows for the gradients of fuel and air to be much less steep, drastically reducing the PM-NO_x tradeoff relationship of mixing controlled combustion.

Approach

The intent of this project is to utilize the long ignition delays of low cetane fuels to create an advanced combustion system that generates premixed (but not homogeneous!) mixtures of fuel and air in the combustion chamber. As reported in several articles, if the local equivalence ratio is below 2 (meaning at most, twice as much fuel as oxidizer) and the peak combustion temperature is below 2,000 K (using EGR to drop the oxygen concentration below ambient 21%, thereby slowing the peak reaction rates and dropping the peak combustion temperature), a combustion regime that is very clean and yet retains reasonably high power density is achieved.

The challenge to this type of combustion system is the metering of fuel into the combustion chamber needs

to be precise, both in timing and amount. If too much fuel is added too early, a "knocking" type of combustion occurs, which creates unacceptably high combustion noise or worse. If not enough fuel is added, ignition may not occur at all and raw hydrocarbons exit the exhaust. Control over the relevant operating parameters is very important – fuel properties, injection strategy, compression ratio and intake temperature all have large influence upon ignition propensity.

Different RON fuels were used during this year; gasolines of 93 RON, 87 RON and 74 RON. In addition, a cetane enhancing additive, ethyl hexyl nitrate was used along with 93 RON fuel to test the use of these additives and compare them to straight fuels – see Figure 1.

Results

Successful operation of 29 different speed/load points, input to Autonomie, was achieved using 87 RON gasoline fuel. The long ignition delay allows for significant premixing, leading to low NO_x formation. The NO_x emissions decrease by 66%-95% compared to equivalent engine-out diesel, while hydrocarbon and CO emissions only slightly increase under the same conditions – see Figure 2. Operating conditions ranged from 1,350 RPM at 2 bar BMEP up to 3,500 RPM at 20 bar BMEP.

Injection strategy was altered in an effort to determine how much premixing is necessary to achieve the DOE goals. Two variations of injection strategy were performed, by varying the middle injection of a three-injection approach. As more fuel was introduced early, the smoke and NO_x production decreased significantly.

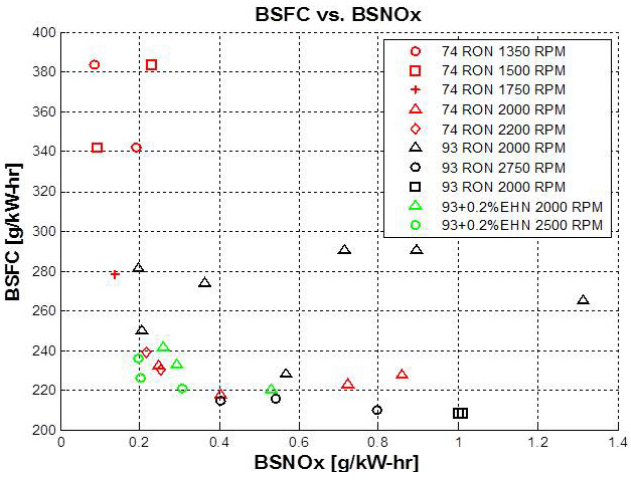

FIGURE 1. BSFC vs. $BSNO_x$ tradeoff for different RON fuels.

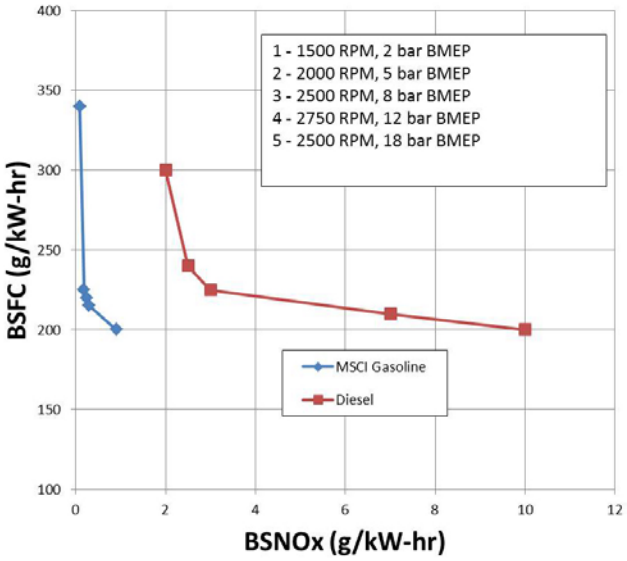

FIGURE 2. BSFC vs. $BSNO_x$ tradeoff comparison between 87 RON gasoline and conventional diesel fuel at the same operating conditions.

Consistent with expectations, the 74 RON fuel displayed high efficiency and low emissions at lower loads (under 10 bar BMEP), the 87 RON fuel appeared to provide the largest operating range of speeds and loads, while the 93 RON fuel performed excellently at loads of 5 bar BMEP and above.

Conclusions

- A wide range (29 different points) of speeds and loads were achieved using stratified gasoline fuel in a compression ignition engine.
- As the ignition propensity was altered by the RON number of the fuel, the operating range was also altered. For example, 74 RON fuel provided so much ignition propensity that the early injection strategies could not be employed without unacceptable combustion noise. This also limited the effective load range for this fuel. See Figure 1 for details.
- Higher RON fuel enabled increased levels of premixing and higher load range for the engine. However, 93 RON fuel was so difficult to autoignite that the engine could not reach loads below 5 bar BMEP. See Figure 1 for details.
- For this configuration of hardware (17.5 CR, 500 bar injection pressure, stock EGR system), 87 RON gasoline provided the optimal compromise of resistance/ease of autoignition for the widest range of operating conditions. See Figure 2 for fuel consumption and emissions performance of 87 RON gasoline compared to conventional diesel.

FY 2012 Publications/Presentations

1. ***Ciatti, S. A.,*** (September 2012) Invited Presentation by Bengt Johansson for the Gasoline Compression Ignition session of SAE International Powertrain, Fuels and Lubricants Conference, "Multizone Stratified Compression Ignition (MSCI) – A Practical Approach to High Efficiency and Low Emissions", Malmo, Sweden.

2. ***Ciatti, S.A.,*** Subramainian, S., Ferris, A (May 2012) –ASME ICES2012-81067, "Effect of EGR in a Gasoline Operated Diesel Engine in LTC mode," ASME ICE Division Conference, Torino, Italy.

3. Das Adhikary, B., Ra, Y., Reitz, R., and ***Ciatti, S.***, (April 2012) - SAE Technical Paper 2012-01-1336, "Numerical Optimization of a Light-Duty Compression Ignition Engine Fuelled With Low-Octane Gasoline," SAE World Congress, Detroit, MI.

4. Knizley, A. A., Srinivasan, K. K., Krishnan, S. R., ***Ciatti, S. A.,*** (April 2012) "Fuel and diluent effects on entropy generation in a constant internal energy-volume (uv) combustion process", *Energy,* Volume 43, Issue 1, July 2012, Pages 315-328.

5. ***Ciatti, S. A.,*** Subramanian, S. (Oct. 2011) – ASME ICEF2011-60014, "Low Cetane Fuels in a Compression Ignition Engine to Achieve LTC", ASME IC Engine Division Conference, Morgantown, WV.

II.17 Collaborative Combustion Research with Basic Energy Science

Stephen Ciatti (Primary Contact),
S. Scott Goldsborough, Sreenath B. Gupta
and Michael V. Johnson
Argonne National Laboratory
9700 S. Cass Avenue
Bldg 362
Argonne, IL 60439

DOE Technology Development Manager:
Gurpreet Singh

Overall Objectives

- Collaborate with combustion researchers within DOE's Office of Science Basic Energy Science and Energy Efficiency Renewable Energy Vehicle Technologies programs to develop and validate predictive chemical kinetic models for a range of transportation-relevant fuels.
- Acquire ignition delay, and other valuable combustion data using Argonne National Laboratory's (ANL's) rapid compression machine (RCM) at conditions representative of today's and future internal combustion engines, including high pressure (p = 15-80 bar) and low to intermediate temperature (T = 650-1,100 K).

Fiscal Year (FY) 2012 Objectives

- Upgrade ANL's RCM facilities to utilize a range of transportation-relevant fuels, especially liquid formulations that cover the boiling range of gasoline. Improve experimental capabilities to quantify stable combustion intermediates via physical gas sampling and gas chromatograph/mass spectrometer analysis. Implement new modeling frameworks for mechanism validation efforts which can reduce uncertainties.
- Acquire data for baseline research grade gasoline, and blends of 4- and 5-component gasoline surrogates.

Accomplishments

- Designed and fabricated new experimental hardware to improve gas conditions in the twin-piston machine's reaction chamber (e.g., minimized fluid dynamic motion and dead volume, tighter sealing at high and low pressures, greater thermal uniformity).
- Validated reduced-order model calculations of the RCM using experimental chemical thermometry techniques employing cyclochexene.
- Developed guidelines through bench-top experiments for the successful implementation and utilization of aerosol fueling methodologies which facilitate the use of involatile, diesel-relevant components and blends in RCM experiments.
- Acquired autoignition data for a 4-component gasoline surrogate at stoichiometric conditions in 21% oxygen diluted with argon at 30 bar with temperatures from 690 to 870 K.

Future Directions

- Develop, refine and validate additional reduced-order, physics-based models for RCM processes in order to improve fundamental understanding, as well as reduce uncertainties in chemical kinetic modeling. Develop additional metrics for mechanism validation, including rate of heat release.
- Acquire additional data for baseline research-grade gasoline, and blends of 4- and 5-component gasoline surrogates. Identify deficiencies in detailed chemical kinetic models, and work to improve these.
- Acquire data for blends of iso-octane + various cetane enhancers, and gasoline + cetane enhancers relevant to a range of low-temperature combustion (LTC) concepts; develop/validate chemical kinetic models for these.
- Develop and validate a control-oriented model capable of predicting autoignition timing over wide range of conditions, including various fuel reactivities applicable to advanced combustion concepts.

Introduction

Accurate, predictive combustion models are necessary in order to reliably design and control next-generation fuels and future engines which can meet mandated fuel economy and emissions standards, while achieving reductions in development times and costs for new configurations [1]. The imprecision of available models prevents the adoption of detailed simulation techniques within current design processes. Existing engineering-scale models can achieve satisfactory performance at some operating points, however they

are not sufficiently robust to cover complete ranges of conventional engine operation, or when novel or advanced combustion concepts are utilized. Towards this, there is a critical need to improve the understanding of the multiple physical and chemical processes that occur within combustion engines, some of which include chemical ignition, fluid-chemistry interactions and pollutant formation/decomposition. To advance these understandings collaborations are necessary across multiple disciplines, for example between combustion engineers within DOE's Vehicle Technologies Program and scientists who are supported through DOE's Basic Energy Science program. Through these interactions fundamental, engine-relevant data can be acquired with low experimental uncertainties, while predictive models can be developed and validated based on these datasets.

Approach

RCMs are highly sophisticated, experimental tools that can be employed to acquire fundamental insight into fuel ignition and pollutant formation chemistry, as well as fluid-chemistry interactions, especially at conditions that are relevant to advanced, LTC concepts [2]. They are capable of creating and maintaining well-controlled, elevated temperature and pressure environments (e.g., T = 600 to 1,100 K, P = 5 to 80 bar) where the chemically-active period preceding autoignition can be monitored and probed via advanced in situ and ex situ diagnostics. The ability to utilize wide ranges of fuel and oxygen concentrations within RCMs, from ultra-lean to over-rich (e.g., ϕ = 0.2 to 2.0+), and spanning dilute to oxy-rich regimes (e.g., O_2 = 5 to >21%), offers specific advantages relative to other laboratory apparatuses such as shock tubes and flow reactors, where complications can arise under such conditions. The understanding of interdependent chemico-physical phenomena that can occur at some conditions within RCMs is a topic of ongoing investigation within the combustion community, while interpretation of facility influences on datasets is also being addressed [2]. Approaches to implement novel diagnostics which can provide more rigorous constraints for model validation compared to integrated metrics such as ignition delay times, e.g., quantification of important stable and radical intermediates such as H_2O_2 and C_2H_4 [3,4], are under development by many combustion researchers.

Argonne's existing twin-piston RCM is utilized in this project to acquire data necessary for chemical kinetic model development and validation, while improvements to the facility's hardware and data analysis protocol are undertaken to extend its current capabilities and fidelity. Collaborations are undertaken with Basic Energy Science-funded scientists at ANL and other U.S. laboratories, as well as with researchers at national and international institutions, including complementary RCM facilities.

Results

Argonne's twin-piston RCM has been used extensively in the past for laser ignition studies of natural gas relevant fuel components and blends [5]. Because the intent of the current project is to investigate the autoignition behavior of a range of fuels relevant to the transportation industry, changes needed to be made in the configuration to facilitate this. The geometric compression ratio was increased from 9.5:1, through re-design of the pistons, to cover a range from 13.5:1 to 20:1; heat loss during piston compression results in slightly lower effective compression ratios. A wide range of compressed conditions is now possible through manipulation of the physical compression ratio as well as the diluent heat capacity. The reaction chamber, piston crevices and seals were also reconfigured in order to minimize dead volume and adverse fluid dynamic motion, as well as inadequate sealing at maximum compression. A new thermal management system was designed in order to prevent partial distillation of fuel blends and improve the thermal uniformity of the reactive gas mixture during recharging of the experiment and post-compression. Finally, a gas sampling system was fabricated in order to quantify concentrations of combustion intermediates to be used as rigorous metrics for chemical kinetic model validation.

To facilitate the utilization of involatile, diesel boiling-range surrogate components and blends, an aerosol fueling system has been investigated by collaborators [6,7]. This experimental approach is similar to one that has been designed and validated for a shock tube at Stanford University [8], but configured for conditions seen in RCMs. The aerosol-fueled RCM, once fabricated, will provide data that is complementary to, and inaccessible via the aerosol shock tube. Bench-top experiments have been used to develop guidelines for the successful implementation of this approach. To achieve adequate fuel vaporization during piston compression (i.e., 'wet compression'), it has been determined that very small droplets (d_0 <5 μm) must be used. In addition, high concentrations are required in order to achieve adequate fuel loading at 21% O_2 conditions. Generating and supplying this to the aerosol-RCM is challenging but is expected to be resolved.

In order to reduce uncertainties associated with modeling of the chemical kinetic processes within the RCM, new physics-based, reduced-order models for the RCM need to be implemented [9]. These models can take into account effects of fluid flow and heat loss which alter

the thermodynamic state of the reacting mixture, and have cost and other advantageous relative to conventional methodologies which employ empirical representations of the heat loss based on experiments using analogous non-reacting mixtures. Reduced-order models are required in order to utilize large, detailed chemical kinetic mechanisms in the simulations. The physics-based models to be utilized with this project are currently integrated with a homogeneous reactor model, where this framework assumes that the fuel/oxygen/diluent mixture is only reactive within the adiabatic core of the reaction chamber. In the future, a stratified reactor model [10] could be used instead in order to account for boundary layer reactivity, which can be important at some conditions, e.g., in the negative temperature coefficient regime. Experimental validation of predictions using the physics-based model was conducted using chemical thermometry techniques where cyclochexene was employed. Physical gas samples indicated the extent of cyclohexene decomposition, and thus the temperature of the gas mixture in the reaction chamber. Only very high compressed temperatures could be covered with these experiments due to the slow pyrolysis of cyclohexene at lower temperatures.

Ignition delay data were acquired for a 4-component gasoline surrogate where this consisted of a blend of n-heptane, iso-octane, toluene and 2-pentene with molar fractions of 0.16, 0.57, 0.23 and 0.04, respectively. Stoichiometric conditions were utilized in the experiments with 21% oxygen diluted in argon. The geometric compression ratio was 9.5:1, since the tests were conducted before the machine modifications were completed. Compressed pressures of approximately 30 bar was used with temperatures ranging from 690 to 870 K. For some of the compressed conditions substantial heat release occurred during the compression process, thus making determination of the ignition delay time challenging. Utilization of physics-based models, such as those described previously, can address this challenge, and this will be undertaken for future experiments. The experimental measurements are presented in Figure 1 where homogeneous reactor model simulations results using the detailed gasoline surrogate mechanism from Lawrence Livermore National Laboratory [11] are also indicated.

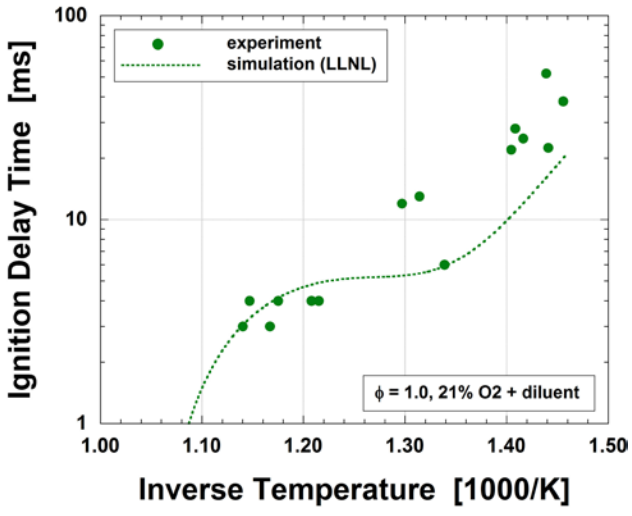

FIGURE 1. Measured and computed ignition delay times for stoichiometric mixtures of a 4-component gasoline surrogate + 21% O_2 + 79% Ar.

Conclusions

- Ignition delay data was acquired for a 4-component gasoline surrogate using Argonne's twin-piston RCM at conditions that are representative of internal combustion engines.
- Chemical thermometry techniques were used to validate reduced-order modeling of the RCM at high temperatures.
- Argonne's twin-piston RCM facility has capability to acquire data for a range of fuels and fuel surrogates that are of interest for the design and development of advanced combustion engines.

References

1. Basic Research Needs for Clean and Efficiency Combustion of 21st Century Transportation Fuels. (http://science.energy.gov/~/media/bes/pdf/reports/files/ctf_rpt.pdf)

2. S.S. Goldsborough, D. Longman, M.S. Wooldridge, R.S. Tranter and S. Pratt, "1st International RCM Workshop Meeting Report," August 28–29, 2012. (http://www.transportation.anl.gov/rcmworkshop)

3. C. Bahrini, O. Herbinet, P.-A. Glaude, C. Schoemaecker, C. Fittschen and F. Battin-Leclerc, "Quantification of hydrogen peroxide during the tow-temperature oxidation of alkanes," J. Am. Chem. Soc. (139) 11944-11947, 2012.

3. I. Stranic, S.H. Pyun, D.F. Davidson, R.K. Hanson, "Multi-species measurements in 1-butanol pyrolysis behind reflected shock waves," Combust. Flame (159) 3242-3250, 2012.

4. S.B. Gupta, R.R. Sekar, G.M. Klett and M. Ghaffarpour, "Ignition characteristics of methane-air mixtures at elevated temperatures and pressures," SAE Paper 2005-01-2189, 2005.

5. S.S. Goldsborough, M.V. Johnson, G.S. Zhu and S.K. Aggarwal, "Gas-phase saturation and evaporative cooling effects during wet compression of a fuel aerosol under RCM conditions," Combust. Flame (158) 57-68, 2011.

6. S.S. Goldsborough, M.V. Johnson, G.S. Zhu and S.K. Aggarwal, "Fuel and diluent property effects during wet compression of a fuel aerosol under RCM conditions," Fuel (93) 454-467, 2012.

7. D.R. Haylett, D.F. Davidson and R.K. Hanson, "Ignition delay times of low-vapor-pressure fuels measured using an aerosol shock tube," Combust. Flame (159) 522-561, 2012.

8. S.S. Goldsborough, C. Banyon and G. Mittal, "A computational efficient, physics-based model for simulating heat loss during compression and the delay period in RCM experiments," Combust. Flame (159) 3476-3492, 2012.

9. J. Kodavasal, S.-H. Keum, and A. Babajimopoulos, "An extended multi-zone combustion model for PCI simulation," Combust. Theo. Mod. (15) 893-910, 2011.

10. https://www-pls.llnl.gov/?url=science_and_technology-chemistry-combustion-gasoline_surrogate

FY 2012 Publications/Presentations

1. S.S. Goldsborough, T.A. Smith, M.V. Johnson and S.S. McConnell, "Evaluation of ignition timing predictions using control-oriented models in kinetically-modulated combustion regimes," SAE Paper 2012-01-1136, 2012.

2. M.V. Johnson, S.S. Goldsborough, T.A. Smith and S.S. McConnell, "Trends in simulated ignition timing across a wide range of conditions including fuel reactivity," ASME ICES 2012-81079, 2012.

3. G. Mittal and S. Gupta, "Computational assessment of an approach for implementing crevice containment in rapid compression machines," Fuel (102) 536-544, 2012.

II.18 Expanding Robust HCCI Operation with Advanced Valve and Fuel Control Technologies

James P. Szybist (Primary Contact) and K. Dean Edwards
Oak Ridge National Laboratory (ORNL)
2360 Cherahala Blvd
Knoxville, TN 37932

Matt Foster, Wayne Moore, and Keith Confer
Delphi – Advanced Powertrain
3000 University Drive
Auburn Hills, MI 48326

DOE Technology Development Manager:
Gurpreet Singh

Overall Objectives

- Determine limits of conditions conducive to robust homogeneous charge compression ignition (HCCI) operation and the engine controls most effective at controlling HCCI.
- Develop robust model of negative valve overlap (NVO) HCCI combustion with GT-Power.
- Operate multi-cylinder engine with cam-based valve train under HCCI conditions, demonstrating the widest-possible HCCI operating regime.

Fiscal Year (FY) 2012 Objectives

- Install a laboratory air handling system for the ORNL single-cylinder engine with hydraulic valve actuation (HVA) to enable boosted operation and external exhaust gas recirculation (EGR).
- Determine engine efficiency and emissions as the high-load limit is approached.
- Characterize the sensitivity of the available engine controls for HCCI under boosted conditions.

Accomplishments

- Published study in SAE International Journal of Engines on expansion of the low-load limit of HCCI combustion.
- Expanded HCCI load range up to 650 kPa net indicated mean effective pressure ($IMEP_{net}$) with indicated thermal efficiency of greater than 40%.
- Operated newly installed laboratory air handling system to an intake manifold pressure of 190 kPaa with external EGR of up to 30%.
- Characterized the independent effect of boost, external EGR, and NVO duration on HCCI.

Future Directions

This Cooperative Research and Development Agreement (CRADA) came to a natural and successful conclusion at the end of FY 2012. ORNL and Delphi maintained a good working relationship throughout the project. The CRADA participants are interested in continuing collaborations in the future, and a follow-on CRADA for FY 2013 between the two organizations was proposed. Discussion for additional collaboration will continue as research needs and opportunities present themselves.

Introduction

HCCI combustion has a great deal of promise for improved efficiency and reduced emissions, but faces implementation barriers. This study aims to better understand the engine conditions that are conducive to HCCI combustion, and the operational sensitivity to engine controls. Specifically, we aim to develop an understanding of engine parameters that can provide robust control and are applicable to a production intent engine with a versatile cam-based valve train.

Approach

Experiments were conducted with the ORNL single-cylinder engine shown in Figure 1. The engine is equipped with a gasoline direct injection fueling system and with HVA which allows full control over valve timing, duration and lift. This versatile research tool can be used to identify and characterize engine operating conditions that are conducive to HCCI combustion, and because of its versatility it can perform parametric studies with valve train parameters that are not possible with a cam-based system. In order for this study to be as relevant as possible to production-intent cam-based valve trains, the intake and exhaust valve lift are held constant at 4 mm and opening and duration is held constant at 98 crank angle (CA, measured at a valve lift of 0.8 mm).

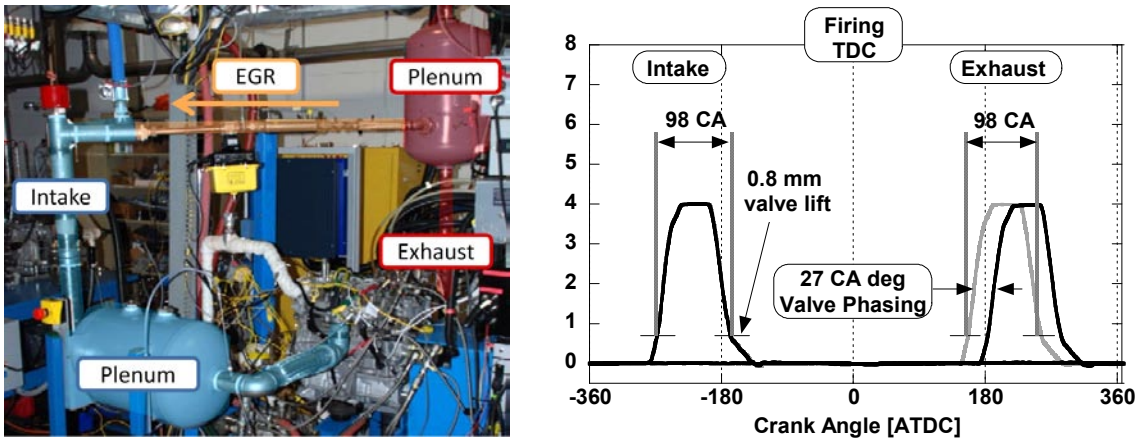

CA - crank angle; TDC - top-dead center; ATDC - after top-dead center

FIGURE 1. Photograph of the experimental engine (left) and valvetrain strategy implemented in the current set of experiments (right).

The exhaust valve phasing is changed throughout the study as needed, with a total required range of 27 CA deg, also shown in Figure 1. This range of valve phasing is within the range of current technology cam-based valve trains with cam phasing.

The engine is operated with a laboratory air handling system to simulate boosted operation with a turbocharger. Pressurized air is metered to the engine using a mass air flow controller and a constant pressure differential of 10 kPa is maintained between the exhaust and intake manifolds. The engine is equipped with separate electro-mechanical valves for backpressure and external EGR, allowing independent control of intake manifold pressure, exhaust manifold pressure, and EGR. Cooled EGR mixes with fresh air upstream of an air heater, followed by the intake plenum and then the intake manifold. Boost and external EGR are increased with engine load to maintain a combustion noise level at or below 94 dB.

Results

Both external EGR and boost enable increases in engine load compared to naturally aspirated conditions while maintaining low oxides of nitrogen (NO_X) emissions and high thermal efficiency. Using boost up to 190 kPaa with 30% external EGR, engine loads as high as 6.5 bar $IMEP_{net}$ were investigated at 2,000 rpm. The required intake manifold pressure, indicated thermal efficiency, and NO_X emissions are shown in Figure 2 as a function of engine load. It can be seen that the intake pressure requirement rises sharply with engine load. Indicated thermal efficiency (ITE) is high throughout, with ITE increases up to a load of 600 kPa $IMEP_{net}$. NO_X emissions are highest for the naturally aspirated condition, but are very low at the higher loads under boosted conditions.

The effect of external EGR on the HCCI combustion process is shown in Figure 3 for two different engine load/manifold pressure conditions at an engine speed

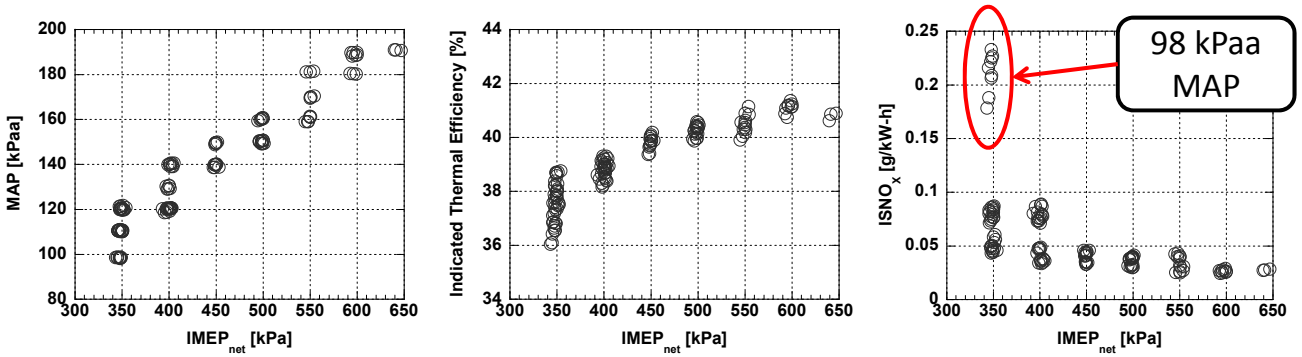

MAP - manifold absolute pressure; ISNOx - indicated specific oxides of nitrogen

FIGURE 2. Intake manifold pressure, indicated thermal efficiency, and NO_X emissions as a function of HCCI engine load at 2,000 rpm.

of 2,000 rpm. As EGR increases, advancement of fuel injection timing is required to maintain combustion phasing. However, when compared as a function of the CA50 combustion phasing, the EGR fraction has little difference on combustion noise, NO_X emissions, combustion stability, maximum heat release rate, and many other parameters. Interestingly, exhaust temperature is one area where there was a repeatable trend with external cooled EGR, and that was that exhaust temperature increased with EGR.

The effect of boosted operation is shown in Figure 4 for two different engine load/EGR conditions. Similar to the effect observed with increasing EGR in Figure 3, increasing boost requires that injection timing be advanced to maintain a constant combustion phasing. However, unlike the effect observed with increasing EGR, a higher level of boost leads to a reduction in combustion noise and a reduction in NO_X emissions. There was no impact of higher boost on thermal efficiency for a given engine load observed in this study.

The duration of the NVO, and specifically the exhaust valve closing angle, is a highly sensitive parameter in terms of controlling combustion phasing. Figure 5 shows the relationships between combustion phasing and start of injection timing. At a relatively light load of 4.0 bar $IMEP_{net}$, a change in exhaust valve closing

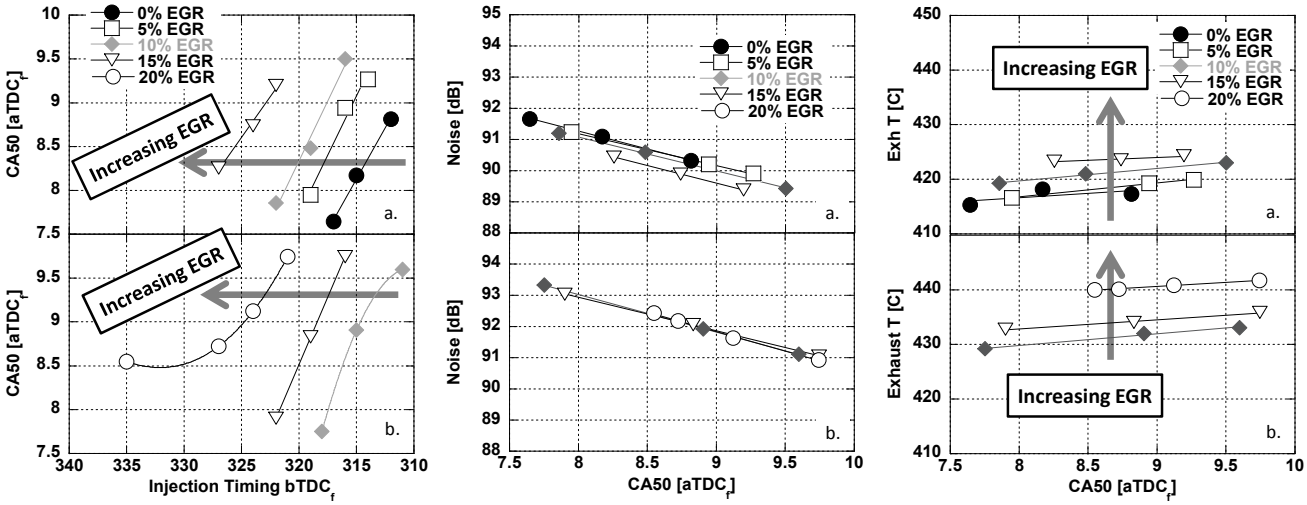

bTDC - before top-dead center

FIGURE 3. Combustion phasing as a function of injection timing, and noise and exhaust temperature as a function of combustion phasing for three different levels of external EGR for (a) 3.5 bar $IMEP_{net}$ at a boost pressure of 110 kPaa, and a load of 4.0 bar $IMEP_{net}$ at a boost pressure of 120 kPaa.

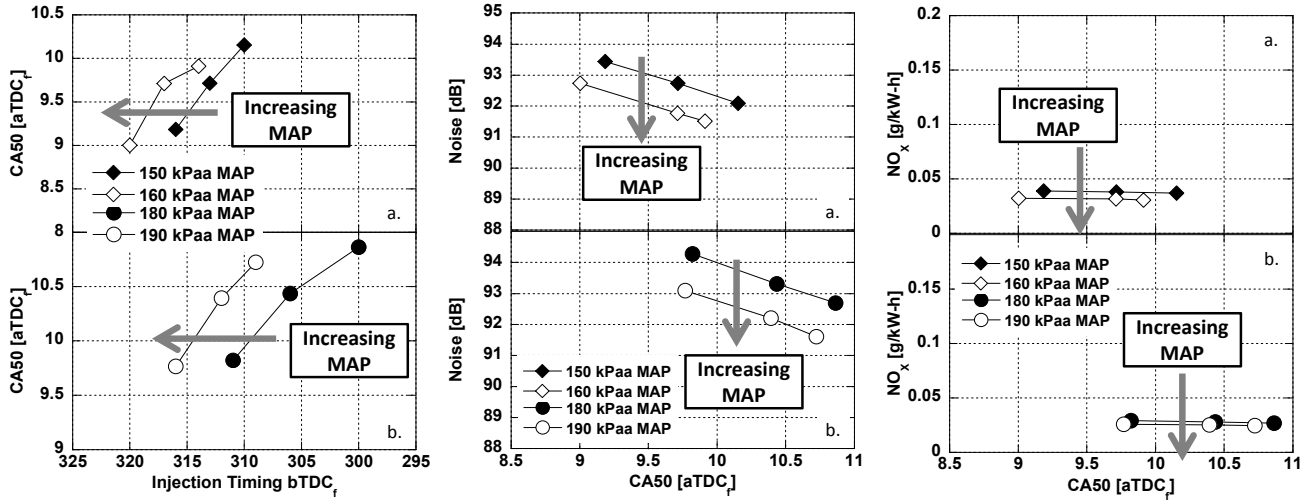

FIGURE 4. Effect of manifold pressure on combustion phasing, noise, and NO_X emissions at (a) an engine load of 5.0 bar $IMEP_{net}$ and 20%, and (b) an engine load of 6.0 bar $IMEP_{net}$ and 25% external EGR at 2,000 rpm.

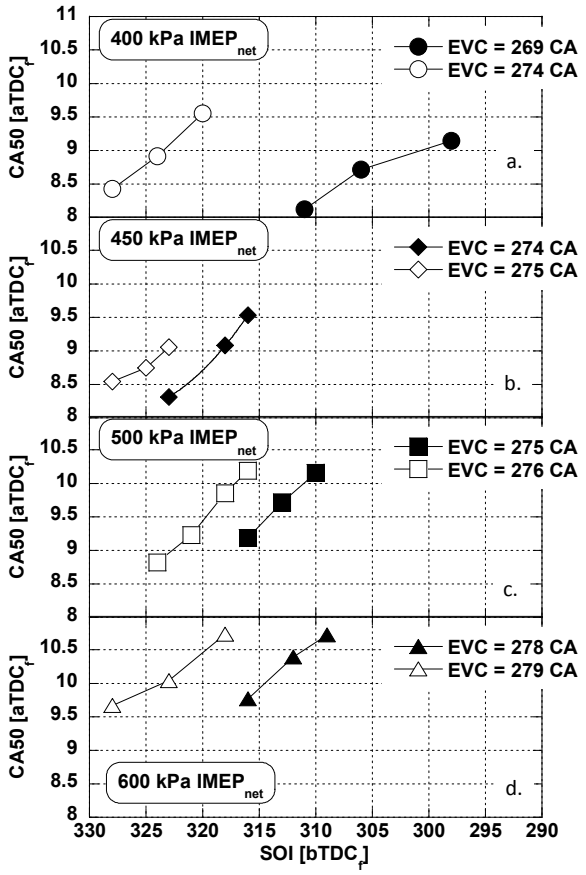

FIGURE 5. Effect of exhaust valve closing (EVC) angle on combustion phasing and noise.

angle of 5 CA degrees requires a change in the start of injection timing of 20 CA degrees. This relationship becomes much more sensitive as load increases where, at an engine load of 6.0 bar $IMEP_{net}$, a change in exhaust valve closing angle of 1 CA degree requires a change in injection timing of 10 CA degrees. This illustrates that although stable HCCI combustion is possible at these relatively high load conditions with low NO_X emissions and high efficiency, combustion phasing and overall operation becomes more sensitive to engine controls.

The parameter used to quantify engine noise has not been standardized for researchers studying different advanced combustion regimes. Commonly cited metrics include maximum pressure rise rate (MPRR), ringing intensity (RI), and combustion noise as measured by an AVL noise meter. However, a consensus is beginning to form that the AVL noise meter provides the best metric for combustion noise, and it is supported by data from noise chambers. Figure 6 shows the MPRR and RI as functions of combustion noise as measured by the AVL noise meter. In all cases, there is trend-wise agreement that noise increases with both the MPRR and RI.

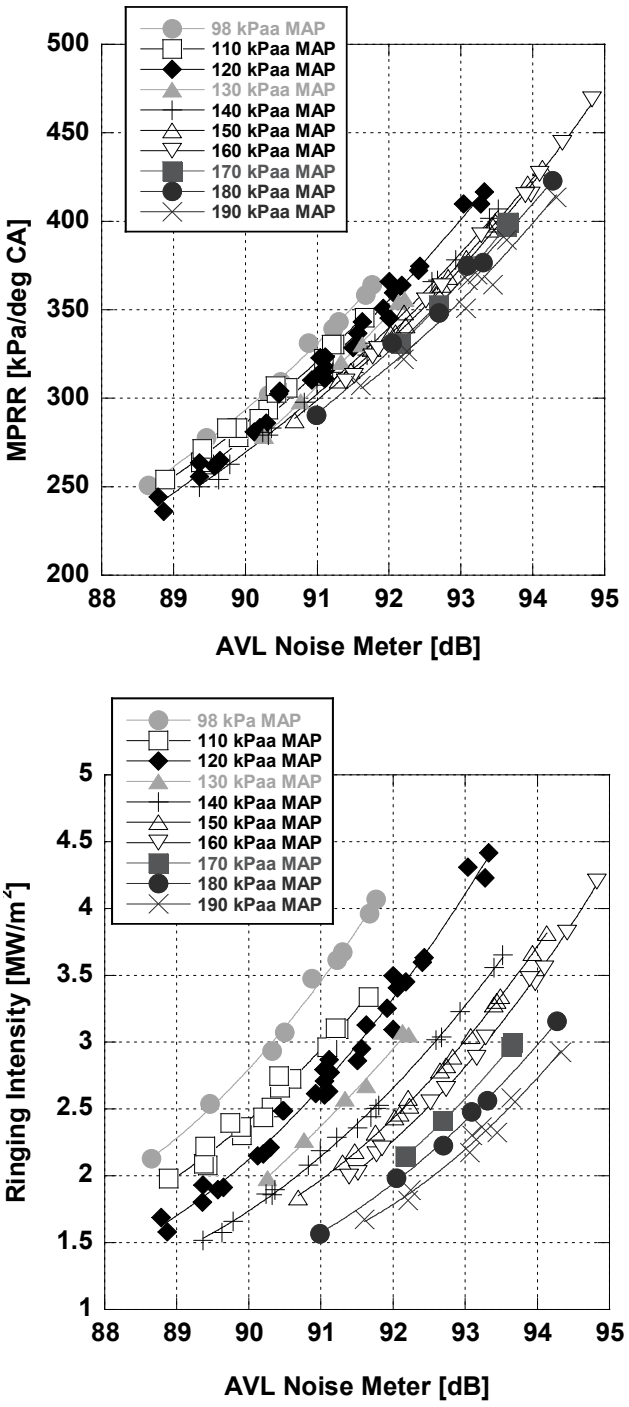

FIGURE 6. MPRR and RI as functions of noise as measured by the AVL noise meter.

However, it is observed that increasing manifold pressure has the effect of decreasing the MPRR and RI more than combustion noise as measured by the AVL noise meter. Thus, if RI is the only noise metric being used, it is possible that combustion noise will be under-predicted by a large margin under boosted conditions.

To summarize, the investigations conducted during the final year of this CRADA revealed a great deal of information about the sensitivity of EGR, boost, injection timing, and manifold pressure on HCCI combustion. While previous researchers have exceeded the engine loads achieved in this study, this investigation provides the most in-depth publically-available study on the ability to control HCCI combustion with the available engine controls.

Conclusions

- Both increasing the overall dilution with boost and increasing external EGR at constant overall dilution are independent enablers for HCCI load range expansion:
  - Increasing dilution with boost requires that fuel injection timing be advanced while mitigating noise and NO_X emissions.
  - Increasing EGR at a constant overall dilution level requires that fuel injection timing be advanced with little effect on noise and NO_X emissions.
- Combustion phasing has an increasing sensitivity to engine controls as engine load is increased:
  - This is particularly true of exhaust valve closing angle, which can be considered the "coarse" control compared to fuel injection timing which can be considered the "fine" control.
- Both MPRR and RI under-predict combustion noise as measured by the AVL combustion noise meter under boosted conditions:
  - Under-prediction with RI is more severe than with MPRR.

FY 2012 Publications/Presentations

1. Weall, A., Szybist, J., Edwards, K., Foster, M. et al., "HCCI Load Expansion Opportunities Using a Fully Variable HVA Research Engine to Guide Development of a Production Intent Cam-Based VVA Engine: The Low Load Limit," *SAE Int. J. Engines* 5(3):1149-1162, 2012, doi:10.4271/2012-01-1134.

2. Szybist, J., Edwards, K., Foster, M., Confer, K., and Moore, W., "Characterization of Engine Control Authority on HCCI Combustion as the High Load Limit is Approached," To be presented at the 2013 SAE World Congress.

II.19 Cummins-ORNL Combustion CRADA: Characterization and Reduction of Combustion Variations

Bill Partridge[1] (Primary Contact), Sam Geckler[2], Jon Yoo[1], Anthony Perfetto[2], Jim Parks[1], Maggie Connatser[1], Vitaly Prikhodko[1], Rodrigo Sanchez-Gonzalez[1]

[1]Oak Ridge National Laboratory (ORNL)
2360 Cherahala Blvd.
Knoxville, TN 37932

[2]Cummins Inc., Columbus, IN

DOE Technology Development Manager:
Ken Howden

Overall Objectives

- Improve engine efficiency through better combustion uniformity.
- Develop and apply diagnostics to resolve combustion-uniformity drivers.
- Understand origins of combustion non-uniformity and develop mitigation strategies.
- Address critical barriers to engine efficiency and market penetration.

Fiscal Year (FY) 2012 Objectives

- Develop exhaust gas recirculation (EGR) probe capable of quantifying spatial EGR uniformity with cylinder-resolved temporal resolution.
- Assess spatiotemporal EGR probe performance in ORNL engine lab.
- Apply EGR probe at Cummins Technical Center (CTC) for assessing advanced intake architectures consistent with achieving next-generation engine efficiency.
- Improve EGR probe to enable multiplexed operation and improved concentration measurements in environments with fluctuating pressure and temperature.

Accomplishments

- Developed EGR probe capable of quantifying transient engine EGR uniformity:
  - Resolves cylinder-specific and fast (ca. 2 ms) EGR on-engine variations.
  - Resolves spatial EGR uniformity in engine applications.
  - Cylinder misfire detected via ex-cylinder EGR probe measurements and correlated with combustion figure of merit.
- Applied EGR probe at CTC to development of EGR mixer design consistent with achieving next-generation engine efficiencies.
- Further EGR probe improvements initiated:
  - Laser-based excitation for improved CO_2 linearity and accuracy in environments with fluctuating temperature and pressure.
  - Multiplexed EGR probes for simultaneous multi-point measurements.
  - High-temperature EGR probe for exhaust applications.

Future Directions

- Apply EGR probe at CTC to development of advanced-intake architectures consistent with achieving next-generation engine efficiencies:
  - Assess hardware performance.
  - Assess performance of numerical design tools.
- Improve EGR probe to achieve Cooperative Research and Development Agreement (CRADA) goals:
  - Exhaust temperature applications.
  - Fast temperature and pressure measurements and corrections.
- Identify and develop diagnostics for addressing efficiency barriers.

Introduction

A combination of improved engine and aftertreatment technologies are required to meet increased efficiency and emissions goals. This CRADA section focuses on engine and combustion-uniformity technologies, while a parallel section (NO_x Control and Measurement Technology for Heavy-Duty Diesel Engines) focuses on emissions and catalyst technologies. Improved efficiency, durability and cost can be realized via combustion-uniformity improvements which enable reduction of engineering margins required

by nonuniformities; specifically, these margins limit efficiency. Specific needs exist in terms of reducing cylinder-to-cylinder and cycle-to-cycle combustion variations. For instance, combustion variations mandate system-calibration tradeoffs which move operation away from optimum efficiency points. Combustion variations are amplified at high EGR conditions which are expected in advanced engine systems. Advanced efficiency engine systems require understanding and reducing combustion variations. Development and application of enhanced diagnostic tools is required to realize these technology improvements, and is a major focus of this CRADA.

Approach

The CRADA applies the historically successful approach of developing and applying minimally invasive advanced diagnostic tools to resolve spatial and temporal variations within operating engines and catalysts. Diagnostics are developed and demonstrated on bench reactors and engine systems (as appropriate) at ORNL prior to field application at Cummins.

Diagnostics are applied at ORNL and Cummins to study the nature and origins of performance variations. For example, this may be manifested in cylinder-to-cylinder CO_2 variations due to nonuniform fueling, air and/or EGR charge, fuel spray, component tolerance stacking, or other variations. Detailed measurements are used to assess the performance of specific hardware designs and numerical design tools, and identify nonuniformity origins and mitigation strategies, e.g., hardware and control changes.

Results

An EGR probe, Figure 1, requiring only single-point access was developed and applied to study spatiotemporal EGR distributions. This probe is more broadly applicable and suitable to further developed and packaged engine systems, and is thus capable of more broadly straining the development barriers, e.g., there are many situations requiring measurement and development in which two-point access is not practically possible, such as internal EGR and integrated intake runners. The probe is based on a 3/8-in outside diameter (OD) tube with two flowing measurement cells. Two hollow waveguides and three optics (window, lens and mirror) function to pitch and catch the measurement light across the flowing-cell measurement regions, and deliver it to a dedicated detector. The probe is mounted to the engine via a standard bore-through SwageLok tube union boss, and positioned via a nonswaging ferrule. Figure 1 shows (an early single-cell version of) the EGR probe positioned for spatiotemporal EGR measurements in an intake manifold. The probe has been used with both mid-infrared (MIR) light-emitting diode (LED) (4.3 μm) and laser (2.7 μm) excitation sources.

On-engine measurements at ORNL were used to develop and demonstrate the ability of the EGR probe to resolve transient spatial EGR distributions. The ORNL engine platform used for development and assessment was a GM 1.9-L, 4-cylinder, direct-injection diesel engine with Bosch common rail fuel injection, variable geometry turbo, electronic EGR valve, an intake swirl actuator, and a full-pass Drivven control system. Figure 1 shows the EGR probe mounted in the intake manifold of this engine and the two runners per cylinder associated with the variable swirl.

The EGR probe exceeds the temporal resolution required to resolve cylinder-specific events as demonstrated on the ORNL engine. The left two plots in Figure 2 show natural CO_2 transients associated with engine operation at 1,200 and 1,600 RPM and ca. 12% EGR. Fast transient EGR fluctuations synchronous with the engine timing are observed and associated with specific cylinder exhaust events. The right-hand plot in Figure 2 shows transient CO_2 fluctuations associated with cylinder-selective fuel addition; addition fuel was added to cylinders 1 and 3 and 1 and 4 in the black and red curves, respectively. These results clearly demonstrate fast (ca. 4-8 ms t_{10-90}) temporal response and the ability to resolve cylinder-specific events. This fast temporal response has broad development applications which we intend to pursue in the CRADA including closed-loop control implementation and evaluation, dynamic EGR charge impacts such as misfire, incomplete combustion and knock, and temporal EGR mixing. In similar cylinder-selective fueling variation experiments, the EGR probe measurements indicate misfire with the lowest 20% fueling. Specifically, the EGR probe intake CO_2 measurements correlated with the corresponding cylinder's in-cylinder pressure measurements, further indicating a correlation with this ex-cylinder measurements and a combustion figure of merit; and demonstrates capability to apply the EGR probe to assess cylinder-specific and in-cylinder combustion variations.

The EGR probe was also used to demonstrate intake-manifold EGR spatial nonuniformities on the ORNL engine. The intake hardware orientation consisted of the throttle, EGR inlet, and intake manifold with four EGR probe ports (P1, P2, P3, P4) nominally positioned at the cylinder-runner-pair locations; and with P1 and P4 closest and furthest from the EGR inlet, respectively. The EGR probe was translated across the ca. 75-mm inside diameter intake manifold duct, nominally above each runner set and in an orientation with respect to the runners as described in Figure 3a; this schematic relates to the intake photograph in Figure 1, for which the EGR probe was in the P2 location. Figure 3b

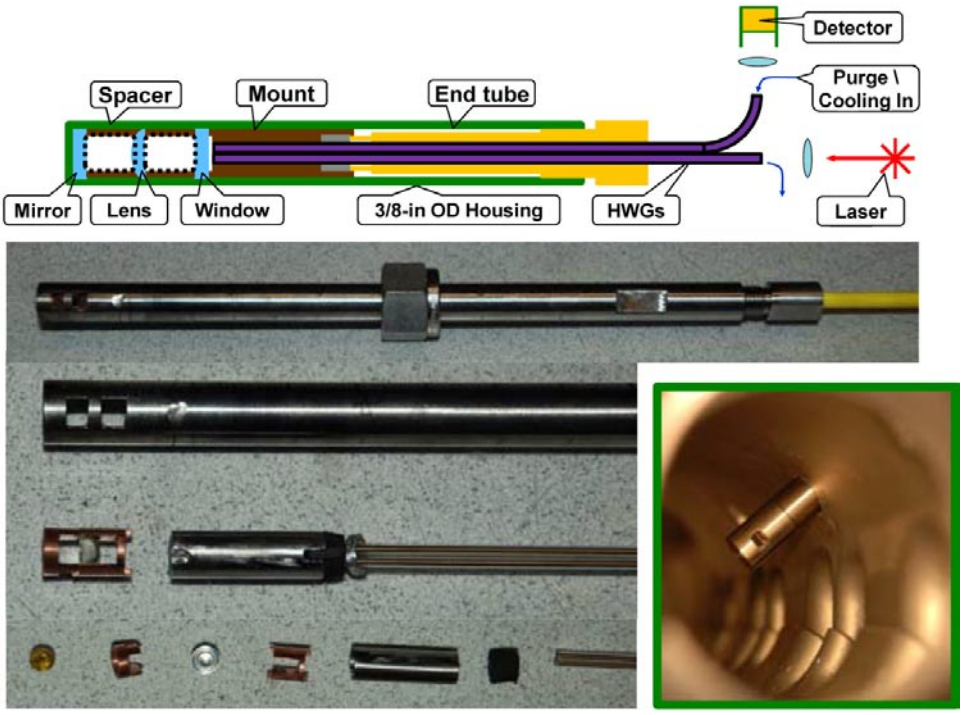

FIGURE 1. EGR probe schematic, exploded-view picture, and installation in an intake manifold. Hollow waveguides pitch and catch the probe light to the measurement flowing cells defined by the space between three optics. The probe is based on a 3/8-in OD tube and positioned via a standard SwageLok union boss and a non-swaging graphite ferrule.

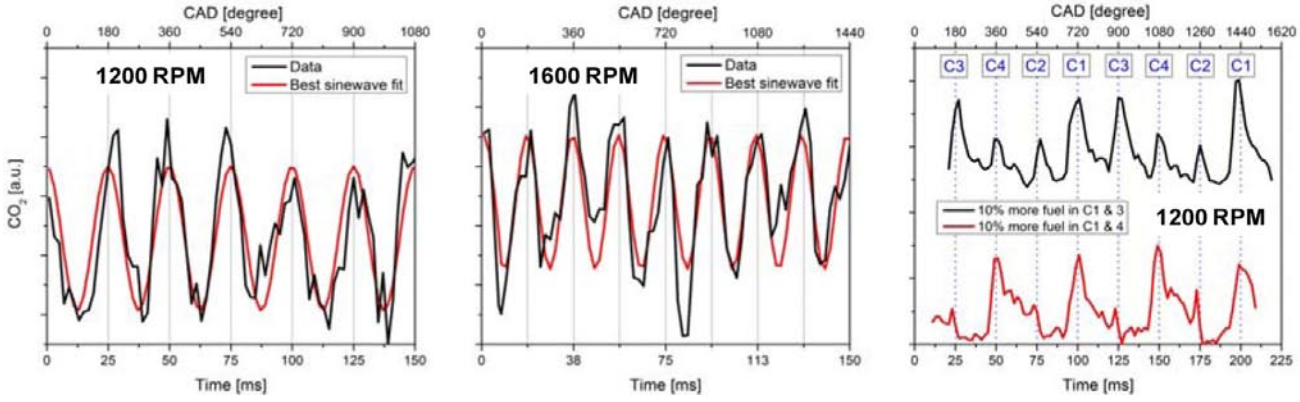

CAD - crank angle degree

FIGURE 2. Transient EGR fluctuations; natural at different engine speeds (left two figures); associated with cylinder-selective fuel addition (right figure)

shows the EGR distribution across the intake duct at the P1 and P3 locations. Notably, at the P1 (cylinder 4) location an extreme EGR nonuniform distribution is observed where ca. 100% undiluted exhaust is observed to flow along the intake-manifold tube wall near where the cylinder runners breathe. Indeed, this 'exhaust river' flowing along the intake manifold tube wall is ca. 15-mm thick , or ca. 20% of the tube diameter. After about a quarter of the distance across the intake manifold tube at this P1 location, the EGR is relatively flat (uniform) at the commanded ca. 20% EGR value. Contrary to the nonuniformity at the P1 location, the EGR is rather uniform at the commanded EGR value by the P3 (cylinder-2 runner) location. Based on these measurements, we expect cylinder 4 to have a significantly greater actual EGR value than the commanded or that of cylinders 3-1. Certainly such EGR nonuniformities can drive cylinder-to-cylinder combustion uniformities and limit overall engine efficiency. Practically, the EGR probe performed very

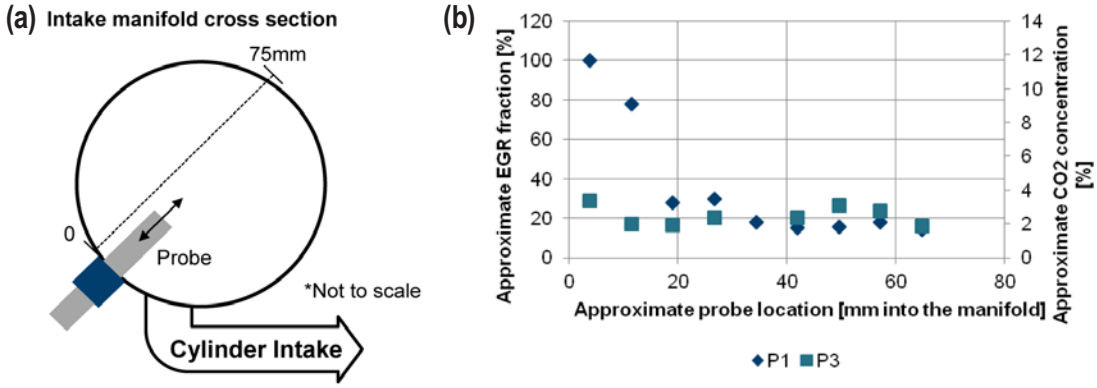

FIGURE 3. EGR uniformity measurement in the General Motors diesel engine. (a, left) EGR probe sampling geometry, (b, right) EGR spatial uniformity measurements at cylinder runners 4 (P1) and 2 (P3).

well and was able to operate for several hours without significant window fouling at the most particulate matter challenging (P1) location and the entire day at the P3 location. When significant fouling was observed, the probe was simply removed and cleaned before continuing measurements. Moreover, there were no significant vibration-induced errors detected.

The EGR probe was used to assess the air handling system and specific EGR mixing hardware of a development engine at Cummins Technical Center. The picture in Figure 4 shows Oak Ridge Associated Universities Postdoctoral Associate, Dr. Jon Yoo adjusting the EGR probe on the engine at Cummins for spatial EGR mapping. The hollow waveguides used to guide the ca. 4.3-um MIR LED light to and from the EGR probe are apparent in the Figure 4 picture. Two EGR mixer designs were assessed at high and low EGR and high and low engine load conditions. The bar graph in Figure 4 shows that Mixer2 provided 34-54% better spatial EGR uniformity compared to the Mixer1 design. These results along with other CRADA-protected insights resulting from this joint campaign are being used to assess specific hardware designs, control parameters and the numerical design tools used in development of next-generation efficiency engines at Cummins.

EGR probe improvements were started to enable improved accuracy in environments with temperature and pressure fluctuations, simultaneous measurement of CO_2, temperature and pressure fluctuations, implementation of simultaneous multiple EGR probes, and applications in high-temperature exhaust applications. Use of a 2.7-μm laser rather than the spectrally broad MIR LED excitation source enables many of these improvements. By probing a single absorption transition the laser enables more accurate and pressure-independent measurements, and implementation of wavelength-modulation spectroscopy which enables better detection limit via improved signal-to-noise ratio, and further negates potential low-frequency interferences such as window fouling. The narrow laser approach also enables high-speed local temperature measurements via two-line approaches. Another laser benefit is having

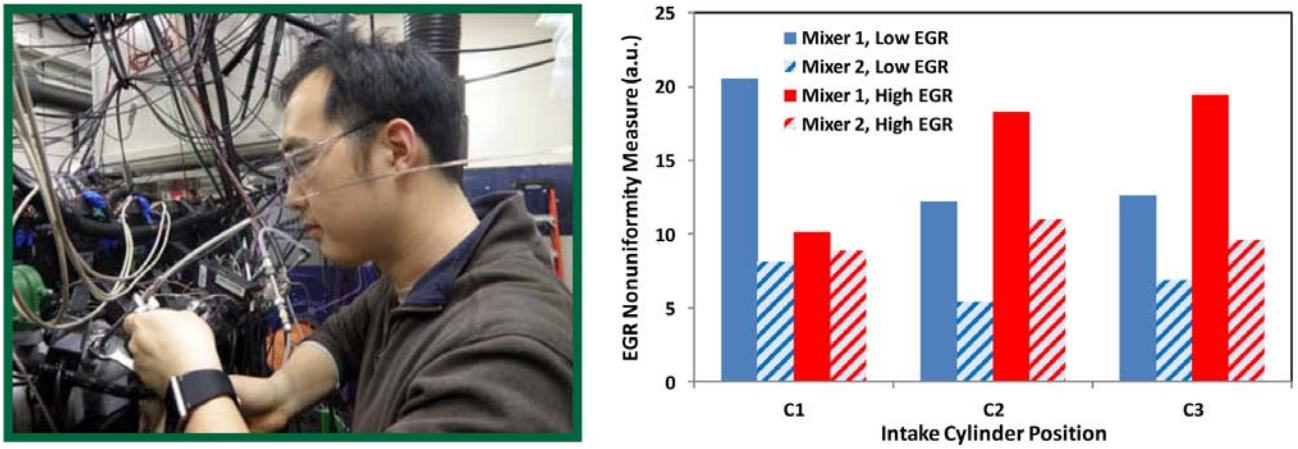

FIGURE 4. EGR probe application for development engine air-handling and EGR-mixer assessment at the Cummins Technical Center.

orders of magnitude more photons, which enable probe multiplexing or deploying multiple probes for simultaneous measurements at multiple locations in the engine system; this allows more extensive mapping of the engine system performance for accelerated development to achieve DOE efficiency objective faster and with lower development costs. The 2.7-µm laser and 4-probe multiplexing hardware have been assembled and are being evaluated and developed as necessary. In addition, the initial high-temperature EGR probe design, which incorporates purge and coolant flow through the hollow waveguides, has been designed, manufactured and evaluated; additional design improvements are ongoing based on evaluation results. Adding exhaust-side measurements allows for improved combustion assessment, control applications, and assessment of EGR-air system transport delays and temporal mixing.

Conclusions

- EGR probe functions well in actual engine applications:
  - Single-point minimally invasive probe access
  - Ready translation, positioning and cleaning
  - Particulate matter fouling and vibrations are practically nonissues
- EGR probe resolves actual engine variations:
  - Fast (ca. <2 ms) cylinder-specific events
  - Single-cylinder misfire events
  - Spatial EGR nonuniformities
- EGR probe enhances development of next-generation efficiency engines:
  - Applied to development engine at Cummins
  - Used to assess hardware designs
  - Used to assess control parameters
  - Applied to assess numerical design tools used in development
- Further EGR probe development further speeds development of engine systems meeting DOE technical goals, reducing development time and cost.

FY 2012 Publications/Presentations

Oral Presentations (2):

1. R. Maggie Connatser, Bill Partridge and Jim Parks. "Facilitating More Precise Control of Selective Catalytic Reduction for Automotive Aftertreatment: Toward Intra-Catalyst Ammonia Detection Using Materials-Modified Optical Fiber Sensors," 58th International Instrumentation Symposium, La Jolla, California, June 5, 2012.

2. Jonathan Yoo, William Partridge. "Spatiotemporal distribution of EGR in an intake manifold using HWG," 58th International Instrumentation Symposium, La Jolla, California, June 6, 2012.

Poster Presentations (3):

1. J. Yoo, J.S. Choi and W.P. Partridge. "Spatiotemporally-Resolved OFDR-Based Measurements of Transient Temperature Distributions within Operating Monolithic Catalysts," CAPoC9 (Ninth International Congress on Catalysis and Automotive Pollution Control), Brussel, Belgium, August 29-31, 2012.

2. J. Yoo, J.S. Choi and W.P. Partridge. "OFDR-Based Measurements of Transient Temperature Distributions within Operating Monolithic Catalysts," 7th International Conference on Environmental Catalysis (ICEC 2012), Lyon, France, September 2-6, 2012.

3. Inchul Choi, William P. Partridge, James Parks. "Diesel Exhaust NO_x/NH_3 Transients Measurement for Fast SCR Reaction," 34th International Symposium on Combustion, Warsaw University of Technology, Warsaw, Poland, July 29 – August 3, 2012.

Special Recognitions & Awards/Patents Issued

Invited Lecture:

1. Jon Yoo, Jim E. Parks, Vitaly Prikhodko , William P. Partridge, Sam Geckler. "An Absorption Spectroscopy Probe for Diagnosing EGR Spatial Uniformity & Cylinder-Resolved Exhaust Transients," Crosscut Workshop on Lean Emissions Reduction Simulation (CLEERS) Teleconference (intra- and international attendance via teleconference) Oak Ridge National Laboratory, June 19, 2012. ***Invited***

Patents:

1. J.E. Parks, W.P. Partridge "Oxygen Concentration Sensors and Methods of Rapidly Measuring the Concentration of Oxygen in Fluids," United States Patent, Patent No. US 8,248,612 B2, Date of Patent August 21, 2012.

Patents Pending (2):

1. R. Maggie Connatser, William P. Partridge, James E. Parks, II, "On-Engine Ammonia Detection Using Evanescent Fields," 9/6/2011. ID-2694 , Patent Pending; USPTO Serial Number 61/654,321; Filed June 1, 2012.

2. Bill Partridge, Jim Parks, Jon Yoo, "EGR Probe based on MIR Spectroscopy using Modulated LEDs and a Single-Port-Access Optical Probe," ID-2759, Patent Pending; USPTO Serial Number 61/657,205; Filed June 8, 2012.

II.20 Engine Benchmarking CRADA Annual Report

Steve McConnell (Argonne National Lab, Primary Contact), David Lancaster (GM), Tom Leon (Ford), John Opra (Chrysler)
Argonne National Laboratory
9700 South Cass Avenue
Argonne, Il 60439
United States Council for Automotive Research (USCAR)
1000 Town Center Drive
Suite 300
Southfield, MI 48075

DOE Technology Development Manager: Gurpreet Singh

Subcontractor:
David Gian, FEV, Auburn Hills, MI

Overall Objectives

- Identify state-of-the-art engine and vehicle technologies currently in production, such as 2-stage lift exhaust valves, advanced turbochargers, spray-on engine liners and advanced engine controls.
- Quantify the benefits of the state-of-the-art vehicle technologies currently in production.
- Optimize vehicle performance using advanced vehicle level modeling such as Autonomie® and the performance maps advanced technologies evaluated in the Cooperative Research and Development Agreement (CRADA).
- Accelerate the development of high efficiency internal combustion engines for light-duty vehicle applications, while meeting the future emission standards, using numerical simulations.
- Support DOE programs with data and analysis of advanced vehicle technologies.

Fiscal Year (FY) 2012 Objectives

- Identified and procured two vehicles with multiple advanced technologies for testing.
- Supplied five data sets from the engine benchmarking data base for USDRIVE goal setting.
- Currently testing two vehicles and evaluating the advanced technologies within each vehicle.

Accomplishments

- Attained the 2012 Audi A4 with twin variable geometry turbochargers, direct injection and variable valve lift 2.0 liter engine for testing.
  - The vehicle level testing is complete and the vehicle has been torn down for engine level and component testing.
  - The engine level testing is complete with an emphasis on speed/load areas where the variable geometry turbo and variable valve lift are operated.
- Attained the 2012 Mini Cooper with a 1.6 liter turbocharged direct injected variable valve timing engine.
  - Vehicle and engine level testing are complete. Final reports will be supplied by the end of November 2012.
- Supplied vehicle data sets for BMW 530i, Toyota Prius and Toyota Auris to the vehicle systems group for the USDRIVE goal setting exercise.

Future Directions

- Evaluate new technologies such as the Nissan Micra (1.4 liter turbocharged direct injected engine) and another vehicle to be identified.
- Analyze the new emerging technologies and how they are used.
- Conduct analysis on the new and emerging technologies to determine their maximum fuel saving potential.

Introduction

The goal of the engine benchmarking CRADA is to accelerate the development of high efficiency internal combustion engines for light-duty vehicle applications, while meeting the future emission standards, using numerical simulations. The CRADA will support this goal by gathering engine and engine component data for use in DOE's programmatic efforts.

Approach

The CRADA partners continuously research current and future model engines and vehicles with new features to assist the USCAR and laboratory members in selecting

vehicles for investigation. The CRADA will provide a brief one-page summary of published specifications and features for each vehicle under consideration.

Once procured, the vehicle baseline testing will then be conducted followed by instrumentation and the vehicle-level investigation. The vehicle investigation may include electronic control unit (ECU) mapping to determine calibration settings. The testing will document the engine controller features, inputs and outputs with an ECU analysis report. The powertrain will then be removed from the vehicle and prepared for engine dynamometer testing. The engine, in the as-installed vehicle configuration, would be installed in an engine test cell for full-load performance and a full engine map to investigate emission characteristics, fuel consumption, performance and implementation of engine control hardware. As an option, additional motored strip-down engine tests could be conducted to analyze friction losses following the thermodynamic investigations. The final step in the engine investigation will be a detailed design analysis and documentation of all of the engine components. The entire engine will be disassembled and the parts will be documented and described in detail with regard to their function and geometry.

Results

- Attained the 2012 Audi A4 with twin variable geometry turbochargers, direct injection and variable valve lift 2.0 liter engine for testing.
  - Vehicle and engine level testing are complete. Final reports will be supplied by the end of November 2012.
- Attained the 2012 Mini Cooper with a 1.6 liter turbocharged direct injected variable valve timing engine.
  - Vehicle and engine level testing are complete. Final reports will be supplied by the end of November 2012.
- Supplied vehicle data sets for BMW 530i, Toyota Prius and Toyota Auris to the vehicle systems group for the USDRIVE goal setting exercise.

Conclusions

- Engine maps provided by this CRADA aided the USDRIVE goals setting team in developing its goals by showing the possibilities of various technologies and their effects on engine efficiency.
- Engine maps provided by this CRADA have been used to support the Government Performance Results Act study so that DOE program managers can tailor their portfolio of research technologies. The state-of-the-art engine maps help establish the baseline performance for present technologies and give a better idea of where the technology could evolve. This is done by simulating low-, medium- and high-technology cases from 2015 out to 2045.
- Engine maps provided by this CRADA have aided in the goal setting and research roadmap development for the Advanced Combustion and Emissions Control Tech Team at USCAR.

FY 2012 Publications/Presentations

1. Due to the confidential nature of the data, the USCAR Engine Benchmarking Team has decided to keep the information generated in this CRADA confidential.

II.21 Neutron Imaging of Advanced Transportation Technologies

Todd J. Toops (Primary Contact),
Charles E.A. Finney, Eric J. Nafziger,
Josh A. Pihl
Oak Ridge National Laboratory (ORNL)
2360 Cherahala Boulevard
Knoxville, TN 37932

DOE Technology Development Manager:
Gurpreet Singh

Objectives

- Develop non-destructive, non-invasive neutron imaging technique and implement it to improve understanding of advanced vehicle technologies.
- Improve understanding of regeneration behavior in diesel particulate filters (DPFs) through comprehensive, quantitative device analysis:
  - Fuel penalty associated with regeneration.
  - Ash build-up.
  - Validation of full-scale modeling.
- Provide complementary analytical tool to guide internal and external fluid flow properties in fuel injectors:
  - Internal cavitation occurrences in commercial fuel injectors.

Accomplishments

- Improved visualization tools to enable identification of particulate from DPF walls:
  - Illustrated dense particulate pattern could be independently visualized from DPF wall.
- Identified particulate depth as a function of length, radius, and particulate loading:
  - Particulate filters filled to 3, 5, and 7 g/L.
  - Imaged with neutrons to identify particulate profile.
  - Completed investigation of sequential regeneration and proposed conceptual model.
- Built portable spray chamber with high pressure fluid delivery system for diesel injectors:
  - No windows necessary; aluminum transparent to neutrons.
  - Efforts focused on integrating spray timing with neutron detector shutter.

Future Directions

- Incorporate ash-laden and catalyzed samples into DPF study:
  - Implement neutron sensitive ash.
  - Investigate impact on soot loading and regeneration.
  - Study NO_2 passive oxidation on catalyzed samples.
- Move to fluid dynamic study within fuel injectors:
  - Requires stroboscopic approach with detector shutter and fuel injector coordination.
  - Focus on cavitation studies.
  - With improved resolution, correlate internal injector dynamics to near nozzle spray patterns.

Introduction

Unlike X-rays, neutrons are very sensitive to light elements such as hydrogen atoms and can penetrate through thick layers of metals (Figure 1a) [1]. These two properties suggest neutrons are well suited to probe engine system components such as diesel particulate filters, exhaust gas recirculation coolers, fuel injectors, oil in engines, oil residues in filters, etc., as illustrated in previous investigations [2-5]. Neutron imaging is based on the measurement of a beam attenuated by a given sample, i.e. it is a comparison of an open beam, with all neutrons in a given pathway, versus a beam affected by the sample of choice. The attenuation is caused by absorption and scattering of neutrons within the sample, such as would be the case with hydrogen containing hydrocarbons. A two-dimensional position-sensitive detector placed behind the sample can measure the transmitted neutron flux, as illustrated in Figure 1b. When combined with a well-controlled rotational stage it is possible to perform computed tomography scans and thus generate three-dimensional images of working fluids inside real devices. Samples can be analyzed at one cross-section, or a complete reconstruction can provide a cross-section of the entire sample at a resolution of the detector (currently ~50 microns). An example of this can be seen in Figure 2, where a destructively obtained cross-sectional image showing a catalyst washcoat in a DPF (Figure 2a) is matched to a virtual cross-section

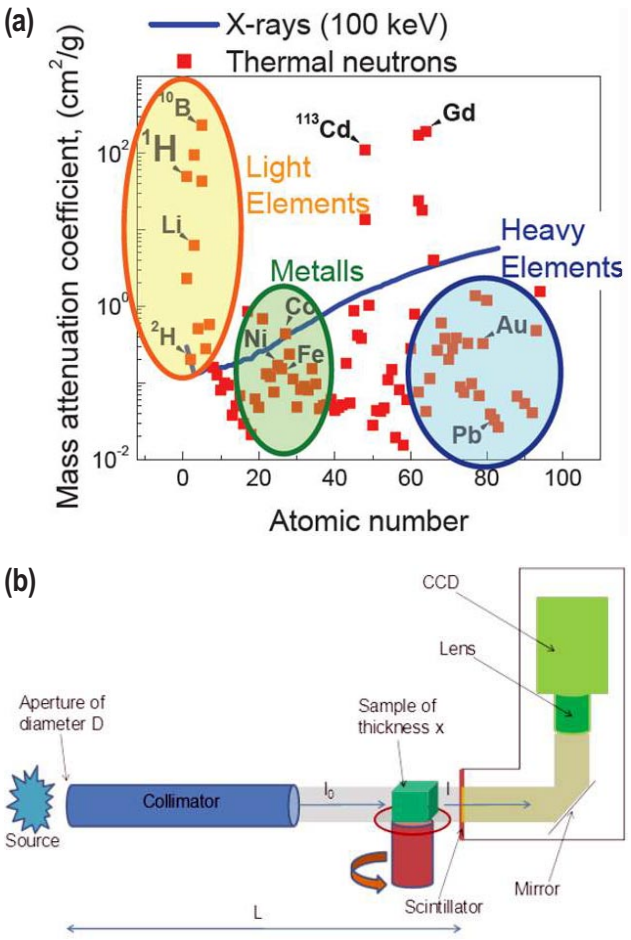

FIGURE 1. (a) Mass attenuation coefficients of a range of elements as a function of atomic number. Comparison given between neutron (squares) and X-rays (line). (b) Schematic of a neutron imaging facility at ORNL.

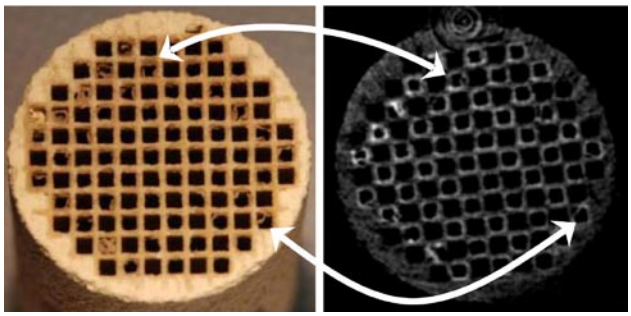

FIGURE 2. (a) Catalyzed DPF was cut open to verify washcoat morphology was pulling away from walls. (b) Virtual slice at approximately same depth reveals the morphology is captured by the reconstruction.

obtained by neutron imaging prior to cutting open the device (Figure 2b). This non-destructive technique can be applied to a wide range of processes in advanced combustion engine systems to advance the knowledge-base and to help validate or redefine models.

Approach

This project is focused on using this unique technique to advance the understanding of two components being employed in modern diesel vehicles: the DPF and the in-cylinder diesel injector. DPFs are a key component of the emissions control system for modern diesel engines, yet there remain significant questions about the basic behavior of the filters. In particular, understanding the progression of the soot cake layer during regeneration is of particular interest. The results of these measurements will provide critical data to the aftertreatment modeling community on the evolution of soot profiles, which are important factors in modeling the fuel intensive regeneration of the DPF. Additionally, efforts are aimed at investigating intra-nozzle fuel injector flow and cavitation during dynamic spraying. These efforts are designed at improving understanding of how external conditions influence internal dynamics, especially as it relates to advanced combustion regimes and injector durability. In carrying out these studies we work closely with industrial partners to obtain relevant systems and devices. The close proximity of our research facility to the neutron beam allows for iterative studies when appropriate (such as with the DPF).

Results

Three different silicon carbide DPFs were loaded to 3, 5, and 7 g particulate per liter of DPF. In our previous study investigating a single particulate loading in a cordierite filter, there was a very distinct layer of soot observed as the soot particulate had strong contrast compared to the cordierite wall [2]. In the silicon carbide DPFs in this study, the contrast was minimal between the soot particulate and the wall making it difficult to measure the transition and thus the particulate layer. However, the reconstructed DPFs revealed that the open cross-sectional area of the inlet channels was measurably less than the outlet channels. This enabled the use of a simple geometric formula to account for the area differences between the inlet channel and its adjacent outlet channels. Applying an area calculating algorithm for each virtual slice allowed the determination of thickness of the particulate layer, T_p, for each channel. For simplicity, the T_p for each inlet was averaged over the entire slice and thus it could be plotted as a function of length along the channel, as shown in Figure 3. Averaging over the entire DPF reveals an average soot cake thickness of 57, 96, and 131 µm for the silicon carbide PFs loaded to 3, 5, and 7 g/L. Converting these thicknesses into soot cake density, it was determined that

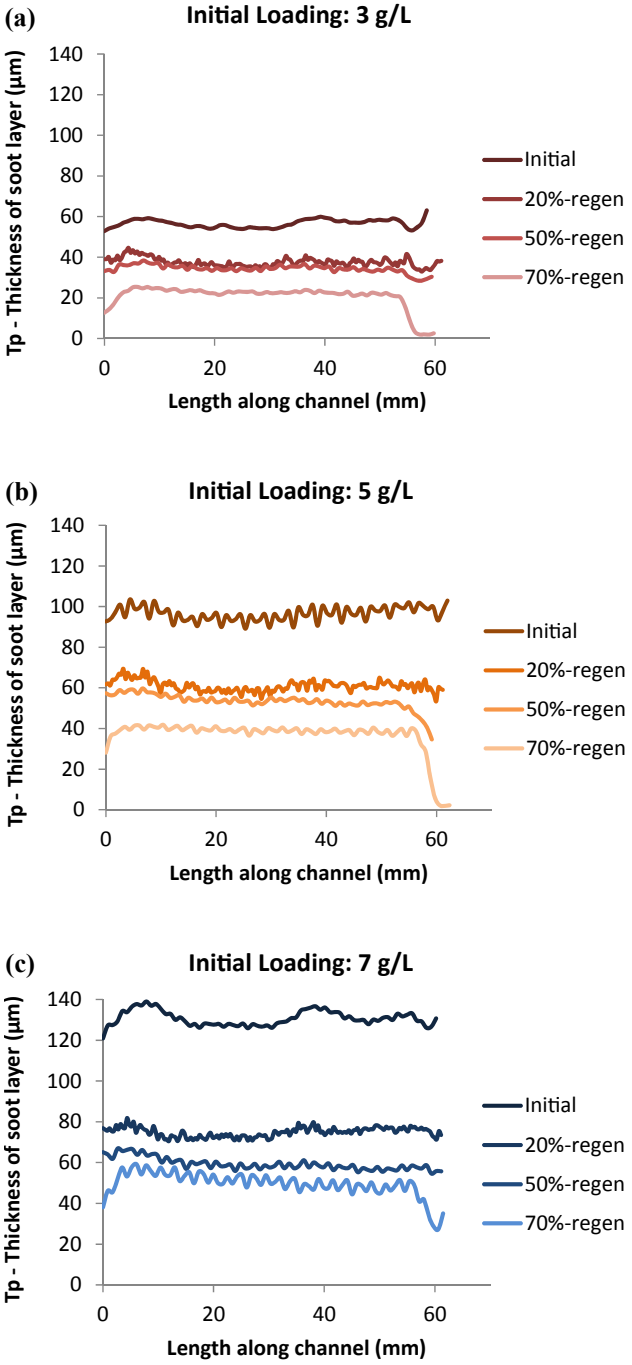

FIGURE 3. The average soot cake layer thickness of all channels in a given virtual slice is plotted as a function of length for the DPFs. The samples are initially loaded to (a) 3, (b) 5, and (c) 7 g/L, followed by sequential nominal regeneration to 20%, 50% and 70% levels.

the soot cake of all three initial samples were statistically identical ("initial" bar in Figure 4).

Following this investigation of the initial soot layers, a controlled sequential regeneration procedure was initiated. Figure 3 shows that the soot cake layer decreased in thickness sharply during the initial 20%

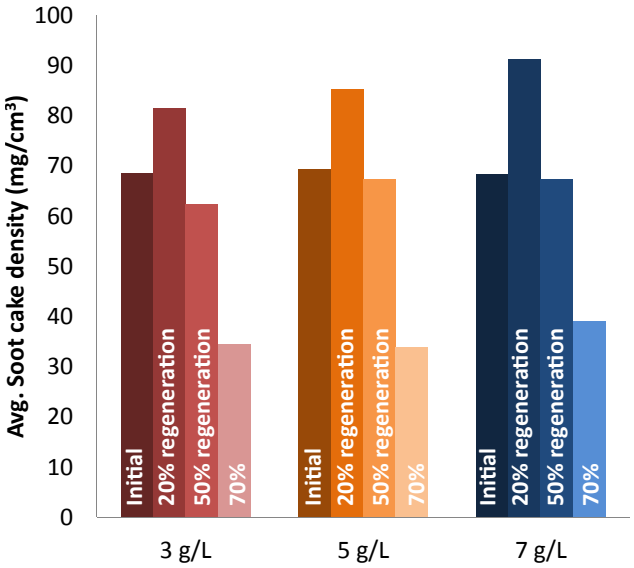

FIGURE 4. Calculated values of the average soot cake density for the profiles in Figure 3.

regeneration for all three samples, which is also reflected in the sharp rise in the soot cake density in Figure 4, i.e. the thickness decreased more than would be predicted from a simple monotonic regeneration. Analysis at 50% regeneration shows that the soot cake thickness has not changed significantly, and as the samples are regenerated to 70% the decrease from 20 to 70% is not as significant as it was in the first 20% regeneration (Figure 3). These observations continue to be illustrated in the density calculations in Figure 4, i.e. the soot cake density only increases in the first step, and then decreases sharply as the volume is not decreasing as fast as the mass. Additionally, it is observed that the first area that is fully regenerated is occurring in the rear of the inlet channels; signs of this are seen in all three samples. These observations have led to a conceptual model of the regeneration process, as illustrated in Figure 5. A uniform particulate layer is observed for the initially loaded sample. After regenerating 20% of the sample the soot cake layer thickness decreases significantly, but the density of the layer increases greatly. At 50% regeneration average soot cake density decreases sharply as pores open in the layer; this process continues through 70% regeneration. The DPF is fully regenerated at the rear of the inlet channels first.

In addition to the DPF study, the neutron imaging approach is being employed to study fluid dynamics in diesel fuel injectors. Initial efforts are aimed at defining the spatial and temporal resolution possible with our current setup and identifying areas needed for further improvement. Figure 6a shows how the technique is able to convey internal geometries of the commercial injector,

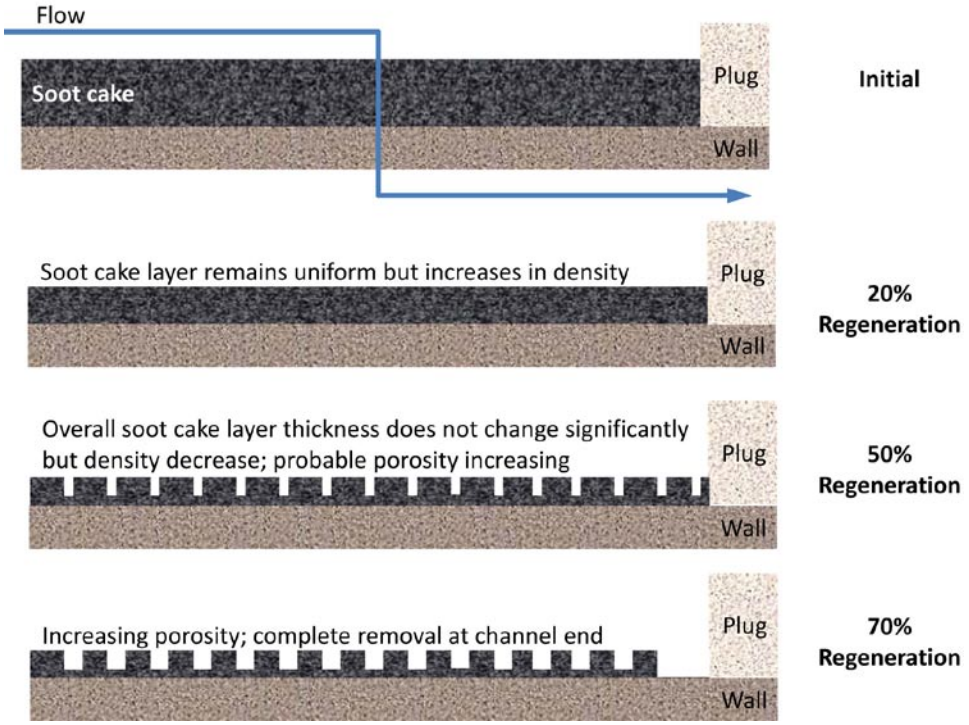

FIGURE 5. Conceptual model of progression during soot cake layer during regeneration.

with the areas of highest contrast being associated with the non-metal regions where the hydrocarbons flow. Figure 6b shows how computed tomography scans can be employed to investigate cross-sections of the fuel injector and highlight areas where voids can occur. This void is significantly larger than the cavitations that are expected to occur during dynamic operation, but this illustrates the potential of the technique. Cavitation is a major contributor to injector failure and impacts the combustion flame front; understanding the conditions and injector geometries that lead to cavitation is important as new, high-efficient combustion strategies are investigated. This is expected to have a broad impact as in-cylinder injectors are starting to become more prevalent in gasoline vehicles (gasoline direct injection). Recent efforts have moved to dynamic spraying and imaging of both intra-injector flow and near nozzle spray dynamics.

Conclusions

Neutron imaging has been successfully employed to capture key particulate layer behavior during a sequential DPF regeneration. The results are currently being shared with academic and industrial modelers as the quantitative results generated in this study are directly applicable as model inputs. Improved resolution will be necessary to capture particulate penetration into the wall of the DPFs. Applying this technique to fuel injectors offers an opportunity to obtain information that is difficult to measure using current approaches with X-rays, without altering the materials or fluids being used, and thus can help to answer key questions regarding fluid flow inside the injector.

References

1. N. Kardjilov's, "Absorption and phase contrast neutron imaging", Imaging and Neutrons 2006, Oak Ridge, TN, October 23–25, 2006; http://neutrons.ornl.gov/workshops/ian2006/MO1/IAN2006oct_Kardjilov_02.pdf

2. A. Strzelec, H.Z. Bilheux, C.E.A. Finney, C.S. Daw, D.E. Foster, C.J. Rutland, B. Schillinger, M. Schulz, SAE Technical Paper 2009-01-2735 (2009).

3. G.D. Harvel, J.-S. Chang, A. Tung , P. Fanson, M. Watanabe, SAE Technical Paper 2011-01-0599 (2011).

4. B. Ismail, D. Ewing, J.S. Cotton, J.-S. Chang, SAE Technical Paper 2004-01-1433 (2004).

5. M.J. Lance, C.S. Sluder, H. Wang, J.M.E. Storey, SAE Technical Paper 2009-01-1461 (2009).

FY 2012 Publications/Presentations

1. Todd J. Toops, Charles E.A. Finney, Josh A. Pihl, Hassina Z. Bilheux, Sophie Voisin, Jens Gregor, "Non-destructive Neutron Imaging to Analyze Particulate Filters", 2012 Directions in Engine-Efficiency and Emissions Research Conference (DEER), Dearborn, MI, October 18, 2012.

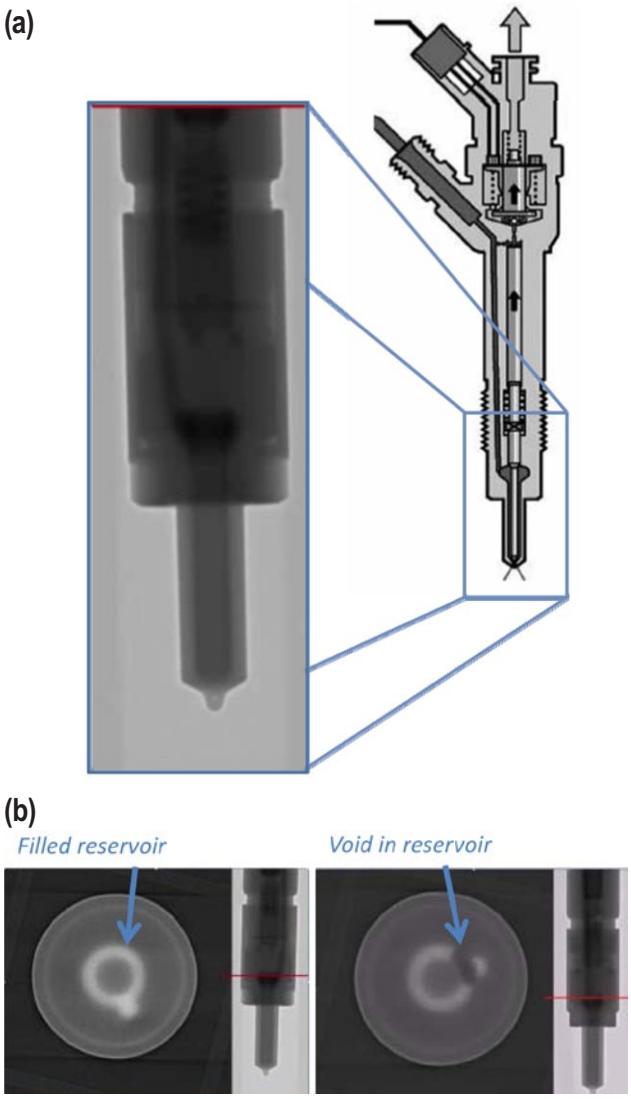

FIGURE 6. (a) Cutaway diagram of a commercial diesel fuel injector and the corresponding image obtained with neutron radiography. Areas of highest contrast are associated with hydrocarbons inside metal fuel injector. (b) Virtual cross-section of two fuel injectors, one with the reservoir filled (left) and another with a void (right).

2. Todd J. Toops, Charles E.A. Finney, Eric J. Nafziger, Josh A. Pihl, "Neutron Imaging of Advanced Transportation Technologies", 2012 DOE Annual Merit Review, Crystal City, VA, May 14–18, 2012.

3. Todd J. Toops, Hassina Bilheux, Sophie Voisin, Jens Gregor, Charles E.A. Finney, Josh A. Pihl, Andrea Strzelec, "Non-destructive, Non-invasive Neutron Imaging of Soot, Ash and Washcoat Deposition in Particulate Filters", 2012 Cross-cut Lean Exhaust Emissions Reduction Simulations (CLEERS) Workshop, Dearborn, Michigan, April 30 – May 2, 2012.

4. Todd J. Toops, Hassina Bilheux, Sophie Voisin, Jens Gregor, Charles E.A. Finney, Josh A. Pihl, Andrea Strzelec, "Non-destructive, Non-invasive Neutron Imaging of Soot, Ash and Washcoat Deposition in Particulate Filters", 2012 SAE World Congress, Detroit, Michigan, April 24-26, 2012.

5. T.J. Toops, C.E.A. Finney, A. Strzelec, H. Bilheux, S. Voisin, and J. Gregor, "Imaging of Diesel Particulate Filters using a High-Flux Neutron Source", presented at the DOE 2011 17th Directions in Engine-Efficiency and Emissions Research (DEER) Conference, Detroit, Michigan, October 3–6, 2011.

II.22 Detailed Assessment of Particulate Characteristics from a Low-Temperature Combustion Engine

Kyeong O. Lee (Primary Contact), Heeje Seong
Argonne National Laboratory
9700 South Cass Ave.
Argonne, IL 60439

DOE Technology Development Manager:
Gurpreet Singh

Subcontractor:
Engine Research Center, University of Wisconsin, Madison, WI

Overall Objectives

- Evaluate particulate emission data measured by a scanning mobility particle sizer (SMPS) and transmission electron microscopy (TEM).
- Investigate effects of biofuels on particulate emissions from low-temperature combustion (LTC) and spark ignited direct injection (SIDI) engines, in terms of morphology, particulate matter (PM) mass and nanostructure.
- Provide the thermo-physico-chemical properties of particulate emissions for the development of future particulate filtration systems, targeting LTC and SIDI engines.

Fiscal Year (FY) 2012 Objectives

- Assess nanoparticles from LTC by comparison of particle sizes measured by an SMPS and TEM.
- Examine LTC soot morphology and nanostructures to better understand soot formation mechanisms in LTC modes.
- Evaluate the effects of biodiesel-blended fuels on particulate emissions from LTC modes.

Accomplishments

- Revealed by comparison of SMPS data with TEM results that aggregate particles smaller than 10 nm, which were found to be abundant in the LTC engine emissions, are not solid carbon particles.
- Demonstrated that LTC soot particles are much smaller in both primary and aggregate particle sizes than those from conventional diesel engines.
- Illuminated that soot oxidation is insignificant during the LTC process by examination of nanostructures as well as morphology.
- Found that biodiesel soot appears to be much smaller in both primary and aggregate sizes than does ultra-low sulfur diesel (ULSD) fuel soot, which results in the reduced total soot mass.

Future Directions

- Evaluate the effects of engine operating parameters, such as injection timing, air-fuel ratio and engine load, on morphology, nanostructures of SIDI soot emissions by using a TEM.
- Assess nanoparticles from SIDI engines with alcohol-blended fuels, in comparison with particles from gasoline combustion.
- Evaluate thermo-physico-chemical properties of SIDI soot by using a thermogravimetric analyzer, a Raman microscope, and a TEM.

Introduction

Many researchers are working on in-cylinder combustion studies, aiming to lowering the exhaust emission levels along with high thermal efficiency, by means of introducing new types of combustion technologies, inclusive of homogeneous charge compression ignition (HCCI), reactivity controlled compression ignition (RCCI), and LTC. In comparison with conventional diesel engines, LTC engines typically use a lower compression ratio to operate at low combustion temperatures. With increasing interest in LTC, researchers have investigated the characteristics of PM emission formation by measuring particle sizes and concentrations at various LTC conditions, and reported new findings: the number of nucleation mode particles significantly increased at LTC modes, while the mass of PM emissions was reduced, compared with those from conventional diesel engines. Since these nano-sized nucleation mode particles are measured by means of commercial measurement instruments, such as SMPS and electric low-pressure impactor, it is very difficult to clarify whether they are solid carbon particles called soot or a saturation of volatile components like hydrocarbons, sulfate, water, and organics. Because the commercial instruments count all the particles involved

in the measurement, it is necessary to separate carbon particles from other chemical compounds dissolved in the emissions. Electron microscopy can identify these components in a qualitative basis, which helps us better understand the soot formation process in LTC. Because LTC conditions generate less thermal energy than do conventional diesel engines, the properties of soot particles, such as morphology and nanostructures, are anticipated to be quite different from those from conventional engines. However, the detailed properties of LTC soot particles have rarely been reported. Therefore, the Argonne research team has worked on assessing the detailed morphology and nanostructures of particulates emitted from an LTC engine by using a TEM.

Approach

This work has been conducted in collaboration between Argonne National Laboratory (ANL) and University of Wisconsin (UW)-Madison. The Engine Research Center at UW-Madison investigated particulate emissions from a single cylinder LTC engine using an SMPS, in terms of particle size distribution and number density, and provided engine combustion data at various operating conditions. ANL collected soot samples from the LTC engine at UW-Madison by a novel thermophoretic sampling system. Then, the primary and aggregate sizes of the LTC particles were measured by means of a TEM and a custom image/data acquisition system. The particle sizes obtained by TEM analyses were compared with those by SMPS measurements. Fractal geometry was also analyzed to verify the soot formation models of an LTC engine previously proposed on the basis of SMPS data. In addition, nanostructures of LTC soot were examined in detail at different experimental conditions to reveal any differences in particle internal structures. The engine was operated at various fuel injection times (22, 26 and 30° before top-dead center, BTDC) with various fuels (ULSD, soy methyl ester 20% + ULSD 80% blend [SME20], and palm-oil methyl ester 20% + ULSD 80% blend [PME20]).

Results

In order to examine particulate emissions, the engine was operated at a 2,000 rpm and 5.5 bar indicated mean effective pressure condition. Particulate number distributions were measured by an SMPS instrument at different injection timings with the three different fuels, as a function of mobility diameter (Figure 1). The profiles display bimodal distributions where both nucleation and accumulation mode particles appeared to exist. An important observation is that the curves of those nucleation mode particles smaller than 10 nm are almost identical, despite different fuel types and injection timings. There is a gradual shift to a smaller size at the junction of the two modes with injection timing. Also, the maximum number of particles was observed to be around 75 nm, regardless of fuel type and injection timing. Overall, the differences in size distribution dependent on fuel type diminish with advancing fuel injection timing, thereby showing an almost identical profile among the three fuels. It is shown that the mean diameter gradually diminishes, from approximately 80 nm to 60 nm, because the number of particles between 10 nm and 15 nm increases while that of particles with the largest population decreases with advancing injection timing.

Direct observations of LTC soot particles have been conducted with TEM images. As observed in Figure 2, the majority of soot aggregates appear to be chain-like structures in shape, where individual primary particles closely agglomerate each other. This particle morphology was shown for soot particles from conventional diesel combustion as well. With this analytic methodology, meanwhile, one could rarely observe any soot particles

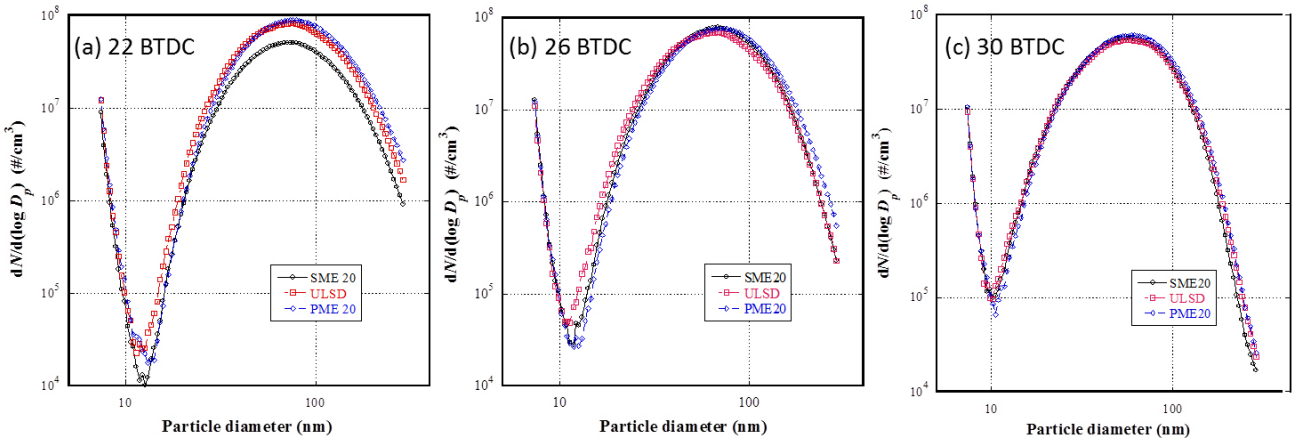

FIGURE 1. Particle Size Distributions Measured by an SMPS with Advancing Injection Timing

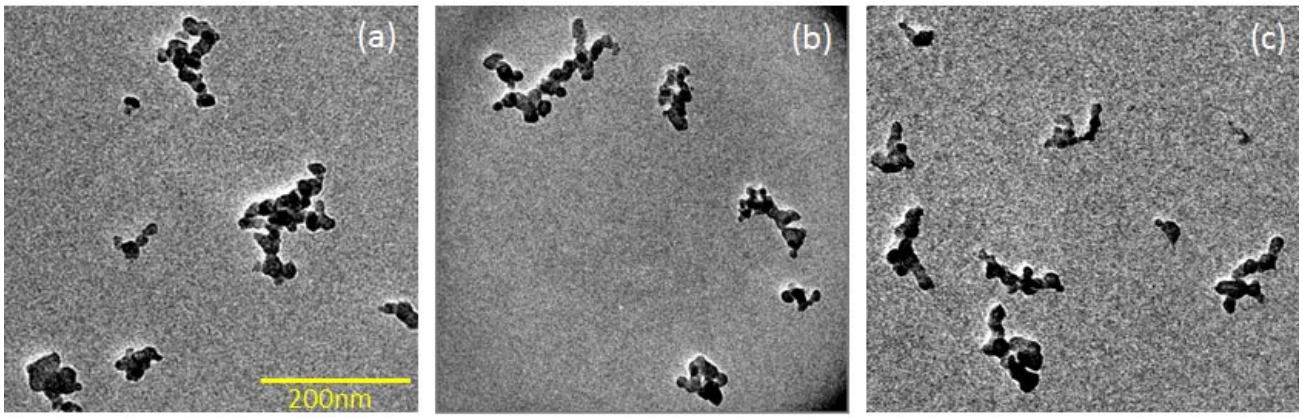

FIGURE 2. TEM Images of LTC Soot Aggregates for (a) SME20, (b) PME20, and (c) ULSD

smaller than 10 nm. This observation offers an important implication for the particle size distributions measured by the SMPS. It is quite apparent that most of the nucleation mode particles measured by the SMPS, of which the size was ranged smaller than 10 nm, should not be solid carbon soot particles.

This visual observation by the TEM was quantified by accurately measuring the sizes in terms of the primary particle diameter and radius of gyration of aggregates. The sizes of aggregate particles were analyzed by the image/data acquisition system in terms of radius of gyration (R_g), and their distributions were compared for different fuels and injection timings, as shown in Figure 3. Figure 3(a) shows that the radii of gyration ranged from approximately 8 nm to 75 nm, regardless of fuel type. The largest population of aggregates for ULSD was found to be in the R_g range of 15 nm to 25 nm. In comparison, aggregates for SME20 showed the most abundance in the size range of 10 nm to 20 nm, while those for PME20 were observed to be the most between 20 nm and 35 nm. The effects of injection timing on size distributions were also examined, as displayed in Figure 3(b). With advancing injection timing, it was clearly shown that the largest population of aggregates moves toward larger aggregate sizes. Also, the population of large aggregates increased with advancing injection timing: at 30° BTDC large aggregates over 70 nm of R_g were often found, while at 22° BTDC those large aggregates were rarely observed. Therefore, it is obvious that advancing injection timing shifted the overall size

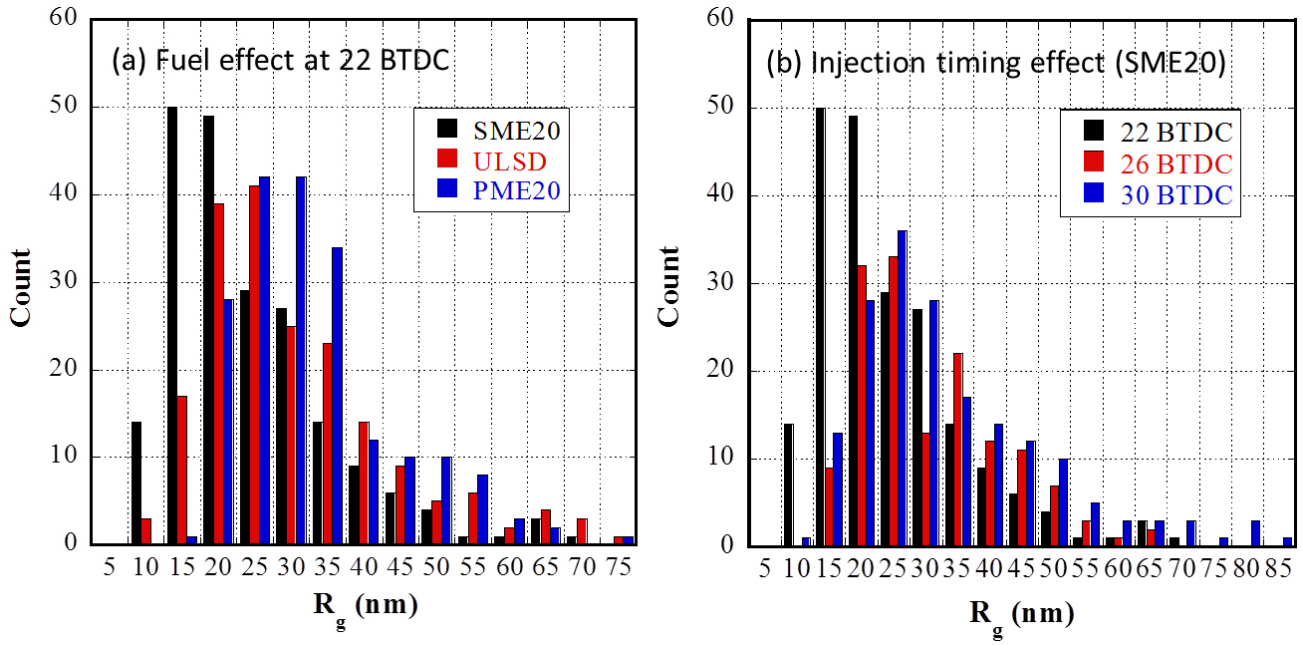

FIGURE 3. Size Distributions of Soot Aggregates in Terms of Radius of Gyration

distribution to the right, which ultimately increased the number of large aggregate particles. For reference, our previous studies revealed that with conventional diesel engines, the radii of gyration were distributed between 20 nm to 180 nm. Obviously, this indicates that soot aggregates from LTC modes are by far smaller than those from conventional modes.

Table 1 lists the average primary particle diameters, radii of gyration, and fractal dimensions for SME20, PME20, and ULSD at different fuel injection timings. The sizes represent the physical dimensions of soot particles — apparently different from those aerodynamic- or mobility-equivalent diameters measured by commercial size-measurement instruments. In addition, the commercial size-measurement instruments cannot measure the primary particle size. As seen in the table, the primary particle diameter varied in a range of approximately 13 nm to 17 nm with advancing injection timing, indicating that the 30° BTDC injection timing apparently increased the particle size. Meanwhile, the size of aggregate particles also increased in the ranges of 22 nm to 31 nm in terms of R_g, with advanced injection timing. According to many studies, the average diameters of primary particles range between 20 nm and 50 nm for conventional engine modes. Therefore, it is apparent that soot particles from LTC modes are much smaller in both sizes of primary particles and aggregates than those from conventional engine modes.

TABLE 1. Average Primary Particle Diameters and Radii of Gyration

Fuel	Injection timing (°BTDC)	Primary particle diameter (d_p), nm	Radius of gyration (R_g), nm	Fractal dimension (D_f)
SME20	22	14.4	22.1	1.73
	26	13.2	28.2	1.70
	30	16.9	31.0	1.62
PME20	22	10.9	25.0	1.58
ULSD	22	14.8	28.0	1.57

As shown in Table 1, the fractal dimension slightly decreased from 1.73 to 1.70 and 1.62 with advancing injection timing. This difference between 1.73 and 1.70 seems to be in the same range of uncertainties. Still, however, the lower value of the fractal dimension at 30° BTDC suggests that the soot aggregates became more chain-like structures with advancing injection timing to some degree. Also, the fractal dimensions (D_f) were evaluated to be 1.73, 1.58 and 1.57 for SME20, PME20, and ULSD, respectively. This result implies that the aggregate particles became more compact in shape with SME20 than with PME20 and ULSD. This range of fractal dimensions falls in that of conventional light-duty diesel engines. Therefore, the fractal geometry of particles from the LTC engine used in this work resembles that of conventional diesel particles, although the sizes of LTC soot particles turned out to be smaller than those of conventional diesel particles

Figure 4 shows high-resolution TEM (HRTEM) images of LTC primary soot particles. The images, taken at 600,000x, provide a glimpse of how LTC soot particles are formed during the combustion process. Each primary particle with approximately 10-nm to 20-nm diameter has a single nucleus, similarly for both SME20 and ULSD particles collected at 22° BTDC injection. The fringe layers within a primary particle are stacked concentrically around a nucleus. However, they are very low-degree graphitic structures showing short-ranged fringe layers and rough outer surface, especially for SME20 soot, compared to conventional diesel soot (see Figure 4(c)). The lowered soot emissions from the LTC engine would give less opportunity for soot surface to grow under the low in-cylinder temperature. Also, low combustion temperature has an impact not only on soot surface growth during soot formation, but also on the realignment of fringe layers during soot oxidation.

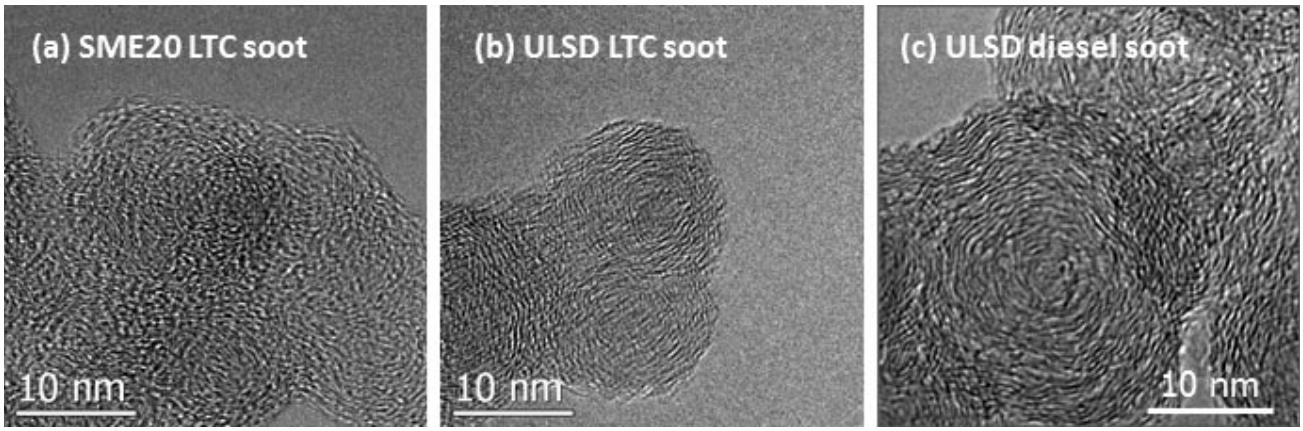

FIGURE 4. HRTEM Images of Soot Particles

Therefore, the rough outer surfaces of particles and short-ranged fringe layers observed in LTC soots are a clear indication that LTC soot has not undergone significant soot oxidation.

Conclusions

Particle sizes from LTC modes were measured by an SMPS and a TEM for two biofuel mixtures (SME20 and PME20) and ULSD at different injection timings.

- Based on the TEM examinations, aggregate particles smaller than 10 nm were rarely observed. Hence, the nucleation mode particles measured by the SMPS are to be condensed volatile organics.
- LTC soot particles were found to be smaller in both primary and aggregate particle sizes than those from conventional diesel engines.
- LTC soot particles represent chain-like fractal geometry, similar to that for conventional diesel soot.
- Examinations of nanostructures as well as morphology propose that soot oxidation was insignificant during the LTC process. Therefore, the degree of graphitic structures appeared to be relatively low.

FY 2012 Publications/Presentations

1. Heeje Seong, "Morphology and Nanostructures of Soot Particles from Various Reciprocating Engines," 2012 Joint Workshop on Advanced Particulate Filtration Technologies (ANL, MIT, and Tokyo Tech), Argonne, IL. August 2012.

2. Kyeong Lee, Heeje Seong, and Yuki Kameya, "Examination of Particulate Emissions from Various Combustion Sources," The United States Council for Automotive Research (USCAR), Southfield, MI. July 2012.

3. Kyeong Lee, Heeje Seong, Cory Adams, and David Foster, "Detailed Assessment of Particulate Characteristics from Low-Temperature Combustion Engines," DOE Merit Review, Arlington, VA. May 2012.

4. Heeje Seong, Kyeong Lee, Seungmok Choi, Cory Adams, and David Foster, "Characterization of Particulate Morphology, Nanostructures, and Sizes in Low-Temperature Combustion with Bio-Fuels," SAE paper, 2012, 2012-01-0441.

II.23 Improved Solvers for Advanced Combustion Engine Simulation

Matthew McNenly (Primary Contact), Salvador Aceves, Daniel Flowers, Nick Killingsworth, Geoffrey Oxberry, William Piggott III, Guillaume Petitpas, and Russell Whitesides

Lawrence Livermore National Laboratory (LLNL)
7000 East Ave. (L-140)
Livermore, CA 94550

DOE Technology Development Manager:
Gurpreet Singh

Overall Objectives

- Deepen understanding of the complex fluid and chemistry interactions that are essential to accelerate the rate of development and deployment of high-efficiency clean combustion engine concepts.
- Improve the physical accuracy of combustion simulations by enabling the use of large chemistry mechanisms for real transportation fuels.
- Reduce the time and resource cost for combustion simulations by designing efficient algorithms guided by the applied mathematics that are at the foundation of the numerical methods in use.
- Develop truly predictive combustion models and software that are computationally efficient enough to impact the engine design cycle.

Fiscal Year (FY) 2012 Objectives

- Create a new thermochemistry library that is able to be distributed by LLNL, offers better data structures to take advantage of future computing architectures, and increases the rate at which new solvers are developed and adopted.
- Continue to develop, rigorously test and validate the adaptive preconditioning concept as a means to accelerate the traditional chemistry solvers in current use with no loss in accuracy.
- Implement the new thermochemistry library and adaptive preconditioner solver in a multidimensional computational fluid dynamics (CFD) code.
- Meet with industrial partners to determine paths for new solver development and adoption throughout the research and design community.

Accomplishments

- Created a new thermochemistry library that is faster than other open source libraries: three times faster than Cantera, and ten times faster than OpenFOAM®.
- Developed a chemistry solver based on adaptive preconditioning that reduces the computational time to integrate large mechanisms by orders of magnitude.
- Reduced computation time for the ignition delay of the 7,200 species 2-methylalkane mechanism from one day using traditional solvers (e.g. those found in Kiva3V, OpenFOAM® and Converge 1.4) to 30 seconds with this project's new solver.
- Implemented and validated the new chemistry solver in the multidimensional CFD software packages Converge and OpenFOAM®.
- Reduced computation time for the chemistry portion of the Converge-multizone CFD simulation using the nearly 900 species iso-octane mechanism by an additional factor of 50 beyond the 6-fold speedup achieved through the LLNL multizone model (total speedup 300-fold).

Future Directions

- Continue efforts to distribute the project's new solvers and libraries to industrial and academic partners, and to the multidimensional CFD software packages they use.
- Improve the fluid transport calculation for a large number of reacting species and other simulation bottlenecks that occur now that the chemistry solver is substantially faster.
- Investigate new nonlinear solvers and stiff integration strategies that would enable fewer timesteps to solution, accelerating the chemistry calculation for all mechanism sizes.
- Explore a more robust error theory for reduced order models used in combustion to ensure that physical accuracy is maintained in a rigorous manner.
- Develop algorithms based on the new chemistry solver for graphical processing units, which are widely available, low-cost, energy efficient, highly-parallel computing architectures.

Introduction

The aim of this project is to fill the present knowledge gap through substantial improvements in the performance and accuracy of the combustion models and software. Specifically, the project is focused largely on the applied mathematics underpinning efficient algorithms, and the development of combustion software on new computing architectures. It is a natural complement to the other LLNL projects in the quest to gain fundamental understanding of the new engine modes investigated under the Vehicle Technologies Program. The other LLNL projects include the multidimensional engine modeling project led by Flowers (see II.A.7), and the high-fidelity chemical reaction mechanisms developed for real transportation fuels by Pitz (see II.A.12). The long-term goal of this project is to develop truly predictive combustion software that is computationally fast enough to impact the design cycle and reduce the deployment time for new high-efficiency, low-emissions engine concepts. Toward this goal, the project developed a new thermochemistry library and chemistry solver that achieves multiple orders of magnitude speedup over the traditional approaches found in multidimensional solvers in current use like Kiva3V [1], OpenFOAM® [2] and Converge (v1.4) [3] without any loss of accuracy. Further, the new library and solver are even 15 times faster than sophisticated commercial solvers. As a consequence of this project, it is now possible to begin modeling high-fidelity chemical mechanisms in multidimensional engine simulations (*i.e.* thousands of species and tens of thousands of reactions).

Approach

This project is focused on creating combustion software able to produce accurate solutions in a short time relative to the design cycle using widely available computing architecture. The creation of fast and accurate simulation tools enables the development and deployment of new engine combustion strategies. In the past, simply demonstrating that it is possible to couple detailed chemical kinetics with fluid dynamics in an engine simulation was a feat unto itself. As a consequence, the effort in designing combustion software was focused solely on getting existing tools and models to work together in a single code (e.g. fluid solvers, stiff integrators, and Lagrangian spray tracking). Now that this type of coupled physics capability is more readily available, it is necessary to take a step back and study how the individual code components can be made more efficient, more accurate and better integrated.

The approach taken in this project to produce accurate and efficient combustion software has several different facets. Major bottlenecks in the software are identified through detailed code profiling. New algorithms for the rate limiting portions of the code are developed from the study of the applied mathematical theory affecting the numerical behavior. Moreover, these new algorithms are developed with an emphasis on exploiting the nature of the physical phenomenon while maintaining mathematical consistency with the model equation. This approach leads to efficient, grid independent and reproducible solutions, which are then validated against existing experimental and computational results. Once rigorously tested, the new models and solvers are distributed to industrial and academic partners as standalone libraries or coupled with larger multidimensional CFD software packages.

Results

In FY 2012, this project focused on developing an improved chemistry solver for standard computer architectures. Faster combustion chemistry solvers enable much wider use of the large detailed mechanisms recently developed at LLNL under the Vehicle Technologies Program project led by Pitz [4-6]. The chemistry solver responsible for integrating these large mechanisms (thousands of species and tens of thousands of reactions) typically accounts for well over 90% of the total computational cost in traditional implementations found in multidimensional simulation codes. Therefore, substantial improvements to this solver have a major impact on the physical accuracy and computational efficiency. Motivated by this fact, the project made three key improvements this year to the chemistry solver that greatly increase the practicality of using detailed chemistry coupled with multidimensional fluid dynamics. First, a new thermochemistry library has been developed to enhance the solver development effort and increase the ultimate usability of any improvements discovered. Second, the thermochemistry library has been combined with the adaptive preconditioner concept demonstrated by this project in FY 2011. Third, the chemistry solver based on the adaptive preconditioner concept was implemented in the multidimensional CFD solvers OpenFOAM® and Converge. These three improvements led to a reduction in computation time by multiple orders of magnitude for both zero-dimensional well-stirred reactor simulations and multidimensional simulations of premixed charge compression ignition engine combustion.

The thermochemistry library contains the set of functions needed to evaluate the time rate of change of the thermodynamic state (*e.g.* pressure, temperature and chemical composition) of the reacting flow. It includes functions for evaluating internal energy, enthalpy, entropy, Gibbs free energy, reaction rates of progress, and species creation and destruction rates.

There are several reasons motivating the development of a new thermochemistry library. Existing open source libraries included with OpenFOAM® and Cantera [7] do not have data structures well suited for developing combustion software on new highly parallel architectures like graphical processing units. In addition, they can be inefficient (in terms of computation time and development time) when used to access certain parts of the thermochemistry data structures needed to study solver components and help debug the next generation of very large mechanisms. Commercial thermochemistry software is even further restrictive both in terms of making necessary algorithm improvements and distributing new combustion software throughout the engine design community. The new thermochemistry library developed this year avoids these problems in development and distribution while markedly improving performance. Figure 1 shows the necessary time to evaluate the rate of change of the species mass fractions and temperature for several large chemical kinetic mechanisms representing transportation fuels and surrogates. The LLNL thermochemistry solver is ten times faster evaluating the rate of change of the thermodynamic state than OpenFOAM® and even three times faster than Cantera. These performance gains are due to improvements in the data structures, vectorized transcendental functions and automatic code generation for greater compiler optimization.

As stated earlier, traditional chemical kinetic solvers account for over 90% of the computation time in multidimensional CFD calculations with large chemical mechanisms. Within the context of the chemical kinetic solver, the linear solver used in the stiff integrator can account for 99% of the cost of the chemistry. Stiff integrators developed at LLNL [8] are able to take advantage of much more efficient linear solvers based on iterative techniques like the generalized minimum residual method named GMRES [9]. Iterative approaches to the linear solver converge very rapidly to the same solution as direct methods if the matrix is "well-conditioned" in the sense that the eigenstructure of the system has tightly clustered eigenvalues far from the origin (see Chap. 35 in Trefethen and Bau [10]). The linear systems occurring in the chemistry solver do not naturally enjoy this well-conditioned property, and thus require a preconditioner matrix to be applied to the system to achieve rapid convergence. The selection of optimum preconditioners unfortunately remains an art, though the general guidance is to find a related linear system that captures the dominant characteristics of the original problem (*i.e.* eigenstructure) while being much simpler to solve than the original system (see Chap 40 in [10]). Consequently, there is no universal preconditioning approach and creating good preconditioners typically requires some insight in the underlying physical processes represented by the linear system.

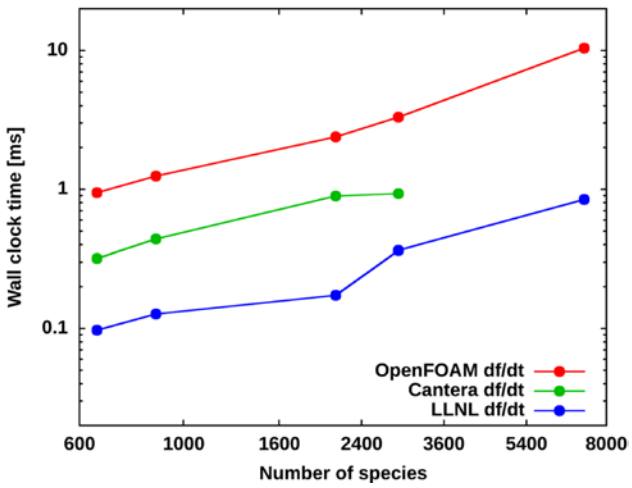

FIGURE 1. The new LLNL thermochemistry library is faster than other open source alternatives – three times faster than Cantera and ten times faster than OpenFOAM®.

The linear system in the chemistry solver is related to the set of ordinary differential equations (ODEs) governing the evolution of the thermodynamic state of the reacting composition. Specifically, the matrix of the linear system is a scaled form of the Jacobian matrix of the ODEs (see [8] for more details). It is reasonable to assume that the Jacobian matrix of a similar but simpler set of ODEs would make an effective preconditioner provided that the simple set retained the key features of the original system. In fact, this has been demonstrated to be true for the linear systems associated with many ODEs including the system of coupled well-mixed reactors studied previously by McNenly et al. [11]. For the case of a single well-stirred considered here, the Jacobian of the ODEs associated with a reduced chemical mechanism would be an obvious candidate for preconditioning the linear system of the complete mechanism.

In this project we have developed a preconditioning approach that can be considered a local reduction of the complete mechanism in some sense. Typically, a reduced mechanism must maintain some degree of global accuracy throughout the combustion process; however, the preconditioner need only represent the key features over a small segment of time. Allowing the preconditioner to adapt in time to include the most important reactions (or species coupling) at any instance greatly reduces the computational cost of applying the preconditioner in the iterative solver. Since the iterative linear solver remains under the same error control as the integrator, the adaptive preconditioner based solver is able to maintain the same accuracy as the traditional approach.

Figure 2 shows the simulation time improvements for the LLNL adaptively preconditioned solver relative to other methods. For mechanisms greater than 30 species, the computational performance of the adaptive preconditioner (blue line) is shown to be faster than the traditional chemistry solvers (red line). The wall clock time represents the elapsed time to solution for calculating the evolution of the thermodynamic state of a single well-stirred reactor over one second of simulated time. The true power of the new solver is observed as the mechanism size increases. For mechanisms greater than 300 species, the computational speedup is greater than a factor of ten. At 7,200 species (2-methylalkane [4]), the computational speedup is greater than a factor of a thousand. A single well-stirred reactor calculation with this mechanism would take the traditional solver used in Kiva3V, OpenFOAM® and Converge 1.4 over a day. It now just requires 30 seconds using the adaptive preconditioner based solver, which is over 15 times faster than even the sophisticated commercial solver (black line) shown in Figure 2. Since the adaptive preconditioner remains under the same integrator error control as the traditional solver, the ignition delay times agree to at least 7 digits (using relative and absolute tolerances of 10^{-8} and 10^{-20} respectively). The new solver developed in this project delivers substantial performance gains with no loss of accuracy.

Furthermore, the adaptive preconditioner solver has demonstrated its robustness by successfully generating a new database of 65,000 detailed iso-octane cases for an artificial neural network in less than 2 cpu-days (varying initial pressure, temperature, equivalence ratio and exhaust gas recirculation levels). The same database required more than 200 cpu-days when generated with the traditional approach.

Improving the performance of a well-stirred reactor not only makes generating large ignition delay databases easier, it also directly impacts the cost of multidimensional CFD simulations with reacting flow. This is due to the fact that most CFD solvers (including Kiva3V, OpenFOAM® and Converge) use a physics-splitting approach when solving the reacting flow equations. In the physics splitting approach, an inert fluid dynamic timestep is taken to update the bulk flow properties followed by a chemistry timestep that integrates the change in the thermodynamic state of a fluid dynamic cell due to the reactions. The chemistry timestep for each fluid dynamic cell is essentially the same as integrating a well-stirred reactor. It is therefore straightforward to incorporate the new adaptive preconditioner solver into OpenFOAM® and Converge. Figure 3 shows the computational speedup of the new solver when compared to the traditional approach used in Converge 1.4. After consulting with LLNL at the end of FY 2012, Converge was able to update the chemistry solver to a more sophisticated iterative approach

Conclusions

In FY 2012, this project was able to make substantial progress toward the goal of bringing truly predictive combustion software to the computational level needed to impact the engine design cycle for new high-efficiency clean combustion operating modes. Key achievements included:

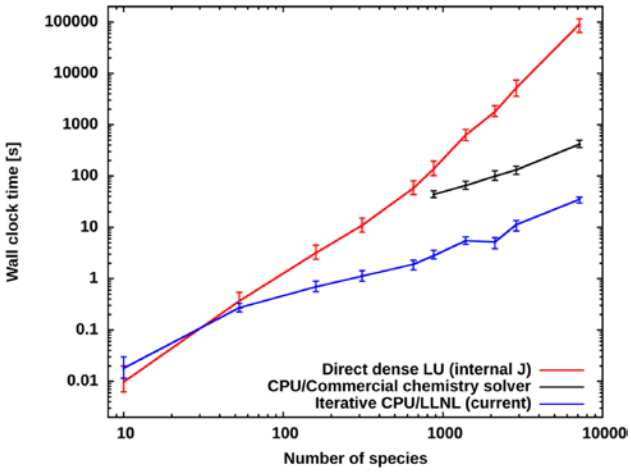

FIGURE 2. The new LLNL chemistry solver, based on adaptive preconditioners, achieves multiple orders of magnitude speedup over traditional chemistry solvers found in Kiva3V, OpenFOAM® and Converge 1.4 for large mechanisms, and it is even 15 times faster than sophisticated commercial chemistry solvers.

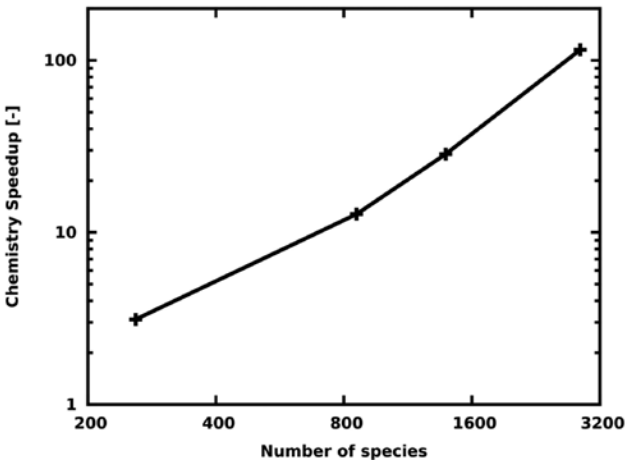

FIGURE 3. The new LLNL solver is able to accelerate the chemistry calculation time of the multidimensional Converge CFD code enabling large detailed mechanisms to be used in engine simulations.

- Creating a new thermochemistry library that is faster than other open source libraries: three times faster than Cantera, and ten times faster than OpenFOAM®.
- Developing a chemistry solver based on adaptive preconditioning that reduces the computational time to integrate large mechanisms by orders of magnitude.
- Implementing and validating the new chemistry solver in the multidimensional CFD software packages Converge and OpenFOAM®.

In FY 2013, we will continue our efforts to distribute the high performance solvers and libraries developed by this project to industrial and academic partners, and explore new algorithms to further accelerate combustion software.

References

1. Hessel, R., Babajimopoulos, A., Foster, D., Aceves, S., Davisson, M, Espinosa-Loza, F.J., Flowers, D.L., Pitz, W., Dec, J., Sjoberg, M., " Modeling Iso-octane HCCI using CFD with Multi-Zone Detailed Chemistry; Comparison to Detailed Speciation Data over a Range of Lean Equivalence Ratios, SAE Paper 2008-01-0047.

2. Website http://www.openfoam.org/.

3. Raju, M.P. *et al*.,"Acceleration of Detailed Chemical Kinetics Using Multi-zone Modeling for CFD in Internal Combustion Engine Simulations," SAE Paper 2012-01-0135.

4. Sarathy, S.M. *et al*., "Comprehensive chemical kinetic modeling of the oxidation of 2-methylalkanes from C7 to C20," Combust. Flame, 2011.

5. Sarathy, S.M., Yeung, C., Westbrook, C.K., Pitz, W.J., Mehl, M. and Thomson, M.J. " An experimental and kinetic modeling study of n-octane and 2-methylheptane in an opposed-flow diffusion flame," Combust. Flame, 2011.

6. Mehl, M., Pitz, W.J., Westbrook, C.K. and Curran, H.J., "Kinetic modeling of gasoline surrogate components and mixtures under engine conditions", Proceedings of the Combustion Institute, 2011.

7. Goodwin, D.G, "Cantera C++ User's Guide," California Technical Institute, 2002.

8. Hindmarsh, A.C and Serban, R., "User Documentation for CVODE v2.6.0," Lawrence Livermore National Laboratory, UCRL-SM-208108, 2009.

9. Byrne, G.D., "Pragmatic Experiments with Krylov Methods in the Stiff ODE Setting," Computational Ordinary Differential Equations, Cash, J. and Gladwell, I., eds., Oxford University Press, Oxford, 1992.

10. Trefethen, L.N. and Bau, D., Numerical Linear Algebra, SIAM, Philadelphia, 1997.

11. McNenly, M. J., Havstad, M.A., Aceves, S.M., and Pitz, W.J., "Integration strategies for efficient multizone chemical kinetics models," SAE International Journal for Fuels and Lubricants, 2010.

FY 2012 Publications/Presentations

1. Kodavasal, J., McNenly, M.J., Babajimopoulos, A., Aceves, S.M., Assanis, D.N., Havstad, M.A., and Flowers, D.L., "An Accelerated Multi-zone for Engine Cycle Simulation (AMECS) of HCCI combustion," in review, 2012.

2. Flowers, D.L., "Simulation of High Efficiency Clean Combustion Engines and Detailed Chemical Kinetic Mechanisms Development," 18th Directions in Engine-Efficiency and Emissions Research (DEER) Conference, Dearborn, MI, Oct. 15–19, 2012.

3. Kodavasal, J., "A Methodology to Capture Thermal Stratification in a Multi-zone HCCI Combustion Model," AEC/HCCI Working Group Meeting, Livermore, CA, Feb. 14–16, 2012.

4. McNenly, M.J. and Whitesides, R.A. "Improving Combustion Software for Modeling Detailed Chemical Kinetics," AEC/HCCI Working Group Meeting, Livermore, CA, Feb. 14–16, 2012.

5. Whitesides, R.A., McNenly, M.J., Piggott III, W.T., Hessel, R.P., Flowers, D.L. and Aceves, S. M., "Advances in Multi-dimensional Modeling of Clean & Efficient Engine Concepts," AEC/HCCI Working Group Meeting, Detroit, MI, June 19–21, 2012.

6. McNenly, M.J., Whitesides, R.A., Flowers, D.F. and Aceves, S.M., "Improving Combustion Software to Solve Detailed Chemical Kinetics," GE Workshop on High Performance Computing for Combustor Turbine Systems, Niskayuna, NY, June 25–26, 2012.

II.24 University Consortium on Efficient and Clean High-Pressure Lean-Burn (HPLB) Engines

Margaret Wooldridge
University of Michigan (UM)
Mechanical Engineering
2156 GGB
Ann Arbor, MI 48109-2125

DOE Technology Development Manager:
Gurpreet Singh

NETL Project Manager: Ralph Nine

Subcontractors:
- Massachusetts Institute of Technology (MIT), Cambridge, MA
- University of California, Berkeley (UCB), Berkeley, CA

Overall Objectives

- Explore new HPLB combustion strategies that can enable future gasoline engines with 20-40% improved fuel economy.
- Determine the fuel economy benefits of engines and engine cycles designed to utilize advanced combustion modes.

Fiscal Year (FY) 2012 Objectives

- Develop and apply analytical tools to integrate knowledge acquired in the consortium to assess system level vehicle fuel economy gains made possible by advanced, multi-mode combustion and novel fuel properties.
- Determine effects of stratification and equivalence ratio in a stratified engine. Develop models of auto-ignition applicable to highly stratified, turbulent combustion as it applies to gasoline direct injection (DI)/homogeneous charge compression ignition (HCCI) engines.
- Experimentally explore flame and auto-ignition heat release in spark-assisted compression ignition (SACI). Determine the effects of composition and temperature on the critical combustion characteristics such as heat release rate and stability. Develop and refine computational fluid dynamics (CFD) models of SACI combustion and validate with experimental data.
- Determine effects of fuel properties such as octane number on HCCI combustion. Explore effects of fuels blends on HCCI and SACI combustion and autoignition chemistry.

Accomplishments

- A phenomenological quasi-dimensional model of SACI has been developed for eventual use for system level simulations of engine control strategies and vehicle fuel economy improvement. This multi-mode combustion model employs a two-zone thermodynamic approach. For the flame zone existing spark-ignition flame models are employed, supplemented by a new laminar flame speed correlation developed earlier in the consortium for highly dilute, high preheat and pressure SACI conditions. The auto-ignition zone is modeled using single-zone chemical kinetics and an experimentally derived scaling correlation for the auto-ignition burn rate (in progress) to account for real engine effects, such as temperature gradients and mixture stratification.
- To assist in the development of the auto-ignition correlation, an engine data analysis tool has been developed. The Advanced Combustion Engine Heat Release analysis program identifies and quantifies the crank angle location and duration of the flame and auto-ignition zones from experimental in-cylinder pressure traces. Comparisons with KIVA simulations for HCCI and SACI operation (developed previously as part of this work) showed good accuracy.
- The effects of fuel stratification in a small bore diesel engine using gasoline have been determined for high (19:1) and low (14:1) compression ratios. At the high compression ratio, ignition occurs in the low temperature regime, which exhibits more sensitivity to temperature and less sensitivity to fuel stratification; at the low compression ratio, ignition occurs in the negative temperature coefficient (NTC) regime, where fuel stratification is more important than temperature. Thus fuel stratification is able to mitigate maximum pressure rise rate (MPRR) in this regime.
- The flamelet-based combustion submodels including the spray vaporization effect have been implemented and validated in DI/HCCI engine conditions. The results show that for modeling ignition of late

injection, stratified mixtures, the flamelet based model gives significantly better agreement with data than current multizone approaches. This identifies an apparent acceleration of ignition/burn rate due to small scale turbulence and mixing effects, not previously well understood.

- Experiments on SACI in the fully flexible valve actuation (FFVA) engine were carried out to quantify the effect of composition and charge temperature at time of spark. The results showed significant changes in the flame heat release rates with in-cylinder oxygen concentration. Temperature at the time of spark was shown to affect the rate of flame heat release consistent with its effect on laminar flame speeds. End gas temperature at the time of auto-ignition was relatively constant. Further analysis is underway. The data are being used to validate the KIVA-CFMZ (Coherent Flamelet Multi Zone) model and calibrate the phenomenological SACI model under development.
- Significant progress has been made with the full KIVA-CFMZ model of SACI. Detailed comparisons with experimental data have been made with an improved computational grid. One finding showed that the auto-ignition event occurred at roughly the same end gas temperature regardless of the fraction of flame generated heat release. In preparation for more realistic open cycle simulations, an improved sub-model was developed for fuel droplet boiling to facilitate further study of the influence of mixture preparation on heat release rates.
- Studies with a microwave-assisted spark plug were carried out in a constant-volume chamber aimed at characterizing mixture composition, turbulence, and pressure effects using Schlieren imaging. Results show improved flame kernel growth and uniformity with microwave addition. Analytical work is underway to develop a chemical kinetic mechanism for microwave-assisted spark plug operation in terms of plasma-assisted ignition.
- New image analysis tools have been developed for rapid and automated processing of optical engine imaging data into quantitative metrics on ignition and flame propagation in HCCI and SACI systems. The tools have been applied to recent studies of ethanol/indolene blends under SACI conditions.
- High speed imaging data of ethanol/indolene blends during HCCI and SACI operation have been used to identify qualitative and quantitative links between flame propagation initiated by spark and heat release rates. Ethanol generally improved engine performance yielding higher indicated mean effective pressure and improved stability.
- Fuels with lower octane numbers were tested in the FFVA engine. Results showed an increase in maximum load with lower octane as well as an increase in burn rate, possibly due the tendency of lower octane fuels to demonstrate NTC behavior, these and other effects are the subject of further studies.
- Fundamental lean flammability limits were determined as a function of dilution in rapid compression facility (RCF) studies of iso-octane/air/diluent mixtures. Flame/autoignition interactions were documented in RCF studies of the same mixtures. The results provide important data for model validation.
- Gas sampling speciation experiments in the UM RCF were compared to kinetic models in a study of autoignition with n-heptane at end of compression conditions of 9.1 atm pressure and 660 to 707 K gas temperature. In a related study, the effect of diluent gas composition effects on autoignition were investigated using ignition experiments and CHEMKIN simulations for an iso-alkane, a n-alkane, a methyl ester, and an alcohol. The results quantify the kinetic effects of diluent gas composition on autoignition.

Future Directions

- Expand thermodynamic and system analyses of mixed combustion modes in a representative turbocharged engine system to include realistic combustion constraints, different compression ratios, and if time, hybridization. Assess the potential benefit of lean/dilute burn, high pressure engine operation under optimal engine-vehicle drive train scenarios.
- Bring together experimental work on SACI with recently completed models to provide new insight. Perform additional experiments as necessary.
- Assess the validity of the flamelet-based combustion submodels in mixed-mode combustion under HPLB conditions. Conduct parametric studies to identify sensitivities of key control variables.
- Investigate effects of varying turbulent intensities, transient phenomena, and expanded operating range using newly configured optically accessible DI engine.
- Explore opportunities for improved engine efficiency through chemistry and properties of novel fuels and fuel blends. Carry out engine experiments with fuels characterized in RCF studies.

Introduction

Low-temperature combustion (LTC) is a desirable thermodynamic regime that can provide improved fuel efficiency in gasoline engines with low emissions, because the properties of the working fluid are best at lower temperature and because oxides of nitrogen (NOx) emissions are reduced. Unfortunately, practical and reliable combustion under these dilute conditions has traditionally been unattainable due to spark ignition limits. HCCI is one method to achieve good combustion; the method works by increasing the charge temperature to induce auto-ignition and by diluting the mixture to reduce heat release rates. Because of the limited loads possible with HCCI, advanced combustion modes such as SACI, stratified or dual fuel mixtures are being considered as a way to increase achievable engine loads. At the same time turbocharging is another means of improving fuel economy, by capturing some wasted exhaust energy, but more importantly and in combination with engine downsizing, by permitting an increase of engine load without excessive temperatures while also reducing the relative importance of friction.

As seen in previously reported results shown in Figure 1, thermodynamic analysis indicates that advanced combustion modes at high pressures can provide vehicle fuel economy gains of up to 55%, exceeding the DOE Vehicle Technologies Program target of 20-40% improvement. Accordingly, the goal of the consortium is to explore how this improvement can be achieved; in particular to look at means of enabling the required advanced combustion under the highly dilute, boosted high pressure conditions necessary for optimal engine-vehicle fuel economy.

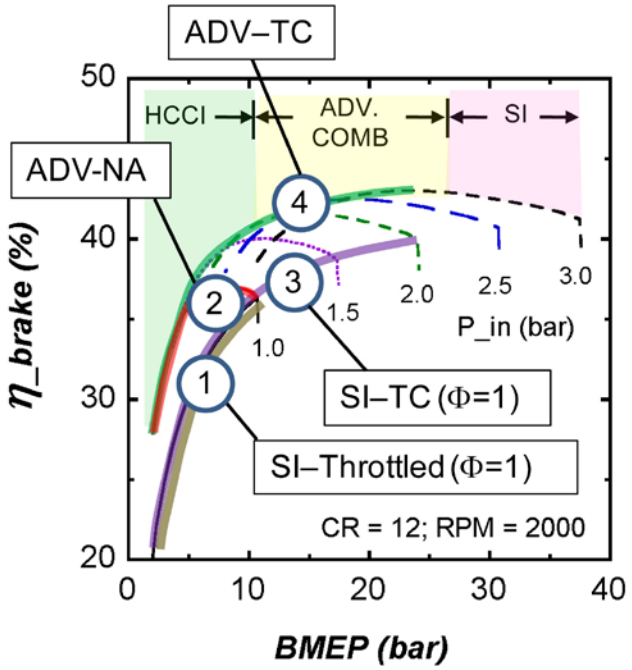

FIGURE 1. Brake efficiency vs. brake mean effective pressure (BMEP). Projected efficiency gains for advanced combustion (ADV) and turbocharged (TC) boosting strategies compared with stoichiometric (Φ =1) spark ignited (SI) systems, both naturally aspirated (NA) and turbocharged. Results are for compression ratio (CR) of 12 at 2,000 revolutions per minute (RPM). (Lavoie et al., 2012).

Approach

Our research program, now at the end of its third year, combines experiments and modeling at three university research centers in order to acquire the knowledge and technology to explore the HPLB advanced combustion regime, which is key to achieving optimal fuel economy. To accomplish this, both single cylinder and multi-cylinder engine experiments are being used to investigate direct fuel injection strategies, fuel and thermal stratification, turbo/supercharging, advanced ignition and combustion modes as well as the ignition characteristics of alternate fuels and blends with gasoline.

At the same time an array of modeling tools are being developed and refined, and brought to bear on the specific limit problems of importance. These models cover a range of detail from system models for engines and vehicles, through fully coupled CFD/kinetic models, to detailed chemical mechanisms. Our intent is to take advantage of the broad range of capabilities of the university partners and the collaborative relationships among the partners and their connections with industry and U.S. federal research facilities.

The overall technical approach is focused on light-duty automotive engine application using primarily gasoline and gasoline blends with alcohols as the fuel. The research agenda addresses the following areas:

- Thermodynamics of engines and engine cycles operating in advanced combustion modes.
- Fuel and thermal stratification and their interaction with fuel properties and heat transfer.
- Advanced multi-mode ignition and combustion.
- Novel fuel opportunities for improved efficiency.

Results

New Zero Dimensional Model of SACI

GT-Power® was used as a programming environment to develop a new phenomenological model of SACI for use in fast engine and vehicle oriented fuel economy assessments for which the drive cycle framework has been developed previously (Ortiz-Soto et al., 2011). The new model is a quasi-dimensional multi-mode

combustion formulation and employs a turbulent flame calculation which has as its primary input, laminar flame speed correlations for highly dilute flames reported previously (Martz et al., 2011, Middleton et al., 2012). The chemical kinetics in the end gas is computed, either by an auto-ignition integral or by direct detailed kinetics until auto-ignition occurs, after which, the remaining heat is released with a rate determined according to an empirical correlation derived from experimental data. For this purpose a special heat release analysis tool was developed to reliably separate the flame generated heat release from the end gas autoignition event. Figure 2 shows preliminary comparison of simulation results vs. experimental data for three sets of inlet temperature and spark timings. The results clearly show the influence of the flame heat release and demonstrate that spark assist can compensate for changes in input conditions.

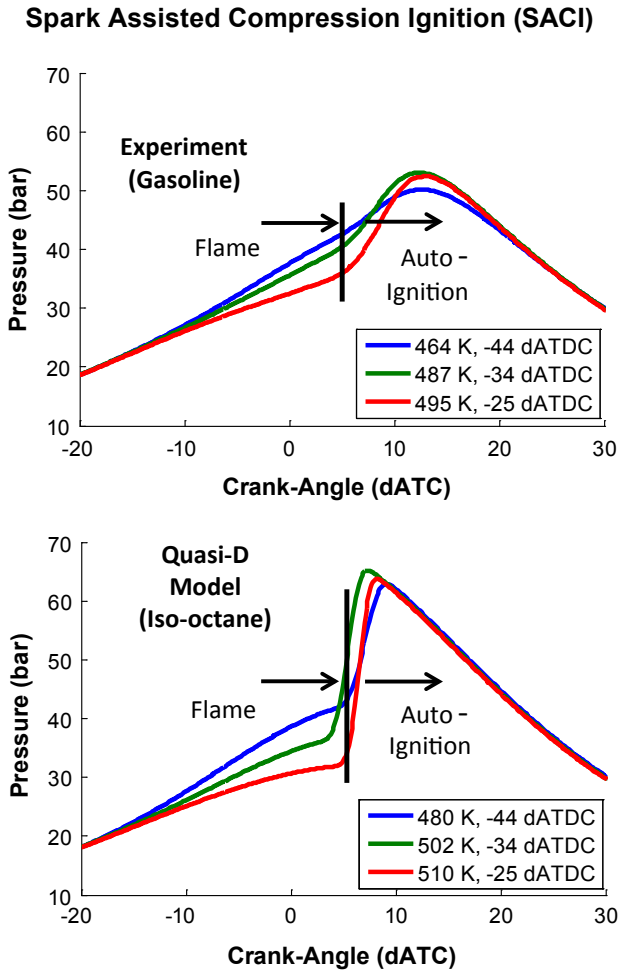

FIGURE 2. Preliminary SACI simulation results from zero-dimension model compared to experiment. (See Figure 4 for comparison with KIVA simulations). The legend indicates the preheat temperature of the air and the timing for spark assist.

Charge Stratification Studies

The objectives of this task are first to experimentally study stratification strategies for HPLB engines and the interaction between fuel properties, heat transfer and stratification, and second to develop advanced simulation tools to predictively describe the combustion characteristics in the presence of temperature and composition inhomogeneities arising from stratified charge, exhaust/residual gas recirculation, and wall heat loss.

In engine experiments, fuel stratification has been found previously not to be effective in mitigating the MPRR and knock tendency of the HCCI engine. The behavior is hypothetically attributed to the fact that the engine is operating at a high compression ratio (19:1) so that the charge density is high and ignition occurs at the low temperature region (i.e. at the right hand side of the traditional ignition delay versus inverse temperature curve). In this region, the ignition delay is insensitive to the fuel concentration but sensitive to temperature. Thus sequential ignition of the charge is determined mainly by the temperature and not the concentration gradient. The presence of fuel concentration gradient would worsen the MPRR since the region with more fuel than the average value would ignite with a more intense heat release.

To verify this hypothesis, the engine compression ratio has been lowered (to 14:1). With the lower charge density, ignition can be expected to occur in the NTC region where the ignition delay is less sensitive to temperature but sensitive to fuel concentration. Preliminary results using change of direct injection timing to control the fuel stratification shows that MPRR indeed decreases with fuel stratification. Thus the results support the hypothesis of the regime change with the lowering of the compression ratio.

In modeling work, a detailed study was carried out comparing flamelet and multizone (MZ) combustion models. To accomplish this, the flamelet-based combustion submodels developed previously including the spray vaporization effect have been implemented in an engine model simulating a DI engine for different spray injection conditions.

Full-cycle engine simulations were conducted by employing spray-interactive flamelet models in the KIVA-3V code. As a validation of the developed models, simulations were conducted for two parametric conditions: early injection (partially premixed compression ignition) and late injection (DI). The results were compared with those from KIVA-multizone (KIVA-MZ) calculations as well as experimental data. The results confirmed our expectation in that, while the two alternative models yielded comparable fidelity for

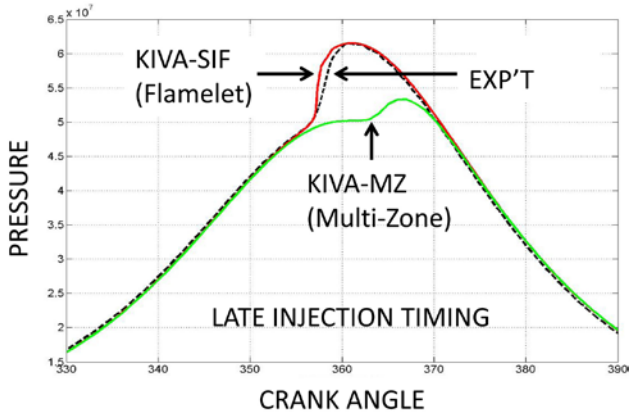

FIGURE 3. KIVA-spray-interactive flamelet (SIF) model gives improved results compared to multi-zone (MZ) model under late injection (stratified) conditions.

the early injection condition, as the injection timing was further delayed, the flamelet approach showed better agreement with experimental results for late injection (Figure 3). The improved fidelity for the flamelet model is attributed to the ability to capture the effects of subgrid scale fluctuations on chemical reactions. Further analysis of detailed distribution of temperature and reaction rates is underway in order to provide more complete understanding of the differences in the two combustion submodels.

Multi-Regime Ignition Strategies

Significant progress has been made applying the previously developed KIVA-CFMZ model of SACI to experimental results from the FFVA engine using an exact mesh. The modeling work focused on explaining significant changes in the peak experimental heat release rate while crank angle at 50% burned (CA50) was maintained constant by trading off charge temperature at intake valve closing with spark timing. For mixtures with lower initial charge temperatures, the spark was advanced, allowing for increased end-gas compression due to deflagrative heat release. Near the onset of autoignition, mean unburned charge temperatures were shown to be comparable. The decrease in the peak heat release rate for the lower initial charge temperatures with the most advanced spark timing resulted in part from the reduction in end-gas mass available for heat release, in addition to the lower peak end-gas temperatures. Results are shown in Figure 4. Future work will focus on open cycle simulations in an attempt to improve agreement with the experimental results by incorporating thermal and compositional stratification resulting from the valve events.

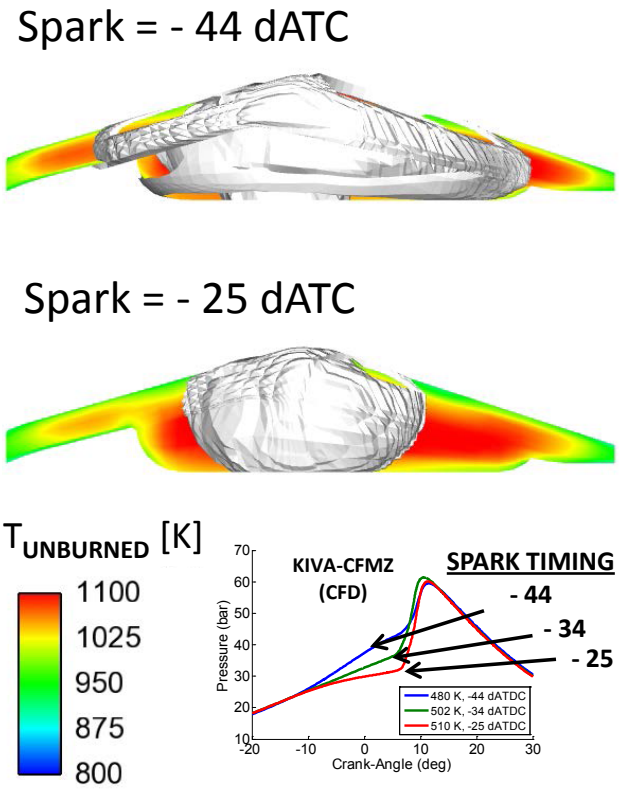

FIGURE 4. CFD results with KIVA-CFMZ (Coherent Flamelet Multi-Zone) model of SACI combustion. Images show computed flame progress at beginning of autoignition for two spark timings.

A series of experiments were carried out in the FFVA engine. The work was focused on identifying the effects of composition and temperature on the relative amounts of heat release induced by flame and auto-ignition processes. The results indicate that oxygen concentration tends to accelerate the flame heat release and exhaust gas recirculation (EGR) tends to decelerate the auto-ignition heat release. Estimates of the end gas temperature at ignition are approximately constant regardless of the fraction of flame heat release.

In other work, preliminary open cycle simulations using the FFVA KIVA mesh indicate that the charge motion and mixture stratification introduced by negative valve overlap and DI have a significant effect on the resulting heat release rates. Further study into these issues is currently in progress.

Experiments in the optical engine focused on the behavior of 100% indolene and 70% indolene/30% ethanol blends on ignition and combustion properties in SACI mode. The spark assist effects were compared to base line HCCI for each blend by varying spark timing at different fuel/air equivalence ratio (Φ = 0.4–0.6). High speed imaging was used to understand the effects of flame propagation on heat release rates. Ethanol

generally improves engine performance with higher indicated mean effective pressure and higher stability compared to 100% indolene. SA advances phasing within a range of ~5 crank angle degrees (CAD) at lower engine speeds (700 rpm) and ~11 CAD at higher engine speeds (1,200 rpm). SA does not affect heat release rates until immediately (within ~5 CAD) prior to autoignition. Unlike previous studies, flames were not observed for all fuel blends and SA conditions. During SA operation, more fuel mass was burned by flame propagation with gasoline compared to 30% ethanol.

The engine images were analyzed to determine the effect of spark timing on flame radius during SACI combustion. The effective flame radius is shown in Figure 5 for three spark timings along with the base case (no spark), i.e. pure HCCI. Each spark assisted case shows an initial kernel development phase leading into more robust propagation and transitioning into full auto-ignition with a rapid rate similar to the HCCI case. (Note: flame radii plateau at the approximate window radius). These results are consistent with the modeling work described above.

Concurrent with the optical engine studies, experiments were conducted in a spark plug equipped RCF using high-speed optical and pressure diagnostics. Fast image processing algorithms were coupled with pressure measurements to determine key quantitative metrics of reaction fronts initiated by the spark discharge, and propagated into premixed iso-octane and air. Depending on the state conditions and composition of the mixtures, the presence of flames accelerated ignition compared to conditions when no flames were initiated and sustained. The predicted adiabatic flame temperature has been identified as a good indicator of the effect of spark on the autoignition timing. A spark-initiated lean flammability limit of $\Phi = 0.4$ was determined for inert to oxygen dilution levels of 3.76:1 to 7.47:1, temperatures of 963 ± 10 K, and pressures of 8.0 ± 0.3 atm.

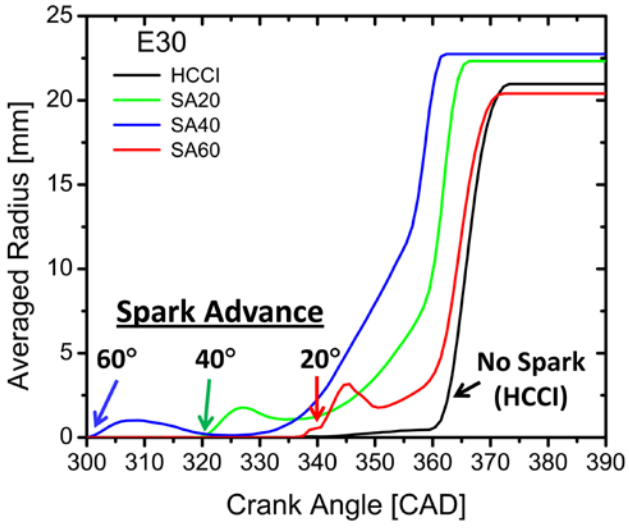

FIGURE 5. Effective flame front radii during SACI, measured in optical engine with varying spark timing for 30/70 blend of ethanol and gasoline (E30).

Microwave Assisted Spark Plug

To complement previously reported results of enhanced microwave assisted ignition in a CFR engine, tests have been carried out on methane-air mixtures in a constant volume bomb equipped with Schlieren imaging and spectroscopy. The studies have provided additional insight into the effects of pressure, mixture composition, turbulence, and microwave input duration. Flame kernel size increases, and the kernel growth rate is higher and more uniform with microwave addition. The enhancement was found to be most effective at lean mixture compositions, lower pressures, and at higher levels of turbulence. Additionally, microwave energy input is only effective when the flame kernel remains near the spark plug. Experimental improvements are ongoing including a multi-electrode microwave-assisted spark plug for a more-robust ignition event than the single-electrode plug.

On the modeling side, coding has begun to incorporate plasma chemical kinetic capabilities into a one-dimensional flame code for numerical study of microwave-enhanced flame behavior. At the same time a method was developed for reducing the size of the microwave plasma chemical kinetic mechanism for improved computational speed with preserved computational accuracy. Implementation of the method has begun.

Fuel Chemistry for Improved Engine Efficiencies

Extending HCCI to higher loads offers potentially higher engine efficiency. To determine if fuel ignition characteristics can influence the maximum load, experiments were carried out in the UM FFVA engine with three fuels with different octane numbers: iso-octane (Research Octane Number, RON=100), RD387 gasoline (RON=90.5), and a 40/60 blend of RD387 and n-heptane, designated NH40 (RON=~53). For each fuel, operating maps were constructed by varying fueling rate and combustion phasing. In this way the limits were determined for early phasing (knock, i.e. ringing intensity > 5 MW/m^2) and late phasing (normalized mean effective pressure coefficient of variation > 3%) for each fueling rate. The maximum load was established where the knock and stability limits converged. The results showed that higher load could be achieved with lower octane fuel in part because the combustion

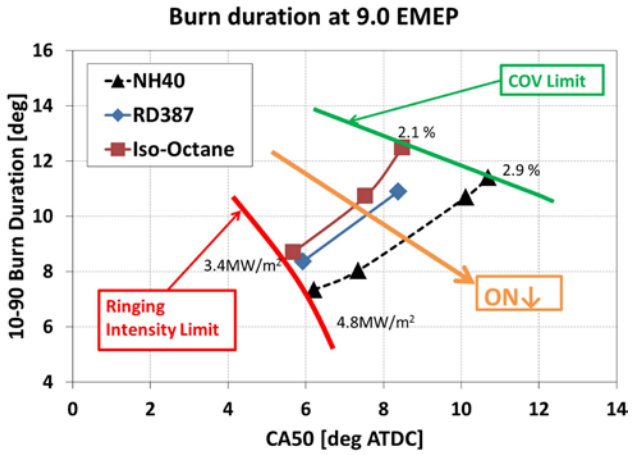

FIGURE 6. Effect of fuel octane number (ON) on HCCI burn duration as a function of combustion phasing. Fuel energy input per cycle was held constant at 9.0 bar energy mean effective pressure (EMEP). Limit lines shown for ringing intensity and coefficient of variation (COV) of IMEP.

could be retarded more without loss of stability. This is thought to be partially due to the shorter burn durations observed for the lower octane fuel as is shown in Figure 6 where 10-90 burn durations are shown as a function of combustion phasing for three fuels at equal fueling energy of 9.0 bar EMEP where EMEP is the fuel energy per cycle normalized by displacement volume (Hagen et al., 2012). A possible explanation is that the increased NTC behavior of the low octane fuel reduces the temperature sensitivity and as a result, reduces the effect of natural thermal stratification in the chamber. Another explanation may also be related to lower levels of internal EGR required for ignition, and the subsequent reduction in thermal stratification. Work is underway to better understand this effect.

In other work, diluent gas composition effects on auto-ignition were investigated using CHEMKIN simulations for an iso-alkane, an n-alkane, a methyl ester, and an alcohol. Results of the study highlight the chemical and thermal effects of diluent composition. In particular, autoignition delay time data acquired using different experimental approaches (namely shock tubes and rapid compression facilities) are subject to uncertainties in the collision efficiencies of the diluents gases, which can have significant effects on autoignition delay time and heat release rates. On the other hand, the computational results indicate chemical effects of the diluents gas composition on autoignition times using EGR levels expected in engine operation are not significant. The results of this work are being compiled in the form of sensitivity coefficients that can be used to interpret experimental data and guide modeling e.g. via ignition correlations.

We have completed the ignition study of n-heptane. Working with Dr. Charles Westbrook, we have identified significant discrepancies in the low temperature chemistry of this important reference fuel. We are currently revising the n-heptane reaction mechanism to address the issues in the low temperature chemistry. The deficiencies in the reaction chemistry were identified using the UM RCF gas sampling data, indicating how important it is to have rigorous targets to benchmark reaction chemistry. Further, RCF studies of n-heptane/n-butanol fuel blends have identified fuel component interactions that are not captured using an integrated reaction mechanism. Fuel blends remain an important source of uncertainty in combustion chemistry, and this work helps interpret the results of the engine studies of fuel blends. Current work for the studies of fuel chemistry effects include developing quantitative metrics that can be used to assess the uncertainties in fuel chemistry on engine simulations.

Conclusions

- The consortium has made considerable progress towards assembling the knowledge and tools needed to achieve the fuel economy goals of the Vehicle Technologies Program for gasoline engines.
- Studies of fuel stratification in a small bore diesel engine using gasoline have shown that the mitigating effect of fuel stratification on heat release rate is higher at low compression ratio than high due to the fact that ignition occurs in the NTC regime where fuel concentration is important.
- Controlled engine experiments on SACI have shown that the combustion event is composed of two relatively independent processes: flame and autoignition, the latter being advanced by the flame generated heat release. Experiments have identified a sensitivity of the flame heat release to spark timing and oxygen concentration consistent with calculations of laminar flame speeds at those conditions. Over the range of conditions studied the end gas temperature at the time of autoignition is relatively constant.
- Improvements in the KIVA-based SACI model (KIVA-CFMZ) have been made to include a fuel spray evaporation model to enable realistic open cycle simulations. Initial results show significant sensitivity to the injection event and the subsequent stratification.
- A low octane fuel (40/60 blend of n-heptane in gasoline) was shown to exhibit a higher load limit than pure gasoline, possibly due to increased NTC behavior. In other experiments ethanol was found to extend the lean HCCI limit when compensation is

made for evaporative cooling effects. Fuel chemistry studies have identified composition effects of EGR on autoignition time are small at typical engine levels of dilution. Additionally, the effects of fuel blends on autoignition chemistry are not well understood and can be large at low temperatures, particularly for interactions between NTC and non-NTC fuels.

FY 2012 Publications/Presentations

1. Bansal, G., and Im, H.G. (2011) Auto-ignition and front propagation in low temperature combustion engine environments. Combustion and Flame, Vol. 158, No. 11, 2105-2112, doi:10.1016/j.combustflame.2011.03.019.

2. Bansal, G., Im, H.G., and Bechtold, J.K. (2012) Flame-flow interactions and flow reversal. *Combustion and Flame,* Vol. 159, No. 4, 1489-1498, doi:10.1016/j.combustflame.2011.11.021.

3. DeFilippo, A., Saxena, S., Rapp, V.H., Ikeda, Y., Chen, J-Y, Dibble, R.W., (2011) Extending the lean flammability limit of gasoline using a microwave assisted sparkplug, SAE Paper no. 2011-01-0663, doi: 10.4271/2011-01-0663.

4. Fatouraie, M., Keros, P., Wooldridge, M.S., (2012) "A Comparative Study of the Ignition and Combustion Properties of Ethanol-Indolene Blends during HCCI Operation of a Single Cylinder Engine," SAE Paper No. 2012-01-1124, pp. 1-17, doi: 10.4271/2012-01-1124.

5. Gupta, S., Im, H.G., Valorani, M., (2011), "Classification of Ignition Regimes in HCCI Combustion using Computational Singular Perturbation," Proceedings of the Combustion Institute, v. 33, pp. 2991-2999. http://dx.doi.org/10.1016/j.proci.2010.07.014.

6. Hagen, L.M., Manofsky-Olesky, L., Bohac, S.V., Lavoie, G., and Assanis, D., (2012) Effects of a Low Octane Gasoline Blended Fuel on HCCI Load Limit, Combustion Phasing and Burn Duration, ASME Fall Technical Conference ICEF2012, Vancouver, BC, Canada, September 23–26, 2012, paper ICEF2012-92155.

7. Karwat, D.M.A., Wagnon, S.W., Teini, P.D., and Wooldridge, M.S. (2011) On the Chemical Kinetics of n-Butanol: Ignition and Speciation Studies. The Journal of Physical Chemistry A, Vol. 115, No. 19, 4909-4921, doi:10.1021/jp200905n.

8. Keum, S., Im, H.G., and Assanis, D.N. (2012) A Spray-Interactive Flamelet Model for Direct Injection Engine Combustion. *Combustion Science and Technology,* Vol. 184, No. 4, 469-488, doi:10.1080/00102202.2011.647141.

9. Lavoie, G., Ortiz-Soto, E., Babajimopoulos, A., Martz, J., and Assanis, D. (2012) Thermodynamic sweet spot for high efficiency, dilute, boosted gasoline engine operation. *Int. J. Engine Res*. First published August 16, 2012, doi: 10.1177/1468087412455372.

10. Manofsky, L., Vavra, J., Babajimopoulos, A., and Assanis, D. (2011) Bridging the Gap between HCCI and SI: Spark-Assisted Compression Ignition. SAE Technical Paper 2011-01-1179, doi:10.4271/2011-01-1179.

11. Martz, J.B., Kwak, H., Im, H.G., Lavoie, G.A., Assanis, D.N., (2011), "Combustion Regime of a Reacting Front Propagating into an Auto-Igniting Mixture," Proceedings of the Combustion Institute, v. 33, pp. 3001-3006.doi: http://dx.doi.org/10.1016/j.proci.2010.07.040.

12. Martz, J., Middleton, R., Lavoie, G., Babajimopoulos, A., and Assanis, D. (2011) A computational study and correlation of premixed isooctane-air laminar reaction front properties under spark ignited and spark assisted compression ignition conditions. Combustion and Flame, Vol. 158, No. 6, 1089-1096. http://dx.doi.org/10.1016/j.combustflame.2010.09.014.

13. Martz, J.B., Lavoie, G.A., Im, H.G., Middleton, R.J. Babajimopoulos, A., Assanis, D.N., (2012)"The Propagation of a Laminar Reaction Front During End-Gas Auto-Ignition," Combustion and Flame, doi:10.1016/j.combustflame.2012.01.011.

14. Middleton, R.J., Martz, J.B., Lavoie, G.A., Babajimopoulos, A., and Assanis, D.N. (2012) A computational study and correlation of premixed isooctane air laminar reaction fronts diluted with EGR. Combustion and Flame, Vol. 159, No. 10, 3146-3157. http://dx.doi.org/10.1016/j.combustflame.2012.04.014.

15. Ortiz-Soto, E., Assanis, D., and Babajimopoulos, A. (2011) A Comprehensive Engine to Drive-Cycle Modeling Framework for the Fuel Economy Assessment of Advanced Engine and Combustion Technologies. *Int. J. Engine Res.,* Vol. 13, No., 287-304, doi:10.1177/1468087411411615.

16. Rapp, V.H., et al. (2012) Extending Lean Operating Limit and Reducing Emissions of Methane Spark-Ignited Engines Using a Microwave-Assisted Spark Plug. *Journal of Combustion,* Vol. 2012, No., 8, doi: 10.1155/2012/927081.

17. Walton, S.M., Karwat, D.M., Teini, P.D., Gorny, A., and Wooldridge, M.S., (2011) "Speciation Studies of Methyl Butanoate Ignition," *Fuel*, 90, pp. 1796-1804, doi: 10.1016/j.fuel.2011.01.028.

18. Zigler, B.T., Keros, P.E., Helleberg, K.B., Fatouraie, M., Assanis, Dimitri, and Wooldridge, M.S., (2011) "An Experimental Investigation of the Sensitivity of the Ignition and Combustion Properties of a Single-Cylinder Research Engine to Spark-Assisted HCCI," *Int. J. Eng. Res*., 12, pp. 353-375. doi: 10.1177/1468087410401286.

II.25 Optimization of Advanced Diesel Engine Combustion Strategies

Profs. Rolf Reitz (Primary Contact),
David Foster, Jaal Ghandhi, Dave Rothamer,
Christopher Rutland, Mario Trujillo,
Scott Sanders
Engine Research Center
University of Wisconsin-Madison
1500 Engineering Drive
Madison, WI 53706

DOE Technology Development Manager:
Gurpreet Singh

NETL Project Manager: Nicholas D'Amico

Objectives

- Development of high efficiency internal combustion engines with goals of improved fuel economy by 20-40% in light-duty and 55% brake thermal efficiency in heavy-duty engines.
- Develop methods to further optimize and control in-cylinder combustion processes, with emphasis on compression ignition engines.

Fiscal Year (FY) 2012 Accomplishments

- Optimum spray and combustion chamber design recommendations made for improved efficiency of heavy-duty and light-duty diesel engines. Gross thermal indicated efficiencies of ~60% in heavy-duty and ~50% in light-duty engines demonstrated.
- Improved thermal efficiency over stock manufacturer light-duty engine achieved without the need for oxides of nitrogen (NOx) and particulate matter after-treatment using gasoline compression ignition and dual-fuel reactivity-controlled compression ignition (RCCI) combustion.
- Validated combustion and realistic fuel vaporization submodels developed for biofuels and gasoline/diesel surrogates for engine optimization and concept evaluation.
- Methodology formulated for efficient engine system transient control strategies appropriate for engine speed/load mode transitions.

Introduction

This is the final report of a 3-year effort under DOE grant DE-EE0000202 at the University of Wisconsin Engine Research Center. The work addressed DOE's program goals of a 20-40% improvement in fuel efficiency in a light-duty vehicle and the attainment of 55% brake thermal efficiency in heavy-duty engine systems. The objectives were pursued through experimentation and the development of advanced combustion regimes and emission control strategies, coupled with advanced petroleum and non-petroleum fuel formulations. To meet the project goals it was necessary to improve the efficiency of expansion work extraction, and this required optimized combustion phasing and minimized in-cylinder heat transfer losses. To minimize fuel used for diesel particulate filter (DPF) regeneration, soot emissions were also minimized. Because of the complex nature of optimizing production engines for real-world variations in fuels, temperatures and pressures, the project applied high-fidelity computing and high-resolution engine experiments synergistically to seek low-emission, fuel-efficient engine designs. The experiments were conducted using representative single- and multi-cylinder automotive and truck diesel engines.

Approach

The projects focused on advanced low-temperature combustion and lean-burn strategies, and on the development of advanced modeling tools. The work was divided into four main tasks with 12 subprojects, featuring experimental and modeling components:

A. Combustion Strategies for Increased Thermal Efficiency
B. Fuels as an Enabler for Fuel Efficiency Improvement
C. Multi-Scale Predictive Tools for Understanding Combustion and Emissions
D. System-Level Engine Optimization (air, fuel, emissions, after-treatment)

A main focus of Tasks A, B and C was to improve fundamental understanding to overcome technology barriers that control fuel efficiency. The impact of advanced combustion technologies on engine performance linked with the after-treatment system was also considered in Tasks C and D. Fully instrumented research diesel engines were used to reveal combustion fundamentals and to explore methods of controlling and optimizing fuel efficient combustion under steady-state and transient operation. Information from the engine experiments was incorporated in computational

fluid dynamics (CFD) codes (KIVA3V with large eddy simulation [LES] turbulence models and detailed chemistry using CHEMKIN) and system models (GT-Power and associated control algorithms). The developed models and experimental methods were used to explore methods to optimize diesel engine fuel efficiency while maintaining low emissions.

Results

Task A: Combustion Strategies for Increased Thermal Efficiency

Dual-fuel RCCI is a new combustion strategy developed during the research. It was implemented using port injection of low reactivity fuel, and optimally timed multiple in-cylinder injections of high reactivity fuel. It was found that RCCI can operate over a wide load range with near-zero NOx and soot emission, acceptable pressure rise rate and ringing intensity, and with very high indicated efficiency. For example, in the Engine Research Center heavy-duty engine a peak gross indicated efficiency of 57% was observed with gasoline-diesel at 9.3 bar indicated mean effective pressure (IMEP) and 1,300 rev/min. Comparisons between RCCI and conventional diesel showed a reduction in NOx by three orders of magnitude, a reduction in soot by a factor of six, and an increase in gross indicated efficiency of 18% (i.e., 9% more of the fuel energy is converted to useful work).

Reductions in engine heat rejection were found to be a key enabler to increase engine efficiency. Piston oil jet gallery cooling had a negative impact on efficiency. Without oil cooling it was found that RCCI is nearly adiabatic, achieving 95% of the theoretical maximum cycle efficiency (air standard Otto cycle efficiency). The results shown in Figure 1 were obtained with a high compression ratio piston (18.7:1) using a very dilute charge with E85 (low reactivity fuel — 85% ethanol, 15% gasoline fuel blend) and gasoline with 3% ethylhexylnitrate (high reactivity fuel). With reductions in heat transfer and improved combustion control, 60% gross thermal efficiency has been achieved.

The light-duty engine experiments demonstrated high efficiency and low emissions single fuel operation with gasoline compression ignition over a wide load/speed range (1,500-2,500 rev/min, 3-17.8 bar net IMEP), as shown in Figure 2. The low-temperature combustion (LTC) was controlled with multiple injections, variable injection pressure, oxygen concentration (exhaust gas recirculation, EGR) and boost pressure with maximum rates of pressure rise less than 10 bar/deg. NOx emissions and particulate matter emissions were less than 1 and 0.1 g/kg-fuel, respectively, and the indicated specific fuel

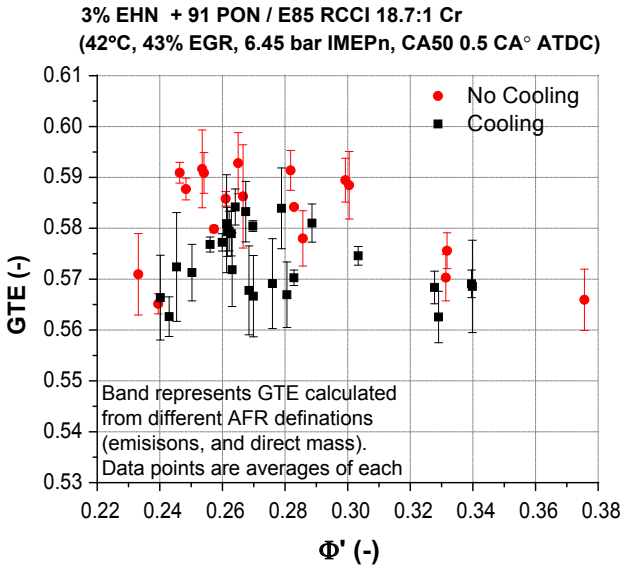

FIGURE 1. Close to 60% gross indicated efficiency achieved in heavy-duty diesel engine operating with optimized RCCI at 1,300 rev/min

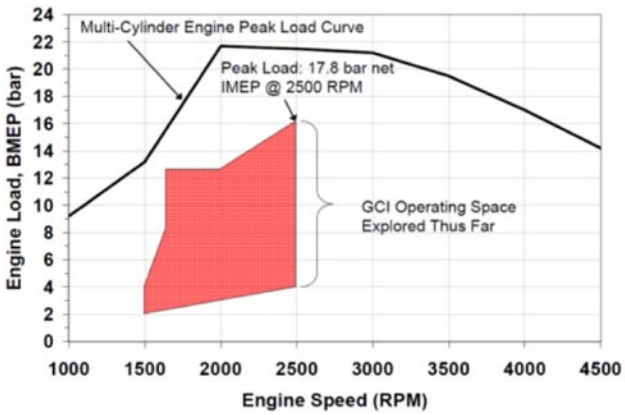

FIGURE 2. Gasoline direct injection compression ignition operation range for light-duty engine

consumption ranged between 175 and 190 g/kW-hr. At the 16 bar IMEP operating point the indicated thermal efficiency was in excess of 47%. A high load injection strategy was also formulated using an initial injection to establish a premixed base charge, a second injection to manipulate the start of combustion, and a third injection to tailor the load. A combustion mode switch study was also carried out using full engine cycle analysis (including intake and exhaust) using an LES model in the KIVA code.

Task B: Fuels as an Enabler for Fuel Efficiency Improvement

A focus of the study was to understand the role of fuel chemistry on RCCI combustion. The experiments

used an optically accessible, single-cylinder light-duty diesel engine. Premixed (low reactivity) fuels were investigated, including pure isooctane, a primary reference fuel (PRF) 90 blend of *n*-heptane and isooctane, and E85. The high-reactivity fuel was low-sulfur diesel fuel. The heat release duration is a function of the reactivity difference between the two fuels. PRF90, which has reactivity closest to diesel fuel, the highest peak heat release and the shortest overall duration. E85, which has the largest reactivity difference from diesel fuel, has the lowest peak heat release and the longest overall duration. High-speed optical movies confirmed that combustion occurs in a staged manner from the high-reactivity zones located at the periphery of the chamber, to low-reactivity zones in the field of view, as shown in Figure 3. In-cylinder laser/optical diagnostics were also used to investigate extended-lift-off diesel combustion in a small bore diesel engine. The results showed the possibility of achieving extended-lift-off combustion (ELOC) for at least limited durations. High swirl ratios were shown to benefit to ELOC due to increased mixing before ignition and the resulting significant temperature non-uniformities near top-dead center.

Task C: Multi-Scale Predictive Tools for Understanding Combustion and Emissions

An efficient reduced chemistry mechanism called MultiChem was developed that models realistic fuels by introducing a physical surrogate, group chemistry representation. A 31-component physical surrogate component data base was used to account for the major species in most hydrocarbon fuels, and MultiChem includes chemistry mechanisms for biodiesel surrogates. The new models enhance the applicability and reliability of engine simulations with multi-component fuels. Advanced spray and fuel film models for selective catalytic reduction after-treatment were also developed in this subtask. Calculations were performed of urea-water-solution sprays and their subsequent vaporization, solidification and urea decomposition. The solver accurately predicted both stages of the vaporization process, which is initially dominated by the presence of water, and gradually becomes governed by the urea content as the water is depleted from the interfacial region. The model also predicted the entrapment of water, which results from the rapid enrichment of urea at the gas-liquid interface.

Task C included high-resolution in-cylinder scalar concentration measurements to study fundamental turbulence and mixing processes and help improve the LES combustion models of Task A. The measurements resolved all turbulence length scales and provided the first direct measurements of dissipation scales of engine flows near top-dead center. Crank-angle-resolved species and temperature measurement diagnostics were also developed for improved understanding of chemistry and mixing. An emission Fouier transform infrared technique was developed and applied to in-cylinder RCCI measurements, as shown in Figure 4. The study demonstrated that the combustion duration in RCCI is controlled by details of the fuel reactivity gradients in the combustion chamber and provided validation data for CFD modeling.

Task D: System-Level Engine Optimization (air, fuel, emissions, after-treatment)

This task established guidelines for efficient transition between LTC and high load combustion. Measurements included performance data and cycle-resolved emissions sampling in a multi-cylinder light-duty diesel engine. A low-pressure EGR system was implemented and sub-system response times were assessed and compared. Operating variables that caused differences between actual transient performance and quasi-steady approximations of the transient

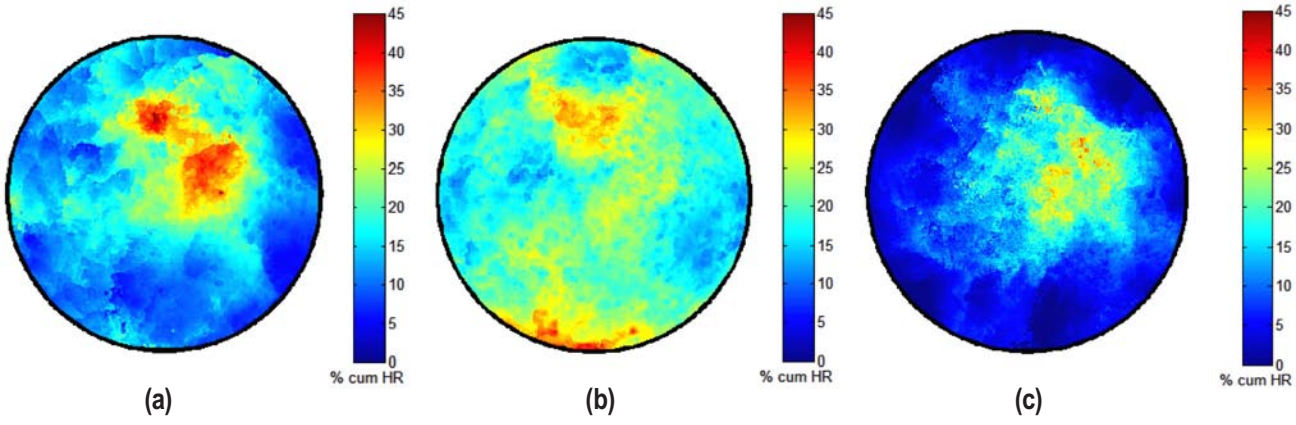

FIGURE 3. RCCI ignition maps for direct injection diesel with premixed (a) Isooctane, (b) PRF90, and (c) E85

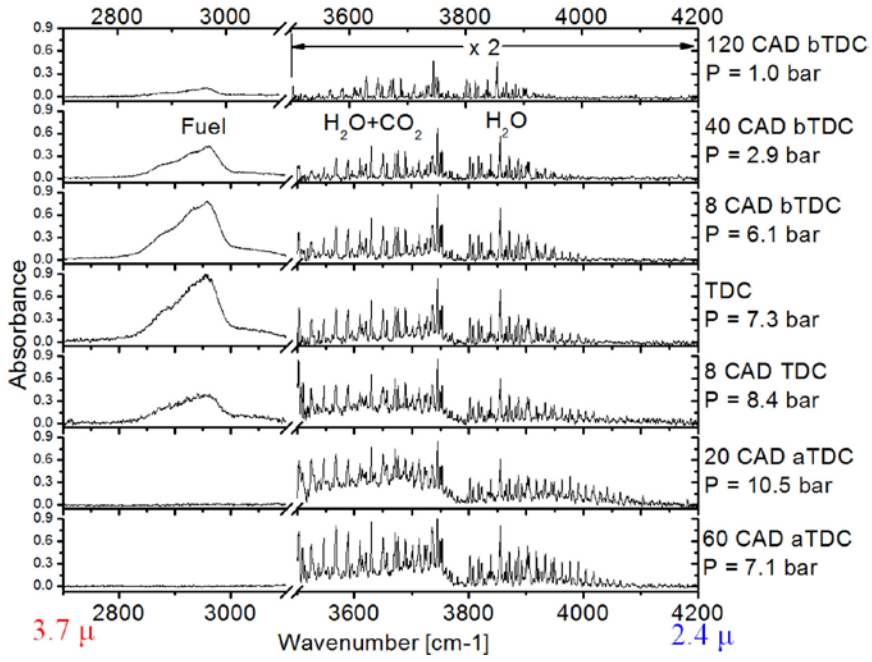

FIGURE 4. In-cylinder Fourier transform infrared measurements of fuel, H_2O and CO_2 absorption spectra

were identified. For example, reproducing intake O_2 concentration alone does not account of all of the differences observed between transient and steady-state operation. Differences in component temperatures (which have a long time constants) were found to have a measurable contribution, and standard diesel combustion had a higher sensitivity to long term thermal transients than LTC. System simulations and after-treatment optimization modeling was used to guide the transient engine experiments and to study engine–after-treatment options for low fuel consumption. System-level engine after-treatment component models with diesel oxidation catalyst, DPF and advanced controllers were used to explore emissions control. Work focused on developing improved control models for transient control, exploring hydrocarbon slip through a diesel oxidation catalyst and its impact on DPF performance, and exploration of pulsed DPF regeneration strategies.

Conclusions

- Novel diagnostics, fuel types, injection concepts and optimized piston geometries were explored together with advanced CFD models and coordinated engine experiments to identify efficient low temperature combustion concepts.
- The study identified advanced combustion regimes with optimized control of fuel/air/diluent mixture preparation and control of fuel reactivity distributions that offer substantial improvements in engine efficiency (>50% gross indicated thermal efficiency) while meeting emissions mandates without the need for after-treatment.

FY 2012 Publications/Presentations

1. Kokjohn, S.L., Reitz, R.D., Splitter, D.A., and Musculus, M.P.B., "Investigation of Fuel Reactivity Stratification for Controlling PCI Heat-Release Rates Using High-Speed Chemiluminescence Imaging and Fuel Tracer Fluorescence," SAE paper 2012-01-0375, 2012.

2. Splitter, D.A., Wissink, M., Kokjohn, S.L., and Reitz, R.D., "Effect of Compression Ratio and Piston Geometry on RCCI Load Limits and Efficiency," SAE paper 2012-01-0383, 2012.

3. Hanson, R.M., Curran, S., Wagner, R., Kokjohn, S.L., Splitter, D.A., and Reitz, R.D., "Piston Bowl Optimization for RCCI Combustion in a Light-Duty Multi-Cylinder Engine," SAE paper 2012-01-0380, 2012.

4. Kaddatz, J., Andrie, M.J., Reitz, R.D., and Kokjohn, S.L., "Light-duty Reactivity Controlled Compression Ignition Combustion using a Cetane Improver," SAE Paper 2012-01-1110, 2012.

5. Nieman, D.E., Dempsey, A.B., and Reitz, R.D., "Heavy-Duty RCCI Operation Using Natural Gas and Diesel," SAE paper 2012-01-0379, 2012.

6. Dempsey, A.B., Adhikary, B. Das, Viswanathan, S., and Reitz, R.D., "Reactivity Controlled Compression Ignition (RCCI) using Premixed Hydrated Ethanol and Direct Injection Diesel," J. Eng. Gas Turbines Power, 134, 082806, 2012.

7. Ra, Y., Loeper, C.P., Andrie, M.J., Krieger, R.B., Foster, D.E., Reitz, R.D., and Durrett, R., "Gasoline DICI Engine Operation in the LTC Regime using Triple-Pulse Injection," SAE Paper 2012-01-1131, 2012.

8. Glewen, W., Heuwetter, D., Foster, D., Andrie, M., Krieger, R., "Analysis of Deviations from Steady State Performance During Transient Operation of a Light Duty Diesel Engine," SAE Int. J. Engines 5(3):909-922, 2012, doi:10.4271/2012-01-1067.

9. Blessinger, M., Stein, J. and Ghandhi, J.B., "An Optical Investigation of Fuel Composition Effects in a Reactivity Controlled HSDI Engine," SAE Int. J. Engines 5(2):2012, doi:10.4271/2012-01-0691.Also published as SAE Paper 2012-01-0829, 2012.

10. Ryddner, D.T. and M.F. Trujillo (2012) "A Fully Resolved UWS Droplet Simulation," 24th Annual Conference on Liquid Atomization and Spray Systems, May, San Antonio, TX.

11. Ryddner, D.T. and M.F. Trujillo (2012) "UWS Droplet Vaporization," (to be submitted to Int. J. Heat and Mass Transfer).

12. Zhang, Y. and Rutland, C.J. 2012, "A Mixing Controlled Direct Chemistry (MCDC) Model for Diesel Engine Combustion Modeling using Large Eddy Simulation," Combustion Theory and Modelling, Vol.16, Issue.3, pp.571-588. DOI:10.1080/13647830.2011.642819.

13. Banerjee, S. and Rutland, C.J., "Numerical Investigation of High Powered Diesel Mode Transition Using Large Eddy Simulations", SAE 2012-01-0693, SAE World Congress, Detroit, MI, April 2012.

Special Recognitions & Awards/Patents Issued

1. Ra, Y., Loeper, P., Reitz, R.D., Krieger, R.B., Foster, D.E., Durrett, R.P., Gopalakrishnan, V., Plazas, A., Peterson, R., and Szymkowicz, P., "Study of high speed gasoline DICI engine operation in the LTC regime," SAE Paper 2011-01-1182, named SAE Horning Award winner for 2011.

2. Reitz, R.D., 2012 DOE Vehicle Technologies R&D Award

II.26 Flex Fuel Optimized SI and HCCI Engine

Guoming (George) Zhu (Primary Contact) and Harold Schock
Michigan State University (MSU)
Mechanical Engineering
Energy and Automotive Research Lab
1497 Engineering Research Court, Room E148
East Lansing, MI 48824

DOE Technology Development Manager:
Gurpreet Singh

Subcontractors:
Chrysler, LLC, Auburn Hill, MI

Overall Objectives

- Demonstrate a spark ignition (SI) and homogeneous charge compression ignition (HCCI) dual-combustion mode engine for a blend of gasoline and E85 (85% ethanol, 15% gasoline) for the best fuel economy.
- Develop a cost-effective and reliable SI and HCCI dual-combustion mode engine.
- Develop a control oriented (real-time) SI, HCCI and SI-HCCI combustion model and implement it into a hardware-in-the-loop (HIL) simulation environment.
- Develop model-based combustion mode transition control strategies for smooth mode transition between SI and HCCI combustions.
- Utilize closed-loop combustion control to minimize efficiency degradation with satisfactory engine out exhaust emissions under any blend of gasoline and E85.

Fiscal Year (FY) 2012 Objectives

- Complete the target optical engine integration and tests in HCCI combustion mode.
- Complete the target metal multi-cylinder engine integration and baseline tests.
- Continue improving the engine modeling and control strategies.

Accomplishments

- The design and fabrication of the optical engine, capable of HCCI combustion, is completed. Both SI and HCCI tests were conducted on the optical engine. The test data was used to calibrate both engine model and control strategy.
- A test bench of the electrical variable valve timing (EVVT) system was designed and fabricated, and the model-based EVVT control strategy was developed and validated on the test bench and also on the optical engine.
- The engine HIL simulation model was further improved, including new physics-based charge mixing model and updated calibrations based upon optical engine test data.
- The target four-cylinder metal engine was modified to fit the two-lift valvetrain and electrical cam phasing system. The engine piston was also redesigned to achieve desired compression for HCCI combustion.
- The prototype metal engine and the Opal-RT prototype controller were integrated and installed in the MSU dynamometer room and the engine is ready for baseline mapping and future tests.
- Over the past year, two journal and two conference papers were published.

Future Directions

In FY 2013, our plan is to complete the project and to demonstrate the smooth combustion mode transition between SI and HCCI operations on the four-cylinder metal engine. The following is a list of tasks for the next fiscal year:

- Complete HCCI closed-loop combustion control dynamometer tests, along with the determination of the HCCI operational range.
- Develop the final test plan and complete the final performance and emission tests.
- Complete the test data analysis and final project report.

Introduction

To obtain the benefit of high efficiency of compression ignition (CI) engines and low emissions of SI engines, there has been a rekindled interest in HCCI engines in recent years. The major advantage of HCCI engines is realized by eliminating the formation of flames and results in a much lower combustion temperature [1-5]. As a consequence of the low-temperature combustion, the formation of oxides of

nitrogen is greatly reduced. The lean-burn nature of the HCCI engine also enables un-throttled operation to improve vehicle fuel economy. The main challenge of HCCI engines is the accurate control of the start of combustion and combustion duration. The practical application of the HCCI principle to gasoline engines is envisioned in a dual-mode combustion engine concept. At partial load conditions, the engine would operate under an un-throttled HCCI combustion mode; and at low- or high-load conditions, the engine operation needs to transit to the conventional SI combustion mode to avoid engine misfire or knocking. The objective of this project is to demonstrate an SI and HCCI dual-mode combustion engine for a blend of gasoline and E85. The operating efficiencies shall be obtained through closed-loop control, which will result in minimal efficiency degradation when E85 fuel or any blend of gasoline and E85 are used.

Approach

This research activity adopts model-based control approach to develop control strategies for smooth mode transition between SI and HCCI combustions with the support from our industrial partner, Chrysler, LLC. The following methodology is and has been used in this research activity:

- Understand and optimize the HCCI and SI-HCCI hybrid combustion processes through optical engine study.
- Develop a control oriented combustion model that unifies SI, HCCI, and SI-HCCI combustion, as well as the entire engine model, and calibrate it based upon GT-Power simulation results and optical/metal engine experiments.
- Utilize the developed control oriented engine model to study SI and HCCI combustion modes as well as the SI-HCCI hybrid (spark assistant) combustion mode during combustion mode transition.
- Develop the closed-loop combustion control strategy for hybrid combustion and SI to HCCI combustion mode transition under a blend of gasoline and ethanol and validate it through HIL simulations.
- Validate the developed control strategy on the multi-cylinder metal engine for smooth mode transition between SI and HCCI combustions.

Results

- To develop a model-based control strategy for the system, an EVVT test bench was designed and constructed, and an EVVT plant model was also developed to closely match the physical system [6]. An output covariance constraint (OCC) controller was designed based upon the developed model. Different reference signals were used to test the controller performance. The test results showed that the OCC controller improves the EVVT response time over the conventional proportional controller with reduced phase delay. The bench test results also show that the EVVT response time is fast enough for the SI and HCCI combustion mode transition (20 degree phasing within three engine cycles); see Figure 1 for optical engine test results.
- After the optical engine was rebuilt early this year with the modified engine head equipped with the two-step valve and EVVT systems (see Figure 2), optical engine tests were conducted in both SI and HCCI combustion modes. Figure 3 shows the optical engine combustion images at 0.1 degree after top-dead center (TDC) under different air-to-fuel ratios, and Figure 4 provides the optical engine HCCI combustion images. This indicates that the optical engine is capable of SI and HCCI combustion.
- The engine HIL model developed in FY 2011 was improved by adding physics-based charge mixing model and validating it in the MSU HIL simulation environment. The modeling results were presented at 2012 American Society of Mechanical Engineers Dynamic System Control Conference [7]. The

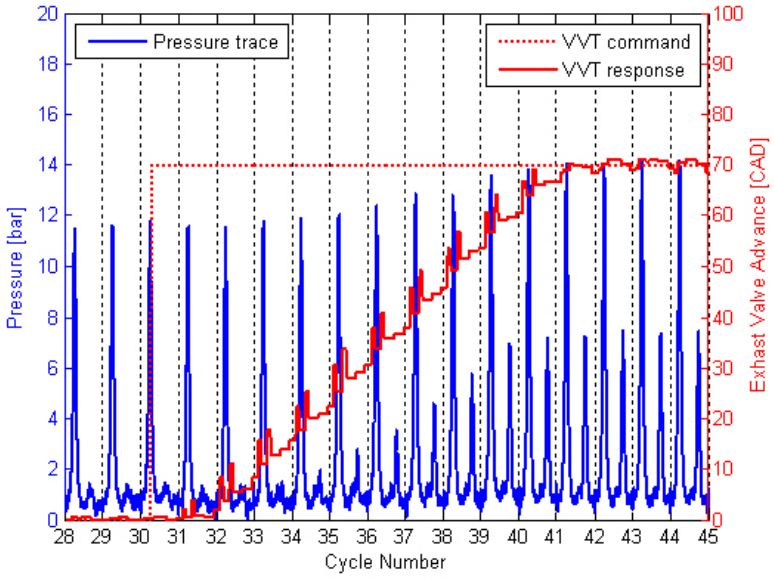

FIGURE 1. EVVT Response with 70 Crank Angle Degree (CAD) Exhaust Advance

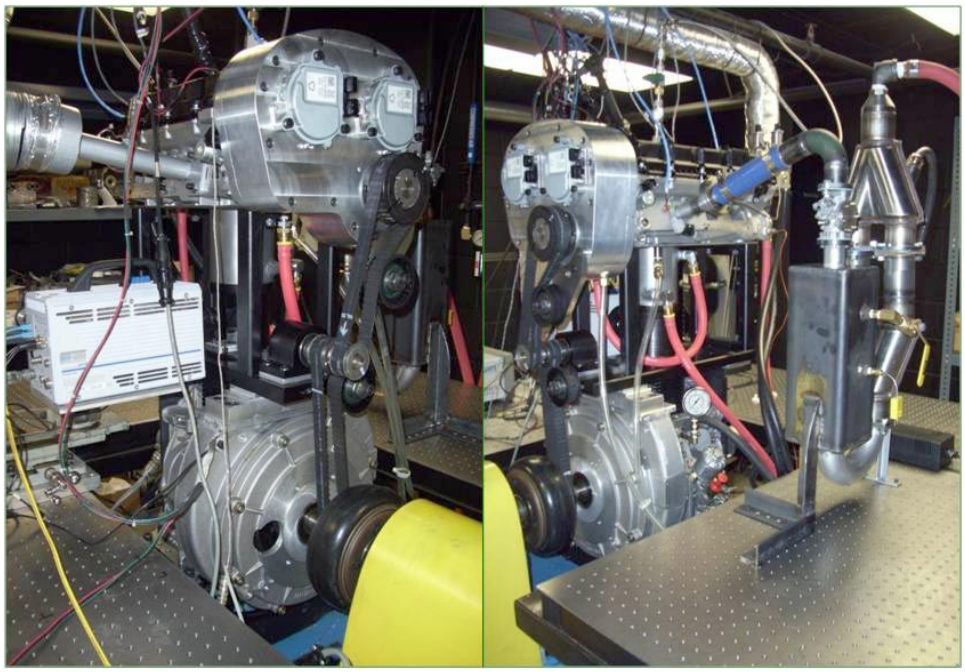

FIGURE 2. Assembled Optical Engine capable of SI and HCCI Combustion

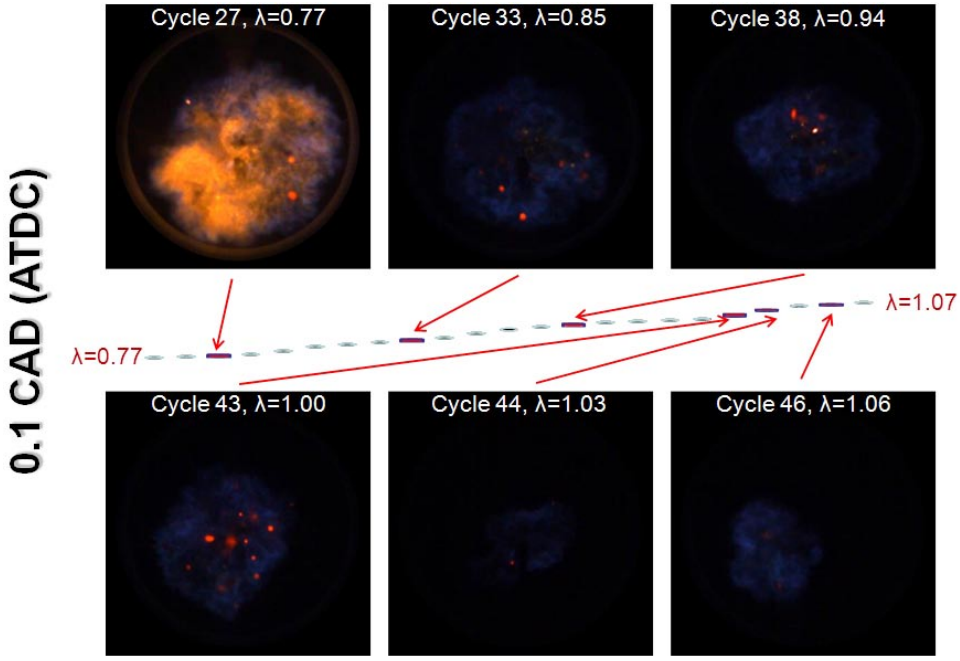

FIGURE 3. Optical Engine Combustion Images at 0.1 Degree after TDC under Different Air/Fuel Ratios

improved HIL model was also recalibrated based upon the optical engine test data.

- It was also learned from the optical engine combustion tests that cycle-to-cycle variation of charge mixing is quiet large and the infrared imaging technique was used to study the intake charge and trapped exhaust gas recirculation mixing process. Infrared images show that at a given engine crank location these images are quite different (see Figure 5), indicating large charge mixing cycle-to-cycle variations. This makes the mode transition control quite difficult. The study results have be summarized into a paper submitted to 2013 American Control Conference [8].

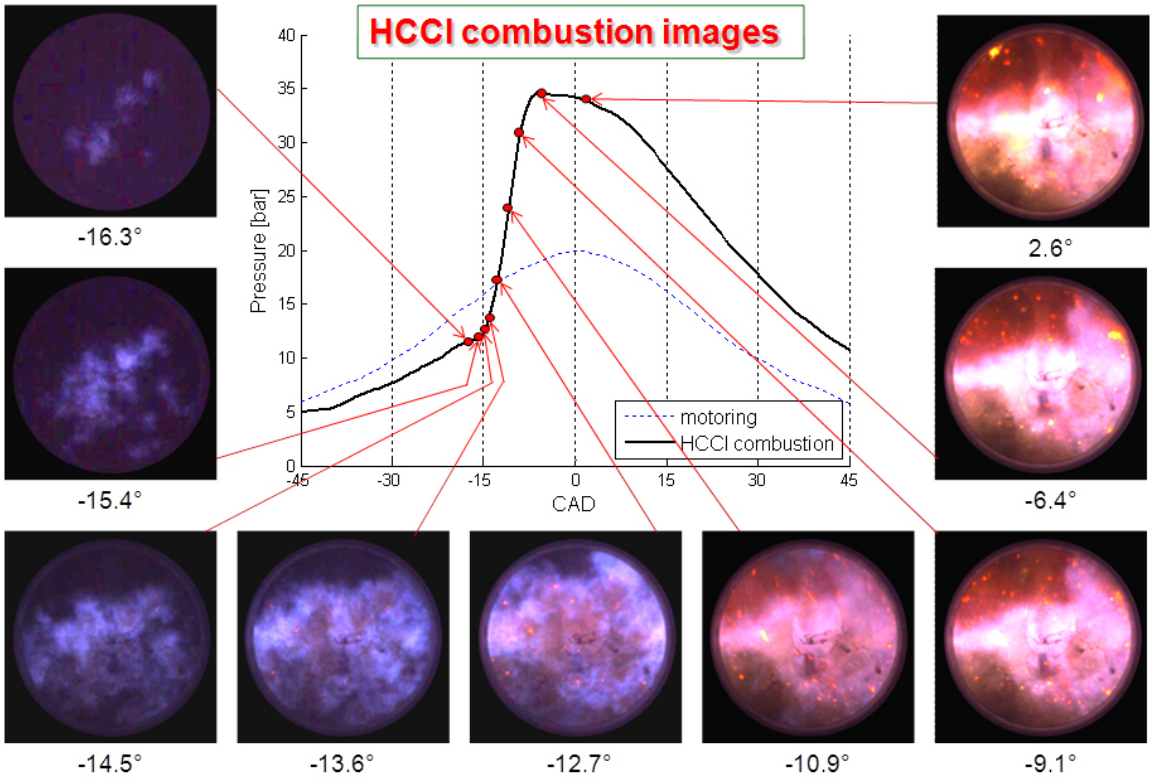

FIGURE 4. Optical Engine HCCI Combustion Images

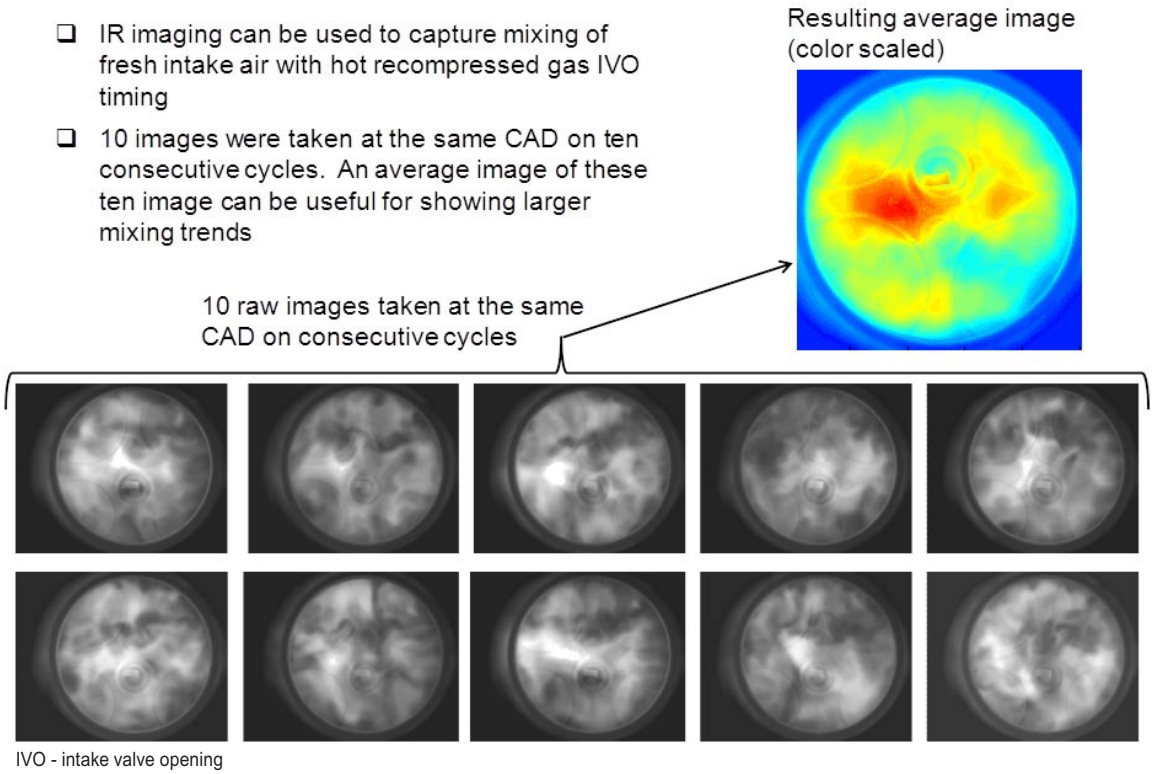

FIGURE 5. Infrared Images of the Charge Mixing for 10 Engine Cycles

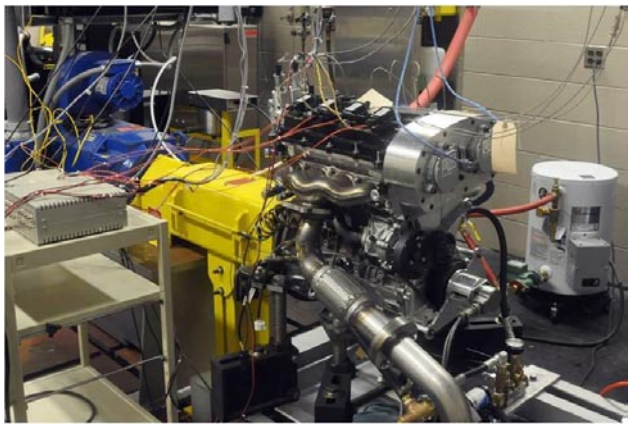

FIGURE 6. Target Metal Engine installed in the MSU Dynamometer Room

- One of the key achievements of FY 2012 is that integration of the target four-cylinder metel engine is completed and the engine has been installed in the MSU dynamometer room (see Figure 6). SI combustion mode was validated in the dynamometer. The original four-cylinder engine, provided by Chrysler, was upgraded through increased compression ratio, the two-step valve lift system with dual cam profile, and fast electrical cam phasing system. The engine is ready for baseline mapping in SI and HCCI combustion modes.

Conclusions

The research conducted in FY 2012 has shown the progress toward the development, implementation, and demonstration of the proposed technology. Specific accomplishments are listed below:

- Both bench and optical engine test results show that the response time of the selected electrical VVT system is satisfactory for combustion mode transition control.
- Simplified charge mixing model is not accurate enough for HIL simulations and physics-based charge mixing model is required.
- Optical engine test data can be used for calibrating the HIL models.
- Large cycle-to-cycle variation of charge mixing was found using the infrared imaging technique, indicating the challenge of smooth combustion mode transition.
- With the normal progress on the project, we are confident that we will be able to complete the project in the next fiscal year (FY 2013).

References

1. G. Shibata, K. Oyama, T. Urushihara, and T. Nakano, (2004) "The Effect of Fuel Properties on Low and High Temperature Heat Release and Resulting Performance of an HCCI Engine," SAE 2004-01-0553.

2. G. Haraldsson, J. Hyvonen, P. Tunestal, and B. Johansson, (2004) "HCCI Closed-Loop Combustion Control Using Fast Thermal Management," SAE 2004-01-0943.

3. H. Persson, M. Agrell, J.-O. Olsson, and B. Johansson, (2004) "The Effect of Intake Temperature on HCCI Operation Using Negative Valve Overlap," SAE 2004-01-0944.

4. G.M. Shaver, et al, (2005) "Dynamic Modeling of Residual-Affected Homogeneous Charge Compression Ignition Engines with Variable Valve Actuation," ASME Journal of Dynamics, Measurement, and Control, Vol. 127, pp. 374-381.

5. G.M. Shaver, (2005) "Physics Based Modeling and Control of Residual-Affected HCCI Engines using Variable Valve Actuation," PhD thesis, Stanford University.

6. Z. Ren and G. Zhu, "Modeling and control of an electrical variable valve timing actuator," *Submitted to ASME Journal of Dynamic Systems, Measurement and Control* (*August, 2012*).

7. S. Zhang, G. Zhu, Y. Yoon, and Z. Sun, "A control oriented charge mixing and HCCI combustion model for internal combustion engines," *2012 ASME Dynamic System Control Conference, Ft. Lauderdale, FL, October, 2012.*

8. Y. Yoon, Z. Sun, S. Zhang, and G. Zhu, "Development of control-oriented charge mixing model and experimental validation using graphical analysis," Submitted to *2013 American Control Conference, Washington DC, June, 2013.*

FY 2012 Publications/Presentations

1. X. Yang and G. Zhu, "A control oriented hybrid combustion model of an HCCI capable SI engine," *Proceedings of the Institution of Mechanical Engineers, Part D, Journal of Automobile Engineering, 226(10), 2012, pp. 1380-1395* (DOI: 10.1177/0954407012443334).

2. X. Yang and G. Zhu, "SI and HCCI combustion mode transition control of a multi-cylinder HCCI capable SI engine," *IEEE Transaction on Control System Technology* (*Accepted in May, 2012,* DOI: 10.1109/TCST.2012.2201719).

3. S. Zhang, G. Zhu, Y. Yoon, and Z. Sun, "A control oriented charge mixing and HCCI combustion model for internal combustion engines," *2012 ASME Dynamic System Control Conference, Ft. Lauderdale, FL, October, 2012.*

4. X. Yang and G. Zhu, "Air-to-fuel ratio regulation during SI to HCCI combustion mode transition using the LQ tracking control," *Proceedings of 2012 American Control Conference, Montreal, Canada, June, 2012.*

5. G. Zhu and H. Schock, "Flex Fuel Optimized SI and HCCI Engine," *DOE Vehicle Technology Program Annual Merit Review, Arlington, VA, May, 2012.*

6. G. Zhu and H. Schock, "Update on flex fuel optimized HCCI engine project," DOE ACE/HCCI working group meeting, San Francisco, CA, February 15, 2012.

7. G. Zhu, and H. Schock, "Update on flex fuel optimized HCCI engine project," *ACE Working Group Meeting, Southfield, MI, June, 2012.*

8. Y. Yoon, Z. Sun, S. Zhang, and G. Zhu, "Development of control-oriented charge mixing model and experimental validation using graphical analysis," Submitted to *2013 American Control Conference, Washington DC, June, 2013.*

III. EMISSION CONTROL R&D

III.1 CLEERS Aftertreatment Modeling and Analysis

George Muntean (Primary Contact),
Maruthi Devarakonda, Feng Gao, Ja Hun Kwak,
Jin-Yong Luo, Chuck Peden, Mark Stewart,
Janos Szanyi, Diana Tran
Institute for Integrated Catalysis
Pacific Northwest National Laboratory (PNNL)
902 Battelle Boulevard
Richland, WA 99352

DOE Technology Development Manager:
Ken Howden

Overall Objectives

- Promote the development of improved computational tools for simulating realistic full-system performance of lean-burn engines and the associated emissions control systems.
- Provide the practical and scientific understanding and analytical base required to enable the development of efficient, commercially viable emissions control solutions for ultra-high efficiency vehicles.

Fiscal Year (FY) 2012 Objectives

- Lead and contribute to the Cross-Cut Lean Exhaust Emissions Reduction Simulations (CLEERS) activities, e.g. lead technical discussions, invite distinguished speakers, and maintain an open dialogue on modeling issues.
- Develop improved modeling capabilities for selective catalytic reduction (SCR) and diesel particulate filter (DPF) through fundamental experiments.
- Develop a fundamental understanding of SCR and lean-NOx trap (LNT) catalysts with primary focus on reaction mechanisms and material characterization.

Accomplishments

- Obtained kinetic parameters for small-pore zeolite-based Cu SCR catalysts.
- Determined an optimum K loading for overall and best high temperature performance for K-based LNT catalysts.
- Developed and validated a Cu SCR model considering a single NH_3 storage site, based on CLEERS SCR transient protocol data from Oak Ridge National Laboratory (ORNL).
- Began development of a new SCR model with two NH_3 storage sites in order to better reproduce effects observed in experimental data.
- Proposed an improved unit collector model for prediction of number efficiency in exhaust particulate filters.

Future Directions

- Continue detailed kinetic and mechanistic studies for NO reduction over the state-of-the-art small-pore zeolite-based Cu SCR catalysts.
- Continue fundamental studies of novel high-temperature LNT formulations.
- Characterize current production and advanced DPF substrates through advanced image and statistical analysis of high resolution computed tomography data and extend these studies to include DPFs coated with SCR catalysts for integrated DPF/SCR systems.
- Develop and validate SCR aging models based on CLEERS transient protocol data.

Introduction

CLEERS is a research and development focus project of the Diesel Cross-Cut Team. The overall objective is to promote the development of improved computational tools for simulating realistic full-system performance of lean-burn engines and the associated emissions control systems. Three fundamental research projects are sponsored at PNNL through CLEERS: DPF, SCR, and LNT. Resources are shared between the three efforts in order to actively respond to current industrial needs. In FY 2012, primary emphasis continued to be placed on the SCR activities because of urgent application issues associated with these technologies.

Approach

SCR: State-of-the-art Cu-CHA zeolites perform differently from previous generations of SCR catalysts. In addition to higher overall NOx reduction rates, higher N_2 selectivity, and better resistance to aging effects, they appear to be significantly more flexible with respect to operating parameters such as NO/NO_2 ratios. While significant progress has been made, global kinetics models originally developed for older

SCR catalyst systems must be further refined in order to allow this technology to realize its full potential in new vehicles. Robust models must also be developed to describe the effects of various aging phenomena, so that system performance can be accurately predicted and controlled over a vehicle's lifetime. We are studying the physicochemical properties of the latest commercial Cu-zeolite catalyst with respect to hydrothermal aging in great detail. We also updated PNNL's SCR model to examine the effects of hydrothermal aging on kinetic parameters to quantitatively describe the changes induced by the aging process.

LNT: The LNT technology is based on the ability of certain oxides, such as alkaline and alkaline earth oxide materials, to store NOx under lean conditions and reduce it during rich engine operation cycles. Our project is aimed at developing a fundamental understanding of the operation of the LNT technology especially with respect to the development of new LNT materials able to operate at significantly higher and lower temperatures than the current generation of LNT materials.

DPF: A number of micro-scale filter modeling studies have been carried out at PNNL to date, which have helped explain fundamental filter behavior and guide the development of improved filter technologies. Since these detailed three-dimensional simulations are too computationally intensive for routine system design tasks, a bridge must also be developed to lower order models, such as the commonly used unit collector model. The ability of standard unit collector models to predict number efficiency over a range of particle sizes is currently being evaluated. Another area of current interest is the development of multi-functional filter technologies, where filters also contain high loadings of catalysts (such as SCR, three-way catalyst, or LNT).

Results

SCR Catalyst Model: PNNL's one-dimensional global kinetic model was adapted to fit steady-state experimental results obtained by ORNL (using the CLEERS SCR transient reactor protocol) and then validated against transient data. The global kinetic model, which employs a single NH_3 storage site, was able to match experimental observations well enough for use in system design and model-predictive control. The same model was also adapted to achieve a similar level of agreement with the performance of aged samples. Figure 1 shows a preliminary model fit to the experimental data. An effort is also being made to develop a rational model for the effect of aging on the storage site populations.

SCR Fundamentals Research: During FY 2012, we continued our studies of the effects of hydrothermal aging on various Cu-zeolite catalysts to better understand the nature of Cu species. We have especially focused on the structure and oxidation state of the active Cu sites in the catalysts as a function of various treatments. In addition, we have carried out extensive kinetics studies of the performance of these catalysts as a function of Cu loading and catalyst aging conditions for several key reactions including "standard" and "fast" SCR, and NO and NH_3 oxidation (by O_2).

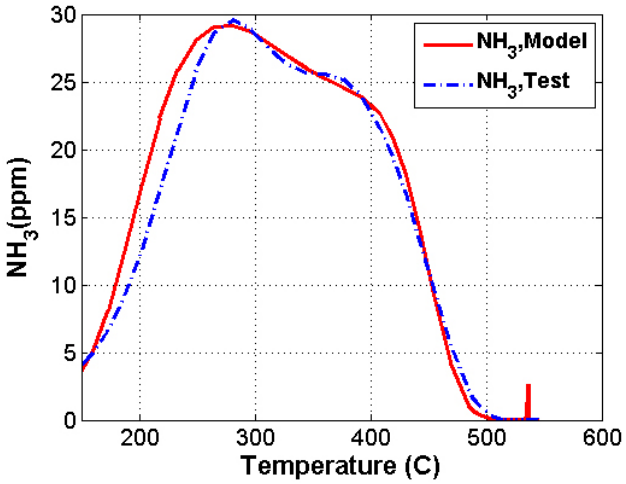

FIGURE 1. Two-Site Adsorption Model Fit to TPD Data

The effects of Cu loading in Cu/SSZ-13 catalysts were also characterized by a variety of techniques, including H_2-temperature-programmed reduction (TPR), Fourier transform infrared (FTIR), and electron paramagnetic resonance. The results obtained are consistent with the presence of Cu ions in two distinct cationic positions of the SSZ-13 framework. For example, Figure 2 displays the H_2-TPR results obtained on Cu-SSZ-13 samples with different Cu ion exchange levels and then calcination at 500ºC. These results provide good evidence that there are two different Cu^{2+} species present in SSZ-13, and that their distribution changes with Cu loading.

LNT Fundamentals Research: Our fundamental studies of possible new LNT formulations able to function at higher temperatures than the current generation of Ba-based materials has focused on changes in the composition of both the NOx storage and support materials. In particular, substituting K for Ba as the NOx storage material is known to provide higher temperature performance. During FY 2012, we examined the effects of LNT catalyst supports and K-loading on the NOx reduction performance of K-based catalysts.

With regard to NOx storage-reduction performance of Pt-K_2O/Al_2O_3 samples, the temperature of maximum NOx uptake (T_{max}) is 573 K up to a potassium loading of

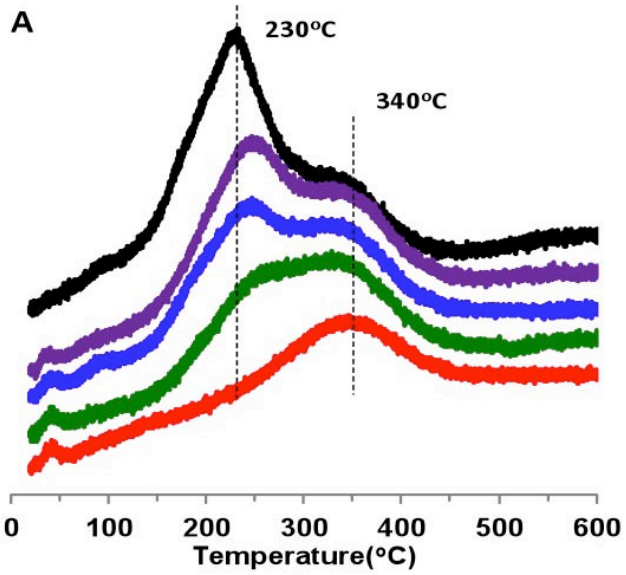

FIGURE 2. H_2 consumption profiles during H_2-TPR on 500°C-calcined Cu/SSZ-13 ($wt_{cat.}$ = 50 mg; heating rate = 10°C/min; total flow rate = 60 ml/min of 2%H_2/Ar. Cu ion exchange levels: 20% (red), 40% (green), 60% (blue), 80% (purple), and 100% (black) – bottom to top).

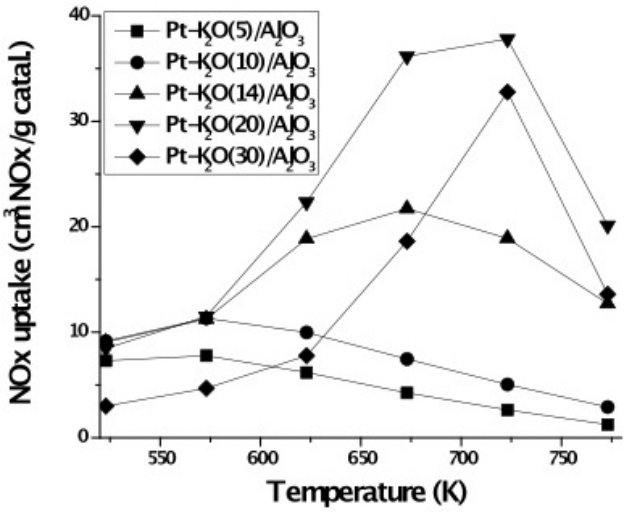

FIGURE 3. Percent NOx Uptake over Pt-BaO/Al_2O_3 and Pt-BaO/$MgAl_2O_4$

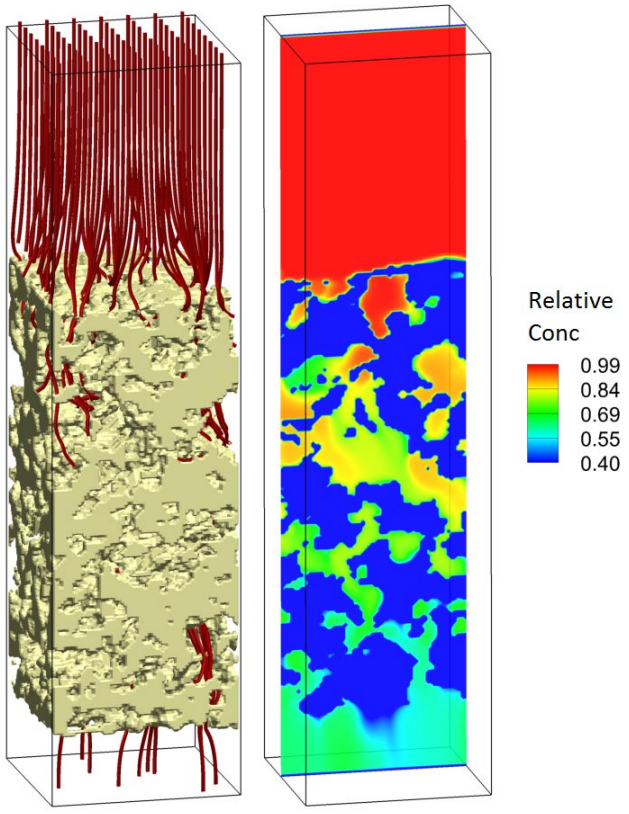

FIGURE 4. Eulerian-Eulerian Filter Simulation of a Cordierite DPF

10 wt% (Figure 3). As the potassium loading increases from 10 wt% to 20 wt%, T_{max} shifted from 573 K to 723 K. Moreover, the amount of NO uptake (38 cm^3 NOx/g catal) at T_{max} increased more than three times, indicating that efficiency of K in storing NOx is enhanced significantly at higher temperature, in good agreement with the NO_2 TPD and FTIR results. Thus, a combination of characterization and NOx storage performance results demonstrates an unexpected effect of potassium loading on nitrate formation and decomposition processes; results important for developing Pt-K_2O/Al_2O_3 for potential applications as high temperature NOx storage-reduction catalysts.

DPF Modeling: Unit collector filter models have been used successfully in DPF system design for a number of years, but they have not typically been used to predict number efficiency over the range of particle sizes encountered in filter exhaust. Standard unit collector filtration models were evaluated against size-resolved number filtration data collected with current DPF substrates, and could not be fit to the size-resolved filtration data collected. It was found that an alternate form of the unit collector model which was developed using micro-scale simulations did a better job matching observed DPF filtration efficiency across the particle size spectrum.

The PNNL micro-scale filter model has been adapted to use the Eulerian-Eulerian approach. The results of one such simulation of a cordierite DPF are depicted in Figure 4, where relative concentration of particulates penetrating along a cross-section through the filter wall is shown. This tool has since been used to support studies of hypothetical filter materials requested by industrial partners in cooperative research projects.

Conclusions

- Cu-CHA zeolites display a number of enhanced properties compared to other zeolite-based catalysts, including improved selectivity (low N_2O production), significantly better hydrothermal stability, and less sensitivity to NO_2/NOx ratio.
- A Cu-CHA SCR model considering a single NH_3 storage site was developed and validated using CLEERS SCR transient protocol data from ORNL.
- Standard unit collector filtration models over-predict capture efficiency of small particles which can dominate number counts in automotive exhaust, but unit collectors with terms modified using micro-scale models appear to perform better across the particle size spectrum.
- On K-based LNT catalysts the optimum (both in terms of overall performance and the highest temperature for maximum performance) K-loading on Al_2O_3 supports was ~15%.

FY 2012 Publications/Presentations

Invited Presentations

1. C.H.F. Peden, "Chemical and physical properties of Cu-SSZ-13 catalysts for the selective catalytic reduction of NOx with NH_3: Implications for the reaction mechanism," 243rd National Meeting of the ACS, San Diego, CA, April 2012.

2. J. Szanyi, "In situ spectroscopy studies on Cu-SSZ-13 SCR catalysts," 244th National Meeting of ACS, Philadelphia, PA, August 2012.

3. C.H.F. Peden, "Some Future Challenges for Catalytic Vehicle Emission Control," Symposium on "The Future of Catalysis", Palo Alto, CA, September 2012.

Contributed Presentations

1. J.H. Kwak, D.N. Tran, J. Szanyi, C.H.F. Peden, and J.H. Lee, "Nature of Cu Species and NO Reduction Kinetics over Cu-SSZ-13," 243rd National Meeting of the American Chemical Society, San Diego, CA, April 2012.

2. J.H. Kwak, F. Gao, E.M. Karp, J.H. Lee, J.Y. Luo, J. Szanyi, D.N. Tran, H. Zhu, C.H.F. Peden, "Chemical and physical properties of small-pore Cu-zeolite catalysts for the selective catalytic reduction of NOx with NH_3: Implications for the reaction mechanism," DOE CLEERS Workshop, Dearborn, MI, April 2012.

3. H. Zhu, J.H. Kwak, C.H. F. Peden, J. Szanyi, "Selective Catalytic Reduction of NOx over Cu-SSZ-13: a combined in situ DRIFTS/MS study," 4th International Congress on Operando Spectroscopy, Upton, NY, May 2012.

4. J.H. Kwak, J.H. Lee, J. Szanyi, H. Zhu, D. Tran, C.H.F. Peden, "Comparative behavior of Cu-zeolite catalysts for the selective catalytic reduction of NOx with NH_3: Nature of the Cu species by temperature-programmed reduction and structural studies," CTEC2012 – Calorimetry and Thermal Effects in Catalysis, Lyon, France, June 2012.

5. J.H. Kwak, J.H. Lee, J. Szanyi, H. Zhu, D. Tran, C.H.F. Peden, "Chemical and physical properties of Cu-SSZ-13 catalysts for the selective catalytic reduction of NOx with NH_3: Implications for the reaction mechanism," 15th International Congress on Catalysis, Munich, Germany, July 2012.

6. F. Gao, E.D. Walter, E.M. Karp, J.Y. Luo, R.G. Tonkyn, J.H. Kwak, J. Szanyi, C.H.F. Peden, "Probing Structure-Activity Relationships in NH_3-SCR over Cu-SSZ-13: Reaction Kinetics and EPR Studies," 2012 Pacific Coast Catalysis Society Meeting, Santa Barbara, CA, September 2012.

Selected Publications

1. J.H. Kwak, D.N. Tran, S.D. Burton, J. Szanyi, J.H. Lee, C.H.F. Peden, "Effects of Hydrothermal Aging on NH_3-SCR reaction over Cu/zeolites." *Journal of Catalysis* **287** (2012) 203-209.

2. J.H. Kwak, R. Tonkyn, D. Mei, S.J. Cho, L. Kovarik, J.H. Lee, C.H.F. Peden, J. Szanyi, "Size-Dependent Catalytic Performance of CuO on γ-Al_2O_3: NO Reduction Versus NH_3 Oxidation," *ACS Catalysis* **2** (2012) 1432-1440.

3. J.H. Kwak, D.H. Kim, J. Szanyi, S.J. Cho, C.H.F. Peden, "Enhanced High Temperature Performance of $MgAl_2O_4$-Supported Pt-BaO Lean NOx Trap Catalysts," *Topics in Catalysis* **55** (2012) 70-77.

4. J.H. Kwak, D. Tran, J. Szanyi, C.H.F. Peden, J.H. Lee, "The Effect of Copper Loading on the Selective Catalytic Reduction of Nitric Oxide by Ammonia Over Cu-SSZ-13," *Catalysis Letters* **142** (2012) 295-301.

5. A. Yezerets, C.H.F. Peden, J. Szanyi, I. Nova, and W.S. Epling, "Preface: Special Issue on Catalytic Control of Lean-Burn Engine Exhaust Emissions," *Catalysis Today* **184** (2012) 1.

6. J.H. Kwak, H. Zhu, J.H. Lee, C.H.F. Peden, J. Szanyi, "Two different cationic positions in Cu-SSZ-13?," *Chemical Communications* **48** (2012) 4758-4760.

7. H. Zhu, J.H. Kwak, C.H.F. Peden, J. Szanyi, "In situ DRIFTS-MS studies on the oxidation of adsorbed NH_3 by NOx over a Cu-SSZ-13 zeolite," *Catalysis Today* (2013) in press.

8. M.N. Devarakonda, J.H. Kwak, J.A. Pihl, S. Daw, J.H. Lee, "Effects of hydrothermal aging on commercial Cu SCR catalyst," Directions in Engine-Efficiency and Emissions Research Conference, Detroit, MI, October 2011.

9. A. Strzelec, T.J. Toops, C.S. Daw, R. Vander Wal, "Investigation of NO_2 Oxidation Kinetics and Burning Mode for Medium Duty Diesel Particulate: Contrasting $O_2$and NO_2 Oyxidation," Directions in Engine-Efficiency and Emissions Research Conference, Detroit, MI, October 2011.

10. A. Strzelec, T.J. Toops, C.S. Daw, R. Vander Wal, "Trends in Particulate Nanostructure," Directions in Engine-Efficiency and Emissions Research Conference, Detroit, MI, October 2011.

11. M.N. Devarakonda, G.G. Muntean, J.A. Pihl, S. Daw, "Modeling Aging Effects on Reaction Pathways in Cu-CHA Urea SCR Catalysts," DOE CLEERS Workshop, Dearborn, MI, April 2012.

12. M.L. Stewart, "Exhaust Filtration for High Number Efficiency," DOE CLEERS Workshop, Dearborn, MI, April 2012.

III.2 Enhanced High-Temperature Performance of NOx Reduction Catalyst Materials

Feng Gao, Do Heui Kim, Jin-Yong Luo, George Muntean, Chuck Peden (Primary Contact)
Institute for Integrated Catalysis
Pacific Northwest National Laboratory (PNNL)
P.O. Box 999, MS K2-12
Richland, WA 99354

DOE Technology Development Manager: Ken Howden

Cooperative Research and Development Agreement (CRADA) Partners:
- Neal Currier, Krishna Kamasamudram, Ashok Kumar, Junhui Li, Randy Stafford, Alex Yezerets, - Cummins Inc., Columbus, IN
- Mario Castagnola, Hai-Ying Chen, Howard Hess - Johnson Matthey, Taylor, MI

Overall Objectives

Identify approaches to significantly improve the high temperature performance and stability of the catalytic oxides of nitrogen (NOx) reduction technologies via a pursuit of a more fundamental understanding of:

- The various roles for the precious metals.
- The mechanisms for these various roles.
- The effects of high temperatures on the precious metal performance in their various roles.
- Mechanisms for higher temperature NOx storage performance for modified and/or alternative storage materials.
- The interactions between the precious metals and the storage materials in both optimum NOx storage performance and long term stability.
- Modes of thermal degradation of new generation chabhazite zeolite (CHA)-based selective catalytic reduction (SCR) catalysts.
- The sulfur adsorption and regeneration mechanisms for NOx reduction catalyst materials.

Fiscal Year (FY) 2012 Objectives

- Experiments probing the thermal stability and sensitivity to sulfur of model high temperature NOx storage and reduction (NSR) catalysts will continue.
- Continue catalyst characterization of these model high-temperature NSR catalysts with a variety of state-of-the-art methods.
- Initiate studies of model Cu/CHA-based catalysts for ammonia SCR.

Accomplishments

Two Research Thrusts Continued this Year

- Fundamental studies of high-temperature NSR catalysts prepared by PNNL (primary activity – will be the focus of this report):
  - Model catalysts were prepared at PNNL based on materials described in the open literature.
  - Detailed studies of the sensitivity to high temperatures (required for desulfation) of these model catalysts were performed this year.
  - Specific new results on the mechanisms of Pt stabilization by the novel support material, $MgAl_2O_4$, were obtained.
- Mechanisms for high- and low-temperature performance stability of CHA-based zeolites:
  - Based on prior literature reports, several synthesis efforts were carried out at PNNL to prepare model CHA-based catalysts.
  - Catalysts were characterized before and after incorporation of Cu by X-ray diffraction (XRD), electron paramagnetic resonance (EPR) and temperature programmed reduction (TPR).
  - Baseline reactivity measurements were performed on these catalysts in preparation for mechanistic studies of high- and low-temperature performance loss.

Future Directions

- Studies aimed at determining performance limitations, sulfur sensitivity and desulfation behavior of candidate alternative support and NOx storage materials that provide improved high-temperature performance will continue. An overall goal of the work will continue to be to develop a deeper understanding of the mechanisms of NOx storage and reduction activity, and performance degradation of materials that have been reported to show good NSR performance at temperatures considerably higher than BaO/alumina-based

materials. As have the initial studies to be described here, these fundamental studies will be carried out in conjunction with baseline performance and stability experiments on fully formulated catalysts provided by Johnson Matthey.

- Mechanisms for low- and high-temperature performance loss as a function of operation conditions of new generation CHA-based NH_3 SCR catalysts. For these studies, we will utilize the model catalysts prepared via methods studied in FY 2012.

Introduction

Two primary NOx after-treatment technologies have been recognized as the most promising approaches for meeting stringent NOx emission standards for diesel vehicles within the Environmental Protection Agency's 2007/2010 mandated limits, NSR and NH_3 SCR; both are, in fact being commercialized for this application. Small pore copper ion exchanged zeolite catalysts with a CHA structure have recently been shown to exhibit both remarkable activity and very high hydrothermal stability in the NH_3 SCR process [1]. The NSR (also known as the lean-NOx trap, LNT, or NOx absorber) technology is based upon the concept of storing NOx as nitrates over storage components, typically barium species, during a lean-burn operation cycle, and then desorbing and subsequently reducing the stored nitrates to N_2 during fuel-rich conditions over a precious metal catalyst [2]. However, in looking forward to 2015 and beyond with expected more stringent regulations, the continued viability of the NSR technology for controlling NOx emissions from lean-burn engines such as diesels will require at least two specific, significant and inter-related improvements. First, it is important to reduce system costs by, for example, *minimizing the precious metal content* while maintaining, even improving, performance and long-term stability. A second critical need for future NSR systems, as well as for NH_3 SCR, will be significantly *improved higher and lower temperature performance* and stability. Furthermore, these critically needed improvements will contribute significantly to minimizing the impacts to fuel economy of incorporating these after-treatment technologies on lean-burn vehicles. To meet these objectives will require, at a minimum an improved scientific understanding of the following things:

- The various roles for the precious and coinage metals used in these catalysts.
- The mechanisms for these various roles.
- The effects of high temperatures on the active metal performance in their various roles.
- Mechanisms for higher temperature NOx storage performance for modified and/or alternative storage materials.
- The interactions between the precious metals and the storage materials in both optimum NOx storage performance and long-term stability.
- The sulfur adsorption and regeneration mechanisms for NOx reduction materials
- Materials degradation mechanisms in CHA-based NH_3 SCR catalysts.

The objective of this CRADA project is to develop a fundamental understanding of the above-listed issues. Model catalysts that are based on literature formulations are the focus of the work being carried out at PNNL. In addition, the performance and stability of more realistic high temperature NSR catalysts, supplied by Johnson Matthey, are being studied in order to provide baseline data for the model catalysts that are, again, based on formulations described in the open literature.

For this short summary, we will primarily highlight representative results from our recent studies of the stability of candidate high-temperature NSR materials.

Approach

In microcatalytic reactor systems, catalyst performance is evaluated in two separate fixed bed reactors. In the NSR technology, the state of the system is constantly changing so that performance depends on when it is measured. Therefore in studies at PNNL, we obtain NOx removal efficiencies as "lean conversion (30 minutes)," which measures NOx removal efficiencies for the first 30 minutes of a lean period that follows multiple lean-rich cycles to insure consistent behavior. We have established a reaction protocol, which evaluates the performance of samples after various thermal aging and sulfation condition. In this way, we could identify optimum de-sulfation treatments to rejuvenate catalyst activities.

Based on formulations and synthesis procedures described in the literature, PNNL has prepared model NSR and NH_3 SCR catalysts. Activity and performance stability measurements were performed. State-of-the-art catalyst characterization techniques and temperature programmed desorption/reaction (TPD/TPR) were utilized to probe the changes in physicochemical properties of the PNNL-prepared model catalyst samples under deactivating conditions; *e.g.*, thermal aging and SO_2 treatment.

Results

High-Temperature NSR Catalysts Prepared by PNNL

K-loading studies of Pt-K/$MgAl_2O_4$: We have studied various characteristics of Pt$K/MgAl_2O_4$ LNT catalysts including the effect of K loading on nitrate formation/decomposition, NOx storage activity, and durability [3]. Upon the adsorption of NO_2 on $K/MgAl_2O_4$ samples, potassium nitrates, formed at Mg-related sites on the $MgAl_2O_4$ support material surface, are observed in addition to the two (ionic and bidentate) potassium nitrate species observed to form on Al_2O_3-supported samples. Based on NO_2 TPD and Fourier transform infrared results, the Mg-bound KNO_3 species thermally decompose at higher temperatures than Al-bound KNO_3, implying its superior thermal stability. At a potassium loading of 5 wt% on $MgAl_2O_4$, the temperature of maximum NOx uptake (T_{max}) is 300ºC (Figure 1). Increasing the potassium loading from 5 wt% to 10 wt% results in a monotonic shift in the T_{max} to 450ºC, demonstrating an unexpectedly significant dependence of T_{max} on the potassium loading. Further increases in potassium loading above 10 wt%, however, only give rise to a reduction in the overall NOx storage capacity. This dependence on K-loading on $MgAl_2O_4$ support materials is qualitatively similar to our recent observations on Al_2O_3-supported K-based LNT catalysts [4-6]. It remains a significant research challenge to explain this unusual loading dependence. For the Al_2O_3-supported Kbased LNT catalysts, moderate K loadings of 10% were found to provide an optimum balance between KNO_3 stability and the availability of exposed Pt sites, thereby exhibiting the best NOx uptake capacity. Thus Pt-K/Al_2O_3 catalysts with 10% K loading were chosen for detailed studies of thermal stability in these candidate LNT materials.

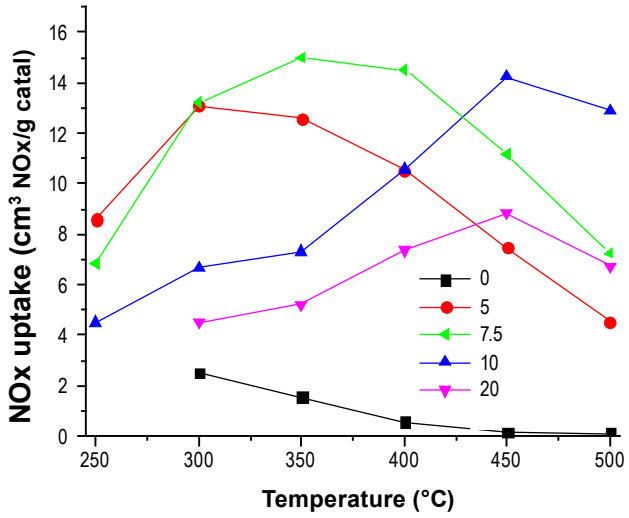

FIGURE 1. The amount of NOx uptake with respect to temperature over Pt-K(x)/$MgAl_2O_4$ (x=0, 5, 10 and 20 wt%) catalysts.

Thermal deactivation of Pt-K/Al_2O_3: Thermal aging at 800ºC severely deactivates the Pt/K/Al_2O_3 catalysts due to Pt sintering; compare the black (fresh) and red (aged) curves shown in Figure 2 [6]. Interestingly, a reduction treatment of the aged catalyst is able recover up to half of the NOx storage capacity of the fresh catalyst at 400ºC and above as shown by the blue curve in Figure 2. Using both XRD and transmission electron microscopy, we determined that a modest fraction of Pt species sinter to form large metallic Pt particles during thermal aging of $K/Pt/Al_2O_3$ catalysts, whereas a significant amount of Pt strongly interacts with K and stays finely dispersed. Upon reduction, these Pt species can be re-activated, resulting in the partial recovery of NOx storage capacity as demonstrated in Figure 2. This behavior differs significantly from similar Pt/Al_2O_3 catalysts, where similar oxidation/reduction treatments result in very large Pt particles that give generally poor performance.

Synthesis of Model Cu-CHA Zeolite Catalysts at PNNL

SCR catalysts with the best performance (activity, hydrothermal stability, etc.) are CHA zeolite materials, with Cu/SSZ-13 and Cu/SAPO-34 being two specific

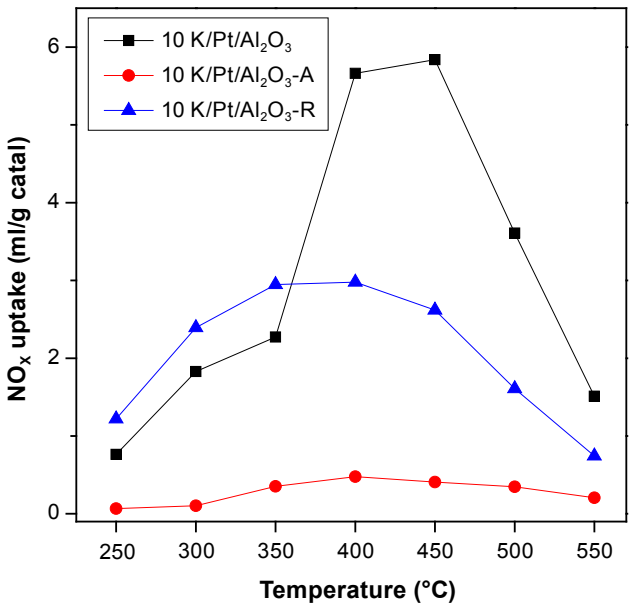

FIGURE 2. NOx uptake as a function of temperature on Pt-K(10)/Al_3O_3 samples after various treatments: freshly prepared (black squares); after oxidation at 800ºC for 4 h in air (red circles); and after reduction in 4% H_2/He at 800ºC for 1 h (blue triangles).

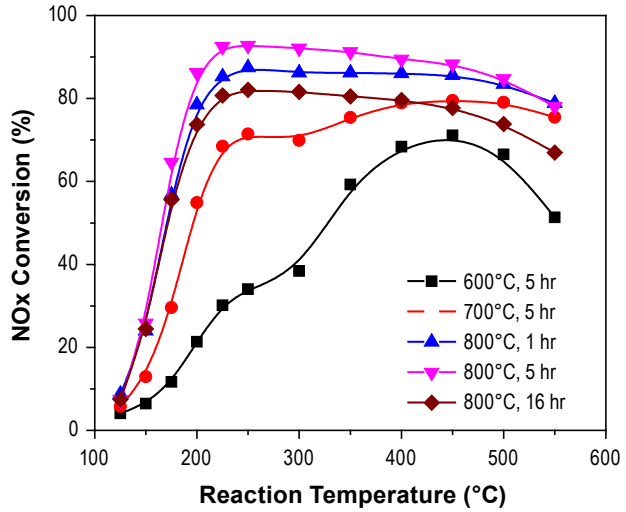

FIGURE 3. NOx conversions of solid state ion exchange Cu (1.2%)/SAPO-34 catalysts after various calcination conditions.

examples. While the synthesis of Cu/SSZ-13 is rather straightforward, Cu/SAPO-34 preparation is significantly more complicated. For example, SAPO-34 is prone to hydrolysis in both acidic and basic solutions; therefore, care must be taken during solution ion exchange. In our recent studies [7], we have systematically investigated two commonly used Cu/SAPO-34 preparation methods; i.e., solution ion exchange and solid state ion exchange using SAPO-34 substrates generated with various structure directing agents including tetraethyl ammonium hydroxide, triethyl amine, diethyl amine, morpholine, and their mixtures. NH_3-SCR reaction studies, coupled with various catalyst characterizations allow us to elucidate the key factors in obtaining highly active and selective catalysts. For example, Figure 3 displays NOx conversions as a function of reaction temperature for a series of solid state ion exchange catalysts with the same Cu loading (1.2 wt%) but calcined at different temperatures. We find that a calcination temperature of 800ºC is needed for complete solid state ion exchange.

Conclusions

PNNL and its CRADA partners from Cummins Inc. and Johnson Matthey have been carrying out a CRADA project aimed at improving the higher temperature performance and stability of candidate NOx reduction technologies. Results obtained this year demonstrate that a $MgAl_2O_4$ support material provided especially promising NOx uptake performance. When K is used as storage element on this support, we show that an optimum K loading is 10%. Additionally, K seems to play a role in stabilizing the precious metal, Pt, towards sintering under high-temperature oxidizing conditions. Finally, we have also recently initiated studies of CHA zeolite-based SCR catalysts. Our first experiments are aimed at preparation of model Cu/SAPO34 catalysts where we find that a solid-state synthesis method provides a useful approach for realizing reproducible and active SCR catalysts.

References

1. Kwak, J.H.; Tran, D.; Burton, S.D.; Szanyi, J.; Lee, J.H., Peden, C.H.F. J. Catal., 287 203-209 (2012).

2. W.S. Epling, L.E. Campbell, A. Yezerets, A., N.W. Currier, J.E. Parks, *Catalysis. Review.–Science and Engineering* 46 (2004) 163.

3. D.H. Kim, K. Mudiyanselage, J. Szanyi, H. Zhu, J.H. Kwak, C.H.F. Peden, "Characteristics of Pt-$MgAl_2O_4$ Lean NO_x Trap Catalysts." *Catalysis Today* 184 (2012) 2-7.

4. D.H. Kim, K. Mudiyanselage, J. Szanyi, J.H. Kwak, H. Zhu, C.H.F. Peden, "Effect of K Loading on Nitrate Formation/Decomposition on and NOx Storage Performance of $PtK_2O/\gamma Al_2O_3$ NOx Storage-Reduction Catalysts," *Applied Catalysis B* (2013) submitted for publication.

5. G.G. Muntean, M. Devarakonda, F. Gao, J.H. Kwak, J.Y. Luo, C.H.F. Peden, M.L. Stewart, J. Szanyi, D.N. Tran, "CLEERS Aftertreatment Modeling and Analysis," in *Advanced Combustion Engine Research and Development: FY2012 Progress Report*, in press.

6. J.Y. Luo, F. Gao, C.H.F. Peden, "Effects of potassium loading and thermal aging on $K/Pt/Al_2O_3$ high-temperature lean NO_x trap catalysts", *Applied Catalysis B*, submitted for publication.

7. F. Gao, E.D. Walter, S.D. Burton, N.M. Washton, I. Arslan, J.H. Kwak, J. Szanyi, C.H.F. Peden, abstract submitted to the 23rd Meeting of the North American Catalysis Society.

FY 2012 Publications/Presentations

1. D.H. Kim, J.H. Kwak, J. Szanyi, C.H.F. Peden, "Isothermal desulfation of pre-sulfated Pt-BaO/γ-Al_2O_3 lean NO_x trap catalysts with H_2: the effect of H_2 concentration and the roles of CO_2 and H_2O." *Applied Catalysis B* 111-112 (2012) 342-348.

2. D.H. Kim, X.Q. Wang, G.G. Muntean, C.H.F. Peden, K. Howden, N. Currier, J. Li, R.J. Stafford, A. Yezerets, H.-Y. Chen and H. Hess, "Enhanced High Temperature Performance of NOx Storage/Reduction (NSR) Materials" in *Advanced Combustion Engine Research and Development: FY2011 Annual Progress Report*, 182-187.

3. D.H. Kim, K. Mudiyanselage, J. Szanyi, H. Zhu, J.H. Kwak, C.H.F. Peden, "Characteristics of Pt-$MgAl_2O_4$ Lean NO_x Trap Catalysts." *Catalysis Today* 184 (2012) 2-7.

4. D.H. Kim, A. Yezerets, N. Currier, J. Li, H.-Y. Chen, H. Hess, M.H. Engelhard, G.G. Muntean, C.H.F. Peden, "Effect of sulfur loading on the desulfation chemistry over a commercial lean NOx trap catalyst." *Catalysis Today* **197** (2012) 3-8.

5. J.K. Jeon, H. Kim, Y.K. Park, C.H.F. Peden, D.H. Kim, "Regeneration of field-spent activated carbon catalysts for low-temperature selective catalytic reduction of NOx with NH_3," *Chemical Engineering Journal* **174** (2011) 242-248.

6. J.Y. Luo, F. Gao, C.H.F. Peden, "Effects of potassium loading and thermal aging on $K/Pt/Al_2O_3$ high-temperature lean NO_x trap catalysts", *Applied Catalysis B*, submitted for publication.

7. D. H. Kim, G.G. Muntean, C.H.F. Peden, N. Currier, J. Li, R. Stafford, A. Yezerets, H.Y. Chen, H. Hess, "Enhanced High Temperature Performance of NOx Storage/Reduction (NSR) Materials", presentation at the DOE Combustion and Emission Control Review, Washington DC, May 2012.

8. D.H. Kim, K. Mudiyanselage, J. Szanyi, J.H. Kwak, C.H.F. Peden, "Water-induced morphology changes in KNO_3 formed on K_2O/gamma-Al_2O_3 NOx storage materials: in situ FTIR and TR-XRD study," presentation at the 15th International Congress on Catalysis, Munich, Germany, July 2012.

III.3 Emissions Control for Lean Gasoline Engines

Todd J. Toops (Primary Contact), Josh A. Pihl, and James E. Parks
Oak Ridge National Laboratory (ORNL)
2360 Cherahala Boulevard
Knoxville, TN 37932

DOE Technology Development Manager:
Ken Howden

Overall Objectives

- Assess and characterize catalytic emission control technologies for lean gasoline engines.
- Identify strategies for reducing the costs, improving the performance, and minimizing the fuel penalty associated with emission controls for lean gasoline engines.

Fiscal Year (FY) 2012 Objectives

- Install a lean gasoline engine on an engine dynamometer to establish an engine research platform for the project.
- Evaluate the feasibility of a passive SCR approach for various three-way catalyst (TWC) formulations on a flow reactor.

Accomplishments

- Determined the effect of lean-rich timing on a commercial lean-NOx trap (LNT) as it impacts lean oxides of nitrogen (NOx) reduction as well as NH_3 and N_2O production.
- Evaluated a series of catalyst formulations and demonstrated impact of platinum-grade metal (PGM) content on NH_3 production as a function of temperature and air/fuel ratio (AFR).
- Demonstrated high NOx conversion with a TWC/selective catalytic reduction (SCR) passive SCR setup under lean/rich cyclic operation on a flow reactor.
- Characterized the control of a representative lean gasoline engine vehicle (European BMW 120i) and installed that engine with a custom controller in an engine dynamometer laboratory to establish a research platform for on-engine studies.

Future Directions

- Continue evaluation of TWC formulations for NH_3 generation, especially ones that have NOx storage component included.
- Conduct studies on the lean gasoline engine research platform to understand real exhaust effects on processes observed in flow reactor studies (with simulated exhaust mixtures).
- Determine catalytic NH_3 production viability under rich engine operation for SCR reactions.

Introduction

Currently, the U.S. passenger car market is dominated by gasoline engine powertrains that operate at stoichiometric AFRs (sufficient fuel is mixed in air such that all of the oxygen in the air is consumed during combustion). Stoichiometric combustion leads to exhaust conditions suitable for TWC technology to reduce NOx, CO, and hydrocarbon emissions to extremely low levels. Operating gasoline engines at lean AFRs (excess air) enables more efficient engine operation and reduces fuel consumption; however, the resulting oxygen in the exhaust prevents the TWC technology from working. It is relatively straightforward to operate an engine lean over a significant portion of the load and speed operating range; so, the largest challenge preventing fuel-saving lean combustion in gasoline applications is the control of emissions, primarily NOx. This project addresses the challenge of reducing emissions from fuel-saving lean gasoline engines in a cost effective and fuel efficient manner to enable their market introduction.

Approach

This project will utilize the full suite of capabilities available at ORNL's Fuels, Engines, and Emissions Research Center, including: a lean gasoline engine on an engine dynamometer, a vehicle equipped with the same engine on a chassis dynamometer, flow reactors for detailed catalyst evaluations under carefully controlled operating conditions, and vehicle system level modeling. The engine platform and vehicle have been obtained and work is underway to develop autonomous control over the engine. While efforts to develop this experimental platform are ongoing, research has continued on a flow reactor with gas mixtures simulating lean gasoline engine exhaust.

The lean gasoline vehicle that we obtained employs a LNT for NOx reduction. The LNT operates by adsorbing NOx during lean (excess oxygen) operation, and then releasing and reducing the NOx to N_2 during rich (excess fuel) operation. Although this engine and aftertreatment combination met the 2009 emissions regulations in Europe, as configured it does not meet the current U.S. emissions standards. LNTs have, however, been successfully deployed in the U.S. on vehicles powered by diesel engines. There are two primary characteristics of lean gasoline engine exhaust that make it more challenging for LNTs than diesel exhaust: high temperatures and high NOx concentrations (in excess of 1,000 ppm). High temperatures reduce the NOx storage capacity, and high NOx concentrations saturate the storage capacity more quickly. The combination of lower storage capacity and higher inlet NOx requires more frequent LNT regeneration events, increasing the fuel penalty associated with LNT operation. Efforts on LNT technology are focused on understanding the limitations and challenges of this technology in the lean gasoline application; in particular, with respect to reducing NOx at high temperature and with high NOx concentrations.

In diesel applications, the most common emissions control system for NOx reduction is NH_3-based SCR using a Cu-zeolite catalyst and a urea solution as the source of NH_3. While this approach has been demonstrated to be durable with very high NOx conversions over a wide temperature window for diesel applications, there are several factors that suggest this approach will not be viable in the U.S. for lean gasoline vehicles. The primary concerns are associated with cost of the urea injection system, high urea consumption (which scales with NOx concentration), and infrastructure limitations. Therefore, our study is investigating alternative onboard NH_3 generation techniques employing both LNTs and TWCs. This approach can eliminate the costs and complexity of NH_3 delivery via urea systems while still taking advantage of the durable and active commercial SCR catalysts. The key to the approach is to generate NH_3 over the TWC/LNT under rich conditions and then store it on a downstream SCR. When returning lean operation, the stored NH_3 reduces NOx that is not converted over the TWC/LNT. A major consideration with this approach is to minimize additional costs associated with PGM in LNTs and TWCs and thus target similar levels of PGM content as in stoichiometric gasoline applications.

This report highlights results from flow reactor experiments in FY 2012 focused on understanding NH_3-generation behavior over a series of TWCs and LNT formulations. In particular, we sought to determine at what temperatures NH_3 could be generated under rich conditions and while cycling between lean and rich conditions. Additionally, the SCR chemistry was studied for two formulations with a particular emphasis on NH_3 storage capacity and NOx reduction performance. Finally, a demonstration of the potential of the approach was performed using a flow reactor system that could simulate a close-coupled TWC with an underfloor SCR.

Results

Data from operation of the BMW LNT for 60 seconds lean and either 5, 10 or 15 seconds rich on the flow reactor is shown in Figure 1. The rich reductant concentrations were adjusted to have the same fuel penalty for each case, i.e. the reductant concentrations were a factor of three lower for the 15 seconds rich time than for the 5 seconds rich time. The results illustrate that high NOx conversion can be achieved between 300 and 450°C (Figure 1a). Depending on the rich timing, up to 45% of the NOx stored under lean conditions can be converted to NH_3 (Figure 1b). Unfortunately, under these same conditions there is a 6-9% yield of N_2O (Figure 1c), averaging 30-45 ppm N_2O over the entire cycle. This is a significant concern due to upcoming greenhouse gas regulations and suggests a typical LNT mode of operation will not be sufficient for this application.

From these initial LNT efforts, the project began evaluation of NH_3 generation over TWCs. Four formulations were investigated, three of which were taken from a state-of-the-art dual-zone TWC. The front portion of the TWC contained only Pd (with no Pt or Rh) and did not contain ceria (designated Pd-only); the rear portion was a Pd/Rh formulation with significant ceria content (Pd/Rh+Ce). These two compositions were evaluated individually and as a combined material as originally designed (combo). Additionally, the BMW LNT was evaluated as if it were a TWC; it contained Pt/Rh with ceria and barium (Pt/Rh+Ce+Ba). To evaluate the NH_3 production on these four formulations, the catalyst cores were evaluated at inlet temperatures ranging from 200-550°C (corresponding to 350-750°C midbed temperatures), and gas concentrations that replicated AFRs of 14.0-14.8. To achieve these AFRs in the flow reactor, O_2 concentrations were varied from 0.79% to 1.65% while the other reactants were fixed at 1,200 ppm NO, 1.8% CO, 6,000 ppm H_2, and 1,000 ppm C_3H_6. Figure 2 shows how the catalyst outlet composition varied with AFR. At stoichiometric conditions (~1.54% O_2), there is essentially 100% conversion of all reactants as expected. Increasing the O_2 content, i.e. AFR, as little as 0.1% results in a significant breakthrough of NO and N_2O, with the Pd-Only TWC (Figure 2a) having significantly more slip than the Pd/Rh+Ce TWC (Figure 2b). Under rich conditions, significant NH_3 is generated from the fed NOx for all four catalysts; in fact, the Pd-only TWC converts 100% of the NOx to NH_3 at a steady-state AFR of 14.3 (1.25% O_2).

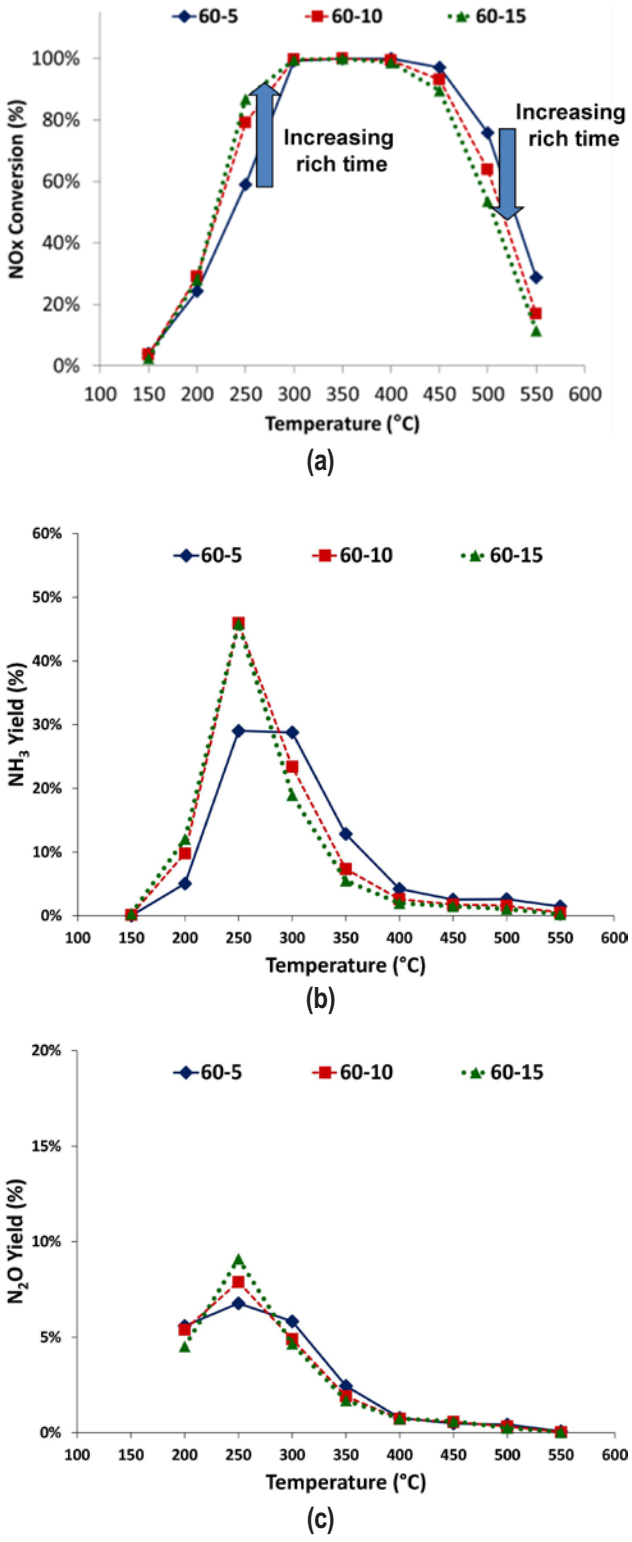

FIGURE 1. (a) NOx conversion, (b) NH_3 yield and (c) N_2O yield for the BMW LNT at 30,000 h^{-1} gas hourly space velocity (GHSV) while cycling for 60 s lean (10% O_2, 500 ppm NO) and either 5 s (2.0% CO, 0.67% H_2, 0.11% C_3H_6), 10 s (1.0% CO, 0.34% H_2, 0.056% C_3H_6) or 15 s (0.67% CO, 0.22% H_2, 0.037% C_3H_6) rich conditions (5% H_2O and 5% CO_2 flowing continuously).

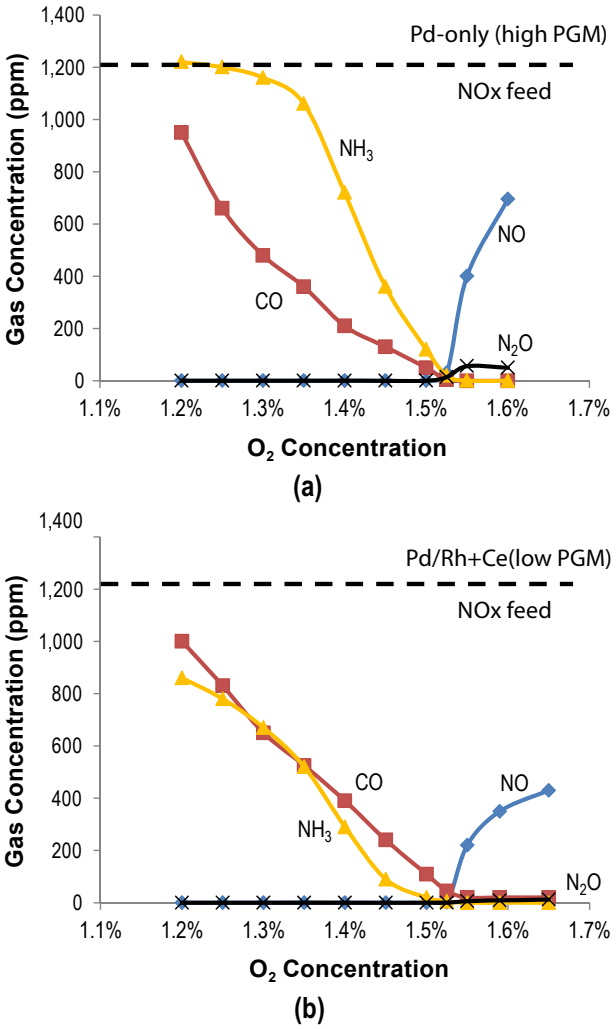

FIGURE 2. Evaluation of the ability of (a) a Pd-only TWC and (b) a Pd/Rh+Ce TWC to convert NOx into NH_3 as a function of O_2 concentration under steady-state conditions (non-cycling). Stoichiometric O_2 concentration is at ~1.54%, with 1.1% O_2 representing an AFR of ~14.2. Reactor conditions: 450-500°C, 75,000 h^{-1} GHSV, 1200 ppm NO, 1.8% CO, 6000 ppm H_2, 1000 ppm C_3H_6, variable O_2, 5% H_2O and 5% CO_2.

Figure 3 compares the four formulations over a range of relevant temperatures while holding the AFR constant at 14.0 (0.79% O_2). It highlights the NH_3 generation capability of the Pd-only TWC, while also illustrating that the addition of Rh decreases the NH_3 selectivity. Comparison to Figure 2b shows that the high temperature selectivity shifts from NH_3 to N_2 rather than slipped NOx or N_2O. Further investigations with the Pd-only TWC showed the interplay between catalyst temperature and AFR in determining NH_3 selectivity under rich operation (Figure 4). Relatively high AFRs can be used to generate NH_3 at low catalyst temperatures. As the TWC temperature is increased, richer conditions must be used to maintain high NH_3 selectivity.

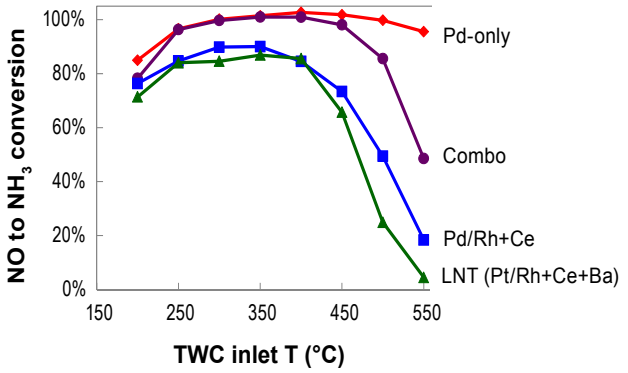

FIGURE 3. NH_3 production for the 4 catalyst formulations studied as a function of temperature. Results are shown for an AFR of ~14.0. Temperature shown is for TWC inlet; reactions over the TWC generated an exotherm of ~150-200°C, so NH_3 was produced at midbed temperatures in excess of 600°C. Reactor conditions: 75,000 h^{-1} GHSV, 1,200 ppm NO, 1.8% CO, 6,000 ppm H_2, 1,000 ppm C_3H_6, 0.79% O_2, 5% H_2O and 5% CO_2.

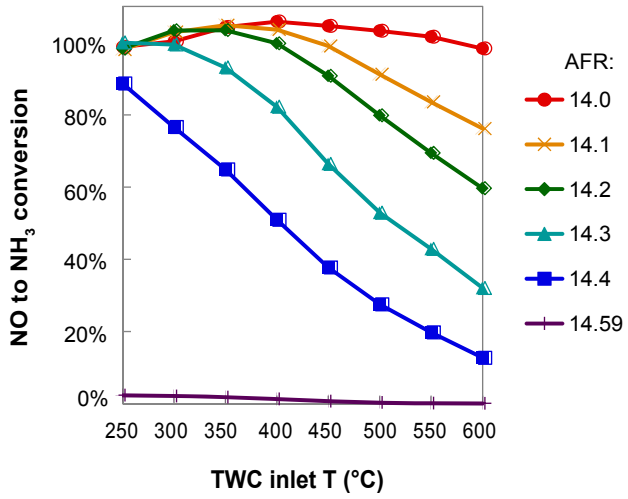

FIGURE 4. NH_3 production for the Pd-only TWC as a function of AFR and temperature. Reactor conditions: 75,000 h^{-1} GHSV, 1,200 ppm NO, 1.8% CO, 6,000 ppm H_2, 1,000 ppm C_3H_6, variable O_2, 5% H_2O and 5% CO_2.

For this approach to work there has to be synergy between NH_3 production over the TWC and NH_3 storage on the SCR. Figure 5a shows the distribution of temperatures observed in the close-coupled TWC and the underfloor catalyst during a Federal Test Procedure drive cycle. This histogram illustrates that the close-coupled catalyst operates within the temperatures where NH_3 is generated in Figures 2-4. Additionally, Figure 5a shows that the underfloor catalyst maintains a temperature between 175 and 375°C. Figure 5b shows the capacity of a Cu-zeolite SCR to store NH_3 under both lean (blue) and rich (red) conditions. A comparison between the two plots in Figure 5 reveals that an underfloor Cu-zeolite SCR catalyst should have significant NH_3 storage

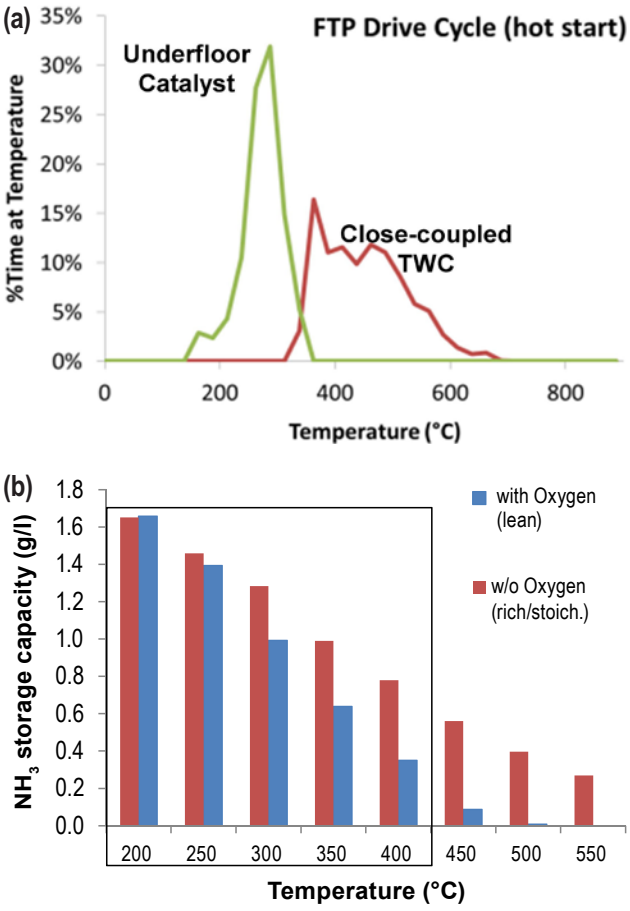

FIGURE 5. (a) Temperature histogram of a close-coupled catalyst and an underfloor catalyst during the FTP drive cycle of a lean gasoline vehicle. (b) NH_3 storage capacity under lean and rich conditions illustrating the potential synergy between the high temperature NH_3 production in the close-coupled catalyst and the low temperature storage in the underfloor catalyst.

capacity over most of the drive cycle. This synergy was further investigated using a two furnace approach that allows us to mimic the close-coupled and underfloor catalyst positions. The Pd-only TWC and a Cu-zeolite SCR were used for this experiment. The lean/rich timing was adjusted to optimize the NOx reduction while minimizing NH_3 slip. These preliminary results show a cycle averaged NOx reduction of more than 99.5% even with NOx inlet conditions in excess of 1,000 ppm (Figure 6). Minimal NH_3 and N_2O slip were observed.

Conclusions

ORNL has made significant progress toward establishing a lean gasoline engine research platform. In the meantime, we have utilized flow reactor experiments to demonstrate high conversion (up to 100%) of NOx to NH_3 over a TWC with moderately rich conditions (AFR~14) over a wide range of temperatures. This

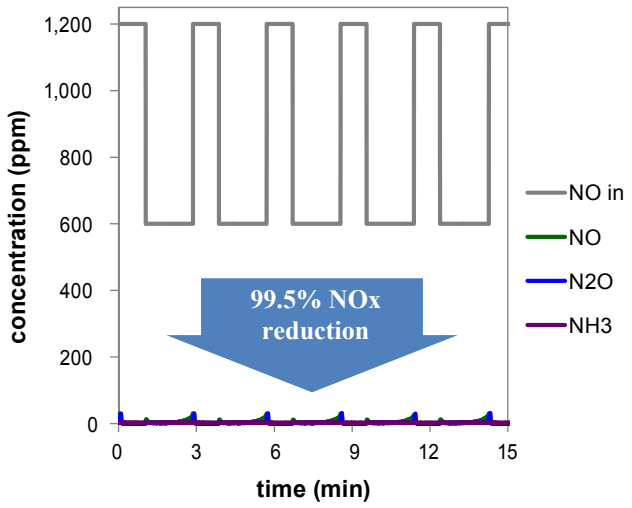

FIGURE 6. Illustration of the potential of the TWC+SCR technique using a two reactor system that mimics the two catalyst positions in a vehicle. Reactor conditions: TWC: 450°C inlet, 70,000 h^{-1} GHSV, SCR: 300°C, 28,000 h^{-1} GHSV; 60s rich: 1,200 ppm NO, 1.8% CO, 6,000 ppm H_2, 1,000 ppm C_3H_6, 0.79% O_2, 5% H_2O, 5% CO_2, AFR = 14; 110s lean: 500 ppm NO, 10% O_2, 5% H_2O, 5% CO_2, AFR ~24.

NH_3 can be stored on the underfloor SCR and used to reduce NOx during lean conditions. Depending on the temperature of the TWC and SCR catalysts, greater than 99.5% of the overall NOx produced can be removed with minimal N_2O production or NH_3 slip. Research efforts are ongoing with emphasis on reducing system costs and the fuel penalty associated with rich operation through alternative catalyst formulations, controlling CO emissions, and demonstrating the approach on a lean gasoline engine at ORNL.

FY 2012 Publications/Presentations

1. J.A. Pihl, J.A. Lewis, J.E. Parks, T.J. Toops, "Lean NOx Trap Chemistry under Lean-Gasoline Exhaust Conditions: Impact of High Temperature and High NOx Operation", submitted to Topics in Catalysis, May 2012.

2. T.J. Toops, J.A. Pihl, J.E. Parks, C.D. DiGiulio, M.D. Amiridis, "NH_3 generation over commercial Three-Way Catalysts and Lean-NOx Traps", 2012 Directions in Engine-Efficiency and Emissions Research Conference (DEER), Dearborn, MI, October 18, 2012.

3. C.D. DiGiulio, M.D. Amiridis, J.A. Pihl, J.E. Parks, T.J. Toops, "An investigation of in situ NH3 generation for use in a downstream NH_3-SCR catalyst", American Institute of Chemical Engineers 2012 Annual Meeting, Pittsburgh, PA, October 29, 2012.

4. T.J. Toops, J.E. Parks, J.A. Pihl, S. Huff, V. Prikhodko, "Emissions Control for Lean Gasoline Engines", 2012 DOE Annual Merit Review, Crystal City, VA, May 14–18, 2012.

5. J.A. Pihl, J.E. Parks, T.J. Toops, "Lean NOx Trap Chemistry under Lean-Gasoline Exhaust Conditions: Impact of High Temperature and High NOx Operation", 9th International Congress on Catalysis and Automotive Pollution Control (CAPoC9), August 29–31, 2012, Brussels, Belgium.

III.4 Cummins-ORNL SmartCatalyst CRADA: NOx Control and Measurement Technology for Heavy-Duty Diesel Engines

Bill Partridge[1] (Primary Contact), Neal Currier[2], Jae-Soon Choi[1], Josh Pihl[1], Jim Parks[1], Xavier Auvray[3], Louise Olsson[3], Krishna Kamasamudram[2], Alex Yezerets[2]

[1]Oak Ridge National Laboratory (ORNL)
2360 Cherahala Blvd.
Knoxville, TN 37932

[2]Cummins Inc., Columbus, IN

[3]Chalmers University of Technology, Göteborg, Sweden

DOE Technology Development Manager:
Ken Howden

Overall Objectives

- Understand the fundamental chemistry of automotive catalysts.
- Identify strategies for enabling self-diagnosing catalyst systems.
- Address critical barriers to market penetration.

Fiscal Year (FY) 2012 Objectives

- Develop improved understanding of NH_3 storage distributions and utilization.
- Investigate nature of dynamic NH_3 inhibition.
- Apply SpaciMS data to develop model of steady-state selective catalytic reduction (SCR) performance distributions.
- Identify basic and practical performance characteristics consistent with enabling self-diagnosing catalyst systems.

Accomplishments

- Advanced understanding of NH_3 utilization and its influencing parameters:
  - The maximum NH_3 capacity (determined by the inlet conditions) is used over the majority of the SCR zone; i.e., the front catalyst region over which SCR occurs.
  - The NH_3 capacity drops below the maximum at the SCR-zone back end.
  - There is zero utilized NH_3 capacity downstream of the SCR zone (assuming complete NH_3 conversion), because there is zero gas-phase NH_3 to utilize any available capacity.
  - These various capacity utilization zones are controlled by the adsorption isotherm, unique to a given catalyst formulation, and the gas-phase NH_3 concentration distribution imposed by the SCR reaction.
- Developed and participated in collaboration which developed a kinetic model of distributed SCR performance based on SpaciMS measurements:
  - Kinetic parameters in excellent agreement with independent literature values.
  - Kinetic model provides spatial performance predictions in good agreements with measurements for multiple temperature SCR conditions.
  - Demonstrates rich nature of SpaciMS data for kinetic data and model applications in addition to the other uniquely valuable insights highlighted elsewhere.
- Elucidated nature of SCR catalyst dynamic inhibition:
  - Dynamic inhibition appears to occur where surface-NH_3 buildup is high; e.g., at the front of the catalyst where NH_3 concentration is high, and/or when SCR is slow allowing high NH_3 concentrations to exist deeper into the catalyst.
  - Inhibited steady-state SCR conditions can be accessed without passing through a conversion inflection indicative of obvious dynamic inhibition; apparently depending on the relative rate of surface-NH_3 buildup.
- In collaboration with Professor Louise Olsson at Chalmers University of Technology, Master student Filipa Coelho modeled the spatially distributed intra-SCR performance measured previously in this Cooperative Research and Development Agreement (CRADA).
- In collaboration with Professors Enrico Tronconi and Isabella Nova of the Politecnico di Milano started effort to investigate fundamental reactions relevant to SCR performance; as part of this collaboration Politecnico di Milano PhD student Maria Pia Ruggeri is spending six months at ORNL as a Visiting Student Researcher focused on this effort.
- Worked in collaboration with the Cross-Cut Lean Exhaust Emissions Reduction Simulations group and the Institute of Chemical Technology, Prague (ICTP)

to identify N_2O formation pathways in lean-NO_x trap catalysts; hosted visiting scientist Dr. Petr Kočí, and ICTP PhD student Šárka Bártová.

Future Directions

Quantify spatiotemporal performance of a commercial Cummins SCR catalyst under degreened and field aged conditions.

Introduction

A combination of improved technologies for engine and aftertreatment control of oxides of nitrogen (NO_x) and particulate emissions are required to efficiently meet increasingly stringent emission regulations. This CRADA section focuses on catalyst technologies, while a parallel section (Characterization and Reduction of Combustion Variations) focuses on combustion and engine technologies. Improved catalyst-system efficiency, durability and cost can be achieved through advanced control methodologies based on continuous catalyst-state monitoring; the overarching goal of this CRADA section is to enable self-diagnosing or smart catalyst systems. Self-diagnosing catalyst technologies are enabled by basic and practical insights into the transient distributed nature of catalyst performance, improved catalyst models, insights suggesting control methodologies, and instrumentation to demonstrate and drive advanced control technologies. These catalysis advances require development and application of enhanced diagnostic tools to realize these technology improvements. While the CRADA has a strong diagnostic focus, it is involved, often through synergistic partnerships, in the other enabling research activities discussed above.

Approach

The CRADA applies the historically successful approach of developing and applying minimally invasive advanced diagnostic tools to resolve spatial and temporal variations within operating engines and catalysts. Diagnostics are developed and demonstrated on bench reactors and engine systems (as appropriate) at ORNL prior to field application at Cummins. In some cases discrete-sensor technology is a stepping stone and may be further developed and integrated in system components; e.g., to create self-diagnosing smart catalyst systems.

Diagnostics are applied at ORNL and Cummins to study the detailed nature and origins of catalyst performance variations; this may be spatial and temporal variations unique to each catalyst function (e.g., SCR, NH_3 storage and parasitic oxidation, NO_x storage and reduction, oxygen storage capacity, water-gas shift) during operating and how these vary with ageing (e.g., thermal, hydrocarbon, sulfur). This detailed information is applied to understand how catalysts function and degrade, develop device and system models, and develop advanced control strategies.

Results

New catalyst insights resulting from the CRADA research were published regarding spatially distributed NH_3 utilization and inhibition in a Cu-Beta zeolite SCR catalyst. Specifically, the NH_3 capacity is effectively saturated over the major SCR zone, or major region of the catalyst used for SCR. Furthermore, spatially distributed dynamic inhibition was demonstrated for the first time for this catalyst type, and its nature was interpreted in the context of the other distributed catalyst parameters allowing several observations relative to dynamic inhibition. Dynamic inhibition conversion inflections are due to suitably fast NH_3 coverage buildup and thus occur to a greater extent at the catalyst front where high gas-phase NH_3 concentrations drive fast coverage buildup; dynamic inhibition is apparent at low-conversion (e.g., 200°C) conditions because high NH_3 survives deeper into the catalyst where measurements were made; dynamic inhibition is predicted to exist at the higher-conversion higher temperature conditions studied, but very close to the catalyst inlet where conversion gradients are high; and, a steady-state inhibited condition can be accessed without transitioning through a conversion inflection if the coverage buildup rate is suitably slow. These new insights have fundamental and practical relevance including enabling improved catalyst models, design tools, control and onboard diaganostic strategies, and are thus supportive of the DOE objectives for improved efficiency and durability.

Further analysis of the published SCR data focused on understanding the nature of incomplete capacity utilization at the SCR-zone back end. This analysis uses the terms total capacity, TC, and dynamic capacity, DC. Total capacity is the fractional NH_3 coverage at the catalyst temperature and inlet NH_3 concentration, and represents the maximum NH_3 coverage throughout the catalyst at those conditions. The DC is the local NH_3 coverage under SCR conditions; DC cannot be greater than TC, and any difference in TC and DC represents unused capacity, UC. The basic conclusion of the published CRADA research is that DC is maximized (equal to TC) over the major portion of the SCR zone, or spatial catalyst region where the SCR reaction occurs. Figure 1 shows the published spatial performance data for the model Cu-Beta zeolite SCR catalyst at 200 and 325°C, and highlights the Major SCR Zone where NH_3

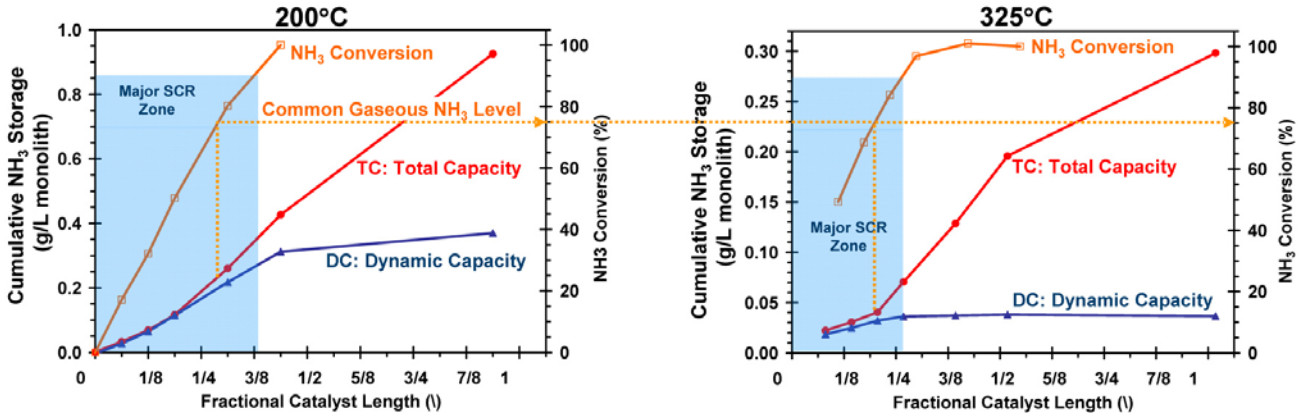

FIGURE 1. Spatially distributed performance of the Cu-Beta Zeolite SCR catalyst, under standard SCR conditions and at 200 and 325°C. The DC drops below the TC at the back of the SCR zone. And despite the notable differences in spatial performance at the two temperatures, the DC-TC split occurs at a common gaseous NH_3 level.

is primarily consumed, and the spatially distributed TC and DC profiles. As reported, the NH_3 coverage is maximized (DC=TC) for these conditions at the front of the major SCR zone, DC drops below the TC at the SCR-zone back, and is zero downstream of the SCR zone where NH_3 is fully consumed. Despite the major differences in spatially distributed performance at these two temperatures, it is apparent that the DC-TC split (point where DC drops below TC) occurs at a common gaseous NH_3 concentration; which happens to be ca. 50 ppm NH_3 for this catalyst. Such commonality in the distributed NH_3 coverage nature is also apparent in the spatial performance of the commercial 2010 Cummins Inc. Cu-SAPO 34 SCR catalyst based on data from a separate DOE-funded catalyst project; this project was led by Gordon Parker at Michigan Tech University, and Josh Pihl at ORNL, and the CRADA team is grateful for the opportunity to incorporate this data in the analysis. Figures 2A and 2B show the spatially distributed performance for the commercial 2010 Cummins Inc. catalyst at three temperatures and under standard and fast SCR conditions, respectively. Notably, despite the profound spatial performance differences between these various conditions, the DC-TC split occurs at a common gaseous NH_3 concentration for both standard and fast SCR reaction, and for all temperatures; for this catalyst the split occurs at ca. 175 ppm NH_3. Indeed, this is a unique case where standard and fast SCR are similar. This overriding commonality indicates the distributed NH_3 coverage utilization is independent of the specific SCR reaction and temperature, and suggests it is controlled by a catalyst-unique adsorption isotherm, and that the NH_3 coverage equilibrium reactions are much faster than even the fast SCR reaction. The catalyst-specific nature of the adsorption isotherm accounts for the differing NH_3 concentration at the DC-TC split for the model Cu-Beta zeolite and commercial SCR catalysts.

An adsorption isotherm indicates the equilibrium NH_3-coverage variation with gaseous NH_3 concentration, and its general shape can explain the general DC spatial trends observed for the model and commercial catalysts. Figure 3 shows a simple single-site Langmuir isotherm fit to measured TC values for the commercial 2010 Cummins Inc. SCR catalyst; furthermore, no coverage-dependence is assumed. The NH_3 coverage is zero at zero NH_3, such as exists at the catalyst outlet and any point within the catalyst downstream of the SCR zone, and has an increasingly greater value at higher NH_3 concentrations, such as exist closer to the catalyst inlet; thus, moving from catalyst front to back through the SCR zone corresponds to moving from right to left in Figure 3. Near the catalyst front where NH_3 is high, the coverage variation is relatively flat and thus DC is practically equal to TC in this region; the horizontal black line in Figure 3 indicates the TC at 200°C, and the arrow indicates the UC (or the difference between TC and DC). Although the isotherm indicates that DC must actually be less than TC for moving into the SCR zone and any NH_3 conversion, there is a region of the catalyst where these capacity values are practically equal as indicated by the green box arrow in Figure 3; e.g., because of the low coverage gradients, and practical measurement limitations. There is a distinct change in the coverage gradient at the isotherm knee, which should generally correspond to the DC-TC separation point. The SCR-zone back, where NH_3 concentrations are approaching zero, corresponds to the high-gradient region of the isotherm causing the DC and TC to further separate as indicated by the purple box arrow in Figure 3. The shape of the adsorption isotherm is dictated by the nature of the specific catalyst; e.g., number and type of NH_3 sites, coverage dependence, etc. Thus, the model and commercial catalyst have differing NH_3 concentrations corresponding to the adsorption-isotherm knee, or DC-TC separation point; similarly, the

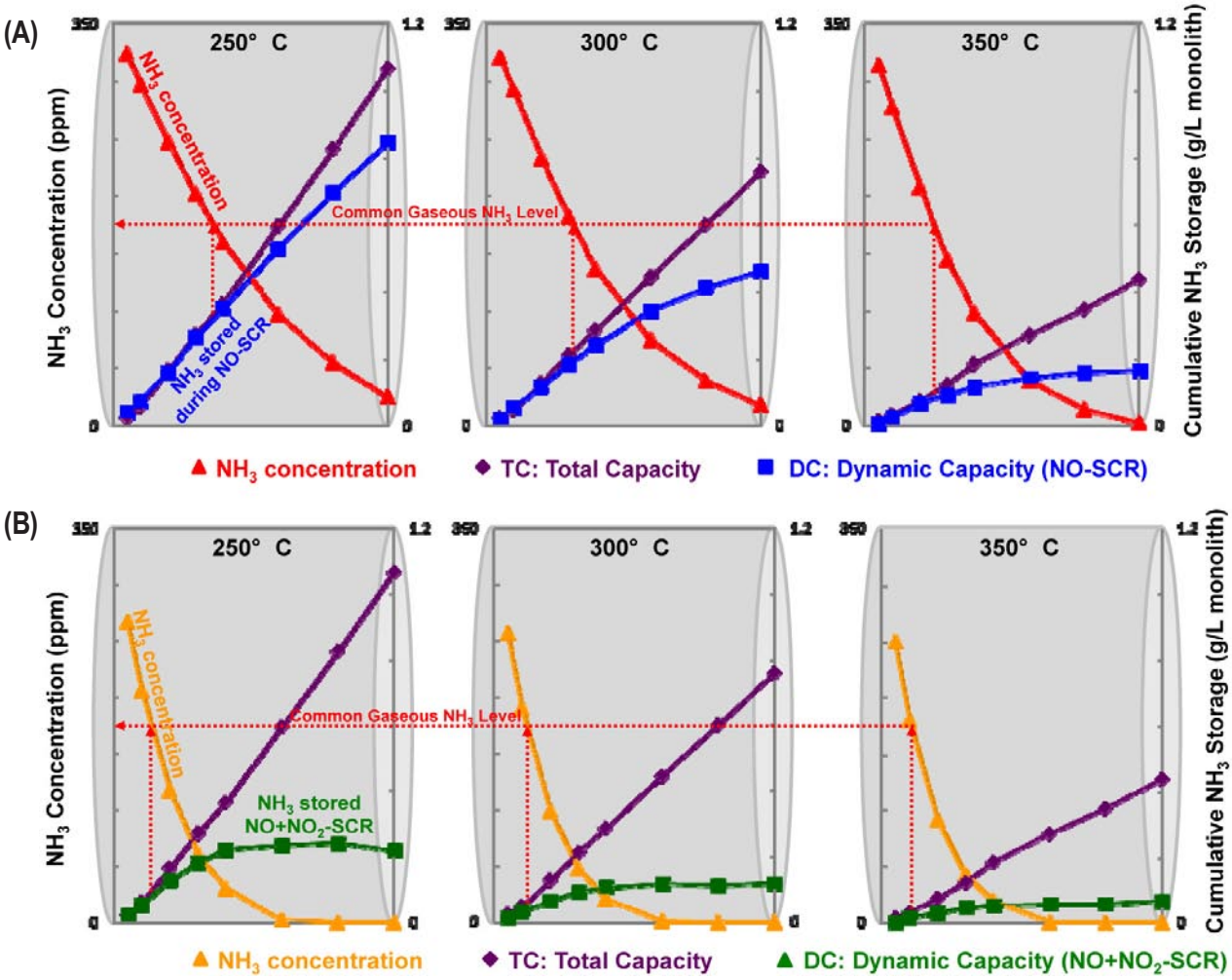

FIGURE 2. Spatially distributed performance of a commercial 2010 Cummins Inc. Cu-SAPO 34 SCR catalyst, under standard (A) and fast (B) SCR conditions and at 250, 300 and 350°C. The DC-TC split occurs at a common gaseous NH_3 level for both Standard & Fast SCR conditions. (This data is from Josh Pihl at ORNL and resulted from the DOE-funded Michigan Tech. University Heavy-Duty Emissions Control project, Gordon Parker PI. The analysis presented here was jointly supported by the Cummins CRADA and MITech projects.)

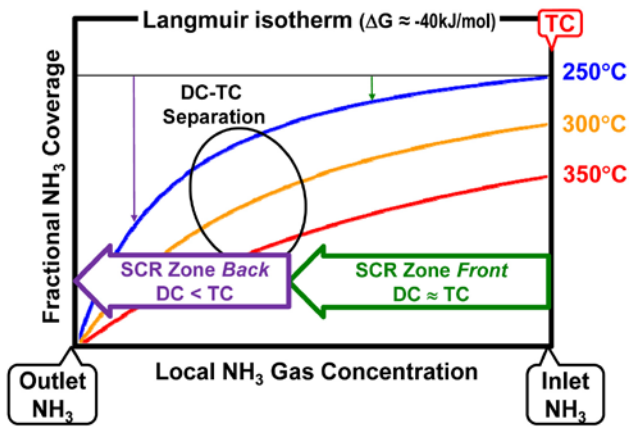

FIGURE 3. Simple single-site Langmuir isotherm fit to measured TC values for the commercial 2010 Cummins Inc. SCR catalyst.

DC-TC separation point is at a common value for the commercial catalyst under different SCR reactions and temperatures. The specific SCR reaction (e.g., standard vs. fast) does not change the adsorption isotherm, but rather only changes the catalyst spatial zones over which the three regions highlighted in Figure 3 exist. Specifically, the specific temperature and SCR reaction can spatially stretch or compress the various zones within the catalyst, but not change the underlying nature of the isotherm controlling the local NH_3 coverage. More generally, the specific temperature and SCR reaction mechanism modify the spatial gaseous NH_3 profile along the catalyst axis, which in turn dictates the local coverage via the adsorption isotherm. The general NH_3 coverage trends in Figure 2A are consistent with coverage estimates resulting from applying the Figure 2A NH_3 concentration distributions to the simple single-site

Langmuir isotherm of Figure 3. The actual isotherm is more complex, and presumably a more rigorous storage model would more fully capture the distributed-coverage behavior.

Conclusions

- The NH_3 capacity utilization is maximized over the major SCR zone.
- NH_3 capacity distribution is dictated by the catalyst-specific adsorption isotherm and the gas-phase NH_3 gradient imposed by the distributed SCR reaction:
  - DC-TC separation occurs at the adsorption isotherm knee.
- NH_3 coverage equilibrium reactions are much faster than even the fast SCR reaction.
- Dynamic inhibition is driven by high coverage buildup rates.
- Inhibited steady-state conditions can be accessed without transitioning through a dynamic inhibition conversion inflection.
- SpaciMS data provides rich foundation for kinetic model development:
  - Excellent agreement of resulting kinetic parameters with literature.
  - Excellent intra-catalyst spatial performance of model results.

FY 2012 Publications/Presentations

Archival Publications:

1. Xavier Auvray, William P. Partridge, Jae-Soon Choi, Josh A. Pihl, Aleksey Yezerets, Krishna Kamasamudram, Neal W. Currier, Louise Olsson (2012). "Local ammonia storage and ammonia inhibition in a monolithic copper-beta zeolite SCR catalyst," Applied Catalysis B: Environmental 126, 144–152; http://dx.doi.org/10.1016/j.apcatb.2012.07.019.

Oral Presentations (four Poster Presentations):

1. Petr Koci, Sarka Bartova, Milos Marek, Josh Pihl, Jae-Soon Choi, William Partridge, "Modelling of N_2O Formation During the Regeneration of NO_x Storage Catalysts," MODEGAT II (2nd International Symposium on Modeling of Exhaust-Gas After-Treatment), Bad Herrenalb/ Kalrsruhe, Germany, September 19, 2011.

2. Jae-Soon Choi, Bill Partridge, Josh Pihl, Petr Koci, Miyoung Kim, Stuart Daw, "Spatiotemporal Distribution of NO_x Storage: a Factor Controlling NH_3 and N_2O Selectivities over a Commercial LNT Catalyst," Environmental Catalysis Session, 17th DEER Conference, Detroit, Michigan, October 5, 2011.

3. Petr Kočí, Šárka Bártová, Miloš Marek, Josh A. Pihl, Mi-Young Kim, Jae-Soon Choi, William P. Partridge. "N_2O Formation Pathways During the Regeneration of Lean NO_x Trap," SAE World Congress, Emissions/Environment/ Sustainability Gaseous Engine Emissions Session, Detroit, Michigan, April 26, 2012.

4. W.P. Partridge, J.-S. Choi, J.A. Pihl, N. Currier, A. Yezerets, K. Kamasamudram, "Cummins/ORNL FEERC Emissions CRADA: NO_x Control & Measurement Technology for Heavy Duty Diesel Engines," 2012 DOE Vehicle Technologies Program Annual Merit Review, Arlington, Virginia, May 17, 2012.

5. Jae-Soon Choi, Petr Kočí, Josh A. Pihl, William P. Partridge, Mi-Young Kim, C. Stuart Daw. "Hydrocarbon Impact on N_2O Selectivity during the Regeneration of a Ba-based Lean NO_x Trap Catalyst with Hydrogen," 15th International Congress on Catalysis, Munich, Germany, July 2–6, 2012.

7. P. Kočí, Š. Bártová, D. Mráček, M. Marek, J.-S. Choi, J. A. Pihl, C. S. Daw and W. P. Partridge. "Effective Model for Prediction of N_2O Formation during the NO_x Storage Catalyst Regeneration with H_2, CO and Hydrocarbons," CAPoC9 (9th International Conference on Catalysis and Automotive Pollution control), Brussel, Belgium, August 29–31, 2012.

8. William Partridge, Josh Pihl, Xavier Auvray, Louise Olsson, Todd Toops, Jae-Soon Choi, Stuart Daw, Krishna Kamasamudram, Alex Yezerets and Neal Currier. "Local Ammonia Storage in a Monolithic SCR Catalyst: Comparing Commercial & Model Catalyst Performance," CAPoC9 (Ninth International Congress on Catalysis and Automotive Pollution Control), Brussel, Belgium, August 29–31, 2012.

9. Galen B. Fisher, Jae-Soon Choi, L. Curt Maxey, William P. Partridge. "Propane PO_x over Rh with and without Sulfur: Spatially Resolved Species & Temperature Determination," 7th International Conference on Environmental Catalysis (ICEC 2012), Lyon, France, September 2–6, 2012.

10. William Partridge, Josh Pihl, Xavier Auvray, Louise Olsson, Todd Toops, Jae-Soon Choi, Stuart Daw, Krishna Kamasamudram, Alex Yezerets and Neal Currier. "Local Ammonia Storage in a Monolithic SCR Catalyst: Comparing Commercial & Model Catalyst Performance," 7th International Conference on Environmental Catalysis (ICEC 2012), Lyon, France, September 2–6, 2012.

Special Recognitions & Awards/Patents Issued

Invited Lecture:

1. Bill Partridge, Jae-Soon Choi, "Understanding Ammonia Formation and Utilization & Sulfation of Lean NO_x Trap Catalysts via Intra-Reactor Spatiotemporal Diagnostics," IFP (French Institute of Petroleum) Énergies nouvelles (IFPEN), Lyon, France, September 7, 2012. ***Invited***

III.5 Cross-Cut Lean Exhaust Emission Reduction Simulation (CLEERS): Administrative Support

Stuart Daw
Oak Ridge National Laboratory (ORNL)
National Transportation Research Center
2360 Cherahala Boulevard
Knoxville, TN 37932-6472

DOE Technology Development Manager:
Ken Howden

Key ORNL personnel involved in this activity are Stuart Daw, Vitaly Prikhodko, Charles Finney, and Zhiming Gao.

Fiscal Year (FY) 2012 Objectives

Coordinate the CLEERS activity for the DOE Advanced Engine Crosscut Team to accomplish the following:

- Promote development of improved computational tools for simulating realistic full-system performance of lean-burn engines and associated emissions controls.
- Promote development of performance models for emissions control components such as exhaust manifolds, catalytic reactors, and sensors.
- Provide consistent framework for sharing information about emissions control technologies.
- Help identify emissions control research and development (R&D) needs and priorities.

FY 2012 Accomplishments

- Continued co-leadership the CLEERS Planning Committee and facilitation of the CLEERS focus group teleconferences, which continue to have strong domestic and international participation.
- Initiated expansion of database and information repository for experimental engine exhaust and aftertreatment measurements and simulation algorithms and modeling tools.
- Identified an advisory team to oversee database activities.
- Coordinated further refinement of lean-NOx trap (LNT) and selective catalytic reduction (SCR) catalyst characterization protocols.
- Coordinated current DOE national lab projects associated with CLEERS to bring them into closer alignment with the updated CLEERS industry partner priority surveys.
- Provided regular update reports to DOE Advanced Combustion Engine Crosscut Team.
- Organized the 2012 CLEERS workshop at University of Michigan, Dearborn on April 30-May 2, 2012.
- Maintained CLEERS website (www.cleers.org) including functionalities, security, and data to facilitate web meetings and serve focus group interactions.
- Increased utilization of models and kinetic parameters produced by CLEERS projects in full system simulations of alternative advanced powertrain options.
- Worked with the U.S. DRIVE Advanced Combustion and Emissions Control low-temperature task force to promote awareness of emerging aftertreatment barriers associated with low temperature exhaust from advanced engines.

Future Directions

- Continue co-leading the CLEERS planning and database advisory committees.
- Continue co-leading the focus groups.
- Implement plans for expanded experimental and modeling tools database and hiring of ORNL post-doctoral researcher to assist in the database coordination.
- Organize and conduct the 2013 CLEERS workshop in the spring of 2013.
- Continue expanding basic data and model exchange between CLEERS and other Office of Vehicle Technologies projects.
- Continue maintenance and expansion of CLEERS website.
- Continue providing regular update reports to the DOE Advanced Combustion Engine Crosscut team.
- Implement an updated CLEERS industry survey in 2013.

Introduction

Improved catalytic emissions controls will be essential for utilizing high efficiency lean-burn engines without jeopardizing the attainment of much stricter

emission standards that will begin taking effect after 2013. Simulation and modeling are recognized by the Advanced Engine Crosscut Team as essential capabilities needed to address the continually evolving regulatory environment and advances in combustion engine and emissions control technology. In response to this need, the CLEERS activity was initiated several years ago to promote improved computational tools and data for simulating realistic full-system performance of lean-burn engines and the associated emissions control systems. Specific activities supported under CLEERS include:

- Public workshops on emissions control topics.
- Collaborative interactions among Crosscut Team members, emissions control suppliers, universities, and national labs under organized topical focus groups.
- Development of experimental data, analytical procedures, and computational tools for understanding performance and durability of catalytic materials.
- Establishment of consistent frameworks for sharing information about emissions control technologies.
- Recommendations to DOE and the DOE Crosscut Team regarding the most critical emissions control R&D needs and priorities.

ORNL is involved in two separate DOE-funded tasks supporting CLEERS:

- Overall administrative support; and
- Joint development of benchmark emissions control catalyst kinetics in collaboration with Sandia National Laboratories (SNL) and Pacific Northwest National Laboratory (PNNL) and university and industry partners.

Approach

In the administrative task, ORNL coordinates the CLEERS Planning Committee, the CLEERS Database Advisory Team, the CLEERS focus groups, CLEERS public workshops, the biannual CLEERS industry survey, and the CLEERS website (http://www.cleers.org). ORNL acts as a communication hub and scheduling coordinator among these groups and as the spokesperson and documentation source for CLEERS information and reports. The latter includes preparation and presentation of status reports to the Advanced Engine Crosscut Team, responses to requests and inquiries about CLEERS from the public, and summary reports from the biannual industry surveys.

Results

Plans have been initiated for an updated industry survey in 2013. Modifications to the survey format and list of key technical topics have been made based on participant feedback. Additional modifications are expected based on recent input from individual industry partners and members of the U.S. DRIVE Advanced Combustion and Emissions Control Technical Team.

Key issues that have been identified in these discussions include:

- The need to develop catalysts and emission control devices capable of functioning at engine exhaust temperatures as low as 150°C. The relevance of catalyst function at such low temperatures for current and advanced combustion modes is illustrated in Figure 1.
- The need to expand public access to pre-proprietary data on engine exhaust properties, realistic values for kinetic reaction rate parameters for well-established reference catalysts, basic computational tools for analyzing experimental data and predicting basic drive cycle emission control trends, and accurate experimental transient measurements of aftertreatment device performance.
- Better coordination and leveraging among DOE's Energy Efficiency and Renewable Energy Program and Basic Energy Science Program so that the results from basic research can be more rapidly translated into vehicle-oriented applications.

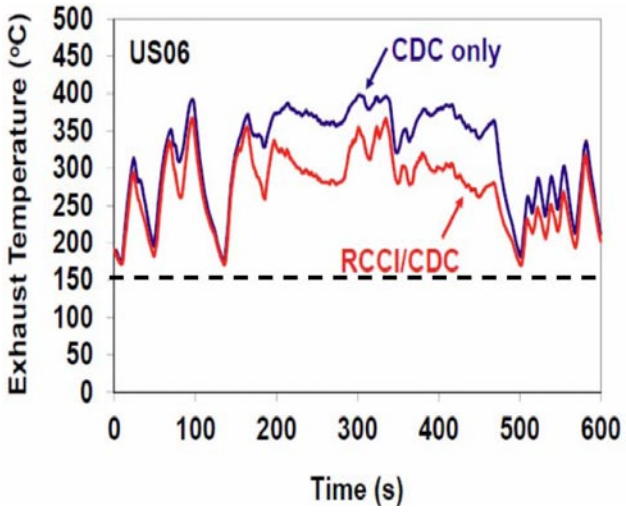

FIGURE 1. Example engine-out US06 cycle exhaust temperature transients from ORNL simulations of a mid-size diesel passenger car with the capability for reaction-controlled compression ignition (RCCI) combustion compared with conventional diesel combustion (CDC). Low exhaust temperatures from advanced combustion modes pose increasing challenges for aftertreatment.

CLEERS technical teleconferences this year included presentations by a range of experts in emissions control experimentation, modeling, and simulation. Presenters included Andy Wereszczak (ORNL), Mike Zammit (Chrysler), Steve Schmieg (General Motors), Chang Kim (General Motors), John Yoo (ORNL), Mark Crocker (University of Kentucky), and Dick Blint (N2Kinetics, formerly General Motors). We have continued to restrict teleconference attendance to members of the Advanced Engine Crosscut Team and their direct collaborators, because these teleconferences sometimes include unpublished or sensitive information. Attendance has recently increased and is typically between 25 and 40 participants. We continue to have several international participants, mostly from Europe.

The 2012 (15th) CLEERS workshop was held April 31-May 2, 2012 at the Institute of Advanced Vehicle Studies on the Dearborn campus of the University of Michigan. This year's program included four invited speakers: Isabella Nova (Politecnico di Milano) - "Development and Validation of a Chemically and Physically Consistent Mathematical Model of Dual-Layer Ammonia Slip Catalysts;" Christine Lambert (Ford) - "Future Directions in SCR Systems;" Milos Marek (Institute for Chemical Technology in Prague) - "Overview of LNT Modeling Approaches;" and Alex Sappok (Massachusetts Institute of Technology) - "Fundamental Processes Controlling Ash Accumulation in Diesel Particulate Filters and Impacts on DPF Performance." There were also 29 contributed talks and 10 posters. One of the associated key discussion topics was the CLEERS SCR protocol illustrated in Figure 2.

As in recent years, we also had an industry panel discussion at the CLEERS Workshop. This year the topic of the panel discussion was "Challenges and Perspectives on Simulating the Relationship Between Emissions Controls and Fuel Efficiency." Panel members were: Neal Currier (Cummins), Houshun Zhang (Environmental Protection Agency), Haifeng Liu (General Motors), Ilya Kolmanovsky (University of Michigan, formerly Ford), Denesh Upadyay (Ford), and Bernd Krutszch (Daimler). Key observations by the panel included the following:

- Many levels of modeling are required to optimize the complex multi-dimensional tradeoffs in meeting emissions regulations, customer needs, and cost.
- Without accurate modeling tools, this complex optimization would not be tractable.
- Industry needs a variety of modeling tools suitable for different purposes that span detailed dynamic models, reduced order models, embedded models, integrated vehicle systems, power trains, subsystems, and aftertreatment component scales.
- Low-order models are best when they are derived from higher-order models.

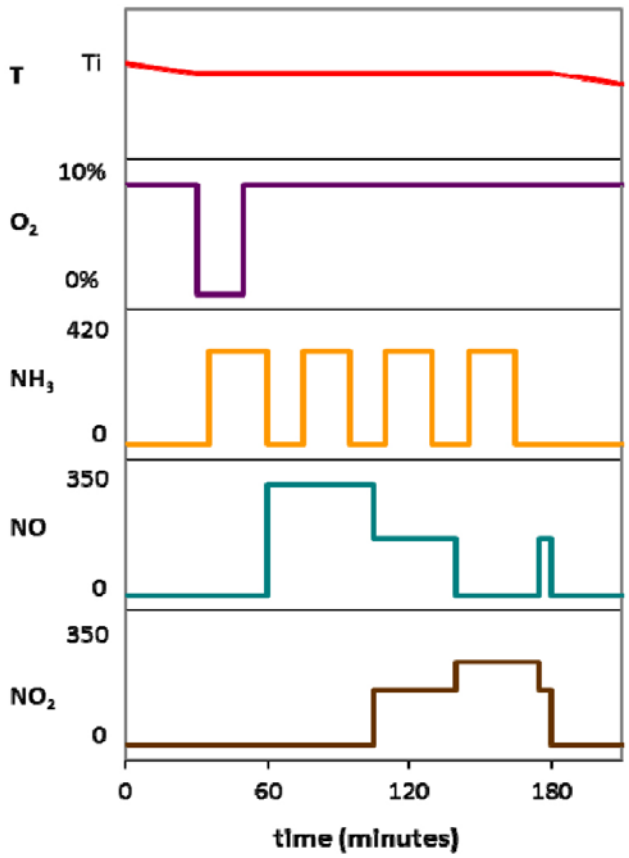

FIGURE 2. Simulated exhaust temperature and concentration transients depicted here in the CLEERS SCR catalyst protocol reveal key information about NO and NO_2 reduction, NO oxidation, NO_2 decomposition, N_2O formation, and NH_3 storage and oxidation needed to develop accurate simulation models.

- Models will be critical to reduce industry testing costs for new products, especially when the impacts of on-board diagnostics are considered.

Ken Howden, from DOE's Office of Vehicle Technologies, provided an update on new challenges in emissions controls technology on the second evening of the workshop. Details of the technical program and presentation downloads are available on the CLEERS website [1] under the 2012 (15th) workshop heading.

ORNL's collaborations with SNL and PNNL under CLEERS have involved significant transitions this year. The joint LNT modeling effort with SNL was concluded with the publication of an SNL technical report [2] and an article in Chemical Engineering Journal [3]. Rich Larson, the key SNL staff member involved in CLEERS modeling activities, retired this year and discussions are underway to identify an appropriate new SNL CLEERS collaborator and directions for a new research focus. ORNL's collaboration with PNNL has continued to center on the characterization and modeling

of commercial chabazite copper-zeolite SCR catalysts, especially in regard to the effects of aging. A summary of recent results from this work has been submitted to the 2013 SAE Congress [4]. We are now reassessing the detailed focus of PNNL's SCR modeling efforts in light of research staff changes at PNNL, but we expect one of their main modeling objectives to remain the development of lower-order models for simulating SCR performance in vehicle drive cycles.

We also have continued active collaborations with university and industry partners in both the U.S. and Europe. Our university partners include Petr Koci at the Institute for Chemical Technology in Prague, Louise Olsson at Chalmers University of Technology, and Isabella Nova at Politecnico di Milano. We will shortly be hosting student researchers from both Prague and Milano, who will be conducting experiments in the Fuels, Engines, and Emissions Research Center catalyst labs as part of these collaborations. A recent new industry partner is Gamma Technologies, who are using CLEERS experimental data to generate improved modeling parameters for the CLEERS Umicore reference LNT catalyst and also the LNT catalyst in the BMW series 120i sedan, which recently underwent extensive chassis dynamometer measurements at ORNL. Gamma has offered to share their results with the CLEERS community in the expanded CLEERS database and to provide reference simulations using the resulting LNT model from their commercial vehicle simulation software.

Conclusions

CLEERS continues to provide a unique coordination link for emissions control R&D across industry, national labs, and universities. Recent efforts to expand a repository of shared, pre-proprietary data as well as reference computational algorithms and modeling components is intended to reduce duplication of effort and more effectively target fundamental research at the national labs and universities. CLEERS also provides a mechanism to identify the leading technical challenges faced by industry in transforming the best available transportation technology into commercial reality. We continue to have heavy participation from industry, labs, and universities in the public workshops and the technical focus meetings. Results from the above interactions provide DOE and the DOE Advanced Engine Crosscut Team with the latest information for updating their strategic plans.

References

1. 2012 (15th) CLEERS Workshop agenda and presentations at http://www.cleers.org.

2. Richard S. Larson, V. Kalyana Chakravarthy, Josh A. Pihl, and C. Stuart Daw, "Microkinetic Modeling of Lean NO*x* Trap Storage and Regeneration," Sandia Technical Report No. SAND2011-9090, December 2011.

3. Richard S. Larson, V. Kalyana Chakravarthy, Josh A. Pihl, and C. Stuart Daw, "Microkinetic modeling of lean NOx trap chemistry," Chemical Engineering Journal, vol. 189-190, 2012, pp. 134-147.

4. Maruthi Devarakonda, Josh Pihl, Jong Lee, George Muntean, and Stuart Daw, "1D Model of a Cu-CHA SCR Catalyst Based on CLEERS Transient SCR Protocol," Submitted to 2013 SAE Congress.

FY 2012 Publications/Presentations

1. 2012 (15th) CLEERS Workshop agenda and presentations at http://www.cleers.org.

2. "CLEERS Coordination & Joint Development of Benchmark Kinetics for LNT & SCR," J.-S. Choi et al, 2012 DOE Hydrogen Program and Vehicle Technologies Annual Merit Review, Washington, DC, May 14–18, 2012.

3. Maruthi Devarakonda, Josh Pihl, Jong Lee, George Muntean, and Stuart Daw, "1D Model of a Cu-CHA SCR Catalyst Based on CLEERS Transient SCR Protocol," Submitted to 2013 SAE Congress.

4. "CLEERS Updates to the DOE Advanced Engine Crosscut Team," C.S. Daw, W. Li, and R. Blint, Nov. 10, 2011; March 15, 2012; May 10, 2012; July 19, 2012; Sept. 13, 2012 (limited distribution).

5. "2011 CLEERS Industry Priorities Survey Final Report: Analysis, Summary, and Recommendations," C.S. Daw, October, 2011.

6. Richard S. Larson, V. Kalyana Chakravarthy, Josh A. Pihl, and C. Stuart Daw, "Microkinetic modeling of lean NOx trap chemistry," Chemical Engineering Journal, vol. 189-190, 2012, pp. 134-147 and SAND2011-9090, December 2011.

III.6 Cross-Cut Lean Exhaust Emissions Reduction Simulations (CLEERS): Joint Development of Benchmark Kinetics

Stuart Daw (Primary Contact), Jae-Soon Choi, Josh Pihl, Bill Partridge, Mi-Young Kim
Oak Ridge National Laboratory
2360 Cherahala Boulevard
Knoxville, TN 37932-1563

DOE Technology Development Manager:
Ken Howden

Overall Objectives

Collaborate with Pacific Northwest National Laboratory (PNNL), and Sandia National Laboratories (SNL) in the development of kinetics information needed for aftertreatment component simulation through the following:

- Provide benchmark laboratory measurements of oxides of nitrogen (NOx) reduction chemistry and reaction rates in lean-NOx traps (LNTs) and selective catalytic reduction (SCR) catalysts under realistic operating conditions.
- Correlate lab measurements of LNT and SCR catalysts with test-stand/vehicle studies.
- Develop and validate global chemistry and low-order models for LNT and SCR kinetics.
- Utilize results from fundamental research to develop new approaches for advanced catalysts (e.g., with enhanced low-temperature function).

Fiscal Year (FY) 2012 Objectives

- Investigate impacts of reductant composition and spatial reaction distributions on LNT regeneration efficiency and product selectivity, including N_2O generation.
- Exercise CLEERS Transient SCR Protocol to generate benchmark model calibration data on a commercial copper zeolite SCR catalyst.
- Quantify impacts of hydrothermal aging on the catalytic properties of a commercial copper zeolite SCR catalyst.
- Provide mechanistic insights and experimental data for model development and calibration to collaborators.
- Investigate unique new approaches for low-temperature oxidation catalysts.

Accomplishments

- Initiated flow reactor characterization of a new commercial CLEERS LNT reference catalyst used in the lean gasoline direct injection-equipped BMW 120i sedan.
- Collaborated with Gamma Technologies to develop and share kinetic parameter estimates for the new CLEERS BMW reference catalyst.
- Developed a global kinetic model that predicts N_2O and NH_3 formation in LNTs over a wide range of reductant composition, temperature, and regeneration period.
- In collaboration with ORNL's Center for Nanophase Materials Sciences and Chonbuk National University, characterized novel catalysts with enhanced low-temperature oxidation activity.
- Continued collaborative kinetic measurements and analysis of LNT and SCR catalysts with ICT Prague, Chalmers University of Technology, and Politecnico di Milano.
- With PNNL, continued developing global kinetics for a commercial Cu-zeolite SCR catalyst and evaluating the impact of hydrothermal aging on the catalyst function.

Future Directions

- Continue evaluation of the BMW LNT catalyst kinetic parameters and distribute results on the CLEERS website.
- Refine the set of kinetic and aging parameters for the commercial small-pore Cu-zeolite SCR catalyst under joint investigation by ORNL and PNNL.
- Continue identification of rate-determining steps, key surface species, and associated catalyst sites in SCR zeolite catalysts through flow reactor and surface spectroscopy experiments.
- Extend the available laboratory characterization data for LNT and SCR catalysts to include temperatures down to 150°C.
- Utilize above results to improve models for simulating LNT and SCR NOx reduction performance under both laboratory and vehicle drive cycle conditions.
- Continue investigations of novel low-temperature oxidation catalysts.
- Develop modeling and lab characterization approaches for passive sorbers.

Introduction

Improved catalytic emissions controls will be essential for utilizing high-efficiency lean-burn engines without jeopardizing the attainment of increasingly strict emission standards. Simulation and modeling are recognized by the DOE Diesel Crosscut Team as essential capabilities needed to achieve this goal. In response to this need, the CLEERS activity was initiated to promote improved computational tools and data for simulating realistic full-system performance of lean-burn engines and the associated emissions control systems [1].

ORNL is involved in two separate DOE-funded tasks supporting CLEERS:

- Overall administrative support; and
- Joint development of benchmark aftertreatment kinetics with SNL and PNNL.

Approach

In the benchmark kinetics task (covered by this report), ORNL collaborates with SNL and PNNL and other CLEERS partners to produce kinetic information for catalytic aftertreatment devices. The current focus is on LNT and SCR lean-NOx reduction catalysts. In addition to open presentations and publications, results are rapidly shared among the CLEERS focus groups, with individual industry and university collaborators, and with the DOE Advanced Engine Crosscut Team, which collectively oversees CLEERS. All of these interactions help ensure that the DOE-funded research remains relevant to the most pressing challenges to achieving maximum vehicle fuel efficiencies. Specific lab activities include:

- Regular direct interactions among ORNL, PNNL, and SNL.
- Experimental measurements of LNT and SCR chemistry and kinetics on laboratory reactors, engine test stands, and chassis dynamometers.
- Analysis and reconciliation of experimental data from different sources with predictions from computer simulations.
- Journal publications, public presentations, and postings on the CLEERS website.

Results

ORNL assisted SNL in completing and publishing a micro-kinetic chemical reaction mechanism for NOx storage and regeneration in LNT catalysts in the Chemical Engineering Journal. Further efforts on LNT modeling are now being directed at re-evaluation and globalization of the key parameters needed to simulate the available BMW LNT catalyst measurements, which include extensive laboratory measurements based on the CLEERS LNT protocol as well as vehicle measurements made on a chassis dynamometer. With the retirement of Rich Larson at SNL, our primary LNT modeling collaborators are now ICT Prague and Gamma Technologies. The Gamma team will be using the resulting kinetic parameter estimates in aftertreatment component models that will be distributed with their GT Power software package for vehicle simulation. These parameters will also be posted on the CLEERS website, along with reference simulations.

One particular aspect of LNT function that is of high concern is the production of N_2O, a potent greenhouse gas. This year we investigated the impact of hydrocarbons (HCs) on the chemistry of N_2O formation over the CLEERS Umicore reference LNT catalyst. In this study, we focused on the regeneration chemistry with propylene and propane. As can be seen in Figure 1, both hydrocarbons significantly increased N_2O yield at temperatures in the range of 200-350°C. We conjecture that this trend results from differences in the "speed" of the reductant front and the "light-off" characteristics of H_2 and HCs. These results were presented at the 15th International Congress on Catalysis in Munich in July and other conferences.

Our detailed spatial measurements of N_2O and NH_3 reactions in the Umicore LNT catalyst have led to a global reaction mechanism that our ICT Prague collaborators have used to accurately predict observed trends in N_2O and NH_3 formation over a wide range

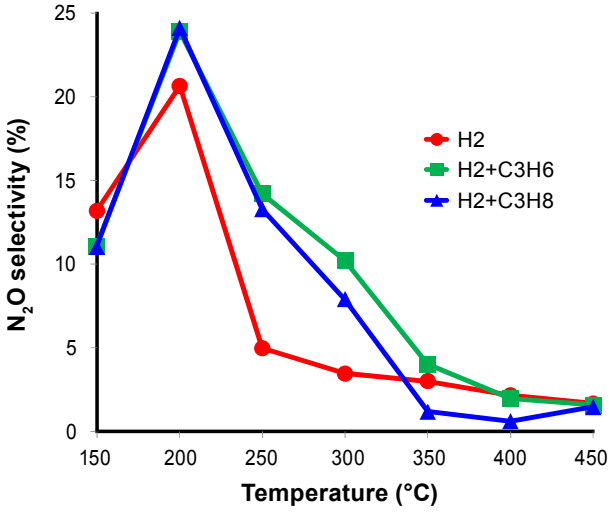

FIGURE 1. Observed variation in N_2O selectivity with addition of C_3H_6 or C_3H_8 during fast-cycle H_2 regeneration of the CLEERS Umicore reference LNT catalyst.

of regeneration conditions. The mechanism appears to explain the effects of the rich regeneration mixture composition (including H_2/CO/C_3H_6), local temperature, and length of regeneration period. The mechanism further implies that the redox state of platinum-group metals and spatial distribution of NO_x storage are needed to accurately predict selectivity for N_2O and NH_3 during regeneration.

This year we investigated a novel oxidation catalyst concept in collaboration with the ORNL Center for Nanophase Materials Sciences (a Basic Energy Sciences user facility) and Chonbuk National University in Korea. The oxidation catalysts being investigated are based on platinum supported on metal-oxide-coated silica. We found that coating the silica support with titania or zirconia leads to significantly enhanced dispersion, stability, and redox capacity of the platinum. Furthermore, the coating promotes surface acidity but not basicity, which is favorable for sulfur tolerance, i.e. low and weak sulfur adsorption. These positive properties are reflected in enhanced low-temperature CO oxidation under fresh, sulfated, and hydrothermally aged conditions.

Experiments with the commercial small-pore Cu-zeolite SCR catalyst revealed that hydrothermal aging reduced high temperature NH_3 storage capacity. To better understand the specific changes occurring in the catalyst active sites that caused the reduction in NH_3 stability on the surface, we conducted a series of NH_3 adsorption/temperature programmed desorption (TPD) experiments that probed the effects of water, catalyst oxidation state, and degree of aging. The observed TPD desorption profiles (Figure 2) were complex, implying a range of storage site adsorption energies. The relative distribution of the site energies changed with pretreatment oxidation/reduction, indicating that they might be associated with different states of Cu in the catalyst. Specifically, aging decreased the NH_3 associated with the high adsorption energy sites and increased the NH_3 desorbed from the low adsorption energy sites, consistent with conversion of more stable storage sites into less stable sites. Additional analyses indicate that the variation in equilibrium NH_3 storage can generally be described with simple multi-site Langmuir or single-site Temkin isotherms. We are using these models to understand how best to interpret the observed changes in NH_3 adsorption with catalyst preparation and aging and, ultimately, to understand how these changes in NH_3 storage capacity might affect optimal control strategies for aged catalysts.

The N_2O decomposition properties of the above SCR catalyst were also studied. N_2O decomposition is of interest because it might provide a mechanism to reduce N_2O emissions from upstream components. As illustrated in Figure 3, the SCR catalyst decomposes

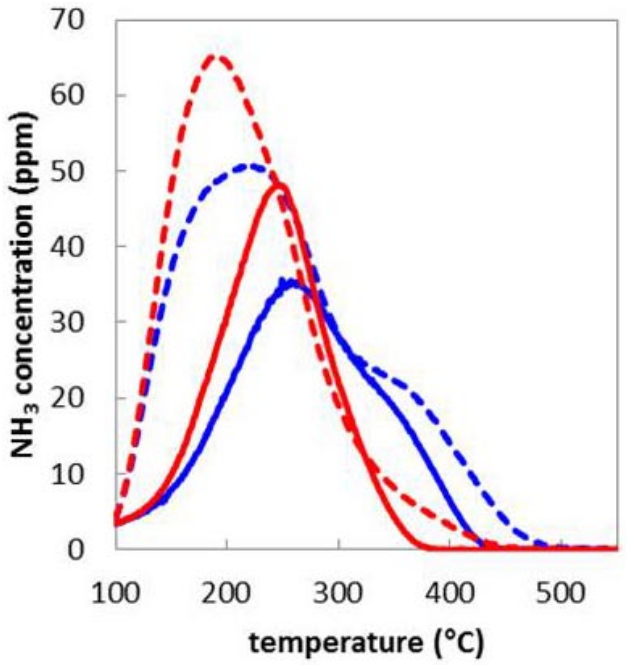

FIGURE 2. Measured outlet NH_3 concentrations during NH_3 TPD from a commercial small-pore Cu-zeolite SCR catalyst aged at 700°C for 4 h (blue lines) and 800°C for 16 h (red lines). Experimental conditions for dashed lines were: 30,000 hr^{-1} gas hourly space velocity with (1) pretreatment: 10% O_2, 5% CO_2; 550°C; (2) adsorption: 350 ppm NH_3, 5% CO_2; 100°C; (3) isothermal desorption: 5% CO_2; 100°C; (4) TPD: 5% CO_2; 100-550°C at 2°C/min. Solid lines also included 5% H_2O in all steps.

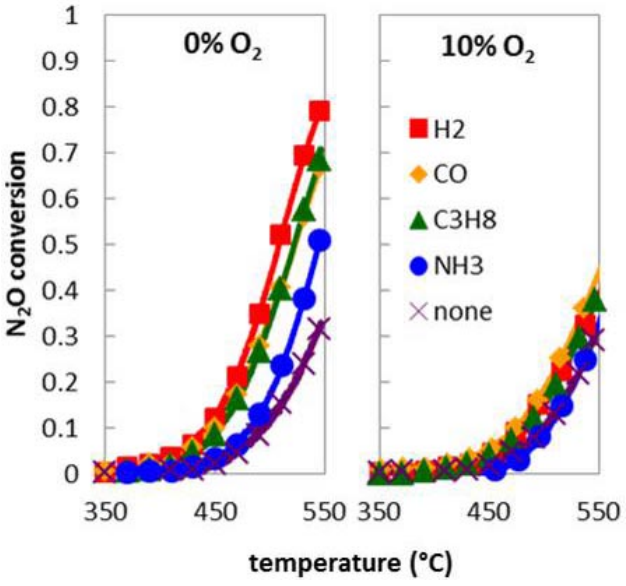

FIGURE 3. Conversion of 100 ppm N_2O over the commercial Cu-zeolite catalyst in the (a) presence and (b) absence of 10% O_2 with 1,000 ppm H_2, 1,000 ppm CO, 100 ppm C_3H_8, 667 ppm NH_3, or no reductant. All cases included 5% H_2O and were run at 30,000 hr^{-1} gas hourly space velocity.

N_2O at temperatures above 450°C even under oxidizing conditions. In the presence of excess oxygen, C_3H_8, CO, and H_2 slightly increase the rate of N_2O decomposition. However, in the absence of O_2, these reductants result in significant N_2O conversions. Moderate N_2O reduction is also observed with NH_3. This insight will aid in the design of operating strategies for hybrid catalyst configurations such as LNT/SCR and three-way catalyst/SCR.

Conclusions

Ongoing collaborations between ORNL and partners at PNNL, SNL, Gamma Technologies, ICT Prague, Chalmers University of Technology, and Politecnico di Milano continue to reveal new insights into the rate controlling mechanisms in lean-NOx control with LNT and urea-SCR catalysts. The resulting experimental data, kinetic parameter estimates, and device simulation models are providing critical information for guiding vehicle and system simulations studies as well as development of more fuel efficient, lower cost emissions control options for advanced combustion engines. Interactions with the CLEERS Focus Groups, industry partners, and the DOE Advanced Engine Crosscut Team updates are helping to maintain commercial relevance.

References

1. "2011 CLEERS Industry Priorities Survey Final Report: Analysis, Summary, and Recommendations," C.S. Daw, October, 2011, http://www.cleers.org.

FY 2012 Publications/Presentations

1. M. Devarakonda, J. Pihl, J. Lee, G. Muntean, S. Daw, submitted to 2013 SAE Congress.

2. P. Kočí, Š. Bártová, D. Mráček, M. Marek, J.-S. Choi, M.-Y. Kim, J.A. Pihl, W.P. Partridge, submitted to Topics in Catalysis.

3. R.S. Larson, V.K. Chakravarthy, J.A. Pihl, C.S. Daw, Chemical Engineering Journal, Vol. 189-190, pp. 134-147, 2012, and SAND2011-9090, December 2011.

4. J.-S. Choi, W.P. Partridge, J.A. Pihl, M.-Y. Kim, P. Kočí, C.S. Daw, Catalysis Today, Vol. 184, pp. 20-26, 2012.

5. N.A. Ottinger, T.J. Toops, J.A. Pihl, J.T. Roop, J.-S. Choi, W.P. Partridge, Applied Catalysis B: Environmental, Vol. 117-118, pp. 167-176, 2012.

6. Z. Gao, S. Daw, J. Pihl, M. Devarakonda, poster, 17th DEER Conference, Detroit, October 3–6, 2011.

7. J.-S. Choi, W.P. Partridge, J.A. Pihl, P. Kočí, M.-Y. Kim, C.S. Daw, oral, 17th DEER Conference, Detroit, Michigan, October 3–6, 2011.

8. M.-Y. Kim, J.-S. Choi, T.J. Toops, V. Schwartz, J. Chen, E.-S. Jeong, S.-W. Han, poster, Center for Nanophase Materials Sciences User Meeting, Oak Ridge, Tennessee, September 13–14, 2012.

9. M.-Y. Kim, J.-S. Choi, T.J. Toops, V. Schwartz, J. Chen, E.-S. Jeong, S.-W. Han, oral, 7th International Conference on Environmental Catalysis, Lyon, France, September 2–6, 2012.

10. J.-S. Choi, J.A. Pihl, W.P. Partridge, M.-Y. Kim, C.S. Daw, P. Kočí, Š. Bártová, M. Marek, poster, 7th International Conference on Environmental Catalysis, Lyon, France, September 2–6, 2012.

11. P. Kočí, D. Mráček, Š. Bártová, M. Marek, J.-S. Choi, J.A. Pihl, C.S. Daw, W.P. Partridge, oral, 9th International Congress on Catalysis and Automotive Pollution Control, Brussels, Belgium, August 29–31, 2012.

12. Š. Bártová, D. Mráček, P. Kočí, M. Marek, J.A. Pihl, J.-S. Choi, W.P. Partridge, poster, 20th International Congress of Chemical and Process Engineering CHISA, Prague, Czech Republic, August 25–29, 2012.

13. J.-S. Choi, P. Kočí, J.A. Pihl, W.P. Partridge, M.-Y. Kim, Š. Bártová, C.S. Daw, poster, 15th International Congress on Catalysis, Munich, Germany, July 1–6, 2012.

14. M.-Y. Kim, J.-S. Choi, T.J. Toops, V. Schwartz, E.-S. Jeong, S.-W. Han, poster, 15th International Congress on Catalysis, Munich, Germany, July 1–6, 2012.

15. J.A. Pihl, C.S. Daw, oral, CTI 4th International Conference on NOx Reduction, Detroit, MI, June 19–20, 2012.

16. J.-S. Choi, invited seminar, Heesung Catalysts Corporation, Shiheung, Korea, June 8, 2012.

17. C.S. Daw, J.-S. Choi, J.A. Pihl, V.Y. Prikhodko, C.E.A. Finney, M. Kim, T.J. Toops, W.P. Partridge, M.J. Lance, oral, DOE Vehicle Technologies Program Annual Merit Review, Crystal City, VA, May 14–18, 2012.

18. J.A. Pihl, C.S. Daw, oral, CLEERS Workshop, Dearborn, MI, April 30 – May 2, 2012.

19. M.-Y. Kim, J.-S. Choi, T.J. Toops, oral, CLEERS Workshop, Dearborn, MI, April 30 - May 2, 2012.

20. J.-S. Choi, J.A. Pihl, W.P. Partridge, M.-Y. Kim, C.S. Daw, P. Kočí, Š. Bártová, M. Marek, poster, CLEERS Workshop, Dearborn, MI, April 30 - May 2, 2012.

21. P. Kočí, Š. Bártová, M. Marek, J.A. Pihl, M.-Y. Kim, J.-S. Choi, W.P. Partridge, oral, SAE World Congress, Detroit, Michigan, April 26, 2012.

III.7 Development of Advanced Diesel Particulate Filtration Systems

Kyeong Lee
Argonne National Laboratory
9700 S. Cass Ave.
Argonne, IL 60564

DOE Technology Development Manager:
Ken Howden

Overall Objectives

- Characterize diesel particulate filter (DPF) filtration/regeneration processes and evaluate the performance.
- Develop technologies to reduce pressure drops across the DPF membrane.
- Measure the thermo-physicochemical properties of diesel particulate mass (PM) emissions for future numerical calculations.

Fiscal Year (FY) 2012 Objectives

- Evaluate the characteristics of soot oxidation with various reactant gases using a thermogravimetric analyzer (TGA).
- Evaluate DPF filtration/regeneration performance with various reactant gases.
- Examine the filter micro pore-structures using an optical imaging technique.
- Develop numerical models for flow dynamics in DPF filters.

Accomplishments

- The effects of exhaust emission components were evaluated on soot oxidation.
- Detailed DPF filtration/regeneration processes were characterized.
- An optimized filter design was proposed in consideration of correlations between pore geometry and size.
- A numerical code was developed to predict flow dynamics in a filter with potential to calculation of soot loading profiles.

Future Directions

- Characterize the physical and chemical properties of gasoline direct injection engine particulates.
- Design and fabricate a bench-scaled gasoline particulate filter (GPF) system.
- Evaluate filtration and regeneration characteristics in a GPF with different filter materials.
- Perform numerical modeling for soot loading in filtration.

Introduction

DPF systems offer the effective control of PM emissions that help diesel engines meet the stringent PM emission standards. However, they still need improvement in design and operating logics to deliver high regeneration performance. Development of high-performance DPF systems require detailed understanding of soot oxidation kinetics in relation to exhaust emission components and ambient conditions. To achieve this goal, we need to accurately evaluate the kinetic parameters that govern soot oxidation at different engine operating conditions (i.e., different concentrations of gaseous emissions). Effective control of thermal runaway also requires this information, because it enables us to predict the amount of transient heat release during DPF regeneration. Based on this fundamental information, filtration and regeneration processes are needed to be characterized in terms of oxidation behaviors for different reactant gases, such as NO_2 and O_2. Filter design is another essential factor to be required for developing advanced DPF systems. Detailed analysis of pore structures and geometry will give an insight into developing advanced filter materials.

Approach

The Argonne research team conducted soot oxidation experiments with different compositions of gaseous reactants, using a TGA. As a result, oxidation rates and activation energy were evaluated to define the oxidation effects of different gaseous reactants. With these data, DPF filtration and regeneration experiments were performed to find out correlations between pressure drops across the filter and visualized images recorded in the filtration/regeneration processes. Pore microstructures in the filter walls were also analyzed by an optical measurement technique. Finally, numerical

modeling for a clean filter was conducted to illuminate the aerodynamics of gas flows in filter channels.

Results

Soot Oxidation Using TGA

Effects of Inert Gases - Isothermal/Non-Isothermal Kinetic Analysis

The temporal variations of activation energy (E_a) during soot oxidation were evaluated for three different inert balance gases (N_2, Ar, and He) in air. Each data set displays the variation in activation energy for instantaneous sample mass, which includes all the activation energies evaluated at three different isothermal conditions, 500°C, 550°C, and 600°C. The non-isothermal kinetic analysis by the differential method represented a result that the activation energy converges to a single value, 155 kJ/mole at a heating rate of 1.0°C/min: this indicates that activation energy is independent of inert gases. For details, see publication [1].

Effects of Reactant Gases Simulating Diesel Exhaust Emissions on Soot Oxidation (refer to publication [1])

Figure 1 illustrates the effects of oxygen on soot oxidation in a temperature range up to 900°C. The figure shows that the increased oxygen concentration remarkably contributed to the soot oxidation in the relatively high temperature range (≥400°C). The oxidation effects of oxygen diminished with further concentration increases up to 8 vol%.

Figure 2 shows the effects of NO_2 concentrations (0 to 450 ppm) on soot oxidation, as CO_2 and O_2 concentrations remained constant. Soot oxidation was promoted as the NO_2 concentration increased. With higher NO_2 concentrations, the main oxidation started at lower temperatures, which implies the oxidation range was extended to the lower temperature.

Figure 3 shows soot oxidation kinetics displayed for various gas mixtures in a form of Arrhenius plot. Each oxidation curve showed two different linear gradients when NO_2 is present in the mixture. Activation energy for each gas mixture was evaluated in the two separate temperature ranges by using the non-isothermal differential method, as summarized in Table 1. These activation energies agree quite well with those from other investigators (see reference [1]). The activation energy significantly decreased as NO_2 concentration increased.

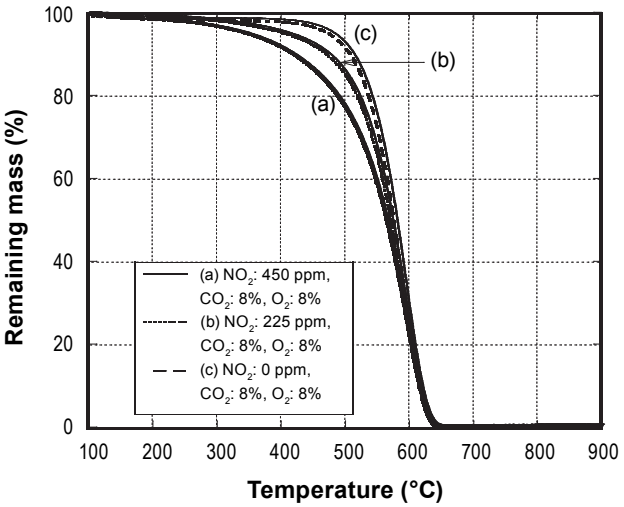

FIGURE 2. Effects of NO_2 concentration on soot oxidation.

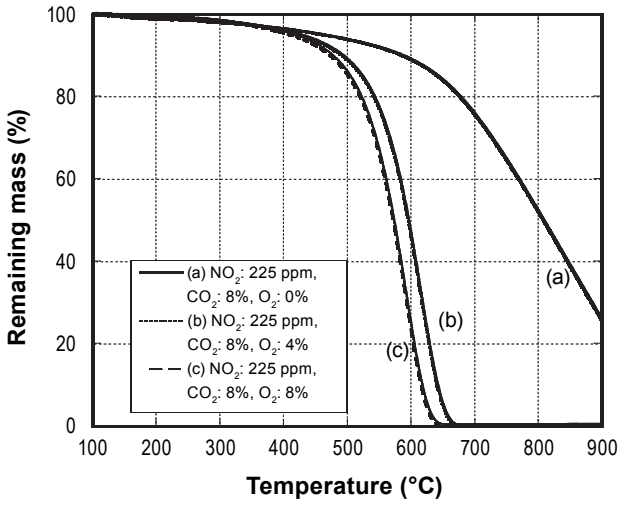

FIGURE 1. Effects of oxygen concentration on soot oxidation.

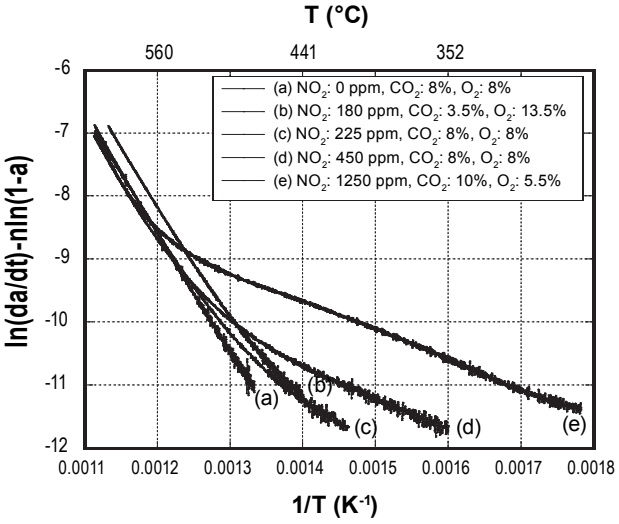

FIGURE 3. Arrhenius plots of soot oxidation for various mixture compositions (in the range of 5 to 95% conversion).

TABLE 1. Activation Energy for Different Mixture Compositions Simulating Diesel Emissions

Compositions (NO_2: ppm, CO_2 & O_2: vol%)	Low temperature zone			High temperature zone		
	T (°C)	E_a (kJ/mole)	*n*	T (°C)	E_a (kJ/mole)	*n*
NO_2: 0, CO_2: 8, O_2: 8	T: 477 – 625, E_a: 153, *n* = 0.83					
NO_2: 180, CO_2: 3.5, O_2: 13.5	441–491	**105**	1	515–610	**154**	0.85
NO_2: 225, CO_2: 8, O_2: 8	410–471	**67**	1	526–625	**157**	0.80
NO_2: 450, CO_2: 8, O_2: 8	352–471	**44**	1	550–626	**154**	0.80
NO_2:1250, CO_2: 10, O_2: 5.5	288–500	**39**	1	575–616	**159**	0.85

n – reaction order

However, the activation energy in the high temperature oxidation zone changes insignificantly with changes in gas emissions composition.

DPF Filtration/Regeneration (For details, see reference [2])

Filtration

Measured pressure drops and soot loading mass were synchronized with the soot loading images to find out correlations, as shown in Figure 4. From the soot loading images corresponding to specific filtration conditions (marked on the pressure drop trace), three distinct filtration stages were clearly identified during the filtration: depth filtration, transition filtration, and soot cake formation.

Regeneration

Regeneration tests were conducted under three different exhaust gas conditions: 9.8 vol% O_2 (existing in the exhaust emissions) at 500°C, and 1,000 ppm NO_2-added at two different temperatures, 400°C and 500°C. NO_2 gases are known to be an oxidant more reactive than O_2 for soot, which can promote soot oxidation in a passive way of DPF regeneration. The graph shown in Figure 5 exhibits pressure drop traces for the three different regeneration conditions. All the three regeneration experiments showed three distinct regeneration stages as shown above, regardless the emissions conditions. Corresponding soot oxidation images are also displayed in the figure below. Results show that the soot images are quite similar between the two corresponding inlet conditions at the same regeneration stages. These qualitative observations

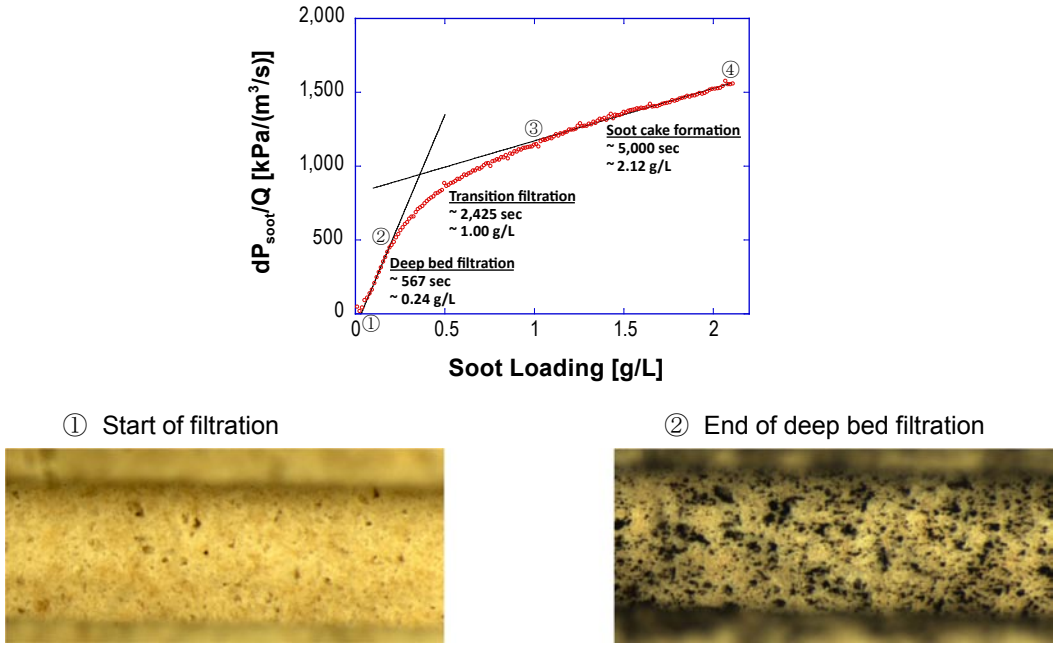

FIGURE 4. Pressure drop trace during filtration process and visualized images at different filtration stages.

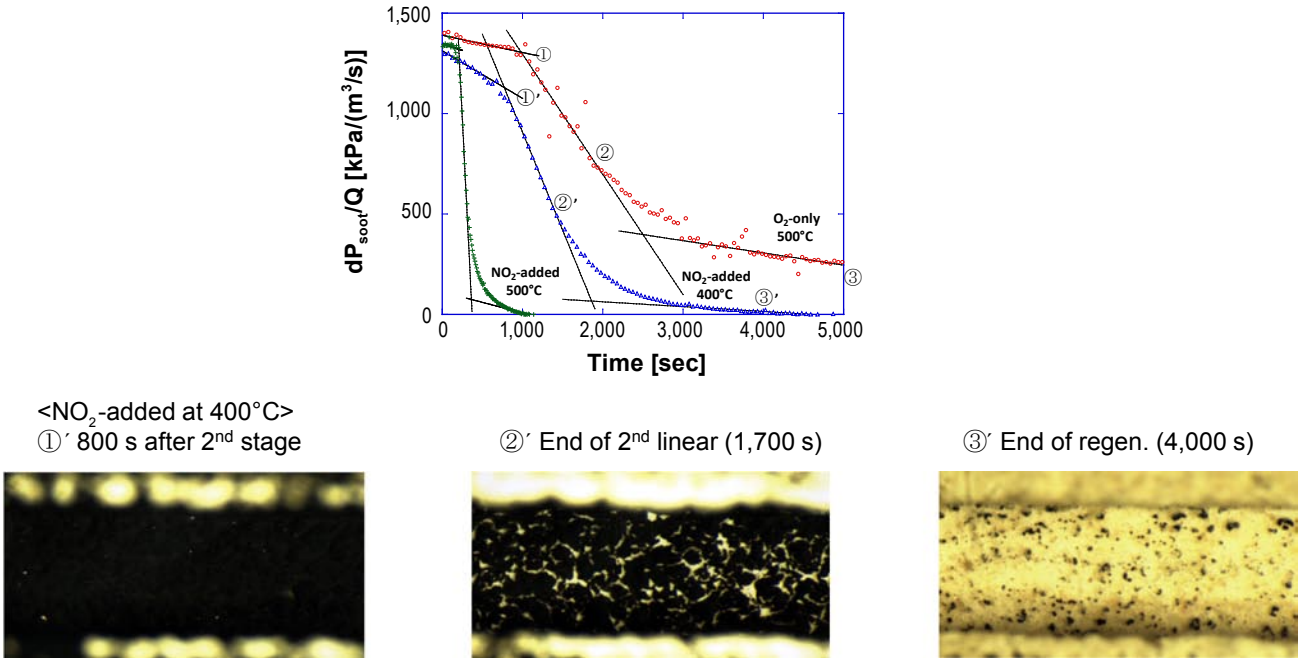

FIGURE 5. Pressure drop traces during regeneration process under three different inlet gas conditions and visualized images for regeneration with 1,000 ppm NO_2-added emissions at 400°C.

indicate that the actual soot oxidation characteristics can be well correlated at each regeneration stage identified by the pressure drop, regardless inlet gas conditions. A noticeable result is that the degree of oxidation rate appears to be quite a bit higher with NO_2-added emissions than does with 9.8 vol% O_2 emissions, indicated by the higher gradient of pressure drops. This behavior is verified by the quantifications of oxidation times.

Optical Examination of Filter Pore Structures

Micro-pore structures of a cordierite filter were examined by a high-resolution stereo-microscope and image processing software (see Figure 6). The filter specimens were polished with a depth of 5 micrometers for the observation. The two-dimensional (2-D) images were then reconstructed to make a three-dimensional (3-D) image and analyze the subsequent 2-D images at desired cross sections. The analysis was conducted to evaluate the total pore area, perimeter, circularity, Feret ratio, and finally propose a way of reducing pressure drop in a filter by finding correlations between the circularity and pore size. For correlations in results between optical and X-ray examinations, refer to publication [3].

Numerical Modeling of Flow Dynamics in Filter Channels

A 3-D computational fluid dynamics code has been developed to predict flow dynamics and pressure drop characteristics in a filter. Flow profiles were predicted for two incoming and two outgoing channels with no soot loading. Prediction of soot deposition and pressure distributions along the channels will be a future plan to be conducted.

Conclusions

Non-isothermal soot oxidation experiments revealed that O_2 and NO_2 effects on soot oxidation are quite significant and temperature dependent. With a constant NO_2 concentration, the increased O_2 concentration significantly enhanced soot oxidation in the temperature range higher than 400°C. In the case of a constant O_2 concentration, increasing the NO_2 concentration promoted soot oxidation in a fairly low temperature range, while the NO_2 effects appeared to be insignificant in the higher temperature range. Each Arrhenius data set exhibited two distinct linear regression lines when NO_2 was present in the mixture. The evaluated activation energy significantly decreased from 153 to 39 kJ/mole with increasing NO_2 concentrations in the low temperature range.

Three consecutive filtration stages were clearly identified: depth filtration, transition filtration, and soot cake formation. Each stage illustrated the different degrees of pressure drop in the filtration process. The regeneration experiments also identified three distinct regeneration stages: the first stage where soot oxidation occurred in deep pores as well as on the wall surface,

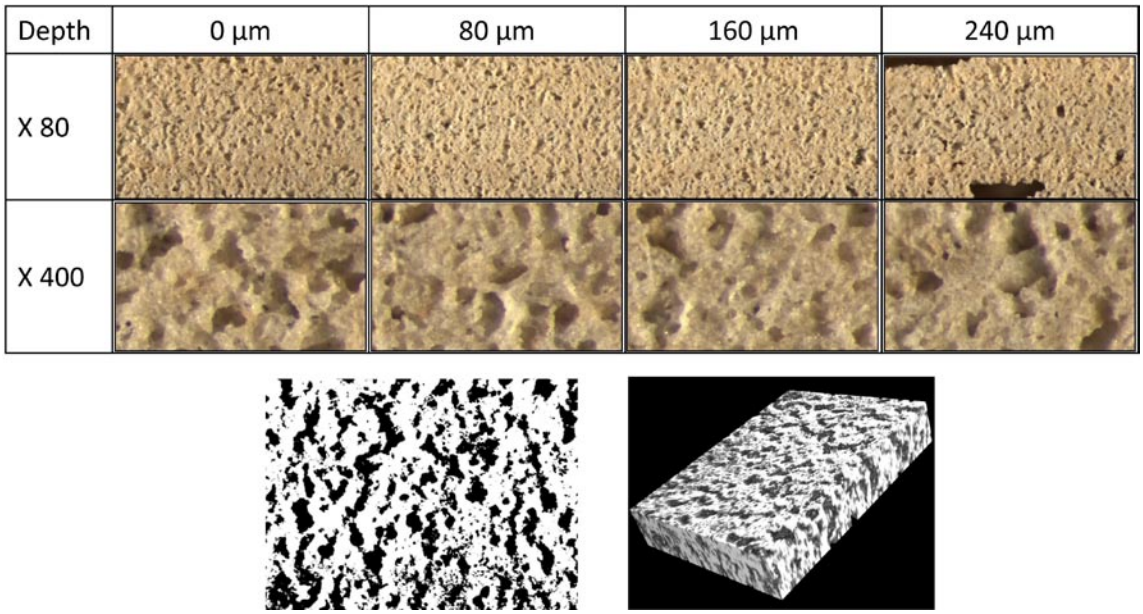

FIGURE 6. Optical images of micro pores of a cordierite DPF filter in 2-D and 3-D (reconstructed).

the second stage where a highest rate of pressure drop appeared with the continuous opening of effective pores, and finally the third regeneration stage where the remaining soot cake was completely cleaned up. The regeneration experiments with three different inlet gas conditions illuminated that corresponding soot oxidation behaviors were quite similar, regardless of inlet gas condition, which were also proved by the microscopic visualization images. Finally, NO_2 significantly promoted soot oxidation in regeneration.

The examination of filter micro-pores by an optical imaging system enabled us to propose the optimal design of filter pore-structures aiming to lowering the pressure drop. The initial 3-D computational modeling showed a potential to further predict soot deposition and pressure distributions along the channels.

References

1. J. Jung, J.H. Lee, S. Song, K.M. Chun, Int J Auto Tech 9:4 (2008) 423-428.

2. S. Choi and K. Lee, 2012 FISITA World Automotive Congress, Beijing, China, Nov. 27-29, 2012.

FY 2012 Publications/Presentations

1. Lee, K., Seong, H., and Choi S.: "Detailed Analysis of Kinetic Reactions in Soot Oxidation by Simulated Diesel Exhaust Emissions," 34th International Symposium on Combustion (2012).

2. H. Seong and K. Lee: "Kinetic Study on Soot Oxidation by Simulated Diesel Gas Emissions," 2012 CLEERS Workshop (2012).

3. Choi, S., Lee, K, and Seong H., "Characterization of Pore Structures in Diesel Particulate Filters by Mercury Intrusion Porosimetry, Optical Imaging, and X-ray Micro-tomography," AFS 2012 Annual Conference (2012).

4. Chong, H., Aggarwal, S., Lee, K., Yang, S., and Seong, H.: "Experimental Investigation on the Oxidation Characteristics of Diesel Particulates Relevant to DPF Regeneration," Journal of Combustion Science and Technology (2012).

III.8 Combination and Integration of DPF-SCR After-Treatment

Kenneth G. Rappé (Primary Contact),
Mark L. Stewart, Gary D. Maupin
Pacific Northwest National Laboratory (PNNL)
Post Office Box 999
Richland, WA 99354

DOE Technology Development Manager:
Ken Howden

Overall Objectives

- Develop a fundamental understanding of the integration of selective catalytic reduction (SCR) and diesel particulate filter (DPF) technologies for on-road heavy-duty diesel applications.
- Probe DPF-SCR interactions with a view to proper function and greater integration.
- Determine system limitations and define basic design requirements for efficient onboard packaging and integration with the engine to minimize impact on vehicle efficiency.

Fiscal Year (FY) 2013 Objectives

- Continue working to quantify the effect of the presence of the SCR reactions on the passive soot oxidation activity exhibited in the integrated SCR-DPF system.
- Continue to develop an understanding of how to optimize the passive soot oxidation activity exhibited in the integrated system in the presence of the SCR process, while retaining a high level of SCR activity.
- Develop an intimate understanding of the dynamics of the SCR process in the integrated system.
- Continue developing integrated DPF and SCR technologies (SCRF) model based on input from empirical studies.

Accomplishments

- Developed an understanding of the primary reaction driver(s) in the SCRF system.
- Developed an understanding of strategies that can be employed for facilitating improved passive soot oxidation in the system in the presence of the SCR process.
- Developed the ability to accurately predict how changes in active species concentrations will affect system performance.

Future Directions

- Pursue investigating alternative DPF substrates for inclusion in the technology, including possibly silicon carbide, aluminum titanite, and others. Consider quick screening studies for comparison to cordierite wash coating results.
- Continue to interrogate passive soot oxidation feasibility in the integrated device, including continued parametric investigations interrogating the effect of NO_2, oxides of nitrogen (NOx) ratio, SCR catalyst loading, NH_3:NOx ratio.
- Continue model development activities.

Introduction

Exhaust after-treatment is considered an enabler for widespread adoption of more fuel efficient diesel engines. In the last decade extensive research has resulted in the development and advancement of many after-treatment technologies. However there are still many unanswered questions that relate to how these technologies can work together synergistically, especially when tightly integrated. It is anticipated that in the future there will be a need to minimize the volume and mass of after-treatment systems on ever increasingly more complex truck platforms. However, to date research focused on combining technologies into an integrated system has been relatively sparse. With the inevitable need to consider how SCR and DPF technologies will function in synergy to reduce both NOx and particulate matter (PM), as well as how CO and hydrocarbons (HCs) need to be managed, an integrated investigation and approach is essential. The determination of important synergies will require study both under steady-state and through transient conditions.

Approach

PNNL and PACCAR will execute a project to understand the critical developmental gaps and subsequently close these for a single container DPF-SCR system. The primary thrust in the project is to study the synergies of DPF-SCR systems in order to develop a pathway to a singular catalytic brick that combines

the function of both a DPF-SCR. It is not envisioned that a flow-through monolith would have sufficient contact with PM in order to reach future U.S. heavy-duty diesel engine PM emission regulations. As such, wall flow filters will be the focus of the study. Corning has provided proprietary ultra-high porosity cordierite as the current subject of study for the DPF. BASF has worked intimately with the project to coat the Corning DPF filters with Cu-zeolite SCR catalyst. These samples are the subject of the investigations presented in the work reported on here.

DPF samples were directionally loaded by BASF with the intent to locate the catalyst predominantly on the downstream portion of the filter microstructure. The samples were empirically tested for SCR of NOx and passive soot oxidation. For passive soot oxidation empirical studies, samples were loaded with soot to an initial loading of 4 g/L of soot.

For the SCRF modeling development, a single flat wall was used with exhaust flow in the normal direction to the wall. Channel scale transport effects and axial variations were ignored. A simplified SCR reaction network was employed developed in collaboration with Oak Ridge National Laboratory, and included the NH_3 oxidation reaction, the standard SCR reaction (NO only) and the fast SCR reaction (equimolar NO and NO_2). A simplified porous media model was employed with similar porosity and tortuosity as the SCRF samples used in the empirical studies. Catalyst distribution employed in the model included 90 g/L of SCR catalyst evenly distributed throughout the wall plus 60 g/L of SCR catalyst on the downstream channel wall surface. A Lattice-Boltzmann model was used to solve for the gas flow field. A soot oxidation kinetic model was employed by Messerer et al, 2006. Soot was presented as a cake layer on the upstream channel was surface, and was assumed 50% oxidized.

Results

SCRF modeling efforts were pursued to (i) assist in developing a more intimate understanding of the interactions of the various reaction processes, (ii) attempt to quantify the magnitude of change in the passive soot oxidation process as result of the SCR process and vice versa, and (iii) begin to develop a tool for proper control of a deployed SCRF system. Figure 1 shows the NO, NO_2 and NH_3 species distributions in the inlet channel and across the filter wall as predicted by the SCRF model. With inclusion of the SCR process, this facilitates gradients in the active species concentrations across the wall which facilitates increased component diffusion effects that have significant impact to the system. Specifically for NO_2, increased diffusion effects penetrate upstream into the inlet channel, decreasing NO_2 concentration upstream from the wall. This explains the effect off decreased passive soot oxidation exhibited in the system, even though the soot is located on the upstream portion of the filter wall upstream from the SCR catalyst. Passive soot oxidation is temperature dependent; the model predicts a maximum of ~35% reduction at 350°C as a result of the presence of the SCR process.

A vast amount of empirical studies were performed on the SCRF system to help develop an intimate understanding how the presence of the passive soot oxidation and SCR processes affect one other and compare to each process in the absence of the other.

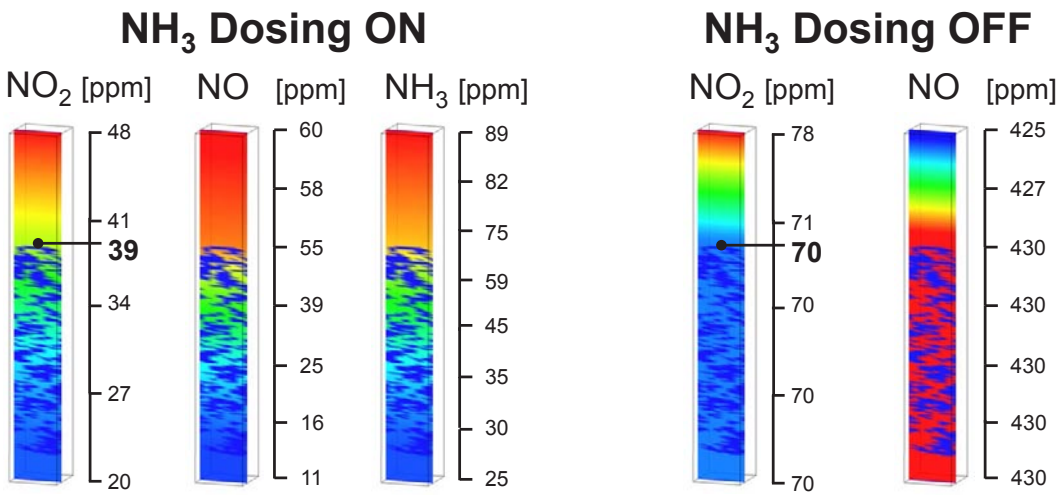

FIGURE 1. NO, NO_2 and NH_3 concentration distributions (in ppm) across the DPF filter wall and in the inlet channel as predicted by the SCRF model in the presence (left) and absence of SCR reactions.

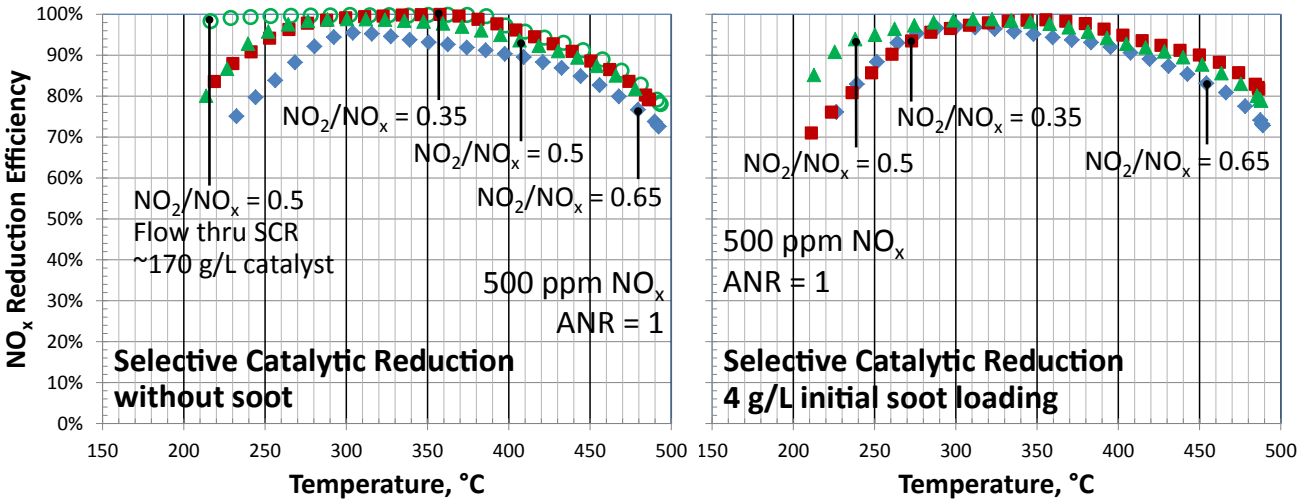

FIGURE 2. SCR NOx reduction performance versus temperature with 4 g/L soot (right) and without soot (left) at 500 ppm NOx, NH_3/NOx (ANR) ratio = 1 and varying NO_2/NOx fraction.

These studies will also be used to help guide the SCRF modeling efforts. Figure 2 shows the results of empirical studies focused on the SCR NOx reduction efficiency performance for the SCRF system. As expected from a Cu-chabazite catalyst, in the absence of soot SCR performance is minimally adversely effected by NO_2 fraction 0.5 and less. However, a detrimental effect of greater than 0.5 is seen. Additionally, a slight detrimental effect of wall flow versus flow through configuration is seen at less than ~275°C.

The presence of soot does not significantly affect the SCR performance of the wall-flow configured system. A slight activity improvement is shown at elevated NO_2 fraction (>0.5). It is expected that this is likely attributed to participation of the passive soot oxidation process and subsequent reduction of NO_2 to bring that NO_2 fraction down.

Temperature programmed oxidation studies were performed to characterize the passive soot oxidation performance of the SCRF. The results of these studies are presented in Figures 3, 4 and 5; Figures 3 and 4 present the data as relative pressure drop across the SCRF sample as a function of temperature. Figure 3 shows the results of varying the NO_2/NOx ratio while keeping the total NOx concentration constant and at a constant NH_3/NOx ratio. With increased NO_2 fraction, improved passive soot oxidation capacity is exhibited in the SCRF system. With a constant NOx concentration, this is facilitated by both an increase in the NO_2 fraction as well as an increase in the total NO_2 concentration.

Figure 4 (in comparison to Figure 3) separates the NO_2 concentration and NO_2 fraction analyses by holding the NO_2 concentration constant and varying the NO_2/NOx fraction by varying the total NOx

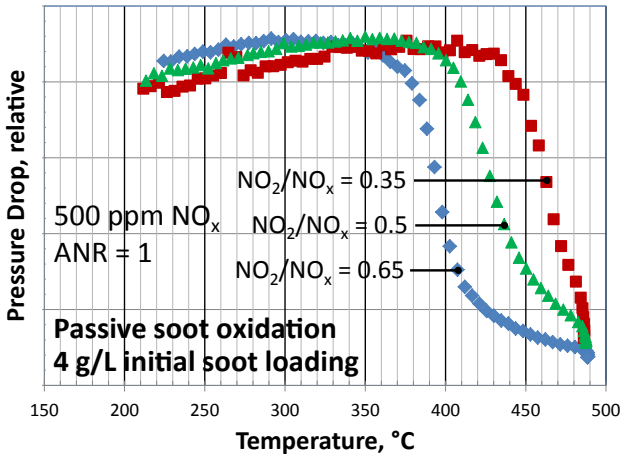

FIGURE 3. Temperature programmed oxidation studies of SCRF at 500 ppm total NOx constant, an ANR = 1, and varying NO_2/NOx fraction, presented as relative pressure drop versus temperature, with 4 g/L initial soot loading.

concentration. The detrimental effect of the presence of the SCR process is obvious by comparing the results of tests conducted with NH_3 dosing versus without. Comparing results of tests conducted in the presence of the SCR process, it can be seen that no improvement in passive soot oxidation is exhibited by the system by increasing NO_2/NOx fraction from 0.33 to 0.5. However, increasing the NO_2/NOx fraction greater than 0.5 results in significant measureable improvement.

To further elaborate upon the results presented in Figure 4, Figure 5 shows the relative makeup of the NOx-slip out of the system from analogous tests. This figure displays the relative fraction of NOx slip that is NO versus NO_2; it does not provide information on total NOx

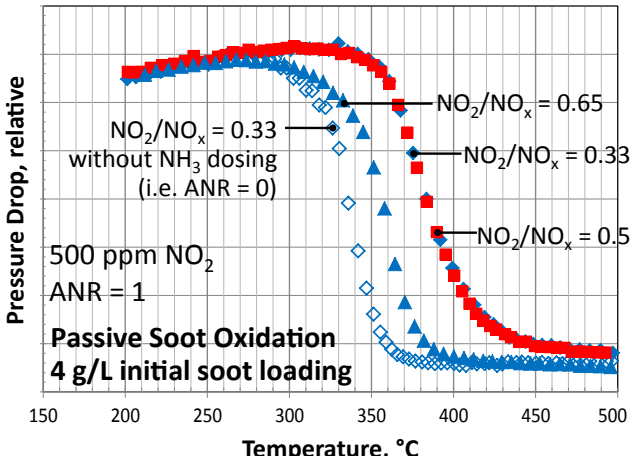

FIGURE 4. Temperature programmed oxidation studies of SCRF at 500 ppm NO_2 constant, an ANR = 1, and varying NO_2/NOx fraction, presented as relative pressure drop versus temperature, with 4 g/L initial soot loading.

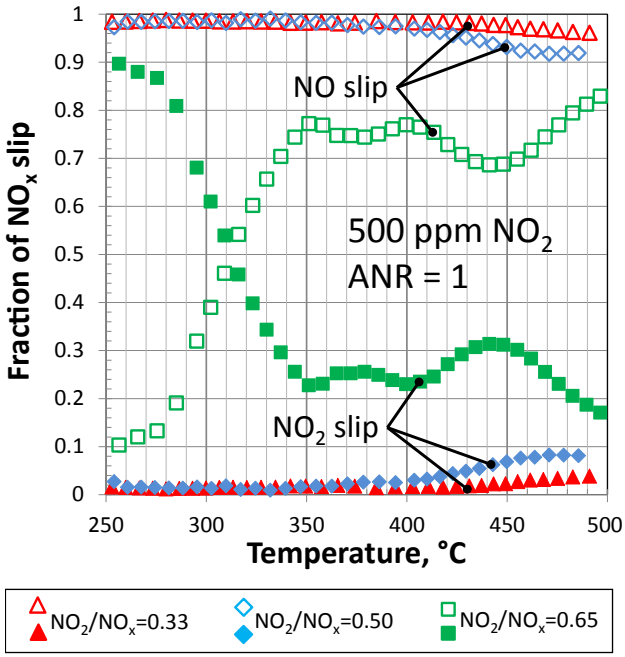

FIGURE 5. Make-up of NOx slip out of SCRF for data in Figure 4, presented as fraction of total NOx slip as a function of the temperature.

slip. At NO_2/NOx fractions of 0.5 and less, the NOx slip is almost entirely NO. However at an NO_2/NOx fraction of >0.5 (0.65), a significantly greater fraction of NO_2 in the NOx slip is observed versus an NO_2/NOx fraction of 0.5 and less.

The passive soot oxidation and SCR processes compete for NO_2 via reaction competition. The results in Figure 3, 4 and 5 demonstrate the importance of the NO_2 balance in the system. Specifically, the results help identify the most significant reaction driver contributing to the NO_2 balance in the system: the fast NO:NO_2 equimolar SCR reaction.

Conclusions

SCRF modeling efforts and empirical studies are helping to provide understanding of fundamental operation of the integrated device. The on-going modeling efforts are helping to gain insight as to how the soot oxidation and SCR processes interact with one another, affecting active species concentration profiles across the filter wall and upstream into the inlet channel. Empirical studies are helping to understand and quantify the primary reaction drivers in the SCRF system. The system is dominated by reaction competition; specifically the fast SCR reaction that consumes equimolar NO:NO_2 is the most significant reaction driver in the SCRF system.

FY 2012 Publications/Presentations

1. K. Rappe, "Combination and Integration of DPF – SCR Aftertreatment Technologies", 2012 DOE Hydrogen Program and Vehicle Technologies Program Annual Merit Review and Peer Evaluation Meeting (Crystal City, VA; May 2012).

2. K. Rappe, G. Muntean, M. Stewart, "PNNL-PACCAR CRADA: SCRF Development", Presentation given to DOW at Pacific Northwest National Laboratory (Richland, WA; September 2012).

3. K. Rappe, "Status: SCRF CRADA", Presentation at PACCAR Technical Center (Mount Vernon, WA; October 2012).

4. K. Rappe, M. Stewart, G. Maupin, "Combination & Integration of DPF – SCR Aftertreatment", 2012 Directions in Engine Efficiency and Emission Research Conference (Dearborn, MI; October 2012).

III.9 Deactivation Mechanisms of Base Metal/Zeolite Urea Selective Catalytic Reduction Materials, and Development of Zeolite-Based Hydrocarbon Adsorber Materials

Feng Gao, Ja Hun Kwak, Jong H. Lee,
Diana Tran, Chuck Peden (Primary Contact)
Institute for Integrated Catalysis
Pacific Northwest National Laboratory (PNNL)
P.O. Box 999, MS K8-93
Richland, WA 99354

DOE Program Manager: Ken Howden

Cooperative Research and Development Agreement (CRADA) Partners: Yisun Cheng, Jason Lupescu, Giovanni Cavataio, Christine Lambert, Robert McCabe;
Ford Motor Company, Dearborn, MI

Overall Objectives

- Develop an understanding of the deactivation mechanisms of the urea selective catalytic reduction (urea-SCR) catalysts used in diesel aftertreatment systems.
- Understand similarities and differences between actual field aging and aging under laboratory conditions, information essential in developing a rapid assessment tool for emission control technology development.
- Determine the role of the various aging factors impacting long-term performance of these catalyst systems, in order to provide information about what operating conditions should be avoided to minimize catalyst deactivation.
- Help fuel-efficient advanced combustion engines meet the current and future hydrocarbon (HC) emission standards with effective, inexpensive and reliable HC adsorber technologies.
- Improve the understanding of interaction between engine-out HCs and HC adsorber materials during the cold-start and the catalyst warm-up periods.

Accomplishments

- Completed studies of the differing effects of SO_2 to SO_3, including identification of the mechanism of poisoning by SO_3.
- Characterized the nature and distribution of phosphorus deposits observed on engine-aged urea SCR catalysts.
- Performed studies aimed at an understanding of unusual hydrothermal aging of zeolite-based urea SCR catalysts observed at Ford.
- Investigated the physicochemical properties of model zeolite materials with respect to hydrothermal aging.
- Evaluated the effects of physicochemical properties of model zeolite materials on the adsorption and desorption of ethanol.

Future Directions

This project was completed in FY 2012.

Introduction

Reducing oxides of nitrogen (NOx) emissions and particulate matter (PM) are primary concerns for diesel vehicles required to meet current Low Emission Vehicle (LEV) II and future LEV III emission standards which require 90+% NOx conversion. Currently, urea-SCR as the NOx reductant [1] and a catalyzed diesel particulate filter (CDPF) are being used for emission control system components by Ford Motor Company for 2010 and beyond diesel vehicles. Because the use of this technology for vehicle applications is new, the relative lack of experience makes it especially challenging to satisfy durability requirements. Of particular concern is being able to realistically simulate actual field aging of the catalyst systems under laboratory conditions. This is necessary both as a rapid assessment tool for verifying improved performance and certifiability of new catalyst formulations, and to develop a good understanding of deactivation mechanisms that can be used to develop improved catalyst materials.

In addition to NOx and PM, the HC emission standards are expected to become much more stringent during the next few years. Meanwhile, the engine-out HC emissions are expected to increase and/or be more difficult to remove. Since HC can be removed only when the catalyst becomes warm enough for its oxidation, three-way catalyst (TWC) and diesel oxidation catalyst (DOC) formulations often contain proprietary zeolite

materials to hold the HC produced during the cold-start period until the catalyst reaches its operating temperature (e.g., >200°C). Unfortunately, much of trapped HC tends to be released before the catalyst reaches the operating temperature. Among materials effective for trapping HC during the catalyst warm-up period, siliceous zeolites are commonly used because of their high surface area and high stability under typical operating conditions. However, there has been little research on the physical properties of these materials related to the adsorption and release of various hydrocarbon species found in the engine exhaust. For these reasons, automakers and engine manufacturers have difficulty improving their catalytic converters for meeting the stringent HC emission standards.

In this collaborative project, scientists and engineers in the Institute for Integrated Catalysis at PNNL and at Ford Motor Company have investigated laboratory- and engine-aged SCR catalysts, containing mainly base metal zeolites. These studies are leading to a better understanding of various aging factors that impact the long-term performance of SCR catalysts and improve the correlation between laboratory and engine aging, saving experimental time and cost. We have also studied materials effective for the temporary storage of HC species during the cold-start period. In particular, we have examined the adsorption and desorption of various HC species produced during the combustion with different fuels (e.g., gasoline, E85 [85% ethanol, 15% gasoline], diesel) over potential HC adsorber materials, and measured the kinetic parameters to update Ford's HC adsorption model.

Since this project has now been completed, in this annual report we will provide very brief summaries of most of the work carried out on this CRADA over the last several years.

Approach

This project has focused on the characterization of catalyst materials used in the urea-SCR and HC absorber technologies with special attention to changes in the materials properties under conditions of laboratory (e.g., oven and laboratory reactor) and realistic (e.g., engine dynamometer and vehicle) aging protocols. Ford has provided both fresh and aged catalyst materials used in the urea-SCR technology, and made experimental measurements of changes in the catalytic performance of these materials before and after the aging. PNNL has utilized state-of-the-art analytical techniques to investigate the surface and bulk properties of these catalysts as well as the changes in these properties induced by the aging process. In particular, catalyst characterization techniques such as X-ray diffraction (XRD), X-ray photoelectron spectroscopy (XPS), transmission electron microscopy (TEM)/energy-dispersive spectroscopy, Brunauer-Emmett-Teller (BET)/pore size distribution, and ^{27}Al solid state nuclear magnetic resonance (NMR) have been utilized to probe the changes in physicochemical properties of SCR catalyst and HC absorber samples after various pretreatments. This work has been performed on a group of model and development catalysts. Specifically, we have utilized a variety of zeolites, a class of microporous aluminosilicate materials that include a wide range of natural minerals. For SCR, Cu-exchanged beta and SSZ-13 zeolite catalysts have been exposed to deactivating conditions; *e.g.*, hydrothermal aging at various temperatures. For HC absorbers, we used candidate catalytic materials that are effective for the temporary storage of HCs produced from different fuels during the cold-start period or advanced combustion processes. Various silicate and aluminosilicate materials, including novel zeolites, were evaluated with respect to hydrophobicity, surface area, pore size and connectivity for the adsorption and desorption of hydrocarbon species found in the engine exhaust. These characterization measurements were complimented by studies at Ford that included performance testing following a variety of laboratory and realistic engine aging protocols.

Results

Physicochemical Investigations of the Degradation Mechanisms for SCR Catalysts

NMR Studies of Hydrothermally Aged Cu/Zeolite SCR Catalysts with Urea: The effects of hydrothermal aging of Cu/zeolite urea-SCR catalysts on their reactivity and material properties was assessed by performance tests and multiple characterization techniques that included ^{27}Al NMR and XRD [2]. Three aging protocols were used that consisted of varying temperature during hydrothermal aging with or without exposure to aqueous urea solution. Differences in behavior were even found for samples hydrothermally aged immediately following exposure to the urea solution or if the sample was dried overnight before hydrothermal aging. The combination of urea and high temperature exposure increased the deactivation of Cu/zeolite SCR catalysts beyond that observed by hydrothermal aging alone, with an immediate high temperature exposure following wetting of the catalyst core with aqueous urea causing the most significant deterioration in performance. The impact of urea on SCR catalyst durability was also found to increase with the aging temperature. NMR analysis suggested that aging with urea resulted in relatively more dealumination of the zeolite for the SCR catalysts in this study.

The Different Impacts of SO_2 and SO_3 on Cu/Zeolite SCR Catalysts: The different impacts of SO_2 and SO_3 on Cu/zeolite SCR catalysts were investigated by SCR performance tests and multiple characterization techniques including temperature programmed desorption (TPD), XPS and X-ray absorption fine structure [3]. The results indicate that a larger amount of highly dispersed $CuSO_4$ formed in the zeolite catalysts (Z-$CuSO_4$) upon SO_3 poisoning, explaining the much more significant deactivation of the Cu/zeolite catalysts that were exposed to SO_3 compared to poisoning by SO_2. In these studies, we provided the first demonstration that active sites of Cu/zeolite SCR catalysts involved in the storage and removal of sulfur can react with SO_2 and SO_3 in very different ways. In particular, the significant differences in the extent of sulfur uptake account for the considerably different impacts of SO_2 and SO_3 poisoning on the performance of Cu/zeolite SCR catalysts. The Cu/zeolite SCR catalyst used in this study was a fully-formulated cordierite monolith with Cu/zeolite washcoat from a catalyst supplier.

Non-Uniform Aging on Super-Duty Diesel Truck Aged Cu/Zeolite Urea SCR Catalysts: Previous studies have shown that deactivation of engine aged SCR catalysts is not uniform, with the inlet section of the catalyst brick deactivating the most. To better understand this non uniform aging phenomena, a set of Cu/zeolite SCR catalysts aged for 50,000 miles on a super-duty diesel truck were investigated with postmortem analyses emphasizing studies of the inlet section [4,5]. The analyses included catalyst activity evaluation and catalyst characterization, such as BET surface area, TPR, XRF, XPS and TEM. The results suggest that the inlet section of the brick experienced all the aging factors in the most severe way, and that this section deactivates in a more complicated manner than the rest of the brick which mainly deteriorated due to hydrothermal aging. This is demonstrated in Figure 1 which shows a comparison of steady-state SCR NOx conversion of cores taken from the middle of the brick, labeled as "M", from the 1st, 2nd, 3rd, and 5th inch of inlet gas direction. Changes of Cu state and high levels of C, P and Zn impurities in very front region might explain the more severe deactivation of the inlet section of the SCR catalyst. For example, Figure 2 shows the levels of these three impurities as a function of distance from the front of the catalyst monolith obtained by XPS.

Unusual Performance Behavior for Cu-zeolite SCR Catalysts After Mild Hydrothermal Aging: The hydrothermal stability of Cu/beta NH_3 SCR catalysts, with respect to their interesting ability to maintain and even enhance high-temperature performance for the "standard" SCR reaction after modest (900°C, 2 hours) hydrothermal aging, was studied [6]. Characterization of the fresh and aged catalysts was performed with an

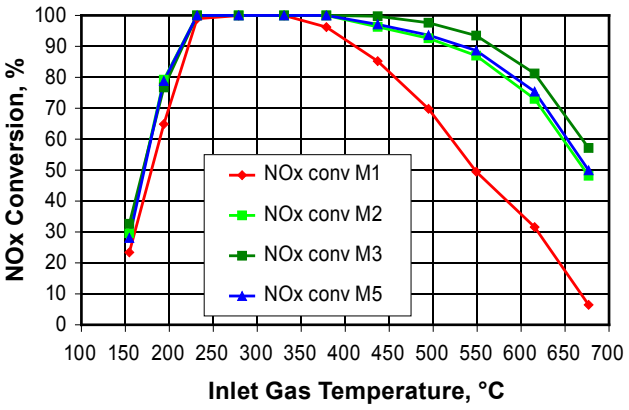

FIGURE 1. Steady-state NOx conversions of engine-aged Cu/CHA SCR catalysts.

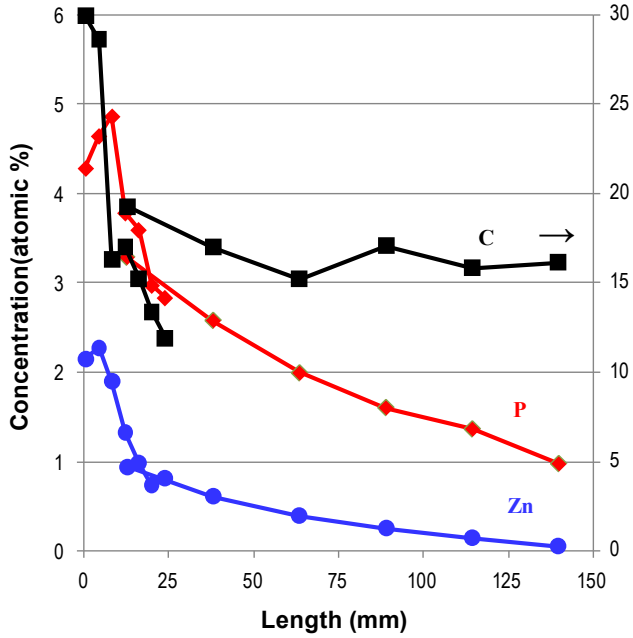

FIGURE 2. XPS intensities of carbon (C), phosphorus (P), and zinc (Zn) as a function of distance from the front of a vehicle aged (50,000 miles) Cu/zeolite SCR catalyst.

aim to identify possible catalytic phases responsible for the enhanced high temperature performance. In particular, XRD, TEM and ^{27}Al NMR all showed that the hydrothermal aging conditions used in our studies resulted in almost complete loss of the beta zeolite structure between 1 and 2 hours aging. While the ^{27}Al NMR spectra of 2 and 10 hour hydrothermally-aged catalysts showed significant loss of a peak associated with tetrahedrally-coordinated Al species, no new spectral features were evident. Two model catalysts, suggested by these characterization data as possible mimics of the catalytic phase formed during

hydrothermal aging of Cu/beta, were prepared and tested for their performance in the "standard" SCR and NH_3 oxidation reactions. The similarity in their reactivity compared to the 2-hour hydrothermally-aged Cu/beta catalyst suggests possible routes for preparing multi-component catalysts that may have wider temperature windows for optimum performance than those provided by current Cu/zeolite catalysts.

Deactivation of Cu/Zeolite SCR Catalysts Caused by Phosphorous: A specific role for phosphorus in the loss of SCR performance of Cu/Zeolite was investigated by reactivity tests and catalyst characterization measurements as a function of aging conditions with and without phosphorus [7]. While these studies were not completed during the project, they did demonstrate a possible concern if significant quantities of this species accumulated on the SCR catalyst as a result of the breakdown of engine lubricants. In particular, addition of small amounts of phosphorus species to the gas mixture used during laboratory aging resulted in a small but significant drop in NOx reduction performance at both low and high temperatures for a state-of-the-art Cu/zeolite catalyst. ^{31}P NMR studies tentatively identified two types of phosphorus species that are present as a function of impurity P levels. This is demonstrated in ^{31}P NMR spectra shown Figure 3 for samples that were aged in low (black curve) and high (red curve) P levels. At low levels, the P species appears to be in the form of a monomeric phosphate-like species while the spectrum obtained for the sample with higher P levels is consistent with the presence of a bulk-like phosphate species.

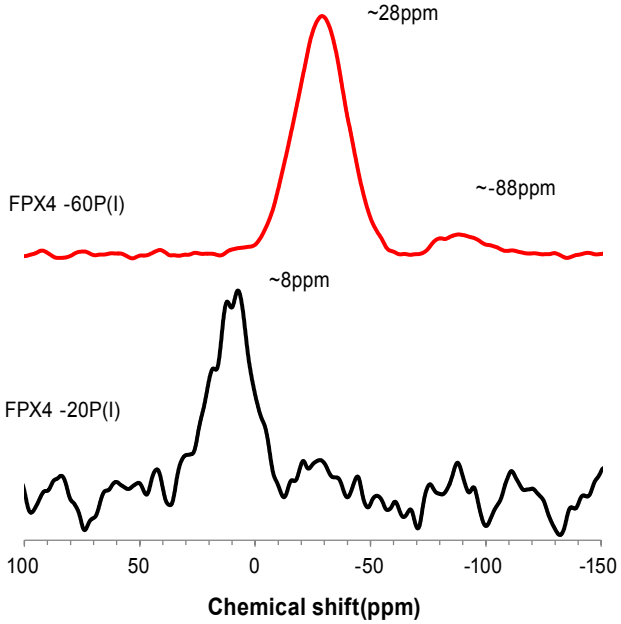

FIGURE 3. ^{31}P solid state NMR spectra of a state-of-the-art Cu/zeolite after laboratory aging with various levels of P in the feed: low (black curve) and high (red curve) P loading.

Physicochemical Investigations of HC Absorber Materials

For the last two years of this project, HC adsorbers have been investigated with a focus on understanding the effects of various physicochemical properties of zeolite materials. In particular, three model zeolite materials were obtained to probe the effects of different pore size and connectivity: beta (large pore, three-dimensional pore connectivity); ZSM-4 (medium pore, three-dimensional pore connectivity); and ZSM-12 (large pore, one-dimensional pore structure). The effects of hydrothermal aging on their physicochemical properties were then examined using various analytical techniques, including XRD and NH_3-TPD. Studies of performance as a function of laboratory aging conditions were carried out at Ford using complex, realistic mixtures of hydrocarbons of various types. At PNNL, detailed catalyst characterization was performed in addition to model studies of performance with gas mixtures containing a single hydrocarbon type. As an example of the studies performed, Figure 4 shows TPD data obtained after exposure of a beta zeolite material to ethanol. Both unreacted ethanol (EtOH) and a reaction product, ethylene (C_2H_4), were observed in the TPD data. Figure 4 also shows that the amount of these two species on the zeolite depends on the order of water and ethanol exposure, with a post-dose of water leading to the removal of a significant fraction of the adsorbed hydrocarbon species (EtOH and C_2H_4) [8].

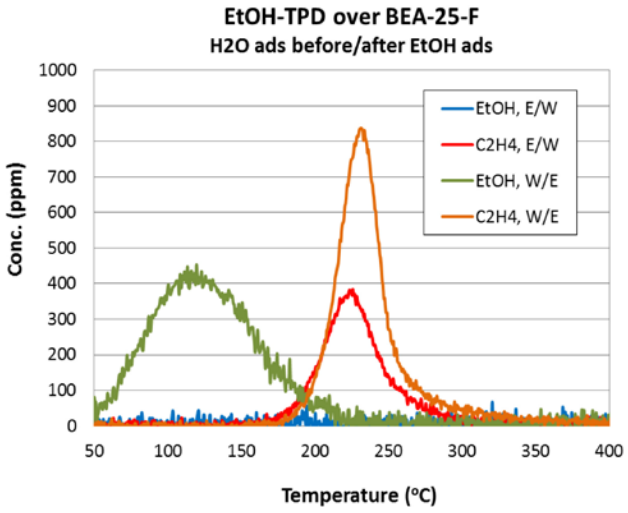

FIGURE 4. TPD data obtained after exposure of a beta-zeolite material to ethanol at room temperature. Ethanol exposures were performed before (E/W) and after (W/E) a separate water exposure to probe the relative stability of these two species.

Conclusions

PNNL and its CRADA partners from Ford have carried out a project to study the properties and mechanisms of deactivation of SCR and HC-absorber materials arising from thermal aging. Because the catalytically active sites certainly include isolated and very small (even mono-atomic) ion-exchanged metals in the zeolite cages, we have pursued a molecular-level understanding of the deactivation mechanisms related to the activity degradation by using a number of state-of-the-art catalyst characterization techniques. The effects of hydrothermal aging on physicochemical properties of model zeolite hydrocarbon trap materials have also been examined. In particular, the adsorption and desorption of ethanol on model zeolite materials were investigated with respect to physicochemical properties.

References

1. S. Brandenberger, O. Krocher, A. Tissler, R. Althoff, Catal. Rev.-Sci. Eng. 50 (2008) 492-531.

2. Y. Cheng, J. Hoard, C. Lambert, J.H. Kwak, C.H.F. Peden, *Catalysis Today* 136 (2008) 34-39.

3. Y. Cheng, C.K. Lambert, D.H. Kim, J.H. Kwak, S.J. Cho, C.H.F. Peden, *Catalysis Today* 151 (2010) 266-270.

4. Y. Cheng, H. Jen, M. Jagner, C.K. Lambert, J.H. Kwak, D.H. Kim, C.H.F. Peden, Oral presentation made by Yisun Cheng at the *2010 DEER Conference* (September, 2010).

5. Y. Cheng, M. Jagner, H. Jen, C.K. Lambert, J.H. Kwak, D.H. Kim, C.H.F. Peden, Oral presentation made by Yisun Cheng at the *22nd Meeting of the North American Catalysis Society* (June, 2011).

6. C.H.F. Peden, J.H. Kwak, S.D. Burton, R.G. Tonkyn, D.H. Kim, J.H. Lee, H.W. Jen, G. Cavataio, Y. Cheng, C.K. Lambert, *Catalysis Today* 184 (2012) 245-251.

7. Y. Cheng, D. Dobson, C.K. Lambert, J.H. Kwak, C.H.F. Peden, unpublished results.

8. J.H. Kwak, J.H. Lee, C.H.F. Peden, D.N. Tran, Y. Cheng, J. Lupescu, G. Cavataio, C. Lambert, R. McCabe, presentation made by Chuck Peden at the *DOE Combustion and Emission Control Review* (May, 2012).

FY 2012 Publications/Presentations

1. C.H.F. Peden, J.H. Kwak, S.D. Burton, R.G. Tonkyn, D.H. Kim, J.H. Lee, H.W. Jen, G. Cavataio, Y. Cheng, and C.K. Lambert, "Possible Origin of Improved High Temperature Performance of Hydrothermally-Aged Cu/Beta Zeolite Catalysts", *Catalysis Today* **184** (2012) 245-251.

2. J.H. Kwak, J.H. Lee, D.H. Kim, S. Li, D.N. Tran, C.H.F. Peden, K. Howden, Y. Cheng, J. Lupescu, G. Cavataio, C. Lambert, R. McCabe, "Deactivation Mechanisms of Base Metal/Zeolite Urea Selective Catalytic Reduction Materials, and Development of Zeolite-Based Hydrocarbon Adsorber Materials", in *Advanced Combustion Engine Research and Development: FY2011 Annual Progress Report*, 231-237.

3. J.H. Kwak, J.H. Lee, C.H.F. Peden, D.N. Tran, Y. Cheng, J. Lupescu, G. Cavataio, C. Lambert, R. McCabe, "Deactivation Mechanisms of Base Metal/Zeolite Urea Selective Catalytic Reduction Materials, and Development of Zeolite-Based Hydrocarbon Adsorber Materials", presentation at the DOE Combustion and Emission Control Review, Washington, DC, May, 2012.

III.10 Fuel-Neutral Studies of PM Transportation Emissions

Mark Stewart (Primary Contact), Alla Zelenyuk
Pacific Northwest National Laboratory
902 Battelle Boulevard
Richland, WA 99352

DOE Technology Development Manager:
Ken Howden

Subcontractors:
- University of Wisconsin Engine Research Center, Madison, WI
- Pennsylvania State University, University Park, PA

Overall Objectives

- Systematically characterize particulates generated by single-cylinder test engines, guided by industry.
- Seek to shorten development time of filtration technologies for future high-efficiency engines.
- Develop modeling approaches relevant to the likely key challenge for spark ignition direct injection (SIDI) filtration – high number efficiency at high exhaust temperatures.

Fiscal Year (FY) 2012 Objectives

- Conduct second round of cooperative experiments at University of Wisconsin Engine Research Center (ERC):
  - Collect detailed particulate data from SIDI test engine running on gasoline and ethanol blends.
  - Collect particulate data from gasoline direct-injection compression ignition (GDICI) test engine.
  - Examine soot from reactivity-controlled compression ignition (RCCI) test engine.
- Evaluate the suitability of commonly used unit collector models for design of gasoline particulate filtration systems to meet number regulations.
- Explore the use of micro-scale simulations to improve device scale modeling and assist in the development of filter systems for advanced gasoline vehicles.

Accomplishments

- Extensive particulate characterization using advanced test engines:
  - Two cooperative campaigns with University of Wisconsin ERC
  - Four fuel blends examined to date, including E20, E85 (20% and 85% ethanol in gasoline, respectively)
  - Three engine technologies: SIDI, RCCI, and GDICI
  - Dozens of experiments at various relevant engine operating points
- Aftertreatment technology development:
  - Effect of filter coatings on filtration performance has been evaluated
  - Improved unit collector models have been applied for prediction of number efficiency
  - Pore-scale simulations have been carried out to evaluate potential filter technologies

Future Directions

- Complete analysis of second campaign data and publish findings.
- Employ micro-scale modeling to explore other possible approaches to achieve high filtration efficiency in high temperature exhaust.
- Use improved unit collector models to explore tradeoffs between parameters such as number efficiency, backpressure, and unit volume in SIDI applications.
- Conduct experiments to evaluate candidate filter technologies for SIDI.
- Apply advanced particulate characterization to subsequent generations of engines – leaner operation, higher fuel efficiency.

Introduction

New gasoline engine technologies such as SIDI, GDICI, and RCCI offer the possibility of dramatically increasing the fuel efficiency of future vehicles. One drawback to these advanced engines is that they have the potential to produce higher levels of exhaust particulates than current port fuel injection (PFI) engines. Regulation of engine particulate emissions in Europe is moving from mass-based standards toward number-based standards. Due to growing health concerns surrounding nano-aerosols, it is likely that similar standards will eventually be applied in the United States. This would place more

emphasis on the reliable removal of smaller particles, which make up the vast majority of the particulates generated on a number basis. While diesel particulate filters (DPFs) have become standard, different filter systems would likely be required for advanced gasoline vehicles, due to factors such as differing particulate properties and higher exhaust temperatures. High exhaust temperatures can limit the accumulation of a soot cake, which performs most of the actual filtration in a typical DPF system.

Approach

The first phase of this effort has focused on characterization of particulates from advanced combustion engines, especially SIDI gasoline engines. To that end, a wide variety of standard and advanced techniques were applied to examine particulate size, shape and composition. These included in-line aerosol methods as well as advanced particle-by-particle analysis including high resolution transmission electron microscopy (HRTEM) and other techniques.

The second stage of the project will focus on development of mitigation technologies through targeted filtration experiments and modeling efforts. Optimal design of filter systems to meet number limits would require accurate prediction of filtration efficiency across the whole particle size range seen in engine exhaust. Standard unit collector models commonly used for design of DPFs were evaluated against this criterion, as well as models modified using input from micro-scale filter simulations. Micro-scale simulations were also carried out to demonstrate the effect of coatings on filtration efficiency.

Results

A second campaign of cooperative experiments was carried out at the University of Wisconsin ERC. Several SIDI experiments conducted during the first campaign with ethanol-free gasoline were repeated to confirm consistency with previous results. New experiments were also carried out at a number of operating points using E20 and E85 ethanol blends. In addition to SIDI, a smaller number of experiments were also carried out with GDICI and RCCI test engines.

The SIDI test engine at the University of Wisconsin ERC was rebuilt and upgraded between the first and second experimental campaigns. Nevertheless, most observations from the first round of experiments were confirmed and expanded in the second. The diameter of the primary spherules which made up the fractal exhaust particles was again observed to vary over a wide range. This can be seen in Figure 1, which shows the

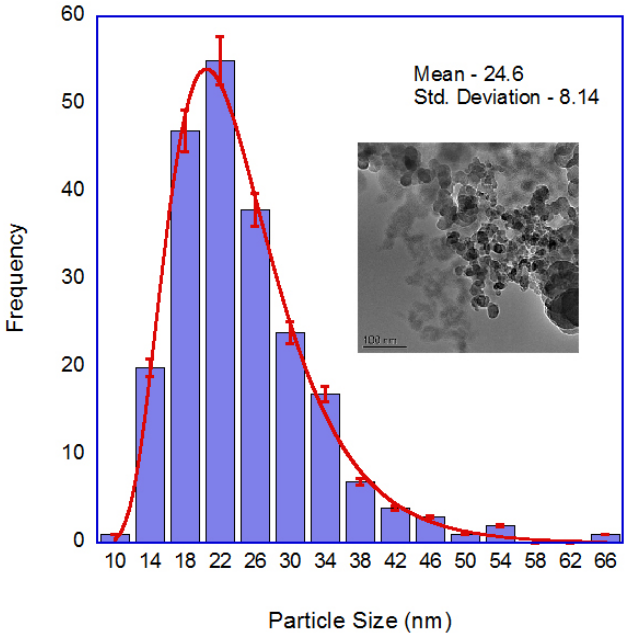

FIGURE 1. Primary Particle Size Distribution in SIDI Exhaust Under Heavy-Load Conditions

primary particle size distribution from a low-resolution TEM survey for a heavy load condition. Most of the primary particle size populations observed were well fit by log-normal distributions. Both the means and standard deviations varied significantly between different operating conditions.

SIDI particle aggregate size and shape were again observed to vary significantly as a function of engine operating parameters. Figure 2 shows particulate mobility size distributions at various end of injection (EOI) times. The total number of particles observed passed through a minimum at around 250° before top-dead center (bTDC). The figure also shows the lower size limit for particle counting defined in the European Particle Measurement Program at 23 nm and the approximate lower size limit of the SPLAT II instrument, which provides particle vacuum aerodynamic diameter and composition. It can be observed that the particle size distribution may peak at or below the European Particle Measurement Program (PMP) lower size limit. Diesel particulate mobility size distributions generally peak at somewhat larger sizes, with relatively fewer particles at the small end [1].

Ethanol blends generally resulted in lower SIDI particulate production, as exemplified in Figure 3, which shows a similar EOI sweep with E85. Particulate production again varied with EOI, but the trend was somewhat different. SPLAT mass spectra showed high proportions of organics in all of the SIDI soot, but

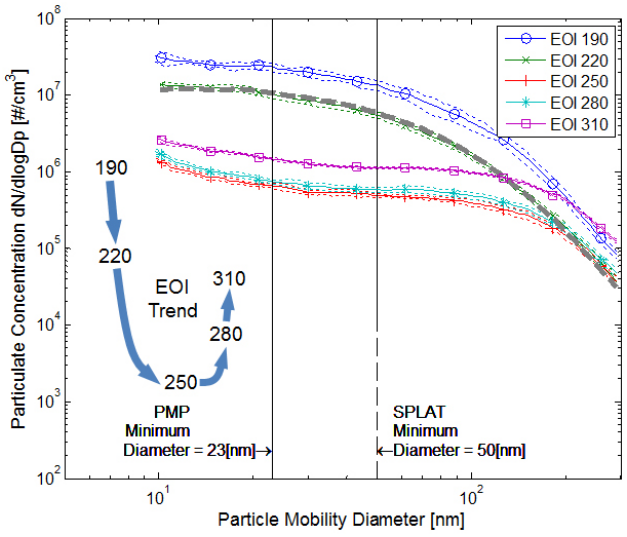

FIGURE 2. SIDI Particle Mobility Size Distributions from E0

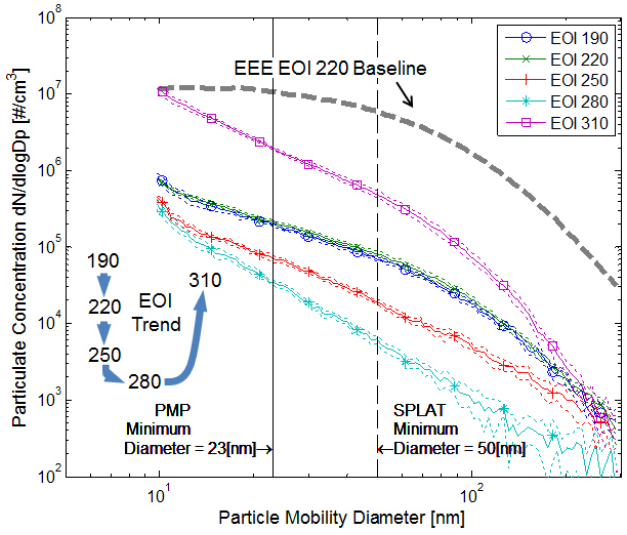

FIGURE 3. SIDI Particle Mobility Size Distributions from E85

organics were considerably higher in the particulates produced by ethanol blends. For example, during medium rail pressure experiments, organic plus polycyclic aromatic hydrocarbon content comprised 77% of particulate mass from E85, 57% from E20, and 46% from E0.

X-ray photoelectron spectroscopy and attenuated total reflectance fourier transform infrared spectroscopy conducted at Pennsylvania State University confirmed the high organic content of SIDI soot particles and suggested that the organics are distributed throughout the soot primary particles, rather than present as a film on top of an inorganic carbon framework. This conclusion was also supported by the highly amorphous nano-

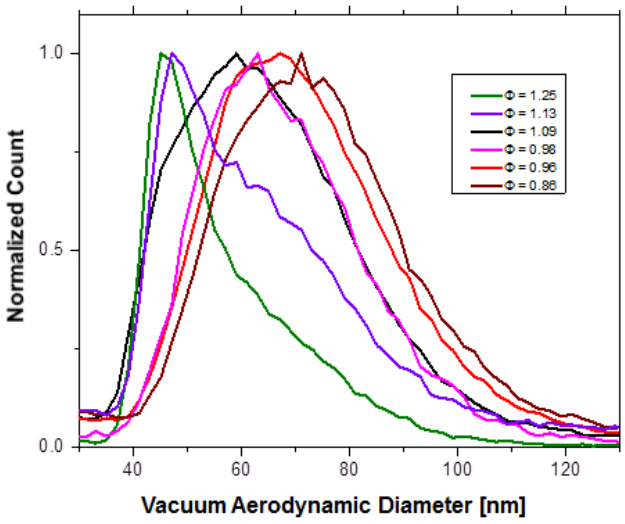

FIGURE 4. Normalized SIDI Vacuum Aerodynamic Size Distributions

structure of primary particles observed by HRTEM, and by the previously observed difficulty in removing the organics by volatilization [2].

Under some experimental conditions, two distinct modes could be observed in the vacuum aerodynamic diameter distributions. Figure 4 shows normalized aerodynamic size distributions from E20 experiments at various equivalence ratios (Φ). Lower equivalence ratios resulted in larger aerodynamic diameters, while higher equivalence ratios resulted in smaller diameters. At intermediate points, the aerodynamic size distribution could be represented as a sum of the two distinct modes. Similar behavior was observed for EOI sweeps with E0. SPLAT mass spectra indicate that the compositions of the two modes are nearly identical. Fractal dimension and average primary particle size can be calculated from vacuum aerodynamic size distributions of mobility-selected particles. The two modes were found to have similar fractal dimensions, with significantly different mean primary particle sizes. Judging from the engine operating conditions under which the two modes appear, it is thought that regions of rich air/fuel mixture may lead to particulates with smaller primary particles, while the larger primary particles may be linked to wall/piston impingement.

In addition to SIDI, experiments were performed with two other test engines at the University of Wisconsin, Madison. The GDICI engine operates in a manner similar to a diesel cycle engine. GDICI particulate matter (PM) varied significantly in character depending upon engine load. Under low-load conditions PM is dominated by compact organic particles with smaller (~30%) contribution of fractal soot particles with average primary spherule diameter of 40 nm.

Under high-load conditions, PM consists of fractal soot agglomerates with nearly identical fractal dimension but smaller spherule diameter (26 nm). The RCCI engine injects gasoline and diesel separately. Like SIDI engines, this engine produced fractal particles with primary spherules of widely varying sizes. Under one of the test conditions examined, the particulates exhibited some unusual hollow structures (Figure 5), possibly indicating a somewhat different soot formation mechanism than is typically observed in other internal combustion engines.

The ability of classical unit collector filter models [3] to predict filtration efficiency over the particle size ranges observed in SIDI exhaust was evaluated by comparing with experimental data. It was found that the classical form of the model over-predicts the removal efficiency of the small particles which dominate number counts. An alternate form of the diffusion term, which was developed using micro-scale simulations [4], was found to describe the experimental data better. This alternate form of the unit collector model was then used to help evaluate the benefit of filter coatings and conduct parametric studies to show how filtration efficiency could be expected to change as the result of changes in substrate parameters such as porosity and pore size.

Micro-scale simulations can also be used directly to explore filter technology options and illustrate trends and mechanisms. Figure 6 shows the results of four lattice-Boltzmann filter simulations of a cordierite filter wall coated on the upstream surface with various thicknesses of a fine-grained material. The particle-laden exhaust is flowing downward through the porous wall cross-section. The smaller pores and higher surface area of the coating make it more effective than the base substrate at removing the small particles (100 nm mobility diameter) considered in these simulations. The uncoated filter has an overall diffusion capture efficiency of 37% for this particle size, while the thickest coating results in an efficiency of 51%.

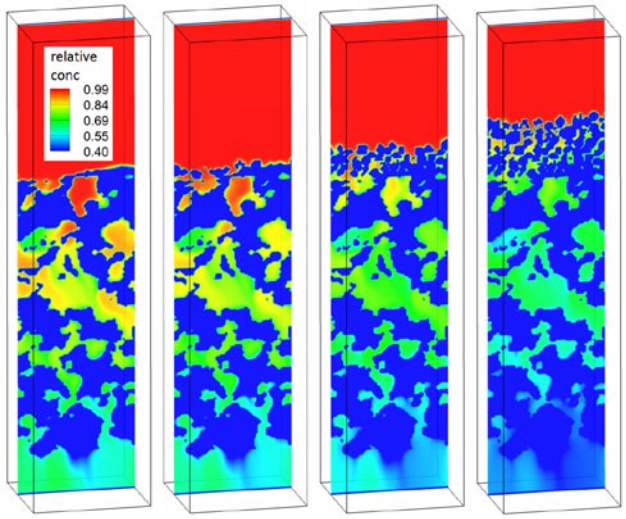

FIGURE 6. Micro-Scale Simulations of Cordierite Filters with Surface Coatings

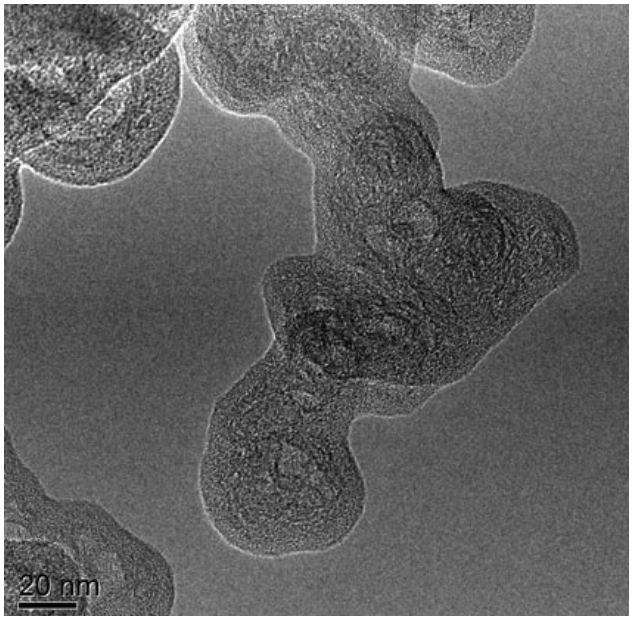

FIGURE 5. HRTEM Image of RCCI Particulates

Conclusions

- Primary particle size and aggregate morphology in SIDI particulates are highly variable and depend upon engine operation.
- SIDI soot resulting from all fuels tested had very high organic content, which was tightly integrated with the inorganic carbon.
- Ethanol blends generally produced fewer particles with higher proportions of integrated organics.
- Two distinct modes were observed in SIDI primary particle size under some conditions, suggesting two separate particle formation regimes.
- The RCCI test engine produced soot which generally looked similar to that observed in SIDI exhaust.
- The nature of GDICI particulates was very dependent on engine load, with relatively large numbers of hydrocarbon droplets under low load conditions.
- Modified unit collector models appear to better describe experimental data on size-dependent filtration efficiency than the classical models.
- The effect of coatings on filtration efficiency could play an important role in filter system design for future high-efficiency vehicles.

References

1. Kolodziej, C., E. Wirojsakunchai, D.E. Foster, N. Schmidt, T. Kamimoto, T. Kawai, M. Akard, and T. Yoshimura, "Comprehensive Characterization of Particulate Emissions from Advanced Diesel Combustion". *SAE*, 2007. 2007-01-1945.

2. Matthias, N., C. Farron, D. Foster, M. Andrie, R. Krieger, P. Najt, K. Narayanaswamy, A. Solomon, and A. Zelenyuk, "Particulate Matter Sampling and Volatile Organic Compound Removal for Characterization of Spark Ignited Direct Injection Engine Emissions". *2011 JSAE Powertrains, Fuels and Lubricants*, 2011. JSAE 20119383, SAE 2011-01-2100.

3. Konstandopoulos, A. and J.H. Johnson, "Wall-Flow Diesel Particulate Filters - Their Pressure Drop and Collection Efficiency". *SAE*, 1989. 890405.

4. Long, W. and M. Hilpert, "A Correlation for the Collector Efficiency of Brownian Particles in Clean-Bed Filtration in Sphere Packings by a Lattice-Boltzmann Method". *ENVIRONMENTAL SCIENCE & TECHNOLOGY*, 2009. 43(12): p. 4419-4424.

FY 2012 Publications/Presentations

1. A Strzelec, TJ Toops, CS Daw, R Vander Wal, "Trends in Particulate Nanostructure," Directions in Engine-Efficiency and Emissions Research Conference, Detroit, MI, October 2011.

2. Beranek, J., D. Imre, et al. (2012). "Real-Time Shape-Based Particle Separation and Detailed in Situ Particle Shape Characterization." Analytical Chemistry 84(3): 1459-1465.

3. ML Stewart, "Exhaust Filtration for High Number Efficiency," DOE CLEERS Workshop, Dearborn, MI, April 2012.

4. ML Stewart. "Fuel-Neutral Engine Particulate Filtration Studies", General Motors Technical Center, Warren, MI, April 2012.

5. CK Gaddam, RL Vander Wal, "Emissions from Ethanol – Gasoline Blends: Physical & Chemical Characterization of SIDI Particulates," DOE CLEERS Workshop, Dearborn, MI, April 2012.

6. ML Stewart, "Fuel-Neutral Studies of Particulate Matter Transport Emissions", 2012 DOE Hydrogen and Vehicle Technologies Merit Review, Washington, DC, May 2012.

7. A Zelenyuk, P Reitz, ML Stewart, M Hageman, A Maier, S Sakai, D Foster, D Rothamer, M Andrie, R Krieger, K Naranayaswami, P Najt, A Solomon, "Characterization of Pre-commercial Gasoline Engine Particulates Through Advanced Aerosol Methods," Directions in Engine-Efficiency and Emissions Research Conference, Detroit, MI, October 2012.

Acknowledgements

General Motors Corporation: Kushal Naranayaswamy, Paul Najt, Arun Solomon, Michael Viola, Wei Li

University of Wisconsin Madison: David Foster, David Rothamer, Matthew Coyne, Michael Andrie, Mitchell Hageman, Roger Krieger, Axel Maier, Stephen Sakai, Rolf Reitz, Nicholas Ryan Walker

Pennsylvania State University: Randy Vander Wal, Chethan Kumar Gaddam

PNNL: Andrea Strzelec, Josef Beranek, Paul Reitz, John Lee, Shelley Carlson, Maruthi Devarakonda, Sarah Suffield

A portion of the research was performed using EMSL, a national scientific user facility sponsored by the Department of Energy's Office of Biological and Environmental Research and located at Pacific Northwest National Laboratory.

III.11 Investigation of Mixed Oxide Catalysts for NO Oxidation

Larry R. Pederson (Primary Contact),
Ja Hun Kwak, Donghai Mei, Darrell R. Herling,
George G. Muntean, Charles H.F. Peden
Pacific Northwest National Laboratory (PNNL)
902 Battelle Blvd, P.O. Box 999
Richland, WA 99352

DOE Technology Development Manager:
Ken Howden

Overall Objectives

- Develop and demonstrate mixed metal oxide-based catalysts as a low-cost replacement for platinum in the oxidation of NO to NO_2 in lean engine exhaust, an essential first step in controlling oxide of nitrogen (NO_x) emissions.
- Improve the understanding of the nature and structure of active sites of mixed metal oxide catalysts for NO oxidation in diesel oxidation (DOC) and lean-NO_x trap (LNT) catalysts.

Fiscal Year (FY) 2012 Objectives

- Determine the structure and active site density for fresh and laboratory-aged mixed metal oxide catalysts prepared by partner General Motors (GM).
- Investigate the mechanism of reaction between NO and O_2 on mixed metal oxide catalysts, including the effects of metal oxide substitution and catalyst aging.
- Perform computational studies, including density function theory (DFT) calculations, to probe interactions between reactants and potentially active sites.

Accomplishments

- Identified mixed metal oxide catalyst compositions and forms that show high activity for NO oxidation, and may serve as a suitable replacement for platinum-based catalysts for exhaust gas treatment.
- Demonstrated that the ceria support both decreased the required temperature for formation and increased the quantity of labile oxygen needed for NO oxidation.
- Showed that mixed metal oxide catalysts produced using a simple incipient wetness method compared favorably to those prepared by co-precipitation.
- Established DFT methods to help investigate interactions between reactants and potentially active sites.

Future Directions

- Optimize mixed metal oxide catalyst compositions and forms for NO oxidation, to enable the noble metal content of DOC and LNT catalysts to be reduced or eliminated.
- Perform a detailed characterization of mixed metal oxide catalysts using state-of-the-art analytical and computational techniques to develop a thorough understanding the nature of active centers on those catalysts.

Introduction

The oxidation of engine-generated NO to NO_2 is an important step in the reduction of NO_x in lean engine exhaust because NO_2 enhances the activities of both ammonia selective catalytic reduction (SCR) [1] and LNT [2]. For SCR catalysts, an NO: NO_2 ratio of 1:1 is most effective for NO_x reduction, whereas for LNT catalysts, NO must be oxidized to NO_2 before adsorption on the storage components. However, NO_2 typically constitutes less than 10% of NO_x in lean exhaust, so catalytic oxidation of NO is essential. Platinum has been found to be especially active for NO oxidation, and is widely used in diesel oxidation and LNT catalysts. However, because of the high cost and poor thermal durability of Pt-based catalysts, there is substantial interest in the development of alternatives. The objective of this project, in collaboration with partner General Motors, is to develop mixed oxide catalysts for NO oxidation, enabling lower precious metal usage in emission control systems.

Approach

This Cooperative Research and Development Agreement (CRADA) project with GM and PNNL is aimed at replacing or reducing platinum usage in DOC and LNT catalysts, and was initiated in 2012. This project builds on success achieved recently by GM researchers, who reported excellent NO oxidation efficiency over substituted lanthanum-based mixed oxides, such as $LaCoO_3$ and $LaMnO_3$, when compared to a commercial Pt-based DOC [2].

Well-coordinated and complementary research activities are being performed at GM and PNNL. The principal focus of GM research is on catalyst formulation, evaluation of catalytic activity under conditions relevant to lean engine exhaust, and catalyst aging. State-of-the-art analytical and computational techniques are applied at PNNL to characterize the structure of the catalysts and to determine the concentration and nature of active sites. Surface and bulk properties of catalyst materials are established as a function of catalyst composition, and correlated to trends in catalytic activity. Computational analyses of active sites and possible reaction mechanisms are probed using DFT, which provides information concerning the interaction between reactants and active sites. It is anticipated that this research will lead to the development of low-cost, durable, and active catalysts for the oxidation of NO to NO_2.

Results

Mixed metal oxide catalysts containing manganese and cerium oxides were identified that show significant activity for NO oxidation. The catalysts were prepared at GM by co-precipitation methods and at PNNL by an incipient wetness method, and their structure and catalytic properties evaluated. The mixed metal oxides formed a single crystalline phase, with no evidence of phase separation. The surface areas of mixed metal oxide catalysts were substantially higher and crystalline domain sizes considerably smaller than could be achieved for single oxides. Lattice parameters were established by X-ray and electron diffraction, which revealed a lattice contraction with increased manganese loading, as was intended. Figure 1 provides transmission electron microscopy images and electron diffraction results for co-precipitated cerium oxide and one manganese-cerium oxide composition (Mn/(Mn+Ce) = 0.5). Electron diffraction is particularly effective in obtaining lattice parameters of materials having very small crystalline domains.

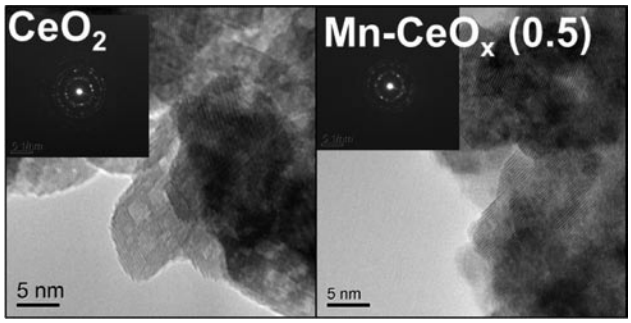

FIGURE 1. Transmission electron microscopy images and electron diffraction of CeO_2 and Mn-CeO_x(0.5).

The cerium oxide support was found to substantially lower the temperature at which manganese oxide could be reduced, which supports oxidation of NO to NO_2. This finding is based on a series of measurements made using temperature-programmed reduction for single and mixed metal oxides that had been prepared by multiple methods, for which typical results are shown in Figure 2. Pure MnO_x shows two hydrogen consumption peaks at ~330°C and 430°C, which are assigned Mn^{4+} to Mn^{3+} and Mn^3+ to Mn^{2+} reduction, respectively. From the relative 1:2 ratio of the peak area, it is apparent that the oxidation state of the original MnO_x is consistent with a ~1:1 mixture of MnO_2 and Mn_2O_3 phases. Hydrogen consumption peaks for MnO_x supported on CeO_2 shifted to lower temperatures by nearly 100°C for mixed oxide catalysts prepared by co-precipitation (red) and incipient wetness (black). Further, relative reduction peak areas for ceria-supported catalysts changed substantially: the peak corresponding to Mn^{4+} to Mn^{3+} grew relative to the peak corresponding to Mn^3+ to Mn^{2+} reduction. This behavior suggests that the ceria support, which incorporates manganese oxide in solid solution, is involved in hydrogen consumption and therefore also is partially reduced along with manganese. Ceria alone shows negligible catalytic activity for NO oxidation, and undergoes the first reduction step (Ce^{4+} to Ce^{3+}) at temperatures >350°C. Clearly, synergism between manganese and cerium oxides leads to a lowering in the reduction temperature and an increase in labile oxygen availability, both of which are important for NO oxidation reactions.

Mixed oxide catalysts prepared by the incipient wetness method, where manganese oxide is introduced to a ceria support of high surface area, show a higher surface concentration of manganese oxide than catalysts prepared by co-precipitation. Despite this difference, catalysts prepared by the two methods gave indistinguishable activities for NO oxidation, as is shown in Figure 3. That is, manganese oxide deposited onto the surface of the ceria support remains as active for NO oxidation as manganese oxide in solid solution with ceria. This is useful because it is substantially simpler to synthesize catalysts of high surface area by the incipient wetness method than by co-precipitation or various other methods. By 300°C, these catalysts achieved the thermodynamic limit for NO conversion, an improvement over properties obtained for a commercial platinum-based LNT catalyst [2]. At 250°C, NO conversion was greater than 80%. The mixed metal oxide catalysts are additionally expected to exhibit improved tolerance to sulfur than noble metal-based catalysts.

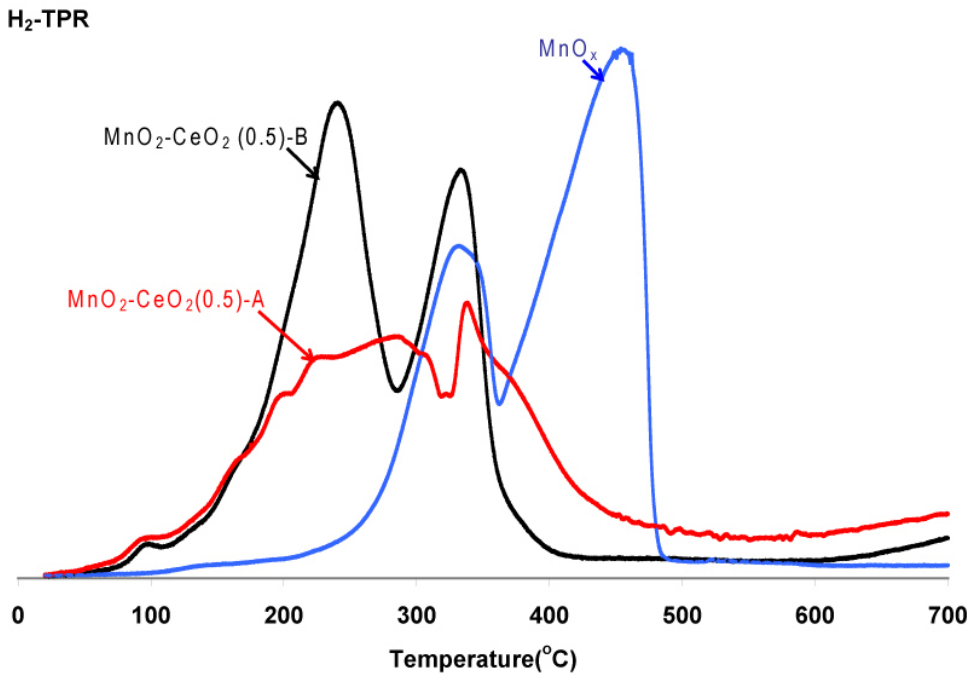

FIGURE 2. Hydrogen consumption profiles during temperature-programmed reduction for mixed metal oxide catalysts prepared by incipient wetness methods (A), by co-precipitation (B), and for MnO_x. The presence of the cerium oxide support lowered temperatures required for reduction.

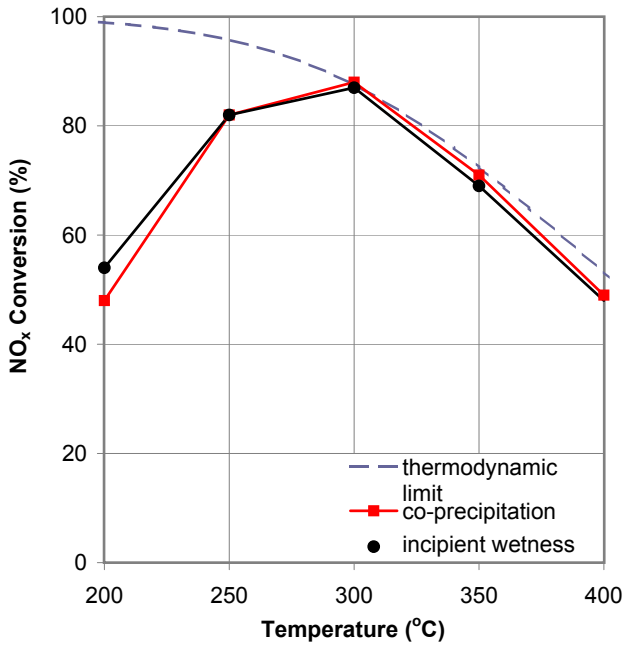

FIGURE 3. NO oxidation activity profiles for Mn-CeO_2 (0.5) catalysts prepared by co-precipitation and by incipient wetness methods.

Conclusions

- Mixed metal oxide catalyst compositions and forms were identified that show high activity for NO oxidation, and may serve as a suitable replacement for platinum-based catalysts for exhaust gas treatment. NO oxidation to NO_2 is important because the activities of both LNT and SCR are enhanced.
- The ceria support was shown to both lower the minimum temperature for manganese oxide reduction and to increase the quantity of labile oxygen available for NO oxidation.
- Mixed metal oxide catalysts made by incipient wetness methods and containing enriched surface manganese were shown to perform similarly to compositionally homogeneous forms made by co-precipitation. The former method is a considerably simpler process.
- DFT methods were established to help investigate interactions between reactants and potentially active sites.

References

1. M. Koebel, G. Madia, and M. Elsener, Catalysis Today 73, 239 (2002).

2. C.H. Kim, G.S. Qi, K. Dahlberg, and W. Li, Science 327, 1624 (2010).

FY 2012 Publications/Presentations

1. Muntean, G., Kwak, J.H., Mei, D. and Herling, D. "Investigation of Mixed Oxide Catalysts for NO Oxidation," 2012 DOE Vehicle Technologies Program Annual Merit Review and Peer Evaluation Meeting, May 14–18, 2012, Washington, D.C.

III.12 Development of Optimal Catalyst Designs and Operating Strategies for Lean NOx Reduction in Coupled LNT-SCR Systems

Michael P. Harold (Primary Contact, University of Houston), Mark Crocker (University of Kentucky)
University of Houston
Dept. of Chemical & Biomolecular Engineering
S325 Engineering Building 1
Houston, TX 77204

DOE Technology Development Manager:
Ken Howden

Overall Objectives

The overarching goal of this project is to identify the oxides of nitrogen (NOx) reduction mechanisms operative in lean-NOx traps (LNTs) and in situ selective catalytic reduction (SCR) catalysts, and to use this knowledge to design optimized LNT-SCR systems in terms of catalyst architecture and operating strategies. The project is split into three phases.

Phase 1

- Elucidate the mechanism of the non-NH_3 pathway for NOx reduction by means of bench-scale reactor, in situ diffuse reflectance infrared Fourier-transform spectroscopy (DRIFTS) reactor, and temporal analysis of products (TAP) reactor studies.
- Map LNT selectivity to NH_3 as a function of catalyst composition (ceria content and type) and relevant process parameters (NOx loading, purge duration, purge lambda and space velocity).
- Develop a microkinetic LNT model that takes into account the catalyst composition (storage component such as ceria and barium loading as well as precious metal such as Pt loading/dispersion) and H_2, CO, and C_3H_6 reductants.
- Develop low-dimensional models for the LNT and the coupled LNT-SCR unit for different catalyst architectures incorporating microkinetics.

Phase 2

- Determine optimum ceria type and content in model LNT catalysts to achieve best net NOx conversion in serial LNT-SCR catalysts.
- Determine the level of Pt-grade metal (PGM) reduction possible in the serial LNT-SCR catalyst system while providing equivalent performance to the corresponding LNT-only system.
- Establish the optimal operating strategy of serial and double layer catalyst systems with respect to NOx conversion level and fuel penalty.
- Develop microkinetic SCR model that includes non-NH_3 mechanism.
- Carry out experimental optimization study of segmented LNT-SCR catalyst configurations.
- Perform simulations of the LNT and coupled LNT-SCR unit using the low-dimensional models to examine the performance features and to identify optimal periodic operation and how it depends on the axial and transverse distribution of the catalytic components.

Phase 3

- Study the surface chemistry and dynamics associated with NH_3 storage and consumption during LNT-SCR lean-rich cycling.
- Quantify the NO*x* storage-reduction behavior of aged LNT-SCR systems so as to pin-point the effects of aging on the different catalyst functions.
- Complete microkinetic model for the LNT-SCR system.
- Carry out modeling study of the LNT-SCR systems for real-time simulation and optimization.
- Experimentally verify model predictions of different segmented LNT-SCR reactor configurations.
- Use low-dimensional models to identify the optimal catalyst architectures and operating strategies of the overall LNT-SCR unit.

Accomplishments

To date the project has been productive in completing project tasks. During the third year of the project most of the Phase 1 and 2 objectives were completed with near completion of Phase 3 objectives. Since project inception, about 25 peer-reviewed publications have appeared or are in print and about the same number of presentations have been delivered at conferences. The latter includes at least two invited "keynote" lectures. The project has supported the doctoral thesis research of about seven doctoral students and one post doc at the University of

Houston and University of Kentucky. Two of the students completed their degrees in 2012 (University of Kentucky students Pranit Metkar, now working in DuPont Central Research, and Yi Liu, now working at Cummins Inc.). Another student will defend his doctorate in the next few months (University of Kentucky student Vence Easterling). By the no-cost extension end date, four additional doctoral students will have completed their degrees. So the project has also been productive in terms of training new researchers, several of whom have taken positions in the emissions area.

Highlights of activities over the year are as follows:

- NOx Storage and Reduction: Regeneration Mechanisms, Kinetics, and Ammonia Generation
  - Isotopic TAP study of NO reduction by NH_3 on Pt to elucidate the pathways towards N_2 production.
  - Elucidation of NOx reduction via isocyanate route on LNT catalysts through a combination of steady-state, transient, and DRIFTS experiments.
  - Modeling of the LNT in order to check on the predictive capability of the model and to better understand the link between catalyst properties and operating conditions.
  - Elucidation of the effect of cycle timing on NOx conversion and NH_3 selectivity through a combination of experiments and modeling.
  - Application of crystallite-scale LNT model to simulate spatially resolved capillary inlet mass spectrometer SpaciMS experiments for LNT monolith.
- Selective Catalytic Reduction: Kinetics, Mechanisms, and Catalyst Comparisons
  - Experimental studies (steady-state, transient) of NOx reduction on Cu/chabazite monolith catalyst using propylene to understand the role of hydrocarbon.
  - Experimental studies of combined NH_3 and propylene reductant mixtures on the performance of Cu-chabazite catalyst.
  - Modeling of the dual component SCR catalyst containing Fe- and Cu-exchanged zeolite to determine the optimal loading and architecture of the two catalysts.
  - Evaluation of the reactivity of N_2O on Cu-chabazite.
- Coupled LNT/SCR
  - Spatio-temporal study using SpaciMS for the LNT-SCR.
  - Cycling experiments involving combined LNT-SCR double-layer and dual-brick catalysts with profiling of ceria to compare the two catalyst architectures and possible performance enhancements with ceria.
  - Development and application of a LNT/SCR serial and segmented model to elucidate the basic features of the reactor in terms of NOx conversion and product distribution.
  - Development of a dual layer LNT/SCR model to elucidate the experimental findings and to identify optimal dual layer compositions and operating conditions.

Future Directions

The project team will converge on critical tasks related to experimental and modeling studies of the LNT/SCR technology. The main focus of the remaining months of the project (no-cost extension period) will be to complete experiments on the LNT/SCR sequential and double-layer configurations, and to make further upgrades in the kinetic and reactor models of these systems.

Introduction

The effective removal of NOx from lean exhaust represents a continuing challenge to the automotive industry. The LNT is a promising technology, particularly for light-duty diesel and gasoline lean-burn applications. Literature studies have shown that the performance of the LNT can be significantly improved by adding an in situ SCR catalyst in series downstream. SCR catalysts promote the selective reduction of NOx with ammonia (NH_3) in the presence of excess oxygen. An in situ SCR catalyst refers to a system where the NH_3 is generated in the upstream LNT and subsequently stored on the SCR catalyst where it reacts with NOx that breaks through the LNT. The overarching goal of this project is to advance our understanding of the LNT/SCR technology and to identify the best reactor designs and operating strategies for reducing NOx with NH_3 generated from engine-out NOx.

Approach

The project activities encompass catalyst synthesis and characterization, kinetics and reactor modeling, vehicle exhaust testing, and systems integration (Figure 1). In Phase 1 of the project, the studies focus on two main goals: first, elucidating the mechanism of

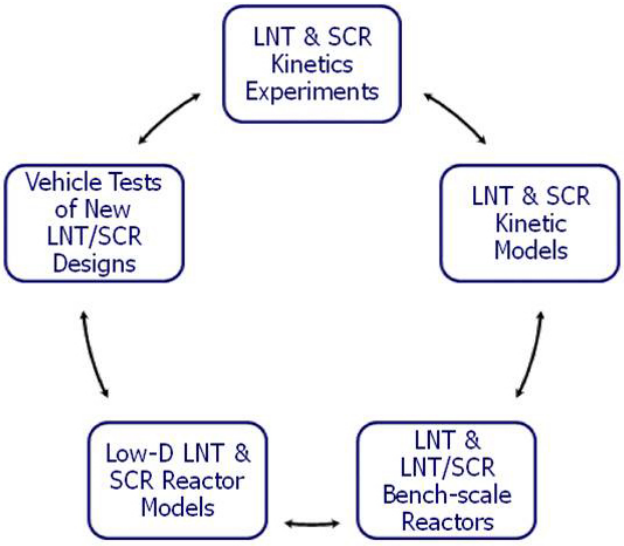

FIGURE 1. Organization of activities carried out by the project team.

the non-NH_3 pathway for NOx conversion in LNT-SCR systems and second, developing mechanistic-based kinetic models that describe the dependence of LNT selectivity to NH_3 and of NOx reduction with NH_3 as a function of relevant process parameters and catalyst composition. In Phase 2, efforts are directed towards improving the individual LNT and SCR catalyst functions in terms of NH_3 generation and NOx to N_2 conversion, respectively, and in elucidating the synergies between the LNT and SCR functions during periodic operation of the LNT/SCR. This is accomplished through targeted kinetics, catalyst synthesis, bench-scale reactor, TAP and DRIFTS measurements and complementary modeling studies, all with the goal of establishing the optimal catalyst architectures (Figure 2) and operating strategies of LNT-SCR catalyst systems that maximize NOx conversion to N_2. A low-dimensional LNT-SCR model is developed that incorporates the main NH_3 reduction pathway and is used to quantify NOx conversion for different architectures, including an assessment of potential PGM reduction in the LNT-SCR catalyst. Additional activities include the synthesis of dual-layer SCR and LNT/SCR catalysts. In Phase 3 of the project, a LNT/SCR reactor model based on refined LNT and SCR models is used to evaluate different catalyst architectures spanning segmented zone and dual-layer catalysts. Complementary bench-scale reactor studies are conducted, for model verification and testing of promising designs predicted by the model. Bench-scale and vehicle exhaust tests are also conducted using aged LNT-SCR systems, with the aim of assessing system durability.

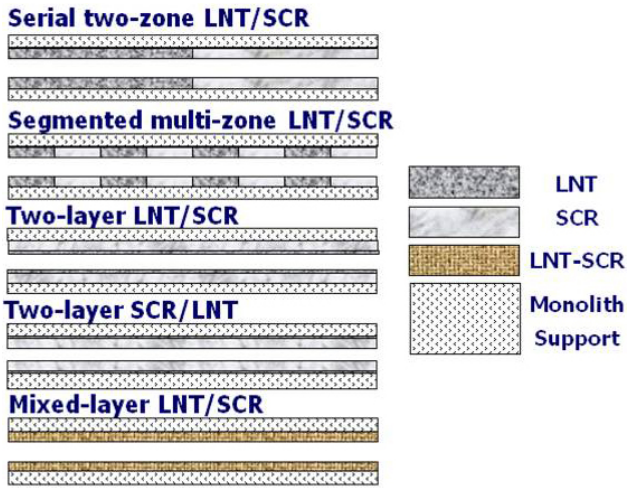

FIGURE 2. Several catalyst formulations and architectures evaluated in the project.

Results

Selected results are reported to illustrate activities that have been completed or are in progress.

NOx Storage and Reduction: Regeneration Mechanisms, Kinetics, and Ammonia Generation

Experimental and Modeling Study of Ammonia Generation in LNT: Effect of Cycle Timing

In the combined LNT-SCR system, NH_3 generated in the LNT is consumed in SCR. The performance of such integrated system depends on the quantity of NH_3 that can be produced in the LNT. Therefore, it is essential that the NOx stored in LNT is selectively reduced to NH_3 rather than N_2. In this study, the effect of cycle timing on the performance of selected 3% and 8% dispersion $Pt/BaO/Al_2O_3$ LNT catalysts was assessed to identify the conditions that yield higher NH_3 production with reasonable NOx conversion. Two sets of experiments were performed. In the first set (set 1), the effect of rich phase duration was studied by varying the rich time while delivering the same moles of reductant for a fixed lean time. In the second set (set 2), the total cycle time was varied while maintaining a fixed lean to rich time ratio. The results were compared to literature data and interpreted on the basis of a model that includes crystallite scale details; i.e. accounts for diffusion of stored NOx. In agreement with the data, the model predicts an increase in NOx conversion and decrease in NH_3 selectivity with increasing rich time (set 1) and a decrease in NOx conversion with overall cycle time (set 2) at 300°C. (Representative results are shown in Figure 3 with catalyst properties and experimental conditions provided in Table 1.) The model shows that for

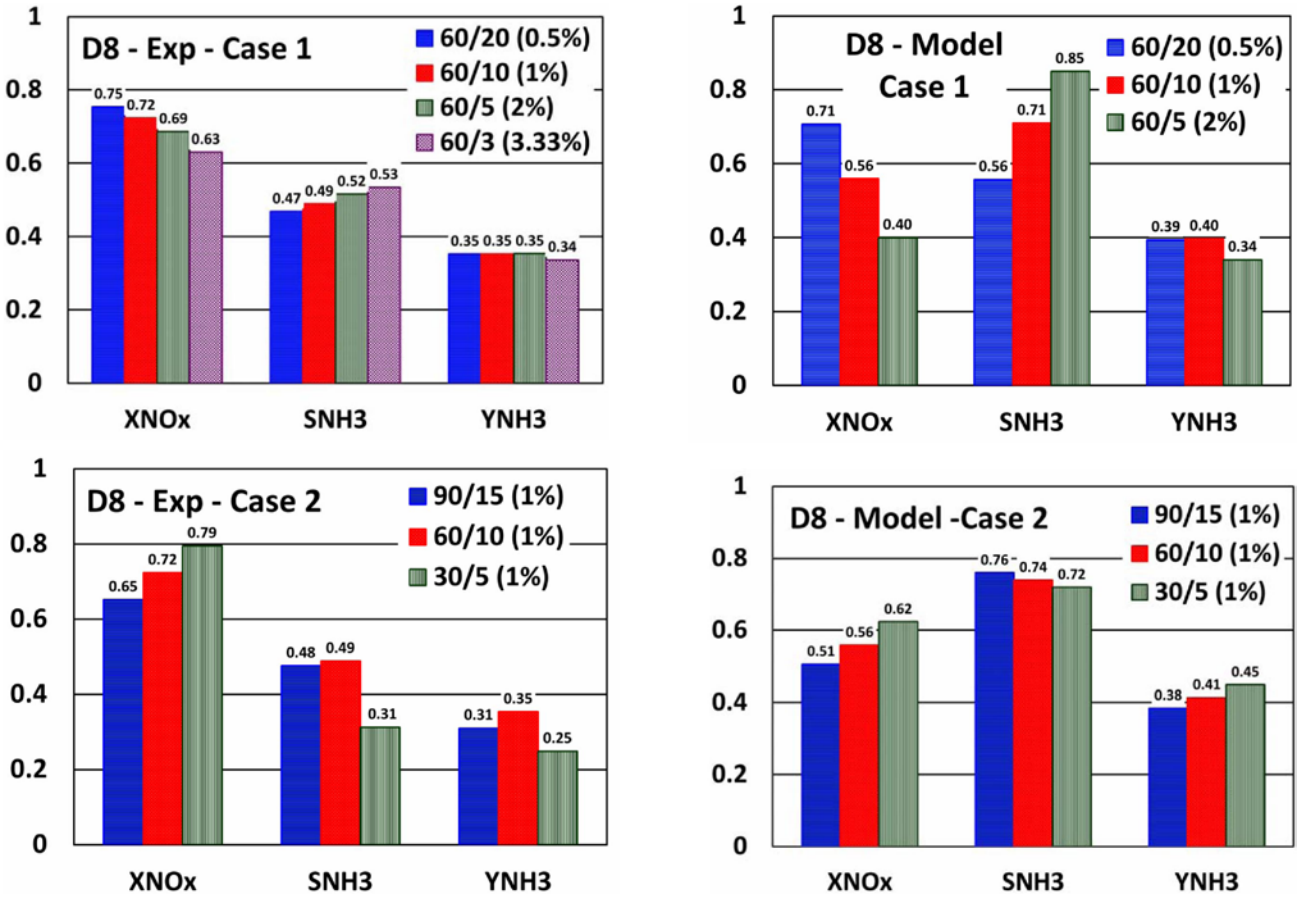

FIGURE 3. Cycle-averaged NOx conversion, NH_3 selectivity and yield obtained for different lean and rich times for D8 catalyst at 300°C. Left column represent experimental result and right column represent calculated result. The experimental conditions are given in Table 1.

TABLE 1. Catalyst properties and experimental conditions corresponding to the results shown in Figure 3.

Sample	Pt (wt%)	BaO (wt%)	Pt Dispersion (%)	Measured Pt size particle (nm)	m_{wc} (g)	C_{Pt} (mol active Pt/m^3_{wc})
D8	2.48	13.0	8.0	12.5	0.13	14.9
D3	2.48	13.0	3.2	30.0	0.13	6.0

Case 1	Lean time (s)	Rich time (s)	H_2 in rich (%)
60/20	60	20	0.5
60/10	60	10	1.0
60/5	60	5	2.0
60/3	60	3	3.3
Case 2			
90/15	90	15	1.0
60/10	60	10	1.0
30/5	30	5	1.0
Lean Feed	: 500 ppm NO and 5% O_2. Balance: Ar		
GHSV	: 60,000 hr^{-1}		
Temperature	: 300°C		

the intermediate dispersion catalyst (8%), the decrease in NH_3 selectivity for longer and diluted regeneration is due to the initial consumption of NH_3 downstream in the reactor, whereas a shorter, more concentrated regeneration results in less downstream NH_3 consumption. Other trends were successfully predicted, indicating that under some conditions and especially for low dispersion LNT catalysts, stored NOx diffusion is a key rate limiting process. This underscores the need to account for this level of detail in any LNT catalyst optimization.

Application of SpaciMS to the Study of Ammonia Formation in LNT Catalysts

SpaciMS was employed to understand the factors influencing the selectivity of NOx reduction in two fully formulated LNT catalysts, both degreened and thermally aged. Both catalysts contained Pt, Rh, BaO and Al_2O_3, while one of them also contained La-stabilized CeO_2. The amount of reductant required to fully regenerate each catalyst was first determined experimentally based on the oxygen storage capacity (OSC) of the catalyst and the NOx storage capacity (NSC). In this way a correction was made for the change in catalyst OSC and NSC after aging, thereby eliminating these as factors which could affect catalyst selectivity to NH_3. For both catalysts, aging resulted in an elongation of the NOx storage-reduction (NSR) zone due to a decrease in the concentration of NOx storage sites per unit catalyst length. In addition to decreased lean phase NOx storage efficiency, stretching of the NSR zone affected catalyst regeneration. Three main effects were identified, the first being an increase of the NOx "puff" that appeared during the onset of the rich front as it traversed the catalyst. Spatially, NOx release tracked the NSR zone, with the result that the NOx concentration peaked closer to the rear of the aged catalysts. Hence the probability that NOx could re-adsorb downstream of the reduction front and subsequently undergo reduction by NH_3 (formed in the reduction front) was diminished, resulting in higher rich phase NOx slip. Second, the stretching of the NSR zone resulted in increased selectivity to NH_3 due to the fact that less catalyst (corresponding to the OSC-only zone downstream of the NSR zone) was available to consume NH_3 by either the NH_3-NO_x SCR reaction or the NH_3-O_2 reaction. Third, the loss of OSC and NOx storage sites, along with the decreased rate of NO_x diffusion to Pt/Rh sites (as a result of Pt/Rh-Ba phase segregation), led to an increase in the rate of propagation of the reductant front after aging. This in turn resulted in increased H_2:NO_x ratios at the Pt/Rh sites and consequently increased selectivity to NH_3. Representative SpaciMS results are shown in Figure 4 in which aged LNT catalysts produce more NH_3 than degreened LNT catalysts.

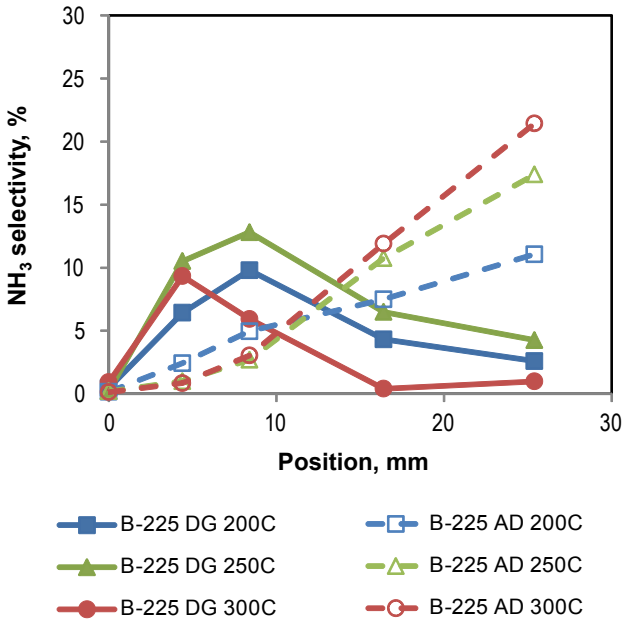

FIGURE 4. Ammonia selectivity profiles for degreened and aged LNT catalysts showing that with aging more ammonia is produced.

NOx Storage and Reduction Properties of Model Ceria-based LNT Catalysts

Three kinds of model ceria-containing LNT catalysts, corresponding to Pt/Ba/CeO_2, Pt/CeO_2/Al_2O_3 and Pt/BaO/CeO_2/Al_2O_3, were prepared for comparison with a standard LNT catalyst of the Pt/BaO/Al_2O_3 type. In these catalysts ceria functioned as a NOx storage component and/or a support material. The influence of ceria on the microstructure of the catalysts was investigated, in addition to the effect on NOx storage capacity, regeneration behavior and catalyst performance during lean/rich cycling. The Pt/Ba/CeO_2 and Pt/BaO/CeO_2/Al_2O_3 catalysts exhibited higher NOx storage capacity at 200 and 300°C relative to the Pt/BaO/Al_2O_3 catalyst, although the latter displayed superior storage capacity at 400°C. Catalyst regeneration behavior at low temperature was also improved by the presence of ceria, as reflected by temperature-programmed reduction measurements. These factors contributed to the superior NOx storage-reduction performance exhibited by the Pt/Ba/CeO_2 and Pt/BaO/CeO_2/Al_2O_3 catalysts under cycling conditions in the temperature range 200-300°C. Overall, Pt/BaO/CeO_2/Al_2O_3 (which displayed well balanced NOx storage and regeneration behavior), showed the best performance, affording consistently high NOx conversion levels in the temperature range 200°C to 400°C under lean-rich cycling conditions.

Experimental Study of NOx Storage and Reduction with CO as the Reductant

This study provided insight into the role of intermediate isocyanates during the cyclic reduction of NO by CO in the presence and absence of excess water on a Pt-Rh/Ba/Al_2O_3 LNT catalyst. At low temperatures (150-200°C), CO is ineffective in reducing NOx and acts as a poison due to its excess coverage of precious metal sites. However, at temperatures higher than 200°C, CO efficiently reduces NOx to N_2 and N_2O. N_2 is the most selective reduction product (selectivity > 70%) at all the temperatures and reductant concentrations studied and its selectivity increases with temperature. Also,

at these higher temperatures addition of water has a significant promoting effect on NOx conversion while leading to a slight drop in the conversion of CO. NH_3 is also produced in addition to N_2 and N_2O on the addition of water which is due either to isocyanate hydrolysis or reduction of NOx by H_2 formed by the water gas shift chemistry. The product evolution trends observed in this study suggest that isocyanate intermediates play a major role in the cyclic reduction of NOx by CO both in the absence and presence of water and further react with stored NOx to give N_2 and N_2O. The addition of excess CO_2 has a negative impact on NOx conversion particularly at 250°C due to the formation of carbonates on the storage component, decreasing the storage capacity of the catalyst and consecutively leading to a drop in the conversion of NOx. At higher temperatures the detrimental effect of CO_2 is not very evident and the product selectivity to NH_3 rises at the expense of N_2 and N_2O due to a rise in the ratio of surface concentration of NCO/NOx. Based on the results, an overall mechanism for the cyclic reduction of NOx by CO under dry and wet conditions is constructed. The mechanism is depicted schematically in Figure 5.

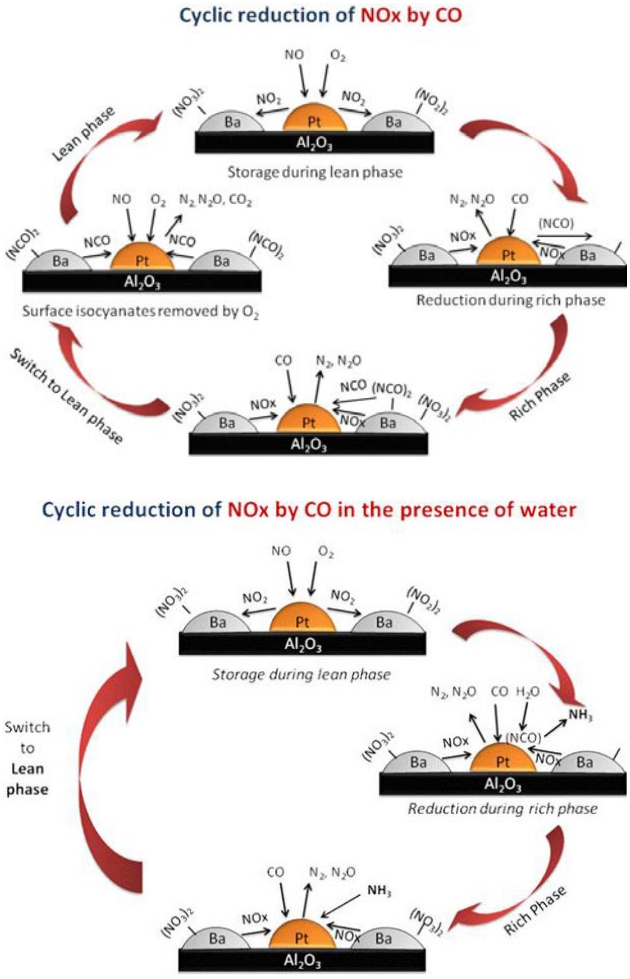

FIGURE 5. Schematic of the proposed mechanism for cyclic reduction of NOx by CO in the absence of water (top) and presence of water (bottom).

Isocyanate Formation and Reactivity on a Ba-Based LNT Catalyst Studied by DRIFTS

Complementary with the above study, DRIFTS and mass spectrometry (MS), coupled with the use of isotopically-labeled $^{15}N^{18}O$ and ^{13}CO, were employed to study the formation of isocyanate species during NOx reduction with CO, as well as isocyanate reactivity towards typical exhaust gas components. DRIFTS demonstrated that both Ba-NCO and Al-NCO were simultaneously formed during NOx reduction by CO under dry lean-rich cycling conditions. The Ba-NCO band was more intense than that of Al-NCO, and became comparatively stronger at high temperatures. During rich purging at 300 and 400°C, a near linear relationship was found between the increase in Ba-NCO band intensity and the decrease in Ba-NO_3 band intensity, suggesting that Ba-NCO is directly derived from the reaction of Ba nitrate with CO. Both temperature-programmed surface reaction and isothermal reaction modes were utilized to study the reactivity of isocyanate species under lean conditions. Simultaneous DRIFTS and mass spectrometric measurements during temperature-programmed surface reaction indicated that isocyanate reaction with H_2O, O_2, NO and NO/O_2 took place almost immediately the temperature was raised above 100°C, and that all NCO species were removed below 300°C. The evolution of the NCO infrared bands during isothermal reaction at 350°C demonstrated that the kinetics of NCO hydrolysis are fast, although a delay in N_2 formation indicated that N_2 is not the initial product of the reaction. In contrast, immediate N_2 evolution was observed during NCO reaction with O_2. Overall, it can be inferred that under dry cycling conditions with CO as the sole reductant, N_2 is mainly generated via NCO reaction with O_2 after the switch to lean phase conditions, rather than being evolved during the rich phase. However, in the presence of water, isocyanate undergoes rapid hydrolysis in the rich phase, N_2 generation proceeding via NH_3.

Isotopic TAP Study of Pt-Catalyzed NO Reduction With NH_3

Another isotopic study was conducted, this time in conjunction with a TAP study, with the focus on one of the key reactions occurring in the NOx trap during the regeneration, namely Pt-catalyzed anaerobic NO reduction by NH_3. The effects of temperature, pulse timing, and feed composition were varied to quantify the conversion and product selectivities on both Pt sponge and Pt/Al_2O_3 catalysts. Isotopically labeled nitric oxide (^{15}NO) was used to follow reaction pathways to

molecular nitrogen and nitrous oxide. A variation in the delay time between sequential pulses of ^{15}NO and NH_3 has a significant effect on the reaction path to molecular nitrogen. A mixed feed (no delay time) above the light-off temperature resulted in a product mixture nearly balanced between the mixed product ^{15}NN, and the two single-source products $^{15}N_2$, and N_2. With increased delay time the selectivity of ^{15}NN decreased significantly in favor of $^{15}N_2$, and N_2. The data suggest at least two major routes to nitrogen formation, one involving direct NO decomposition on reduced Pt sites and the other involving reaction between NHx and NO. There is also kinetic evidence for a slower, third minor route involving an unidentified surface complex. The alumina support is shown to suppress this effect of delay time through ammonia adsorption, serving as a source-sink.

Selective Catalytic Reduction – Non-NH_3 and NH_3 Based Pathways

Global SCR Kinetic Model for Fe-ZSM-5 and Cu-Chabazite with Application to Fe-Cu Dual Component Catalysts

A comprehensive experimental and modeling study of selective catalytic reduction of NOx with NH_3 was carried out on Fe-ZSM-5 and Cu-chabazite (CHA) catalysts. The experiments reveal that Cu-CHA catalyst has a higher NH_3 storage capacity and activity for NH_3 oxidation and standard SCR compared to Fe-ZSM-5. The NOx reduction activity on the Fe-ZSM-5 catalyst was found to be strongly dependent on the NO_2 feed fraction in contrast to Cu-CHA catalyst for which NOx conversion was much less sensitive to NO_2. In the presence of excess NO_2, both N_2O and ammonium nitrate were produced on both catalysts although Fe-ZSM-5 catalyst had a higher selectivity towards these byproducts compared to Cu-CHA. For different feed conditions (NO_2/NOx = 0 to 1), Cu-CHA was a more active NOx reduction catalyst at lower temperatures (≤350°C) while Fe-ZSM-5 was more active at higher temperatures (≥400°C). Global kinetic models were developed to predict the main features of several SCR system reactions investigated experimentally. The models account for NH_3 adsorption, NH_3 oxidation, NO oxidation, standard SCR, fast SCR, NO_2 SCR, ammonium nitrate formation and its decomposition to N_2O N_2O decomposition and N_2O reduction by NH_3. The 1 + 1 dimensional reactor model accounts for potential washcoat diffusion limitations. The model accurately predicts the steady-state NOx and NH_3 conversions and the selectivity of the different products formed during these reactions. The model was used to predict the performance of standard and fast SCR reactions on combined systems of Fe- and Cu-zeolite monolithic catalysts which were found to have higher NOx conversion activity over a wider temperature range than with individual Fe- and Cu-zeolite catalysts as reported in our earlier study. Among various configurations of the combined catalysts, either a single brick made up of a dual-layer catalyst with a thin Fe-zeolite layer on top of a thick Cu-zeolite layer or a sequential arrangement of short Fe-ZSM-5 brick followed by longer Cu-CHA brick resulted in high NOx removal efficiency over a wide temperature range of practical interest. Representative results are shown in Figure 6.

LNT/SCR Studies – Understanding Synergies of NH_3 Generation and NOx Reduction

A Non-NH_3 Pathway for NOx Conversion in Coupled LNT-SCR Systems

NOx storage-reduction experiments were performed using a coupled LNT-SCR system consisting of a low-precious metal loaded Pt/Rh LNT catalyst and a commercial Cu-zeolite SCR catalyst. Cycling experiments revealed that when a $CO+H_2+C_3H_6$ mixture or C_3H_6 by itself was used as the reductant, the NOx conversion over the SCR catalyst exceeded the conversion of NH_3 over the same catalyst. This is explained by the presence of propene, which slipped through the LNT catalyst and reacted with the LNT NOx slip. Separate experiments, conducted under continuous flow and lean-rich cycling conditions, confirmed the ability of propene, as well as ethene, to function as a NOx reductant over the SCR catalyst. Cycling experiments also revealed that the SCR catalyst was able to store propene, such that NOx reduction by stored propene continued into the lean phase (after the switch from rich conditions). According to adsorption experiments, significant co-adsorption of NH_3 and propene occurred in the SCR catalyst, while under lean-rich cycling conditions the contributions of NH_3 and C_3H_6 to NOx conversion were found to be essentially additive. These findings suggest that under actual driving conditions, NOx reduction by non-NH_3 reductants (olefins and possibly other hydrocarbons) in the SCR catalyst can contribute to the mitigation of lean and rich phase NOx.

N_2O Mitigation in a Coupled LNT-SCR System

N_2O formation and consumption were investigated over a coupled LNT-SCR system consisting of a low precious metal loaded Pt/Rh LNT catalyst and a commercial Cu-zeolite SCR catalyst. Under lean-rich cycling conditions, N_2O emissions from the LNT were found to be partially mitigated by the downstream SCR catalyst. N_2O decomposition over the SCR catalyst was observed in absence of reductant immediately after the switch to rich conditions, while N_2O reduction occurred after subsequent breakthrough of the reductant from the LNT. Steady-state data indicate that the former process is

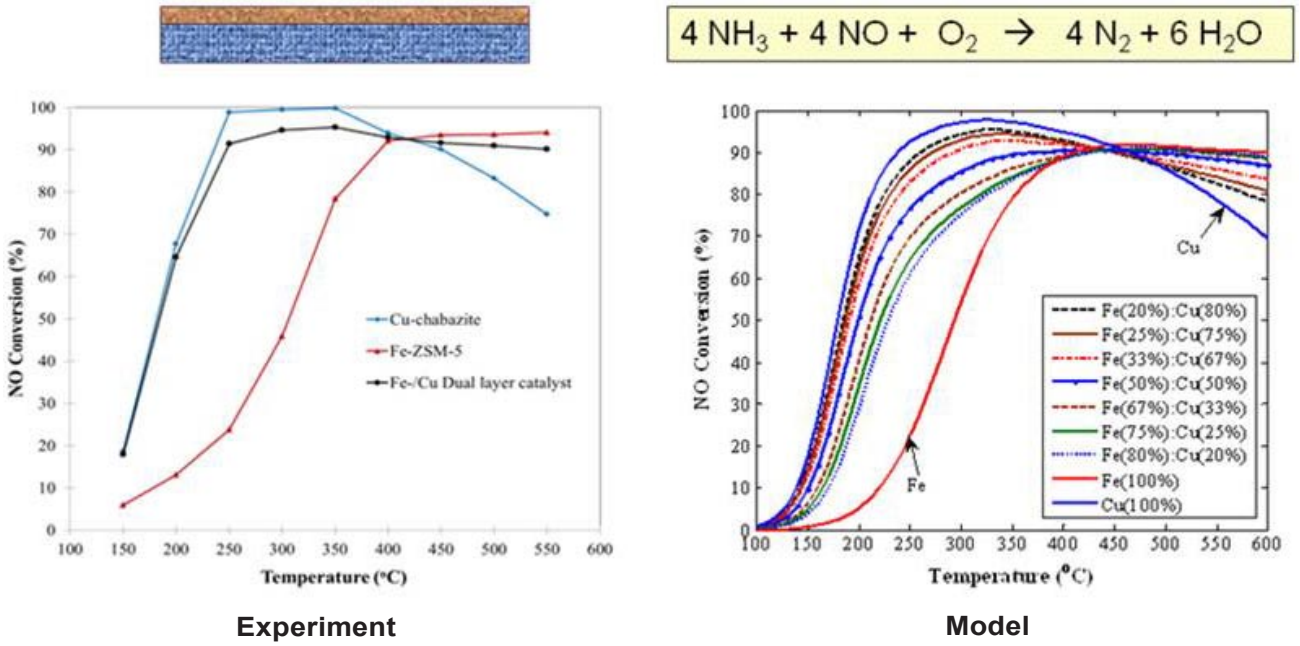

FIGURE 6. Comparison of experiment (left) with model predictions (right) of the NO conversion versus temperature for Cu-, Fe-, and Cu/Fe dual layer catalysts during standard SCR.

weakly promoted by NO which breaks through the LNT at the same time as the N_2O. Steady-state experiments revealed the order $H_2 > NH_3 > CO > C_3H_6$ for the efficacy of N_2O reduction with different reductants. These findings suggest that coupled LNT-SCR systems can not only improve overall NOx conversion levels but can also mitigate N_2O emissions from the LNT catalyst under actual driving conditions.

Experimental Studies of the Dual Layer LNT/SCR Monolithic Catalyst

Lean reduction of NOx (NO and NO_2) was studied using monolith-supported catalysts consisting of a layer of a metal-exchanged (Fe, Cu) zeolite (ZSM-5) SCR catalyst deposited on top of a Pt/Rh/BaO/CeO_2 LNT catalyst. During periodic switching between lean and rich feeds, the LNT layer reduces NOx to N_2 and NH_3. The SCR layer traps the latter, where additional NOx reduction occurs. The dual-layer catalysts exhibited high N_2 selectivity and low NH_3 selectivity over the temperature range of 150 to 300°C. The NOx conversion was incomplete due to undesired side reactions in the LNT layer, such as NH_3 oxidation to N_2O at lower temperature and NOx at high temperature. The NOx conversion and N_2 selectivity of the Cu-exchanged ZSM-5 was higher than the Fe-exchanged ZSM-5. This was due to a higher low temperature SCR activity and a higher NH_3 storage capacity on the Cu-zeolite. The dual-layer catalyst had a higher NOx conversion than the LNT catalyst below 300°C and a higher N_2 selectivity over the entire temperature range when H_2O and CO_2 were present in the feed. The NOx storage capacity and NH_3 generation increased upon addition of CeO_2 to the LNT layer. It also intensified NH_3 oxidation at high temperatures. The addition of ceria mitigated the undesirable migration of Pt between the LNT and SCR layers. Hydrothermal aging had a smaller effect on dual-layer catalysts containing ceria. Representative results are shown in Figure 7, displaying the effectiveness in adding the SCR layer on top of the LNT layer, in terms of converting NH_3 and NO_2 generated by the LNT layer.

A series of experiments were carried out using monolithic catalysts containing CeO_2 and with mixtures of H_2 and CO as the reductant, consisting of a layer of SCR catalyst deposited on top of a LNT catalyst. The LNT catalyst exhibited a rather low NOx conversion below 250°C due to CO inhibition. The top SCR layer comprising Cu/ZSM5 significantly increased the NOx conversion at low temperature by its reaction with NH_3 formed during the regeneration phase. The addition of CeO_2 to the LNT layer promoted the water-gas shift reaction ($CO + H_2O \leftrightarrow H_2 + CO_2$). The water-gas shift reaction mitigated the CO inhibition and the generated H_2 enhanced the low-temperature catalyst regeneration. The ceria addition decreased the performance at high temperatures due to increased oxidation of NH_3. The ceria loading was optimized by applying a non-uniform axial profile. A dual-layer catalyst with an increasing ceria loading axial profile improved the performance over a wide (low and high) temperature range.

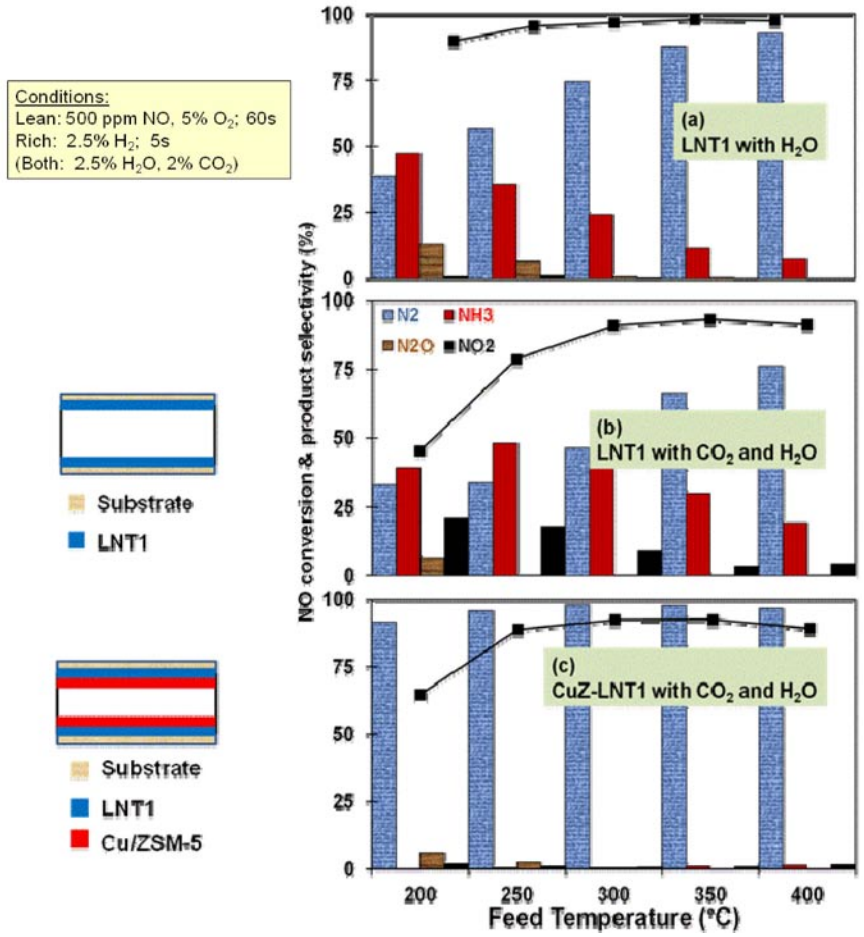

FIGURE 7. Dual-layer LNT/SCR results showing LNT-only data in the top two panels and the LNT/SCR data in the bottom panel. The addition of the SCR layer is effective in converting the NH_3 and unreacted NOx from the LNT.

Additional experiments were carried out to evaluate the effect of CeO_2 on the performance of the dual-layer catalysts. CO poisoning was especially significant below 250°C for the ceria-free LNT catalyst. The low-temperature NOx reduction was increased either by use of an LNT-SCR dual-layer catalyst or deposition of CeO_2 on the LNT catalyst. However, the ceria decreased the high-temperature reductive conversion of NOx due to promotion of the undesired NH_3 oxidation. Ceria zoning o enhanced the monolith NOx conversion. Downstream loading of ceria led to the highest NOx reduction at both low and high temperatures due to the beneficial interaction of the ceria and H_2. The low-temperature NOx conversion of an aged dual-layer catalyst could be increased by a higher SCR catalyst loading. However, at high temperatures NOx reduction was independent of the SCR loading. The ratio of the lean to rich feed duration and the total cycle time were optimized to improve the NOx conversion in a temperature range from 150 to 400°C. The highest cycle-averaged NOx conversion was obtained with a 30 s:5 s lean-rich cycle containing 1.25% total reductant for all CO/H_2 ratios for a lean feed containing 500 ppm NO and 5% O_2.

Modeling of Series and Segmented LNT/SCR Reactor System

Experiments were conducted to determine the NOx reduction by a series of LNT and SCR catalytic bricks. An important goal is to minimize the required precious metal loading in the LNT while keeping the NOx emission below a specified level. Simulations were used to determine the influence of the architecture of the LNT-SCR bricks, non-uniform precious metal loading in the LNT bricks and the cycle time at temperatures in the range of 200°C–350°C. Several findings were obtained: (a) low temperature reduction is the limiting step in the optimization of PGM loading in LNT; (b) the NOx conversion increases as the number of the sequential bricks (with total length fixed) increase and reaches an asymptotic limit. From a practical point of view, there is little incentive in using more than two sequential pairs; (c) non-uniform precious metal loading of the LNT bricks results in only a minor improvement in the $deNO_x$ performance; (d) the cycle time has a significant impact on the NOx conversion. In the simulated example, the NOx conversion at low temperatures is increased by about 15 to 20% by reducing the cycle time by a factor of two; (e) even at low temperature operation, diffusional limitations in the washcoat are most likely to be important in the LNT but not in the SCR operation. The NOx conversion and ammonia selectivity are reduced when washcoat diffusion is dominant in the LNT.

Additional simulations were conducted to optimize the performance of the coupled LNT and SCR catalysts under non-isothermal operating conditions. The architecture of the LNT-SCR bricks, precious metal loading, the cycle time, catalyst length and the support materials were investigated in this work. The simulations lead to the following observations: (a) the non-isothermal operation of the sequence of LNT and

SCR bricks increases the NOx conversion over that of isothermal operation by up to ~10%; (b) the multiple brick architecture increases the NOx conversion by ~4%; (c) the cycle time and pulse duty have a significant impact on the NOx conversion by reducing the overall NOx slip from the coupled catalyst and improving the NOx conversion by ~41% over that of isothermal operation; (d) there is an optimal catalyst length of 2 cm during the non-isothermal operation; (d) metal based monolith support improves NOx conversion by ~2%.

Summary

This project combines kinetics measurements, bench-scale reactor studies, and analytical methods including spatially-resolved mass spectrometry to advance the understanding of LNT, SCR, and LNT/SCR systems. Kinetic models are being developed based on measurements for the LNT and SCR chemistries, to be incorporated into reactor models for design and optimization.

FY 2012 Publications/Presentations

Publications

1. J. Wang, Y. Ji, Z. He, M. Crocker, M. Dearth, R.W. McCabe, "A non-NH_3 pathway for NO_x conversion in coupled LNT-SCR systems", Appl. Catal. B **111-112** (2012) 562.

2. Metkar, P., V. Balakotaiah, and M.P. Harold, "Experimental Study of Selective Catalytic Reduction of NO_x on a Combined System of Fe and Cu-based Zeolite Monolithic Catalysts," Applied Catalysis B: Environmental, **111– 112**, 67– 80 (2012).

3. Joshi, S., Y. Ren, M.P. Harold, and V. Balakotaiah, "Determination of Kinetics and Controlling Regimes for Propylene and Methane Oxidation on Pt/Al_2O_3 Monolithic Catalyst Using High Space Velocity Experiments," Ind. Eng. Chem. Res., ***51*** (22), 7482–7492 (2012).

4. Kota, A., D. Luss and V. Balakotaiah, "Modeling of a Sequence of LNT-SCR Bricks for Lean NOx Reduction", Ind. Engng. Res., **51** ,6686-6696 (2012).

5. Metkar, P., M.P. Harold, and V. Balakotaiah, "Experimental and Kinetic Modeling Study of NO Oxidation: Comparison between Fe and Cu-zeolite Catalysts," Catalysis Today **184** 115– 128 (2012).

6. Dasari, P., R. Muncrief, and M.P. Harold, "Elucidating NH_3 Formation During NO_χ Reduction by CO on $Pt\text{-}BaO/Al_2O_3$ in Excess Water," Catalysis Today, **184**, 43–53 (2012).

7. Shakya, B., M.P. Harold, and V. Balakotaiah, "Crystallite-Scale Model for NOx Storage and Reduction on $Pt/BaO/Al_2O_3$: Pt Dispersion Effects on NOx Conversion and Ammonia Selectivity," Catalysis Today, **184**, 27-42 (2012).

8. Harold, M.P., "NOx Storage and Reduction in Lean Burn Vehicle Emission Control: A Catalytic Engineer's Playground," Current Opinion in Chemical Engineering, **1**, 1-9 (2012).

9. Liu, Y., M.P. Harold, and D. Luss, "Coupled NO_x Storage and Reduction and Selective Catalytic Reduction Using Dual-layer Monolithic Catalysts," Appl. Catal. B. Environmental, **121-122**, 239-251 (2012).

10. C. Shi, Y. Ji, U.M. Graham, G. Jacobs, M. Crocker, Z. Zhang, Y. Wang, T.J. Toops, NOx Storage and Reduction Properties of Model Ceria-based Lean NOx Trap Catalysts", *Appl. Catal. B*, **119-120** (2012) 183-196.

11. V. Easterling, Y. Ji, M. Crocker, M. Dearth, R.W. McCabe, "Application of spaciMS to the study of ammonia formation in lean NOx trap catalysts", *Appl. Catal. B*, **123-124** (2012) 339.

12. J. Wang, M. Crocker, "N_2O Mitigation in a Coupled LNT-SCR System", *Catal. Lett*., **142** (2012) 1167.

13. Zheng, X., A. Kumar, and M.P. Harold, "Isotopic Study of Pt-Catalyzed NO Reduction by NH_3 on Pt Catalysts Using Temporal Analysis of Products," Catalysis Today, 10.1016/j.cattod.2012.06.025 (2012).

14. Metkar, P.S., M.P. Harold, and V. Balakotaiah, "Kinetic Model of NH_3-Based Selective Catalytic Reduction of NOx on Fe-ZSM-5 and Cu-Chabazite, and Dual Layer Fe/Cu Zeolitic Monolithic Catalysts," Chem. Engin. Sci., **87**, 51–66 (2013).

15. Liu, Y., M.P. Harold, and D. Luss, "Lean NO_x reduction on LNT-SCR dual-layer catalysts by H_2 and CO," *Appl. Catalysis B. Environmental*, accepted for publication (2012).

16. Liu, Y., M.P. Harold, and D. Luss, "Lean NO_x Reduction with H_2 and CO in Dual-layer LNT-SCR Monolithic Catalysts: Impact of Ceria Loading," *Topics in Catalysis*, to appear (2013).

Patents

1. Harold, M.P., and P. Metkar, US Provisional Patent Application, "Multi-Component and Layered Formulations for Enhanced Selective Catalytic Reduction Activity," under review, June 6, 2011**.**

Presentations

1. P. Metkar, M. Harold, and V. Balakotaiah, "Experimental and Kinetic Modeling Study of Selective Catalytic Reduction of NOx on Fe- and C-Based Zeolitic Monolithic Catalysts, presented at AIChE Annual Meeting, Minneapolis, 10/11.

2. B. Shakya, M. Harold, and V. Balakotaiah,"Modeling the Effect of Pt Dispersion During Steady-State NO Oxidation and Transient NOx Storage and Regeneration on $Pt/BaO/Al_2O_3$ Lean NOx Trap Catalysts," presented at AIChE Annual Meeting, Minneapolis, 10/11.

3. Y. Liu, M. Harold, and D. Luss). "NOx Storage and Reduction by Multilayer Monolithic Catalysts," presented at AIChE Annual Meeting, Minneapolis, 10/11.

4. P. Dasari, M. Harold, and R. Muncrief, "Studies of NH_3 Formation over $Pt/BaO/Al_2O_3$ LNT Monoliths in the Presence of Excess Water," presented at AIChE Annual Meeting, Minneapolis, 10/11.

5. P. Metkar, M. Harold, and V. Balakotaiah, "Determination of Controlling Regimes for Various SCR Reactions on Zeolitic-Based Monolithic Catalysts," poster presented at AIChE Annual Meeting, Minneapolis, 10/11.

6. M.P. Harold,Y. Liu, and D. Luss, "NOx Reduction in Dual-Layer LNT/SCR Catalysts," CLEERS, Dearborn, MI, 4/12.

7. M.P. Harold, Ninth International Congress on Catalytic Air Pollution Control, Keynote Lecture: "Dual Layer Catalysts for Lean Reduction of NOx by in situ Generated Ammonia," Brussels, Belgium, 8/12.

8. M.P. Harold, Caterpillar Inc., *"Studies of Selective Catalytic Reduction: From Microkinetics through Vehicle Testing,"* Peoria, IL, 9/12.

9. M. Crocker, "Synergy of LNT and Cu-chabazite SCR Catalysts in Coupled LNT-SCR Systems", web presentation given to the CLEERS lean NOx trap working group, August 16, 2012.

10. V. Easterling, M. Crocker, M. Dearth, R. McCabe, "Ammonia formation in Lean NOx Trap Catalysts Studied by SpaciMS", oral presentation at the 7th International Conference on Environmental Catalysis, Lyon, France, September 2–6, 2012.

11. J. Wang, Z. He, Y. Ji, M. Crocker, M.-Y. Kim, J.-S. Choi, "New Insights into the Role of the SCR Catalyst in Coupled LNT-SCR Systems", oral presentation at the 2012 CLEERS Workshop, U. Michigan-Dearborn, MI, April 30 – 2 May, 2012.

III.13 Three-Dimensional Composite Nanostructures for Lean NOx Emission Control

P.-X. Gao (Primary Contact), R. Ramprasad, S.P. Alpay
University of Connecticut
97 North Eagleville Road
Storrs, CT 06269-3136

DOE Technology Development Manager: Ken Howden

NETL Project Manager: Nicholas Damico

Overall Objectives

- Develop three-dimensional (3-D) composite nanostructure array (nano-array) monolithic catalysts as the next generation of lean oxides of nitrogen (NOx) emission control catalysts.
- Demonstrate the ability to significantly reduce or eliminate the usage of Pt-group metals (PGM), while achieve good catalytic performance toward emission aftertreatment in automobiles in the developed 3-D composite nanostructured monolithic nanocatalysts.

Fiscal Year (FY) 2012 Objectives

- Synthesize various 3-D metal oxide nano-arrays on monolith substrates.
- Fabricate PGM and BaO-loaded 3-D mesoporous metal oxide/perovskite composite nano-arrays on monolith substrates.
- Characterize the chemical, morphology and structure of the composite nanostructures using a wide array of electron microscopy and spectroscopy techniques.
- Investigate the (hydro-)thermal and mechanical stability, CO and NO catalytic oxidation performance, S-resistance, and NOx storage and reduction (NSR) performance of fabricated monolithic nano-array catalysts.
- Analyze and understand the materials loading/utilization and catalytic efficiencies of the composite nano-array monolithic catalysts.
- Investigate the perovskite surface catalytic chemistry using first principle thermodynamics and kinetic Monte Carlo (KMC) simulations.

Accomplishments

- Fabricated and characterized the PGM- and BaO-loaded 3-D composite nanowire/rod arrays (such as ZnO/(La,Sr)CoO_3(LSCO) and TiO_2/(La,Sr)MnO_3(LSMO), etc.) on monolith substrates.
- Investigated the (hydro-)thermal and mechanical stability, CO and NO oxidation performance, S-poisoning resistance, as well as NSR performance of the 3-D composite nanostructured catalysts.
- Demonstrated ultra-high materials usage efficiency of 3-D composite nano-array catalysts in both PGM and metal oxides, excellent thermal and mechanical robustness, as well as tunable catalytic performance, showing their good potential to be used as the next-generation automotive catalysts.
- Developed the reliable surface catalytic phase diagrams of perovskite (such as $LaMnO_3$) surfaces through the first principle thermodynamics and KMC simulations.

Future Directions

- Further optimize and quantitatively characterize the PGM and BaO-loaded 3-D composite nano-array based on metal oxides (e.g., ZnO, and TiO_2) and perovskite (e.g., LSMO, LSCO).
- Further investigate, understand and improve the PGM and metal oxide materials utilization and catalytic conversion efficiencies of 3-D composite nano-array catalysts.
- Further evaluate the composite nano-array catalysts on high temperature hydrothermal stability.
- Further evaluate the catalytic performance of 3-D composite nanowires/nanorod arrays on CO and NO oxidations, S-resistance and NSR performance.

Introduction

Nowadays, lean-burn engines are attracting more and more attention due to their higher fuel efficiency and lower CO_2 emission than conventional gasoline engines [1-6]. However, under lean-burn conditions, the NOx emissions cannot be efficiently reduced over the classical three-way catalysts in the presence of excessive O_2 [1,4,7]. The NOx emissions have multi-fold hazards on the atmosphere, environment and human health, due to

the formation of fine particles, ozone smog, acid rain and eutrophication [8]. NSR technology is regarded as one of the most promising exhaust after-treatment technologies for lean-burn gasoline and diesel vehicles. The objective of this project is to develop a new class of oxide-based 3-D nano-array monolithic catalysts for lean burn emission control with drastically reduced materials usage in PGM, and improved catalytic functions.

Approach

Experimentally, low cost and green wet chemical methods are used to synthesize metal oxide nano-arrays on honeycomb substrates, followed by perovskite coating, PGM and BaO loading through sol-gel processes [9]. Post thermal-annealing is used to improve the crystallity and stoichiometry of 3-D composite nanostructures. Structure, morphology and chemical characterization is carried out using X-ray diffraction, transmission electron microscopy (TEM), scanning electron microscopy (SEM), and energy-dispersive X-ray spectroscopy. Catalyst evaluation is conducted using temperature programmable reduction, benchtop tube reactor kinetics testing, thermal and hydrothermal aging testing. Theoretically, the first principles thermodynamics and KMC simulation approaches are used to construct surface phase diagrams of (001) AO- and BO_2 terminated ABO_3 perovskite surfaces involving gaseous O_2 as the principal source of surface oxygen [10].

Results

Pristine metal oxide (such as ZnO, TiO_2, Co_3O_4, etc.) and metal oxide/Pt nano-array based monolithic catalysts have been successfully fabricated using low-cost and green-wet chemical synthesis methods, as highlighted in Figure 1. These monolithic nano-array catalysts have been systematically studied in terms of structure, morphology (Figures 1a-1f), mechanical and thermal stability, materials utilization efficiency, and catalytic CO and NO oxidation performance [9]. Excellent stability and catalytic performance toward CO and NO oxidation have been demonstrated. Furthermore, the materials loading and utilization efficiency in both metal oxide and PGM has been improved by an order of magnitude compared to washcoated powder-form monolithic catalysts, i.e., 10 times reduction of PGM and metal oxide usage was achieved (bottom table in Figure 1) [9]. The highly ordered and facet well-defined, well-separated but densely packed high surface area nano-arrays might have

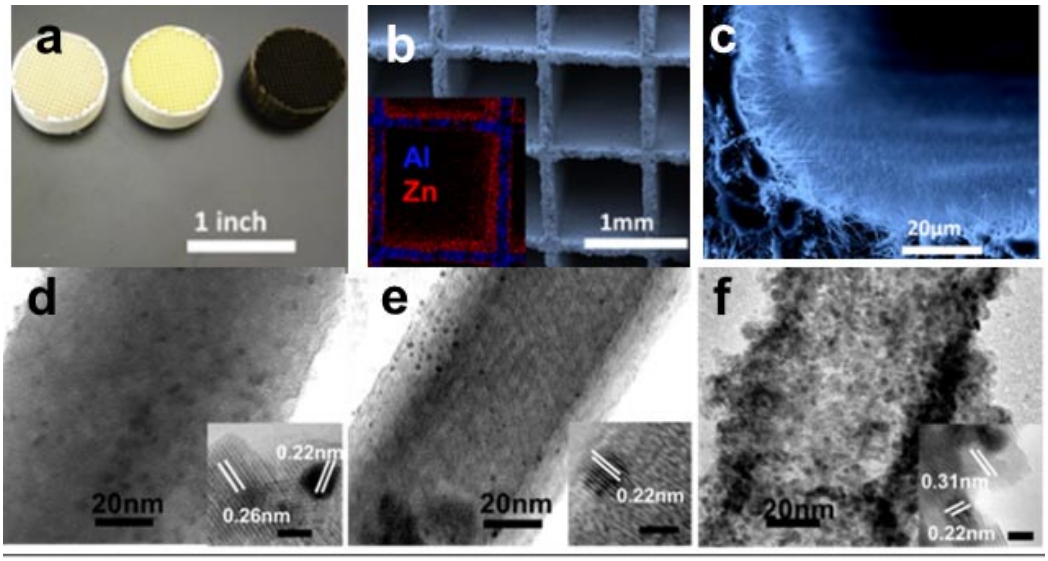

Monolithic Catalysts	PGM (g/L)	Catalyst layer thickness (μm)	Reference
Metal oxide nano-array	*0.5-1.0*	*1-10*	*This project*
Washcoated powder-form (Al_2O_3 based)	*2.0-12.0*	*15-100*	*Open literature*

FIGURE 1. (a) Selected nano-array cordierite monolithic catalysts. (b)-(f) SEM images of metal oxide nano-arrays on monoliths and corresponding TEM images of Pt-loaded metal oxide nanostructure. Bottom table: materials usage comparison between nano-array and washcoated powder-form monolithic catalysts in open literature.

helped the enabling of the well-defined, highly efficient, robust and tunable catalysts, which provide a potentially next generation of automotive catalysts.

As reported earlier, ZnO/LSCO/Pt nanorod arrays have been successfully fabricated on cordierite monoliths. Using similar process, ZnO/LSCO/BaO/Pt nano-array NSR catalysts was made by additional BaO aqueous precursor deposition. Figure 2a shows the low magnification top-view SEM image of as-prepared ZnO/LSCO/BaO/Pt nano-array catalysts. Zoom-in SEM image in Figure 2b indicated that nanorods are densely packed with a rough surface as a result of an overcoated layer of LSCO/Pt on ZnO nanorods. The NSR performance was investigated on the as-prepared ZnO/LSCO/BaO/Pt nano-array monolithic catalysts. Figure 2c reveals a NO_2 breakthrough after just a few seconds and the NO_2 outlet concentration reaches to a maximum of 160 ppm in about 10 min after NO_2 breakthrough. In a typical storage and reduction cycle (Figure 2d), after NO_2 outlet concentration reaches to a maximum and stable for 10 min, reducing gas (H_2) were induced to the system to start the "rich phase". NO_2 outlet concentration reaches a peak upon introduction of H_2 and then decreases to undetectable level in 10 min. The study on the structure and storage/reduction performance relationship is on-going. The distribution of BaO particles on the nano-array monolith may have played an important role in the NSR performance.

ZnO nano-array based monolithic catalysts demonstrated an excellent stability under extreme high temperature up to 1,000°C. However, in practice, water steam is generally involved in and sometimes could seriously decrease the catalyst performance. Therefore, the hydrothermal stability of ZnO-based nano-array catalysts has been studied using two types of experimental protocols. One is under extreme condition with 100% steam vapor at 120 °C. The structure and morphology analyses after 24 hours aging in boiling deionized water suggested that both the array structure and surface morphology of ZnO, ZnO/LSCO and ZnO/CeO_2 retain very well with no visible morphology change, which suggests as-prepared ZnO nano-array monolithic catalyst is very stable in 100% steam vapor environment. On the other hand, the hydrothermal aging was also conducted at high temperature under 10% steam vapor at 500 °C for 24 hours. Figure 3 shows the morphology evolution before and after hydrothermal aging by SEM imaging. As depicted in Figures 3a and 3b, fresh ZnO/LSCO/Pt nanorods maintained their hexagonal tips individually and good array structure as a whole. The cross-sectional view SEM image (Figure 3c) clearly indicated the uniform LSCO/Pt overcoated layer formed

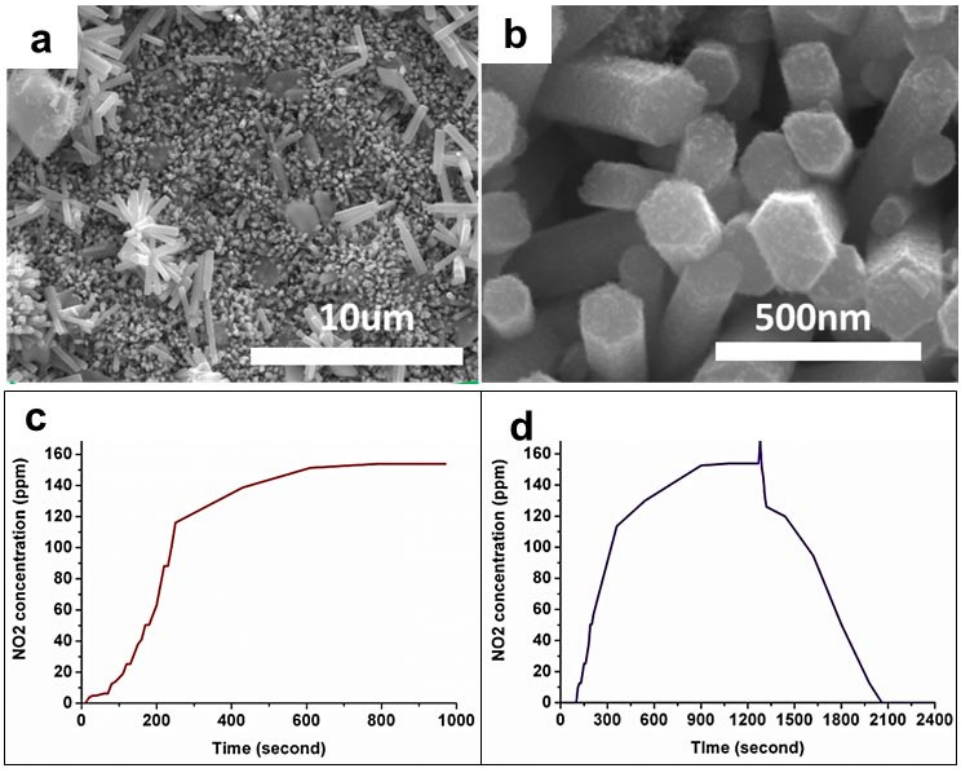

FIGURE 2. Typical top view (a) low magnification and (b) zoom-in SEM images of as-prepared ZnO/LSCO/BaO/Pt nano-array monolithic catalysts; (c) NO_2 storage profile and (d) a full cycle NSR profile of ZnO/LSCO/BaO/Pt nanorods-based monolithic catalysts.

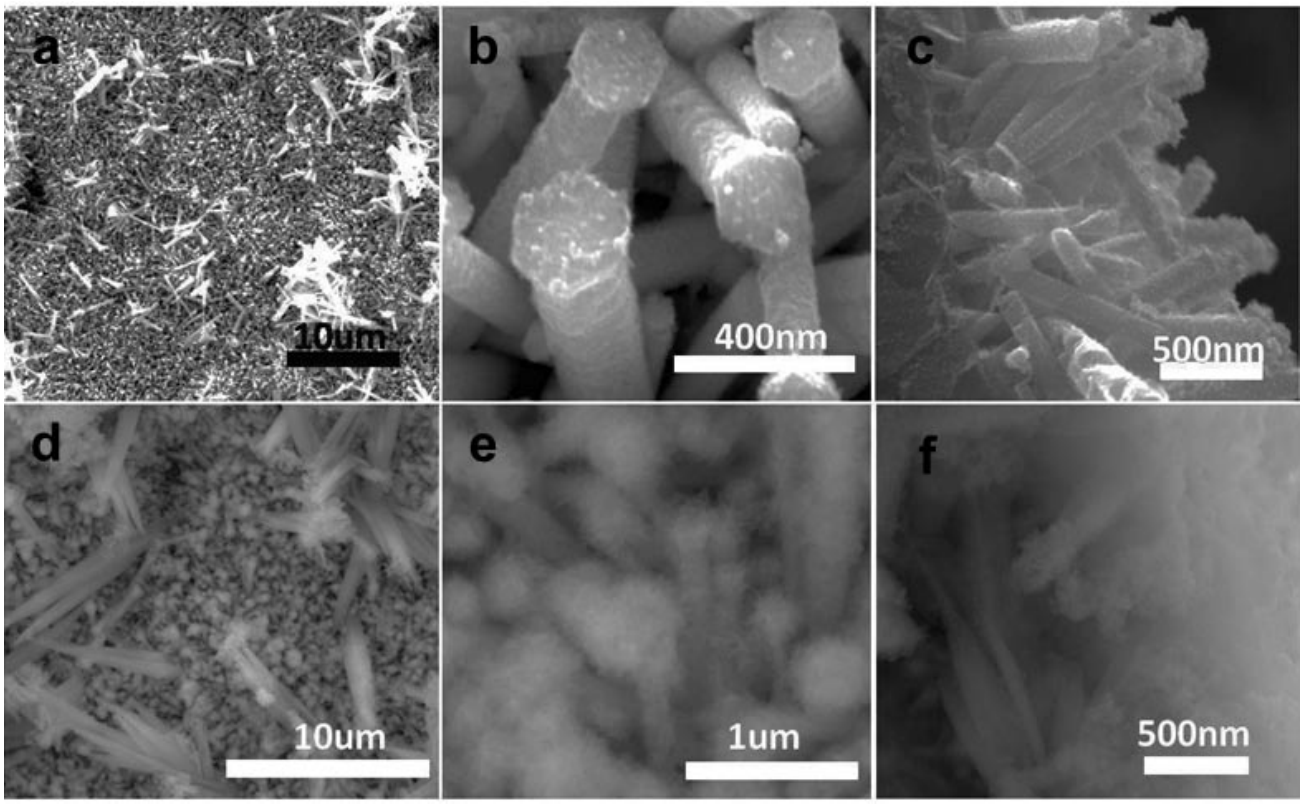

FIGURE 3. SEM images of ZnO/LSCO/Pt nanorods array on cordierite monolith before and after 24 hours aging in 10% stream vapor at 500 °C: (a), (b) and (c) fresh ZnO/LSCO/Pt nanorods array; (d), (e) and (f) ZnO/LSCO/Pt nanorods array after the steam hydrothermal aging.

throughout the side surfaces of individual nanorods. However, after 24 hours annealing at 500 °C in 10% steam vapor (Figure 3d), the distance between adjacent nanorods decreases and the surface of the nanorods become rough (Figure 3e and 3f), a thin silica layer was identified by energy-dispersive X-ray spectroscopy to form on the surface of ZnO/LSCO/Pt nanorods. However, little decrease on NO oxidation performance has been observed, which may be attributed to the passivation of silica layer on the surface.

On the basis of ZnO/LSCO/Pt catalysts, different preparation methods have been found to influence the nano-array catalysts' catalytic performance. It is found that sequentially deposited ZnO/LSCO/Pt nano-array shows higher NO conversion efficiency throughout the temperature range (Figure 4a). Three cycles of NO oxidation were performed on the sequential deposited catalysts to evaluate the stability of as-prepared catalysts (Figure 4b). The first test displayed a lower NO conversion efficiency than the other two, which may be induced by the impurity adsorbates on the catalyst surface. After burning the surface contamination in the first cycle, the second and third tests show almost the same profiles; demonstrating good catalytic stability of ZnO/LSCO/Pt. Figures 4c and 4d show the surface of co-loading ZnO/LSCO/Pt and sequential deposition ZnO/LSCO/Pt, respectively. Compared with co-loading sample, more Pt nanoparticles were observed on the sequential deposited ZnO/LSCO/Pt. Considering the identical Pt mass loading controlled for these two samples, certain amount of Pt may immerse in between LSCO layer and ZnO core during the co-loading process, leading to fewer Pt active sites exposed and compromised its catalytic performance. Therefore, the sequential deposition method may be a good process for preparing high efficient nano-array based monolithic catalysts.

Figure 5 is the NO conversion plots on the Pt/LSCO/ZnO/CH catalyst before and after SO_2 adsorption. After three cycles of NO oxidation tests, the conversion efficiency of the catalyst has no obvious change, which indicates that the catalyst has a very good stability for NO oxidation. After 5 hours of SO_2 adsorption, the conversion efficiency of the catalyst changes little from 65% to 63%. Even after 15 hours of poisoning, the conversion efficiency is ~55%. This indicates that the catalyst has a good S-poisoning resistance. Further investigation was conducted on the effect of S poisoning on the catalyst morphology by SEM, which shows no obvious change even after 15 hours of poisoning. The EDX results indicate no obvious change in other elements

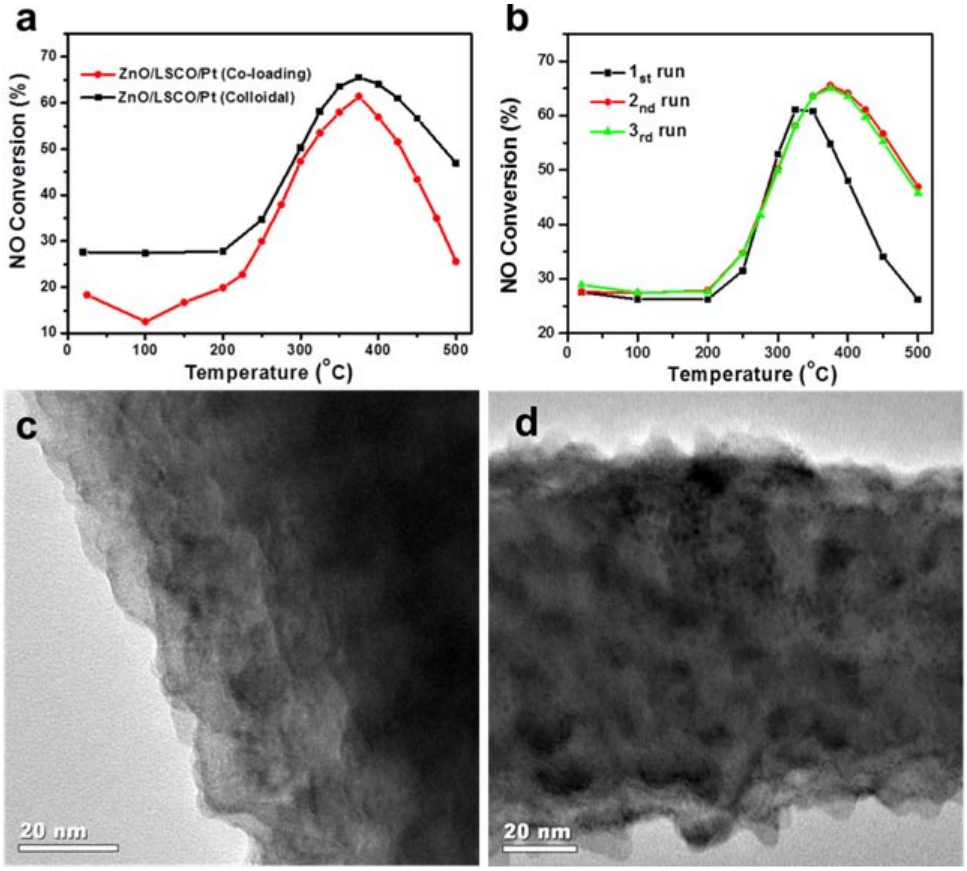

FIGURE 4. NO conversion plots on the ZnO/LSCO/Pt catalysts: (a) NO oxidation on ZnO/LSCO/Pt catalysts made by co-loading and colloidal sequential methods; (b) NO oxidation stability of colloidal deposited ZnO/LSCO/Pt; (c) typical TEM image of co-loading ZnO/LSCO/Pt surface; (d) typical TEM image of sequential deposition ZnO/LSCO/Pt surface.

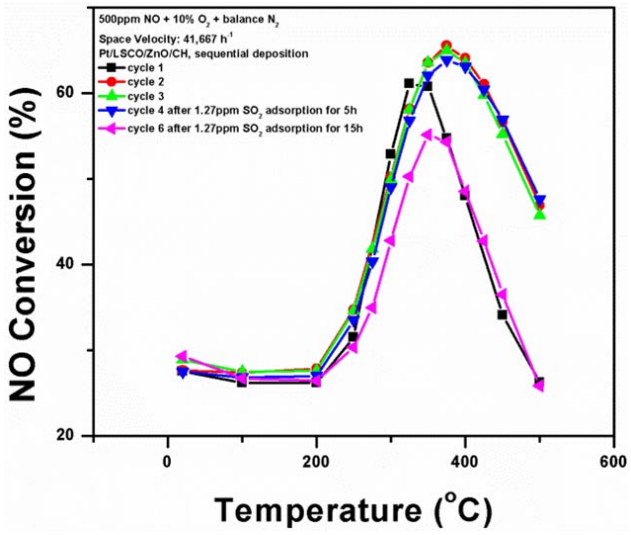

FIGURE 5. NO conversion plots on the Pt/LSCO/ZnO/CH catalyst before and after SO_2 adsorption.

except S, which shows 0.2 at%, before and after 15 hours of poisoning.

Furthermore, first principles methods were successfully employed enabling us to simulate the steady-state catalytic interaction of oxygen with $LaMnO_3$ (001) surface under varying levels of oxidative environment [10]. In the work carried out till date, density-functional theory together with transition-state theory was first used to obtain the energetics and activation barriers of various relevant elementary surface processes. The results were subsequently used in KMC simulations to explicitly account for the correlations, fluctuations, and spatial distributions of the oxygen ad-atoms and ad-molecules at the surface of the catalyst under steady-state conditions. The calculated (*p, T*) surface phase diagram based on purely thermodynamic arguments and the KMC method based equilibrium surface phase diagrams for the surface are computed and found to be in reasonable agreement with each other. In addition to the thermodynamics, the KMC based approach has allowed us to describe the kinetics related effects (such as influence of thermal and chemical history and surface preparation on sample's

behavior) and meta-stable regions on the (*p, T*) phase diagram. We find that the results from our model are in good agreement with available temperature programmed desorption experiments in the literature [11,12].

Thus far, only flat (001) $LaMnO_3$ surface facets have been considered in our *ab initio* models. In the imminent future, we are also going to investigate the surface facets with steps and edges. We note that the surface steps at the (001) facet of various perovskites (*e.g.*, Sr doped $LaMnO_3$ and $SrTiO_3$) [13,14] have indeed been observed experimentally and are known to play an important role in both thermodynamics and kinetics of oxygen interaction with the surface. Owing to the severe under-coordination, the surface atoms at the edges are expected to behave quite differently towards oxygen as compared to their counter parts at the flat surface. It will be interesting compare oxygen ad-atom and vacancy formation energies as well as the activation barrier for oxygen dissociative adsorption at flat surface and at the edges (as illustrated in Figure 6).

Conclusions

In FY 2012, the main accomplishments are listed as follows:

- Synthesized and characterized PGM and BaO-loaded 3-D metal oxide nanowire/rod arrays (such as ZnO/LSCO and TiO_2/LSMO, etc.) on monolith substrates.
- Investigated the (hydro-)thermal and mechanical stability, CO and NO oxidation performance, S-poisoning resistance, as well as initial NSR performance of the above-mentioned 3-D nanostructures.
- Demonstrated the nano-array catalysts' ultra-high materials usage efficiency in both PGM and metal oxides, excellent thermal and mechanical robustness, as well as tunable catalytic performance, showing their good potential to be used as potential next-generation automotive catalysts.
- Investigated the surface catalytic chemistry with perovskite (such as LMO, etc.) surfaces by the first principles thermodynamics and KMC simulations.

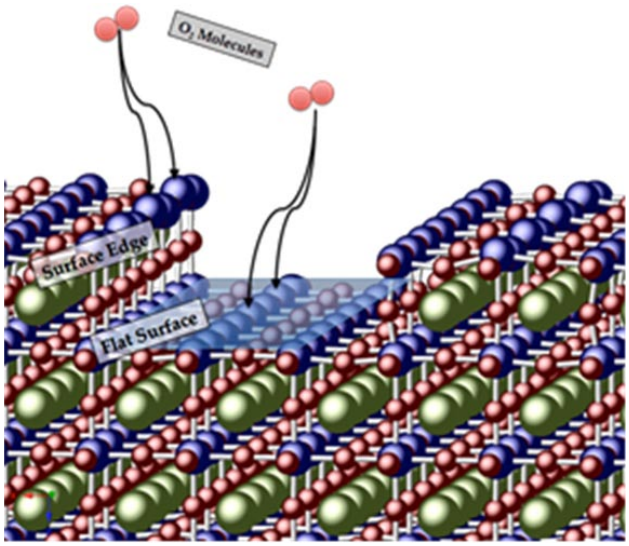

FIGURE 6. An atomic scale model of the MnO_2-terminated $LaMnO_3$ (001) surface with a surface step, illustrating dissociative adsorption of two oxygen molecules from gas phase on to a surface edge and a flat region.

References

1. R.M. Heck, R.J. Farrauto, Catalytic Air Pollution Control, Van Nostrand-Reinhold, New York, 1995.

2. L. Li, J. Chen, S. Zhang, F. Zhang, N. Guan, T. Wang, S. Liu, Environ. Sci. Technol. 39 (2005) 2841.

3. R.D. Clayton, M.P. Harold, V. Balakotaiah, Appl. Catal. B 84 (2008) 616.

4. F. Basile, G. Fornasari, A. Grimandi, M. Livi, A. Vaccari. Appl. Catal. B 69 (2006) 58.

5. Q. Wang, J.H. Sohn, J.S. Chung, Appl. Catal. B 89 (2009) 97.

6. J.E. Parks II, Science 327 (2010) 1584.

7. W.S. Epling, L.E. Campbell, A. Yezerets, N.W. Currier, J.E. Parks II, Catal. Rev. 46 (2004) 163.

8. P.S. Monks et al. Atmospheric Environment 43 (2009) 5268.

9. a) Y.B. Guo, Z. Ren, P.-X. Gao, DEER 2012 conference, Detroit, Oct. 19, 2012. b) P.-X. Gao, Y.B. Guo, Z. Ren, Z.H. Zhang, US non-provisional patent filed, PCT filed, 2012. c) Y.B. Guo, Z. Ren, Z.H. Zhang, W. Xiao, C.H. Liu, H. Sharma, H.Y. Gao, A. Mhadeshwar, and P.-X. Gao, 2012, submitted. d) Z. Ren, Y.B. Guo, Z.H. Zhang, C.H. Liu, and P.-X. Gao, 2012, submitted.

10. G. Pilania, P.-X. Gao, and R. Ramprasad, J. Phys. Chem. C, 2012, dx.doi.org/10.1021/jp3083985.

11. G. Saracco, F. Geobaldo, G. Baldi, Applied Catalysis B: Environmental 20 (1999) 277-288.

12. R. Spinicci, M. Faticanti, P. Marini, S. De Rossi, P. Porta, J. Mol. Catal. Chem., 197 (2003) 147-155.

13. H. Jalili, J.W. Han, Y. Kuru, Z. Cai, B. Yildiz, J. Phys. Chem. Lett. 2, (2011) 801–807.

14. T. Kubo, H. Nozoye, Appl. Phys. A 72, (2001) S277–S280.

FY 2012 Publications/Presentations

1. G. Pilania, P.-X. Gao, and R. Ramprasad, "Surface phase diagram of the MnO_2-terminated $LaMnO_3$ (001) surface in an oxygen environment through ab initio kinetic simulations," *J. Phys. Chem. C*, 2012, dx.doi.org/10.1021/jp3083985.

2. Z.H. Zhang, H.Y. Gao, W.J. Cai, C.H. Liu, Y.B. Guo, and P.-X. Gao, "TPR removal: A generic method for achieving tubular structure devices with good mechanical and structure soundness on substrates," *J. Mater. Chem.*, 2012, DOI:10.1039/C2JM34606K.

3. P. Shimpi, K.-T. Liao, H.J. Lin, P.-X. Gao, "Conversion of functional nanofilm into nanowires using combination of in-situ carbothermal and stress induced recrystallization," *Sci. Adv. Mater.,* 2012, 4, 837-842.

4. P.-X. Gao, P. Shimpi, et al., "Multifunctional Composite Nanostructures for Energy and Environmental Applications," *Int. J. Mole. Sci.,* 2012, 13(6), 7393-7423. (invited review)

5. M. Staruch, H.Y. Gao, P.-X. Gao, and M. Jain, "Low-field Magnetoresistance in $La_{0.67}Sr_{0.33}MnO_3$:ZnO composite film," *Adv. Funct. Mater.*, 2012, DOI: 10.1002/adfm.201200489.

6. Z. Ren, Y.B. Guo, G. Wrobel, D. Knecht, H.Y. Gao, Z.H. Zhang, P.-X. Gao, "Three Dimensional Koosh Ball Nanoarchitecture with Tunable Magnetic Core, Fluorescent Nanowire Shell and Enhanced Photocatalytic Property," *J. Mater. Chem.*, 2012, 22, 6862–6868.

7. Y.B. Guo, Z.H. Zhang, H.Y. Gao, Z. Ren, and P.-X. Gao, "Synthesis and Characterization of TiO_2/(La,Sr)MnO_3 Composite Nanostructures as CO oxidation catalysts," *Catalysis Today*, 2012, 184, 178–183.

8. L. Dong and S.P. Alpay, "Theoretical Analysis of the Crystal Structure, Band Gap Energy, Polarization, and Piezoelectric Properties of ZnO-BeO Solid Solutions", Physical Review B 2011, 84, 035315.

9. P.-X. Gao, and G. Liu, "Helical Nanostructures: Synthesis and Potential Applications," Chapter 7 in *Three Dimensional Nanoarchitectures: Designing the Next Generation Devices,* Weilie Zhou et al. *Eds*, Springer, New York, NY, 2011, 167-204. (invited)

10. P.-X. Gao, *Three-dimensional Composite Nanostructures for Lean NO_x Emission Control*, DOE Vehicle Technology Program Annual Merits Review Meeting, Washington, D.C., May 17, 2012.

11. K.T. Liao, Z. Ren, Z.H. Zhang, P.-X. Gao, *Free standing Cu-Sn alloying via low temperature solution process*, Connecticut Microelectronics and Optoelectronics Consortium (CMOC) Symposium 2012, Storrs, CT, April. 11, 2012.

12. Z. Ren, Y.B. Guo, G. Wrobel, P.-X. Gao, *Hierarchical Koosh Ball Nanoarchitectures: Towards Multifunctional and Three Dimensional Integration of Nanoscale Building Blocks*, CMOC Symposium 2012, Storrs, CT, April 11, 2012.

13. Z.H. Zhang, Y.B. Guo, N. Freedman, and P.-X. Gao, *CeO_2 Nanowire Arrays on 2D and 3D substrates for Lean NOx Automobile Emission Control,* Mateirals Research Society 2011 fall meeting, Boston, MA, Nov. 30, 2011.

14. Z. Ren, Y.B. Guo, G. Wrobel, P.-X. Gao, *ZnO Nanowire Growth Array Growth on Three- Dimensional (3D) Spherical Substrate: Facile Synthesis of Multi-component Koosh Ball Structures*, Materials Research Society 2011 fall meeting, Boston, MA, Nov. 28, 2011.

15. Z. Ren, Y.B. Guo, D. Knecht, P.-X. Gao, *Synthesis of Fe_3O_4/SiO_2 Core-shell Structured Microspheres*, Materials Science & Technology 2011 conference, Columbus, OH, Oct. 17, 2011.

16. L. Dong, and S. P. Alpay, *Effect of Equi-Biaxial In-Plane Strains on GaN Thin Films and InGaN/GaN Superlattices*. Materials Science & Technology 2011 Conference, Columbus, OH, Oct., 2011.

17. S. Glod, Z.H. Zhang, Y.B. Guo, P.-X. Gao, *ZnO Nanowire Arrays Coated With $La_{1-x}Sr_xCoO_3$ Perovskite Nanoparticles for DOC and DeNOx Integration*, Materials Science & Technology 2011 conference, Columbus, OH, Oct. 18, 2011.

18. P.-X. Gao, et al., *Monolithic metal oxide based composite nanowire LNT catalysts*, Directions in Engine-Efficiency and Emissions Research (DEER) Conference 2011, Detroit, Oct. 5, 2011.

19. P.-X. Gao, et al., *Thermal and chemical stability of metal oxide/perovskite/metal nano-interfaces: An investigation of modeled ZnO/(La,Sr)CoO_3/Pt nanowire based catalyst*, DoE Catalysis Science program meeting, Annapolis, MD, Oct. 2, 2011.

Special Recognitions & Awards/Patents Issued

1. K.T. Liao, Z. Ren, Z.H. Zhang, P.-X. Gao, *Free standing Cu-Sn alloying via low temperature solution process*, CMOC symposium 2012, Storrs, CT, April. 11, 2012. (Best student oral presentation award)

2. Z. Ren, Y.B. Guo, G. Wrobel, P.-X. Gao, *Hierarchical Koosh Ball Nanoarchitectures: Towards Multifunctional and Three Dimensional Integration of Nanoscale Building Blocks*, CMOC symposium 2012, Storrs, CT, April 11, 2012. (Best student poster award)

3. P.-X. Gao, Y.B. Guo, Z.Ren, Z.H. Zhang, "Metal oxide nanorod arrays on monolithic substrates", US non-provisional patent filed, PCT filed, 2012.

4. P.-X. Gao, Z.H. Zhang, "Temperature-programmed-reduction Fabrication Method for Tubular Structure Devices", US provisional patent filed, 2012.

5. P.-X. Gao, Y.B. Guo, and Z. Ren, "Ultra-efficient, robust and well-defined nano-array based monolithic catalysts," Invention Disclosure 12-079, University of Connecticut, 2012.

III.14 Experimental Studies for DPF, and SCR Model, Control System, and OBD Development for Engines Using Diesel and Biodiesel Fuels

John Johnson (Primary Contact), Gordon Parker, Jeffrey Naber, Song-Lin Yang
Michigan Technological University
1400 Townsend Drive
Houghton, MI 49931

DOE Technology Development Manager:
Ken Howden

DOE Project Officer: Nicholas D'Amico

Subcontractors:
- Oak Ridge National Laboratory, Oak Ridge, TN
- Pacific Northwest National Laboratory, Richland, WA

Overall Objectives

- Experimentally validated reduced order models and state estimation algorithms.
- Quantify particulate matter (PM) maldistribution, loading, and NO_2/PM ratio effects on passive and active regeneration, bio-fuel blends, and aging for catalyzed particulate filters (CPFs).
- Increased knowledge of ammonia (NH_3) storage behavior, optimal NH_3 loading, hydrocarbon (HC) poisoning, and aging for selective catalytic reduction (SCR) catalysts.
- Understanding effect of sensor type/configuration on state estimation quality.
- Optimal reductant strategies for SCR operation and CPF regeneration.

Fiscal Year (FY) 2012 Objectives

- Calibrate reduced order models with experimental data and quantify the effect of model reduction compared to high-fidelity models.
- Develop state estimation strategies, and understand the effects of different sensor combination/types.
- Conduct studies in CPF PM oxidation kinetics and SCR oxides of nitrogen (NO_X) reduction kinetics.
- Evaluation of diesel oxidation catalyst (DOC) and SCR high-fidelity and reduced order estimator models by industrial partners.

Accomplishments

The most significant accomplishments of this project to date are listed below:

- Multiple sensor technologies studied on the MTU engine/aftertreatment systems to characterize NO_X, NH_3, PM concentration, and PM mass retained.
- A high-fidelity one-dimensional (1-D) CPF model was enhanced for calibration of engine data that is being used for reduced order model/state estimation.
- A lumped CPF model for reduced order model/state estimation was developed and calibrated.
- Completed development and calibration of the DOC high-fidelity and the reduced order estimator models to engine data.
- Completed development and calibration of the SCR high-fidelity model to the reactor data.
- Completed development and calibration of the SCR high-fidelity and the reduced order estimator models to engine data.
- Developed an agreement with four of our industrial partners to use and evaluate MTU codes - the software was released and evaluated.

Future Directions

- Hydrocarbon impact on SCR performance will be tested on the bench reactor at Oak Ridge National Laboratory - HC effect model will be built and calibrated from this.
- Similar estimation strategies to those for the SCR and DOC will be implemented for a CPF along with evaluation of sensor combinations for on-board diagnostics (OBD).
- Passive oxidation testing and the mass retained and concentration sensors study will be performed.
- Perform engine tests to experimentally characterize PM loading maldistribution in the CPF and its dependency on regeneration parameters.
- High-fidelity CPF model will be used to determine optimum PM kinetics from active regeneration and passive oxidation data.
- Transient testing with a Cummins 2010 6.7-L ISB engine SCR system to determine model response as compared to experimental data including NO_X, and NH_3 sensor data.
- ISB SCR testing to determine NH_3 maldistribution as a function of temperature and space velocity.

Introduction

The project focus is to develop experimentally validated DOC, CPF, and SCR models with real-time internal state estimation strategies that support future objectives for aftertreatment systems that minimize the energy penalty of meeting emission regulations. Studying the effects of sensor type and combinations on state estimate quality is an inherent aspect of the process. Two additional phases of this work focus on developing SCR and CPF models in specific, high-impact areas. The CPF research includes PM maldistribution, loading, and passive regeneration over large NO_X/PM ranges for engines using both diesel and biodiesel fuel blends, and optimal active regeneration. The SCR research examines NH_3 distribution, optimal NH_3 loading, and HC poisoning.

Approach

To achieve the goal of DOC, diesel particulate filter (DPF), and SCR state estimation strategies, a mix of simulation and experimental studies with a combination of off-the-shelf and prototype sensor technologies is used. Engine test cell and reactor data along with high-fidelity models are used for reduced order model forms, suitable for state estimation strategy development.

Results

DOC Estimator: The reduced order model-based DOC state estimator was simulated on a surrogate Federal Test Procedure (FTP) cycle. Figure 1 shows the comparison of the DOC outlet NO_2 concentration and temperatures for a closed-loop estimator. The DOC outlet temperature closely follows the response of the measured DOC outlet temperature with less than 0.1% error. With the accurate temperature estimate, the estimator agrees with the measured DOC outlet NO_2 concentration for most parts of the test with a maximum error of 26%.

SCR Estimator: A reduced-order SCR model-based estimator was developed and used for the Extended Kalman Filter-based state estimator. Figure 2 shows a comparison of the SCR outlet NO, NO_2, and NH_3 concentration on the surrogate FTP cycle. From the figure it can be observed that the estimator in a closed loop fits the SCR outlet NH_3 concentration with a maximum error of +/-30 ppm. The improved estimate of the storage and the NH_3 concentration results in reduced error in the NO and NO_2 concentration with a maximum error of +/-30 ppm.

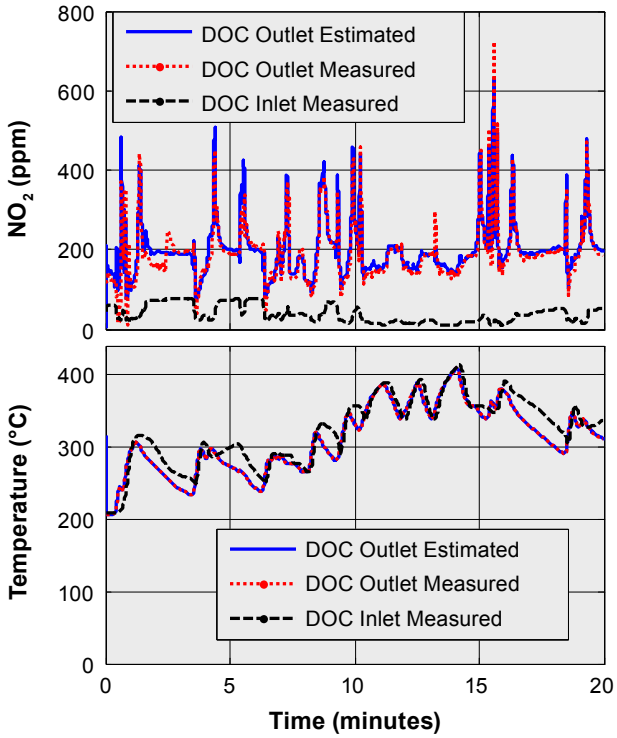

FIGURE 1. Comparison of the DOC outlet NO_2 concentrations and temperatures with the estimator in a closed loop for the ISB surrogate FTP cycle.

CPF High Fidelity Model: The CPF high-fidelity model was calibrated to CPF pressure drops, PM retained in the CPF at the end of different stages and CPF outlet temperatures as well as overall mass-based filtration efficiencies to selected test cases from passive oxidation and active regeneration experiments. Model comparison to experimental values for a passive oxidation test case is shown in Figure 3. Details about the model development and results obtained from two test cases, one passive oxidation and one active regeneration, were included in an SAE International paper. The filtration sub-model developed in this model is being used in a reduced order model being developed and calibrated. This will form the basis for a state estimation model code to be used for control strategy development and OBD for a CPF.

CPF Lumped Model: Development and calibration of the CPF lumped model has been carried out during the last year. The lumped model will be used as the reduced order model for the estimator. The model has incorporated features and filtration with wall PM oxidation sub-models from the CPF high-fidelity model. The model has been calibrated on both the passive oxidation and active regeneration data for ultra-low sulfur fuel and biodiesel. Figure 4 shows a comparison of the CPF pressure drop between the lumped model and the experimental active regeneration data for B10-1. The

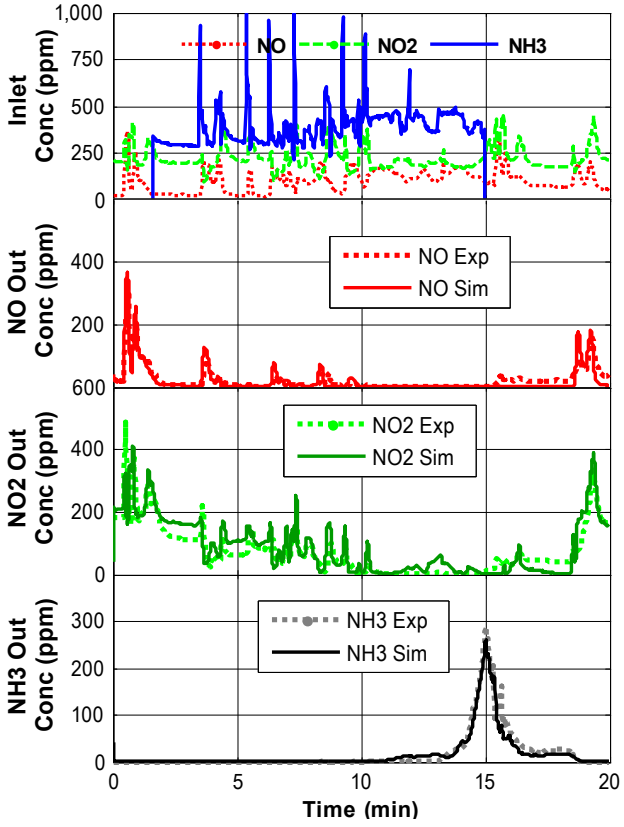

FIGURE 2. Comparison of the SCR outlet NO, NO_2 and NH_3 concentration for the ISB surrogate FTP cycle.

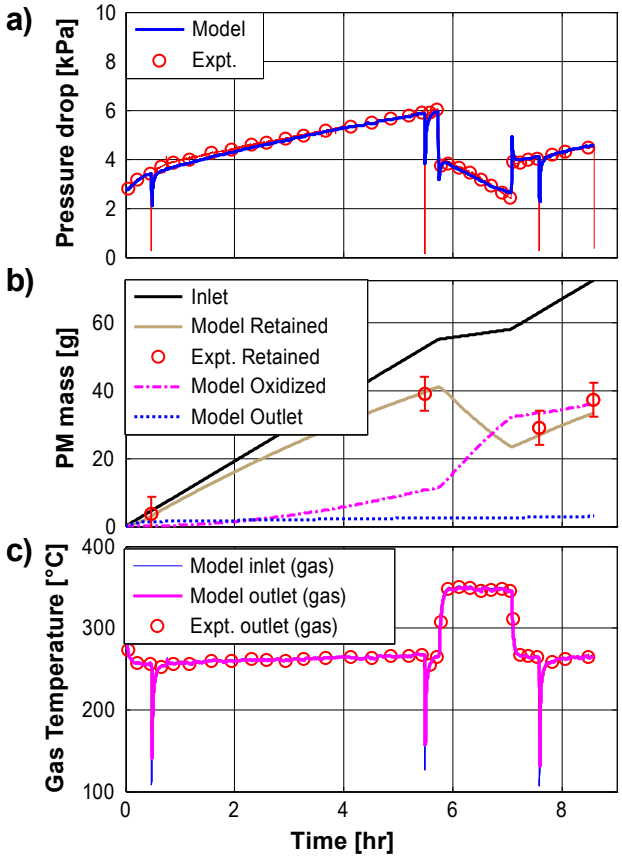

FIGURE 3. ISL passive oxidation test case (test 12) - comparison of CPF model outputs to experimental data: a) experimental vs. model pressure drop vs. time, b) experimental vs. model PM mass retained with model PM mass inlet, PM mass oxidized and PM mass outlet, and c) experimental vs. model outlet gas temperature with model input inlet gas temperature vs. time.

model follows the ΔP data closely in Figure 4 and also the PM mass retained and the NO and NO_2 concentrations out of the CPF. Work has begun on an Extended Kalman Filter for the estimator based upon the CPF reduced order model (lumped).

CPF Maldistribution: The maldistribution research was conducted with filters loaded at MTU using the ISB engine and scanned at Cummins using an Advantest TAS7000 3D Imaging Analysis System using terahertz waves. The Phase 1 maldistribution study has been completed. This study included four tests and seven filter scans of clean and loaded substrates. The TAS7000 scans a substrate using 4,096 sample points with a resolution of a 4 x 4 x 4.3 mm rectangle. This produces data with high enough resolution for accurate PM distribution analysis. An example of a filter scan is shown in Figure 5. A summary of the research results was presented at the 2012 DOE DEER conference.

Sensor Implementation and Characterization: Research has been conducted on mass retained and PM concentration sensors. The Pegasor sensor measures PM concentration and the data correlates with the hot PM filter concentrations measured using the MTU method. The GE Accusolve and Filter Sensing Technologies sensors are mass retained sensors. Both have been shown to correlate to mass retained data obtained by weighting the substrate. Evaluation of the GE Accusolve is ongoing. The Pegasor and GE Accusolve will be used in conjunction with the models once there is confidence built in the results. A PM sensor that is intended to detect CPF failure has been installed downstream of the CPF and is currently being evaluated. A NH_3 sensor was installed downstream of the SCR and being used to measure NH_3 slip.

SCR NH_3 Distribution: NH_3 maldistribution at the SCR inlet is a major difference between the SCR engine and reactor tests. This likely contributes to the differences in kinetic parameters between the SCR high fidelity models separately calibrated to the SCR engine and reactor test data. SCR engine tests were performed to study the maldistribution of NH_3 and NH_3/NO_x ratio (ANR) by measuring the emissions at 25 different positions at the outlet face of the SCR brick with and without the urea injection upstream of the SCR.

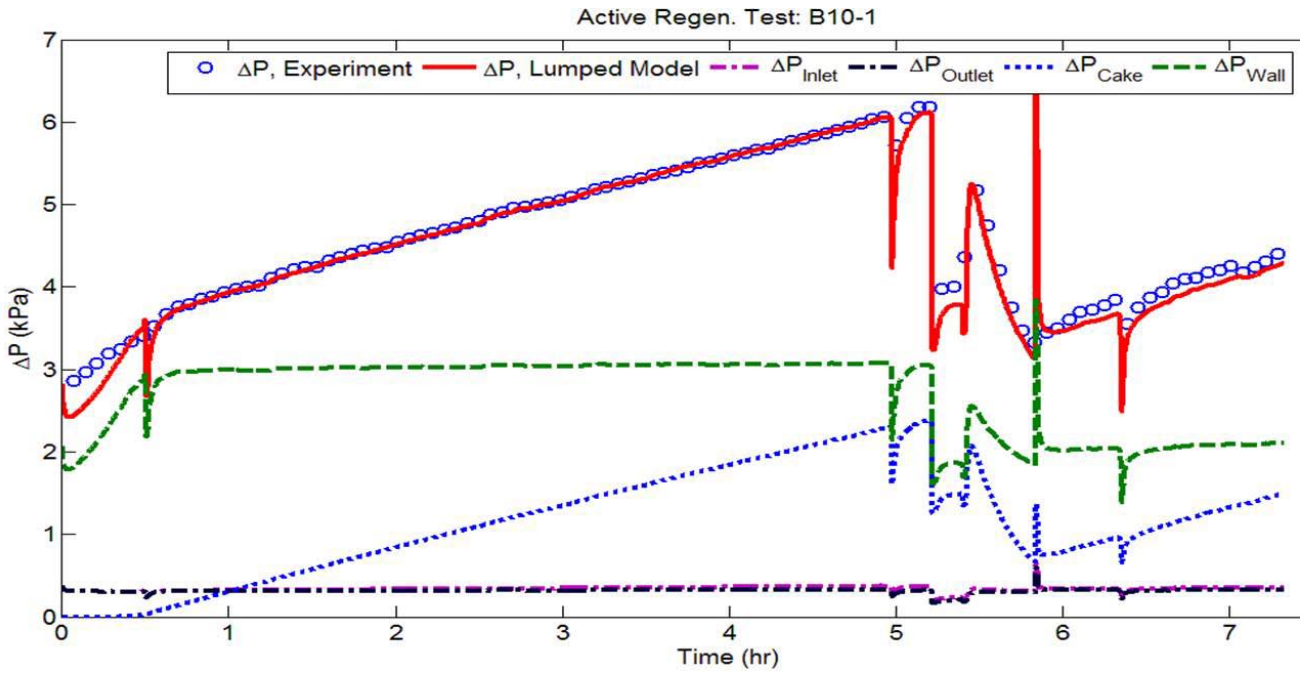

FIGURE 4. CPF Lumped Model Pressure Drop for B10-1 on ISL engine.

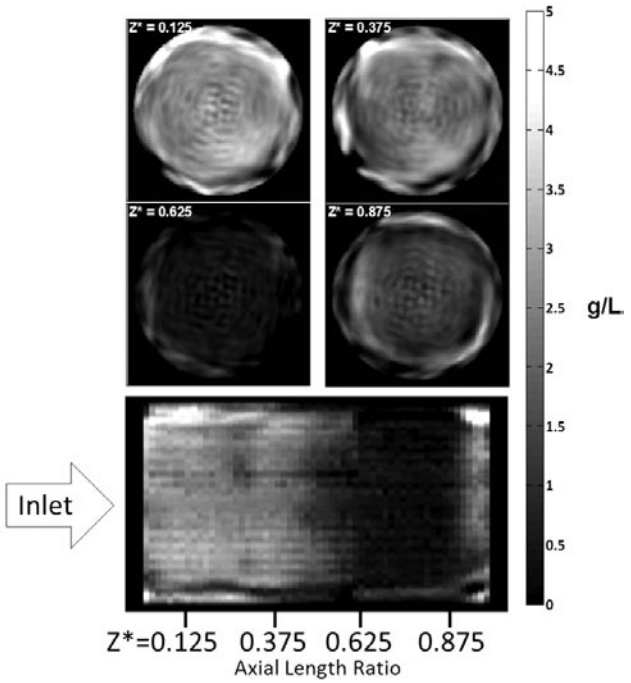

FIGURE 5. PM Distribution in the CPF after a 600°C Active Regeneration with 69% of the PM Oxidized from ISB engine with an initial PM loading of 5.1 g/L.

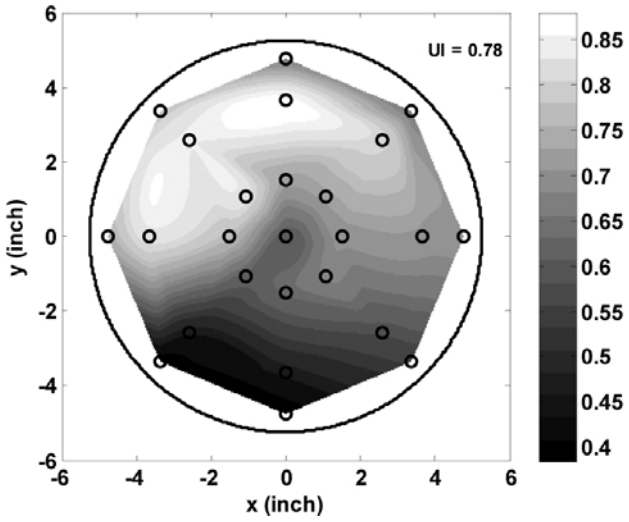

FIGURE 6. Distribution of ANR at the SCR inlet with an average ANR of 0.65 for exhaust mass flow rate of 9.9 kg/min and SCR inlet temperature of 350°C on the ISB Engine.

The measurement positions as well as a determined distribution profile of ANR with the average ANR of 0.65 is shown in Figure 6. The distribution of NOx has been confirmed to be uniform. It can be seen from Figure 6 that the maldistribution of ANR ranges from 0.4 to 0.9 with a uniformity index of 0.78, indicating an obvious level of maldistribution of available NH_3 at the SCR inlet. The maldistribution level at exhaust mass flow rate of 4.2 kg/min was found to be similar to this case.

Conclusions

Specific conclusions are as follows:

- The DOC and SCR models and estimators have been successfully calibrated to the ISB surrogate FTP cycle data.
- The CPF lumped model that will be used with the estimator has been developed and calibrated to the passive oxidation and active regeneration data.
- The CPF high-fidelity model is being used to calibrate to the passive oxidation and active regeneration data for determining the kinetic parameters – the experimental and model resistances are proving useful to understanding the data.
- The Phase 1 maldistribution study has been completed and a method has been developed to scan the substrates and analyze the terahertz wave data.
- A method for determining NH_3 maldistribution has been developed.
- Nine papers have been written for publication in 2013 – seven of those for the SAE 2013 International Congress, one presentation and one poster were prepared for the 2012 DOE DEER Conference.

FY 2012 Publications/Presentations

1. "A Kalman Filter Estimator for a Diesel Oxidation Catalyst, During Active Regeneration of a CPF," H. Surenahalli, G. Parker, J. Johnson, and M. Devarakonda, *American Control Conference,* June 2012.

2. "Experimental Studies for DPF, and SCR Model, Control System, and OBD Development for Engines Using Diesel and Biodiesel Fuels," Oral Presentation, G. Parker, 2012 DOE Vehicle Technologies Annual Merit Review, Washington, D.C.

3. "Engine Test and Analysis Report for the Effects of a Biodiesel Blends on Particulate Matter Oxidation in a Catalyzed Particulate Filter during Active Regeneration," J. Pidgeon, J. Johnson, J. Naber, *Technical Report to DOE*, (October12, 2011).

4. "A Parameterized Iron-Zeolite SCR Model Calibrated to Reactor Data,"S. DeLand, J. Keith, G. Parker, J. Johnson, *AICHE No. 222827-2011*, AICHE Annual Meeting October 2011.

5. "Estimator Strategy Report," H. Surenahalli, G. Parker, J. Johnson, and M. Devarakonda, *Technical Report to DOE* (Jan 27, 2012).

6. "Engine Test and Analysis Report for Catalyzed Particulate Filter Particulate Matter Loading and Passive Oxidation with Ultra Low Sulfur Diesel and Biodiesel Fuels," C. Hutton, J. Johnson, J. Naber, *Technical Report to DOE* (Nov 7, 2011).

7. "Catalyzed Particulate Filter Passive Oxidation Study with Ultra Low Sulfur and Biodiesel Blended Fuel," K. Shiel, J. Naber, J. Johnson, C. Hutton, Michigan Technological University, *SAE Paper No. 2012-01-0837*, SAE International Congress April 25, 2012.

8. "Procedure Development and Experimental Study of Passive Particulate Matter Oxidation in a Diesel Catalyzed Particulate Filter," C. Hutton, J. Johnson, J. Naber, J. Keith, Michigan Technological University, *SAE Paper No. 2012-01-0851*, SAE International Congress April 25, 2012.

9. "Spatial Variations in NH_3 Storage on Copper Zeolite SCR Catalysts," J.A. Pihl, C.S. Daw, *Presentation to the CTI 4th International Conference on NO_X Reduction*, Detroit, MI, June 20, 2012.

10. "A Study of the Effect of Biodiesel Fuel on Passive Oxidation in a Catalyzed Particulate Filter" K. Shiel, Master Thesis, Michigan Technological University, 2012.

III.15 The Advanced Collaborative Emissions Study (ACES)

Dan Greenbaum (Primary Contact),
Rashid Shaikh, Maria Costantini,
Annemoon van Erp
Health Effects Institute (HEI)
101 Federal Street, Suite 500
Boston, MA 02110

DOE Technology Development Manager:
Gurpreet Singh

NETL Project Manager: Carl Maronde

Subcontractors:
- Coordinating Research Council (CRC), Alpharetta, GA
- Lovelace Respiratory Research Institute (LRRI), Albuquerque, NM

Overall Objectives

- Phase 1: Extensive emissions characterization at Southwest Research Institute® (SwRI®) of four production-intent heavy-duty diesel engine and control systems designed to meet 2007 standards for particulate matter (PM) and nitrogen oxides (NOx). One engine/aftertreatment system will be selected for health testing.
- Phase 2: Extensive emissions characterization of a group of production-intent engine and control systems meeting the 2010 standards (including more advanced NOx controls to meet the more stringent 2010 NOx standards).
- Phase 3: One selected 2007-compliant engine will be installed and tested in a specially-designed emissions generation and animal exposure facility at the Lovelace Respiratory Research Institute (LRRI) (Phase 3A) and used in chronic and shorter-term health effects studies to form the basis of the ACES safety assessment (Phases 3B and 3C). This will include periodic emissions characterization during both a core 24-month chronic bioassay of cancer endpoints in rats and biological screening assays in both rats and mice (Phase 3B) as well as emissions characterization during a set of shorter animal exposures and biological screening using accepted toxicological tests after the end of the chronic bioassay (Phase 3C). (NOTE: Only the emissions characterization and biological screening activities during Phase 3 are components of the DOE ACES contract).

Fiscal Year (FY) 2012 Objectives

- Phase 2: Conduct emissions characterization at SwRI® of production-intent engine and control systems meeting the 2010 standards.
- Phase 3: Publish Phase 3A Emissions Characterization report and short-term exposures in mice and rats. Publish Phase 3B Health Testing reports describing those short-term results. Continue the long-term exposures in rats and conduct further intensive exposure characterization campaigns midway and towards the end of the animal exposures.

Accomplishments

Key Accomplishments

- Published reports with results of Phase 3A exposure characterization (HEI Communication 17) and Phase 3B shorter-term bioscreening studies in mice and rats (HEI Research Report 166).
- Initiated Phase 2 emissions characterization of three 2010-compliant engines and completed testing of the first and second engines.
- Participated in the meeting of the International Agency for Research (IARC) on Cancer to ensure that the ACES Phase 3B Report results were integrated into the IARC review of diesel exhaust and carcinogenicity, highlighting the benefits of the new technology.

General Oversight

- Held a third stakeholder workshop to discuss progress in ACES, including additional results from the Phase 3B short-term biological screening exposures in mice and rats (October 2011).
- Presented ACES results at the CRC Real Word Vehicle Emissions Workshop in San Diego (March 2012).
- Held a stakeholder briefing ahead of publication of the Phase 3B interim reports (April 2012).
- Held an ACES Oversight Committee meeting to discuss the remaining work to be performed in ACES, including a decision on extending the bioassay to 30 months (April 2012).
- Presented ACES results at the HEI Annual Conference in Chicago, IL during a plenary session on diesel exhaust (McDonald) and during poster sessions (Bemis, Conklin, Hallberg, McDonald, Sun, and Tennant) (April 2012).

- Presented ACES progress at the 2012 DOE Annual Merit Review Meeting (May 2012).

Phase 2

- Finalized contract negotiation for Phase 2 (comprehensive emissions characterization for 2010-compliant Class 8 Engines) (October 2011).
- Finalized planning with CRC about the start of Phase 2 (comprehensive emissions characterization for 2010-compliant Class 8 Engines) (January 2012).
- Held a site visit to SwRI® to inspect the facility and finalize the testing arrangements for Phase 2. Continued discussions with the CRC Panel on how to accommodate trap regeneration events in the test cycles (May 2012).
- Completed testing of two 2010-compliant engines at SwRI® (September 2012).

Phase 3A

- Published the Phase 3A final report (exhaust characterization at LRRI leading up to the start of the animal exposures) as HEI Communication 17 (February 2012).

Phase 3B

- Completed engine and dynamometer repairs owing to more than usual wear and tear from the 16-hr cycle; continued communication with LRRI and engine manufacturers to ensure the necessary repairs of the drivetrain (December 2011).
- Received revised reports with short-term biological screening results from the five Phase 3B investigators and sent the reports to the Special Review Panel (December 2011).
- Conducted a pathology peer review site visit to evaluate results from the Phase 3B 12-month rat exposures (December 2011).
- Reviewed — and accepted for publication — the revised reports with short-term biological screening results from four Phase 3B investigators (Bemis, Conklin, Hallberg, and McDonald) (January 2012).
- Presented Phase 3B interim results of short-term biological screening in mice and rats during a seminar at the California Air Resources Board (February 2012).
- Received from LRRI a progress report and rodent survival data, as well as plans for remaining work in Phase 3B from the ACES ancillary studies for review by the ACES Oversight Committee (March 2012).
- Published the Phase 3B reports with short-term biological screening results as HEI Research Reports to ensure their consideration in upcoming health reviews of diesel exhaust (HEI Research Report 166) (April 2012).
- Held a site visit to Ohio State University to discuss procedures for tissue evaluation for the ancillary study by Sun (April 2012).
- Conducted the third intensive chemical characterization during the chronic inhalation exposures at LRRI and sent samples to Desert Research Institute for analysis (May 2012).
- Conducted a site visit to LRRI to witness the Phase 3B 24-month interim sacrifice (May 2012).
- Participated in the IARC meeting to ensure that the ACES Phase 3B Report results were integrated into the IARC review of diesel exhaust and carcinogenicity, highlighting the benefits of the new technology; as a result, (June 2012).
- Completed the Phase 3B 24-month interim sacrifice at LRRI and shipped tissue samples to the ancillary studies investigators (June 2012).
- In coordination with Dr. Sun at Ohio State University, made a decision to terminate the study. Discussed potential gaps in Phase 3B health effects testing with the HEI Research Committee (June 2012).
- Published the complete HEI Research Report 166 (including Part 4, the Conklin ancillary study) on the web (September 2012).
- Continued emissions generation and exposure characterization during the Phase 3B chronic testing at LRRI, completing month 28 of 30 (September 2012).

Future Directions

- Discuss with the ACES Oversight Committee whether to commission further analyses in Phase 3B to fill in gaps due to termination of the Sun and Veranth studies.
- Complete the ancillary studies in November 2012 and receive final reports by January 2013.
- Complete Phase 2 testing in December 2012 and receive a draft final report by April 2013.
- Complete Phase 3B exposures at LRRI in December 2012 and receive a final report by June 2013.
- Conduct stakeholder briefing to present final results of Phases 2 and 3B in the Spring of 2013.
- Present ACES activities and results at the DEER meeting in Dearborn, MI in October 2012; the CRC Real World Emissions workshop in San Diego, CA in April 2013, and the HEI Annual Conference in San Francisco, CA in April 2013.

- Peer review and publish the Phase 2 and Phase 3B reports during 2013 (Phase 2) and 2014 (Phase 3B).

Introduction

The ACES is a cooperative, multi-party effort to characterize the emissions and assess the safety of advanced heavy-duty diesel engine and aftertreatment systems and fuels designed to meet the 2007 and 2010 emissions standards for PM and NOx. The ACES project is being carried out by the Health Effects Institute (HEI; contractor) and the Coordinating Research Council (CRC; subcontractor). It is utilizing established emissions characterization and toxicological test methods to assess the overall safety of production-intent engine and control technology combinations that will be introduced into the market during the 2007-2010 time period. This is in direct response to calls in the U.S. Environmental Protection Agency Health Assessment Document for Diesel Engine Exhaust [1] for assessment and reconsideration of diesel emissions and health risk with the advent of new cleaner technologies.

The characterization of emissions from representative, production-intent advanced compression ignition engine systems includes comprehensive analyses of the gaseous and particulate material, especially those species that have been identified as having potential health significance. The core toxicological study includes detailed emissions characterization at its inception, and periodically throughout a two-year chronic inhalation bioassay similar to the standard National Toxicology Program bioassay utilizing two rodent species. Other specific shorter-term biological screening studies also are being undertaken, informed by the emissions characterization information, to evaluate these engine systems with respect to carefully selected respiratory, and other effects for which there are accepted toxicologic tests. It is anticipated that these emissions characterization and studies will assess the safety of these advanced compression ignition engine systems, will identify and assess any unforeseen changes in the emissions as a result of the technology changes, and will contribute to the development of a data base to inform future assessments of these advanced engine and control systems.

Approach

Experimental work under ACES is being conducted in three phases, as outlined in the Objectives. Detailed emissions characterization (Phases 1 and 2) is performed by an existing engine laboratory (SwRI®) that meets the U.S. Environmental Protection Agency specifications for 2007 and 2010 engine testing. In Phase 1, emissions from four 2007-compliant engine/control systems were characterized. One engine was selected for health testing in Phase 3. In Phase 2, emissions from three 2010-compliant engine/control systems are being characterized. In Phase 3, the selected 2007-compliant engine/control system was installed in a specially designed emission generation facility connected to a health testing facility at LRRI to conduct a chronic inhalation bioassay and shorter term biological screening in rats and mice. During the 30-month bioassay, emissions are being characterized at regular intervals throughout the testing.

The emissions characterization work is overseen by the subcontractor (CRC) and CRC's ACES Panel. The health effects assessment is overseen by HEI and its ACES Oversight Committee (a subset of the HEI Research Committee augmented by independent experts from several disciplines), with advice from an advisory committee of ACES stakeholder and other experts. The overall effort is guided by an ACES steering committee consisting of representatives of U.S. Department of Energy, engine manufacturers, Environmental Protection Agency, the petroleum industry, the California Air Resources Board, emission control manufacturers, and the Natural Resources Defense Council. Set up of the emission generation facility at LRRI (for Phase 3) and establishment of periodic emissions characterization throughout Phase 3 has been done with input from the team of investigators who conducted Phase 1 and the CRC ACES Panel.

Results

The results obtained during this reporting period pertain to the ongoing Phase 2 emissions characterization at SwRI® and Phase 3B animal exposures at LRRI. Preliminary results of the first two engines tested at SwRI® indicated that the intended emissions reductions are met. Figure 1 shows that the emissions of key pollutants of the first 2010-compliant engine (Engine X) are considerably lower than emissions from the 2007-compliant engines tested in Phase 1 (Engines A-D), with the exception of N_2O as well as PM measured in the exposure chamber (simulating animal exposures) during the Federal Test Procedure cycle. Due to the expected different regeneration pattern (i.e. less frequent) in the 2010-compliant engines, the CRC ACES Panel, SwRI® scientists, and HEI staff extensively discussed whether or not to have a forced active regeneration before the start of each of the three 16-hour test cycles, as was done in Phase 1. It was decided to induce a forced active regeneration before the first test, but to remove the forced active regenerations between the 16-hour test cycles, in order to capture emissions from some regeneration

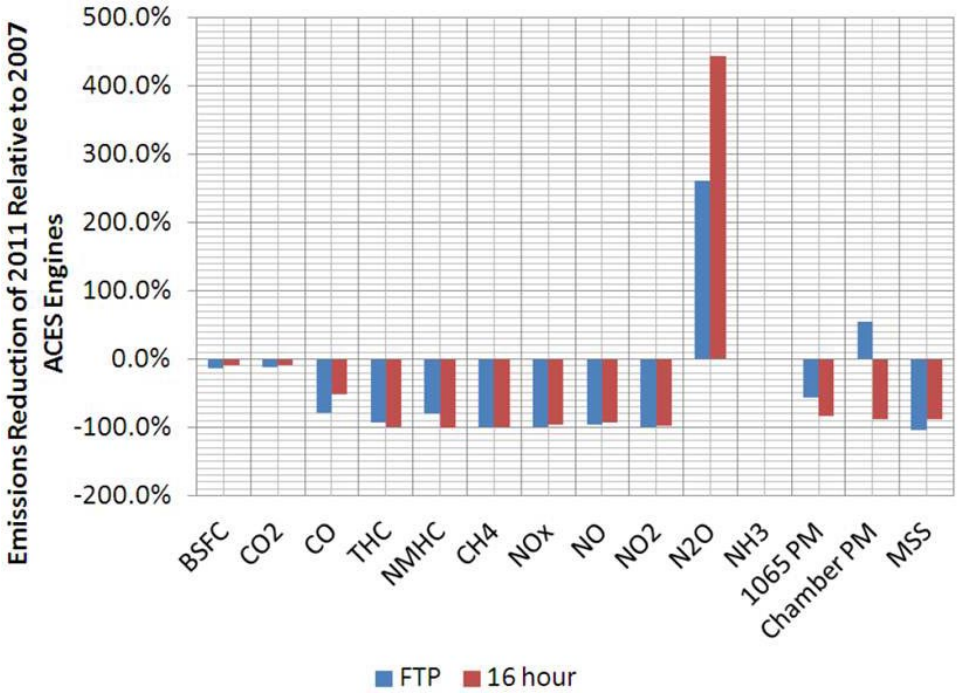

BSFC - brake specific fuel consumption; THC - total hydrocarbons; MSS - micro soot sensor; FTP - Federal Test Procedure

FIGURE 1. 2011 Engine X Emissions Reduction Compared to Average ACES 2007 Engines A, B, C, and D (Disclaimer: these are preliminary results that have not undergone quality control or peer review.)

events, if they occurred during the 48 hours of testing. SwRI® reported that Engine X did not have any active regeneration during the entire period of testing. Preliminary results indicate that Engine Y emissions for NOx, NO_2, N_2O, and CO_2 were higher than those for Engine X but were still below the NOx standard, indicating some differences in how the standard is met. PM emissions or number of regenerations were not yet reported for Engine Y.

Animal exposures and health evaluations at LRRI have made considerable progress during the past year, including completion of 24-month exposures in June 2012. Daily analysis of exposure atmospheres indicates that the 2007-compliant engine system continues to operate reliably and has consistently provided the targeted exposure concentrations (at 4.2, 0.8, and 0.1 ppm of NO_2) (data not shown). There were no exposure-related differences in mortality or clinically-evident morbidity in rats after 12 or 24 months (preliminary findings) of exposure. Similarly as observed after 3 months of exposure, the histologic findings at 12 months showed a small increase in the extent of the tissue changes in the respiratory tract, but the severity of the changes remained mostly minimal and effects were observed only at the highest exposure level (Table 1). Analyses of 24-month results are currently ongoing.

The primary importance of these interim results is their demonstration that: 1) the great majority of health tests showed no effect of exposure; 2) several plausibly coherent responses may indicate early, exposure-related, subclinical impacts on lung inflammation, structure, and function of rats that are consistent with exposure to NO_2; 3) statistically significant effects were observed primarily at the highest exposure level (the lowest level has produced no observable effects to date); and 4) effects have not appreciably progressed from 3 to 12 months of exposure.

TABLE 1. Incidence of selected lung findings in Wistar Han rats after 12 months of diesel exhaust exposure. (Data from HEI Research Report 166, Appendix F)

Male and Female Lung Combined	Control	Low	Mid	High
Epithelium Hyperplasia (Periacinar)	0/20	0/20	0/20	20/20
Macrophage Accumulation	0/20	0/20	0/20	6/20
Interstitial Fibrosis	0/20	0/20	0/20	18/20
Bronchiolization	0/20	0/20	0/20	3/20

Conclusions

Emissions testing of 2010-compliant engines indicates that the standards are met, although some differences exists among engines from different manufacturers. Exposure of rats up to 24 months

indicates that animals do not show exposure related mortality or morbidity. Preliminary results indicate some mild exposure-related changes in the lungs after 12 months of exposure, suspected to be due to the NO_2 exposure. These effects were seen only at the highest concentration of diesel exhaust. Exposures will continue through 30 months, when a full assessment of potential tumor formation will be conducted. All this work has been conducted with input from the ACES stakeholders.

References

1. U.S. Environmental Protection Agency. 2002. Health Assessment Document for Diesel Engine Exhaust. EPA/600/8-90/057F. U.S. Environmental Protection Agency, National Center for Environmental Assessment, Office of Research Development, Washington D.C.

FY 2012 Publications/Presentations

1. Published the Phase 3A final report (exhaust characterization at LRRI leading up to the start of the animal exposures): *Mauderly JL, McDonald JD. 2012. Advanced Collaborative Emissions Study (ACES) Phase 3A: Characterization of U.S. 2007-Compliant Diesel Engine and Exposure System Operation. Communication 17. Health Effects Institute, Boston, MA.*

2. Published the Phase 3B report (short-term biological screening results): *Advanced Collaborative Emissions Study (ACES). 2012. Advanced Collaborative Emissions Study (ACES) Subchronic Exposure Results: Biologic Responses in Rats and Mice and Assessment of Genotoxicity. Research Report 166. Health Effects Institute, Boston, MA.*

3. Platform and poster presentations at the HEI Annual Conference in Chicago, IL, April 2012:

- "Toxicologic Effects of Diesel Emissions: Historical Data and New Technology—Results from the HEI ACES Study" (McDonald - plenary).
- "Micronucleated Reticulocytes as an Indicator of Genotoxicity Following Exposure to Diesel Exhaust" (Bemis – poster).
- "Effects of Diesel Engine Emissions on Systemic Inflammation in Rodents" (Conklin - poster).
- "Assessment of the Genotoxicity of Diesel Exhaust and Diesel Exhaust Particulates from Improved Diesel Engines" (Hallberg - poster).
- "One- and Three-Month Results from Rats and Mice Exposed to 2007-Compliant Diesel Emissions" (McDonald- poster).
- "Diesel Exhaust Exposure and Cardiovascular Dysfunction" (Sun - poster).
- "Status of ACES Phase 2" (Tennant – poster).

4. Seminar at the California Air Resources Board in Sacramento, CA in February 2012 "Biological Response to Inhaled 2007 Compliant Diesel Emissions" (McDonald).

5. Platform presentation at the CRC Real Word Vehicle Emissions Workshop in San Diego, CA in March 2012 "Update on Phase 2 of the Advanced Collaborative Emissions Study (ACES Phase 2)" (Tennant).

6. Platform presentation at the annual DOE Vehicle Technologies Program Annual Merit Review, Washington, D.C. in May 2012: "Advanced Collaborative Emissions Study (ACES)."

IV. HIGH EFFICIENCY ENGINE TECHNOLOGIES

IV.1 Recovery Act: Technology and System Level Demonstration of Highly Efficient and Clean, Diesel Powered Class 8 Trucks

David Koeberlein
Cummins Inc.
P.O. Box 3005
Columbus, IN 47201-3005

DOE Technology Development Manager: Roland Gravel

NETL Project Manager: Ralph Nine

Overall Objectives

- Objective 1: Engine system demonstration of 50% or greater brake thermal efficiency (BTE) in a test cell at an operating condition indicative of a vehicle traveling on a level road at 65 mph.
- Objective 2:
  - Tractor-trailer vehicle demonstration of 50% or greater freight efficiency improvement (freight-ton-miles per gallon) over a defined drive cycle utilizing the engine developed in Objective 1.
  - Tractor-trailer vehicle demonstration of 68% or greater freight efficiency improvement (freight-ton-miles per gallon) over a defined 24-hour duty cycle (above drive cycle + extended idle) representative of real world, line haul applications.
- Objective 3: Technology scoping and demonstration of a 55% BTE engine system. Engine tests, component technologies, and model/analysis will be developed to a sufficient level to validate 55% BTE.

Fiscal Year (FY) 2012 Objectives

- Complete a demonstration of a 50% thermal efficient engine system.
  Complete the build of the 50% freight efficiency demonstration vehicle.
- Complete vehicle component development tests to be used in the demonstrator vehicle.
- Complete waste heat recovery (WHR) vehicle cooling system development tests.

Accomplishments

- Demonstrated the interim milestone of 50% or greater BTE with a combination of hardware demonstration and simulation of optimized components.
- Vehicle cooling testing with a fully integrated waste heat recovery system, demonstrating the recovery and fuel economy improvements.
- Completed build and initial testing of the higher cylinder pressure capability, low pump parasitic engine.
- Completed aerodynamic aid hardware fabrication and follow-on testing of this hardware to correlate with analytical results.
- Completed design and build of the demonstrator #1 vehicle.
- Completed the on-vehicle integration of the intelligent electronic modules comprising the road load management and cycle efficiency manager systems; conducted initial system calibration and vehicle tests.
- Completed build and initial development testing of the advanced heavy-duty transmission.
- Completed the installation and vehicle start-up and initial load testing of the solid oxide fuel cell auxiliary power unit (APU) on the demonstrator #1 vehicle.

Future Directions

- Complete the 50% freight efficiency vehicle demonstration testing.
- Analysis and targeted testing of technologies for achievement of a 55% BTE engine.
- Complete the build of the 68% 24-hour freight efficiency demonstration vehicle.

Introduction

Cummins Inc. is engaged in developing and demonstrating advanced diesel engine technologies to significantly improve the engine thermal efficiency while meeting Environmental Protection Agency 2010 emissions. Peterbilt Motors is engaged in the design and manufacturing of heavy-duty Class 8 trucks.

Together, Cummins and Peterbilt provide a comprehensive approach to achievement of a 68% or greater increase in vehicle freight efficiency over a 24-hour operating cycle. The integrated vehicle demonstration includes a highly efficient and clean diesel engine with 50% or greater BTE including advanced waste heat recovery, aerodynamic Peterbilt tractor-trailer combination, reduced rolling resistance tire technology, advanced transmission, and an efficient solid oxide fuel cell APU for idle management. In order to maximize fuel efficiency, each aspect associated with the energy consumption of a Class 8 tractor/trailer vehicle will be addressed through the development and integration of advanced technologies.

In addition, Cummins will scope and demonstrate evolutionary and innovative technologies for a 55% BTE engine system.

Approach

Cummins and Peterbilt's approach to these project objectives emphasizes an analysis-led design process in nearly all aspects of the research. Emphasis is placed on modeling and simulation results to lead to attractive feasible solutions. Vehicle simulation modeling is used to evaluate freight efficiency improvement technologies. Technologies are evaluated individually along with combination effects resulting in our path to target measure of project status and for setting project direction.

Data, experience, and information gained throughout the research exercise will be applied wherever possible to the final commercial products. We continue to follow this cost-effective, analysis-led approach both in research agreements with the Department of Energy as well as in its commercial product development. We believe this common approach to research effectively shares risks and results.

Results

- Demonstrated the interim milestone of 50% or greater BTE with a combination of hardware demonstration and simulation of optimized components. The demonstration engine was based on the Cummins 15-liter ISX with selective catalytic reduction aftertreatment and WHR system. The demonstration engine showed approximately a 20% reduced friction compared to the current production ISX15 engine. The engine exhibited an improvement in gross indicated efficiency compared to the baseline engine, and a modest improvement in open-cycle efficiency. WHR reduced fuel consumption in the range of 4-5 percent.

  The demonstration engine with the WHR system combined with aftertreatment fueling improvements resulted in an effective BTE of 49.0%; the estimated engine-only BTE from the system is 46.3% BTE. The engine system also showed compliance with current prevailing supplemental emissions test emissions requirements of 0.2 g/bhp-hr. The engine was operated at the 13 supplemental emissions test modes, and the cycle-weighted supplemental emissions test emissions were 0.08 g/bhp-hr system-out.

  The WHR system tested low global warming potential working fluid with results indicating a 0.2% system BTE improvement. Testing was terminated due to a leak that resulted in losing the fluid; additional replacement fluid was not available at the time. The above results do not include these observed low global warming potential fluid formulation benefits.

- Multiple WHR-equipped vehicles are operating in test conditions. The vehicles have each completed cooling tests in a Modine climactic tunnel to understand WHR system performance on-vehicle in varying ambient and various applied heat loads.

  A key objective included generating cooling module performance data to validate analysis and assist in condenser development. The critical question sought during the testing was "is the WHR condenser capacity sufficient to reject the WHR system's highway cruise heat rejection without cooling fan assist?" Also, data was collected to help with understanding of this cooling modules capacity at other ambient temperatures and vehicle velocities.

  Results of an 85ºF ambient condition, fan off and 300-hp engine output, the WHR achieved 15 hp of recovered power, 5% recovery. This result validates a key design point of the cooling module that the cooling module the capacity of rejecting WHR heat at greater than the highway cruise power point without fan assist.

- The build of the integrated Demo 1 truck including a higher efficiency WHR-equipped engine, an advanced transmission and a solid oxide fuel cell was completed. Over the course of three days, the truck ran down the production assembly line to complete its build. Over the next several weeks, custom completion and charging of the WHR system, installation and tests of the battery system and the solid oxide fuel cell were completed. The truck was driven bobtail on local Denton, TX roads to evaluate the advanced transmission. The truck was delivered to Cummins, in Columbus, IN for calibration and development of engine, WHR and route management systems. In late August, Demo 1 returned to Denton

for up-fit of the truck and trailer aero package, tires, and wheels and along with additions for fuel economy test equipment.

- Truck and trailer aero aid fabrications were completed and initial truck on-road evaluations completed. A Model 587/trailer combination was equipped with design intent in preparation for freight efficiency testing. The 65,000 lb ballasted truck with current production super-single tires system achieved a 28% fuel economy improvement over the baseline 2009 Model 386 with a standard trailer.
- A fuel cell APU unit was re-installed and drive tested with full vehicle electrical system's functional, development issues found were remedied in preparation to be available for truck testing. A functional solid oxide fuel cell APU was initially installed on the Demo 1 truck in May 2012 for truck interface, start, and run evaluation. Following successful on-truck trials, the unit was replaced by a non-functional unit and returned for upgrades to replace the desulfurization subsystem with a bypass tube. Rebuild of the system was completed and underwent sulfur conditioning, calibration, and testing. The unit continues to show good performance in idle fuel consumption, noise level and cool down time but recent output and efficiency have suffered in the sulfur-conditioned configuration. An increase in both internal stack temperature and parasitic electrical loads are the general causes for decreased peak power and efficiency.

  The exterior noise level at all recording points was below the 65-dBA target. Measurements inside the cab were less than 50 dBA. The rebuilt unit was re-installed on the Demo 1 truck and will undergo future system level testing.
- The advanced transmission was initially built in November 2011 and since then has been undergoing numerous development tests. The transmission has been subjected to shift tests, full load dyno, lube and cooling tests and installed in a mule truck completing mileage accumulation tests. Shift calibration and software development has been a critical focus of attention, with progressive improvements are being reported with focused jury evaluation vehicle trials. The Demo 1 truck was initially built with the transmission and enabled demonstration of the improvements the transmission will bring to the vehicle, including marked improvements to downsped engine driveability. The transmission has since been completing parallel development tests in lab and vehicle environments.
- A vehicle power train system analysis is a tool to evaluate freight efficiency improvements. The path to target roadmap study involved an analysis of various power train component changes, including both hardware and control algorithms, with their resulting freight efficiency impacts. Figure 1 shows

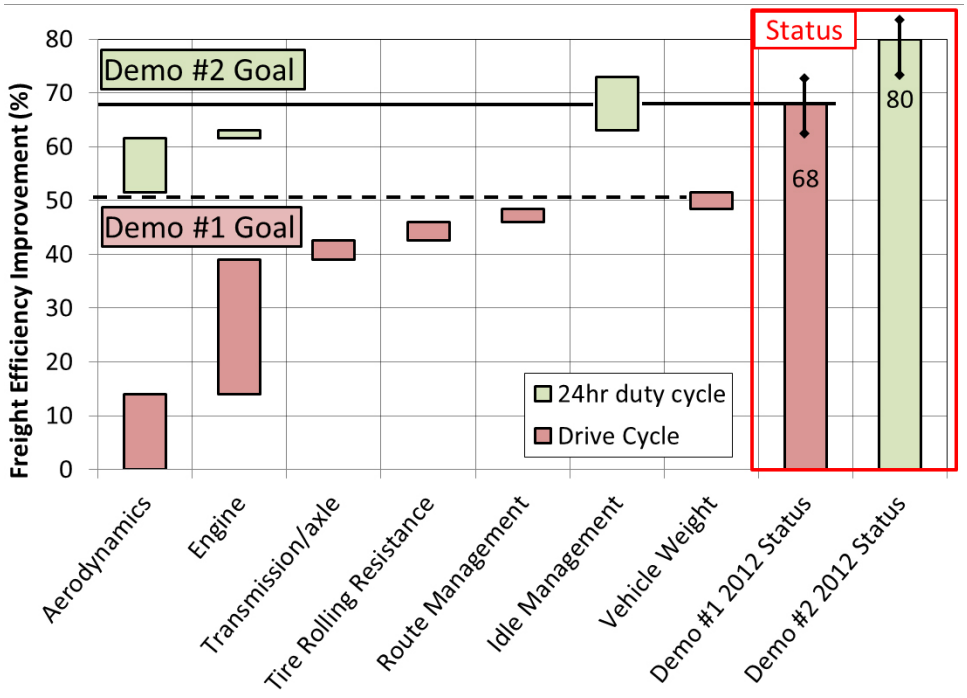

FIGURE 1. Freight Efficiency Roadmap and Status

the path to target roadmap for both the drive cycle 50% improvement and 68% improvement on the 24-hr cycle. This figure also shows current expected status toward both objectives of 68% and 80% respectively, we have determined uncertainty in these values of +/- 5%.

Conclusions

The SuperTruck Engine and Vehicle System Level Demonstration of Highly Efficient and Clean, Diesel Powered Class 8 Truck project has successfully completed the second year of the four-year project. The following conclusions have come from the second year:

- Vehicle power train system analysis shows path to achievement of project freight efficiency goals.
- Demonstrated the interim milestone of 50% or greater BTE with a combination of hardware demonstration and simulation of optimized components.
- The build of the integrated Demo 1 truck including a higher efficiency WHR-equipped engine, an advanced transmission and a solid oxide fuel cell was completed.
- WHR vehicle cooling tests were conducted with fan-off system performance and system power recovery demonstrating results as expected from analysis.
- Truck and trailer aero aid fabrications were completed with initial truck on-road evaluations showing a 28% improvement.

FY 2012 Publications/Presentations

Journal Paper Submissions:

1. Karla Stricker, Lyle Kocher, Dan Van Alstine, *Input Observer Convergence and Robustness: Application to Compression Ratio Estimation*, IFAC Control Engineering Practice, 3/5/2012.

2. L. Kocher, E. Koeberlein, K. Stricker, D.G. Van Alstine, and G.M. Shaver, *Control-Oriented Gas Exchange Model for Diesel Engines Utilizing Flexible Intake Valve Actuation*, J. of Dyn. Sys., Meas., and Control, 10-24-2011.

3. L. Kocher, K. Stricker, E. Koeberlein, D.V. Alstine, and G.M. Shaver, *In-cylinder Oxygen Fraction Estimation for Diesel Engines Utilizing Flexible Intake Valve Actuation*, IEEE Trans. on Control Systems Technology, 11-21-2011.

Conference papers and presentations:

1. Dan Van Alstine*, Lyle Kocher, Ed Koeberlein, Karla Stricker, and Gregory M. Shaver, *Control-Oriented PCCI Combustion Timing Model for a Diesel Engine Utilizing Flexible Intake Valve Actuation and Higher EGR Levels*, presented at the 2012 American Control Conference, 6/2012.

2. Karla Stricker*, Lyle Kocher, Ed Koeberlein, Dan Van Alstine, and Gregory M. Shaver, *Effective Compression Ratio Estimation in Engines with Flexible Intake Valve Actuat*ion, presented at the 2012 American Control Conference, 6/2012.

3. Lyle Kocher*, Karla Stricker, Dan Van Alstine, Ed Koeberlein, and Gregory M. Shaver, *Oxygen Fraction Estimation for Diesel Engines Utilizing Variable Intake Valve Actuatio*n, presented at the 2012 American Control Conference, 6/2012.

4. Lyle Kocher, Karla Stricker, Dan Van Alstine, and Gregory M. Shaver, *Robust Oxygen Fraction Estimation for Diesel Engines Utilizing Variable Intake Valve Actuation*, submitted 3-12-2012 to IFAC Workshop.

5. Karla Stricker, Lyle Kocher, Dan Van Alstine, and Gregory M. Shaver, *Guaranteed Convergence of a High-Gain Input Observer Robust to Measurement Uncertainty: Application to Effective Compression Ratio Estimation*, submitted 3-12-2012 to IFAC Workshop.

6. David Koeberlein, *Cummins SuperTruck Program, Technology Demonstration of Highly Efficient Clean, Diesel Powered Class 8 Trucks,* 2012 DEER conference.

7. Lyle Kocher, *Estimation and Control of Diesel Engine Processes Utilizing Variable Intake Valve Actuation,* 2012 DEER conference.

IV.2 SuperTruck – Improving Transportation Efficiency through Integrated Vehicle, Engine, and Powertrain Research; Fiscal Year 2012 Engine Activities

Kevin Sisken
Detroit Diesel Corporation
HPC A-08
13400 Outer Drive West
Detroit, MI 48239-4001

DOE Technology Development Manager: Roland Gravel

NETL Project Manager: Carl Maronde

Overall Objectives

- Demonstration of a 50% total increase in vehicle freight efficiency measured in ton-miles per gallon, with at least 20% improvement through the development of a heavy-duty diesel engine.
- Development of a heavy-duty diesel engine capable of achieving 50% brake thermal efficiency on a dynamometer under a load representative of a level road at 65 mph.
- Identify key pathways through modeling and analysis to achieving 55% brake thermal efficiency on a heavy-duty diesel engine.

Fiscal Year 2012 Objectives

- Utilizing the results of the comprehensive analytical effort performed in 2011, the 2012 objective was to experimentally demonstrate the technology building blocks that will be used to achieve the 50% engine brake thermal efficiency target.
- As an intermediate project goal, demonstrate 46% brake thermal efficiency, with development plans in place and further progress toward demonstrating 50% brake thermal efficiency in 2013.

Accomplishments

- Demonstrated 46.2% engine brake thermal efficiency in the laboratory on the SuperTruck demonstration engine, meeting the year-2 project targets.
- Development has continued on the core engine, with the best results to date being an engine brake thermal efficiency of 46.8%.
- The waste heat recovery system design was completed, hardware ordered, and system testing initiated. Testing to date has demonstrated an improvement in engine brake thermal efficiency of 1.3% via recovered exhaust energy, bringing the total engine brake thermal efficiency up to 48.1% (46.8% engine + 1.3% from waste heat).

Future Directions

- Demonstrate 50% engine brake thermal efficiency via improvements in the base engine to reach 48% thermal efficiency and an additional 2% increase in thermal efficiency via the waste heat recovery system, which will include energy recovery from the exhaust gas recirculation (EGR) system (current system is exhaust heat only).
- Build and test the final engine system in the SuperTruck vehicle to demonstrate the improvements in the vehicle as part of the 50% vehicle freight efficiency improvement.
- Analytically demonstrate the pathway to reach 55% engine brake thermal efficiency.

Introduction

SuperTruck is a 5-year research and development project with a focus on improving diesel engine and vehicle efficiencies. The objective is to develop and demonstrate a Class-8, long haul tractor-trailer which achieves a 50% vehicle freight efficiency improvement (measured in ton-miles per gallon) over a best-in-class 2009 baseline vehicle, 20% of which shall be demonstrated on a heavy-duty diesel engine tested on a dynamometer under representative loads at 65mph. In FY 2012, SuperTruck completed the second phase of the project and entered Phase 3. Phase 2 targeted the demonstration of 46% engine brake thermal efficiency with Phase 3 (will end March 2013) targeting 50% brake thermal efficiency.

Approach

The approach used in Phase 2 of the project has primarily centered on system analysis through the use of

modeling and simulation, as well as dynamometer bench testing. Specific engine systems being refined for high engine efficiency include the combustion system, air system, fuel system, engine controls, engine parasitics, aftertreatment, and waste heat recovery. In addition, the engine was significantly downsized from the baseline engine in order to improve the engine's efficiency at conditions representative of road load operation.

Results

To date, the SuperTruck project is on track to reach the 50% freight efficiency target, including the engine's target of 50% brake thermal efficiency. Progress toward reaching the engine efficiency target is shown graphically in Figure 1.

Significant progress was made in the core engine development towards reaching the 175 g/kW-hr brake specific fuel consumption (bsfc) target (aka 48% brake thermal efficiency). The current technical package, which enables the high brake thermal efficiency at cruise RPM, includes the following elements:

- Engine downsizing
- Higher engine-out NOx compared to baseline
- Higher engine compression ratio
- Higher peak cylinder pressures
- Re-matched injector spray angle and nozzle flow characteristics
- Re-matched turbocharger
- Low viscosity oil
- Variable speed coolant pump

Many of these items have already been evaluated in Phase 2 and 3, with further improvement measures still to be exploited, including a further compression ratio increase, additional parasitic reductions, air system refinements, as well as electric turbo-compounding.

Research is being conducted in the area of parasitics reduction at the Sloan Automotive Laboratory of the Massachusetts Institute of Technology as part of the SuperTruck sub-contract. One of the sub-goals of this effort on parasitic reduction is fuel economy improvement of Class-8 truck engines through lubrication system improvements. Reduction of in-cylinder friction losses, which amount to 40-50% of the total engine mechanical losses, is an area of primary focus. Technologies related to piston kit friction reduction, oil circuit and flow optimization, and low viscosity oil are being explored, with promising hardware improvements currently being procured for on-engine validation.

A novel method of engine controller is being utilized in this program, and these controls are currently being optimized for engine fuel efficiency improvement measures via dynamometer test cycles representative of over-the-road SuperTruck operation. The SuperTruck engine control logic is based on extensive mapping of engine operation, followed by training of neural network engine performance models. The resulting logic enables the control of engine actuators based on engine-out NOx set-points adapted to the driving conditions. The instantaneous fuel economy benefits measured under steady-state operating conditions have been shown to translate into benefits under transient conditions as well.

Progress has been made in the development of a high efficiency, low back pressure aftertreatment system for

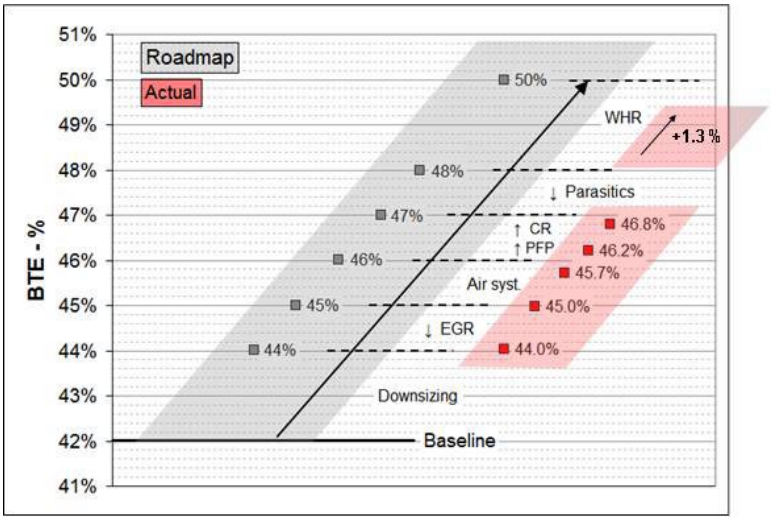

FIGURE 1. Engine Brake Thermal Efficiency (BTE) Improvements

the SuperTruck engine. One of the engine strategies is higher engine out NOx for increased engine efficiency matched to a high efficiency aftertreatment system. A number of aftertreatment designs have been procured and tested, and the final system has been selected which has a significant NOx efficiency improvement over the baseline system while also reducing the system back pressure, which is beneficial for engine efficiency.

The SuperTruck waste heat recovery system will employ a Rankine cycle to harness the heat energy in the engine's exhaust and EGR cooler. Currently, the Rankine heat engine is setup to generate high pressure ethanol vapor utilizing the exhaust heat, which then energizes an expansion machine to turn a generator to produce electrical power. An extensive performance evaluation of the expansion machine and overall Rankine system has been conducted. High component and system efficiencies were demonstrated and a brake thermal efficiency improvement of 1.3% was realized. It is fully expected that this will increase to 2% brake thermal efficiency when the energy from the EGR cooler is also recovered.

Oak Ridge National Laboratory is a partner in the SuperTruck waste head recovery system development, and their efforts are focused on design and development of an efficient generator prototype for use with this waste heat recovery system. The expander driven generator converts mechanical input energy to electrical energy and returns this recuperated energy back to the vehicle's high voltage battery and/or hybrid drive components. The magnetic and mechanical design of the final concept has been completed and the design is in the build phase, with testing to commence shortly.

Conclusions

The intermediate project goal of 46% brake thermal efficiency was achieved and to date, an engine thermal efficiency of 48.1% has been demonstrated. The technical path and plans are in place to extend this to the project goal of 50% thermal efficiency.

FY 2012 Publications/Presentations

1. Sisken, Kevin: "SuperTruck Program: Engine Project Review; Recovery Act –Class 8 Truck Freight Efficiency Improvement Project", Project ID: ACE058, DoE Annual Merit Review, May 17, 2012.

2. Sisken, Kevin: "Daimler's SuperTruck Program; 50% Brake Thermal Efficiency", 2012 Directions in Engine Efficiency and Emissions Research (DEER) Conference, October 18, 2012.

IV.3 Development and Demonstration of a Fuel-Efficient Class 8 Tractor and Trailer

Dale Oehlerking (Primary Contact),
Willy de Ojeda
Advanced Technologies
Navistar, Inc.
2601 Navistar Drive
Lisle, IL 60532

DOE Technology Development Manager:
Roland Gravel

NETL Project Manager: Ralph Nine

Subcontractors:
- Bosch, Farmington Hills, MI
- Behr America, Troy, MI
- Federal-Mogul, Ann Arbor, MI
- Argonne National Laboratory, Argonne, IL
- Wisconsin Engine Research Center, Madison, WI

Overall Objectives

- Demonstrate engine brake thermal efficiency (BTE) improvements which contribute 20 percent (of the total 50 percent required) improvement in the freight efficiency of a combination tractor-trailer as a part of the DOE SuperTruck Project.
- Demonstrate 50 percent BTE at an engine operational point which corresponds to an on-road driving condition of 65 mph.
- Demonstrate a path towards achieving a peak BTE target of 55 percent.

Fiscal Year (FY) 2012 Objectives

Demonstrate base engine improvements through engine technology development and concept readiness.

Accomplishments

To date the project has accomplished the following:

- Demonstrated an engine combustion strategy leading to a BTE improvement from 42 to 45 percent by extending peak cylinder pressure capability (190→220 bar) and using higher injection pressure (2,200→2,900 bar).
- Demonstrated heat recovery using electrical turbo-compounding with advanced air system to further increase the BTE to 46.5 percent.

In addition

- Nearly all base engine components have been procured with expectation to meet 1.5-2.0 percent BTE gain. A systematic engine benchmarking has been initiated.
- Installation of new water and oil pump accessories raised the BTE to 47.3%.
- Variable valve actuation (VVA) has been incorporated in the base engine for benchmarking.
- Towards the 55 percent BTE goal, a dual-fuel engine demonstrator is already operational at Argonne National Laboratory.

Introduction

The overall goal of the DOE-supported SuperTruck Initiative is to demonstrate a 50 percent improvement in freight efficiency (measured in ton-miles/gallon) of a combination tractor-trailer. Truck efficiency improvements will come from improvement to both the engine and the vehicle, with 20 percent of the overall 50 percent improvement coming from engine improvements alone. This establishes a target engine BTE of 50 percent which is an 8 percentage point improvement from the current benchmark of 42 percent attained at an engine operating point equivalent to a 65 mph truck speed. An additional goal of the project is to demonstrate a path towards a 55 percent BTE.

Approach

The Navistar MaxxForce 13-L engine is used to demonstrate engine efficiency improvements through engine technologies. The roadmap and present status towards the target 50 percent engine BTE is shown in Figure 1. The roadmap lays out the efficiency gains that would be achieved, starting from the benchmarked 42 percent BTE through the following approaches:

- Improved fuel injection system
- Improved combustion chamber
- Optimum injection timing
- Updated aftertreatment
- Electrical turbocompounding
- Friction reduction from cooling and lube oil system improvements.

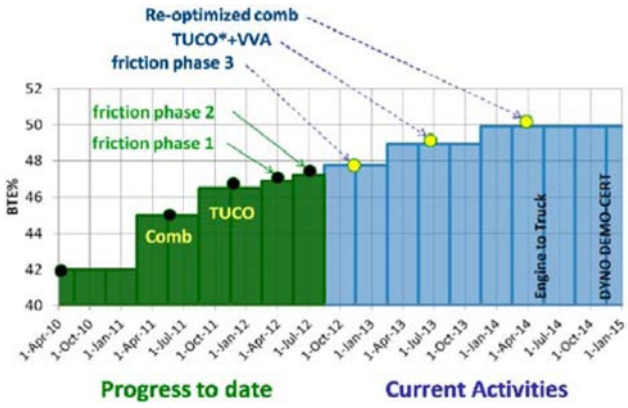

TUCO - turbocompounding

FIGURE 1. Roadmap for Engine Technology Development

Multiple prototype engines were built and set up at various facilities to quantify efficiency gains from engine technology improvements:

- A dedicated engine at Navistar's Melrose Park facility to map out combustion and emissions impact.

Navistar

Combustion Development
Air / cooling system
Emissions
Turbocompounding
EGR-Rankine Cycle

- A second engine at Navistar's Melrose Park facility to demonstrate turbo-compounding hardware integration with the base engine controls and aftertreatment for extensive testing over transient cycles in the dynamometer.
- A dedicated engine at the Bosch Farmington Hills facility to demonstrate improvements with fuel injection hardware and design of piston geometry.

BOSCH

High-injection pressure capability
High Compression ratio
CFD-Engine correlations

- A base engine and power cylinder improvements at Federal-Mogul facility for systematic friction testing and evaluation of friction reduction technologies and improved engine accessories.

Federal Mogul

Friction Benchmark
Power cylinder components

Results

Engine tests demonstrated peak efficiencies of 46.5% from combustion work and the first generation of turbo-compounding hardware. Base engine with friction reduction technologies increased the BTE further to 47.3%.

VVA

The VVA hardware was installed on a base engine and calibration work has been undertaken. Some issues were encountered regarding insufficient lubrication on cam rollers but successfully corrected. The preparatory work has been completed and the engine is ready for performance testing.

Engine Accessories

Testing of engine accessories including the variable displacement oil pump and the variable speed water pump have been initiated on two dedicated engines at Navistar's Melrose Park facility. The variable speed water pump testing showed favorable results, indicating approximately 1.5 percent and 2 percent fuel economy improvement on the U.S. Supplemental Emission Testing (USSET) steady-state and Federal Test Procedure (FTP) transient tests (see Figure 2).

Engine Friction Reduction

Engine friction reduction hardware has been incorporated on the MaxxForce 13-L engine installed at the Federal Mogul facility. The engine is ready for benchmark testing.

Turbo-Compounding and Waste Heat Recovery

The first phase of turbo-compounding testing was completed which included USSET and FTP results under normal and active regeneration modes. BTE improvements of 1.2% over the USSET were measured. Transient testing highlighted the challenge of optimizing fuel economy without compromising transient response.

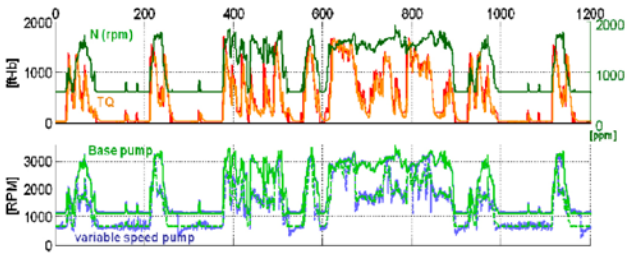

FIGURE 2. Variable Speed Pump Benchmarked Against Base Pump over the FTP

Optimization of the turbos and turbo-generator sizing for the next generation turbo-compounding hardware has been completed. The re-optimized system should provide 1.6% BTE improvement over the USSET.

The Rankine cycle system configuration has been finalized (Figure 3) and all hardware has been ordered. The system includes both exhaust gas recirculation cooler and exhaust boilers to maximize heat capture. An exhaust boiler will be installed downstream of the turbo-compounding unit. Heat exchangers will undergo in parallel thermal and fatigue testing.

Modeling indicates that the system should provide a 3% BTE improvement over the USSET. In the present project the Rankine technology will be limited to dynamometer testing due to concerns of additional weight and limited experience with the dynamic nature of the system.

Dual-Fuel (Diesel and Gasoline) Engine

Navistar is collaborating with Argonne National Laboratory to use "fuel reactivity" to demonstrate a path towards 55 percent BTE. A MaxxForce 13-L engine was set up at Argonne National Laboratory and equipped with added capability to run a second fuel system targeting a high octane number fuel for a more homogeneous charge (Figure 4).

Initial dynamometer tests at Argonne National Laboratory showed great potential for optimization of engine efficiency and engine-out emissions utilizing the fuel properties of gasoline. The gasoline was injected in the port resulting in a highly premixed charge mixture ahead of the diesel injection. This resulted in improved efficiency with very low oxides of nitrogen and particulate matter emissions. Initial results showed 1–2 percent BTE improvement over the baseline at 10 bar brake mean effective pressure (BMEP). Load limitations were encountered at 12 bar.

FIGURE 4. Dual-Fuel Engine Setup at Argonne National Laboratory

Tests results with 85% ethanol in gasoline (E85) and diesel fuel showed large improvement in BTE (reaching above 46 percent) with the base engine configuration (not accounting for waste heat or friction reduction). The oxygenated characteristics of the fuel helped keep soot at very low levels.

Figure 5 below compares a high efficiency diesel operation with the gasoline+diesel (G+D), and the E85+diesel (E85+D) results. The G+D and E85+D can operate with very little emissions up to 12 and 19 bar respectively. In the case of E85, its fuel reactivity allowed for significant improvement in engine efficiency.

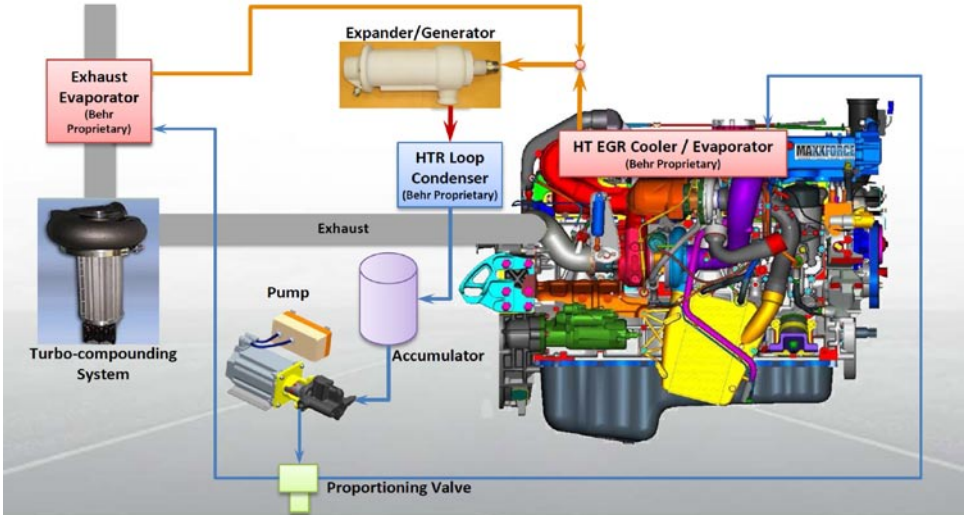

HT - high temperature; HTR - high temoerature Rankine

FIGURE 3. Rankine Cycle System Configuration

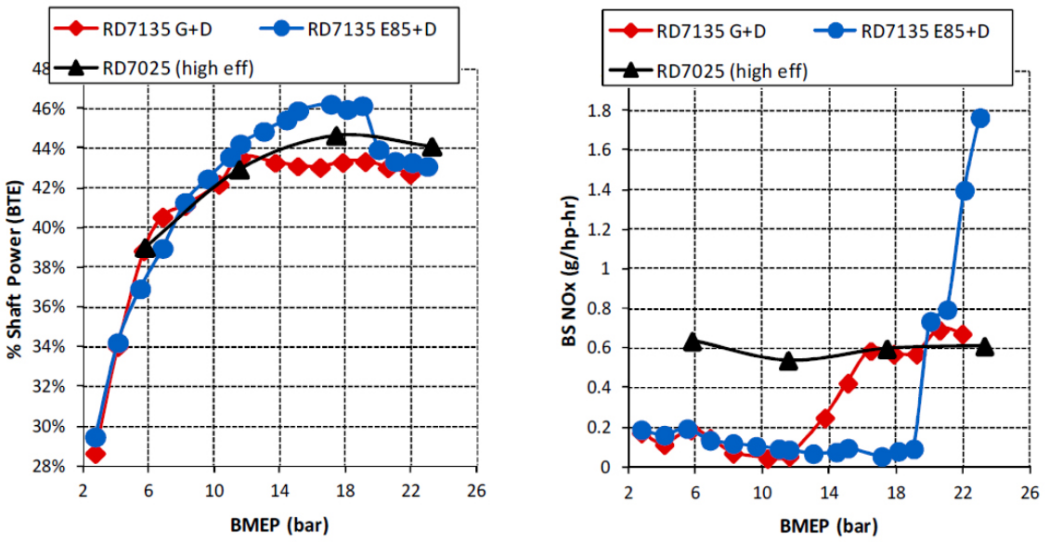

FIGURE 5. Dual-Fuel Engine Results at 1,200 RPM

Conclusion

Work to date has demonstrated efficiency improvements of the base engine from 42% to 47.3% by combustion system improvements and implementation of electrical turbo-compounding. The VVA and friction reduction components have been integrated with the base engine. A pathway to 55 percent BTE is being demonstrated with a dual-fuel engine using a fuel reactivity controlled compression ignition strategy.

FY 2012 Publications/Presentations

1. Dennis W. Jadin, "SuperTruck – Development and Demonstration of a Fuel-Efficient Class 8 Tractor & Trailer - Engine Systems," Annual Merit Review, USDOE, May 17, 2012, Washington, D.C.

2. William de Ojeda, "Development and Demonstration of a Fuel-Efficient HD Engine," Directions in Engine-Efficiency and Emissions Research (DEER) Conference, October 16, 2012, Dearborn, MI.

3. Yu Zhang, et al., "Development of Dual-Fuel Engine for Class 8 Applications," Directions in Engine-Efficiency and Emissions Research (DEER) Conference, October 18, 2012, Dearborn, MI.

IV.4 SuperTruck Initiative for Maximum Utilized Loading in the United States

Pascal Amar (Primary Contact),
Samuel McLaughlin, Arne Andersson,
John Gibble
Volvo
13302 Pennsylvania Avenue
Hagerstown, MD 21742

DOE Technology Development Manager:
Roland Gravel

NETL Project Manager: Ralph Nine

Subcontractor:
Penn State University, State College, PA

Overall Objectives

- Identify concepts and technologies that have potential to achieve 55% brake thermal efficiency (BTE) on a heavy-duty diesel engine as defined in the SuperTruck project. A thorough analysis of the limiting factors and potential areas for improving the engine's efficiency using analytical simulations will be performed. This will include research into alternative thermodynamic cycles, advanced component design, fuel formulation and new engine designs.
- Demonstrate a partially premixed combustion (PPC) combustion concept operating on a specially formulated fuel that can operate in the load, and speed range of a normal diesel engine but with significantly improved thermal efficiency. The aim is to demonstrate 50% BTE in at least some operating points.

Fiscal Year (FY) 2012 Objectives

- Develop and use simulation tools and models for PPC and other new concept.
- Select a concept capable of 55% BTE for further analysis.
- Simulate, test and evaluate PPC combustion.

Accomplishments

Combustion computational fluid dynamics (CFD), transported probability density function (PDF):

- V2 of combustion model PDF code released.
- Validated two skeletal-size n-heptane and n-dodecane chemical mechanisms under Engine Combustion Network (ECN) conditions.

Engine Tests:

- Achieved up to 2% fuel economy improvement in alternative fuel tests (high derived cetane number [DCN]/low aromatics fuels) at heavy-duty engine cruise-like point.
- Attained up to 7% BTE improvement in PCC engine tests.
- PPC tests with 70 octane number demonstrated wide operating range.

Concepts:

- Identified a concept capable of 55 % BTE.

Future Directions

- We are now very close to a working transported PDF combustion CFD that works together with a moving mesh. With that in place we will start the validation work with engine test data.
- Verifying assumptions behind 55% BTE concept.

Introduction

New combustion concepts like PPC and reactivity-controlled compression ignition have demonstrated very high indicated efficiencies together with a potential for low engine-out emissions. But the implementation of those combustion concepts in engine concepts remains a challenge. A number of issues like boosting, load range, exhaust gas recirculation control and transients have to be addressed. Integration of different technologies into an engine concept is done with gas exchange simulations. But how do we model the combustion in the gas exchange simulations when new combustion concepts are utilized?

Iterating with 1-cylinder testing and three-dimensional combustion CFD is time consuming. In order to speed up the concept work we need to exchange the right parameters between the simulation tools and reduce the number of iterations. This can be achieved with a good combustion model in the gas exchange code.

We also need high fidelity combustion simulation capabilities for PPC. In parallel to tests in 1-cylinder test cell with PPC combustion we are developing the simulation tool.

We continue to gain experience from operation of the Organic Rankine Cycle (ORC) waste heat recovery (WHR) system.

Approach

Combustion models of direct injected engines need to capture fuel and thermal stratification. For PPC we need to include the mixing process since the combustion is more or less premixed depending on the load. A stochastic reactor model (SRM) approach addresses the stratification. The state variables are described with a PDF and the cylinder gas mixture are discretized in a number of reactors. The PDF can then be compared with distributions from CFD calculations or from measurements. Typically from 100 to 2,000 reactors are used in the model which allows for a significantly more detailed chemistry than in combustion CFD.

With low-temperature combustion the simulation becomes much more challenging. Ignition delays and lift-off lengths increase and make simulations more sensitive. Those parameters have a very big influence on the final result. The transported PDF combustion CFD model captures the turbulence-chemistry interactions. This will make it possible to do high fidelity combustion simulations with PPC. The importance of this interaction has now been demonstrated in spray bomb simulations.

The full integration of the WHR system is an important step to evaluate and develop the interaction with other systems.

Results

Combustion Model for Engine Concept Simulations

The stochastic reactor model is based on statistical distributions that are generated with combustion CFD (Figure 1). The distributions are well captured in CFD together with computer-aided design resolved turbulence data. Together with test results from the 1-cylinder test rig this enables us to generate good zero-dimension models (Figure 2).

Combustion CFD

Work to date has focused on identification and selection of chemical mechanisms, and on establishing the degree to which turbulent fluctuations in composition and temperature influence the computed ignition event

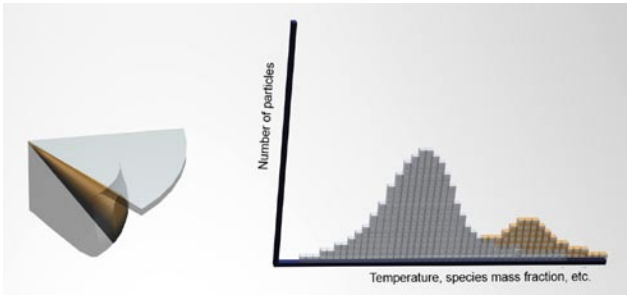

FIGURE 1. Distributions from CFD used in the zero-dimension SRM model.

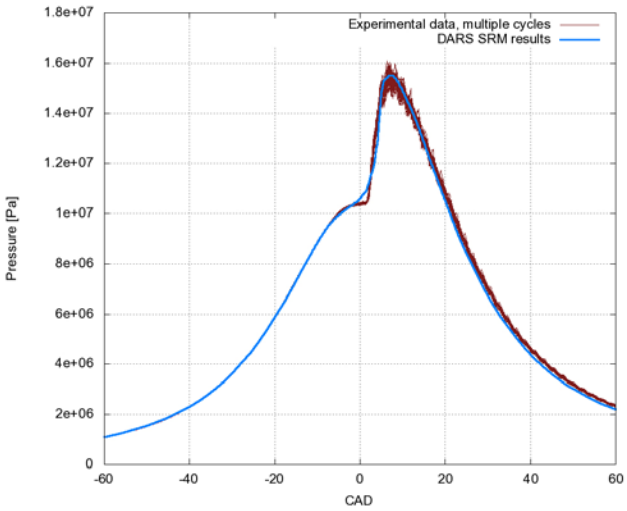

CAD – crank angle degree

FIGURE 2. Graph showing SRM model validation with PPC combustion for a 12-bar indicated mean effective pressure case.

and turbulent flame structure. Figure 3 shows that this influence becomes very important at low-temperature combustion.

Comprehensive CFD study has been accomplished for high-pressure, constant-volume turbulent spray combustion, to validate two skeletal-size n-heptane and n-dodecane chemical mechanisms under ECN conditions (http://www.sandia.gov/ecn/). An example of a simulated spray is shown in Figure 4.

The focus of the modeling activity to date has been in-cylinder combustion modeling. Detailed quantitative comparisons are being made between model results and experimental measurements available through the Volvo engine testing facilities.

Regarding the constant volume combustion chamber experiments, an ignition quality test apparatus (PAC LLC, “CID 510” DCN analyzer) was setup. Fuel characteristic tests were carried out for primary reference fuels and high DCN/low aromatics fuels.

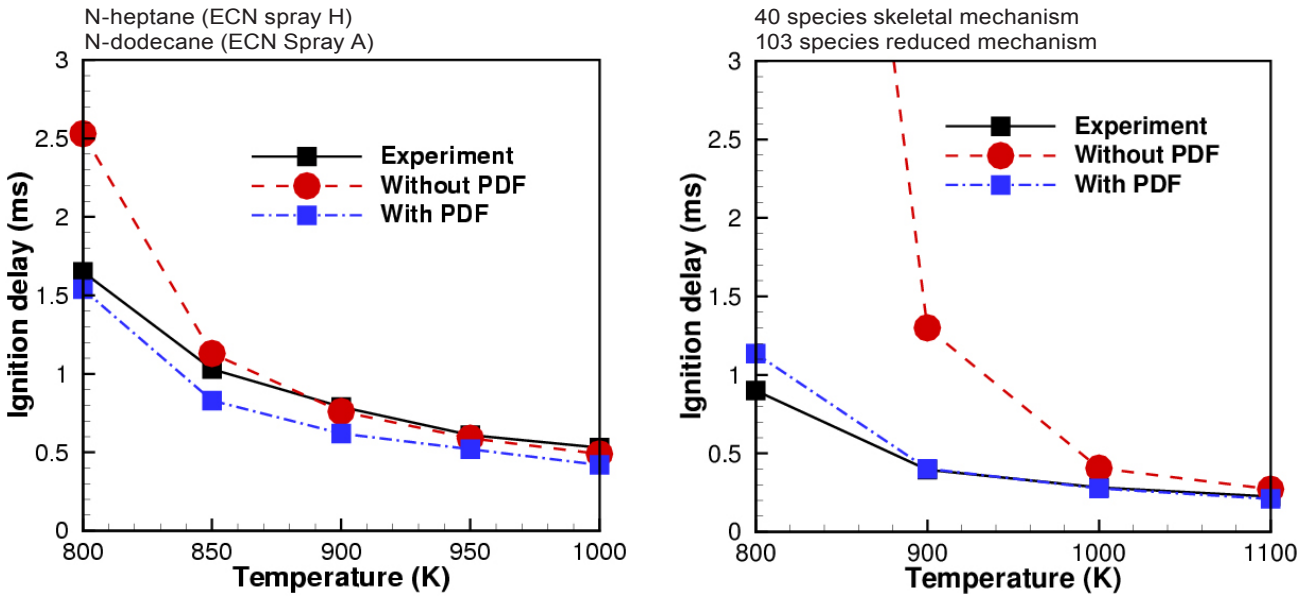

FIGURE 3. Graphs show how much more sensitive the simulation becomes to the turbulence-chemistry interaction when moving into the low-temperature combustion regime.

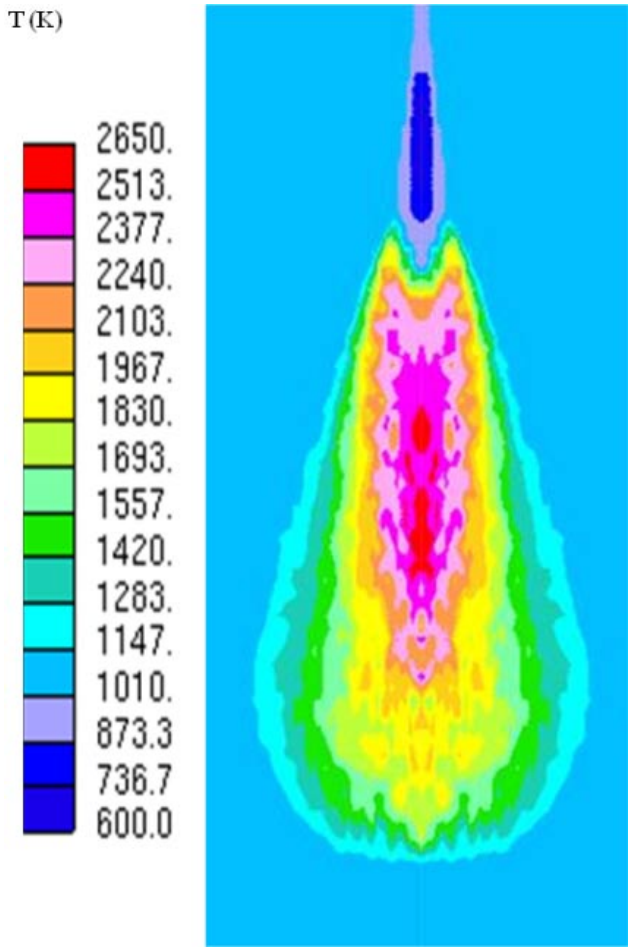

FIGURE 4. N-heptane spray flame predicted with transported PDF model.

Also, optical instrumentation was installed to the CID 510 instrumentation for visualization of spray (digital photography using a borescope) and detection of the onset of chemiluminescence in the chamber (photomultiplier tube with supporting optics).

Test and Modeling of High Performance Pistons

CFD simulations evaluated the impacts of injector nozzle orientation on fuel economy and emissions, subsequent engine tests concluded best performance with 6-hole injectors. An improvement of engine fuel economy up to 2.4% applying ultra-high peak cylinder pressure (240 bar) was shown and up to 1.0% applying high peak injection pressures (3,000 bar).

ORC Design and Simulation Transient Drive Cycle Results

The net fuel economy benefit strongly depends on input conditions to the WHR system. Advancements to combustion systems that improve combustion will generally decrease exhaust gas temperatures. These decreases will negatively impact a WHR system. System and component level simulations of bottoming cycle technologies are being developed to guide future WHR system specifications to take into account the combustion advancements for appropriate integration and maximum return on investment.

A Rankine system is on test in an engine test cell, integrated with the prototype engine designed to achieve 50% brake thermal efficiency as part of the SuperTruck

program. This system will later be installed in chassis for demonstration in 2013. Some test data and simulation key findings are summarized in the following:

- Under low heat input operation the expander is bypassed resulting in drag torque. Bypass mode must be minimized, or drag torque reduced to improve total system efficiency on a drive cycle.
- Under high heat input operation, boiler or expander bypass is required due to excessive heat rejection and limited capacity of expansion machine. Pressure limitation of heat exchangers limits power at high load points since the expander is sized for cruise. Components should all be sized for normal operation under cruise conditions and heat rejection minimized.
- Dynamic stability of the system is challenging. Measures must be taken to reduce speed and torque variation of the powertrain system to stabilize conditions of the available heat for the WHR system.
- Testing has shown the thermodynamic principles of Rankine operation are sound, with results meeting expectations. The technical challenges of the Rankine cycle in a transportation application are surmountable; however feasibility for production remains constrained by cost, weight, packaging and reliability concerns. Future development work will focus on both system efficiency improvement and improvement of these features.
- The total system (engine operation conditions) must be optimized to consider engine load reduction due to WHR addition, aerodynamic improvements, etc. as shown along with some of the aforementioned findings in Figure 5. Methods to improve total system efficiency include downsizing of the powertrain and downspeeding of the engine.

ORC Testing and Controls Development Changes in Speed and Load Test Results

Control of system is challenging due to:

- Thermal inertia
- Flow restriction changes
- Pump delivery with speed
- Expander flow with speed, pressure and temperature

Steady-state operation of the system is difficult to achieve due to variation in working fluid flow caused by changing restriction and thermal inertia of system. Results from integrated WHR system on various duty cycles indicate that the more stable the chassis operation, the greater the integrated benefit found from WHR system addition. Steps must be taken to stabilize engine load demand for further improvements.

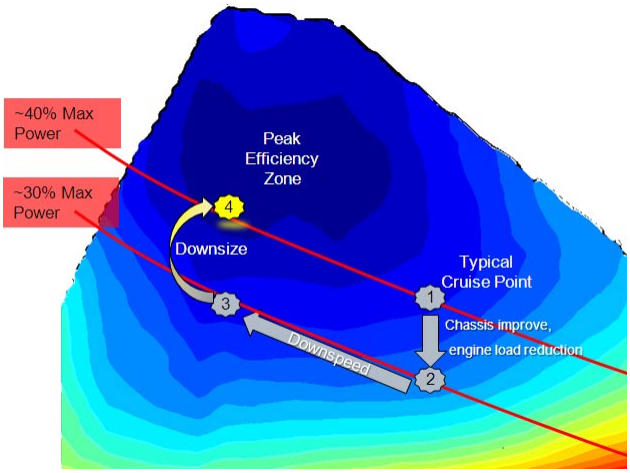

FIGURE 5. Total system optimization in speed-load range including ORC system integration.

Conclusions

Combustion

PPC combustion is very demanding on simulation tools. A practical PPC engine involves combustion modes from premixed charge compression ignition to diffusion combustion.

ORC system

Experience on ORC system operation has been gained. It shows that it is important to leave the saturation dome as quickly as possible, and that heat input management of exhaust stream is a very effective control. It is also important to calibrate the engine and design the powertrain to maximize the zone of useful operation during in-use application.

FY 2012 Publications/Presentations

1. DEER 2012 conference, Arne Andersson – "Combustion Model for Engine Concept Simulation."

2. DEER 2012 conference, Sam McLaughlin – "Impact of Vehicle Efficiency Improvements on Powertrain Design."

3. DEER 2012 conference, Vivek Raja – "Advanced CFD Models for High-Efficiency Compression-Ignition Engines."

4. DEER 2012 conference, Gregory Lilik – "Effects of Ignition Quality and Fuel Composition on Critical Equivalence Ratio."

5. DEER 2012 conference, Matthew Wright, "ORC Closed Loop Control Systems for Transient and Steady State Duty Cycles as it Relates to Class 8 Diesel Trucks."

IV.5 Advanced Gasoline Turbocharged Direct Injection (GTDI) Engine Development

Terry Wagner
Ford Motor Company
2101 Village Road
Dearborn, MI 48121

DOE Technology Development Manager:
Ken Howden

NETL Project Manager: Ralph Nine

Subcontractor:
Michigan Technological University (MTU),
Houghton, MI

Overall Objectives

Ford Motor Company Objectives:

- Demonstrate 25% fuel economy improvement in a mid-sized sedan using a downsized, advanced GTDI engine with no or limited degradation in vehicle level metrics.
- Demonstrate vehicle is capable of meeting Tier 2 Bin 2 emissions on the Federal Test Procedure (FTP)-75 cycle.

MTU Objectives:

- Support Ford Motor Company in the research and development of advanced ignition concepts and systems to expand the dilute/lean engine operating limits.

Fiscal Year (FY) 2012 Objectives

- Multi-cylinder development engines completed and dynamometer development started.
- Demonstration vehicle and components available to start build and instrument.
- Project management plan updated

Accomplishments

Combustion System Development:

- Completed port, chamber, injector, and piston specifications to enable combustion system iteration option (i.e. risk mitigation) during the multi-cylinder engine (MCE) evaluation on dynamometer phase of the project.

Single-Cylinder Build and Test:

- Completed commissioning of surrogate 1.8-L single-cylinder engine (SCE) in test cell.
- Completed combustion system verification testing, provided data for correlation to detailed multi-dimensional engine simulation analyses, and selected injector and spark plug specifications for subsequent 2.3-L SCE.
- Completed installation and commissioning of new 2.3-L SCE in test cell.
- Initiated combustion system verification testing to ensure combustion system meets target metrics, including fuel consumption, stability, oxides of nitrogen (NOx), carbon monoxide (CO), and particulate matter (PM) emissions; testing included part-load, lean and stoichiometric, air-fuel ratio sweeps, injection timing sweeps, cooled EGR sweeps, and cam timing sweeps; testing to date indicates combustion system satisfies target metrics.
- Initiated combustion system testing on alternative injector specifications to enable combustion system iteration option (i.e. risk mitigation) during the MCE evaluation on dynamometer phase of the project.

Engine Design/Procure/Build:

- Completed procurement process in support of May 1, 2012 MCE material required date; completed bill of material, component tooling and piece costs, and supplier request for quote/sourcing process with Ford Prototype Purchasing.
- Completed manufacturing process reviews in support of MCE material required date (e.g. cylinder block casting and machining, cylinder head casting and machining, cover castings and machining).
- Completed assembly process reviews, assembly illustrations, and assembly aids in support of MCE material required date.
- Completed MCE build and first firing of 1st of 12 engines; initiated MCE instrumentation and prep for dynamometer installation; 1st engine planned for combustion system verification testing.
- Initiated MCE build for 2nd, 3rd, and 4th of 12 engines; 2nd engine planned for transient emissions development testing; 3rd engine for calibration/

mapping; 4th engine for mechanical development/ noise-vibration-harshness (NVH).
- Remainder of 12 engines to be built following 1st engine combustion system/mechanical verification.

Engine Development on Dynamometer:

- Initiated dynamometer facility and engine instrumentation planning in support of 2012–2014 development plans.

Vehicle Installation Design and Procurement:

- Completed computer-aided (CAD) design and required computer-aided engineering (CAE) analyses of exhaust system; initiated procurement of exhaust system components.
- Initiated CAD design and required CAE analyses of new advanced integrated powertrain systems, specifically torque converter pendulum damper and active powertrain mounts.

Vehicle Build:

- Milestone "Demonstration vehicle and components available to start build and instrument" deferred from 12/31/2012 to 08/01/2013, due to milestone "Multi-cylinder development engines designed and parts purchased" deferred from 12/31/2011 to 05/01/2012.

Vehicle Cooling Design and Optimization:

- Completed CAD design and required CAE analysis of total engine and vehicle cooling system, with primary emphasis on internal engine cooling flow to optimize the split, parallel, cross-flow cooling configuration.
- Initiated procurement of vehicle cooling system components including pumps, heat exchangers, fittings, lines, etc.

Vehicle Calibration:

- Acquired surrogate vehicle with surrogate GTDI engine; initiated early controls and calibration development tasks to accelerate target vehicle tasks.

Aftertreatment Development:

- Investigated the potential of a three-way catalyst (TWC) + lean-NOx trap/selective catalytic reactor (LNT/SCR) system to satisfy the hydrocarbon (HC) and NOx slip targets.
  - Assessed catalyst volumes, operating temperatures, lean/rich durations, and lean NOx concentrations; estimating system costs and fuel economy benefits.
  - Assessed TWC + LNT formulations with reduced oxygen storage capacity thus enabling reduced rich purge durations; estimated fuel economy benefits.
- Investigated the deSOx capability of an underbody LNT; estimated associated aging impact and tailpipe emission penalties.
  - Determined that reducing TWC oxygen storage capacity levels and employing a lean/ rich wobble deSOx strategy was insufficient to achieve the 700°C target deSOx temperature.
- Investigated the potential of a TWC + passive SCR system to satisfy the HC and NOx slip targets while improving the deSOx capability (vs. the TWC + LNT/SCR system).
  - Assessed catalyst volumes, operating temperatures, lean/rich durations, and lean/rich NOx concentrations; estimated system costs and fuel economy benefits.
- Given the deSOx challenges of a TWC + LNT/SCR system, and the uncertainty of a TWC + passive SCR system, received concurrence on lean aftertreatment transitioning to stoichiometric at the vehicle level.
- Completed additional analytical, laboratory, and dynamometer level assessments to further quantify the attributes of a TWC + passive SCR system.

Combustion Research:

- Progressed all facets of research and development described by the primary tasks i) Advanced Ignition & Flame Kernel Development, ii) Advanced Ignition - Impact on Combustion, iii) GDI Air/Fuel Mixing via PLIF for Fuel Injection Optimization, iv) Combustion Sensing & Control, v) Advanced Knock Detection & Control, and vi) In-Cylinder Temperatures & Heat Transfer.
- Continued development of the high feature combustion pressure vessel, including i) optimization of the dual fans/shrouds for wide range charge motion representing engine-like mean flow and turbulence intensity conditions at the spark plug electrode, and ii) optimization of the variable output ignition system (VOIS) discharge pattern for substantially successful flame initiation and propagation.
- Continued advanced ignition hardware investigations in the 1st 3.5-L EcoBoost engine, including i) optimization of the VOIS, and ii) assessment of the dilute engine operating limits (i.e. cooled EGR) as a

function of VOIS parameters, spark plug electrode gap, and tumble ratio.
- Continued preparation of the 2nd 3.5-L EcoBoost engine for combustion surface temperature measurements, including installation of a wireless telemetry system for piston temperature and heat flux measurements.

Future Directions

- Dynamometer engine development indicates capability to meet intermediate metrics supporting vehicle fuel economy and emissions objectives.
- Demonstration vehicle and components available to start build and instrument.
- Vehicle build, instrumented, and development work started.
- Aftertreatment system development indicates capability to meet intermediate metrics supporting emissions objectives.
- Project management plan updated.

Introduction

Ford Motor Company has invested significantly in GTDI engine technology as a cost effective, high volume, fuel economy solution, marketed globally as EcoBoost technology. This project is directed toward advancing the EcoBoost technology, as well as related additional technologies, in order to achieve the project objectives:

- Demonstrate 25% fuel economy improvement in a mid-sized sedan using a downsized, advanced GTDI engine with no or limited degradation in vehicle level metrics.
- Demonstrate vehicle is capable of meeting Tier 2 Bin 2 emissions on the FTP-75 cycle.

Approach

Engineer a comprehensive suite of gasoline engine systems technologies to achieve the project objectives, utilizing:

- Aggressive engine downsizing in a mid-sized sedan from a large V-6 to a small I-4.
- Mid- and long-term EcoBoost advanced technologies such as:
  - Dilute combustion with cooled exhaust gas recycling and advanced ignition
  - Lean combustion with direct fuel injection and advanced ignition
  - Boosting systems with active and compounding components
  - Cooling and aftertreatment systems
- Advanced friction reduction technologies, engine control strategies, and NVH countermeasures.
- Progressively demonstrate the project objectives via concept analysis/modeling, SCE, MCE, and vehicle-level demonstration on chassis rolls.

Results

The team progressed the project through the Combustion System Development, Single-Cylinder Build and Test, and Engine Design/Procure/Build tasks with material accomplishments. In addition to the prime combustion system completed in Budget Period 1, the team completed a combustion system iteration option which may be employed during the MCE dynamometer evaluation phase. The combustion system iteration option, shown in Figure 1, represents a risk mitigation option and may be employed if the prime combustion system is challenged to satisfy the target metrics.

The team completed commissioning and combustion system verification testing of a 1.8-L SCE and a subsequent 2.3-L SCE. The 1.8-L SCE was used to select injector and spark plug specifications for the 2.3-L SCE (and ultimately the MCE); representative results are shown in Figure 2. The team completed testing of both the 1.8-L and 2.3-L SCEs to ensure the combustion system meets the target metrics, including fuel consumption, stability, NOx, CO, and PM emissions. Representative results are shown in Figure 3, and further testing at additional speed/load points indicates the combustion system satisfies the target metrics.

Lastly, and most notably, the team substantially completed the engine design/procure/build task. The completed engine design in solid model form is shown in Figure 4. Over the course of the budget period, the team completed the procurement process with Ford Prototype Purchasing, completed manufacturing and assembly process reviews, and MCE build and first firing of the 1st of 12 engines. The team also initiated instrumentation and prep for dynamometer installation. The 1st engine is planned for combustion system verification testing, while the remainder of engines are planned for transient emissions development testing, calibration/mapping, mechanical development/NVH, vehicles, and other related tasks. Figure 5 shows the completed 1st engine build, designated as 2.3-L MiGTDI Pre-X0 Engine #1.

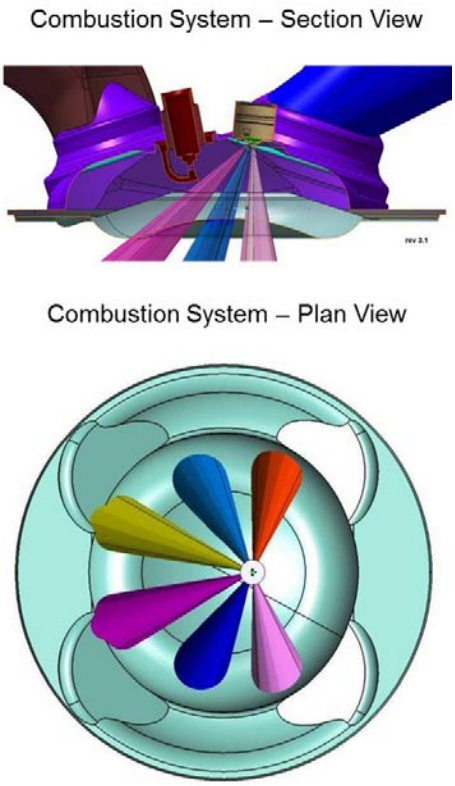

FIGURE 1. Combustion System Iteration Option

Conclusions

- The project will demonstrate a 25% fuel economy improvement in a mid-sized sedan using a downsized, advanced GTDI engine with no or limited degradation in vehicle level metrics, while meeting Tier 2 Bin 2 emissions on FTP-75 cycle.
- Ford Motor Company has engineered a comprehensive suite of gasoline engine systems technologies to achieve the project objectives and progressed the project through the Combustion System Development, Single-Cylinder Build and Test, and Engine Design/Procure/Build tasks with material accomplishments to date.
- Ford Motor Company is in collaboration with Michigan Technological University on a critical facet of the project, specifically advanced ignition concepts.

FY 2012 Publications/Presentations

1. Completed presentation at 2012 U.S. Department of Energy Hydrogen and Fuel Cells Program and Vehicle Technologies Program Annual Merit Review and Peer Evaluation Meeting (AMR), held May 14–18, 2012, Crystal City Marriott, Arlington, Virginia.

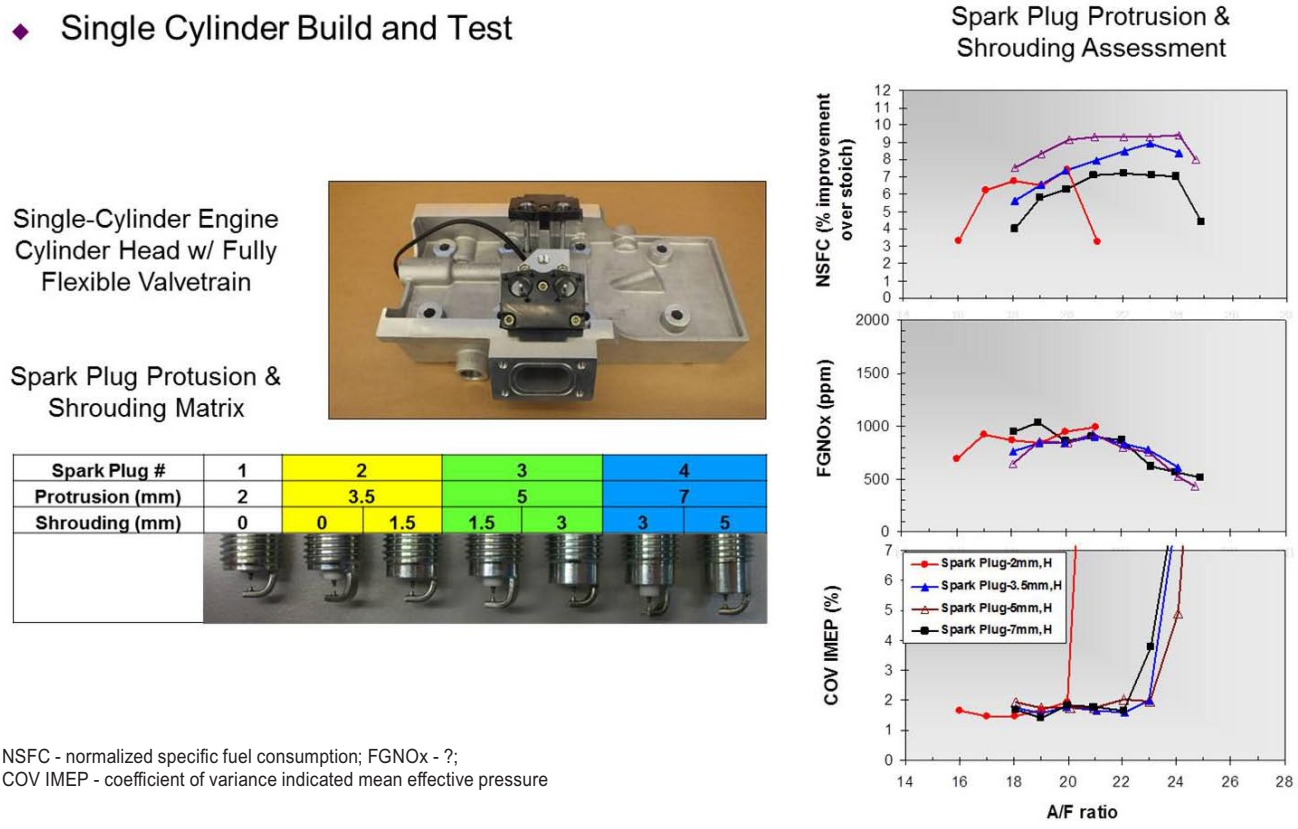

NSFC - normalized specific fuel consumption; FGNOx - ?;
COV IMEP - coefficient of variance indicated mean effective pressure

FIGURE 2. 1.8-L Single-Cylinder Engine

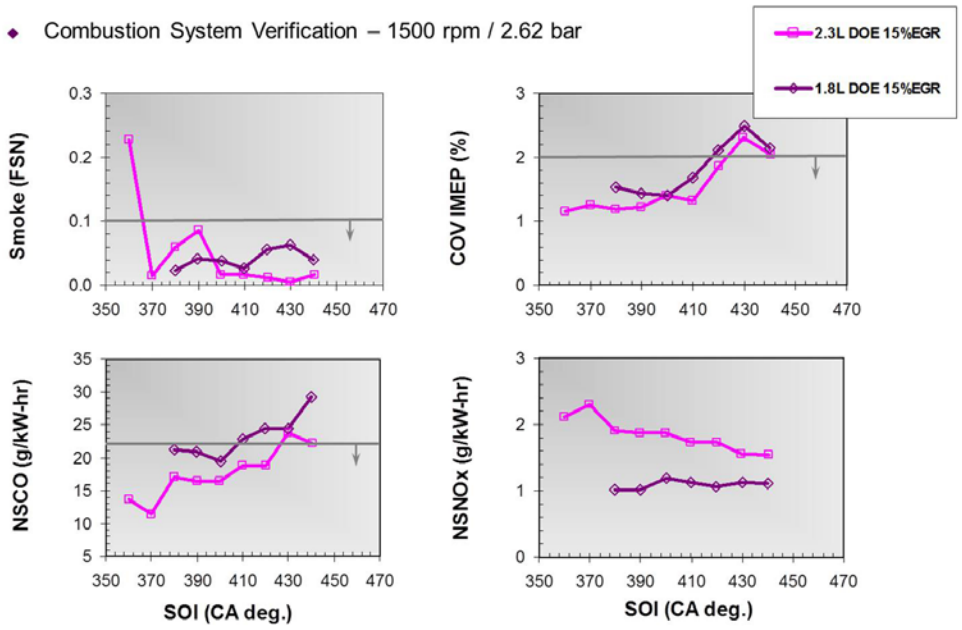

FSN - filter smoke number; NSCO - normalized specific carbon monoxide; SOI - start of injection; CA - crank angle

FIGURE 3. 2.3-L Single-Cylinder Engine

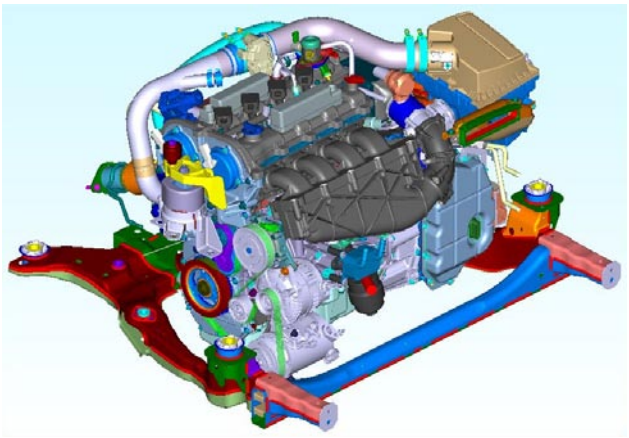

FIGURE 4. Multi-Cylinder Engine Design

FIGURE 5. Multi-Cylinder Engine Build

2. Completed project status presentation for Ralph Nine and Ken Howden at Ford Motor Company on July 16, 2012; reviewed status of all primary tasks and received concurrence on lean aftertreatment transitioning to stoichiometric at the vehicle level. Completed an active mount drive session, a single-cylinder lab tour, and a lean aftertreatment lab tour; due to time constraints, a multi-cylinder build tour was deferred.

Special Recognitions and Awards/Patents Issued

1. Submitted "Using AIS Throttle to Reduce TipOut EGR Overshoot in LPEGR System", ID No 83228949, DOE Case No S-130,540 – 03/08/2012.

2. Submitted "Cooled EGR Operation Under Enrichment Conditions To Circulate Rich Exhaust For Fuel Economy Improvement", ID No 83228424, DOE Case No S-130,541 – 03/08/2012.

IV.6 Lean Gasoline System Development for Fuel Efficient Small Cars

Stuart R. Smith
Powertrain Division
General Motors, LLC
895 Joslyn Avenue
Pontiac, MI 48340-2920

DOE Technology Development Manager:
Ken Howden

NETL Project Manager: Ralph Nine

Overall Objectives

- Develop an advanced lean gasoline combustion engine and aftertreatment system.
- Demonstrate 25% vehicle fuel economy improvement while achieving Tier 2 Bin 2 emissions.
- Comprehend system level integration for an optimal combination of advanced vehicle technologies to provide the highest fuel economy for potential production implementation.

Fiscal Year (FY) 2012 Objectives

- Demonstrate active thermal management fuel economy improvement >1.5%.
- Demonstrate lean gasoline aftertreatment hardware provides emissions <200% w/o particulate matter.
- Demonstrate lean gasoline cold Federal Test Procedure (FTP) and Highway driving cycle fuel economy improvement >13%.

Accomplishments

- Designed, procured and assembled the 2nd generation, lean downsize boost (LDB) gasoline combustion engines that incorporates multiple fuel injection authority and high-energy ignition.
- Developed the lean aftertreatment system hardware configuration and calibration to provide comprehensive oxides of nitrogen (NOx) reduction under all thermal operating conditions.
- Refined the torque-based engine controls architecture and calibration to provide precise EGR control for optimized transitions between lean and stoichiometric operation.
- Achieved the FY 2012 technical target of a lean aftertreatment system capable of emissions within 200% of Tier 2 Bin 2 without particulate mitigations.
- Approached the FY 2012 technical target of City FTP and Highway fuel economy improvement at 9%, with projections to achieve target with the new LDB engine.

Future Directions

- Expand the torque-based controls to support boosted operation.
- Optimize the combustion system to allow extended lean stratified operation under boosted conditions with optimization of the fuel injection and ignition parameters.
- Refine the lean aftertreatment system hardware to incorporate the optimum elements of the active and passive technologies which will yield lowest initial and operational costs.
- Install the optimized LBD engine and final refined lean aftertreatment hardware.
- Integrate the 12-volt stop/start and advanced thermal management systems hardware and functionality.
- Calibrate the 2nd generation LBD engine and 4th generation lean aftertreatment system to provide optimal fuel economy, emissions compliance and seamless drivability.

Introduction

The project accelerates development and synergistic integration of four cost competitive technologies to improve fuel economy of a light-duty vehicle by 25% while meeting Tier 2 Bin 2 emissions standards. These technologies are targeted to be broadly implemented across the U.S. light-duty vehicle product line between 2015 and 2025 and are compatible with future and renewable biofuels. The technologies in this project are: lean gasoline combustion, innovative passive selective catalytic reduction (SCR) lean aftertreatment, 12-volt stop/start and active thermal management. The technologies are initially developed on engine dynamometers, further refined on development vehicles, fully integrated and then calibrated in a mid-size sedan for final demonstration. The project scope additionally includes risk mitigation of downsize boosting and active urea dosing.

Approach

The development approach is structured to garner fundamental understanding of technology areas, innovate novel solutions to challenges and optimize solutions along with implementing risk mitigations to address limitations. The FY 2011 initial concept phase of the project revolved around fundamental modeling, analysis and experimental investigation, leading in to initial hardware designs and control strategies. The FY 2012 refinement phase of the project focused on evaluating the hardware and controls to refine the technology areas, ascertain barriers and subsequently define the hardware to be utilized for final optimization and demonstration phase during FY 2013. Figure 1 depicts the targeted fuel economy improvement technology contributions that evolved from the refinement phase; vehicle integration 4-6%, advanced dilute combustion 3-5%, downsizing 6-10%, lean dilute combustion and aftertreatment 6-10%.

Results

LDB Engine

Boosted lean combustion system development and optimization focused on enhancing the operation and performance of lean stratified gasoline combustion. Test results from boosting the 1st generation SG5 engine indicated that additional fuel economy improvement can be achieved by increasing the air flow capacity of the engine, executing a multiple closely spaced injection pulse strategy and utilizing a higher ignition energy system, Figure 2.

The turbo system is aggressively sized to match the air flow requirements that provides the maximum potential efficiency gain while providing the large mass flow required to support lean operation. The turbo matching has been restricted to selection of a single-stage turbo, where selection is biased to meet low speed stratified operation for peak fuel economy rather than peak power charging requirements. The fuel system and engine controller capability is enhanced to deliver multiple closely spaced injection pulses (up to four injection pulses and less than 0.5 ms spacing between injection pulses). The data illustrates a brake thermal efficiency improvement of 3% can be achieved by boosting the engine along with upgrading the injection strategy with multi-hole solenoid injectors. The ignition system is upgraded to a high energy system. A high-energy ignition system enables higher EGR tolerance at low- and mid-load operation. EGR tolerance is increased from 15 to 35% with constant air/fuel ratio while a 4% brake specific fuel consumption (BSFC) reduction can be achieved at lower load condition. Inclusion of the high-energy ignition will enable improved fuel economy at the same engine-out NOx levels.

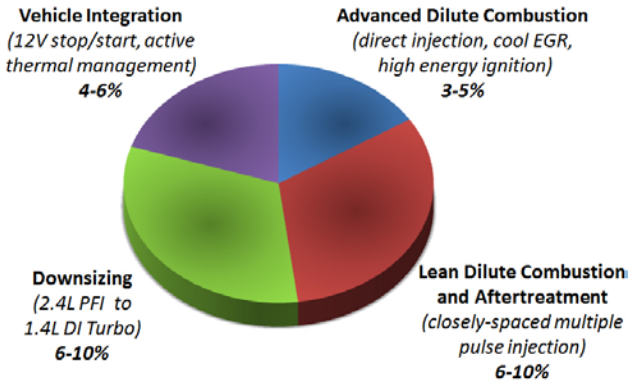

FIGURE 1. Targeted Fuel Economy Improvement

The boosted lean combustion development systems are incorporated in to a 2nd generation lean stratified engine, the LDB engine. The engine is downsized to 1.4-L, incorporates single-stage turbocharging, cooled EGR and a spray-guided combustion system scaled from the 1st generation SG5 engine. The LDB engine is configured to provide the highest level of fuel economy potential with the optimal combination of advanced technologies, Figure 3.

A number of subsystems and components are redesigned to support the integration of the boosted lean combustion system; new spark plug, injector targeting changes, chamber smoothing modifications, cylinder pressure transducer provisions, split intake port cylinder head, intake port deactivation adapter assembly to provide high swirl mixture motion for increased lean dilution tolerance and a close coupled catalyst exhaust system with cooled external EGR exhaust. Additionally, the piston bowl is designed in three different sizes at the same compression ratio of 10.5 to support performance impact assessments at low and high engine load conditions; 2 bar (lean), 10 bar (lean), and 16 bar (stoichiometric) to ensure good lean operation and acceptable high load homogeneous operation.

Lean Aftertreatment

The passive SCR lean aftertreatment system development continued with Gen 3 hardware in an effort to overcome the limitations of excess CO breakthrough during NH_3 generation and insufficient NOx reduction during high thermal operating conditions. The updated Gen 3 hardware included three design changes targeted to improve emissions performance; 1) the front SCR location has been positioned axially rearward by 29 inches to lower temperatures and improve NH_3 storage, 2) the rear SCR configuration was modified to a single 2.0-L SCR with a revised inlet cone, 3) enhanced

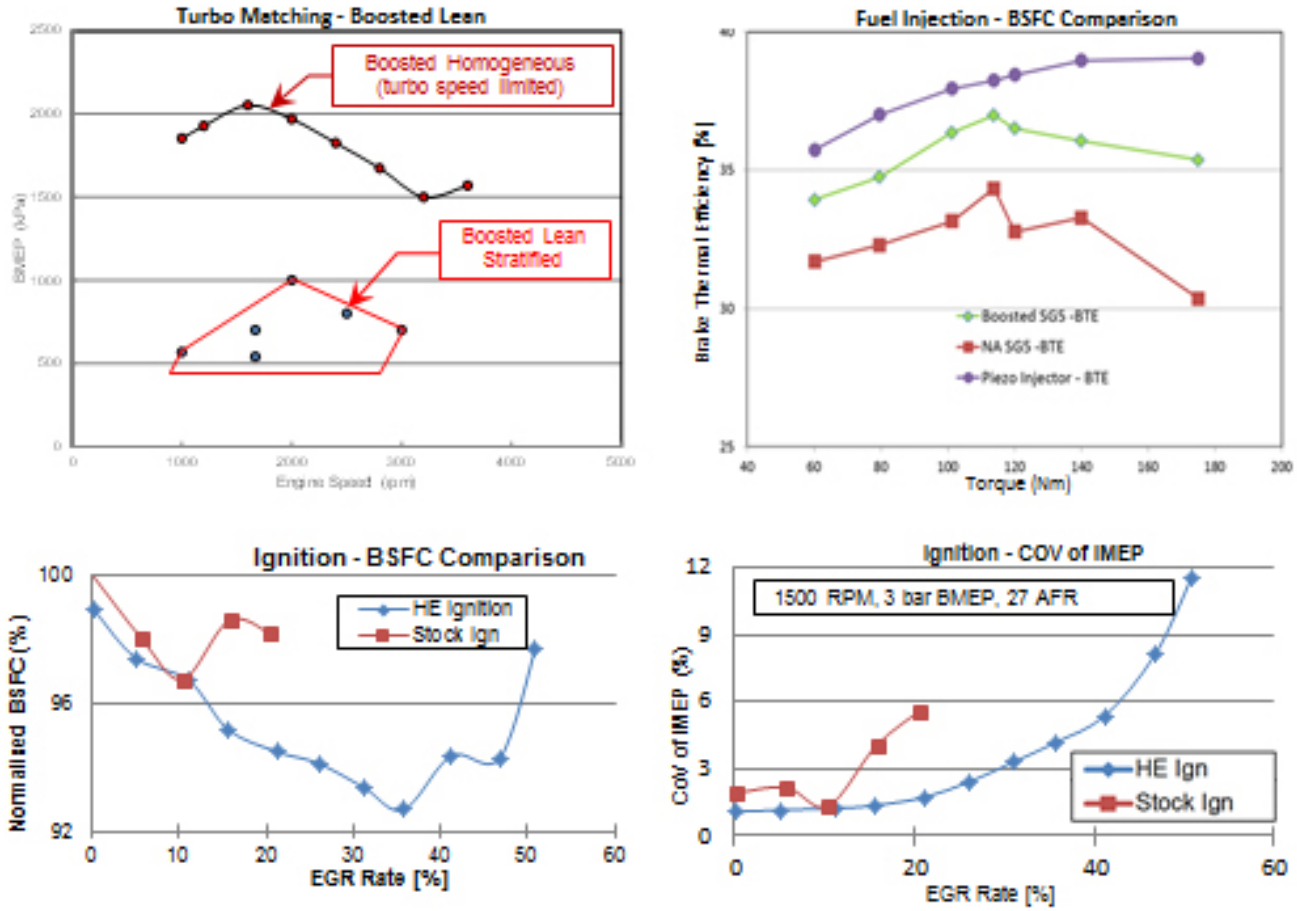

BMEP - brake mean effective pressure; COV - coefficient of variance; IMEP - indicated mean effective pressure; EGR - exhaust gas recirculation; AFR - air/fuel ratio

FIGURE 2. Lean Boost Combustion Development

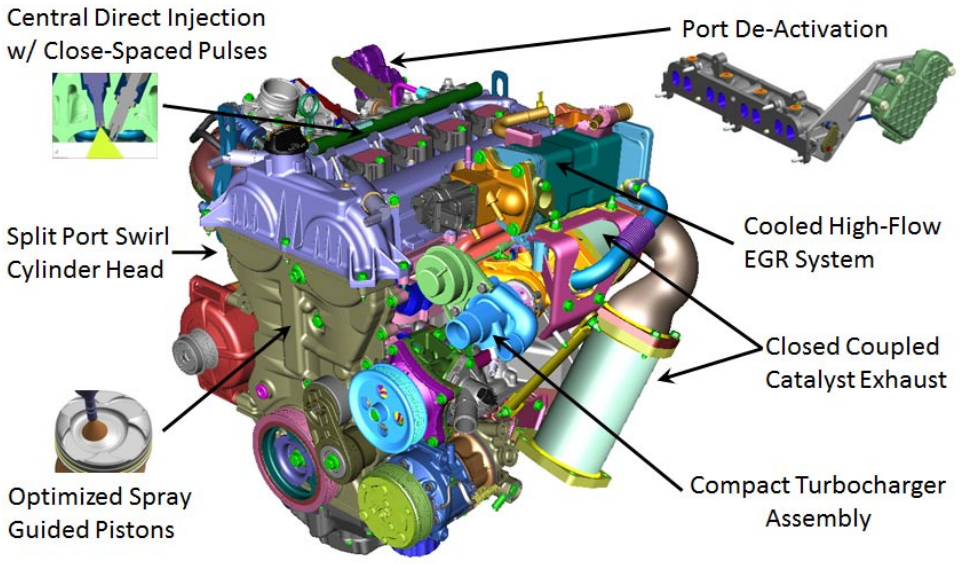

FIGURE 3. 1.4-L Lean Downsize Boost Engine

washcoat technologies were incorporated to optimize NH_3 generation. Unfortunately, the changes were unsuccessful in fully addressing the system limitations and providing the require NOx conversion efficiency, Figure 4. Subsequently, efforts to develop an only passive SCR lean aftertreatment have ceased.

The active urea lean aftertreatment system development continued in the development vehicle to support refinement of the calibration and evaluate the performance under transient vehicle operation. The active urea dosing system utilized copper/iron/iron/copper SCR technology. The vehicle emissions were evaluated with the FTP and Highway test cycles, Figure 5. Overall

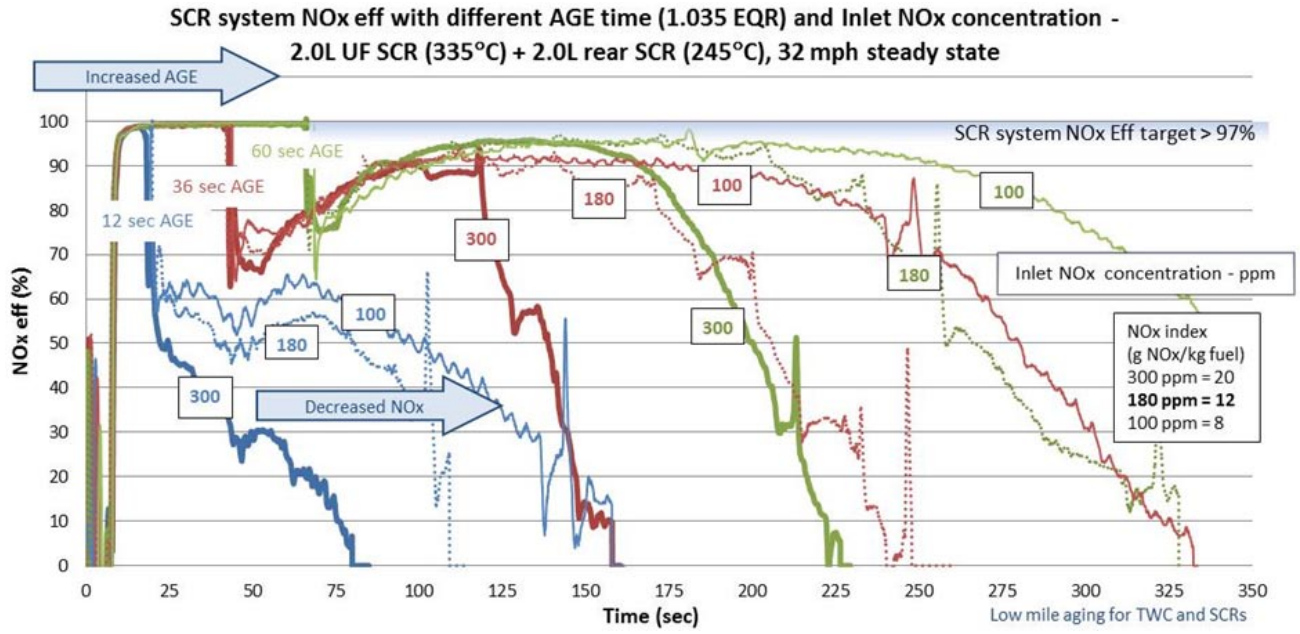

UF - underfloor; TWC - three-way catalyst

FIGURE 4. Passive SCR Lean Aftertreatment NOx Efficiency

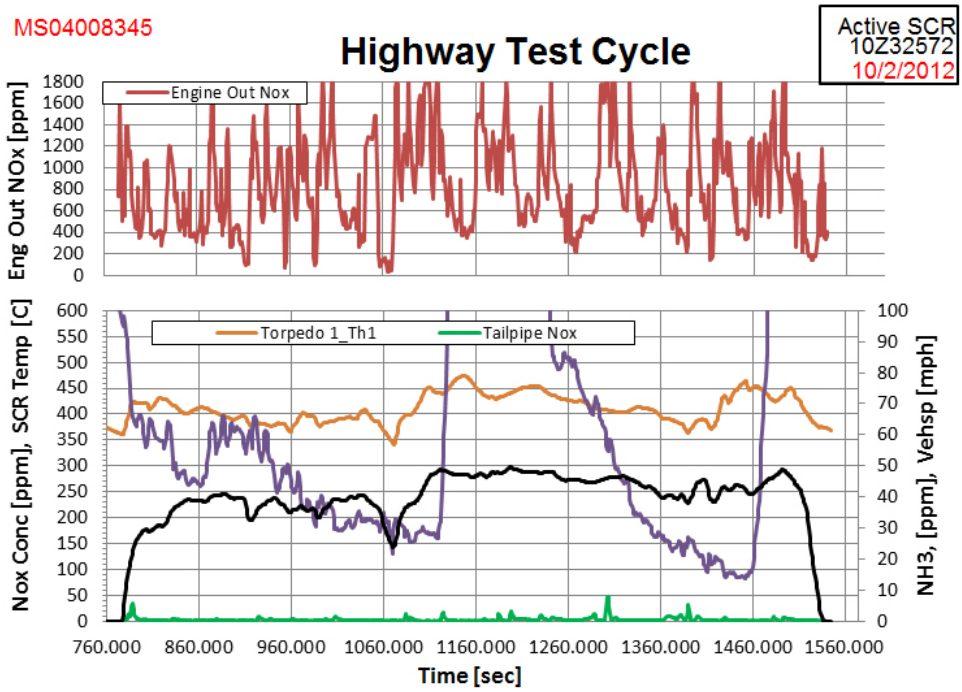

FIGURE 5. Active Urea Lean Aftertreatment NOx Reduction

the system is achieving the engineering emission targets to support lean gasoline engine operation. The combustion is very sensitive to calibration and richer calibrations can meet the standards for hydrocarbons (HCs) and NOx, but at the expense of fuel economy. There is sufficient data available that supports, with a short cold-start strategy, the final engineering target for NOx can be achieved. Increased catalyst volume is needed for complete reduction of CO and HC. NH_3 is still higher than expected, but is due to new catalyst formulation and an immature dosing calibration. Outside of the high temperature release, the NH_3 slip is very good. HC and NOx are very good for the highway fuel economy but CO is still high, extra catalyst volume is required. Additionally, NH_3 slip can be improved with an optimized storage model calibration.

Vehicle Emissions and Fuel Economy

Emissions development during transient operation has progressed with the Malibu development vehicle equipped with a SG5 naturally aspirated lean stratified engine. The focus has been on minimizing HC and CO emissions during engine start/warm-up as well as calibrating the active urea dosing aftertreatment system to minimize NOx emissions. Tailpipe emissions results are shown in Table 1. The lean stratified emissions results achieve the NOx milestone but exceed the HC and CO milestone levels. For conventional gasoline engine and aftertreatment systems, the majority of the tailpipe emissions occur before the engine and catalyst systems reach full operating temperature. In this case, however, the emissions during engine start and warm up are relatively low with the majority of the tailpipe emissions occurring during transitions from homogeneous to lean stratified and lean stratified to homogeneous operating modes.

Calibration and controls refinements focused on EGR algorithms and controls for the naturally aspirated lean stratified vehicles. The recirculated exhaust gas flow control is one of the primary enablers of the lean stratified operation with precise control critical to meeting combustion parameters targeted for seamless transition to stoichiometric operation. To support the precise control of exhaust gas flow, exhaust pressure and temperature sensors were integrated into the electronic control module to allow the EGR valve to respond to changes in environmental conditions. Enabling the ability to react to changing conditions allows the engine to run higher levels of exhaust gas recirculation, thereby maximizing the lean dilute combustion operation.

Fuel economy improvements have been measured on Malibu development vehicle equipped with the SG5 naturally aspirated engine and compared to the same vehicle with the baseline 2.4-L port fuel injected LE5 engine. The level of improvement correlates reasonably well with the simulation results. This simulation results are based on BSFC data for the high density speed-load points that are seen on the FTP City and Highway test schedules. The fuel economy measured on Malibu with the LE5 and SG5 engines as well as the measured and predicted fuel economy improvement are shown in Table 1. Lean stratified gasoline combustion on a naturally aspirated engine yields a combined cold FTP and Highway measured fuel economy improvement of 9% over the baseline engine.

TABLE 1. 2.2-L Naturally Aspirated SG5 Emissions and Fuel Economy

EMISSIONS	NMHC (gm/mi)	CO (gm/mi)	NOX (gm/mi)
T2B2 Standard	.010	2.1	.020
150% of T2B2	.015	3.2	.030
Stoichiometric Homogeneous	.009	2.1	.008
Lean Stratified w/ Active Urea System	.033	3.9	.019

FUEL ECONOMY	LE5 (baseline)	SG5 (2.2L NA)	Measured % Improvement	Simulation % Improvement
City	23.61	26.08	10.5%	11.5%
Highway	41.17	43.68	6.1%	7.9%
Combined	29.22	31.86	9.0%	10.3%

T2B2 - Tier 2, Bin 2

Conclusions

- Naturally aspirated lean stratified gasoline engines can provide significant fuel economy improvements of ~9%, though lean boosting is require to further extend benefit of lean combustion.
- Combined advanced technologies of boosting, multiple fuel injection, high-energy ignition and cooled EGR extend operation of lean gasoline combustion for maximum fuel economy.
- Active thermal management shall provide up to additional 1.5% in fuel economy benefit.
- Passive SCR aftertreatment has fundamental implementation barriers with generating greater than desired CO during NH_3 generation and NH_3 storage during hot operation.
- Active urea dosing lean aftertreatment is a demonstrated technology to enable lean stratified gasoline operation robustly under all operating conditions.

FY 2012 Publications/Presentations

1. Santoso, Halim, "Lean Gasoline System Development for Fuel Efficient Small Car", 2012 U.S. DOE Vehicle Technologies Program Annual Merit Review and Peer Evaluation Meeting, Arlington, VA, May 18, 2012.

2. Yang, Xiaofeng; Solomon, Arun; Kuo, Tang-Wei "Ignition and Combustion Simulations of Spray-Guided SIDI Engine using Arrhenius Combustion, with Spark-Energy Deposition Model". SAE World Congress, April 2012.

IV.7 Recovery Act – A MultiAir/MultiFuel Approach to Enhancing Engine System Efficiency

Ron Reese
Chrysler Group, LLC
800 Chrysler Drive
Auburn Hills, MI 48326

DOE Technology Development Manager:
Ken Howden

NETL Project Manager: Ralph Nine

Subcontractors:
- The Ohio State University, Columbus, OH
- Bosch, Farmington, MI
- Delphi, Troy, MI
- FEV, Auburn Hills, MI
- Argonne National Laboratory (ANL), Argonne, IL

Overall Objectives

- Demonstrate 25% improvement in combined City and Highway Federal Test Procedure (FTP) fuel economy for the Chrysler minivan.
- Accelerate the development of highly efficient engine and powertrain systems for light-duty vehicles, while meeting future emissions standards.
- Create and retain jobs in support of the American Recovery and Reinvestment Act of 2009.

Fiscal Year (FY) 2012 Objectives

- Complete Alpha 1 engine builds. Perform dynamometer tests to demonstrate durability and ability to meet 25% fuel economy improvement goal.
- Select Alpha 2 design content based on Alpha 1 testing and results.
- Develop/implement full vehicle simulation model and demonstrate 4% improvement in fuel economy based on thermal management system improvements.
- Install thermal management system into surrogate vehicle that rapidly warms up coolant, engine and transmission oil after cold start to reduce parasitic losses and contribute 4% fuel economy improvement. Conduct drive cycle fuel economy testing.
- Design and demonstrate controlled charge algorithm to maintain absorbed glass mat (AGM) battery integrity while maximizing fuel economy via smart charging.
- Update design of pendulum crank.
- Develop/test system controls functionality for twin-turbo, cooled exhaust gas recirculation (EGR), secondary air.
- Calibrate/validate the Vehicle Energy Simulator (VES) model.
- Integrate/calibrate the Vehicle Energy Model (VEM).

Accomplishments

- Four Alpha 1 engines built/tested. Engines have proven efficient. Over 1,600 hours testing completed.
- Diesel micro pilot (DMP) engine shows impressive brake specific fuel consumption (BSFC) results at high loads (40% brake thermal efficiency, BTE) but difficult to control due to sensitivities to EGR rate, injection events, temperature and humidity.
- The triple-plug engine demonstrated good fuel efficiency (39% BTE). Significant testing completed with dual-fuel system using port fuel injected (PFI) ethanol.
- Delphi developed/verified algorithms to predict combustion feedback information based on ion-sensed signals from the ignition coils.
- The design for the Alpha 2 engine near completed.
- Conducted drive cycle fuel economy testing with new thermal management system installed on surrogate vehicle. Demonstrated 3.0% increase in unadjusted fuel economy due to rapid warm-up.
- Communication protocol between the powertrain and vehicle determined and gateway software identified.
- Second iteration vehicle crank pendulum with updated design created and tested, eliminating excessive operating noise. New design adapted for Alpha 1 engine includes seven pendulums (three more than original design).
- Developed controlled charge algorithm to optimally charge the AGM battery. Fuel flow savings of up to 0.015 g/s. Controlled charge algorithm demonstrated in surrogate vehicle.
- Delivered feed-forward and feedback twin turbo control software. Delivered and verified direct injection variable injection timing and secondary air control software. Developed control software to

handle ethanol injection in PFI mode and gasoline injection in the direct injection mode.
- Models for electric system, air conditioning system, engine, vehicle, driver, torque converter and transmission thermal, torque converter mechanical and transmission and differential mechanical completed in the VES and the VEM.

Future Directions

- Complete final design, procurement, build and demonstration of targeted improvements for Alpha 2 engine.
- Complete thermal management system, third iteration of vehicle crank pendulum, integrated controlled charge algorithm and install with engine into vehicle.
- Complete control strategies to enable engine calibration, drivability and fuel economy improvements for implemented technologies including twin turbo, cooled EGR, secondary air and multi-fuel.
- Continue DMP combustion learning through continued engine testing and simulation efforts at ANL.
- Complete implementation of the VEM.

Introduction

Purpose of project is to demonstrate 25% improvement in fuel economy while maintaining comparable vehicle performance to the baseline engine – a state-of-the-art 4.0-L V-6. Tier 2, Bin 2 tailpipe emissions will be demonstrated. Will down-size and down-speed the engine through combustion improvements via a combination of engine technologies with concurrent development of other system enhancements.

Main technologies explored as part of development project include in-cylinder combustion improvements, waste heat recovery and thermal management strategies, friction reduction, ancillary load management and emissions controls.

Approach

Complete two engine design/development iterations. Each iteration encompasses two development phases – one for design/simulation efforts, the second for procurement, engine build and test. The combination of Phases 1/2 resulted in the Alpha 1 engine. Phases 3/4 will incorporate learning from early phases to produce the Alpha 2 engine. This engine will be used in Phase 5 fuel economy demonstration.

Results

Mechanical development tests performed to prove the capability of the Alpha 1 engines. Most systems met goals. Results pointed to improving the boosting system, positive crankcase ventilation system and mechanical friction for the Alpha 2 design. Flow restrictions across the air charge and EGR cooler developed frequently on the DMP-equipped engines. Triple-plug engines have shown no significant degradation.

Extensive one-dimensional/3-dimensional (1-D/3-D) engine simulations completed by Chrysler, ANL on the triple-plug and DMP-equipped engine models. The 1-D modeling results indicate design is capable of meeting/exceeding efficiency and performance targets with identified design improvements. Completed 3-D code evaluations, selected Converge™ for future computational fluid dynamics simulation. Enhancements made to improve combustion mechanism to predict spark ignition and DMP combustion events. Correlation established with dynamometer results. Injector spray imaging (ANL's advanced photon source) provided gasoline and diesel direct injection density information for the combustion model.

The original two-stage boosting devices did not perform as model predicted. Thermal energy driving the turbines found to be lower than expected for low-temperature combustion. Highly dilute operation and turbo maps did not fully account for actual turbine and compressor inlet and outlet conditions of the physical hardware. With additional modeling and hardware testing, a revised low-pressure turbine housing design was selected, used in Alpha 2 engines. PFI introduced ethanol as secondary fuel tested to provide combustion phasing, knock relief benefits at high load on triple-plug engine. Dual-fuel system met/exceeded performance goals throughout speed range while allowing gasoline only operation below 14 bar brake mean effective pressure at most speeds (Figure 1). Vehicle modeling shows high loads should only be required for about 30 seconds during the FTP City/Highway cycle so volumetric fuel economy disadvantage of ethanol should be minimal.

DMP ignition demonstrated in Alpha 1 engine testing. Technology provides ability to achieve compression ignition event with very high levels of EGR, resulting in highly efficient engine operation (Figure 2). DMP combustion is sensitive to multiple control parameters: EGR rate, intake manifold temperature, intake cam position. Sensitivity under steady-state

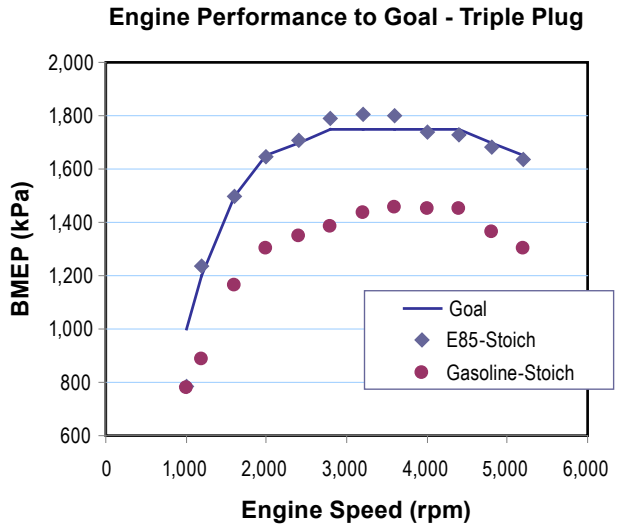

FIGURE 1. Engine Performance to Goal – Triple Plug

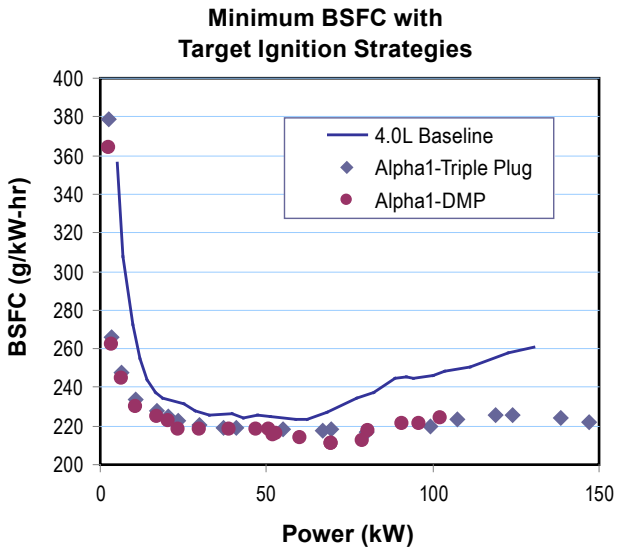

FIGURE 2. Minimum BSFC with Target Ignition Strategies

conditions and difficulty in controlling under in-vehicle transient conditions led to removing DMP from Alpha 2 engine. ANL continues to study DMP combustion.

Delphi gathered combustion data with ion-sensed signals from two dynamometer test cells. Algorithm development, artificial neural network training resulted in reasonable prediction of combustion phasing. Work continues in knock detection, combustion stability and improving combustion phasing measurement. Delphi's cylinder pressure-based combustion feedback system installed for use with production grade cylinder pressure sensors. Results will be compared with ion-based results and used in Alpha 2 engines if ion sense results not sufficient.

Thermal management system installed on surrogate vehicle. Key thermal system features include electronic thermostat with 105°C set point (compared to 95°C), exhaust heat recovery system for rapid coolant warm-up, engine oil heater for rapid engine oil warm-up, transmission oil heater for rapid transmission oil warm-up. The mule vehicle underwent FTP City/Highway drive cycle tests with no thermal management system and with full thermal management. Figures 3 and 4 indicates reduced fluid warm-up times from new thermal management system and associated 3.0% reduction in combined FTP City/Highway fuel economy.

A controlled charge strategy was developed to optimally charge automotive AGM battery to maximize

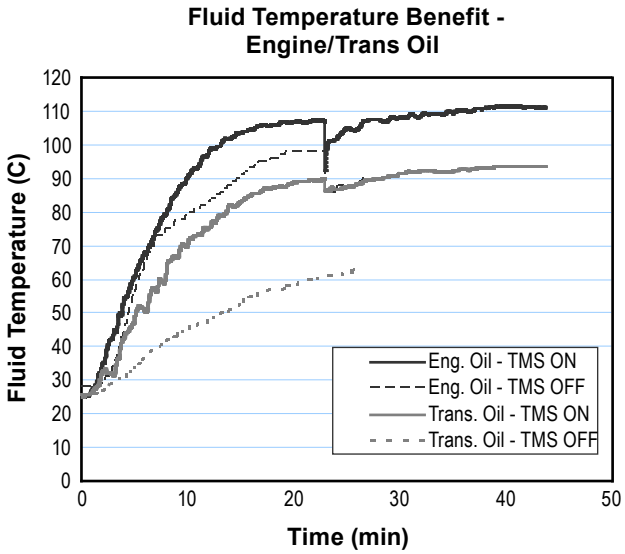

FIGURE 3. Fluid Temperature Benefit – Engine/Trans Oil

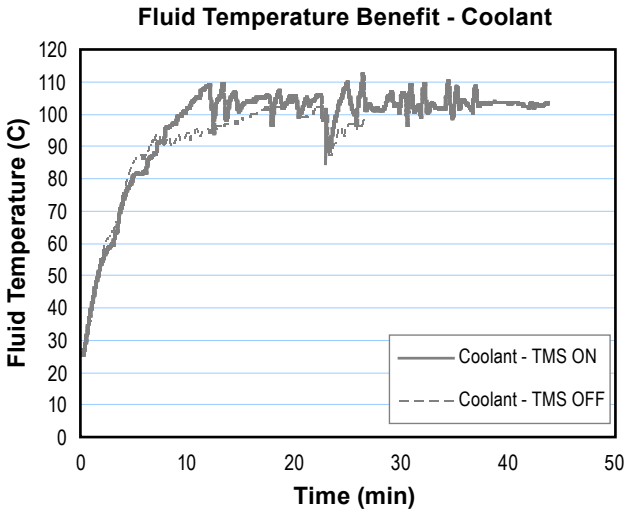

FIGURE 4. Fluid Temperature Benefit – Coolant

fuel economy while maintaining battery integrity. Strategy consists of four states. The regeneration mode is designed to utilize low-cost battery charging opportunities to aggressively charge the battery. Low state of charge mode is to protect battery from extended depletion periods. Passive boost mode lowers engine accessory load during high cost operation. Trickle charge mode maintains the battery state of charge by utilizing battery current feedback to control alternator load. Engine accessory load is decreased by matching battery charge requirements to cost function.

The surrogate vehicle crank pendulum corrects 65% of torsional at light to medium loads. At high load (near wide open throttle), correction is between 45% to 50% (Figure 5). The final pendulum design is quiet over a wider range of engine speeds (850 rpm to 1,250 rpm to max speed).

Conclusions

- There is sufficient data from Alpha 1 modeling, simulation, testing activities to support development of these engine technologies to achieve project goals.
- Engine efficiency at high load is improved with diesel fuel ignition system on gasoline engine. Controlling combustion process is challenging in an automatic control system, especially under transient operation conditions and varied environmental conditions. Addition of secondary fuel system using ethanol enables improved combustion phasing, knocks relief at high loads without the complexity or expense of DMP system.

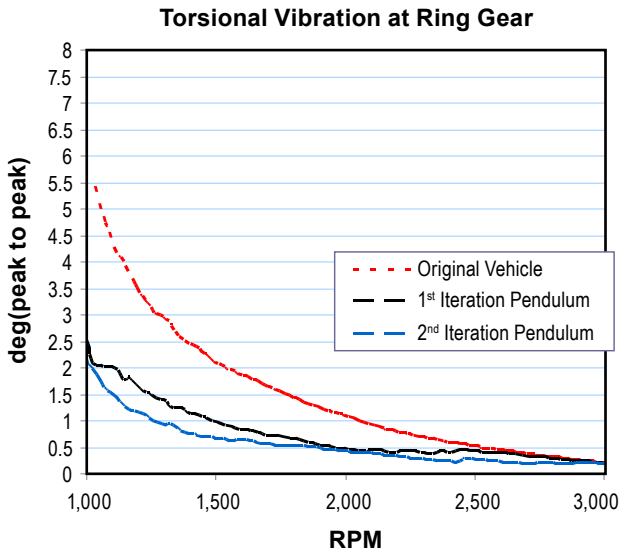

FIGURE 5. Torsional Vibration at Ring Gear

- Controlled charge strategy to optimize AGM battery charge cost and maintain battery integrity provides 0.5% fuel economy gain over the FTP cycle. Requires intelligent battery sensor to provide battery current feedback and battery state of charge.
- Thermal management system sufficiently rejects ~30-40% increased heat load due to EGR cooling and charge air cooling. System is capable of extreme high ambient conditions, towing a trailer up a grade, but only at reduced %EGR levels.
- Thermal management system is effective for improving fuel economy on standard certification drive cycle, by means of rapid oil warm-up. Greater fuel economy benefits are realized in "real-world" cold ambient environments.
- Exhaust heat recovery system not effective at rapidly warming coolant due to distance from engine (exhaust pipe heat losses) and heat exchanger's high thermal inertia. The rapid warm-up strategy for engine/transmission oil sufficient to achieve fuel economy goals.

FY 2012 Publications/Presentations

1. 2012 DOE Vehicle Technologies Program Annual Merit Review, May 2012.

2. Modeling, Validation and Analysis of an Advanced Thermal Management System for Conventional Automotive Powertrains; Neeraj Ravindrakumar Agarwal; Ohio State University; 6/18/2012.

3. Modeling, Analysis, and Open-Loop Control of an Exhaust Heat Recovery System for Automotive I.C. Engines; Ross Owen; Ohio State University; 9/13/2011.

4. Department of Energy Project Review – DOE MAMF Project Team, July 18, 2012.

Special Recognitions & Awards/Patents Issued

1. D. Hornback, K. Laboe, G. Black, "Automotive Engine Coolant Heating System with Integrated EGR Cooler", patent application submitted for Chrysler IDR#708870US1, Dickstein Shapiro LLP.

2. R. Wakeman, "Pendulum Absorber Snubber", patent application submitted for Chrysler IDR# 708946, Dickstein Shapiro LLP.

3. C. Brunstetter, J. Jaye, G. Tallarek, J. Adams, "Battery Trickle Charge Algorithm with Current Feedback", patent application submitted for Chrysler IDR# 709111, Dickstein Shapiro LLP.

IV.8 Advanced Combustion Concepts – Enabling Systems and Solutions

Hakan Yilmaz (Primary Contact),
Oliver Miersch-Wiemers, Alan Mond, Li Jiang
Robert Bosch LLC
38000 Hills Tech Drive
Farmington Hills, MI 48331

DOE Technology Development Manager:
Ken Howden

NETL Project Manager: Ralph Nine

Subcontractors:
- AVL Powertrain, Plymouth, MI
- Emitec, Auburn Hills, MI
- University of Michigan, Ann Arbor, MI
- Stanford University, Palo Alto, CA

Overall Objectives

- Improve fuel economy by 25% with minimum performance penalties.
- Achieve super ultra-low emissions vehicle level emissions with gasoline.
- Demonstrate multi-mode combustion engine management system.

Fiscal Year (FY) 2012 Objectives

- Complete vehicle simulation investigation confirming the fuel economy improvement with proposed combustion and powertrain technologies.
- Complete design for prototype II engine and engine management system.
- Complete concept feasibility with target combustion modes on prototype II engine.

Accomplishments

- Completed vehicle simulations showing greater than 25% fuel economy improvement over the baseline vehicle.
- Completed prototype II engine design and engine management system configuration.
- Demonstrated transient performance of the target combustion modes with closed-loop control via cylinder pressure sensing techniques.
- Initiated demonstration vehicle integration.

Future Directions

- Evaluate fuel economy and emission benefits of target combustion modes on prototype II engine at transient dynamometer.
- Integrate prototype II engine into demonstration vehicle, enabling full spark ignition (SI) capability.
- Complete control strategies for multi-mode combustion, ready for engine management system integration.

Introduction

Due to availability and security of energy resources, environmental concerns, and cost factors, the automotive industry is facing the challenge of improving fuel economy and reducing the emissions without sacrificing performance. Although there are promising developments in electrification of powertrain with hybrid systems, battery electric vehicles and fuel cell electric vehicles; internal combustion engines are expected to be the mainstream power source of future high-efficiency vehicles for the next decade. The feasible future advanced engine and powertrain configuration must address the topics such as emission and fuel economy requirements for worldwide applications, transition to bio fuels, and synergies with future powertrain trends.

The Advanced Combustion Concepts – Enabling Systems and Solutions (ACCESS) project has the primary objective of developing highly capable and flexible advanced control concepts with enabling system, sub-system and component level solutions for the management of multi-mode combustion events in order to achieve 25% fuel economy improvement in a gasoline fueled light-duty vehicle without compromising its performance while meeting future emission standards as outlined in DOE solicitation targets.

Approach

The ACCESS project, through a three-phase approach, addresses the development, testing, and demonstration of the proposed advanced technologies and the associated emission and fuel economy improvement at an engine dynamometer and on a full-scale vehicle. The project investigates the synergistic mainstream advanced combustion and system concepts such as:

- SI combustion with high compression ratio and high boost assisted with cooled external exhaust gas recirculation (EGR).
- Homogenous charge compression ignition (HCCI) assisted with external EGR, spark, and fueling strategies for operation range extension.
- Port assisted direct injection (PDI) – dual injection system for combining the benefits of port fuel injection (PFI) and direct injection (DI).
- Multi-hole direct injection with individual nozzle geometry design for improved mixture preparation and combustion efficiency.
- Start-stop and thermal management systems to eliminate fuel consumption at idling conditions and enhanced engine warm-up behavior.

As a result, a substantial improvement in thermal efficiency by exploiting the advantages of SI/HCCI combustion on a turbocharged downsized engine with high compression ratio is proposed. The target engine, equipped with the capabilities of dual-stage turbocharging, external EGR system, electric dual cam phasing, dual cam profile switching and in-cylinder pressure sensing, enables the investigation and development of combustion and control strategies to maximize engine thermal efficiency.

Results

After successful completion of Phase I experiments with Prototype I, an engine operation map outlining the boundaries of the different combustion modes was generated and confirmed in two of the ACCESS engines, see Figure 1. The combustion modes include a lean, naturally aspirated HCCI mode, a stoichiometric spark-assisted homogeneous charge compression ignition (SA-HCCI) mode, stoichiometric spark ignited mode, and spark ignited mode with externally cooled EGR for the higher loads. The main objective was to clearly define a region at the lower loads of the Federal Test Procedure 75 (FTP75) cycle that was lean enough to avoid generating oxides of nitrogen. The next combustion mode investigated was the stoichiometric SA-HCCI, which goes from approximately 3 bar to 6.5 bar brake mean effective pressure and 1,500 to 3,500 RPM. This advanced combustion mode has demonstrated fuel efficiencies greater than the spark ignited mode in the order of 5%. Based on vehicle simulations, it has been confirmed that the pure HCCI and the SA-HCCI combustion modes should cover the entirety of the FTP75 cycle, leading to measurable gains in fuel economy.

Prototype II has been designed and is under procurement on track to meet the scheduled vehicle build. The Prototype II modification shown in Figure 2 has been fired and initial results have been generated. The modifications comprise a lower flowing direct injector (1), modified camshafts (2), an externally cooled EGR circuit (3), a second generation Delphi control valves for hydraulic cam profile switching (4), and a latest generation three-way catalytic converter (5). Prototype II engine integration into the demonstration vehicle has been initiated in FY 2012. As shown in Figure 3, the design has been completed and all parts have been procured.

Based on vehicle simulations, seven distinct engine speed, load combinations were measured against the baseline engine to measure steady state gains in fuel consumptions, Figure 4. As expected, the highest gains are achieved at the lowest loads where the naturally aspirated HCCI operation benefits from lower pumping

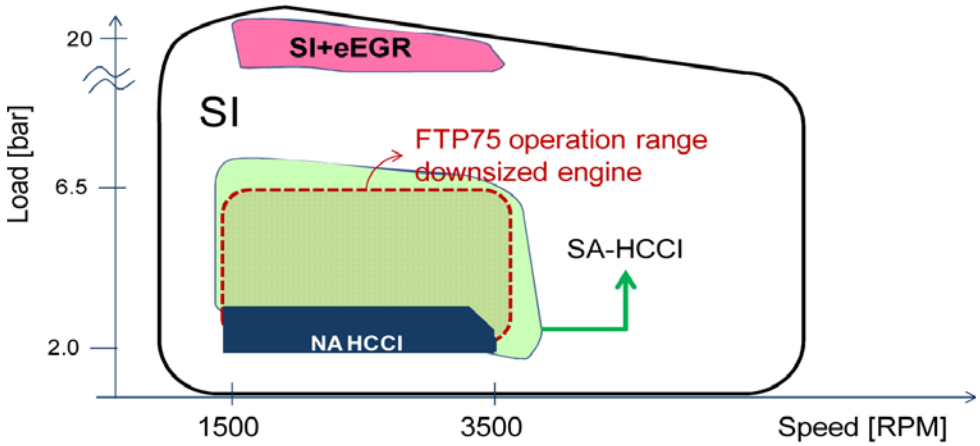

NA - naturally aspirated

FIGURE 1. Combustion Modes for ACCESS Engine

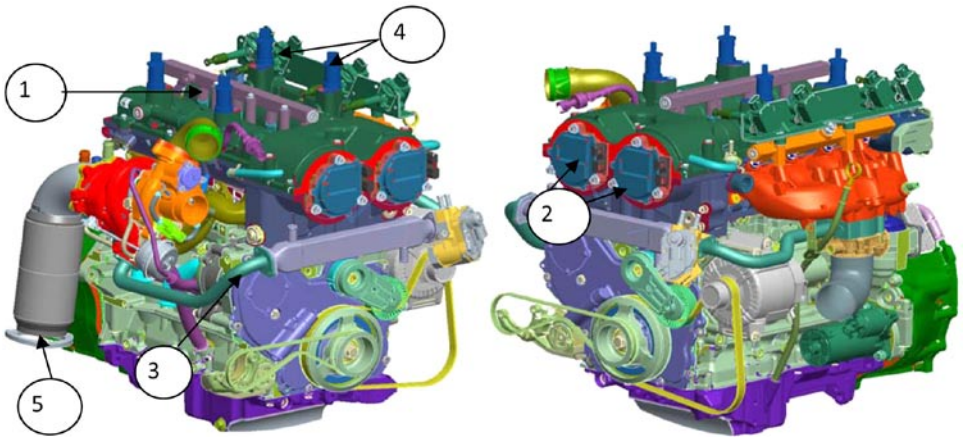

FIGURE 2. Prototype II Engine Configuration

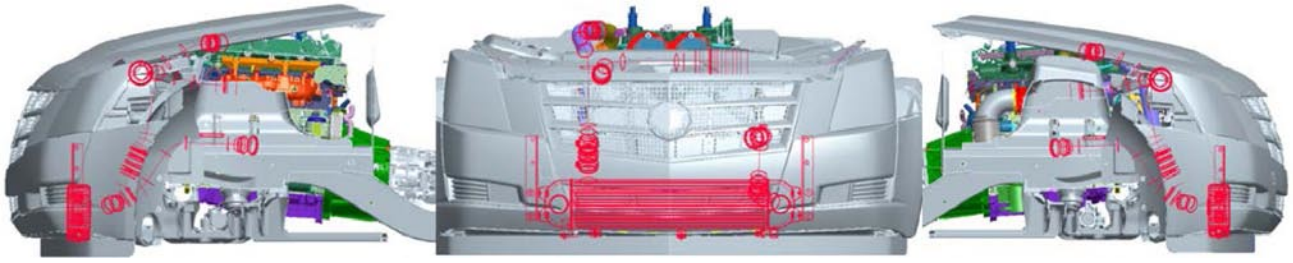

FIGURE 3. Vehicle Integration of Prototype II Engine and Accessories

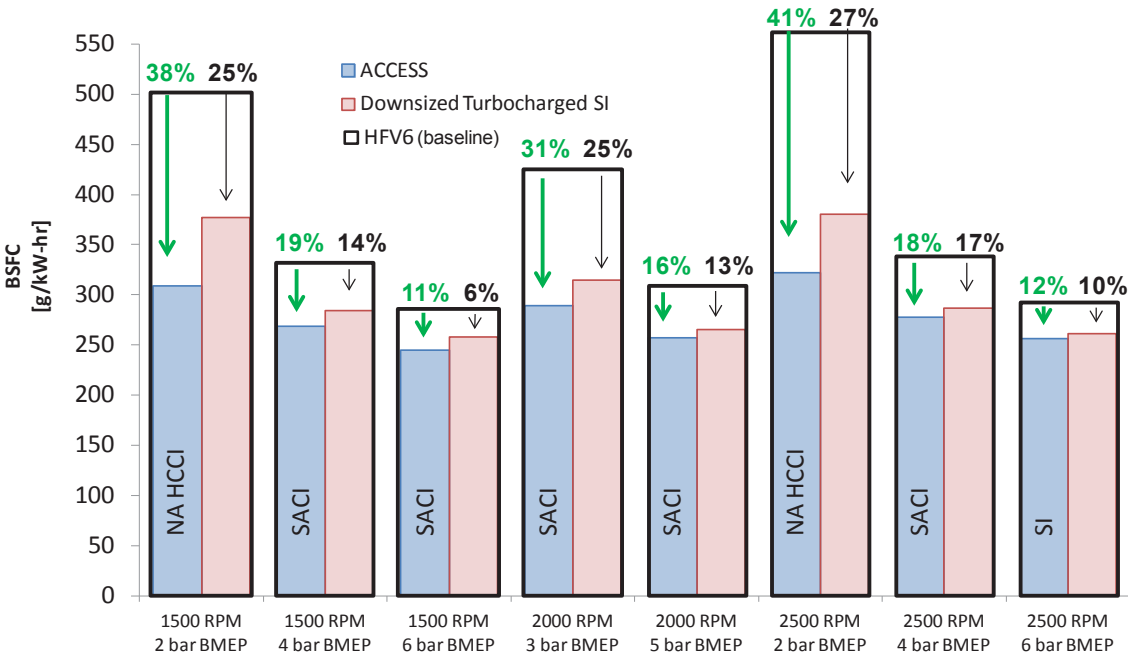

SACI - spark-assisted compression ignition; RPM - revolutions per minute; BMEP - brake mean effective pressure

FIGURE 4. BSFC Improvements over Baseline Engine

losses and increased combustion efficiency due to low temperature combustion. In Figure 3, the downsized turbocharged SI measurements demonstrate the gains achieved by downsizing, while the ACCESS measurements show the reduction in fuel consumption due to low temperature combustion.

For ease of integration of future control functionalities, the Bosch torque-driven modular control architecture, as illustrated in Figure 5, is employed as the base engine management software structure. Given the driver demands, the torque and mode coordinator selects the optimal combustion mode, and commands the key subsystems, including air system, fuel system, and ignition system to set the actuators at appropriate values.

During the HCCI combustion, combustion phasing and torque are the two main control variables. It has been observed during experiments that exhaust valve closing (EVC) and start of injection are the two main actuators for the control of combustion phasing. In this work, the mid-ranging control strategy with cylinder pressure sensing feedback has been employed to coordinate EVC and start of injection for target combustion phasing in crank angle (CA) at 50% mass fraction burn (CA50). Such a mid-ranging control strategy for a two-input single-output system has been proven as effective for actuators with distinctive dynamics and control authorities. To enable fast and reliable transient operation during HCCI combustion, a dynamic model-based feedforward controller is incorporated to compensate for abrupt changes in operation conditions such as fueling level, engine speed, and EVC setting. In addition, cylinder-to-cylinder load balancing is achieved with cylinder-individual fuel injection quantity adjustment with cylinder pressure sensing feedback.

As illustrated in Figure 6, such a combustion phasing controller was validated on the mule engine using rapid prototype techniques. Experiments were conducted at 1,800 RPM during a sudden load transition with a step change in fuelling level. In order to demonstrate the performance of the combustion phasing controller, the cylinder-individual load balancing controller was disabled in the illustrated experiment. It can be observed that the proposed controller is effective in regulating the combustion phasing across different cylinders during such a transient operation.

Conclusions

- Prototype II engine design for target combustion modes, HCCI and spark-assisted HCCI, has been completed with a low-cost three-way catalyst solution.
- Initial experimental data on prototype I engine indicates promising fuel economy and emission improvement, while maintaining adequate performance.
- Model-based combustion phasing controller has been validated on a multi-cylinder engine, during which desirable HCCI transient operations were observed.

FY 2012 Publications/Presentations

1. E. Hellström, A. Stefanopoulou, J. Vavra, A. Babajimopoulos, D. Assanis, L. Jiang, H. Yilmaz, "Understanding the dynamic evolution of cyclic variability at the operating limits of HCCI engines with negative valve overlap," SAE, April 23–26, 2012.

2. E. Hellström, J. Larimore, A. Stefanopoulou, J. Sterniak, L. Jiang, "Quantifying cyclic variability in a multi-cylinder HCCI engine with high residuals," ASME ICES, May 6–9, 2012.

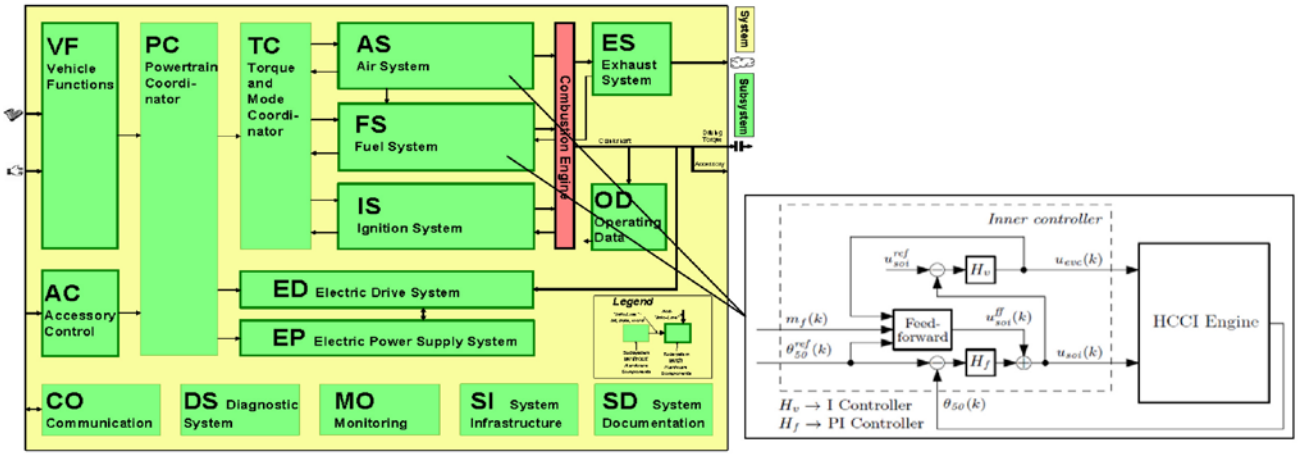

FIGURE 5. Combustion Phasing Controller Integrated into the Bosch Control Architecture

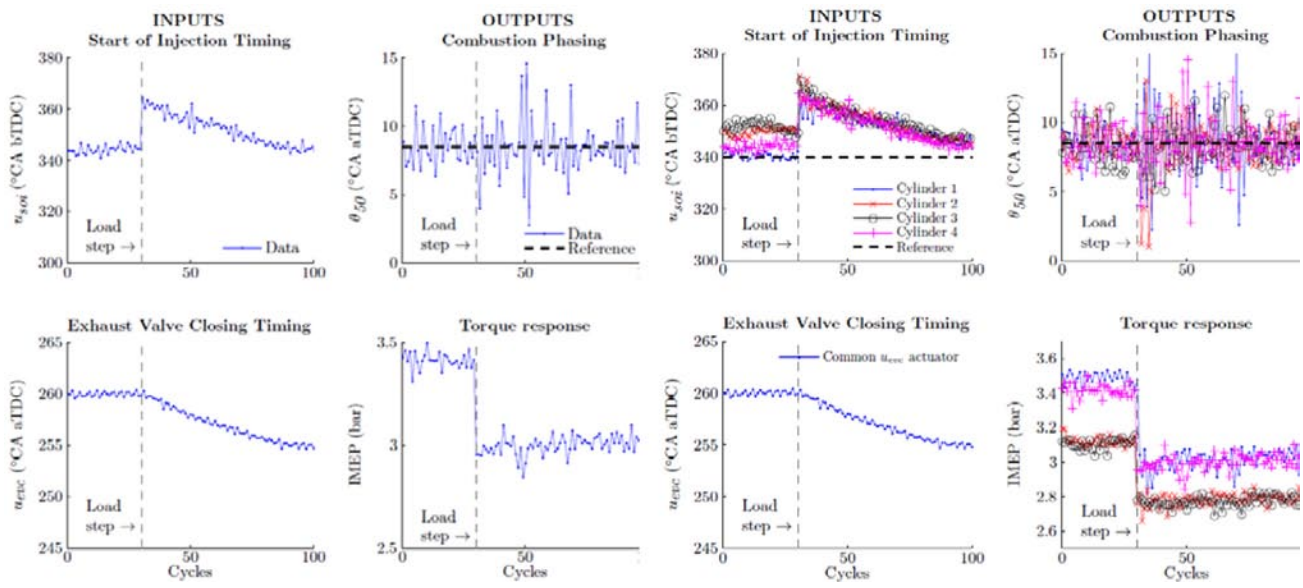

FIGURE 6. Transient HCCI Combustion Behaviors with Controller Enabled

3. P. Gorzelic, E. Hellstrom, L. Jiang, A. Stefanopoulou, "A coordinated approach for throttle and wastegate control in turbocharged spark ignition engines," CDCC, May 23–25, 2012.

4. J. Larimore, E. Hellström, J. Sterniak, L. Jiang, A. Stefanopoulou, "Experiments and analysis of high cyclic variability at the operational limits of spark-assisted HCCI combustion," IEEE ACC, June 27–29, 2012.

5. S. Jade, E. Hellström,L. Jiang, A. Stefanopoulou, "Fuel governor augmented control of recompression HCCI combustion during large load transients," IEEE ACC, June 27–29, 2012.

6. E. Hellström, A. Stefanopoulou, L. Jiang, "Cyclic variability and dynamical instabilities in autoignition engines with high residuals," IEEE Trans. Control Syst. Technol., January 2012.

7. P. Gorzelic, E. Hellstrom, L. Jiang, A. Stefanopoulou, "Model-based feedback control for automated transfer out of SI operation in the SI to HCCI transition," ASME DSCC, October 17–19, 2012.

8. V. Janakiraman, J. Sterniak, D. Assanis, "Modeling the Gasoline HCCI Combustion Dynamics using Recurrent Neural Networks," ASME DSCC, October 17–19, 2012.

9. V. Janakiraman, J. Sterniak, D. Assanis, "Machine Learning Methods for identification of HCCI combustion," ICINCO 2012, July 28–31, 2012.

10. E. Hellström, J. Larimore, A. Stefanopoulou, J. Sterniak, L. Jiang, "Quantifying cyclic variability in a multi-cylinder HCCI engine with high residuals," J. Eng. Gas Turbines Power, September 2012.

11. Hellström, A. Stefanopoulou, J. Vavra, A. Babajimopoulos, D. Assanis, L. Jiang, H. Yilmaz, "Understanding the dynamic evolution of cyclic variability at the operating limits of HCCI engines with negative valve overlap," SAE Int. J. Engines, September 2012.

Patents Issued

1. Pending US Patent(s) on "Compounded Dilution and Air Charging Device"

2. Pending US Patent(s) on "Combustion Mode Switching with a Turbocharger/Supercharged Engine"

3. Pending US Patent(s) on "Method for Modeling Cyclic Variability in Lean Controlled-Autoignition Engines"

4. Pending US Patents Patent(s) on "Fueling Strategy for Controlled-Autoignition Engines"

5. Pending US Patent(s) on "Method for Path Planning during Combustion Mode Switch"

6. Pending US Patent(s) on "Combustion Control with External Exhaust Gas Recirculation (EGR) Dilution"

IV.9 Cummins Next Generation Tier 2 Bin 2 Diesel

Michael J. Ruth
Cummins Inc.
P.O. Box 3005
Columbus, IN 47201-3005

DOE Technology Development Manager:
Roland Gravel

NETL Project Manager: Carl Maronde

Subcontractor:
Johnson-Matthey Inc
Wayne, PA

Overall Objectives

- Demonstrate 40% fuel economy improvement over baseline gasoline V-8 pickup truck.
- Demonstrate Tier 2 Bin 2 tailpipe emissions compliance.

Fiscal Year (FY) 2012 Objectives

- Complete initial evaluation of passive oxides of nitrogen (NOx) adsorber (PNA) with respect to model predictions.
- Demonstrate engine-out emissions target in steady-state operation, test cell environment.
- Upgrade mule vehicle to include operating direct ammonia (NH_3) delivery system and new transmission.
- Complete design and procurement of hardware for new engine system.

Accomplishments

- Completed design and analysis of an all-new engine including all elements required to meet Tier 2 Bin 2 tailpipe emissions (dual-loop exhaust gas recirculation [EGR] and variable swirl control) while meeting a weight target of less than 65 kg/ltr of displacement.
- Procured required hardware to build the new engine and have ready for test in December 2012.
- Demonstration of engine-out emissions of less than 0.4 g/mi NOx, using steady-state operating conditions to approximate the drive cycle without loss of fuel economy.
- Demonstrated mule vehicle with ZF 8-speed automatic transmission and operable direct NH_3 delivery system (DADS) from Amminex at the 2012 DEER conference.

Future Directions

- Develop new engine hardware to meet the intermediate goal of Tier 2 Bin 2 emission levels.
- Integrate the new engine into existing mule vehicle.
- Develop control technology to include the PNA operation to the intended application.
- Develop control technology for the optimization of the DADS with selective catalytic reduction (SCR) on filter (SCRF) as well as under-floor SCR.

Introduction

The overall objective of this project, Cummins Next Generation Tier 2 Bin 2 Diesel, is to design, develop, and demonstrate in a light-duty (1/2-ton pickup truck) a state-of-the-art light-duty diesel engine that meets Environmental Protection Agency light-duty Tier2 Bin2 emission standards and increases fuel efficiency by at least 40% compared with a state-of-the-art port fuel injected gasoline engine.

The U.S. new, personal-use vehicle fleet has changed slightly over the past two years, with car purchases increasing, but by and large, pickup trucks and sport utility vehicles (SUVs) account for nearly half of sales in this segment. An improvement in fuel economy by 40% in the light truck and SUV segment would reduce the U.S. oil consumption by 1.5M bbl/day and reduce greenhouse gas emissions by 0.5 MMT/day.

Approach

The project is a four phase plan. The first phase included the baseline establishment for the target vehicle (2010 Nissan Titan) as well as the fuel consumption and emission rate of the Cummins 2.8-L ISF Euro III engine. Model development in phase one will direct technology test and development to create a technical profile for the new engine design. Phase 2 includes low-level system testing of a mule engine with chosen technologies applied in a laboratory environment. The data from the laboratory testing will be used to refine models and requirements for the final product as well as a platform to track real progress. Phase 2 also includes

the design, analysis and procurement of the new engine. The new engine design will be targeted not only toward meeting emissions and fuel economy but also mitigating the current weight penalty of the diesel engine. Phase 3 will entail the development work required to bring the new engine to achieve Tier 2 Bin 5. Phase 4 will be the optimization of all subsystems, including vehicle systems such as charging and vacuum system as well as fueling and transmission shift logic. The fourth and final phase will be the ultimate goal of Tier 2 Bin 2 emissions with 40% fuel economy improvement over the baseline gasoline power train.

Results

The design team has a completed the new engine design and all parts have completed, detailed designs. The new design has achieved a 63.3 kg (140 lb) weight reduction over the comparably equipped baseline engine. Table 1 is a summary of comparison between the new engine and baseline engine component systems.

Figure 1 is a rendering of the complete new engine assembly. This engine assembly includes a major portion of the aftertreatment, charge air cooler (CAC), and low-pressure EGR system. The CAC is located under a vanity/noise cover (not shown) that highlights the service points; oil check and fill as well as oil and fuel filter.

The new engine is constructed mainly of aluminum, including cylinder block and head. The ladder frame, a major structural component, is cast iron. The accessory drive system utilizes common automotive components and is not specific to any one manufacturer. The transmission fitment to the engine is with an integral transmission adapter (i.e. not a separate, bolt on flywheel housing) and is designed to accept either

TABLE 1. New Engine System Weight Compared to Baseline Engine (all units in kg)

	New 2.8L	Baseline 2.8L
Block System	52.7	65.5
Misc Housings	0	27.1
Head System	23.6	34.4
Rotating and Reciprocating	29.3	31.0
Valve Drive	1.2	5.3
Cam & Drive	7.4	5.9
Balance	6.1	14.6
Sum	120.4	183.7
Sum/L	43.0	65.6

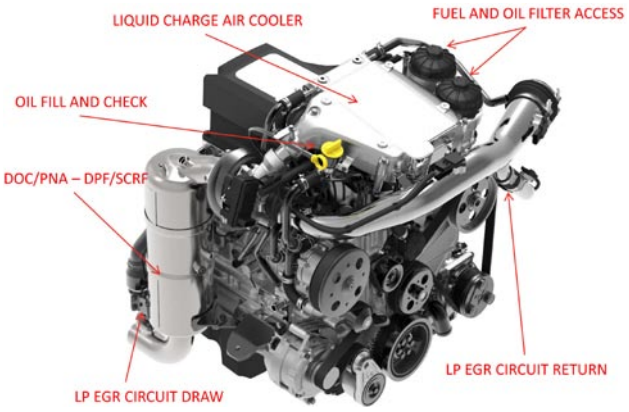

lp - low-pressure

FIGURE 1. New Engine Design

an SAE standard or a ZF pattern (common for several manufacturers).

The team has utilized a baseline 2.8-L engine to vet technology used to reduce engine-out NOx emissions. The engine was built to include dual-loop EGR system that allowed both cooled and un-cooled paths in both EGR routes. Data from the mule vehicle was used to create a set of steady-state operating conditions that could be used to estimate the fuel consumption and emissions over the warm portion of the dynamometer driving cycle, known as LA-4. The development path included several steps to achieve a truly optimized solution (see Figure 2):

- The baseline engine was a Euro IV specific engine fitted with a waste gate turbocharger and low fidelity common rail fuel system. The baseline configuration yielded approximately 24 mpg and nearly 2 g/mi NOx emissions.
- The same engine, when fitted with a piezo fuel system and variable geometry turbocharger, calibrated for the U.S. drive cycle (labeled as

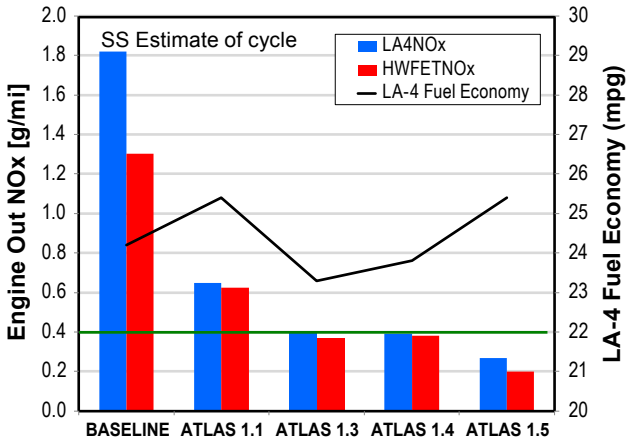

FIGURE 2. Mule Engine Development Path

ATLAS 1.1) yielded an improvement in fuel consumption and reduction in NOx emissions – 25.3 mpg while emitting only slightly more than 0.6 g/mi NOx.

- The initial addition of low-pressure EGR (ATLAS 1.3) proved to dramatically reduce NOx emissions, but also be a fuel economy hit. This initial arrangement proved to meet the goal of 0.4 g/mi NOx, but only achieved 23.3 mpg.
- Further refinement of the EGR system (ATLAS 1.4) included tuning the combustion system with reduced swirl, increased number of injection holes and EGR flow tuning to include cooled low-pressure EGR in unison with un-cooled high-pressure EGR. This dual flow path of EGR showed reduced pumping work for a fixed EGR rate. This configuration recovered 0.6 mpg, achieving 23.9 mpg while maintaining NOx at the target rate of 0.4 g/mi.
- Finally, the turbocharger match was optimized for the new tune of dual EGR flow paths (high-pressure and low-pressure) and lowered compression ratio for added pre-mix combustion operation. The final optimized solution (ATLAS 1.5) was capable of further reducing NOx emissions to less than 0.3 g/mi and more than 25 mpg. Comparing 1.1 to 1.5 shows nearly a 2 to 1 reduction of NOx without a fuel economy penalty.

The catalyst development work was focused on the use of the DADS reductant system with SCRF and the initial evaluation of the PNA. The evaluation of the PNA showed the model predictions were representative of the overall capacity of the PNA. The PNA testing showed the cold-cycle NOx take up to be very effective—very little NOx slip in the very front end of the cycle. As the device gained temperature, the NOx did desorb and eventually purge rapidly as the temperature approached 300ºC. The actual test sample was damaged in the early evaluation due to an uncontrolled thermal event that overheated the part.

The DADS hardware was applied to the SCRF plus SCR system. This system was tested behind the baseline engine (greater than 2 g/mi NOx emissions). The test was a full Federal Test Procedure (FTP)-75 dynamometer driving cycle repeated six consecutive times to indicate there was no preloading of NH_3 pre- or post-test. The system was shown to be capable of being consistently greater than 93% effective at reducing NOx.

The vehicle team completed the intermediate upgrade of the mule vehicle. This upgrade included an engine system that known as ATLAS 1.1 (described previously) and the ZF-supplied 8-speed automatic transmission. The initial vehicle's upgraded calibration was evaluated on the chassis drive cycle. The fuel economy over the FTP-75 (cold start included) was

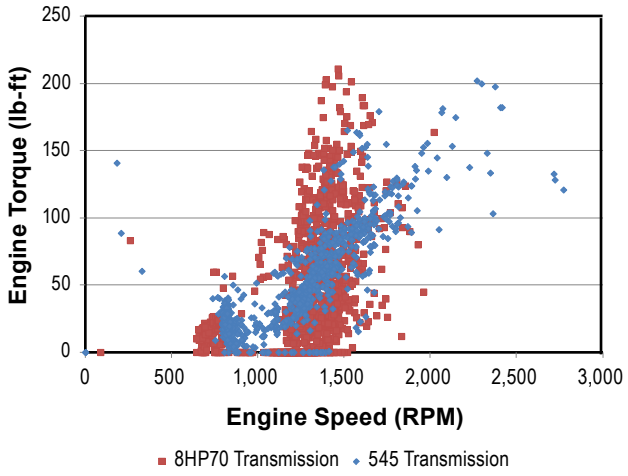

FIGURE 3. Comparison of 8-Speed and 5-Speed Operating Space

25.8 mpg with an engine-out NOx emission rate of 1.0 g/mi. The LA-4 drive cycle yielded a 26.8 mpg with the NOx emission rate of just below 0.80 g/mi. The results from this test demonstrate the improved efficiency of the 8-speed automatic transmission – considering the results from the 5-speed transmission modal results of only 25.3 mpg.

The testing of the upgraded mule vehicle also helped depict how the engine speed and load operating space were affected by moving from the 5-speed to the 8-speed (see Figure 3). Cummins will continue working with ZF on tuning the transmission shift operation to ensure both fuel economy and NOx.

Conclusions

The Cummins next generation Tier 2 Bin 2 light-duty diesel engine project has successfully completed the second year of the four-year project. The follow conclusions have come from the second year of development:

- The design and analysis work has produced a new engine with nearly a 30% reduction in engine weight even with design criteria requiring 40% increase in peak cylinder pressure.
- Low-pressure EGR has proven to be a powerful lever for NOx control given an engine-out particulate matter limit. The development steps to bring engine-out NOx emissions down to the target of 0.40 g/mi can be achieved without incurring a fuel consumption penalty.
- The DADS will be critical toward achieve the goal of Tier 2 Bin 2 tailpipe emissions. Data has shown that even without any NOx storage device, a close-coupled SCRF plus SCR system is capable of

reducing NOx over 93% including the cold phase. These results could be achieved in consecutive FTP cycles.

- The addition of the ZF 8-speed transmission has improved the expected fuel economy of the overall project. The 8-speed does have a dramatic effect on the operating space of the engine over the drive cycle. The lower speed, higher load operation does negatively affect the NOx emissions.

FY 2012 Publications/Presentations

1. Program progress update, DEER conference 2012 (Ruth – High Efficiency Engine Technologies, Part 2)

2. Advanced Technology Light Duty Diesel Aftertreatment System, DEER conference 2012 (Henry – Emission Control Technologies, Part 1)

3. Thermodynamics of a T2B2 Light Duty Diesel, DEER conference 2012 (Suresh – High Efficiency Engine Technologies, Part 2)

4. SAE paper application: Thermodynamics of a T2B2 Light Duty Diesel, Suresh et. al.

IV.10 Development of Radio Frequency Diesel Particulate Filter Sensor and Controls for Advanced Low-Pressure Drop Systems to Reduce Engine Fuel Consumption

Alexander Sappok (Primary Contact),
Leslie Bromberg, Peter Koert
Filter Sensing Technologies, Inc. (FST)
P.O. Box 425197
Cambridge, MA 02141

DOE Technology Development Manager:
Roland Gravel

NETL Project Manager: Trevelyn Hall

Subcontractors:
- Corning, Inc., Corning, NY
- FEV Inc., Auburn Hills, MI
- Maguffin Microwaves, LLC, Andover, MA
- Oak Ridge National Laboratory, Knoxville, TN

Overall Objectives

- Design, develop, and validate radio frequency (RF) sensors for accurate real-time measurements of diesel particulate filter (DPF) loading with low-pressure drop substrates.
- Demonstrate and quantify improvements in efficiency and greenhouse gas reductions through improved DPF sensing, controls, and low-pressure drop components.
- Achieve breakthrough efficiencies via use of advanced combustion modes, alternative fuels, and advanced aftertreatment enabled by improved sensing and controls.
- Develop production sensor designs and commercialization plans on the scale required to significantly impact reduction in greenhouse gas emissions and fuel consumption.

Fiscal Year (FY) 2012 Objectives

- Develop and calibrate RF models to simulate the resonance characteristics of specific filter geometries to guide sensor design and development.
- Finalize/down-select RF sensor designs for prototype development and subsequent testing in FY 2013.

Accomplishments

- Completed RF model development and generated database of material dielectric properties over a range of frequencies and temperatures for typical DPF systems.
- Validated models with experiments and applied results to guide prototype development.
- Down-selected final prototype designs and initiated testing to optimize performance.

Future Directions

- Develop and calibrate RF prototype sensors with reference DPF configuration.
- Evaluate sensor baseline performance and identify/quantify error sources.
- Determine sensor accuracy for various operating conditions and DPF configurations.
- Develop specifications and designs for pre-production sensor.

Introduction

Diesel engines present one of the most promising, readily-available technologies to achieve dramatic efficiency improvements in light-duty applications and are the power plant of choice for most heavy-duty vehicles. However, significant hurdles inhibiting the increased use of diesels are the additional energy consumption and associated costs, driven by the need to use advanced emission controls and aftertreatment systems. Specifically, DPFs are required to reduce particulate matter (PM) emissions to mandated levels. DPFs are common on all on-road vehicles in the U.S. since 2007, as well as a growing number of off-road vehicles and equipment. The DOE's Vehicle Technologies Program Multi-Year Program Plan has identified challenges associated with the use of diesel particulate filters, namely: (1) additional cost and energy usage, (2) lack of "ready to implement" sensors and controls required for sophisticated feedback systems, and (3) demanding durability requirements for both light and heavy-duty applications [1].

This project directly addresses the challenges outlined above by demonstrating a robust RF sensor and control system, for use with next-generation, low-pressure-drop aftertreatment devices, to reduce engine fuel consumption and emissions. This technology leverages advances in RF circuit chips, similar to those found in cell phones and other wireless devices, to obtain a highly accurate measurement of soot and ash levels in the DPF. Compared to current state-of-the-art pressure- and model-based control systems, the proposed technology will enable a step change in engine and aftertreatment system control, and reduce system cost and complexity, while delivering tangible performance benefits. Initiated in July of this year, this three-year project will develop a series of RF sensors and demonstrate/quantify improvements in overall system efficiencies enabled through the use of advanced sensing and controls, in conjunction with next-generation particulate filters.

Approach

This project will leverage knowledge developed from previous internal research and development activities conducted by FST as well as collaborations with national laboratories, industry, and academia. Results of initial sensor development and proof-of-concept testing were first presented at the 2006 CLEERS Workshop [2], with additional follow-on testing at Oak Ridge National Laboratory in 2010 [3]. Further, substantial involvement of industry, including Corning, FEV, and Detroit Diesel is also planned to most efficiently accelerate technology research and development activities to achieve the goals of this project.

This project will be carried out in four phases to achieve the objectives listed above. The following project phases are planned over the course of three years (36 months):

- **Phase 1 – Sensor Development** will build on previous experience to design, develop, and calibrate beta prototype sensor, specifically tailored for use with advanced high porosity, low-pressure-drop filters. The prototype RF sensors will be supplied to industry and national laboratory partners for testing and evaluation in subsequent project phases.
- **Phase 2 – Sensor Testing** will include targeted experiments to quantify sensor accuracy over a wide range of conditions with various DPFs. Bench, test cell, and vehicle testing is planned, and will explore additional benefits when advanced aftertreatment systems and sensors are use with advanced combustion systems and alternative fuels.
- **Phase 3 – System-Level Demonstration** will incorporate input from industry to define sensor performance specifications, resulting in the development of an optimized pre-production sensor, and associated controls. The optimized sensor and control system will be evaluated to quantify benefits using engine test cell and vehicle tests spanning both light- and heavy-duty applications.
- **Phase 4 – Commercialization Planning** will develop system specifications with input from industry, finalize production sensor designs, and develop commercialization plans on the scale required to achieve a significant reduction in greenhouse gas emissions.

The phased approach, outlined above, will progress from design and simulation to component development and testing, with several iterations to optimize the overall system. Substantial involvement of industry partners including Corning, FEV, Maguffin, Oak Ridge National Laboratory, and Detroit Diesel provide considerable expertise to insure successful achievement of project objectives.

Results

Following project kick-off in the third quarter of 2012, work in Phase I has focused on developing and refining the RF system models, conducting bench-top experiments to validate the model results, and applying these results to guide prototype development, in addition to commissioning the experimental setup. Results of previous work at Oak Ridge National Laboratory utilizing FST's alpha prototype sensors showed the RF signal to be well-correlated to DPF soot levels over a range of filter loading and regeneration conditions. Figure 1 presents a comparison of the RF sensor signal (showing total soot accumulated in the DPF) with engine-out soot emissions measured via tapered element oscillating microbalance over the course of a simulated

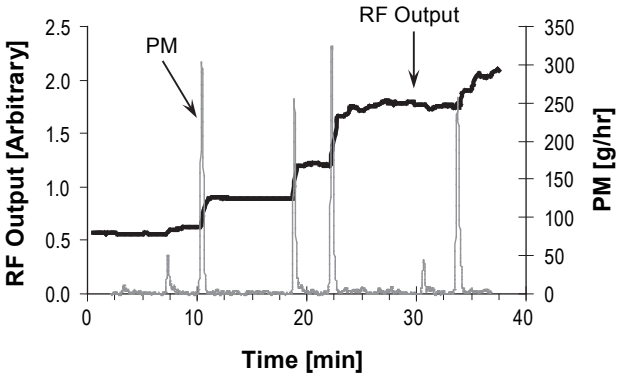

FIGURE 1. Comparison of RF sensor response with measure engine-out soot emissions over simulated transient drive cycle [3].

Federal Test Procedure cycle, using a light-duty GM 1.9-L diesel engine [3].

Work in the initial phase of this project has built on the results and knowledge gained from prior testing with the alpha prototype system to develop a second-generation beta prototype. The RF-based sensing technique utilizes the metallic DPF housing as a microwave resonant cavity. The transmission and subsequent reception of a radio frequency signal through the ceramic particulate filter results in the establishment of resonances at specific frequencies. Each of these resonances, or modes, corresponds to regions of high electric field strength within the filter housing. Proper selection of the sensor operating frequencies, and the resulting spatial distribution of the electric field within the DPF, is thus a key element of the sensor design.

During the first six months of this project, existing RF models previously developed by FST have been refined and improved to more accurately simulate the overall RF signal response and better understand the electric field distribution in the DPF. Relative to typical DPF materials, soot exhibits significantly higher dielectric loss, up to two orders of magnitude. However, the soot dielectric properties may vary with frequency and temperature [4-6]. Initial work focused on compiling soot dielectric properties as a function of temperature, frequency, and composition, in order to improve the inputs to the RF models. Where data from the literature was lacking, measurements were conducted in-house, utilizing both engine-out PM samples as well as standard black carbon reference samples, to obtain the information over the requisite DPF operating temperature range and RF system frequencies.

The RF system models were applied extensively to understand the sensitivity of the cavity resonance to variations in DPF housing geometry and RF antenna design parameters. Additional work is currently ongoing to optimize the antenna design, based on the model results. Figure 2 presents an example of the simulation results for the baseline filter geometry, and shows the variation in electric field strength inside the DPF housing for one particular resonant mode. The baseline DPF configuration consists of a catalyzed, cordierite filter, 200/12 cell geometry, with a total volume of approximately 2.5 liters. The figure clearly shows a region of high electric field in the center of the DPF for this resonant mode.

Additional applications of the RF models included exploring the utility of monitoring additional RF signal parameters, derived from both the transmitted and reflected signal, to improve the sensor performance and measurement range. Figure 3 provides additional simulation results showing the variation in the cavity resonance curves with increasing filter soot loading.

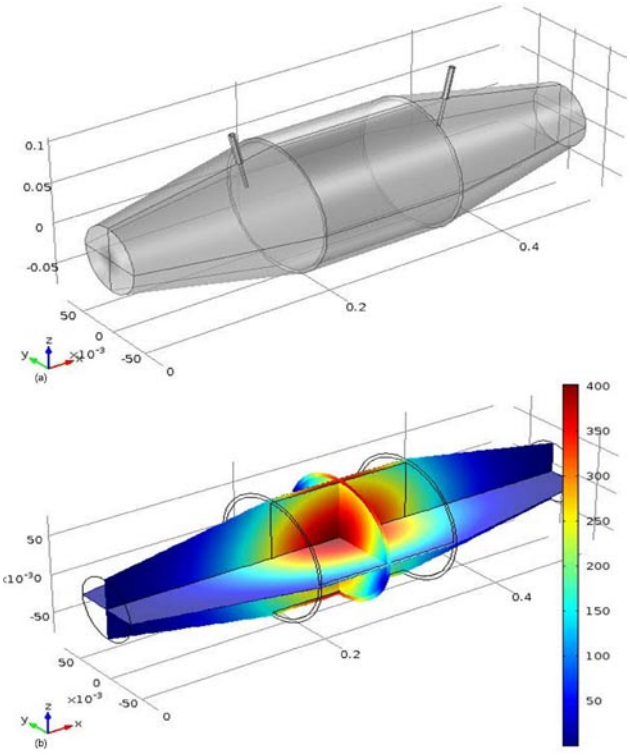

FIGURE 2. DPF housing and antenna model (a) and corresponding simulation results showing electric field distribution (b) for a single resonant mode.

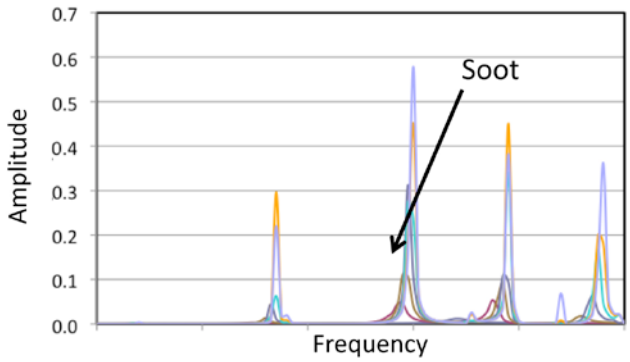

FIGURE 3. Simulation results showing decrease in resonant mode amplitude with increasing soot accumulation in the DPF.

Bench tests were also conducted with the baseline DPF to confirm the simulation results. Initial indications showed significant opportunity for monitoring additional signal parameters (proprietary) to improve measurement accuracy, particularly with high filter soot loads. Work is currently ongoing to further explore these new developments.

Results of the RF system simulations and bench tests were applied to guide key prototype design decisions. A base sensor architecture has been selected and current

work is focused on component-level testing to finalize hardware specifications. This beta system will undergo additional bench tests and iteration prior to delivery to industry and national laboratory partners for initial testing in early 2013.

Work in FY 2013 will focus on developing calibrations for the RF sensor with the reference DPF configuration. Testing at FST, Corning, and Oak Ridge National Laboratory will evaluate baseline sensor performance over a range of engine operating conditions and particulate filter configurations. These test results with be applied to refine sensor calibrations and develop specifications and designs for a pre-production system for evaluation in a subsequent project phase. Ultimately, the performance of the pre-production sensor and advanced control system will be benchmarked against current system to quantify potential efficiency improvements when used with conventional engine technologies, as well as alternative combustion modes and fuels.

Conclusions

Initiation of this project in the third quarter of this year has already resulted in substantial progress to develop an improved RF-based sensing system to provide engine and vehicle manufacturers an additional tool to optimize the combined engine/aftertreatment system for increased efficiency. Specific accomplishments are the following:

- Completed RF model development and generated database of material dielectric properties over a range of frequencies and temperatures for typical DPF systems.
- Validated simulation results with carefully controlled experiments and applied results to guide prototype development.
- Down-selected final prototype architecture and initiated component-level testing to optimize performance prior to delivery to industry and national lab team members.

References

1. U.S. Department of Energy, "Freedom Car and Vehicle Technologies Multi-Year Program Plan: 2006-2011," September 2006.

2. Bromberg, L., Sappok, A., Parker, R., and Wong, V., "Advanced DPF Loading Monitoring with Microwaves," CLEERS Workshop, Dearborn, MI, May 2006.

3. Sappok, A., Bromberg, L., Parks, J., and Prikhodko, V., "Loading and Regeneration Analysis of a Diesel Particulate Filter with a Radio Frequency-Based Sensor," SAE Technical Paper 2010-01-2126, 2010, doi:10.4271/2010-01-2126.

4. Ma, J., Fang, M., Li, P., Zhu, B., Lu, X., and Lau, N., "Microwave-Assisted Catalytic Combustion of Diesel Soot," *Applied Catalysis A: General*, vol.159, Issues 1–2, 9 October 1997, Pages 211–228, 1997.

5. Michel, R., Baican, R., and Schubert, E., "Soot Particle Properties in the Microwave Range," presented at the 23rd European Microwave Conference 1993, vol. 38, Issue: 8, IEEE, pages 959-960, 1993.

6. Suresh, V., Farinash, L., and Seehra, M., "Carbon in Diesel Participate Matter: Structure, Microwave Absorption, and Oxidation," *Journal of Materials Research*, 10, pages 1075-1078, 1995.

FY 2012 Publications/Presentations

1. Sappok, A., Bromberg, L., Parks, J., and Prikhodko, V., "Loading and Regeneration Analysis of a Diesel Particulate Filter with a Radio Frequency-Based Sensor," SAE Technical Paper 2010-01-2126, 2010, doi:10.4271/2010-01-2126.

Special Recognitions & Awards/Patents Issued

1. Bromberg, L., Sappok, A., Koert, Parker, R., and Wong, V., "Microwave Sensing for Determination of Loading of Filters," U.S. Patent # 7679374, 2010.

IV.11 The Application of High Energy Ignition and Boosting/Mixing Technology to Increase Fuel Economy in Spark Ignition Gasoline Engines by Increasing EGR Dilution Capability

Edward J. Keating
General Motors LLC (GM)
GM Powertrain – Pontiac Engineering Center
895 Joslyn Ave
Pontiac, MI 48340

DOE Technology Development Manager:
Roland M. Gravel

NETL Project Manager: Trev Hall

Subcontractor:
Southwest Research Institute®, San Antonio, TX

Overall Objectives

- Apply the enabling technologies of high energy, extended duration ignition [1] and novel intake charge boosting/mixing system to a current GM boosted spark ignition engine.
- Demonstrate that this GM boosted spark ignition gasoline engine operating with extensive, "high quality" exhaust gas recirculation (EGR) dilution [2] achieves a 12% fuel economy benefit relative to a conventional naturally aspirated gasoline engine at equivalent or better performance.
- Demonstrate that the GM boosted spark ignition gasoline engine solution is capable of U.S. introduction packaged in a mid-sized GM vehicle in the near- to medium-term and has the capability of meeting current and anticipated future emission standards while maintaining or exceeding competitiveness with alternate technologies.

Fiscal Year (FY) 2012 Objectives

- Construct and evaluate a one-dimensional engine simulation model with conventional low-pressure loop (LPL) EGR to determine opportunities to recirculate and/or cool various quantities of EGR.
- Update the one-dimensional engine simulation model to explore the application of "high quality" dedicated EGR (D-EGR) and the various boost/mixing system candidates. Evaluate the capability of the candidate systems to supply and cool a sufficient quantity of dedicated EGR to meet the project objectives.
- Apply the resulting engine output characteristics into a vehicle simulation model of a current mid-size GM vehicle. Utilize the vehicle simulation model to determine the operating points for the subject engine configurations to generate fuel economy projections.
- Install the baseline engine in the test cell and conduct testing to determine the fuel consumption and performance baseline.

Accomplishments

- One-dimensional engine simulation models with conventional LPL EGR and D-EGR have been constructed and various boost/mixing system candidates have been evaluated to determine capability of the candidate systems to supply and cool a sufficient quantity of EGR to meet the project objectives.
- Vehicle simulation model of a current mid-size GM vehicle has been evaluated to determine the operating points for the subject engine configurations in order to generate fuel economy projections.
- Baseline engine testing completed to establish the fuel consumption and performance baseline.
- Design work is completed to package the LPL EGR system defined through simulation in the engine compartment of a current GM mid-size vehicle.

Future Directions

- Update and test a GM 2.0-L turbocharged engine updated with the LPL EGR system defined through simulation and packaging studies. The base engine will be updated with increased compression ratio and a novel high energy, extended duration ignition system.
- Design an updated 2.0-L turbocharged base engine to facilitate efficient operation with increased compression ratio and D-EGR. Design features to include:
  - Reduced combustion chamber surface to volume ratio.
  - Increased in-cylinder mixture motion capability.
  - Accommodation for novel ignition concepts including multiple spark plugs.
- Investigate novel boosting/mixing arrangements including:

- Engine driven compressors and various turbocharger concepts.
- Various methods to implement damping of gaseous pulses that are a characteristic of the D-EGR concept.

Introduction

In order to support the federal government's objective of achieving breakthrough thermal efficiencies while meeting U.S. Environmental Protection Agency emission standards, this project focuses on the enabling technologies of high energy, extended duration ignition and a combination boosting and mixing system. These technologies have been shown to enable engine operation with very high EGR dilution levels leading to significant thermal efficiency improvements across the engine operating range. The mechanisms for thermal efficiency improvement include lower thermal losses, improved ideal cycle efficiency, improved combustion phasing, improved combustion efficiency, and reduced pumping losses. The enabling technologies involved are production viable in the near- to medium-term.

The enabling technologies identified offer the potential additional benefit of using increased quantity and quality of cooled EGR for knock suppression at high load. This benefit should permit the specification of a higher compression ratio leading directly to improved thermal efficiency.

Approach

Phase II - Simulation: A one-dimensional engine performance simulation will be developed to evaluate the potential possibilities to generate various quantities and quality of EGR. An output of the engine simulation will be a definition of various options for recirculating EGR that will best support the enhanced EGR dilution tolerance provided by an innovative ignition system. An additional output will be the investigation regarding the capabilities of the potential novel boost systems to efficiently generate charge boosting and enhance mixing with EGR.

A vehicle simulation will be conducted following the engine simulation to define the engine dynamometer test points that will be used to predict vehicle fuel efficiency as installed in a current mid-size GM vehicle.

Phase III - Initial High Energy, Extended Duration Ignition System Development: Components will be designed and procured to update a suitable GM engine with the novel high energy, extended duration ignition system and the EGR system as determined by simulation in Phase II. Design work will confirm that the systems added to the engine will be capable of installation in the engine compartment of a current mid-size GM vehicle. The engine will be installed on the dynamometer and developed to operate at the highest thermal efficiency possible based upon the EGR dilution tolerance established with the novel high energy ignition system.

Phase IV - Initial Boost System/Mixer and further Innovative Ignition Development: Components will be designed and procured to update a GM engine with the novel intake charge boosting/mixing system and the appropriate D-EGR system as determined by simulation in Phase II. Design work will confirm that the systems added to the engine will be capable of installation in the engine compartment of a current mid-size GM vehicle. The engine will be installed on the dynamometer and developed to operate at the highest thermal efficiency possible based upon the EGR dilution tolerance established with the addition of the novel intake charge boosting/mixing system and D-EGR in conjunction with various novel ignition systems.

Phase V - Engine System Development: Component designs will be updated and procured to update a GM engine with a final enabling technology solution based on the results of the first four phases. A final vehicle simulation will be conducted using the engine dynamometer data to establish performance to objectives.

Results

Vehicle Simulation

A vehicle simulation of a current mid-size GM vehicle was conducted using the current U.S. Federal City/Highway/US06 test cycles. The engine speed and load operating points were compiled over these vehicle test cycles and the fuel energy used was determined. Based on this work, 11 engine speed and load operating points were established that represent approximately 95% of the fuel energy used by the mid-size GM vehicle during these test cycles. These engine speed and load points will form the basis for engine testing to establish fuel consumption performance of the current baseline engine and the technologies under study.

Construct One-Dimensional GT-Power Model of the Baseline Engine

This task was conducted to establish initial correlation between simulation results and engine dynamometer test results. The engine simulation model of the baseline engine was acquired from within GM. This engine simulation model was run at the speed and

load test points determined from the vehicle simulation work to establish predicted baseline fuel consumption performance for the mid-sized GM Vehicle.

Install and Test the Baseline Engine

The baseline 2.4-L Ecotec engine was installed in a test cell and the baseline test matrix was fully executed. The engine was instrumented for temperatures, pressures, and flow rates to establish a comprehensive baseline of the engine. The fully instrumented engine was installed in a test cell with control of inlet air temperature/pressure/humidity, exhaust back pressure, and engine speed/load. An emission sampling system was installed for post catalyst and engine-out emissions measurements. Emissions measurements were conducted with a Horiba Mexa 7100DEGR exhaust emissions analysis system. Cylinder pressure analysis was conducted with an internally controlled software program.

The engine test matrix was determined by vehicle simulation (see above) to best represent engine fuel consumption over the Federal City/Highway/US06 drive cycles. This matrix includes 11 modes. Each mode was weighted based on vehicle fuel consumption simulations and the required engine speed and load necessary to match with the vehicle transmission and drive line constraints. Best brake specific fuel consumption (BSFC) points were determined at each of the 11 modes. Best BSFC was determined by performing sweeps of intake and exhaust cam phasers at each speed/load condition. The spark timing was adjusted to minimum for best torque (MBT), or knock limited spark advance. MBT spark advance was used when possible and determined by locating the 50% mass fraction burned location of the engine between 6-8 crank angle degree after top-dead center. The full load curve from 1,250 rpm to 6,700 rpm was acquired to verify performance. Full load data at the test site was found to be 1.3% higher than the published SAE full-load curve on average. This provided high confidence in engine operation and test cell acquisition.

Assessment of the engine model and engine test show strong agreement in terms of BSFC for the 11 mode points. The measured modal average BSFC was within 2% of the simulated estimations, expressing strong fidelity between simulation and experiment.

Construct One-Dimensional GT-Power model of Conventional LPL EGR Engine

The model of the GM turbocharged engine that is the basis for this phase was acquired from within GM. The LPL EGR system (Figure 1) was defined and added to the engine simulation model. The engine simulation model was run at the speed and load test points determined from the vehicle simulation work to evaluate and confirm the capability of the LPL EGR system components to provide the desired EGR flow and cooling performance required to properly evaluate the concept on the test bench and in vehicle.

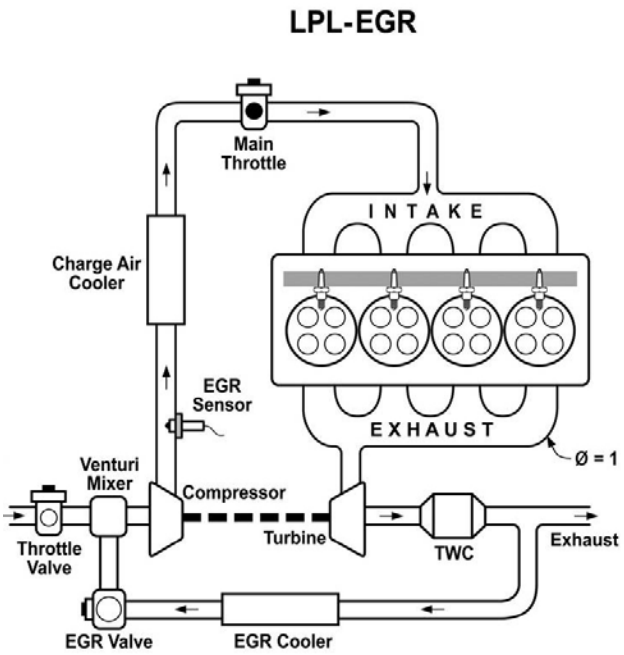

TWC - three-way catalyst

FIGURE 1. LPL EGR System Applied to Turbocharged Engine

Design LPL EGR System that meets Performance Requirements and Packages in Mid-Size GM Vehicle

The packaging development of the LPL EGR system in the vehicle is complete (Figure 2). Per the project objectives, the LPL EGR system to be evaluated meets the packaging requirements of a current GM mid-size vehicle. The various parts required to implement the system are in the process of being manufactured.

Construct One-Dimensional GT-Power model of D-EGR Engine

The model of the GM turbocharged engine that is the basis for this phase was acquired from within GM. The D-EGR system (Figure 3) was defined and added to the engine simulation model. The engine simulation model was run at the speed and load test points determined from the vehicle simulation work to evaluate and confirm the capability of the D-EGR system components to provide the desired EGR flow and cooling performance required to properly evaluate the concept on the test bench and in vehicle.

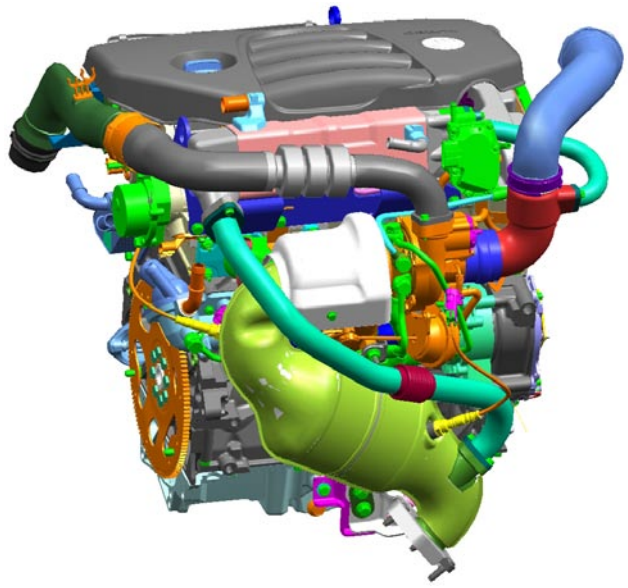

FIGURE 2. LPL EGR System Packaged in GM Mid-Sized Vehicle

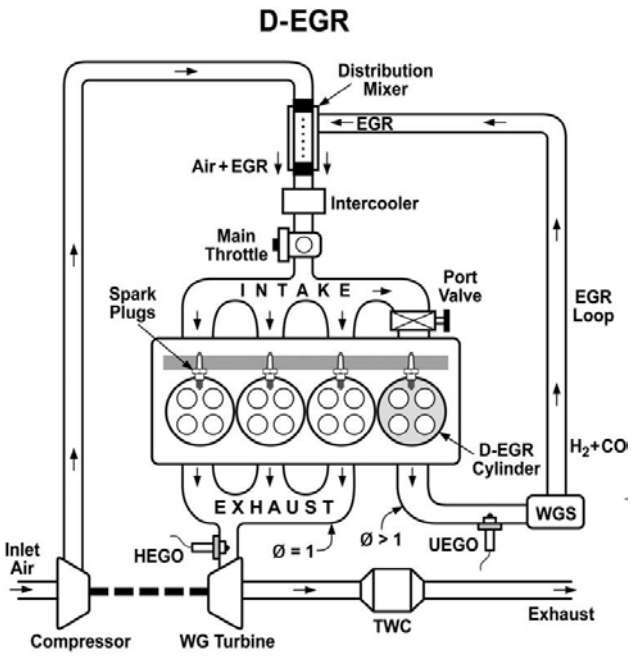

HEGO - heated exhaust gas oxygen (sensor);
UEGO - universal exhaust gas oxygen (sensor);
WG - wastegate; WGS - water-gas shift catalyst

FIGURE 3. D-EGR System Applied to Turbocharged Engine

Conclusions

The project activities conducted to date have supported the basic assumptions used for the project performance improvement projections. The activities have been completed within the constraints of the project timeline. Conclusion of the ongoing design activities and subsequent engine test bench evaluations will establish the performance benefits of the enabling technologies identified.

- The initial one-dimensional GT-Power simulation and subsequent test bench results from the baseline engine achieved excellent correlation to the predicted performance results.
- A LPL EGR system that meets the project EGR performance requirements and packages in a current GM mid-size vehicle has been specified and designed.
- A D-EGR system that meets the project D-EGR performance requirements has been specified.

References

1. T. Alger, B. Mangold, "Dedicated EGR: A New Concept in High Efficiency Engines", SAE paper 2009-01-0694, March 2009.

2. T. Alger, J. Gingrich, B. Mangold, "A Continuous Discharge Ignition System for EGR Limit Extension in SI Engines" Preliminary SAE paper number 2011-01-0661.

IV.12 Heavy-Duty Diesel Engines Waste Heat Recovery Using Roots Expander Organic Rankine Cycle System

Swami Subramanian Ph.D. (Primary Contact), William N. Eybergen

Eaton Innovation Center
Advance Mechanical Systems
26201 Northwestern Hwy
Southfield, MI 48076

DOE Technology Development Manager: Gurpreet Singh

NETL Project Manager: Trevelyn Hall

Subcontractors:

- AVL Powertrain Engineering, Inc., Plymouth, MI
- John Deere, Waterloo, IA
- Electricore, Inc., Valencia, CA

Overall Objectives

- Demonstrate fuel economy improvement through Rankine cycle waste heat recovery (WHR) systems utilizing a roots expander in heavy-duty diesel applications of:
  - 5% (baseline objective) if only energy from the exhaust gas recirculation (EGR) loop is recovered.
  - 8% (target objective) if exhaust energy from downstream of the turbine is also used for recovery.
- Demonstrate green house gas improvement with WHR systems in heavy-duty diesel applications of:
  - 5% (baseline objective) if only energy from the EGR loop is recovered.
  - 8% (target objective) if exhaust energy from downstream of the turbine is also used for recovery.
- Demonstrate that other pollutants, such as oxides of nitrogen (NOx), hydrocarbons, carbon monoxide and particulate matter will not be increased as part of the overall engine/WHR/exhaust after treatment optimization.

Fiscal Year (FY) 2012 Objectives

- Analyze baseline engine for exhaust heat energy availability.
- Quantify the roots-based Rankine cycle fuel economy improvement from simulation and experimental data.
- Optimize the expander configuration to achieve 5% fuel economy improvement.

Accomplishments

- Baseline engine calibration and experimental data collection of EGR, injection timing, air/fuel ratio sweeps and exhaust restriction sensitivity on performance.
- One-dimensional simulation validated against experimental data predicting the enthalpy availability.
- Analytical investigation completed to predict the roots-based Rankine cycle performance.
- Fuel economy improvement of 5% was achieved analytically.
- Roots expander concept design developed based on simulation and analytical results.

Future Directions

- Prototype and evaluate the roots expander first level concept for performance in an ethanol organic Rankine cycle (ORC) system.
- Iterate the roots expander designs based on performance feedback to maximize effectiveness and durability.
- Design a robust roots expander for integration into a heavy-duty diesel engine ORC system.
- Prototype and validate the performance of final roots expander design in an ethanol-based ORC system.
- Design and build a heavy-duty diesel engine Rankine cycle system with integrated roots expander.
- Demonstrate roots-based Rankine cycle system on a heavy-duty diesel engine.

Introduction

Nearly 30% of fuel energy is not utilized and wasted in engine exhaust. ORC WHR systems offer a promising approach on waste energy recovery and improving the efficiency of heavy-duty diesel engines. Typical ORC

WHR systems exploit the engine exhaust energy to evaporate the ORC working fluid through an evaporator. The high pressure heated ORC working fluid is typically expanded through a turbine expander, heat is rejected to the ambient in the condenser, and the cooled working fluid is pumped back into the evaporator. One of the major technological barriers in the ORC WHR system is the turbine expander. A turbine expander is grossly mismatched for use with diesel engine exhaust heat recuperation.

Eaton's solution is to adapt an Eaton designed roots compressor (currently in use for supercharger boosting applications) as an expander of the ORC WHR system. Roots-based expanders will have multiple advantages over turbine expanders, including minor down speeding to match engine speed, caliber to handle multiphase flow, high volumetric efficiency and broad efficiency island. This configuration will enable faster commercialization of ORC WHR technology capable of improving engine fuel efficiency and total power output (performance).

Approach

The present work has been structured to baseline the 13.5-L heavy-duty diesel engine, characterize and quantify the potential waste energy sources for construction of thermodynamic analysis models. The impacts of various WHR heat exchanger layouts on system performance will be assessed, leading to specifications of WHR components. The expander development will utilize computational fluid dynamics analysis, bench testing, calibration, and validation to maximize efficiency and durability. The developed expander with ORC system will be tested on engine operated over the same speed and load conditions of baseline engine. These results will be compared to the baseline engine data at the same NOx emission levels to provide a back-to-back demonstration of the expander technology and impact on fuel efficiency and engine system performance.

Results

A one-dimensional thermodynamic simulation model of the 2012-model year John Deere 13.5-L engine was developed using AVL Boost software. Three steady-state operating points were chosen for the correlation of the model. The baseline test was performed with production calibration for injection event, EGR, air handling systems, and 15 kPa exhaust restriction [1].

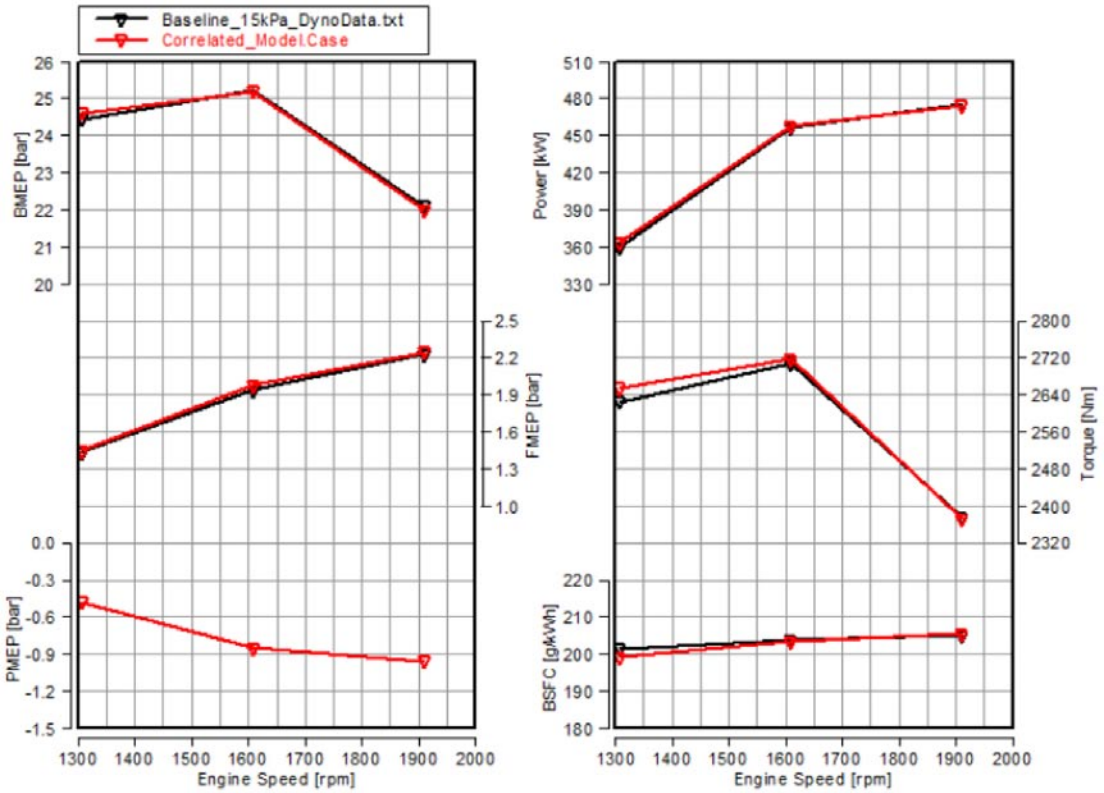

BMEP - brake mean effective pressure; FMEP - friction mean effective pressure; PMEP - pumping mean effective pressure; BSFC - brake specific fuel consumption

FIGURE 1. Comparison of Modeled to Measured Engine Performance Parameters

The baseline engine test data was used for correlation of the simulation model. Figure 1 shows the results of the one-dimensional thermodynamic model correlation efforts. It can be seen that the simulation model closely predicts the measured engine performance parameters data within ~3%.

Engine Energy Balance Analysis

The engine energy balance analysis was conducted based on the experimental engine test data that was summarized earlier [1]. A summary of the energy balances for the engine load points are presented in Table 1. It is seen that combined exergy levels in the 12 load points listed vary from 22 kW (A25) to 152 kW (C100). This shows that the waste heat has high exergy levels for most load points. It is seen that the exergy level of EGR is much higher than that in the exhaust after the turbine.

Working Fluid Selection

The efficiency of the WHR Rankine cycle is dependent on the thermodynamic properties of the working fluid. Three working fluids, R245fa ($C_3H_3F_5$), water and ethanol were selected as candidates from more than 30 working fluids reported in a literature review. Water was eliminated from the candidate list due to having a low condensation pressure (0.3 bar) (sealing concerns), a high freezing point and a significantly higher than desired volume flow rate through the expander stage. Ethanol has advantages over R245fa in reduced system pressure and size of the recuperator. Higher system pressure has significantly impact to the cost of the WHR system for mobile applications because the working fluid pump and the heat exchangers costs increase. The above mentioned considerations led to the selection of ethanol as a working fluid.

ORC Architecture Study

Three concept ORC WHR system architectures were defined for evaluation. The first architect is a simple ORC system for which heat is extracted by cooling the recirculated exhaust gas and no recuperation is used. The second system is the same as the first but with recuperation added. The third system architecture adds post turbine exhaust heat energy to augment the EGR energy and recuperation (Figure 2).

The three systems were compared using consistent boundary conditions. Each system utilized the same target evaporation temperature (120°C), the same target superheat temperature (350°C), the same target condenser temperature (70°C), and the same expander and working fluid pump efficiencies (60% and 50% respectively). The system architecture was evaluated utilizing 25% post turbocharger turbine exhaust energy recovery. Based on evaluation of the three candidate architectures it was determined that the fuel economy advantages of recuperation merit its inclusion. Architecture 1, 2 and

TABLE 1. Energy and Exergy Summary

Load points	A25	A50	A75	A100	B25	B50	B75	B100	C25	C50	C75	C100
Engine speed [rpm]	1307	1307	1307	1307	1609	1609	1609	1609	1910	1910	1910	1910
Brake power [bkW]	89	178	266	355	112	224	337	449	118	235	352	468
BMEP [bar]	6.0	12.0	18.1	24.1	6.2	12.4	18.5	24.7	5.5	10.9	16.3	21.7
Engine torque [Nm]	650	1297	1947	2595	666	1332	1997	2663	588	1174	1760	2339
Parameters affecting waste heat conditions												
EGR rate [%]	33.5	27.4	26.1	25.1	37.0	33.4	31.5	25.9	39.9	36.7	33.8	28.2
Lambda [-]	1.78	1.51	1.44	1.38	1.80	1.56	1.48	1.44	2.02	1.71	1.54	1.44
T_exhaust_bfr-turbine [C]	379	506	595	648	402	522	595	650	379	497	568	647
T_charge_aft-compressor [C]	80	124	173	221	94	153	203	247	111	169	206	232
Engine energy balance												
Brake thermal efficiency [%]	38.0	41.3	41.8	41.6	36.6	40.0	40.6	40.9	33.6	37.5	39.8	40.7
Charge air heat rejection/Fuel Energy [%]	3.5	5.2	7.1	8.6	4.4	6.6	8.5	9.6	5.8	7.9	8.7	9.0
Engine heat rejection/Fuel Energy [%]	26.9	22.9	20.3	18.9	25.9	20.2	17.2	16.5	25.4	19.7	18.1	16.4
EGR cooler heat rejection/Fuel Energy [%]	9.8	9.0	9.9	9.9	12.0	12.6	12.8	10.6	13.6	14.1	13.2	11.6
Net exhaust energy/Fuel energy [%]	21.5	21.7	21.3	21.5	21.1	20.7	20.5	22.0	21.4	20.7	20.5	22.1
Sum [%]	100	100	100	100	100	100	100	100	100	100	100	100
Heat rejections												
Engine heat rejection [kW]	62.2	97.7	127.9	159.8	78.5	112.2	141.3	179.5	88.3	122.1	158.4	187.1
Charge air cooler heat rejection [kW]	8.2	22.0	44.8	72.6	13.2	36.9	69.7	104.8	20.3	48.8	76.2	103.0
EGR cooler heat rejection [kW]	22.6	38.5	62.3	83.5	36.4	70.3	105.3	115.3	47.3	87.6	115.6	132.1
Exhaust enthalpy after turbine [kW]	92.3	158.5	228.1	302.3	120.6	204.9	293.9	402.7	146.4	238.4	319.3	422.4
Exergy (available energy) of EGR before EGR cooler and exhaust after turbine												
Exergy in EGR before EGR cooler [kW]	9	18	31	43	15	33	53	61	20	43	61	71
Exergy in exhaust after turbine [kW]	13	28	42	59	17	34	51	77	18	35	52	81
Total exergy available for WHR (kW)	22	46	73	102	32	67	104	138	38	78	113	152

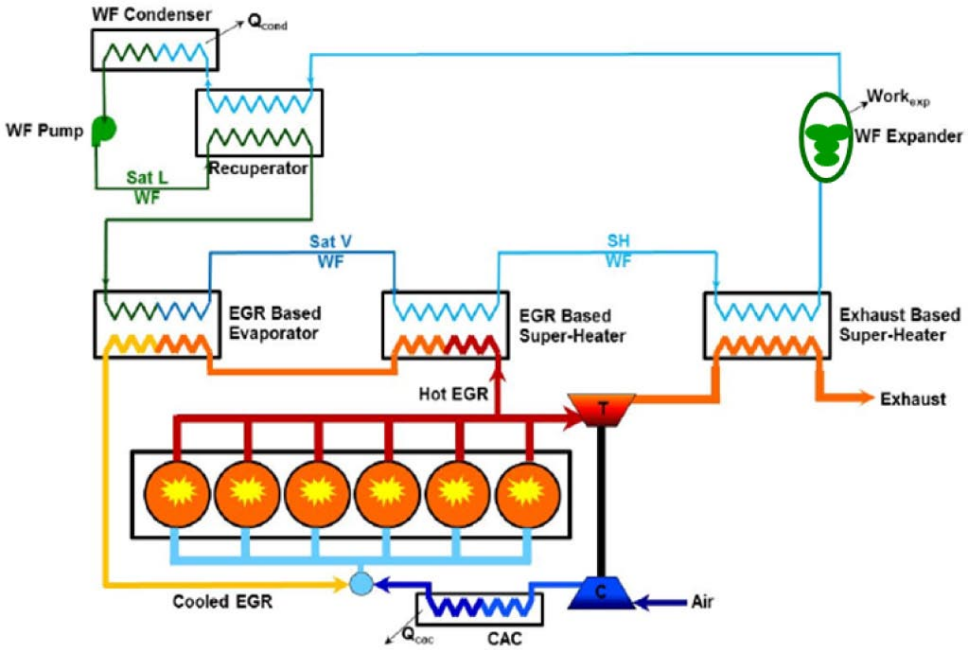

WF - working fluid; Sat L - saturated liquid; Q - heat; CAC - charge air cooler

FIGURE 2. Architecture 3 - Both EGR and Post Turbocharger Turbine Exhaust-Based Recovery

3 BSFC improvements were 2%, 3% and 5% respectively. It was also concluded that the addition of exhaust-based recovery is advantageous from a system fuel economy perspective but the advantages must be weighed against the increase in total system heat rejection including the potential decrease in fuel economy improvement that may occur if ram air cooling of the condenser is not possible. For this reason the basic architecture described in Concept 3 was selected (Figure 2). Table 2 shows that architecture 3 has achieved 5% BSFC improvement over the entire speed and load range.

Expander Development

Table 2 reviews working fluid pressures over 5 bar and temperatures up to 350°C which challenges sealing, bearings, lubrication cooling and material choices. Significant design effort has gone into the selection of static and dynamic seals based on rotational speeds, pressure and temperature. Bearings that will meet the speed and temperature demands have been identified. Lubrication will be separated out of the cooled liquid ethanol and circulated through the gear box of the expander providing cooling and lubrication of the timing gears and bearings. Stainless has been identified as the material for fabrication of the rotors and housing. To evaluate the effectiveness of the components selected a single stage expander mule has been developed as shown in Figure 3. The mule will be tested on an ethanol test stand to evaluate expander efficiency at ideal pressure ratio and flow.

Conclusions

- One-dimensional thermodynamic model of the base engine correlated well with experimental data.
- Ethanol was selected as the working fluid.
- The preliminary architecture study identified the utility of using a recuperator in the system, providing an additional ~1% BSFC improvement.
- Highest BSFC (5% BSFC) improvement is achieved utilizing a roots expander with EGR and post turbine exhaust heat and recuperation.
- An analysis model of the WHR system was constructed, including film heat transfer coefficient capability for emulating the system evaporator and condenser.
- A relatively simple coupling of the WHR system expander to the engine crankshaft appears feasible (variable speed coupling can be avoided).

References

1. Quarterly Report Submitted on July 31 2012.

TABLE 2. BSFC Improvement in Architecture 3

Base Engine Inputs	EGR & Post Turbine Exhaust Recovery / 120C Evaporation, 350C SH, 70C Condenser With Recuperation - 5% bsfc target											
Mode	A25	A50	A75	A100	B25	B50	B75	B100	C25	C50	C75	C100
Speed (rpm)	1307	1307	1307	1307	1609	1609	1609	1609	1910	1910	1910	1910
Torque (N-m)	650	1297	1946	2595	666	1332	1997	2649	587	1174	1760	2331
Power (KW)	88.9	177.6	266.4	355.2	112.3	224.5	336.5	446.3	117.4	234.8	352.1	466.3
bsfc (g/kW-h)	0.225	0.205	0.205	0.206	0.228	0.211	0.210	0.209	0.251	0.226	0.213	0.209
EGR Rate (kg/h)	276.9	287.6	398.4	512.5	404.3	555.7	676.5	744.3	608.5	704.1	976.0	797.5
EGR Temp (C)	397	490	557	615	399	498	548	612	371	467	523	590
Available EGR Q_{rej} (kW)	18.29	32.42	59.09	81.42	27.86	63.09	90.82	108.39	32.95	66.03	97.99	105.12
Exh Rate (kg/h)	503.9	846.4	1165.3	1502.2	639.7	1005.8	1576.3	2045.8	873.3	1383.9	1715.6	2178.9
Exh Temp (C)	325	369	386	408	317	357	364	396	277	321	332	391
Exh Q_{rej} (kW)	45.15	87.75	127.56	175.34	55.76	100.89	161.22	230.15	64.97	122.09	158.07	241.43
Rankine Cycle Inputs												
Evap T (C)	120	120	120	120	120	120	120	120	120	120	120	120
Super Heat T (C)	350	350	350	350	350	350	350	350	350	350	350	350
Condensor Target T (C)	70	70	70	70	70	70	70	70	70	70	70	70
Recuperator Hot Side ε (-)	0.90	0.90	0.90	0.90	0.90	0.90	0.90	0.90	0.90	0.90	0.90	0.90
Expander Eff (-)	60%	60%	60%	60%	60%	60%	60%	60%	60%	60%	60%	60%
Pump Efficiency	50%	50%	50%	50%	50%	50%	50%	50%	50%	50%	50%	50%
Working Fluid Flow (kg/s)	0.0414	0.0827	0.1240	0.1655	0.0523	0.1046	0.1568	0.2080	0.0547	0.1094	0.1640	0.2170
Rankine Cycle Summary												
Total Recovered Heat (kW)	39.69	79.29	118.88	158.67	50.14	100.28	150.33	199.41	52.44	104.88	157.23	208.04
Recovered EGR Heat (kW)	18.29	32.42	59.09	81.42	27.86	63.09	90.82	108.39	32.95	66.03	97.99	105.12
Avail EGR Superheat (kW)	19.79	39.53	59.27	79.11	25.00	50.00	74.95	99.43	26.15	52.30	78.39	103.73
Avail EGR Superheat (kW)	-1.50	-7.11	-0.18	2.31	2.86	13.09	15.87	8.96	6.80	13.73	19.60	1.39
Recovered Post Turb Heat (kW)	21.40	46.87	59.79	77.25	22.28	37.19	59.51	91.02	19.49	38.85	59.24	102.92
Recovered Post Turb Heat (-)	47%	53%	47%	44%	40%	37%	37%	40%	30%	32%	37%	43%
Rejected Heat (kW)	36.84	73.59	110.34	147.27	46.54	93.08	139.52	185.08	48.67	97.35	145.93	193.09
Net Recovered Work (kW)	4.44	8.88	13.31	17.77	5.61	11.23	16.83	22.33	5.87	11.74	17.61	23.30
Expander P_r (-)	5.54	5.54	5.54	5.54	5.54	5.54	5.54	5.54	5.54	5.54	5.54	5.54
Expander In Vol. Flow (m3/hr)	42.12	84.14	126.16	168.38	53.21	106.42	159.53	211.62	55.65	111.31	166.86	220.78
Rankine Cycle Efficiency	11.2%	11.2%	11.2%	11.2%	11.2%	11.2%	11.2%	11.2%	11.2%	11.2%	11.2%	11.2%
Combined Cycle Summary												
Engine Fuel Economy Benefit	5.00%	5.00%	5.00%	5.00%	5.00%	5.00%	5.00%	5.00%	5.00%	5.00%	5.00%	5.00%
δQ_{rej} wrt to Engine Only (kW)	18.55	41.17	51.25	65.85	18.68	29.99	48.70	76.69	15.72	31.32	47.94	87.97

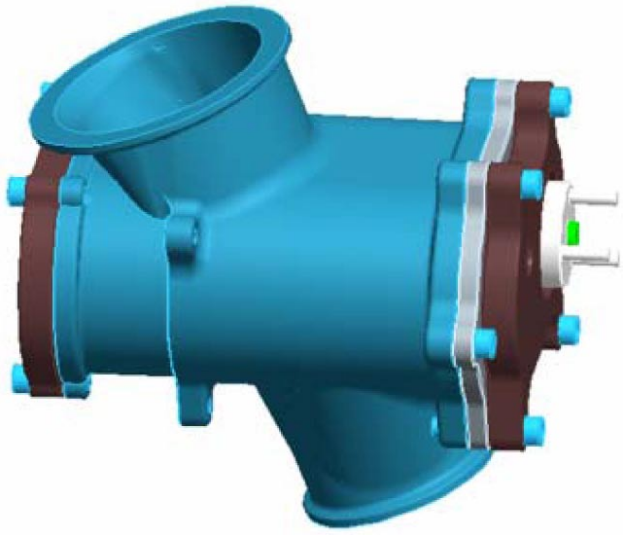

FIGURE 3. Roots Expander Development

IV.13 Next Generation Ultra-Lean Burn Powertrain

Hugh Blaxill (Primary Contact),
Michael Bunce, Kristie Boskey, Luke Cruff,
Eric Smith, Sotirios Mamalis, Aaron Hanson,
Ryan Matulich, and Matthew Williams
MAHLE Powertrain
41000 Vincenti Ct.
Novi, MI 48375-1921

DOE Technology Development Manager:
Roland Gravel

NETL Project Manager: Trevelyn Hall

Subcontractors:
Delphi Corporation, Rochester, NY
Wisconsin Engine Research Consultants, Madison, WI

Overall Objectives

- Demonstrate breakthrough thermal efficiency of 45% on a light-duty gasoline engine platform while demonstrating potential to meet U.S. emissions regulations.
- Demonstrate using ultra-lean burn technology, a 30% predicted vehicle drive cycle fuel economy improvement over an equivalent conventional port fuel injected (PFI) gasoline engine with variable cam phasing.
- Demonstrate potential to maintain typical levels of passenger vehicle performance.
- Demonstrate a cost-effective system, capable of being installed in production engines with minimum modification and showing a clear route to production in the future.
- Develop MAHLE Powertrain's Turbulent Jet Ignition (TJI) concept, in conjunction with turbocharging, as the enabling technology to accomplish these objectives.

Fiscal Year (FY) 2012 Objectives

- Computational fluid dynamics (CFD) analysis of the jet ignition combustion system.
- Design and procurement of jet ignition parts to suit test engine.
- Design and procurement of single-cylinder optical and thermodynamic engine components and single-cylinder engine build.
- Specification and preparation of engine control systems.
- Single-cylinder optical engine and thermodynamic engine testing.

Accomplishments

- Developed single-cylinder optical and corresponding single-cylinder thermodynamic engines as tools to study and optimize TJI hardware, utilizing production engine platforms and incorporating TJI.
- Initiated three-dimensional (3-D) analysis of TJI concept by providing detailed boundary condition parameters synthesized from previous experiments and one-dimensional (1-D) analysis.
- Optimized design of experiments to methodically examine engine performance as a function of TJI hardware variations and to correlate experimental data with 3-D analysis results.

Future Directions

- Complete single-cylinder optical engine build and installation, and acquire high speed imaging and speciation data.
- Complete single-cylinder thermodynamic engine build and installation, and acquire data to evaluate TJI hardware variation effects on engine performance.
- Correlate 3-D analysis results with experimental data from both optical and thermodynamic engines.

Introduction

Regulation and industry trends have sought to produce engines with higher efficiency, lower fuel consumption, and lower exhaust emissions than their predecessors. Lean-burn operation provides thermal efficiency benefits but may result in higher oxides of nitrogen (NOx) emissions, requiring expensive emissions aftertreatment. Ultra-lean burn has been shown to improve thermal efficiency and simultaneously reduce NOx formation by significantly reducing in-cylinder temperatures. However, there are challenges associated with ignition of the charge and combustion stability. In order to improve light-duty spark ignition engine efficiency and vehicle fuel economy, the industry is moving towards downsizing (smaller displacement,

boosted direct injection engines), but these engines typically display poor thermal efficiency. MAHLE Powertrain (MPT) intends to use two key enabling technologies for its ultra-lean burn combustion concept: MPT's TJI system and turbocharging.

Approach

TJI has been under development at MPT for a number of years on a production PFI gasoline base engine. The jet ignition system is a pre-chamber-initiated distributed ignition system that enables reliable ignition of ultra-lean air fuel mixtures. Testing has demonstrated stable and reliable combustion running at lean air fuel ratios exceeding lambda of 2 and has yielded peak indicated net thermal efficiency reaching 42% and near-zero engine-out NOx emissions.

The jet ignition system developed by MPT is characterized by features including: auxiliary pre-chamber fueling, small orifices connecting the main and pre-chamber combustion cavities and a very small pre-chamber volume. The smaller orifice size causes the burning mixture to travel quickly through the orifice, which extinguishes the flame and seeds the main chamber with partially combusted pre-chamber products (radical species). It is then the reacting pre-chamber combustion products which entrain and ignite the main chamber charge through chemical, thermal, and turbulence effects, thus producing multiple distributed ignition sources. During research this system has already displayed thermal efficiencies of 42.8% at some operating conditions, low engine-out NOx emissions and is proven to work over a wide engine operating envelope. The system is also self contained and can be retro-fitted to an existing engine in place of the spark plug with minimal modifications to the existing engine, enabling an easier route to production. This project seeks to further advance this research on a light-duty engine platform.

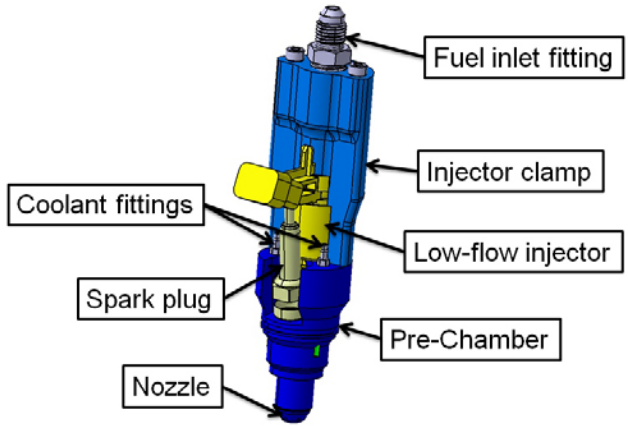

FIGURE 1. MPT TJI

During Phase 1, the directive is to increase the understanding of the TJI concept and to confirm previous experimental achievements. To address the former, a single-cylinder optical engine has been designed and is being built to quantify combustion-related responses to variations in TJI hardware. These responses include jet velocity and penetration and burn rates. In addition, high-speed spectrometry will provide qualification as to which partial-combustion species are most prevalent in the jets immediately post pre-chamber, and will describe their distribution throughout the main chamber. Increased understanding of TJI and the effects of hardware variations will result from comprehensive 3-D analysis. This analysis will be used to guide TJI hardware optimization in subsequent phases.

Phase 1 also includes design and testing of a single-cylinder thermodynamic engine that, in terms of engine platform bases, closely corresponds to the single-cylinder optical engine. These experimental results will, along with the aforementioned optical engine results, provide data against which the 3-D analyses will be correlated. The single-cylinder thermodynamic engine will also be used to confirm the previous experimental thermal efficiency result of 42.8%. A pathway to achieving 45% brake thermal efficiency in subsequent phases will be determined.

Results

During the reporting period, designs for both a single-cylinder optical engine and a single-cylinder thermodynamic engine were developed using production 4-cylinder engines as the bases. TJI will be evaluated using the optical engine to determine the sensitivity of jet velocity and penetration and burn rates to TJI hardware variations. TJI will be evaluated using the

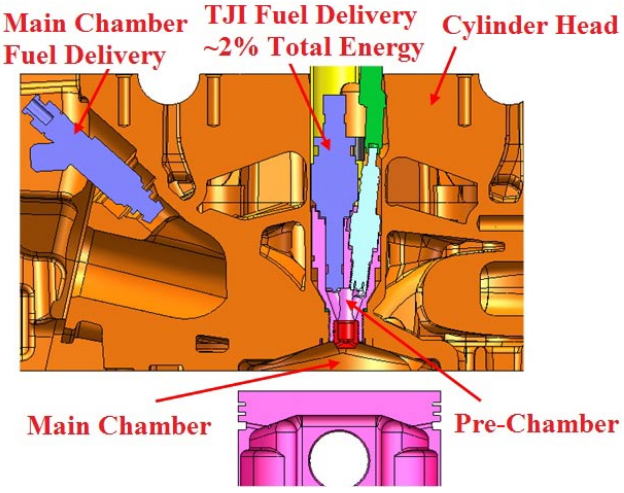

FIGURE 2. Spark Ignition Engine Incorporating MPT TJI

thermodynamic engine to determine the viability of ultra-lean performance with a liquid gasoline-fueled pre-chamber and provide correlation data for 3-D analysis.

During this phase, significant engineering effort was put into design of experiments and planning the test matrices encompassing the course of the entire project, including the analysis approach for 1-D and 3-D simulations required to optimize the TJI pre-chamber design. This will allow methodical iteration of pre-chamber hardware parameters in both modeling and physical testing, thereby providing understanding of engine performance trends resulting from these iterations. Methodical iteration is necessary for TJI hardware optimization in subsequent project phases.

To accomplish the aforementioned stepwise hardware changes in a physical testing environment, the pre-chamber design was updated from that used in previous experiments. The updated design is better suited to provide the robustness, flexibility, ease of access, and ease of service required for this project.

1-D and 3-D simulations play a key role to the fundamental analysis of the TJI concept pursued by the current project. For that reason, 1-D and 3-D analysis tools are being utilized in order to facilitate understanding of the engine and TJI processes. Analysis work began with 1-D modeling of a single-cylinder TJI engine in order to compare predicted performance parameters to those measured in previous experiments. 1-D models were built based on experimental setups and simulations have shown that gas exchange and heat transfer can be successfully described. These simulations provided the boundary conditions necessary for 3-D analysis of TJI.

The MAHLE Flexible electronic control unit was used for this project. This control unit provides an in-house MPT solution for robust control of two fuel injectors per cylinder, and, ultimately, optimized pre-chamber and main chamber fuel injector parameterization. Efforts are ongoing to incorporate the electronic control unit into the test cell.

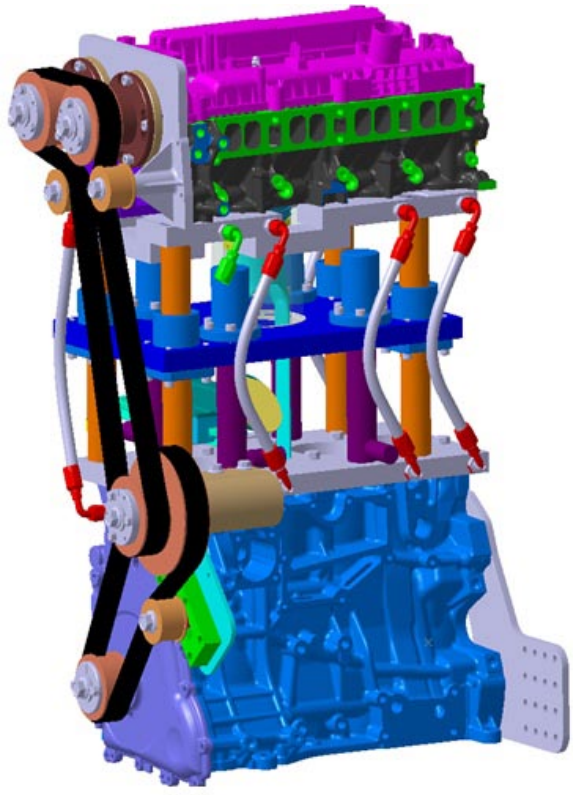

FIGURE 3. MPT Single-Cylinder Optical Engine

Conclusions

Phase 1 of this 3-phase project is ongoing. Test hardware, design of experiments, and 1-D and 3-D analysis plans were developed in preparation for data acquisition and processing later in the phase. Specific accomplishments during the reporting period are:

- Completion of single-cylinder optical engine design incorporating TJI as a tool to better understand combustion sensitivities to TJI hardware by acquiring high speed imaging and speciation data.
- Completion of single-cylinder thermodynamic engine design incorporating TJI as a tool to better understand combustion and engine performance sensitivities to TJI hardware, and to use as a correlation for 3-D analysis.
- Completion of design of experiments to methodically iterate TJI hardware in both physical testing and in 3-D simulation to aid in TJI hardware optimization in subsequent phases.
- Initiation of 3-D analysis of pre-chamber by providing 1-D simulation results as boundary condition inputs to 3-D simulation.

FY 2012 Publications/Presentations

1. B. Mahr, H. Blaxill, W. Attard, “Application and Potential of an Ultra Lean, Low NOx Combustion to Reduce Emission of Nitrogen Oxides and Fuel Consumption”, International Vienna Motorsports Symposium (Vienna, Austria; April 26–27).

2. H. Blaxill, W. Attard, “A Lean Burn Gasoline Fueled Pre-Chamber Jet Ignition Combustion System Achieving High Efficiency and Low NOx at Part Load”, SAE World Congress (Detroit, MI; April 24–26).

IV.14 Gasoline Ultra-Efficient Vehicle with Advanced Low-Temperature Combustion

Keith Confer (Primary Contact), Harry Husted, Mark Sellnau
Delphi
3000 University Drive
Auburn Hills, MI 48326

DOE Technology Development Manager: Ken Howden

NETL Project Manager: Ralph Nine

Subcontractors:
- John Juriga, HATCI, Superior Township, MI
- Dr. Rolf Reitz, WERC LLC, Madison, WI
- Dr. Ming-Chia Lai, Wayne State University, Detroit, MI

Overall Objectives

- Develop, implement, and demonstrate fuel consumption reduction technologies using a new low-temperature combustion process: gasoline direct-injection compression ignition (GDCI).
- Refine and demonstrate several near-term fuel consumption reduction technologies including advanced valvetrain and parasitic loss reduction.
- Design and build engine hardware required.
- Develop engine control strategies.
- Demonstrate benefits of new hardware and refined engine operation.

Fiscal Year (FY) 2012 Objectives

- Calibrate and refine Phase 1 vehicles.
- Test Phase 1 vehicles.
- Continue GDCI simulation.
- Map and refine GDCI operation using single-cylinder engine.
- Design and build Phase 2 multi-cylinder engine hardware.
- Build Phase 2 GDCI multi-cylinder engine.

Accomplishments

- The reduced parasitic loss engine was installed in Phase 1 Vehicle 1 and testing was started. After initial testing, the engine developed a crankshaft main bearing outer race problem. This was resolved and the engine was rebuilt and reinstalled in the vehicle.
- Final debug and test preparation was completed on Vehicle 1.
- A full powertrain calibration was completed for Phase 1 Vehicle 2 using an engine dynamometer engine and the demonstration vehicle. The dynamometer results were integrated into the baseline vehicle calibration.
- While the Vehicle 2's engine control algorithms were completed in 2011, some minor software changes were made during 2012 in response to requests from the vehicle calibration team.
- Vehicle fuel economy and emissions tests were performed. The Environmental Protection Agency (EPA) Federal Test Procedure (FTP) and Highway Fuel Economy Test (HWFET) drive cycles were used for all of the fuel economy testing and combined, unadjusted values were calculated from the test cycle results. All test methods, fuels, vehicle settings and procedures were consistent for Vehicle 1, Vehicle 2 and a baseline port fuel injected (PFI) vehicle.
- For Phase 2, detailed FIRE and KIVA simulations coupled with single-cylinder testing were used to refine the fuel injection, mixing, and combustion processes for GDCI. This information resulted in improved injector and cylinder head designs.
- Detailed computer-aided designs were developed at Delphi for the cylinder head and valvetrain system, boost system, exhaust gas recirculation (EGR) system, intake air coolers, pistons, intake and exhaust manifolds and related components. The enhanced block and related components were designed at HATCI, including a dual oil jet system and a two-stage oil pump.
- All engine hardware was fabricated, finished and bench tested. All valvetrain components for single- and multi-cylinder engines were fabricated and tested on a Delphi valvetrain test bench. The enhanced block and related components were fabricated at HATCI. Engine assembly, final inspection and debug were completed at the Delphi.

Future Directions

- Test Phase 2 technologies on multi-cylinder engines.
- Map GDCI operation on performance dynamometer.
- Develop GDCI engine control systems.

- Continue single-cylinder engine tests and detailed FIRE and KIVA simulations to refine the combustion process and component designs.
- Build Phase 2 vehicle.

Introduction

This project will develop, implement and demonstrate fuel consumption reduction technologies which are focused on improvement of thermal efficiency from in-cylinder combustion complemented by a reduction of friction and parasitic losses.

The investigation includes extensive simulation efforts combined with bench, engine and vehicle testing in a comprehensive four-year project conducted in two phases. The conclusion of each phase is marked by an on-vehicle technology demonstration.

The single largest gain in fuel economy will come from development and demonstration of a breakthrough low-temperature combustion scheme called GDCI to be developed in Phase 2 of the project. Initial steady-state dynamometer testing of this new combustion scheme showed that thermal efficiencies can be greater for GDCI combustion than for diesel combustion. During the project, substantial development work will be done in the areas of combustion control, base engine design, fuel system design and valve train design to fully validate and reduce to practice a combustion scheme implementing GDCI in a gasoline engine which is suitable for mass production. Phase 2 development work spans the full four years of this project.

Phase 1 concentrated on nearer term technologies to reduce friction and parasitic losses. The on-vehicle implementation of these technologies was performed using a systems engineering approach to optimize the collective value of the technologies. The duration of Phase I was two years and was completed in June, 2012.

Approach

Phase 1 technologies were divided into two demonstration vehicles. These two vehicles were equipped with different Phase 1 technologies and hardware. Broadly, Vehicle 1 focused on technologies to reduce engine friction and accessory loads. Vehicle 2 focused on pumping losses and engine idling reduction. Both demonstration vehicles met the same tailpipe emissions standards as the original production vehicle from which they were derived.

For Phase 2, a wide range of analytical and experimental tools were assembled within small expert teams. Detailed FIRE and KIVA simulations were used with spray chamber tests of physical injectors. Single-cylinder engine tests using the design of experiment method were combined with response surface modeling and custom combustion analysis macros to quickly process large amounts test data. GT-Power was used to develop efficient boost systems. While the multi-cylinder engine design work addressed all aspects of the engine, extra design effort was placed on valvetrain, fuel injection, thermal management and boost systems as they are key enablers for the new combustion process. Multi-cylinder GDCI engines were built for both performance dynamometer and engine start-cart development over the past year.

Results

Phase 1

Vehicle 1

All vehicle hardware was debugged and the controls were refined by the end of the first quarter 2012. The vehicle spent the second quarter of the year at HATCI's facility in Michigan for final de-bug and testing (see Figure 1).

The overall fuel economy test results for Vehicle 1 are shown in Figure 1. Fuel economy improvement of 12.6% was achieved for the City drive cycle compared to the PFI baseline vehicle. Highway fuel economy was improved by 13.9% and a combined unadjusted fuel economy improvement of 13.1% was realized for the vehicle (see Figure 2).

Vehicle 2

The demonstration vehicle was completed at Delphi CTCM (see Figure 3) and spent the first quarter of 2012 and part of the second quarter at Delphi's TCR facility in New York for final calibration and de-bug. Final vehicle testing was performed at HATCI.

The overall fuel economy results for Vehicle 2 are shown in Figure 2. A fuel economy improvement of 13.6% was achieved for the city drive cycle compared to the PFI baseline vehicle. Highway fuel economy was improved by 12.8% and the combined unadjusted fuel economy improvement was 13.4% (see Figure 4).

Phase 2

Injector and Fuel System Development

Several injector designs were fabricated and a new fuel system was developed. Sprays were simulated using FIRE and KIVA, and correlated against spray images and

FIGURE 1. Phase 1 Vehicle 1

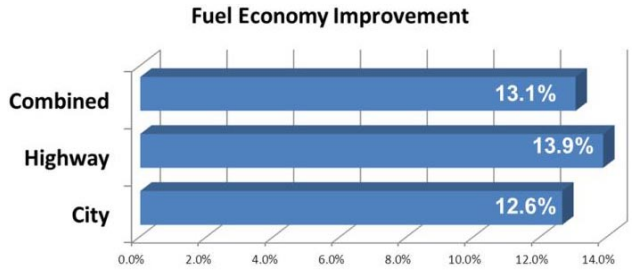

FIGURE 2. Fuel Economy Test Results for Phase 1 Vehicle 1 vs. PFI Baseline

FIGURE 3. Phase 1 Vehicle 2

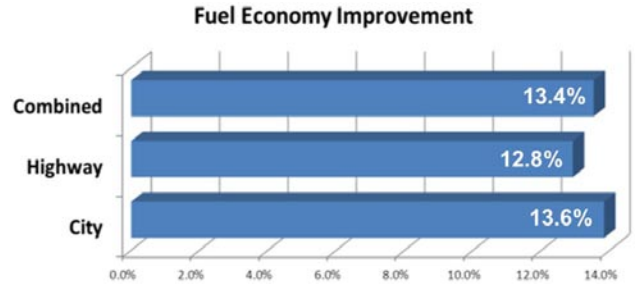

FIGURE 4. Fuel Economy Test Results for Phase 1 Vehicle 2 vs. PFI Baseline

droplet size data from spray chamber tests. The complete fuel system was modeled using AMESIM and GT Fuel, and tested on the bench.

SCE Engine Testing

Tests were conducted on a single-cylinder engine using various injectors and a new piston designed for GDCI. Improved spray characteristics helped reduce indicated specific fuel consumption, oxides of nitrogen, particulate matter, and combustion noise, while also lowering injection pressure (see Figure 5). Burn duration and timing can be controlled to effectively control heat release rate and noise levels.

Boost System Development

Extensive simulations were conducted to develop a practical boost system for GDCI. Various system architectures were studied using maps of boost devices from several suppliers. It was shown that the required boost levels could be achieved. Simulation-based calibration techniques were used to estimate BSFC over the map with good results. Subsequent vehicle simulation showed excellent potential for low fuel consumption for FTP, New European Driving Cycle, and the Worldwide Harmonized Light Duty Driving Test Cycle drive cycles.

Multi-Cylinder Engine Design and Build

Two multi-cylinder engines were assembled and installed in a start cart and a performance dynamometer. The engines were instrumented for combustion analysis and prepared for testing by end of the reporting period.

Conclusions

Phase 1

- The groupings of technologies to reduce engine friction and accessory loads used on Vehicle 1 combined for a 13.1% fuel economy improvement over the PFI baseline vehicle. Engine downspeeding combined with friction reduction, two-step oil pump and cooled EGR were all major contributors to the improvements. The rollerization of the crankshaft was found to have durability concerns and the exhaust heat recovery system (used to pre-heat the engine oil) yielded little fuel economy benefit as mechanized in this study.
- The groupings of technologies to reduce pumping losses and engine idling losses installed on Vehicle 2 combined for a 13.4% fuel economy improvement over the PFI baseline vehicle. An advanced valvetrain system with ePhasers and two-step valve

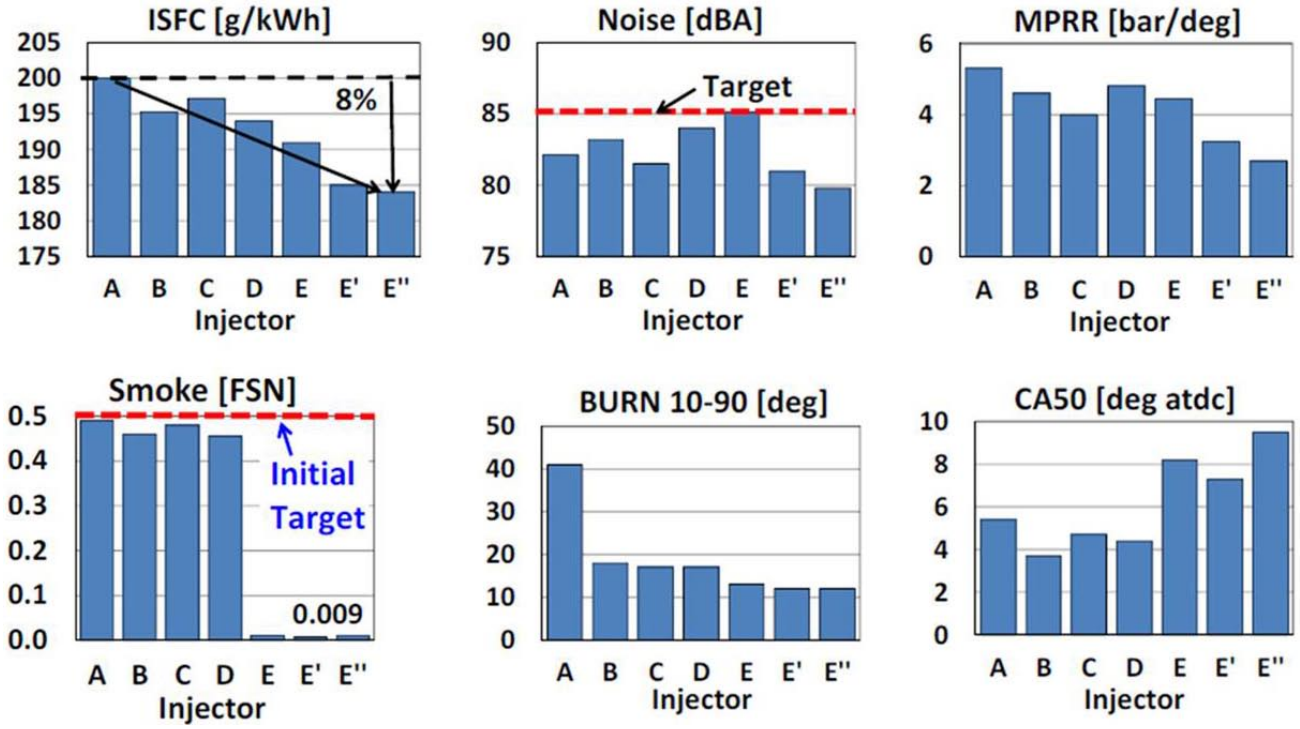

ISFC - indicated specific fuel consumption; MPRR - maximum pressure rate rise; FSN - filter smoke number; CA - crank angle ; atdc - after top-dead center

FIGURE 5. GDCI Single-Cylinder Test Results at 1,500 rpm-6 bar

lift was the largest contributor to the fuel economy improvements. The stop/start system contributed significantly during the city drive cycle.

- Each of the two vehicles demonstrated in excess of 13% improvement in EPA combined fuel economy. Minimal overlap between technologies implemented on the two vehicles suggests that further combination of favorable technologies evaluated in this study would likely offer further improvement on a single vehicle.

Phase 2

- Matching of the latest injector and new piston design resulted in improved fuel consumption and noise at two key test points. GDCI fuel consumption and noise levels show trends similar to diesel, however injection pressures are reasonably low.
- Steady-state engine tests were conducted over the load range from 2 to 18 bar indicated mean effective pressure and demonstrated very low emissions and indicated specific fuel consumption with acceptable combustion noise.

FY 2012 Publications/Presentations

1. *"Gasoline Direct-Injection Compression-Ignition"* M. Sellnau, SAE 2012 High Efficiency IC Engine Symposium, April 2012.

2. *"Full-time Gasoline Direct-Injection Compression Ignition (GDCI) for High Efficiency and Low NOx and PM",* M. Sellnau et al., SAE 2012-01-0384 SAE World Congress, April 2012.

3. *"High Performance Stop-Start System with 14 Volt Belt Alternator Starter", G. Fulks, G. Roth, A. Fedewa,* SAE 2012-01-1041, SAE World Congress, April 2012.

4. UFEV Project Merit Review Presentation, K. Confer, Merit Review, Washington, DC, May 2012.

5. *"Combustion System for Full-time Gasoline Direct-Injection Compression-Ignition (GDCI)",* M. Sellnau, et al., Aachen Colloquium Automobile and Engine Technology, October 2012.

6. *"Development of a High Efficiency Gasoline Vehicle: Program Overview"* K. Confer, et al., US DOE DEER Conference Detroit Michigan, October 2012.

IV.15 Advanced Boost System Development For Diesel HCCI Application

Harold Sun
Ford Motor Company
2101 Village Road
Dearborn, MI 48121

DOE Technology Development Manager:
Ken Howden

Subcontractors:
- Wayne State University, Detroit, MI
- ConceptsNREC, White River Junction, VT

Overall Objectives

The overall objective is to support industry efforts of clean and efficient diesel engine development for passenger and commercial applications. More specifically:

- ConceptsNREC objectives: leads boost system design, optimization, computer-aided engineering stress analysis and fabrication of prototypes as well as flow bench test; provides turbocharger maps for various turbo technologies to support system level simulation/integration.
- Wayne State University objectives: leads computational fluid dynamics analysis and analytical validation of various turbocharger concepts designed by ConceptsNREC.
- Ford Motor Company objectives: leads system integration, cascade system requirement, boost system development design target, validation and demonstration of fuel economy improvement of light duty diesel engine performances on engine test bench.

Fiscal Year (FY) 2012 Objectives

- Actuation system development of compressor active casing treatment.
- Redesign of small turbocharger for light-duty (LD) diesel applications.
- Flow bench test of the advanced turbocharger for LD diesel applications.
- Fabrication of actuation system and the LD turbocharger.
- Engine dyno demonstration of fuel economy improvement on the Federal Test Procedure (FTP) cycle with advanced LD turbo vs. base turbo.
- Redesign, analyses and fabrication of medium-duty (MD) turbocharger on GT37 platform with ruled surface compressor impeller.

Accomplishments

- An IHI production turbo was finally selected as the donor turbo based on the variable geometry turbocharger packaging size in which the advanced mixed flow turbine can fit.
- A production 3.2-L I-5 diesel engine was selected as base engine. The advanced turbocharger based on the IHI donor turbocharger was designed, analyzed and fabricated. The advanced turbo assembly was flow bench tested at the supplier's facility.
- The advanced turbocharger assembly was equipped with an "active casing treatment" to extend flow capacity of the compressor. The active casing treatment is pneumatically controlled in the test cell.
- The advanced compressor design with active casing treatment is a truly technical breakthrough (US Patent 20110173975A1) and has demonstrated 2-4% brake specific fuel consumption (BSFC) improvement on steady-state conditions at part load, even though the advanced turbo was designed for 30% increase in flow capacity over the donor turbo.
- The base Puma I-5 engine was calibrated for Tier 2, Bin 8 tailpipe emissions. Efforts were made to meet Tier 2, Bin 5 tailpipe emissions with the base IHI donor turbocharger. Using the same engine setup and calibration, except the turbocharger change, the newly developed advanced turbocharger demonstrated 3.3% fuel economy improvement over the donor turbocharger.

During 2012, we have made one publication at the DEER conference along with two journal publications in the "Journal of Automobile Engineering."

Future Directions

- All the development work and experimental work have been completed under this contract.
- Additional test data will be organized, analyzed and reported in a final report to DOE.

Introduction

Diesel homogeneous charge compression ignition (HCCI) and low-temperature combustion (LTC) have been recognized as effective approaches to dramatically reduce diesel emissions. However, high level of exhaust gas recirculation (EGR) is needed to achieve homogeneous or partially homogeneous mode, which often drives the compressor and turbine into less efficient or even unstable operation areas.

To support industry efforts of clean and efficient internal combustion engine development for passenger and commercial applications, this project focuses on complete and optimal system solutions to address boost system challenges, such as efficiency degradation and compressor surge, etc, in diesel combustion/emission control system development, and to enable commercialization of advanced diesel combustion technologies, such as HCCI/LTC.

Approach

There are several boosting concepts that have been published and will potentially be helpful to extend operation range with decent efficiency. They are primarily single-stage turbochargers so that they are cost effective, have small package space, small thermal inertia while providing enough EGR that is required by advanced combustion concepts such as HCCI/LTC.

This project has now particularly been focused on the following:

- Optimal compressor impeller design that is focused on efficiency and surge margin improvement.
- The innovative active casing treatment that separates the function of surge and low-end performance from the flow capacity enhancement at full load, which is a major departure from conventional design concept.
- Mixed flow turbine is an attractive option to improve efficiency on turbine side. Base production turbine efficiency at light load and low speed is substantially lower than its peak efficiency. The target of this study will focus on high turbine efficiency at lower speed ratio to improve EGR pumping capacity and vehicle fuel economy on customer driving cycles as well as enhancement of flow capacity.

The above technologies have been fully investigated and well validated through numerical simulations as well as steady-state turbocharger flow bench test and engine dynamometer test on a 6.7-L diesel engine. The advanced compressor impeller, active casing treatment for high compressor efficiency over wide operation range, together with the mixed flow turbine (matched to production variable nozzle geometry turbine and center housing) have demonstrated superior performance at part load and full load. However, the MD turbocharger designed for the 6.7-L diesel has a compressor impeller with arbitrary surface that requires additional manufacturing cost. For the cost sensitive LD diesel market, a low-cost compressor impeller design was pursued, i.e. compressor with ruled surface. As such, the LD turbocharger was focused on compressor impeller optimization with a ruled surface besides the active casing treatment as well as the mixed flow turbine that matched to a production IHI variable geometry turbine.

Results

1. Figure 1 is the comparison of MD compressor impeller with the LD compressor impeller.
2. Figure 2 is schematic illustration of advanced compressor with active casing treatment to address the surge and choke design requirement separately for optimal performance over a wide operation range.
3. Figure 3 shows the comparison of mixed flow turbines of the MD turbocharger and the LD turbo.
4. Figure 4 shows the comparison of compressor efficiencies between the LD and MD designs. The flow capacities of the LD compressors were scaled up to match the flow capacity of the MD compressor.

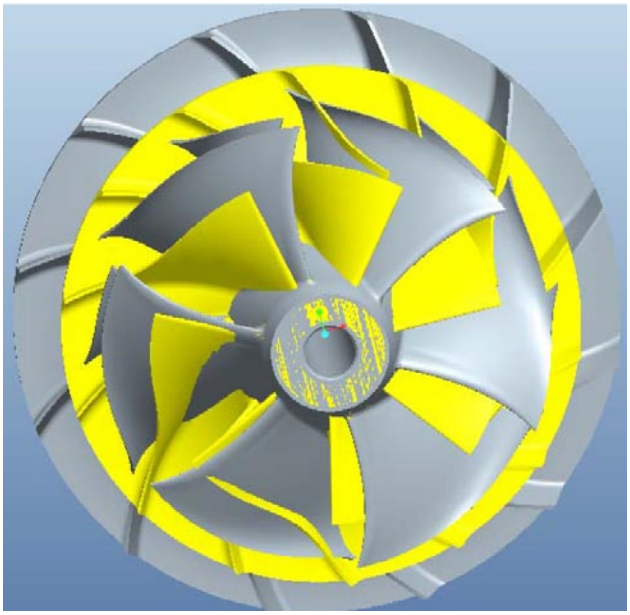

FIGURE 1. Comparison of MD and LD compressor wheel designs.

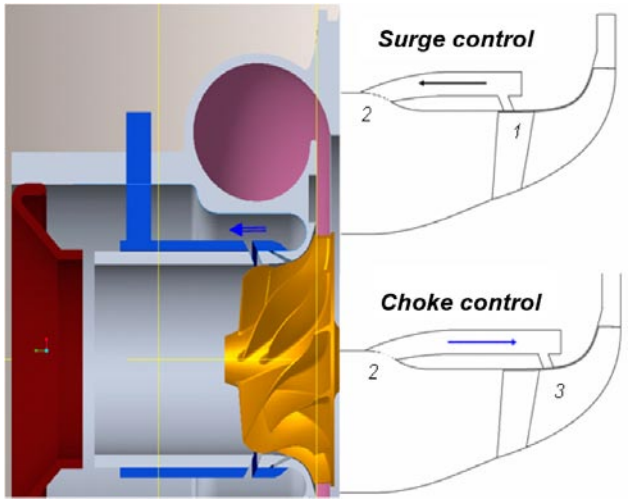

FIGURE 2. Illustration of compressor active casing treatment.

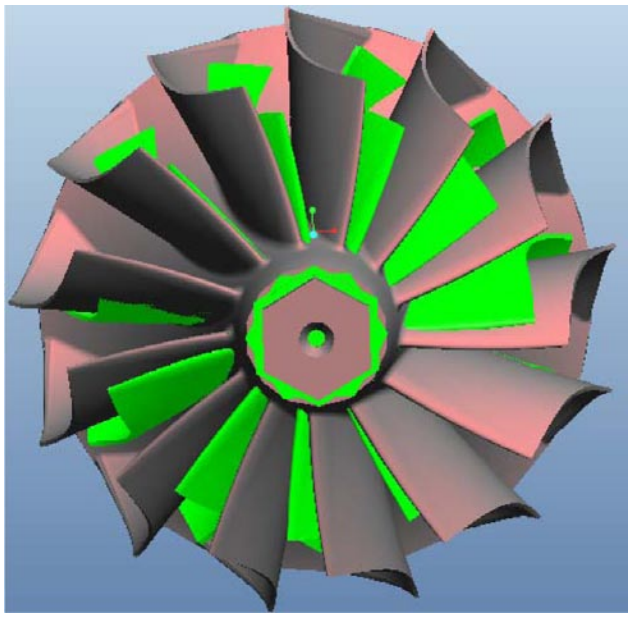

FIGURE 3. Comparison of MD and LD mixed flow turbine designs.

5. Figure 5: The engine dynamometer test at part-load conditions demonstrated BSFC improvement, which is consistent with improvement of compressor efficiency.
6. Figure 6: The engine with advanced TS11 turbocharger demonstrated 3.3% thermal efficiency improvement on the cold FTP cycle over the the base IHI turbo at the Tier 2 Bin 5 tailpipe emission level.

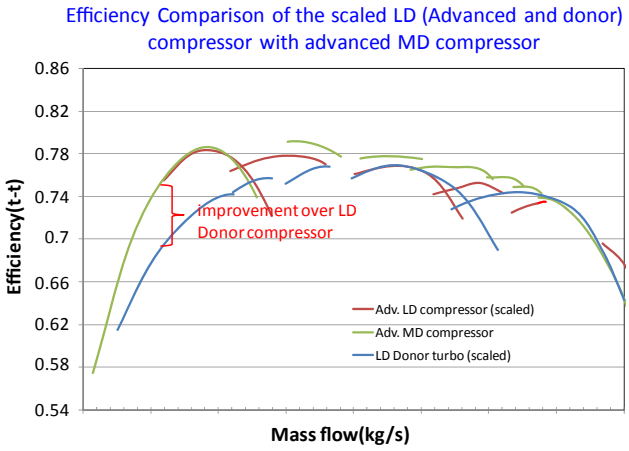

FIGURE 4. Comparison of compressor efficiencies between LD (scaled up to match the flow capacity of MD compressor) and MD designs.

Conclusions

The small turbocharger for LD diesel application is complete. The LD turbocharger was designed for efficiency improvement on both compressor (with ruled impeller surface) and turbine, especially at low compressor mass flow and low turbine speed ratio area where most customer driving cycle will be populated. The back-to-back engine dynamometer test between advanced turbo and base production turbo demonstrated ~2-4% BSFC improvement in part load areas, which was consistent with compressor efficiency improvement. The 3.2-L I-5 engine with the advanced TS11 turbocharger also demonstrated 3.3% improvement in thermal efficiency on a cold FTP transient cycle over the engine performance with the base IHI turbo at Tier 2 Bin 5 emission level, which meets the project target of 3% fuel economy improvement.

FY 2012 Publications/Presentations

1. "New Compressor Concept Improves Efficiency and Operation Range", DEER 2012, October 18, 2012.

2. "SWITCHABLE DUAL-PORT CASING TREATMENT SCHEME FOR ENHANCED TURBOCHARGER COMPRESSOR OPERATING RANGE," Journal of Automobile Engineering, December, 2012.

3. "Numerical and Experimental Investigation of Compressor with Active Self Recirculation Casing Treatment for Wide Operation Range," Journal of Automobile Engineering, December, 2012.

Patents Issued

1. US 20110173975(A1)

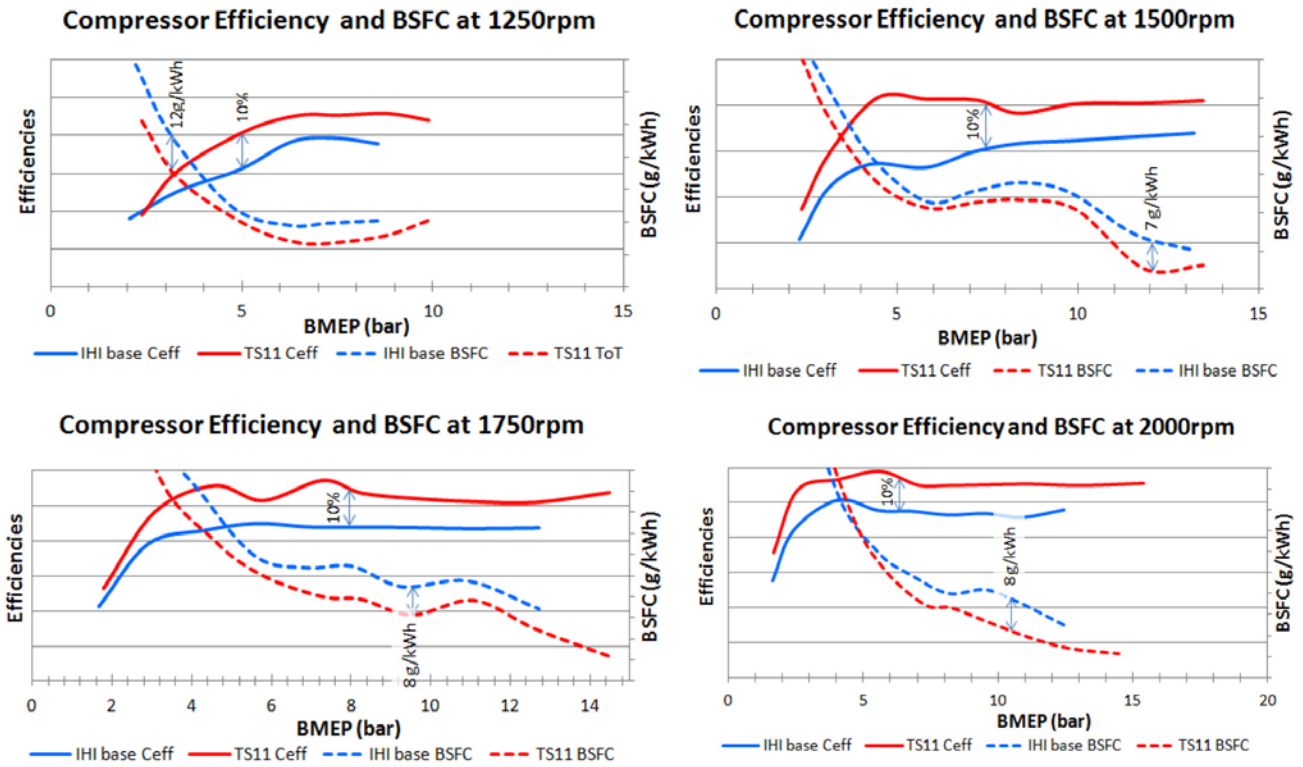

FIGURE 5. Steady-state engine test at part load showing fuel economy and compressor efficiency improvements with advanced turbocharger (TS11) vs. the base turbocharger.

	FTP cycle thermal efficiency
IHI Base Turbo	29.55%
TS11 Adv. Turbo	30.52%
Improvement	3.3%

FIGURE 6. Engine thermal efficiency improvement with TS11 Advanced turbocharger over the base turbo on the cold FTP cycle at the Tier 2 Bin 5 tailpipe emission level.

IV.16 Robust Nitrogen Oxide/Ammonia Sensors for Vehicle Onboard Emissions Control

Rangachary Mukundan (Primary Contact), Eric L. Brosha, Cortney Kreller and Fernando Garzon
Los Alamos National Laboratory (LANL)
MS D429, P.O. Box 1663
Los Alamos, NM 87544

DOE Technology Development Manager: Roland Gravel

Overall Objectives

- Develop prototype oxides of nitrogen (NO_x) sensor based on mixed-potential technology using a $La_{1-x}Sr_xO_{3-\delta}$ (LSC) sensing electrode.
- Develop prototype NH_3 sensor based on mixed-potential technology using an Au sensing electrode.

Fiscal Year (FY) 2012 Objectives

- Demonstrate repeatable and stable heater performance.
- Reproduce performance characteristics of a LANL bulk sensor in an ElectroScience Inc. (ESL)-manufactured platform using commercial mass-manufacturing methods.
- Demonstrate ±5 ppm NO_x and NH_3 sensitivity in two different mixed-potential sensor configurations respectively.

Accomplishments

- Qualitatively reproduced NO_x sensitivity and selectivity of a LANL bulk sensor in a commercially manufacturable device.
- Demonstrated ±5 ppm NH_3 sensitivity in a Pt/ytrria-stabilized zirconia (YSZ)/Au mixed potential sensor.
- Demonstrated ±5 ppm NO_x sensitivity in a Pt/YSZ/LSC mixed potential sensor.

Future Directions

- Evaluate sensing technology under dynamometer conditions at end user site. The work will be continued under a new grant recently awarded by the DOE.
- Analyze the impact of interference gases on NO_x sensor performance.
- Conduct long-term durability studies including thermal cycling.

Introduction

The 2010 Environmental Protection Agency (EPA) emissions regulation for NO_x is 0.2 g/bhr-hr, and the EPA has started to certify vehicles that can actually meet this regulation. Most manufacturers had initially opted instead to meet a family emission limit around 1.2-1.5 g/bhp-hr NO_x with most of their vehicle emissions lying between the two standards [1]. Currently the EPA has certified engines with both the exhaust gas recirculation (EGR) and selective catalytic reduction (SCR) technologies to meet the strict 0.2 g/bhr-hr NO_x standard. While there is only one EGR system that has been certified by the EPA as meeting 2010 emissions regulations (Navistar, Inc.), there are several SCR systems that can meet this requirement (Cummins, Detroit Diesel, Volvo etc.). Moreover the SCR system in addition to meeting emissions regulations can result in a 3 to 5.5% increase in fuel efficiency [2].

The SCR system typically uses a zeolite NO_x adsorption catalyst that can selectively adsorb NO_x molecules during lean burn operation and convert it to N_2 and H_2O with the injection of an urea water solution called diesel exhaust fluid. It is the technology of choice for emissions control in Europe and several manufacturers have adopted this for the United States. SCR systems require tuning to work properly and systems can be tuned with either preexisting engine performance curves or with NO_x/NH_3 sensors. The use of NO_x/NH_3 sensors can provide closed-loop control of the SCR system that can optimize the system for improved NO_x reduction efficiencies and low NH_3 slip. According to a recent review "Reliable and accurate NO_x sensors will be the key to the management of adsorption catalysts" [3]. The optimized use of SCR systems can increase the value for the customer with fuel and diesel exhaust fluid savings (including reduced frequency and costs of the dealer servicing of the emissions system consumables) over the life of the vehicle helping defray the added cost of the system.

Approach

LANL has previously developed a new class of mixed-potential sensors that utilize dense electrodes partially covered with porous and/or thin film electrolytes [4-8]. This unique configuration stabilizes the three-phase (gas/electrode/electrolyte) interface resulting in sensors with exceptional response stability and reproducibility. This configuration also minimizes heterogeneous catalysis resulting in high sensor sensitivity. Moreover, the electrode composition of these sensors can be varied to tune the selectivity relative to desired exhaust gas species. For example, a gold electrode has high NH_3 selectivity while a LSC electrode provides high hydrocarbon or NO_x selectivity. When the sensors using LSC electrodes are operated at open circuit, the voltage response is proportional to non-methane hydrocarbons and when they are operated under a current/voltage bias mode, the response is proportional to total NO_x.

The unique mixed potential electrochemical sensors developed at Los Alamos were experimental, laboratory devices. Moreover, the sensors were bulk, hand-made devices that required a large external furnace for precise temperature control during operation. In this project LANL is working closely with ESL of King of Prussia PA, to apply commercial manufacturing methods to LANL laboratory NO_x sensor configurations. Through an iterative process of prototype preparation at ESL, laboratory testing and materials characterization at LANL, and a free exchange of performance and characterization data between LANL and ESL, the performance of the bulk sensors will be reproduced in a commercially manufacturable device.

Results

Figure 1 is a photograph of the first type of pre-commercial sensors prepared by ESL to LANL specification. Based on LANL-provided concept drawings, ESL designed a high-temperature co-fired ceramic part incorporating the required screen-print patterns for various layers including the heater, heater overcoat, platinum pseudo-reference electrode, and the oxide working electrode. Further, the heater pattern was designed to obtain the required heater resistance utilizing a standard heater ink composition. The design was stepped and repeated to provide a total of 10 sensor parts per substrate. Such a design is conducive for mass production using a 2 × 25 array on a 6″ × 6″ substrate.

The response of a mixed potential electrochemical sensor is dependent on operating temperature. The higher the operating temperature, the more closely the response of the device is to equilibrium electrochemical response. Because both the working and counter electrodes are exposed to the same test gas composition, the voltage produced by the sensor will go to zero as the operating temperature is increased. Therefore, temperature control is crucial and the resistive heater prepared by ESL using commercial manufacturing methods must be robust and stable in order to provide a drift-free sensor response. The heater resistances of the stick sensors were measured in the first lot of parts prepared by ESL. Table 1 lists the room temperature resistances with an average resistance of 13.6 ± 0.3 ohms for the devices fired at 1,450°C and 11.5 ± 0.1 ohms for the set fired at 1,500°C. For preproduction prototypes, this variability is expected and optimization during scale up would tend to reduce the spread in the heater resistance. The heaters (sintered at a particular temperature) needed only one calibration curve

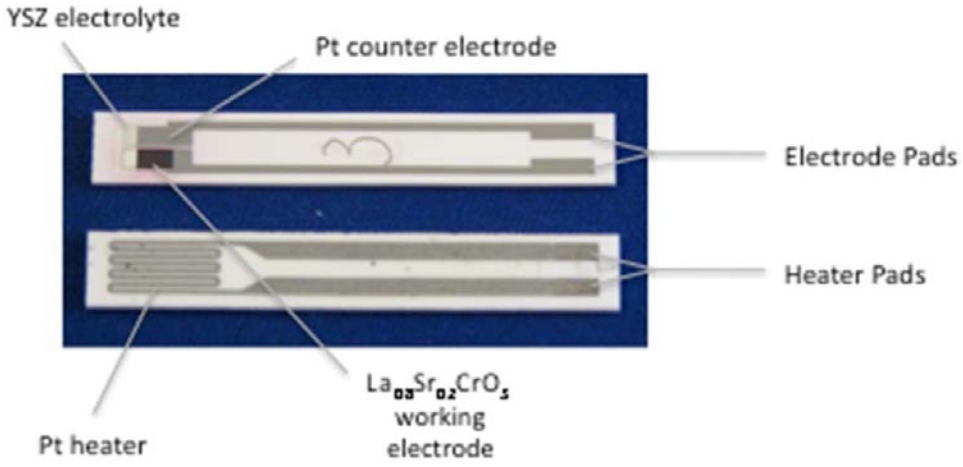

FIGURE 1. Photograph of Pre-Commercial Sensors Prepared by ESL to LANL Specification

TABLE 1. Properties of 10 Electrochemical Sensor Parts obtained from ESL

Table 1 : Properties of Type 1 Sensor Parts, Part No. 42523, Lot No. D-3094-64A

Serial No.	Peak firing Temp.,°C	Length mm	Width mm	Thickness mm	Heater resistance (Ω)
A1	1450	51.5	7.5	1.3	13.8
A2	1450	51.5	7.5	1.3	13.9
A3	1450	51.5	7.5	1.3	13.7
A4	1450	51.5	7.5	1.3	13.4
A5	1450	51.5	7.5	1.3	13.3
A6	1500	51.3	7.4	1.3	11.5
A7	1500	51.3	7.4	1.3	11.6
A8	1500	51.4	7.5	1.3	11.3
A9	1500	51.4	7.4	1.3	11.6
A10	1500	51.3	7.3	1.3	11.5

and provided exceptional temperature stability in up to 1,000 hours of testing.

Several sensors were tested from the first batch of ESL devices and all of the devices except one produced a typical NO_x response illustrated in Figure 2a. One device produced no response to any test gas at any operating voltage and a closer inspection under an optical microscope revealed that the source of this anomalous behavior of this one device was caused by a small crack bisecting the electrolyte between the working and counter electrodes. The sensor response illustrated in Figure 2a shows several characteristics that were seen with the bulk, tape-casted laboratory sensors with excellent NO_2 sensitivity and acceptable hydrocarbon selectivity. The NO sensitivity was lower compared to the previously reported tape cast NO_x sensors [4]. Moreover longer-term testing as illustrated in Figure 2b revealed significant drift in the sensor response over time. For example the baseline response drifted as much as 50% over the 700 hours of testing which is un-acceptable for any sensing application.

LANL performed extensive characterization of the devices including X-ray computed tomography, X-ray fluorescence, X-ray diffraction and scanning electron microscopy. These characterizations revealed multiple defects in the YSZ electrolyte near the three-phase interface area and porosity in the electrode structures, especially the platinum. The reason for the sensor drift observed in Figure 2b was attributed to the changing morphology of the electrodes over time. LANL provided this feedback to ESL and the sensor manufacturing was optimized resulting in the optimized electrode/sensor structure illustrated in Figure 3. The two electrodes are almost dense as seen in the scanning electron microscopy pictures and the YSZ is without any defects as revealed by X-ray computed tomography (not shown). The performance of this optimized sensor is illustrated in Figures 4a and 4b. The sensor response under bias and unbiased conditions is comparable to the previously reported response of the tape cast sensors [4].

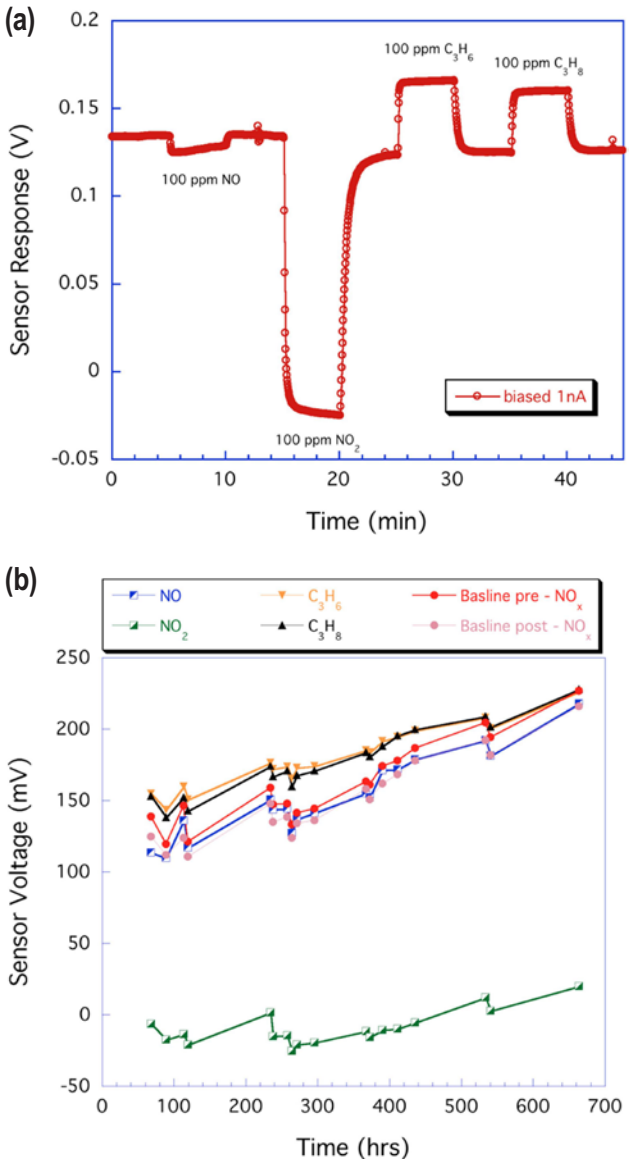

FIGURE 2. a) Performance and b) Stability of First Generation Sensors

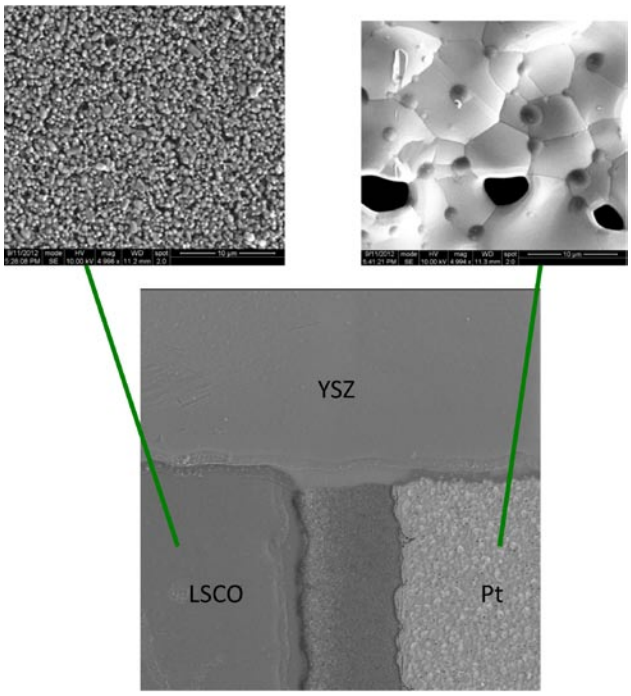

FIGURE 3. Scanning Electron Micrographs of the Optimized Sensors

The sensor behaves like a total NO_x sensor under bias and a hydrocarbon sensor under open circuit conditions. Furthermore, the stability of this sensor is remarkably improved when compared to the first generation devices. These improvements were achieved as a result of LANL's better understanding of the electrode/electrolyte morphology and its effect on mixed potential sensor response, and ESLs ability to manufacture devices with the desired electrode/electrolyte morphology. Further optimization of the electrode morphology is required to meet the stringent stability requirements for automotive applications.

Further advancement of this technology is required before commercialization. LANL will continue to work with ESL to optimize the sensor morphology and therefore the sensor response. The electrode morphology and spacing will be optimized to maximize the NO_x sensor sensitivity, selectivity and long-term stability. Extensive interference measurements need to be carried out and response times characterized in actual dynamometer conditions. LANL will work with an end user to conduct these tests and advance this technology to the next stage of commercialization. Finally, further long-term testing including extensive temperature cycling is required to prove the durability of these sensors over 100,000 miles of operation in an automotive exhaust environment.

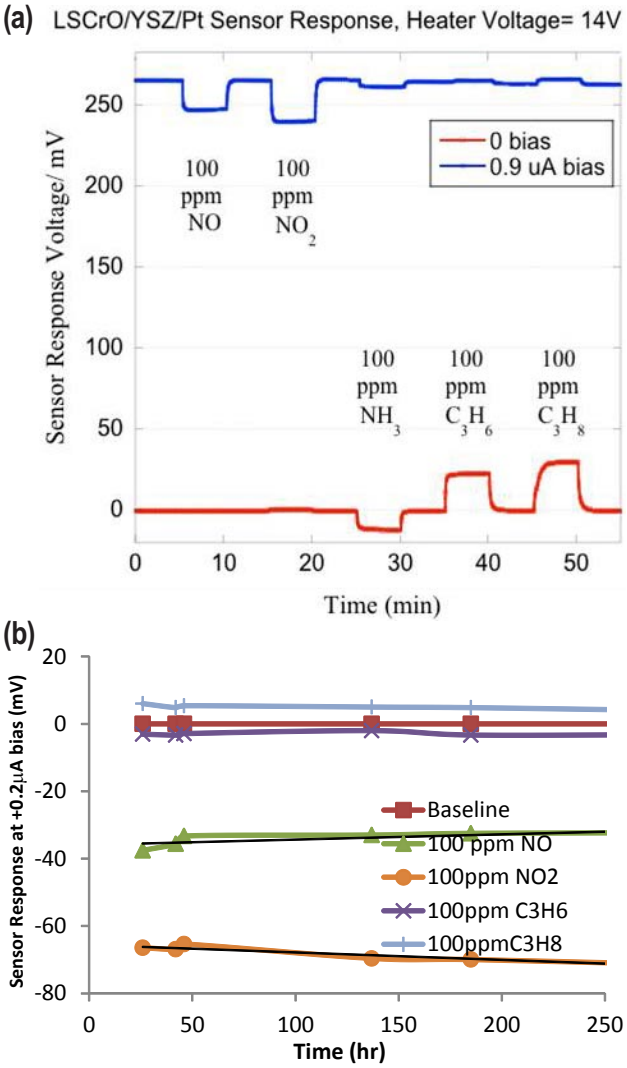

FIGURE 4. a) Performance and b) Stability of Optimized Sensors

Conclusions

- Unique LANL mixed potential sensor has been adapted to low-cost robust NO_x and NH_3 sensors.
- First generation NO_x sensors manufactured by ESL using LANL sensor designs:
  - Interfacial stability issues identified.
  - Morphological instability identified.
- Changes made to processing in iterative fashion result in dramatically improved sensor response:
  - ±5 ppm NO_x sensitivity obtained.
- Heater electronics developed and heater stability confirmed.
- Pathway identified for future development of this technology for transfer to industry.

References

1. Diesel Power: Clean Vehicles for Tomorrow. Vehicle Technologies Program, U.S. Department of Energy, July 2010.

2. T.V. Johnson, "Review of Diesel Emissions and control," International Journal of Engine Research, V10. No 5, 275 (2009).

3. N. Docquier, S. Candel, "Combustion control and sensors: a review", Progress in Energy and Combustion Science, V 28, 107 (2002).

4. R. Mukundan, E.L. Brosha and F.H. Garzon. US Patent # 7,575,709 B2, "Tape Cast Sensors and Method of Making"; August 18, 2009.

5. F.H. Garzon, E.L. Brosha and R. Mukundan. US Patent # 7,264,700, "Thin Film Mixed Potential Sensors"; Sept. 4, 2007.

6. R. Mukundan, K. Teranishi, E.L. Brosha, and F.H. Garzon, "Nitrogen oxide sensors based on Yttria-stabilized zirconia electrolyte and oxide electrodes". *Electrochemical and Solid-State Letters*, **10(2)**, J26-J29 (2007).

7. F.H. Garzon, E.L. Brosha, and R. Mukundan, "Solid State Ionic Devices for Combustion Gas Sensing". *Solid State Ionics*, **175(1-4)**, 487-490 (2004).

FY 2012 Publications/Presentations

1. C.R. Kreller, P.K. Sekhar, R. Mukundan, E.L. Brosha, and F.H. Garzon, "Influence of Design Parameters on Performance of Mixed Potential Sensors" 221st Meeting of the ECS, Seattle WA, May 2012.

2. P.K. Sekhar, E.L. Brosha, F.H. Garzon, and R. Mukundan, "Understanding the Mixed Potential Sensor Response through Four Electrode Measurements", 219th ECS Meeting, Montreal, Canada, May 2011.

IV.17 Variable Compression Ratio (VCR) Assessment to Enable Higher Efficiency in Gasoline Engines

Norberto Domingo
Oak Ridge National Laboratory (ORNL)
2360 Cherahala Boulevard
Knoxville, TN 37932

DOE Technology Development Manager:
Roland Gravel

Subcontractor:
ENVERA, Los Angeles, CA

Overall Objectives

- Under subcontract with Envera LLC, design, prototype, and deliver to ORNL one variable compression ratio (VCR) gasoline direct injection engine (GDI) with combined direct fuel injection and port fuel injection capabilities. Conduct high-load dynamometer testing prior to delivery to ORNL to validate functionality of all mechanical systems.
- Set up VCR engine at ORNL and quantify the fuel economy benefit of VCR engine technology to a modern direct-injection gasoline engine, and the impact on emissions.
- Map VCR engine performance and emissions over multiple control variables, including compression ratio (CR), spark timing, and cam phasing.
- Utilize experimental engine maps as inputs to drive cycle simulation software to estimate the real-world fuel economy and emissions impact.

Fiscal Year (FY) 2012 Objectives

- Continue work on fabrication of prototype VCR research engine. This includes machining of engine bedplate, engine crankshaft cradle, and fabrication of custom crankshaft and other VCR actuation components.
- Deliver all engine components to Automotive Specialist in Concord, North Carolina, for engine build and demonstration testing.
- Conduct a post-test inspection of key engine components by Automotive Specialist and reassemble engine for delivery to ORNL.

Accomplishments

- The Envera VCR engine has been built, and is now being prepared for dynamometer testing. Testing of the engine at Automotive Specialists is scheduled for the week of December 10th, 2012.
- The engine was first preassembled by Envera in Los Angeles, California. Figures 1 and 2 show the VCR engine preassembly. The engine was then disassembled and shipped to Automotive Specialists.
- Automotive specialists then reassembled the engine in North Carolina. Automotive Specialists finalized key mechanical dimensions such as cylinder honing, thrust bearing clearances and cam timing checks. General mechanical functionality was inspected during assembly. Figures 3 and 4 show the Envera VCR engine in the Automotive Specialists engine build room.

FIGURE 1. Envera VCR Engine Preassembly

FIGURE 2. VCR Crankshaft Cradle and Crankshaft Preassembly

FIGURE 3. Front View of the VCR engine at Automotive Specialists

FIGURE 4. Rear View of the VCR Engine at Automotive Specialists

Future Directions

- Conduct demonstration testing of VCR engine including measurements of the engine performance, VCR actuator mechanism response time and fuel consumption at Automotive Specialists in Concord, North Carolina.
- Conduct a post-test inspection of key engine components by Automotive Specialist and reassemble engine for delivery to ORNL.
- Install engine at ORNL dynamometer test facility and conduct experiments to investigate the effect of VCR on engine efficiency at the maximum brake torque (MBT) spark timing over the engine map with a VCR research engine. Engine experiments will combine parametric sweeps of spark timing, CR, and cam phasing to determine the optimal efficiency at each engine speed/load operating condition. Emissions from the engine will also be measured before and after a three-way catalyst.

Introduction

Basic thermodynamics dictate that the efficiency of internal combustion engines is proportional to CR. However, CR of modern gasoline engines is relatively low from a thermodynamic standpoint, in the range of about 8.5 to 12.5, because of practical constraints at higher CR such as engine knock, increased friction work, and increased heat transfer. It is only the knock-prone conditions (low speed, high load) that constrain the engine CR. The efficiency of most part-load engine conditions can be increased by raising the CR, and it is these part-load conditions that have the most direct impact the real-world fuel economy.

Figure 5 illustrates the potential impact of increased part-load efficiency on fuel economy. Figure 5 (a) shows a contour map of engine efficiency as functions of engine speed and load for a Saab Biopower vehicle, and is qualitatively representative of modern engines. Peak engine efficiency is approximately 32%. Figure 5 (b) shows the vehicle speed as a function of time for a Federal Test Procedure (FTP) driving cycle, used in determining “City” fuel economy, which contains numerous decelerations, stops, and accelerations. In Figure 5 (c), data points from the FTP cycle are superimposed on the map of engine efficiency. Nearly all of the driving cycle takes place under low efficiency part-load engine conditions, conditions where higher compression could increase engine efficiency.

There are currently several ongoing investigations aimed at increasing efficiency, at least in part, by utilizing high mechanical CR and reducing the effective CR with late intake valve closing [1,2]; a technique that is particularly attractive for optimizing engines using

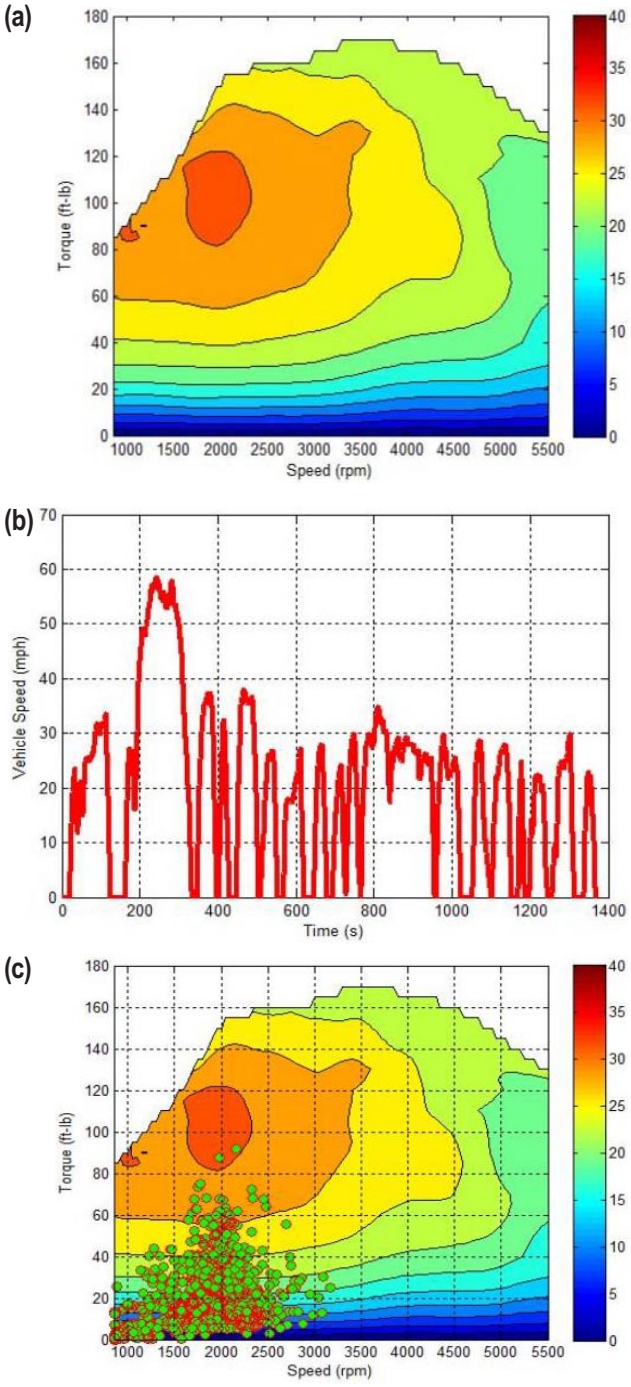

FIGURE 5. (a) Engine efficiency contour plot for the Saab Biopower, (b) Vehicle speed trace for the FTP driving cycle, and (c) Operating points from the FTP driving cycle superimposed on the engine efficiency contour plot. Data collected at the ORNL chassis dynamometer laboratory in 2007.

E85 (85% ethanol and 15% gasoline). However, reducing the effective CR in this manner actually decreases the maximum torque at all engine speeds because of reduced volumetric efficiency, which is a direct result of late intake valve closing. An earlier investigation to increase part-load efficiency was made with a predecessor of the research engine proposed here [3]. The earlier investigation demonstrated proof of principle and showed promise, but did not include a comprehensive study on the effects of variable CR engine emissions and is no longer representative of modern engine technology.

Engine downsizing is viewed by U.S. and foreign automobile manufacturers as one of the best options for improving fuel economy. While this strategy has already demonstrated a degree of success, downsizing and fuel economy gains are currently limited. With new VCR technology however, the degree of engine downsizing and fuel economy improvement can be greatly increased. A small VCR engine has the potential to return significantly higher vehicle fuel economy while also providing high power.

To meet torque and power requirements, a smaller engine needs to do more work per stroke. This is typically accomplished by boosting the incoming charge with either a turbocharger or supercharger so that more energy is present in the cylinder per stroke to do the work. With current production engines the degree of engine boosting (which correlates to downsizing) is limited by engine knock at high boost levels. Engine knock or detonation can be prevented by lowering the CR and using premium octane fuel, but as stated earlier, lowering CR reduces engine efficiency and using premium fuel increases customer cost.

VCR technology eliminates the limitation of engine knock at high load levels by reducing CR to ~8.5:1 (or whatever level is appropriate) when high boost pressures are needed and regular grade fuel is used. By reducing the CR during high load demand periods there is increased volume in the cylinder at top-dead center which allows more charge (or energy) to enter the cylinder without increasing the peak pressure. Cylinder pressure is thus kept below the level at which the engine would begin to knock. When loads on the engine are low the CR can be raised (to as much as 18:1) providing high engine efficiency. It is important to recognize that for a well designed VCR engine cylinder pressure does not need to be higher than found in current production turbocharged engines. As such, there is no need for a stronger crankcase, bearings and other load bearing parts within the VCR engine.

Under the current project, Envera is delivering a prototype gasoline direct-injection VCR engine to ORNL. In the proposed study, ORNL will provide an update of the potential benefit of variable mechanical CR on efficiency and emissions using Envera's state-of-the-art VCR engine technology.

Fuel Efficiency Comparison

The fuel efficiency benefit of downsizing from a naturally aspirated V-8 engine to a turbocharged V-6 engine was assessed by the U.S. Environmental Protection Agency (EPA, A Study of Potential Effectiveness of Carbon Dioxide Reducing Vehicle Technologies, Revised Final Report, June 2008, US EPA) [4] and Ricardo (SAE Paper No. 2007-01-1410) [5]. In Figure 6, engine efficiency projections for an inline 4-cylinder Envera VCR engine are added to the earlier EPA/Ricardo comparison. Figure 6 includes brake specific fuel consumption (BSFC) curves for a gasoline direct injection turbocharged 3.6-L V-6 engine (DI Boost) and a naturally aspirated engine 5.7-L V-8 engine (V8) as reported by EPA. Efficiency projections for the Envera VCR engine (dashed black line) have been added to the graph. All three engine BSFC curves correspond to an engine speed of 2,000 rpm. The Envera VCR engine will operate according to the Atkinson Cycle at light load, with engine calibration settings similar to (or better than) that of the 2010 Toyota Prius. The solid portion of the "--- VCR BOOST" curve is drawn from engine efficiency data presented by Toyota in SAE paper 2009-01-1061 [6]. The data has been scaled from an engine having a displacement of 1.8-L (the stock 2010 Toyota Prius) to 2.2-L so that the peak torque of the Envera VCR engine matches the peak torque of the V-8 engine at 2,000 rpm, which is 445 Nm (328 ft-lb). In this comparison the Envera VCR engine employs turbocharging in order to provide V-8-like power and torque. VCR and variable valve actuation enable the Envera engine to operate according to the high-efficiency Atkinson cycle at light loads and according to the Otto Cycle with aggressive turbocharging at high loads. Data for the three engines is shown in Table 1. At 100 Nm and 2,000 rpm, all three engines produce about 28 horsepower. The V-6 Turbo DI engine is expected to consume 19.6 percent more fuel than the I-4 turbocharged VCR engine at 100 Nm. The V-8 engine is expected to consume 43 percent more fuel than the I-4 turbocharged engine at 100 Nm. At 50 Nm (14 hp) the V-8 engine is expected to consume 67 percent more fuel than the I-4 turbocharged engine. The VCR engine in this comparison has port fuel injection. Even larger gains in fuel efficiency may be attainable for gasoline direct-injection VCR engines. In general, VCR technology enables significantly larger fuel economy gains to be achieved than can be accomplished with fixed CR engines.

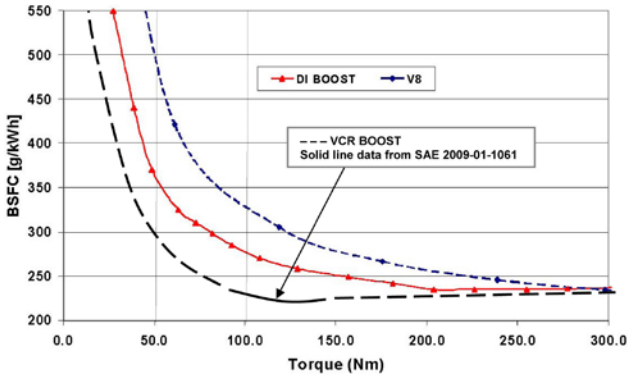

FIGURE 6. Fuel Efficiency Comparison of a 5.7-L V-8, a 3.6-L Turbo DI V-6, and a 2.2-L Turbo-VCR 4-Cylinder Engine (projected data)

TABLE 1. Benefits of Engine Downsizing

Type	V-8	V-6 Turbo DI	I-4 Turbocharged VCR
Displacement	5.7 L	3.56 L	2.2 L
Power	298 kW	283 kW	271 kW
At 2,000 RPM			
Peak Torque	445 Nm	560 Nm	445 Nm
Peak BMEP	9.8 bar	19.7 bar	25.4 bar
Fuel efficiency			
@ 100 Nm	328 g/kWh	276 g/kWh	230 g/kWh
@ 50 Nm	500 g/kWh	362 g/kWh	300 g/kWh

Approach

We propose to investigate the effect of variable CR on engine efficiency at MBT spark timing over the engine map with a VCR research engine designed and built by Envera LLC. This state-of-the-art engine will combine a production cylinder head utilizing direct fuel injection, cam phasers, and a custom engine block containing the VCR mechanism. Specifications for the engine are shown in Table 2.

Engine experiments will combine parametric sweeps of spark timing, CR, and cam phasing to determine the optimal efficiency at each engine speed/load operating condition. Emissions from the engine will also be measured before and after a three-way catalyst.

The experimental data of engine performance and emissions will be used to generate composite engine maps of engine efficiency and emissions (i.e. at best efficiency, constant CR, lowest emissions, etc). The engine maps will be used as inputs for computer simulations of vehicle drive cycles using the PSAT software to determine the real-world impact of VCR on fuel economy and emissions.

TABLE 2. ORNL Envera GDI-VCR Engine Specifications

Cylinders	Inline 4-cylinder
Displacement	1.886 L
Bore/Stroke	81.0/91.5 mm
Compression ratio	Variable
Maximum	18:1
Minimum	8.5:1
Crankcase material	A356 aluminum
Cooling	Electric water pump
Valve train	16-valve DOHC
Phase shifters	Intake and exhaust camshafts
Fuel delivery	Gasoline direct injection
Aspiration	Naturally aspirated as delivered (turbocharged upgrade capable)

Results

The Envera VCR engine has been built and is now being prepared for dynamometer testing. Assembly checks on key mechanical dimensions such as cylinder honing, thrust bearing clearances and cam timing were conducted by Automotive Specialists. Testing of the engine at Automotive Specialists is scheduled for the week of December 10th, 2012.

Conclusions

VCR technology enables significantly larger fuel economy gains to be achieved than can be accomplished with fixed CR engines. Under the current project, Envera is delivering a prototype gasoline direct-injection VCR engine to ORNL. ORNL will then conduct dynamometer tests to independently assess engine efficiency values, and use the engine for efficiency research and benchmarking.

References

1. Confer, K., "E85 Optimized Engine through Boosting, Spray Optimized DIG, VCR, and Variable Valvetrain." Presented at 2008 DOE Vehicle Technology Merit Review, http://www1.eere.energy.gov/vehiclesandfuels/resources/proceedings/2008_merit_review.html#fuels.

2. Yilmaz, H., "DOE Merit Review – Flex Fuel Vehicle Systems." Presented at 2008 DOE Vehicle Technology Merit Review, http://www1.eere.energy.gov/vehiclesandfuels/resources/proceedings/2008_merit_review.html#fuels.

3. Mendler, C. and R. Gravel, "Variable Compression Ratio Engine." Society of Automotive Engineers, 2002, Technical Paper 2002-01-1940.

4. A study of Potential Effectiveness of Carbon Dioxide Reducing Vehicle Technologies, Revised Final Report, June 2008, US EPA.

5. Christie, M. et. al Ricardo Ltd.: DI Boost: Application of a High Performance Gasoline Direct Injection Concept, SAE Paper no. 2007-01-1410, Pub. SAE 2007.

6. Kawamoto, N. et al. Toyota Motor Corporation: Development of New 1.8-Liter Engine for Hybrid Vehicles, SAE Paper 2009-01-1061, Pub SAE 2009.

V. SOLID STATE ENERGY CONVERSION

V.1 Gentherm Thermoelectric Waste Heat Recovery Project for Passenger Vehicles

D. Crane (Primary Contact)[1], J. LaGrandeur[1], C. Maranville[2], J. Maerz[3], M. Miersch[4]

[1]Gentherm Inc.
5462 Irwindale Ave.
Irwindale, CA 91706

DOE Technology Development Manager: John Fairbanks

NETL Project Manager: Carl Maronde

Subcontractors:

[2] BMW, Palo Alto, CA and Munich, Germany
[3] Ford Motor Company, Dearborn, MI
[4] Tenneco GmbH, Grass Lake, MI and Edenkoben, Germany

Overall Objectives

- A detailed production cost analysis for a thermoelectric generator (TEG) for passenger vehicle volumes of 100,000 units per year and a discussion of how costs will be reduced in manufacturing.
- A five percent fuel economy improvement by direct conversion of engine waste heat to useful electric power for light-duty vehicle application. For light-duty passenger vehicles, the fuel economy improvement must be measured over the US06 driving cycle.
- Confirmatory testing of the hardware to verify its performance in terms of fuel economy improvement.
- Build scaled-up TEG for TARDEC Bradley Fighting Vehicle.

Fiscal Year (FY) 2012 Objectives

- Select target vehicle platform and powertrain for TEG integration.
- Begin definition of vehicle system level requirements and boundary conditions.
- Define TEG design architecture.
- Develop one-dimensional (1-D) and three-dimensional (3-D) computer models for TEG design.
- Begin work on TE material model to help define methods and pathways towards TE material improvement.
- Begin work on sublimation and oxidation protection for TE material.
- Initial TE engine development and testing.
- Begin development on scale up TE fabrication methods.
- Kickoff TARDEC project extension.

Accomplishments

- Vehicle platform/powertrain selections have been made by BMW and Ford after extensive fuel efficiency improvement performance trade-off analysis. BMW will use a BMW X5 30i with a 4-cylinder gasoline engine. Ford will use a Ford Explorer with 2-L EcoBoost I-4.
- An initial TEG architecture design concept has been finalized which addresses issues associated with previous TEG designs:
  - Initial subcomponents (cartridges) modeled, built and tested.
  - Computational fluid dynamics (CFD) analysis and finite-element analysis (FEA) has begun along with 1-D MATLAB®/Simulink® modeling to further understand and optimize the design.
  - Work has also begun on TE material scale up methods relating to the cartridge design that will help lower cost and increase manufacturability.
- TE material improvement has begun with the construction of the "holistic performance model" for skutterudite (SKU) TE material.
- Early tests of oxidation/sublimation suppression coating systems indicate potential for success.
- TARDEC project extension kicked off in July 2012.

Future Directions

- Initial SKU cartridge is on schedule to begin test in December 2012.
- Further modeling, including MATLAB®/Simulink® and CFD/FEA, will continue to support a design freeze planned for the end of first quarter of 2013.
- Component, cartridge, and multi-cartridge-level testing to continue, for both performance and durability.
- Vehicle and TEG system requirements to be completed, with significant input from new partner, Tenneco.

- Further work on oxidation/sublimation suppression coating.
- Further development of the TE material model for SKU from Caltech.
- Scale up TE material and cartridge fabrication methods, including tooling and process development, for commercialization quantities.
- Cartridge test at TARDEC lab.

Introduction

Emission regulations continue to become more restrictive and fuel costs continue to rise. The need for vehicles with better fuel economy continues to be very important for vehicle manufacturers. With many fuel economy-saving technologies already implemented, vehicle manufacturers need to search for additional improvements. Waste heat recovery is one potential option with thermoelectric waste heat recovery being a leading candidate.

The objective of this project is to design and implement a 5% improvement in fuel economy for light-duty vehicles based on TE waste heat recovery while providing a path towards commercialization at passenger vehicle volumes of 100,000 units per year. Confirmatory testing of the hardware to verify its performance in terms of fuel economy improvement will be conducted.

In addition to building TEGs for passenger vehicles, an additional project component was added to build and test a TEG for a Bradley Fighting Vehicle for TARDEC. With a similar timeline to the passenger vehicle component, the TEG for TARDEC will be scaled up for the 15-L diesel engine of the Bradley Fighting Vehicle.

Approach

This project has a strong team that provides vital inputs at each stage of the project. The team includes two vehicle manufacturers: BMW and Ford to provide their needs for the TEG component. They will provide important information on the best platform and powertrain selection for successful commercial implementation. The Tier 1 exhaust supplier is Tenneco, who will translate the needs of the vehicle manufacturer into requirements for successful implementation into the exhaust system. Tenneco will also take the TEG subcomponents and package them (canning much like a catalytic converter) effectively into a TEG device that satisfies all of the vehicle and vehicle subsystem constraints. Gentherm, the overall lead of the project, will design, build, and test the TEG subcomponents for the project. These TEG subcomponents will be optimized based on the vehicle and vehicle subsystem requirements and the TE material performance. Extensive 1-D and 3-D modeling will be conducted by the team. 3-D models will be used to best understand the component details with the 1-D models used for comprehensive design optimization and for integration into vehicle system level models. These models will be rigorously validated against targeted experiments.

Gentherm will also spend considerable effort to develop TE material scale up capabilities for the most cost effective designs at 100,000 units per year. Research to development necessary oxidation and sublimation protection will also be conducted. The team also includes TE material improvement efforts from Caltech and 3rd party performance validation from the National Renewable Energy Laboratory.

Results

The Gentherm-led TEG project including subcontractors Ford, BMW North America, Tenneco (starting in Phase 2), Caltech, and the National Renewable Energy Laboratory formally started on October 1, 2011. Building off the successes and lessons learned of the previous DOE-funded project, an initial TEG architecture design concept has been finalized which addresses issues associated with former TEG designs. This new design is based on a more modular, scalable, and cost-effective approach using TEG subcomponents called “cartridges.” The cartridge, see Figure 1, is approximately 1 inch in diameter by 6 inches in length, will make between 25 and 50 watts of power and be “aggregated” to scale up to the required power level in an enclosure. Initial cartridges have been modeled, built and tested (see the test bench and test

FIGURE 1. TEG Cartridge

results in Figures 2 and 3). CFD and FEA analysis has begun along with 1-D MATLAB®/Simulink® modeling to further understand and optimize the cartridge design. An example of the 3-D analysis is shown in Figure 4.

Vehicle platform/powertrain selections have been made by BMW and Ford after extensive trade-off analysis. BMW will use a BMW X5 30i with a 4-cylinder gas engine. Ford will use a Ford Explorer with 2-L EcoBoost I-4.

Work has also begun on TE material scale up methods relating to the cartridge design that will help lower cost and increase manufacturability. TE material improvement has begun with the construction of the "ultimate performance model" for SKU by Caltech and early tests of oxidation/sublimation suppression coating systems indicate potential for success.

The team believes that the new cartridge-based TEG design (an initial concept is shown in Figure 5) will help achieve commercialization goals more readily than previous designs and put the team on a path towards

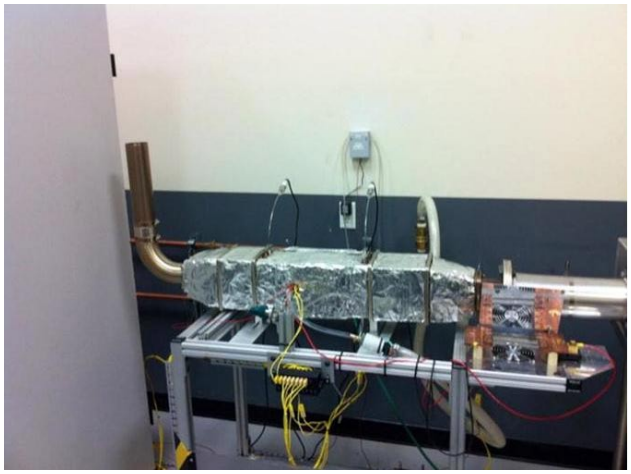

FIGURE 2. TEG Cartridge Test Bench

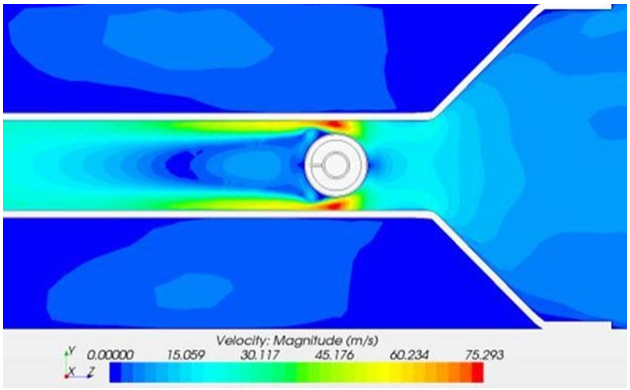

FIGURE 4. Gas Flow Analysis of Single Cartridge

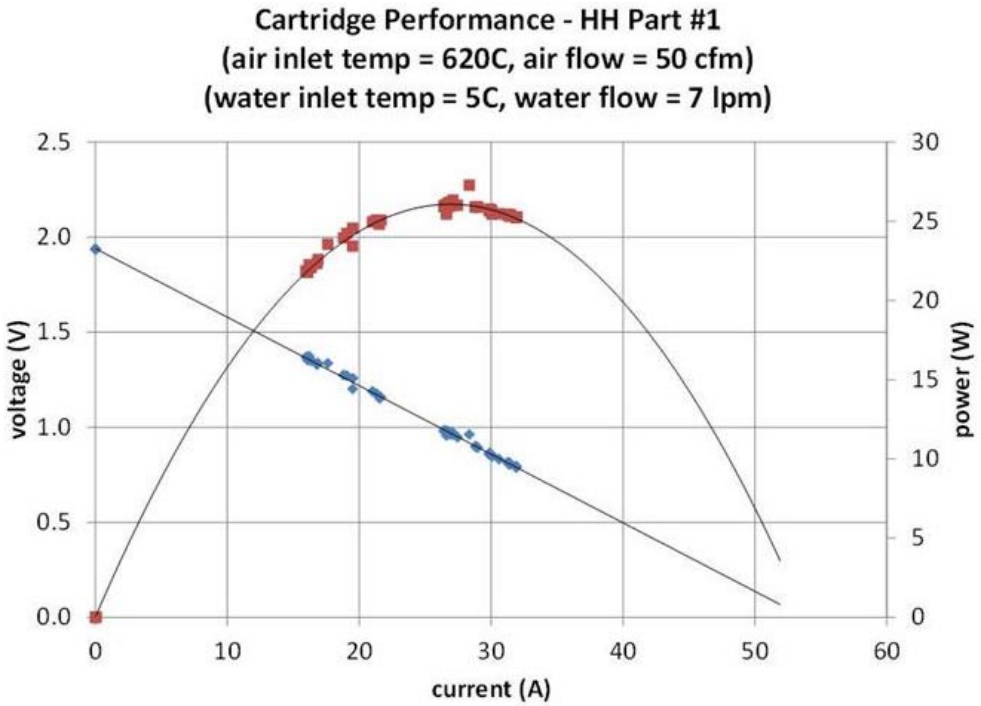

FIGURE 3. Initial TEG Cartridge Performance

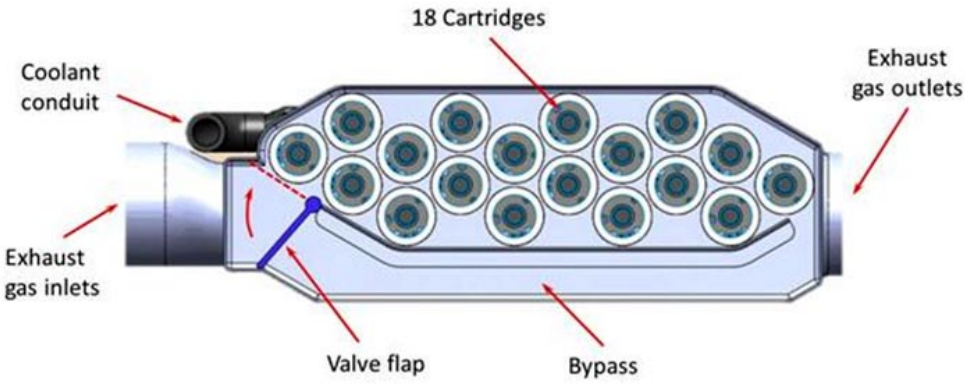

FIGURE 5. Initial TEG Concept Using Cartridge Subcomponents

the project goal of a cost effective TEG for passenger vehicles at a production volume of 100,000 units per year.

Conclusions

This activity has shown progress toward a modular, scalable, and cost-effective TEG design that is on a path to commercialization for the vehicle manufacturers.

- An initial TEG architecture design concept has been finalized which addresses issues associated with previous TEG designs with initial components modeled, built and tested.
- Vehicle platform/powertrain selections made by BMW and Ford after extensive trade-off analysis. BMW will use a BMW X5 30i with a 4-cylinder gas engine. Ford will use a Ford Explorer with 2-L EcoBoost I-4.
- Work has begun on TE material scale up methods relating to the cartridge design that will help lower cost and increase manufacturability.

FY 2012 Publications/Presentations

1. "Thermoelectric Generator Performance for Passenger Vehicles", Doug Crane, John LaGrandeur, March 20, 2012 presented at the Thermoelectric Applications Workshop in Baltimore, MD.

2. "Practical thermoelectric generators for automotive and industrial waste heat recovery", Doug Crane, Dmitri Kossakovski, Vladimir Jovovic, John LaGrandeur, Eric Poliquin, April 24, 2012 presented at SPIE conference in Baltimore, MD.

3. "TEG On-Vehicle Performance & Model Validation & What It Means For Further TEG Development", Doug Crane, John LaGrandeur, Vladimir Jovovic, Marco Ranalli, Martin Adldinger, Eric Poliquin, Joe Dean, Dmitri Kossakovski, Boris Mazar, Clay Maranville, July 11, 2012 presented at the International Conference on Thermoelectrics in Aalborg, Denmark.

4. "TEG On-Vehicle Performance & Model Validation", Doug Crane, John LaGrandeur, Vladimir Jovovic, Marco Ranalli, Martin Adldinger, Eric Poliquin, Joe Dean, Dmitri Kossakovski, Boris Mazar, Clay Maranville, October 18, 2012 presented at the Directions in Engine Efficiency and Emissions Research (DEER) Conference in Dearborn, MI.

V.2 Improving Energy Efficiency by Developing Components for Distributed Cooling and Heating Based on Thermal Comfort Modeling

Jeffrey Bozeman (Primary Contact),
Greg Meisner, Dr. Kuo-Huey Chen,
Dr. Taeyoung Han, E Gundlach, R Leach
General Motors LLC (GM)
30001 Van Dyke Ave
Warren, MI 48903

DOE Technology Development Manager:
Gurpreet Singh

Subcontractors:
- Delphi Thermal, Lockport, NY
- University of California at Berkeley (UC Berkeley), Berkeley, CA
- Faurecia Automotive Seating, Troy, MI
- University of Nevada at Las Vegas. Las Vegas, NV

Overall Objectives

Integrate thermoelectric (TE) technology in an automotive distributed cooling/ heating climate control system:

- Reduce fuel used for occupant comfort by 30% by localized use of TE technology.
- Integrate and test as a system in 5-passenger demonstration vehicle.
- Integrate and test an extended range electric vehicle (Chevrolet Volt).
- Improve TE generators - develop TE materials for engine heat recovery applications (to provide power TE heating, ventilation and air conditioning [HVAC] climate loads).

Fiscal Year (FY) 2012 Objectives

- Comfort model enhancement and validation.
- Finalize distributed TE devices design and testing on vehicle.
- Develop climate system efficiency metrics.
- Develop efficient TE coolant heater for the Chevy Volt's cabin and windshield defrosting system.

Accomplishments

- Team selection criteria lead to a 2012 eAssist Buick LaCrosse for final demonstration.
- All phases of testing benefit from UC Berkeley thermal manikin evaluation; providing detailed localized comfort measurement with an absence of psychological influence.
- Team has finalized the design and test for the Volt coolant TE heat exchanger.
- Volt test data showed the new coolant TE heater with coefficient of performance (COP) = 1 for extremely low temperature (large ΔT) and achieved COP > 2.3 depending on ΔT.
- The developed thermoelectric devices (TEDs) for the Lacrosse are being examined and plan to be modified and retrofitted into Volt demonstration vehicle.

Future Directions

- Phase 3 activities began in October; conclude April, 2013 with focus on commercial design of new comfort components and estimating efficiency improvements for the integrated system.
- Phase 4 activities begin in March 2013, conclude August 2013 with focus on final component integration into demonstration vehicle, test and evaluate distributed HVAC system in vehicle and calculate efficiency improvements of distributed system.
- Chevrolet Volt Phase 2 began in October, 2012 and is planned for completion in August 2013.

Introduction

This project employs human subject thermal testing to characterize the response to localized cooling and heating of human body segments, for inclusion in an automotive thermal comfort math model. The developed math model is used to identify the optimal locations for energy-efficient distributed cooling and heating components by selecting occupant body segments that are most sensitive to thermal comfort and can offset the comfort effects of warmer or cooler cabin ambient temperature. This knowledge is used to develop a distributed HVAC component set to supplement the central HVAC system. This configuration of components is integrated in a 5-passenger demonstration vehicle. The component configuration will be tested to prove the system reduces the energy required by the current centralized system by at least one third while maintaining

equal thermal occupant comfort. The advantage of the TE devices is their ability to integrate into the vehicle cabin with the device closer to the occupant for more efficiently energy transfer into the occupant. TE devices in a traditional vehicle utilize power at a cost of 0.3 mpg per 100 alternator Watts, whereas a traditional air conditioning (AC) compressor utilizes a more efficient crankshaft belt power at 0.2 mpg per 100 crankshaft Watts. This project also has a goal to develop TE materials to improve the efficiency of TE generators for directly converting engine waste heat to electricity. This energy can then be used to improve the efficiency of the climate control.

Approach

The following methodology is and has been used in this project:

1. **Applied Research – Phase 1**: Develop Thermal Comfort model of human responses to potential locations for distributed heating and cooling:
   - Identified locations for distributed HVAC components and measured their physiological and psychological effectiveness.
   - Used UC Berkeley environmental test chamber and mule vehicle to perform human subject testing.
   - Update UC-Berkeley's thermal comfort model as a "key component" of the Virtual Thermal Comfort Engineering computer-aided engineering (CAE) tool.
2. **Exploratory Development – Phase 2**: Develop the initial prototype HVAC components and evaluate on bench & mule vehicle:
   - Computational fluid dynamics (CFD) and vehicle design of experiments analysis.
   - Functional intent component manufacturing and vehicle integration.
   - Define control strategies and algorithms.
   - Build eAssist LaCrosse with design intent localized TE components.
3. **Advanced Development – Phase 3**: Develop final prototype HVAC components and evaluate on bench:
   - Optimize control system to balance comfort and consumption.
   - Estimate HVAC system efficiency improvements.
   - Commercialize TE components for future production application.
4. **Engineering Development – Phase 4**: Integrate final local and central HVAC components into demo vehicle and optimize system performance:
   - Build advanced propulsion demonstration vehicles.
   - Test and evaluate distributed HVAC system.
   - Calculate expected customer efficiency gain.
   - Deliver vehicle and final report.
5. **HVAC Material/Waste Heat Recovery Research – Phase 5**: Develop new TE generator materials (concurrent with phases 1-4) to produce power for the TE HVAC climatic loads

Results

Improving the Thermal Comfort Model

UC Berkeley incorporated the most recent published data about sweat distribution on the human body into their thermal comfort model. The newly published data allows the model to predict skin temperatures in warm conditions more accurately.

Following the changes to physiology modeling for sweat distribution and changes to the overall sensation model, UC Berkeley has been testing the updated model systematically under a matrix of test conditions. We compared the simulations with measured data and verified the improvement. As warm environments generally are the cause of sweat, we use the distributions of sweat under warm conditions. The distributions for the trunk regions (chest, back, and pelvis) are much smaller than the old values, but they are much larger for the hands and feet.

With the new sweat distributions, the simulated skin temperatures under warm conditions (between 30–50ºC) for the chest and pelvis are much higher than the simulated results with the old sweat distributions, and they are much closer to the measured data. As expected, at air temperatures between 30 and 50ºC, the simulated skin temperatures for hands and feet are lower with the new sweat distributions than with the old distributions. For feet, the simulated skin temperatures are closer with the new distributions than with the old distributions while for hands, the simulated skin temperatures with the old distributions are much closer to the measured data.

Development of a Distributed HVAC System and its TE-Based Components

The project team is working on the development and demonstration of the TED sub-assemblies that will provide distributed cooling and heating in the Buick eAssist LaCrosse demonstration vehicle. The team analyzed the individual TED designs to predict their COPs versus the targets of 1.3 and 2.3 respectively in cooling and heating modes. As part of the TED

component selection, the performance of fans and blowers were evaluated, and other parameters such as size were considered. To evaluate the overall system, the team worked on the definition of metrics for human comfort and energy efficiency. Multiple design iterations were analyzed using CFD to optimize the design for low total fan power at the expected airflows. Lower sub-system pressure drop was targeted to keep the parasitic wattage of all the fan low as well as to reduce the system noise. Low energy consumption is of paramount importance to the project objectives. Limitations from fitting a design to an existing vehicle posed significant challenges. The design of the TE sub-assembly is simpler if tailored to a new vehicle design. The presence of many critical vehicle operational and safety components made the design of the TE sub-assembly difficult. Parts were designed to keep new components as common as possible. Insertable metering devices are built into the designs for monitoring flow uniformity and thermal performance as needed during the climatic tunnel tests.

TED Development and Build

Marlow Industries developed optimum solutions for cooling and heating with TEs based upon the requirements specified by the team. The initial design utilized air as a heat transfer fluid on the waste side to provide the heat rejection during cooling and heat utilization. However, after several iterations, it was determined that air on the waste side was not satisfactory in terms of efficiency. Therefore designs were configured to waste side water. A COP vs. cost plot was evaluated to understand the return on more. The rate of return after 400-600 couples demonstrated little benefit. It is also understood that the number of couples and their cost would scale together; therefore, the number of couples is a good indication of the relative cost. Marlow completed detailed drawings of the liquid exchangers; Delphi and Marlow assessed preliminary assemblies and further studied system COPs to determine an optimal matrix of possible combinations. A final set of recommended designs were determined; Table 1 shows the COPs for the TE designs that will be evaluated and compared with the simulated COP values.

Several learnings were discovered early in the build: several iterations of TE devices were needed, the TE cooler with thermal grease had to be placed accurately or the grease smeared into other areas caused problems, and fastening the TED to the liquid heat sink allowing for proper compression was difficult. Marlow found the large TEs had an issue was related to an assembly error that caused one-half of the TE to act as a cooler while the other half was a heater. A recovery plan was developed to deliver large TEs, so as not to delay the project.

Metric Selection for Comfort and Energy Efficiency

Energy efficiency and comfort metrics are required to measure the energy savings from the TE HVAC system under equivalent comfort conditions. Energy efficiency for heat transferred into or out of the occupant is critical.

Human Comfort Metric

Two measurement methods are used for human comfort, the human subject comfort ride and the manikin in-car objective measurement. Both of these methods have been used in prior vehicle testing. The human subject comfort rides using the Thermal Sensation rating and Thermal Comfort ratings as defined by UC Berkeley are the main method of comfort measurement. Tablet data acquisition computers are used to record the comfort ratings in real-time as the riders experience the thermal environment in the tested vehicle. This provides actual, direct comfort assessment of the TE HVAC system. The supporting method of comfort measurement is the objective measurement of the in-car thermal environment using the UC Berkeley manikin. The temperature and heat flux measurement from multiple segments of the manikin body are composited to provide a thermal comfort indicator. From past experience, a whole body equivalent homogenous temperature (EHT) calculated via a direct average of the segmental EHT temperatures is not representative of the in-car comfort. UCB has provided an optimally weighted EHT that better represents the human in-car comfort. The quality of manikin representation deteriorates in a transient thermal

TABLE 1. COP Verses the Number of Thermocouples in the TED

COP with EGW Waste Side	1 Small 224 couples	1 Big 336 couples	2 Small 448 couples	2 Big 672 couples
Seat Heating Lower or Upper 41.9 W at 5.0 CFM	1.9	2.2	2.3	-
Face Cooling 13.4 W at 4.0 CFM	2.5	-	-	-
Lap/Foot Heating 43.6 W at 5.2 CFM	-	2.2	2.3	-
Chest Heating 67.1 W at 8.0 CFM	-	1.8	2.1	2.3

EGW - Ethylene Glycol Water (50% by weight); CFM – cubic feet per minute

environment as the transient thermal response of the manikin is different from that of the human body.

Energy Efficiency Metric

The TE HVAC system automotive energy consumption calculations include all the related components: HVAC blower, compressor, engine cooling fan and the prototype distributed system components: the TE modules, fans, waste heat exhaust fan and coolant pumps, etc. The measured energy saving will be annualized per established SAE International Life Cycle Climate Performance [1] methology to provide annual savings. Steady-state measurement of energy consumption is the main energy efficiency assessment criteria. Accurate and repeatable test data is obtained in the steady-state phase of the vehicle operation. The team expects additional energy savings during the transient phase of the car operation, and these additional savings from the TE comfort components are captured and characterized. Four methods of system energy consumption have been considered: vehicle testing in climatic tunnel, HVAC bench testing, HVAC system simulation, and vehicle testing in emission tunnel. Direct vehicle fuel economy measurement in the emission tunnel method measures the CO_2 discharge rate at the tailpipe to determine the vehicle fuel consumption rate. The baseline fuel consumption and the TE HVAC system enabled vehicle fuel consumption difference will give the energy efficiency impact of the TE HVAC system. However, as a vehicle level measurement method lack resolution, this method may not be able to differentiate the impact from the TE HVAC system accurately. It is thus viewed as an alternative or confirmative method for energy consumption measurement.

Controls Strategy and Hardware

Substantial resources were spent programming and debugging the software for the vehicle development control system (significant impact on project timing) due to the complexity driven by the large number of controllers and the devices that need management. Hardware development included the additional build of devices, packaging of these devices, development of occupant input interfaces, build of wire harnesses, and vehicle integration. User input panels were developed and integrated into the vehicle. These can be seen in Figure 1 and Figure 2.

These input panels provide the occupants a means to make adjustments to the system operation as desired. The front control panels were integrated in the center console with labeling oriented for easy reading from the intended seating position.

FIGURE 1. Front Seat Occupant Climate Control Input Panel

FIGURE 2. Rear Seat Occupant Climate Control Input Panel

Each front seat has five inputs for setting automatic operation, manual operation, or to turn the system off. Light-emitting diodes and switch ring lights provide user feedback on the state of operation. Similarly the rear input panel is mounted in the flip-down armrest in the center of the rear seat. In addition to the functionality of the front control panel, the rear panel also is used to specify whether the rear seating positions are occupied by the user pressing the “Left On” or “Right On” switches. For functional debugging of the software, the team constructed a software test bench (one seat area capable of simulating the TEDs, fans, and human-machine interface). The bench proved indispensable for initial debugging of TE component operations.

Vehicle Build and Instrumentation

The team prepared and completed climatic wind tunnel tests of initial prototype parts on the Buick eAssist LaCrosse demonstration vehicle. The overall basic cooling loop is designed to allow for waste heat removal of each TED. To further control the flow to each TE, a rotameter flow measurement device with feedback control is plumbed into the cooling circuit. The rotameters enable the proper flow to each TE, that being one liter/minute for each. After the flow is delivered to each TE, the coolant will be collected in a manifold that will deliver it to a reservoir prior to going to the waste heat exchanger. The waste heat exchanger will remove the waste heat delivered by the TE, or add heat as appropriate.

Development of Distributed TE HVAC for the Chevrolet Volt EV Application (Second Demonstration Property)

Heating coolant to warm occupants is not the most efficient method to warm an occupant, but it a necessary compromise understanding the need to also defrost the windshield. Front windshield defrosting could be accomplished with an electrical impregnated plastic layer in the composite windshield. This project elected to not utilize this electric heated windshield method as a replacement for coolant heating as 1) it is fully developed technology (usage would not further development of TE technology) and 2) is not considered practical for economical vehicle use. Electric windshields have been shown to cost in excess of $1,000 for field replacement and windshield replacement due to stone damage is 2 times annually common for some customers [2]. This development effort therefore is focused on providing improved heating efficiency beyond the electric vehicle baseline electrical resistive coolant heater. A plate and frame heat exchanger concept is developed that is designed specifically for use in conjunction with TE technology.

The technical challenges addressed include thermal interface, gasket, plate material, and mesh orientation optimization as well as high voltage experimental setup. Compared to the Beta prototype, the Gamma prototype will be safer (bent plate edge), lighter (smaller plates and gaskets), more versatile (shorter), and capable of handling much higher temperatures (gasket material of hydrogenated nitrile butadiene rubber). Figure 3 shows the Gamma prototype.

FIGURE 3. TE Coolant Heater Gamma Prototype

Development of the PC-Based Virtual Thermal Comfort Tool

The GM team is developing an extensive database that characterizes representative vehicles for each GM platform type. For each vehicle, we carefully modeled all AC outlets into the cabin. These includes four main AC panel outlets, two side window outlets, defrost outlet, heater outlets in the driver and front passenger foot well areas, floor outlets under the driver and front passenger seats, and finally outlets on the center console toward to the rear seat (if any). One of the features of the tool is that it provides a user interface to bring in the air velocity and temperature around the manikin and the vehicle panel temperature from an external CFD flow simulation. The team has tested and obtained valuable thermal sensation and comfort data for various spot cooling and heating configurations, and has used CFD to compute the flow and temperature according to the test conditions. In summary, we believe that the tool's thermal comfort prediction for the vehicle in the real world environment is very encouraging, and that these test successfully demonstrate the capabilities of the virtual thermal comfort tool.

Development Activities under the Waste Heat Recovery Objective

The project team made significant progress under the waste heat recovery objectives. Resources focused on high-temperature TE materials research, including the evaluation of melt-spun skutterudite materials, low-cost p-type skutterudite TE materials, and defect diamond-like materials. An evaluation of thermal interface

materials was also performed. Additional details are provided in protected quarterly reports.

Evaluation of Melt-Spun Skutterudite Materials

Magnequench has delivered several different formulations of n- and p-type skutterudite that were prepared by melt spinning of pre-melted charges. From our analysis we conclude that melt spinning combined with spark plasma sintering results in materials with properties comparable to those where annealing was performed. This annealing step can be eliminated, thereby increasing materials throughput and reducing cost and energy inputs for the production processes. In all cases, the as-spun ribbons can be completely converted to pure phase skutterudite in the matter of 20 minutes of processing including the heating ramps.

Low-Cost P-Type Skutterudite TE Materials

With the emphasis on the reduction of rare earth materials due to supply concerns, the current p-type formulations being considered for skutterudites, which are rich in rare earth, are not a long-term sustainable solution for automotive TE applications. With this in mind, we have begun to explore the TE properties of $CaxFe_4$-$yNiySb_{12}$. From the evaluation of transport measurements we find that the approach of altering the Fe to Ni ratio is a more effective approach for controlling the carrier concentration as compared to changing the filling fraction. There is little to no variation in the magnitude and temperature dependence of Seebeck coefficient, and, with the exception of one sample, the resistances are quite similar as well. It has been noted that Fe/Co containing p-type skutterudites have a wider band gap and so these formulations are predicted to undergo the transition to intrinsic conduction at higher temperatures and therefore not be as strongly affected by bipolar diffusion. Experiments were conducted that evaluated the material processing temperatures and hot pressing times. The highest temperatures and longest hot pressing times evaluated during this experiment produced the highest figure of merit (ZT).

Defect Diamond-Like Materials

Various zincblende or chalcopyrite compounds with a wide range of transition metal and tri-al ratios may contain structural vacancies, the amount of which increases with the increasing trial content. We have studied $(Cu_2Te)_{1-x}(Ga_2Te_3)_x$ to find out how the overall TE properties of this material are affected by the vacancy content. All the samples show p-type semiconducting behavior in the temperature dependence of the Seebeck and Hall coefficients. The structural vacancies were found to scatter both phonons and charge carriers. The highest ZT ~1.4 among the samples in this study was found at 840 K. The TE properties can be further tuned by doping. Mn has been found to be an effective dopant.

Evaluation of Thermal Interface Materials

In conjunction with Purdue University, GM R&D has been investigating the effects of carbon nanotube (CNT)-based thermal interface materials on the performance of an off-the-shelf Bi_2Te_3 module. The experiment is set up to measure the steady-state electrical power output of a module under a virtually constant thermal gradient. Initial findings indicate that there are gradual increases in the module open circuit voltage with changing the interface materials from nothing to grafoil to copper to single-sided CNT, and finally, the double-sided CNT array which showed the largest open circuit voltage. The open circuit voltage of the module is a sensitive function of the temperature gradient along the length of the legs. The larger open circuit voltage leads to a higher maximum power output and higher efficiency.

Conclusions

During the past year, the GM-led project team completed the following:

- Significant progress in the development and refinement of the UC Berkeley thermal comfort model, including improvements in the physiology model and further comparisons of the model's predictions with measured data.
- The personal computer version of the virtual thermal comfort tool with additional vehicle data generated for the CFD flow database and further validation of the tool's predictions.
- The team resolved issues with the distributed HVAC application including the TED development and build, built the prototype demonstration vehicle, and resolved unexpected issues with the control system. Climatic tunnel evaluation time of 6.5 weeks resulted in substantial analysis data.
- Two types of seating solutions were evaluated (delaying project completion) to ensure maximum efficiency on this critical customer interface.
- Unique development activities for the second application on the Chevrolet Volt are on track for completion as scheduled. The team addressed issues with the alpha and beta prototype heater design. The team completed construction and testing of the new beta prototype heater, achieving the target COP under certain operating condition, and identified enhancements for a new gamma prototype heater design.

- For the waste heat recovery objectives, the team investigated several high-temperature TE materials to research issues, and also evaluated thermal interface materials. The team investigated melt-spun skutterudite materials and modules, and also evaluated diffusion barriers for skutterudites.

References

1. Papasawa S,, Hill W, "GREEN-MAC-LCCP®: A Tool for Assessing Life Cycle Greenhouse Emissions of Alternative Refrigerants", SAE 2008-01-0828, April 2008, SAE World Congress, Detroit MI. http://papers.sae.org/2008-01-0828

2. Auto Glass Tech Center Knowledge Base, http://www.glasslinks.com/tips/htd1.htm

FY 2012 Publications/Presentations

1. Kaushik S., Han, T and Chen, K-H, "Development of a Virtual Thermal Manikin to Predict Thermal Sensation in Automobiles", SAE 2012-01-0315, April, 2012 SAE World Congress, Detroit, MI.

2. Chen, K-H, Kaushik, S, Han T, Ghosh, D and Wang, M, "Thermal Comfort Prediction and Validation in a Realistic Vehicle Thermal Environment", SAE 2012-01-0645, April, 2012 SAE World Congress, Detroit, MI.

3. A. Thompson, J. Sharp, J. Moczygemba, H. Wang, D. Brown, "Implementation and Performance of Skutterudite based Thermoelectric Generators", Presentation, International Conference on Thermoelectrics (Aalborg, Denmark; August 2012).

4. D. Ghosh, Mingyu Wang, E. Wolfe, K. Chen, S. Kaushik, and T. Han, Energy Efficient HVAC System with Spot Cooling in an Automobile – Design and CFD Analysis, SAE Int. J. Passenger. Cars – Mech. Syst., Vol. 5, pp.885-903, June 2012.

5. Yi Zhang, Xuezhi Ke, Paul R. C. Kent, Jihui Yang and Changfeng Chen "Anomalous Lattice Dynamics near the Ferroelectric Instability in PbTe,", Physical Review Letters 107, 175503 (2011) [appeared in October 21 issue].

V.3 Development of Cost-Competitive Advanced Thermoelectric Generators for Direct Conversion of Vehicle Waste Heat into Useful Electrical Power

Gregory P. Meisner (Primary Contact), James R. Salvador, Michael G. Reynolds, Norman K. Bucknor, Kevin Rober, Edward R. Gundlach, Richard W. Leach, Jennifer M. Stanek*, Joshua D. Cowgill*

General Motors Global Research & Development
(*GM Powertrain)
MC 480-106-224
30500 Mound Road
Warren, MI 48090

DOE Technology Development Manager: John W. Fairbanks

NETL Project Manager: Carl Maronde

Subcontractors:

- Brookhaven National Laboratory, Upton, NY
- Dana Thermal Products, Oakville, Ontario, Canada
- Delphi Electronics & Safety, Kokomo, IN
- Eberspaecher North America, Inc., Novi, MI
- Future Tech, LLC, Troy, MI
- Jet Propulsion Laboratory, Pasadena, CA
- Magnequench, Inc., Singapore
- Marlow Industries, Inc., Dallas, TX
- Michigan State University, East Lansing, MI
- Oak Ridge National Lab, Oak Ridge, TN
- Purdue University, West Lafayette, IN
- University of Washington, Seattle, WA

Overall Objectives

- Overcome major obstacles to the commercialization of automotive thermoelectric generator (TEG) systems.
- Develop an overall TEG system including all necessary vehicle controls and electrical systems and fully integrated onto a light-duty vehicle.
- Demonstrate fuel economy (FE) improvement of 5% over the US06 driving cycle.

Fiscal Year (FY) 2012 Objectives

- Select target vehicle for the project.
- Complete a gap analysis of the target vehicle and TEG system to determine specifications and requirements needed to achieve the 5% FE improvement.
- Conduct TE materials research and development to reduce fabrication costs and improve performance.
- Establish the preliminary requirements and design targets for the TE materials, TEG components, and TEG subsystem for the project.

Accomplishments

- Assessed skutterudite material and module performance.
- Identified parasitic thermal and electrical losses associated with diffusion barriers, thermal interfaces, and electrical interconnects.
- Achieved a projected 10% heat conversion efficiency for skutterudite TE modules in laboratory tests.
- Selected a full-size light duty truck as the project target vehicle.
- Completed the gap analysis that supports establishing the technology development requirements for the overall TEG system and supports the program objective to improve FE in light-duty vehicles by 5%.
- Determined that over 1 kW of TEG power will be needed to improve FE by 5% based on vehicle performance data, vehicle simulations, and system modeling.
- Developed improved modeling tools for a combined system model incorporating (1) an exhaust gas temperature model based on combustion power, (2) the TEG model based on our earlier work on the previous TEG project, and (3) a unified model of the vehicle high voltage electrical power bus.

Future Directions

- Select TE materials for prototype TE modules.
- Establish design targets for TEG components.
- Establish design targets for TEG subsystem.
- Fabricate and test TE modules for the TEG prototype.

Introduction

The development of a practical and fully integrated TEG for a production vehicle will be a significant step forward toward reducing energy consumption and lowering emissions associated with the U.S. transportation sector. Considerable innovation, however, is needed to overcome the major obstacles to TEG technology commercialization. This effort will culminate in the first application of high-temperature TE materials for high-volume use, and it will establish new industrial sectors with scaled up production capability on all needed TEG materials and components. TE waste heat recovery is a new area of commercial technology that will be implemented without the added burden of displacing any existing technology. Moreover, this major effort to commercialize TE based recovery of waste energy has significant potential beyond the automobile industry. Our work on automotive TEGs focuses on several innovative paths: (1) enhancing p-type material performance via band structure modification by doping and other compositional modifications, (2) optimizing TE material fabrication and processing to reduce thermal conductivity and improve fracture strength, (3) accelerating unique and novel routes to high volume production for successful market introduction of skutterudites, (4) incorporating new nanostructures and nanoscale approaches to reduce thermal interface resistances, (5) achieving high efficiency heat flows and optimum temperature profiles under the highly variable exhaust gas flow of typical automotive drive cycles with new and innovative heat exchanger and TEG subsystem designs, (6) developing new modeling and simulation capabilities, and (7) using new highly thermally insulating substances, e.g., aerogels, as potentially inexpensive encapsulation and insulation materials for TE technology. At the completion of this four-year project, we will have created a potential supply chain for automotive TEG technology and identified manufacturing and assembly processes for large-scale production of TE materials and components that include scale-up plans for the production of 100,000 TEG units per year.

Approach

This project benefits from the wealth of knowledge and understanding of advanced TE and automotive technology represented by General Motors (GM) and the members of the project team. GM has many years of experience leading TE projects, both federally [1] and internally funded [2], on new TE materials development, advances in TEG design, fabrication techniques, vehicle integration and testing methods [1], and distributed heating and cooling systems [3]. Vehicle applications of these projects have ranged from conventional light-duty vehicles (Figure 1) to GM's new extended-range

FIGURE 1. The Chevrolet Suburban target vehicle used for our previous TEG development project. The lower panel shows the underside view of the vehicle.

electric vehicle, the Chevrolet Volt. The current project builds on this prior work with the goal of moving advanced TE materials and module fabrication from the laboratory scale to mass production, and to develop a fully integrated and viable TEG design suitable for commercialization by the automotive industry. We have made significant advances in TE material performance through collaborative research and development for more than a decade, and our TE material partners all have extensive accomplishments in advanced TE technology. Our project team's expertise includes (a) TE material research, synthesis, and characterization [4], (b) thermal and electrical interfaces and contacts [5], and (c) skutterudite-based TE module fabrication and testing [1,6]. We are working on improving the performance of TE materials simultaneously with the development of high volume methods of TE material synthesis, TE module production, and thermal interface material fabrication [7]. The team has considerable expertise in heat exchanger design, computational fluid dynamics, and the packaging of automotive exhaust systems, including the design and commercialization of several exhaust gas heat exchangers for other waste heat recovery applications. We will use this technology as a starting point for the design of the TEG heat exchangers to optimize heat extraction for the maximum TE conversion of heat into usable electrical power. We will develop and implement effective strategies for module interconnection and power management that are

crucial to manufacturability and system efficiency, and we will leverage the team's expertise in hybrid electric vehicle technology and integrated circuits to design the electrical subsystem for the TEG and develop integrated circuit solutions for module interconnect and power management hardware that will be focused on durability and low-cost assembly.

We are now analyzing vehicle energy and FE data to help determine the target vehicle for this project. Our results indicate a hybrid vehicle gives the best opportunity for maximum FE improvement using the thermoelectrically generated power. We have examined target vehicle math data to establish packaging constraints, and we have begun modeling studies for the thermoelectric modules, heat exchangers, TEG subsystem, and vehicle system. The TE materials and module development work under this project focuses on optimizing the skutterudites and establishing cost-effective rapid synthesis and fabrication methods. To facilitate this work at GM and in collaboration with our subcontractors, several pieces of high temperature measurement equipment for materials and module assessment are available for this project at the GM Global Research and Development Center. A TE module test stand, for example, is shown in Figure 2.

Results

Our previous prototype skutterudite TE modules yielded a heat to electricity conversion efficiency of 7% for $\Delta T = 450$ K between the hot and cold side heat exchangers [8]. Our current progress on improving the intrinsic TE performance of the skutterudite material and on reducing thermal interface resistances has improved the efficiency to as much as 10% with the same applied ΔT. These results are shown in Figure 3. Additional improvement plus minimizing electrical contact resistances and other parasitic thermal losses are anticipated that should increase TE module efficiency even further.

Our analysis of four potential target vehicles conducted during this reporting period indicated that a large full-size truck (i.e., pickup or sport utility vehicle) with a gasoline engine was most likely to generate sufficient heat plus have a suitable baseline fuel economy for achieving a 5% FE improvement using TEG technology. In addition, this type of vehicle is a likely first application for TEG technology, so the selection (and subsequent development) will possibly speed up its commercial introduction in the automobile industry. For our gap analysis, we enhanced our vehicle modeling and simulation tools and conducted vehicle system simulations of the US06 driving cycle in order to compare baseline powertrain performance to the performance with a TEG installed on the vehicle. The maximum TEG operating temperature was limited to 450°C, and we assumed that TEG power was put on the high voltage bus at 90% efficiency and that there was a constant high voltage load of 350 Watts and 400 Watts of low voltage load. The results are shown in Figure 4 for the TEG initially at ambient temperature (cold) in the upper panel and for the TEG initially at 400°C (hot) in the lower panel. Table 1 summarizes these results, and it can be seen that the higher initial TEG temperature increases the total TEG power output from 532 Watts to 581 Watts and thereby increases the FE gain by nearly 1%, from 2.4% to 3.3%. We also note that additional electrical power consumption via vehicle electrification

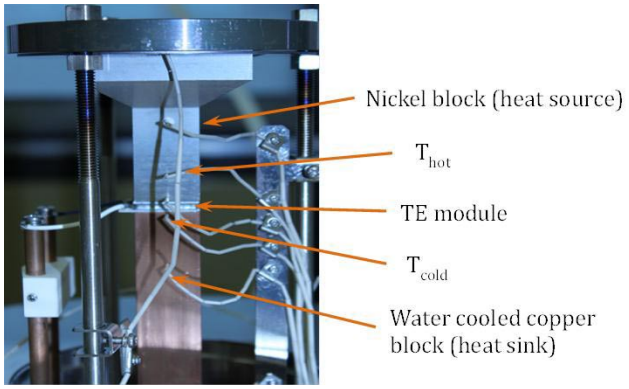

FIGURE 2. Measurement apparatus for TE module characterization. T_{hot} and T_{cold} are measured using thermocouples inserted into the nickel and copper blocks, respectively.

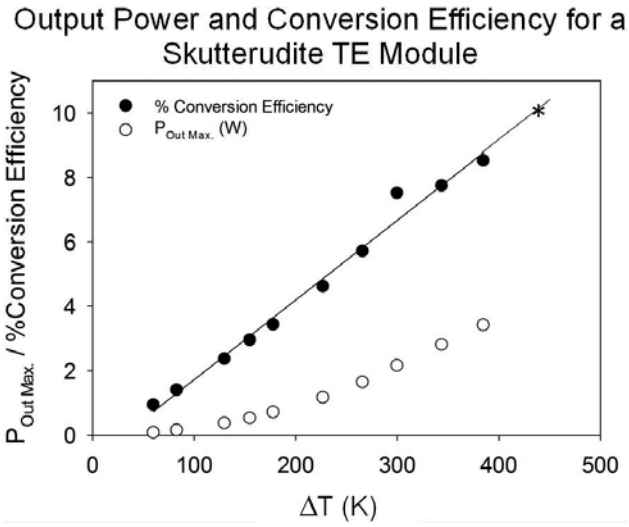

FIGURE 3. Performance of a skutterudite-based TE module with improved intrinsic properties of the TE material and reduced thermal resistances of interfaces between the module and the heat sinks. These data were collected using the apparatus shown in Figure 2. The asterisk (*) indicates an extrapolated TE module efficiency of 10% at $\Delta T = 450$ K.

TABLE 1. Initial simulation of full-size truck powertrain efficiency for a gasoline engine

	Baseline	With TEG	Gain (%)
US06 prep run completed: the engine is hot and the TEG is cold (initially at ambient)			
US06 FE (mpg)	21.7	22.3	2.4%
TEG Energy Out (kJ)	0.0	314	N/A
TEG Average Output Power (W)	0.0	523	N/A
Engine Efficiency (%)	33.2	33.3	0.2%
Powertrain Efficiency (%)	31.7	32.4	2.3%
US06 prep run completed: the engine is hot and the TEG is hot (initial at 400°C)			
US06 FE (mpg)	21.7	22.5	3.3%
TEG Output Energy (kJ)	0.0	352	N/A
TEG Average Power Output (W)	0.0	581	N/A
Engine Efficiency (%)	33.2	33.0	-0.8%
Powertrain Efficiency (%)	31.7	32.7	3.2%

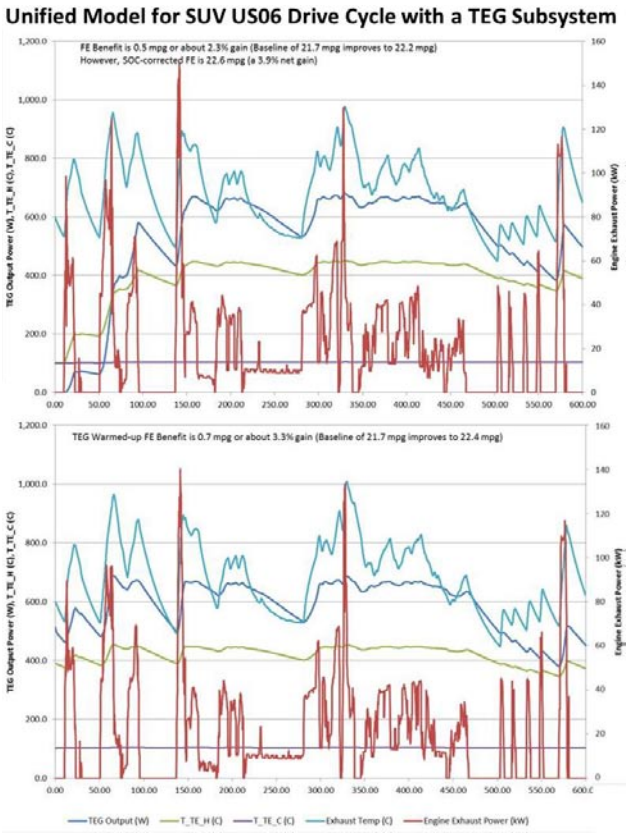

FIGURE 4. Vehicle simulation for a full-size sport utility vehicle over the US06 driving cycle using a TEG subsystem model based on our previous prototype. These results are for a warmed-up engine with the TEG cold (upper panel) and for a warmed up engine with the TEG warmed up to 400°C (lower panel). The TEG hot side high temperature was limited to 450°C (green line).

strategies and battery state of charge considerations will further increase the TEG-based fuel economy improvements.

Further improvements in these simulations and vehicle analyses will guide our TEG design process and will be made using actual vehicle data in the simulation. Data are being collected for this analysis using instrumented test vehicles equivalent to our proposed demonstration vehicle. Preliminary analysis of the physical aspects of the target vehicle determined the overall dimensions of the available space for a TEG located as close to the engine as possible.

Conclusions

- This project is focused on producing a TEG system with all necessary vehicle controls and electrical systems with full integration onto a light-duty vehicle for demonstrating fuel economy improvement of at least 5% over the US06 driving cycle.
- The large number of external partners (subcontractors) constitutes the entire supply chain necessary for the ultimate commercialization of TEG technology.
- We have identified specific barriers to a successful project that require the development of new engineering and materials technologies. Examples are:
  - Low resistance electrical contacts.
  - Low thermal resistance interface materials that operate at high temperatures (550°C).
  - Diffusion barriers for electrical and thermal contact stability within the TE modules.
- Commercial success requires advancement in the areas of:
  - Heat exchanger design, engineering, and manufacturing.
  - Exhaust systems, including vibration and noise control and back pressure mitigation.
  - Electrical power conditioning technology.
  - Vehicle component electrification.
  - Advanced vehicle controls and integration.
- Dual uses for the TEG and other exhaust system components could potentially reduce overall complexity and cost for implementing automotive TEG technology.

References

1. Work supported by GM and by DOE under cooperative agreement DE-FC26-04NT42278, by the Assistant Secretary for Energy Efficiency and Renewable Energy, Office of

Transportation Technologies. (b) Gregory P. Meisner "*Thermoelectric Generator Development for Automotive Waste Heat Recovery*" Directions in Engine-Efficiency and Emissions Research (DEER) Conference, 27–29 September 2010 Detroit MI.

2. GM Thermal Advanced Technology Work (ATW): TE exhaust heat recovery project, studying the technology limitations of readily available TE components and identifying the vehicle integration challenges of a thermoelectric generator (TEG) to a compact vehicle.

3. Work supported by GM and by DOE under cooperative agreement DE-EE0000014, by the Assistant Secretary for Energy Efficiency and Renewable Energy, Office of Transportation Technologies and the California Energy Commission, titled "*Improving Energy Efficiency by Developing Components for Distributed Cooling and Heating Based on Thermal Comfort Modeling*".

4. (a) X. Shi, H. Kong, C. P. Li, C. Uher, J. Yang, J.R. Salvador, H. Wang, L. Chen, W. Zhang, *Appl. Phys. Lett.* 2008, 92, 182101; (b) X. Shi, J. Yang, J.R. Salvador, M.F. Chi, J.Y. Cho, H. Wang, G.Q. Bai, J.H. Yang, W.Q. Zhang, L.D. Chen, *J. Amer. Chem. Soc.* 133(20), 7837 (2011).

5. Purdue's thermal resistance measurements using a photoacoustic technique showed thermal resistances as low as 1.7 $mm^2\ kW^{-1}$ for bonded VACNT films 25–30 μm in length and 10 $mm^2\ kW^{-1}$ for CNTs up to 130 μm in length. See: R. Cross, B. A. Cola, T. S. Fisher, S. Graham, *Nanotechnology*, 2010, *21,*445705.

6. T. Caillat "*Advanced High-Temperature Thermoelectric Devices*" DOE Thermoelectrics Applications Workshop, San Diego, 29 September 2009.

7. K.R. Saviers, S.L. Hodson, T.S. Fisher, L. Kasten, *"Carbon Nanotube Arrays for Enhanced Thermal Interfaces to Thermoelectric Modules,"* proceedings of the International Energy Conversion Engineering Conference, Atlanta, GA, 20 July 2012.

8. J.R. Salvador, J.Y. Cho, Z. Ye, J.E. Moczygemba, A.J. Thompson, J.W. Sharp, J.D. König, R. Maloney, T. Thompson, J. Sakamoto, H. Wang, A. A Wereszczak, G.P. Meisner, *"Thermal to Electrical Energy Conversion of Skutterudite-Based Thermoelectric Modules,"* J. Electronic Materials, DOI: 10.1007/s11664-012-2261-9.

FY 2012 Publications/Presentations

1. J.R. Salvador, G.P. Meisner, J.D. König, J. Moczygemba, J.W. Sharp *"Evaluation of Thermal to Electrical Energy Conversion of High Temperature Skutterudite-Based Thermoelectric Modules,"* presented at Directions in Engine-Efficiency and Emissions Research (DEER) Conference, Detroit, MI, 3 October 2011.

2. G.P. Meisner, *"Thermoelectric Conversion of Exhaust Gas Waste Heat into Usable Electricity,"* presented at the Directions in Engine-Efficiency and Emissions Research (DEER) Conference, Detroit, MI, 3 October. 2011.

3. J.R. Salvador, *"Skutterudite Based Thermoelectric Generator for Waste Heat Recovery in Passenger Vehicles,"* Invited presentation at Department of Physics, Central Michigan University, Mt. Pleasant, MI January 2012.

4. G.P. Meisner, *"Skutterudite Thermoelectric Modules for Waste Heat Recovery,"* presented at the American Physical Society (APS) March Meeting, Boston, MA, 1 March 2012.

5. J.R. Salvador, D.N. Brown, D.J. Miller, H. Wang, A.A. Wereszczak, *"Exploration of Melt Spinning as a Route to Large Volume Production of Skutterudite Thermoelectric Materials,"* presented at 3rd Thermoelectrics Applications Workshop 2012, Baltimore, MD, 20 March 2012.

6. G.P. Meisner *"Skutterudite Thermoelectric Generator for Automotive Waste Heat Recovery,"* presented at the 2012 Thermoelectrics Applications Workshop, Baltimore, MD, 20 March 2012.

7. M. Guch, C.R. Sankar, H. Kleinke, J.R. Salvador, G.P. Meisner, *"Improvements of the thermoelectric properties of PbTe via simultaneous doping with indium and iodine,"* J. Appl. Phys. 111(6) 63706 (2012).

8. S. Kumar, S. Heister, X. Xu, J.R. Salvador, G.P. Meisner, *"Thermal Design of Thermoelectric Generators for Automobile Waste Heat Recovery,"* presented at the ASME 2012 Summer Heat Transfer Conference, Puerto Rico, USA, 8–12 July 2012.

9. S. Kumar, S.D. Heister, X. Xu, J.R. Salvador, G.P. Meisner, *"Thermal Design of Thermoelectric Generators for Automobile Waste Heat Recovery"* Proceedings of the ASME 2012 Summer Heat Transfer Conference, Puerto Rico, USA, 8–12 July 2012.

10. X. Xu, L. Guo, J.R. Salvador, G.P. Meisner, *"Ultrafast Time-Resolved Investigations of Resonant Fillers in Filled Skutterudites,"* presented at the International Conference on Thermoelectrics, Aalborg Denmark July 2012.

11. J.R. Salvador, G.P. Meisner, J.D. König, J.E. Moczygemba, A.J. Thompson, J. W. Sharp, R. Maloney, T. Thompson, J. Sakamoto. *"Thermal to Electrical Energy Conversion of Skutterudite-Based Thermoelectric Modules,"* presented at the International Conference on Thermoelectrics, Aalborg Denmark July 2012.

12. J. Y Cho, M.M. Tessema, R.A. Waldo, J.R. Salvador, J. Yang, W. Cai, H. Wang, *"Thermoelectric Properties of p-type Skutterudites* $Yb_xFe_{3.5}Ni_{0.5}Sb_{12}$ *(0.8<x<1),"* Acta Materialia 60, 2104 (2012).

13. S. Ballikaya, N. Uzar, S. Yildirm, J.R. Salvador, C. Uher, *"High Thermoelectric Performance in In, Yb, Ce Multiple Filled* $CoSb_3$ *Based Skutterudite Compounds,"* J. Solid State Chemistry 193, 31 (2012).

14. K.R. Saviers, S.L. Hodson, T.S. Fisher, L. Kasten, *"Carbon Nanotube Arrays for Enhanced Thermal Interfaces to Thermoelectric Modules,"* presented at the International Energy Conversion Engineering Conference, Atlanta, GA, 20 July 2012.

15. J.R. Salvador, *"Challenges and Opportunities in Meeting 2020 CAFE Standards: The Chemist's Role in Sustainable Mobility,"* Keynote Address at the Two Year College Chemistry Consortium (2YC3) Meeting, Palatine, IL Sept 2012.

16. J.R. Salvador, G.P. Meisner, M.G. Reynolds, J.E. Moczygemba, A.J. Thompson, R. McCarty, D.N. Brown, D.J. Miller, *"Materials, Modules and Systems: An Atoms to Autos Approach to Automotive Thermoelectric Systems Development,"* presented at Directions in Engine-Efficiency and Emissions Research (DEER) Conference, Dearborn, MI, 15 October 2012.

17. J.R. Salvador, J.Y. Cho, Z. Ye, J.E. Moczygemba, A.J. Thompson, J.W. Sharp, J.D. König, R. Maloney, T. Thompson, J. Sakamoto, H. Wang, A.A Wereszczak, G.P. Meisner, *"Thermal to Electrical Energy Conversion of Skutterudite-Based Thermoelectric Modules,"* J. Electronic Materials, DOI: 10.1007/s11664-012-2261-9.

18. J.R. Salvador, G.P. Meisner, M.G. Reynolds, J.E. Moczygemba, A.J. Thompson, R. McCarty, D.N. Brown, D.J. Miller, *"Materials, Modules and Systems: An Atoms to Autos Approach to Automotive Thermoelectric Systems Development,"* presented at the Thermoelectrics Goes Automotive Conference, Berlin, Germany, 23 November 2012.

19. J.R. Salvador, G.P. Meisner, H. Wang, *"Thermoelectric Performance of Rare Earth-Free p-Type Skutterudite Materials,"* presented at the Fall 2012 Materials Research Society Meeting, Boston, MA, 27 November 2012.

Special Recognitions & Awards/Patents Issued

1. United States Patent US 8256220: "*Exhaust Gas Bypass Control for Thermoelectric Generator*" issued 4 September 2012.

2. United States Patent US 82286424: "*Thermoelectric Generator System and Method of Control*," issued 16 October 2012.

V.4 Nanostructured High-Temperature Bulk Thermoelectric Energy Conversion for Efficient Automotive Waste Heat Recovery

Jonathan D'Angelo[1] (Primary Contact), Yanliang Zhang[1], Xiaowei Wang[1], Jian Yang[1] Boris Kozinsky[2], Alan Mond[2], Varun Mittal[2], Steve Gladstein[2,] Zhifeng Ren[3], Jim Szybist[4]

[1]GMZ Energy
11 Wall St.
Waltham, MA 02453

DOE Technology Development Manager: John Fairbanks

NETL Project Manager: Carl Maronde

Subcontractors:
[2] Bosch of North America, Farmington, MI
[3] Boston College, Chestnut Hill, MA
[4] Oak Ridge National Laboratory, Oak Ridge, TN

Overall Objectives

- Develop a robust thermoelectric generation (TEG) system that will provide at least 5% fuel efficiency improvement for a light-duty vehicle platform.

Fiscal Year (FY) 2012 Objectives

- Achieve thermoelectric device level efficiency, i.e. bismuth telluride devices with 4% efficiency between 80°C to 200°C and half-Heusler devices with 4% efficiency between 200°C to 450°C.
- Heat exchanger and thermoelectric system design, including initial model of temperatures.
- Initial vehicle model with preliminary integration of the effects of thermoelectric power generation.
- Initial testing plan including preliminary hardware design for instrumentation and electric power integration.
- Initial cost assessment and production cost analysis with basic raw materials cost and device and system estimates.

Accomplishments

- Achieved and surpassed Phase 1 Go/No-Go milestone. Fabricated bismuth telluride devices with 4.3% efficiency between 80°C to 200°C and half-Heusler devices with 4.3% efficiency between 200°C to 450°C.
- Designed TEG systems that can produce up to 500 W electricity.
- Demonstrated up to 4% fuel economy improvement with simulated TEG power output of 480 W.

Future Directions

- Build reliable thermoelectric modules with >4.5% efficiency.
- Design and build robust heat exchangers with >50% thermal efficiency.
- Build and test thermoelectric generators in selected vehicle platforms and achieve maximum fuel economy improvement with minimum cost.

Introduction

Improvement of automotive engine efficiency is crucial to the conservation of petroleum and energy sustainability. Engine waste heat accounts for >30% of the total energy consumption in a vehicle. Thermoelectric conversion is a solid-state process that can convert waste heat in engine exhaust into useful electricity and thus improve engine efficiency. With recent developments in thermoelectric materials, TEGs bear promises to achieve high-efficiency energy conversion in automotive waste heat recovery applications.

Approach

This project utilizes high performance nanostructured bulk thermoelectric materials developed at GMZ Energy using our unique nanostructuring approach. The team will meet the project goals of 5% fuel economy improvement by direct conversion of engine waste heat to useful electric power for light-duty vehicle application using significantly improved thermoelectric materials and an innovative two-stage cascade design. The TEG will interact with the exhaust gases through post- catalytic converter heat exchangers designed and fabricated to give minimal pressure drop while maximizing the heat transfer from the exhaust stream to thermoelectric systems.

The following methodology has been used in this project:

- Improve thermoelectric material intrinsic efficiency and reduce cost through composition optimization.
- Develop high-temperature thermoelectric module and characterize efficiency, power density and reliability.
- Design and simulation of heat exchanger and thermoelectric systems using computational fluid dynamics and finite element methods.
- Build TEG prototype and integrate it with a light-weight vehicle.
- Perform vehicle test and characterize the fuel economy gain with a TEG.

Results

A significant achievement in material development during Phase 1 was the reduction of the hafnium in the half-Heusler material. Hafnium has the largest cost (450 $/Kg) by an order of magnitude over any other elements in the material system. With work done in collaboration between Boston College and GMZ, the hafnium concentration was reduced from 0.75 to 0.25 without affecting ZT (shown in Figure 1).

During Phase 1, one major milestone for GMZ is to develop power generation devices of 4% efficiency at specified temperature gradient. The TEG device is the core technology that drives the DOE Vehicle Technologies Program project. Without efficient power generation devices the project goal of a 5% fuel efficiency increase cannot be achieved. Table 1 shows measurement results of bismuth telluride and half-heusler devices fabricated and measured at GMZ. The efficiency of 4.3% has been achieved in these devices, which surpassed the Phase 1 Go/No-Go milestone of 4%.

TABLE 1. Bismuth Telluride and Half-Heusler Device Efficiency Measurement Results

	T_{hot} (˚C)	T_{cold} (˚C)	Efficiency (%)	Power Density (W/cm^2)
Bismuth Telluride	200±5%	80±5%	4.3	0.312
half-Heusler	450±5%	200±5%	4.3	2.44

The next important step following thermoelectric devices is TEG system design. In Phase 1, a three-dimensional (3-D) multi-physics thermoelectric system design model has been built using computational fluid dynamics and finite element method in ANSYS. Figure 2 shows electric power output and pressure drop calculated as a function of the heat exchanger fin packing fraction. Based on the exhaust temperature of 600˚C and mass flow rate of 30 g/s, the system shows about 460 W peak power output with about 1 KPa pressure drop. Much higher power output can be achieved by further improving heat exchanger design in Phase 2.

Along with the 3-D model, a one-dimensional (1-D) transient model has been developed by Bosch. This is an initial model that will be further improved and validated in the future. Three modeling approaches were compared: steady state, map lookup, and transient. The power output from the simulation is shown in Figure 3. The mean power output of transient simulation is higher than the map lookup approach, but lower than the steady estimate approach. The preliminary results from this model provide information about the electrical circuit requirements of the device, and the effect of different

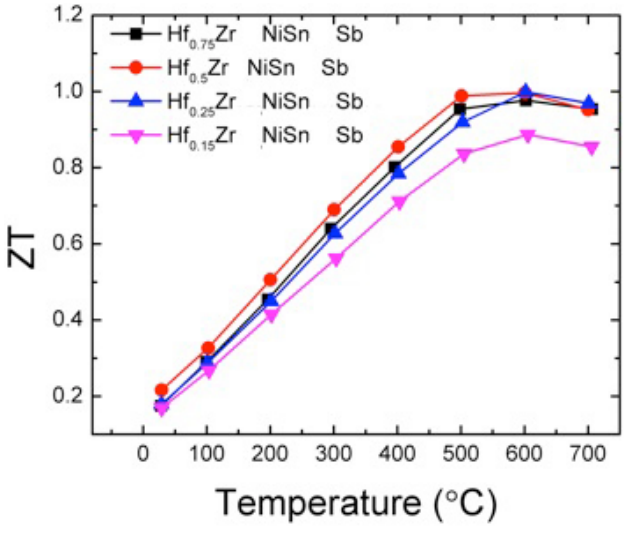

FIGURE 1. Half-Heusler figure of merit (ZT) as a function of hafnium composition.

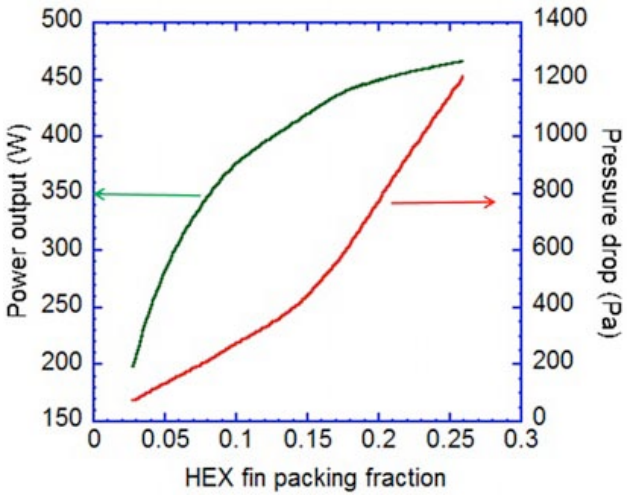

FIGURE 2. Electric power output and pressure drop calculated as a function of the heat exchanger fin packing fraction.

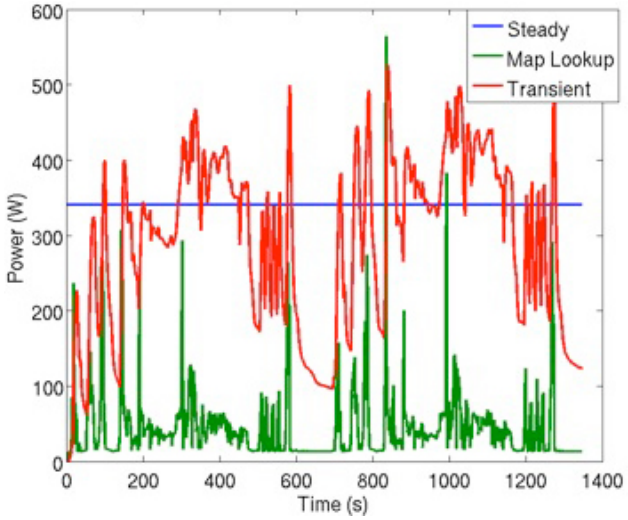

FIGURE 3. Generator power output over the US06 cycle from different modeling approaches.

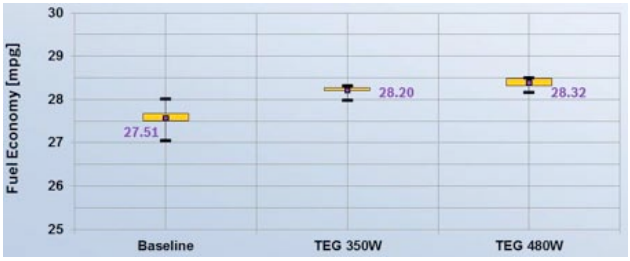

FIGURE 4. Fuel economy measured as a function of power output from a power supply (simulated TEG) over the US06 driving cycle.

module placements. In the following quarters, this 1-D model will be validated against detailed 3-D simulations and experiments.

Figure 4 shows fuel economy measured as a function of power output from a power supply (simulated TEG) over the US06 driving cycle without additional electrical consumers. Since there are two independent methods (electronic control unit and carbon balance based) that can be used to measure the fuel economy, every test is represented twice. Despite measurements exhibiting a large uncertainty, the overall average results of performed tests is given in Figure 4.

The vehicle with baseline configuration has a fuel economy of 27.51 mpg. The fuel economy reaches 28.20 mpg and 28.32 mpg with the power supply of 350 W and 480 W, which correspond to 2.31% and 2.94% fuel economy gain respectively. The highest gain in fuel economy was achieved over the Highway driving cycle of + 2.97 % (330 W) and + 4.07 % (480 W).

Conclusions

In Phase 1, significant progresses have been achieved in material cost reduction, thermoelectric device development, thermoelectric system design and vehicle model test. Specific accomplishments are as follows:

- Material cost is reduced significantly, which is realized through Hafnium reduction from 0.75 to 0.25 atomic concentrations.
- Thermoelectric devices show over 4% efficiency in both low temperature bismuth tellurium device and high temperature half-Heusler device.
- Both 3-D steady-state thermoelectric system model and 1-D transient model have been developed. Initial thermoelectric system design shows 460 W power output with less than 1 KPa pressure drop.

FY 2012 Publications/Presentations

1. J. D'Angelo, Y. Zhang, B. Poudel, G. Joshi, C. Caylor, "High-Temperature Power Generation Devices from Nanostructured Half-Heusler Materials," *International Conference of Thermoelectrics,* Aalborg, Denmark, July 2012.

2. G. Joshi, J. D'Angelo, J. Yang, T. Pantha, Y. Zhang, C. Caylor, B. Poudel, "ZT Enhancement and Developing a Contact Layer on Nanostructured Half-Heuslers," *International Conference of Thermoelectrics,* Aalborg, Denmark, July 2012.

3. Yanliang Zhang, Jonathan D'Angelo, Xiaowei Wang, Chris Caylor, "A comprehensive multi-physics model on thermoelectric generators for waste heat recovery applications", *Directions in Engine-Efficiency and Emissions Research (DEER) Conference*, Michigan, Oct., 2012.

4. Jian Yang, Giri Joshi, Jonathan D'Angelo, Yanliang Zhang, Chris C. Caylor, Bed Poudel, "Enhancement of Thermoelectric Figure-of-merit and Development of Metallization on Half-Heuslers", *Material Research Society Fall Meeting*, Boston, Nov. 2012

Special Recognitions & Awards/Patents Issued

1. Patent application number 61664012, "Thermoelectric Power Generation System Using Gradient Heat Exchanger", Y. Zhang, June 25, 2012.

V.5 NSF/DOE Thermoelectrics Partnership Project SEEBECK: Saving Energy Effectively by Engaging in Collaborative Research and Sharing Knowledge

Dr. Joseph P. Heremans
The Ohio State University (OSU)

Dr. Guo-Quan Lu
Virginia Tech (VT)

Dr. Mercouri G. Kanatzidis
Northwestern University (NU)

Objectives

The goal is to advance work in the thermoelectric (TE) field by focusing on (a) materials research (OSU/NU) to develop advanced TE materials made from cheap, environmentally friendly and earth abundant elements (b) thermal management system design to minimize losses by minimizing the number of interfaces, the amount of material used and maximize the durability of the product (c) optimize interfaces (VT/ZTPlus): metallization of the TE materials, device interconnection and flexible bonding to increase durability and reduce performance losses. OSU chose to work on Mg_2X systems and NU on PbS as most attractive materials (synthesis and characterization) while VT is working to identify a suitable diffusion barrier to silver (Ag) and demonstrate the sintering of nanoscale Ag paste as an attachment technique and evaluate its bonding quality.

Approach and Accomplishment

Mg_2Sn: Theoretical calculation from collaborators of AGH-University (Poland) shows that Ag, copper (Cu) and zinc (Zn) are resonant impurities and might distort the density of state of Mg_2Sn, suitable for high thermopower (S). We synthesized pure Mg_2Sn and doped it with Ag, Cu, Zn and Indium (In) as a reference impurity. Thermomagnetic and galvanomagnetic measurement show that Ag-doped samples are p-type with a maximum power factor of 18μ $Wcm^{-1}K^{-2}$, a maximum figure of merit (zT) of 0.25 at 540 K and a high effective mass of 0.9 m_o.

PbS: By using our endotaxial approach to nanostructure PbS using SrS or CaS as the second phases we produce spectacular reductions in the thermal conductivity (κ_l) of PbS. Nanoscale precipitates and point defects play an important role in reducing κ_l but the contribution from nanoscale precipitates of SrS is greater than that of CaS, whereas the contribution from point defects in the case of CaS is greater than that of SrS. κ_l at 723 K can be reduced by ~50% by introducing up to 4 at% of either SrS or CaS. zT values as high as 1.3 at 923 K can be achieved for p-type PbS with 3 at% SrS and 1.2 for n-type PbS with 4% SrS. No deterioration was observed after a 15 d annealing, indicating their excellent thermal stability. PbS is extremely environmentally stable and pound for pound the least expensive thermoelectric material under consideration today.

Titanium-Tungsten Alloy (Ti10W90wt%) as a Barrier Diffusion: The diffusivity of Ag in Ti-W thin films deposited on silicon (Si) substrate by sputtering is calculated by Sauer–Freise–den Broeder inverse solution and is about 1×10^{-15} cm^2/s at 793 K suggesting that Ti-W barrier can efficiently prevent Ag diffusion. Roughness and concentration profile are also characterized after annealing.

Sintered Nano-Ag Paste to Attach Mechanical Chips on Ag-Coated Substrates: Bonding quality was characterized by die-shear testing. The study of the effect of processing parameters using a fractural factor design experiment shows that pressure and time during drying and sintering influence the bonding quality, separately, with little coupling effect. Microstructure of the bondline fabricated under different drying pressure show that the porosity of sintered Ag can be controlled by varying pressure in the drying stage.

A new type of nano Ag paste (nanoTach-X) was developed to eliminate sintering pressure. Mechanical chips were used for device attachment. It produces excellent bonding quality (~25 MPa die-shear strength and free of large voids).

Status

There are two challenges to overcome to obtain higher zT in Mg_2Sn. Firstly, S of Ag-doped samples bend over at 500 K. As a potential waste recovery heat system, it is recommendable that maximum S reaches 700 K implying the need to widen the bandgap. Secondly, lattice κ_l is dominant in Mg_2Sn. So, phonon scatterings are required. Future research will focus on the use of Si to overcome these two challenges since experimentally, addition of Si greatly reduced κ_l P-type $Mg_2Sn_{1-x}Si_x$ will be studied.

We will work closely with our partners and the industrial colleagues to integrate our findings with their latest development in TE materials and devices. Specifically we will focus our effort on the following two tasks. (a) The thermal and electrical properties of nano-Ag sintered bonding layer between TE element and heat exchanger will be characterized. The goal is to develop a bond layer with an electrical contact resistance $<10^{-5}\Omega cm^2$ and a thermal contact resistance $<10^{-3}KW^{-1}cm^2$. (b) Thermomechanical reliability of nano-Ag sintered bonding layer will be tested. The goal is to fulfill the integration and packaging of TE devices with an overall performance that is not degraded by more than 20% over the theoretical performance of the material, with a 10-year lifetime, and the capability to withstand 10^6 thermal cycles from 773 K to 300 K.

Published

1. K. Xiao, J. Calata, K. Ngo, D. Ibitayo and G-Q Lu, "Large-Area Chip Attachment by Sintering Nanosilver Paste: Process Improvement by Nondestructive Characterization," *Transactions of the Japan Institute of Electronics Packaging*, **2011**, *4*,101.

2. Biswas, K.; Zhao, L.D.; Kanatzidis, M.G. Tellurium-Free Thermoelectric: The Anisotropic n-Type Semiconductor Bi2S3, *Advanced Energy Materials*, **2012**, *2*, 634.

3. Zhao, L.D.; He, J.Q.; Hao, S.Q.; Wu, C.I.; Hogan, T.P.; Wolverton, C.; Dravid, V.P.; Kanatzidis, M.G. Raising the Thermoelectric Performance of p-Type PbS with Endotaxial Nanostructuring and Valence-Band Offset Engineering Using CdS and ZnS, *Journal of the American Chemical Society*, **2012**, *134*, 16327.

4. Zhao, L.D.; He, J.Q.; Wu, C.I.; Hogan, T.P.; Zhou, X.Y.; Uher, C.; Dravid, V.P.; Kanatzidis, M.G. Thermoelectrics with Earth Abundant Elements: High Performance p-type PbS Nanostructured with SrS and CaS, *Journal of the American Chemical Society*, **2012**, *134*, 7902.

5. Zhao, L.D.; Lo, S.H.; He, J.Q.; Li, H.; Biswas, K.; Androulakis, J.; Wu, C.I.; Hogan, T.P.; Chung, D.Y.; Dravid, V.P.; Kanatzidis, M.G. High Performance Thermoelectrics from Earth-Abundant Materials: Enhanced Figure of Merit in PbS by Second Phase Nanostructures, *Journal of the American Chemical Society*, **2011**, *133*, 20476.

Conferences/Proceeding (underlined presenting author):

1. H. Zheng, J. Calata, K. Ngo, S. Luo, and G-Q Lu, "Low-pressure (<5 MPa) Low-temperature Joining of Large-area Chips on Copper Using Nanosilver Paste," in *Proceedings of International Conference on Integrated Power Electronics Systems* (CIPS) 2012, Nuremberg, Germany, (March 6–8).

2. K. Xiao, J. Calata, H. Zheng, K. Ngo, and G-Q Lu, "Large-area Nanosilver Die-attach by Hot-pressing Below 200°C and 5 MPa," International Conference and Exhibition on High Temperature Electronics (HiTEC) 2012, Albuquerque, New Mexico, USA, 2012 (May 8–10).

3. S. Kim, E. Evola, M.D. Nielsen and J.P. Heremans "The search for resonant levels in Mg2Sn", paper B4.10, *Material Research Society fall meeting* (MRS), 2012, Boston, Maryland, USA (November 25–20).

Submitted

1. K. Xiao, J. Calata, H. Zheng, K. Ngo, and G-Q Lu, "Simplification of the Nanosilver Sintering Process for Bonding Large-Area Semiconductor Chips: Reduction of Hot-Pressing Temperature below 200°C", submitted to *Transactions on Components, Packaging and Manufacturing Technology* (Sept, **2012**).

2. H. Zheng, J. Calata, D. Berry, K. Ngo, S. Luo and G-Q Lu, "Low-pressure Joining of Large Area Devices on Copper Using Nanosilver Paste", submitted to *Transactions on Components, Packaging and Manufacturing Technology* (Sept, **2012**).

V.6 NSF/DOE Thermoelectrics Partnership: Purdue – GM Partnership on Thermoelectrics for Automotive Waste Heat Recovery

Xianfan Xu (Primary Contact),
Timothy S. Fisher, Stephen D. Heister,
Timothy D. Sands, and Yue Wu
Purdue University

This research project is in collaboration with the General Motors Global R&D (GM) to develop thermoelectric generators (TEGs) for automotive waste heat recovery. The focus areas of our research are:

1. Advancing the performance of skutterudites through phonon engineering.
2. Development of nanowire thermoelectric materials.
3. Development of metal-semiconductor laminate thermoelectric materials.
4. Development of efficient heat exchanger and system level thermal modeling
5. Development of thermal interface materials.

The following describes approaches and achievements of each research areas:

1. Advancing the performance of skutterudites through phonon engineering: We employ ultrafast pump-probe technique to investigate the dynamics of energy carriers including electrons, holes and phonons in partially filled skutterudites. Skutterudites with different compositions were investigated for the different carrier dynamics. It was shown that in misch-metal filled skutterudites, lattice thermal conductivity is significantly reduced due to the interaction of the fillers and the host lattice. On the other hand, in multiple-filled skutterudites, several host-lattice interaction modes were found, which scatter a broader spectrum of phonons. The current status of the study is to focus on the dynamics of photo induced carriers, electrons and holes, in skutterudites with different compositions and filling ratios. This will help to understand the differences in electrical and thermal conductivity among different types of partially filled skutterudites, particularly p-type materials which have a relatively low thermoelectric figure of merit (ZT) at high temperatures.
2. Development of nanowire thermoelectric materials: The objective of this task is to identify the suitable materials and nanostructures for mass production and large-scale deployment of TEGs to improve energy efficiency. The approach we take is through the analysis of the abundance, the cost, the performance, and the toxicity of each individual elements in the common thermoelectric materials as well as the development of solution-phase scalable synthetic methods to mass produce advanced thermoelectric nanostructures at low cost. Our accomplishments up to date include (1) identifying materials for high temperature thermoelectric; (2) developing solution-phase method to synthesize chalcogenide nanowires with thermoelectric performance better than the state of the art; and (3) exploring complex metal sulfides as potential candidates to replace tellurides and antimonides for mid temperature range thermoelectric application.
3. Development of metal-semiconductor laminate thermoelectric materials: Work is currently focused on TiN/(Al,Sc)N as a potential high temperature thermoelectric materials system. iN/(Al_xSc_{1-x})N superlattices (with $0.6<x<0.8$ and periods ranging from 8-40 nm) were deposited on (001) MgO, (0001) sapphire and (001) Si substrates. High-resolution X-ray diffraction analysis along with reciprocal space X-ray mapping indicates that the growth is epitaxial and pseudomorphic with columnar morphology on the MgO substrates. Superlattices grown on sapphire and Si are polycrystalline with local epitaxy internal to the grains. X-ray reflectivity analysis indicates sub-nanometer surface and interface roughness of the samples grown on MgO substrates, while the roughness values are much lager for samples grown on sapphire and Si substrates. Cross-plane electrical transport studies indicate metallic transport within a small temperature range of 30-170°C. Efforts are underway to study the high temperature thermoelectric properties, including the Seebeck coefficient, electrical conductivity and thermal conductivity of these superlattices for their potential applications in thermoelectric devices.
4. Development of efficient heat exchanger and system level thermal modeling: A multidimensional computational model of the TEG has been created with the objective of defining optimal topologies and overall power production for given design conditions. The model includes heat transfer from exhaust gas to fins or walls of the TEG, as well as through the various wall elements and legs of the thermoelectric modules (TEMs). Rectangular, hexagonal, and circular topologies have been studied

using skutterudite and bismuth-telluride TEMs and optimal configurations have been identified for each topology. Detailed modeling of the TEM legs is underway in order to include the effects of ZT changes with leg type (p vs. n leg), leg area, and leg length. Using this improved tool, a complete optimization of the TEM/TEG system can be conducted.

5. Development of thermal interface materials: A key area in the system level integration of a thermoelectric module is the interface between each material. A metrology technique to measure interface resistance is currently being developed. The first design has been completed, achieving 150°C, and currently a redesign phase is in process to achieve higher interface temperatures (up to 700°C). Thermal interface material (TIM) development is also progressing, utilizing vertically aligned carbon nanotube (CNT) arrays. Currently, the focus is on CNTs synthesized on copper foil and graphitic foil of thicknesses 100 µm and 130 µm, respectively. A copper foil TIM with CNTs on both sides placed on the external face of a TE module on the hot side has resulted in an interface resistance of 17 mm^2K/W, which corresponds to a 60% relative increase in TE module efficiency compared to a condition with no interface material and a 25% relative improvement compared to a bare copper foil. To increase the thermal stability of the material, boron nitride doping of CNTs has been achieved, thus increasing the thermal decomposition temperature. The chemical doping process is currently being refined to increase the thermal stability further.

List of Publications

1. Guo, L., X. Xu, J.R. Salvador, and G.P. Meisner, Resonant Oscillations in Multiple-Filled Skutterudites, presented at the 31st International & 10th European Conference on Thermoelectrics. Also, submitted to Journal of Electronic Materials.

2. Wang, Y., Qiu, B., McGaughey, A., Ruan, X., and Xu, X., Mode-Wise Thermal Conductivity of Bismuth Telluride, J. Heat Transfer, accepted.

3. Kumar, S., Heister, S., Xu, X., Salvador, J.R., and Meisner, G.P., "Thermal Design of Thermoelectric Generators for Automobile Waste Heat Recovery", ASME-HT2012-58129, ASME Heat Transfer Conference, Rio Grande, Puerto Rico.

4. Kumar, S., Heister, S., Xu, X., Salvador, J.R., and Meisner, G.P., Thermoelectric Generators for Automotive Waste Heat Recovery Systems, Part I. Numerical Modeling and Baseline Model Analysis, submitted to Journal of Electronic Materials.

5. Kumar, S., Heister, S., Xu, X., Salvador, J.R., and Meisner, G.P., Thermoelectric Generators for Automotive Waste Heat Recovery Systems, Part II. Parametric Evaluation and Topological Studies, submitted to Journal of Electronic Materials.

6. Saviers, K., Hodson, S., Salvador, J., Kasten, L., and Fisher, T., "Carbon Nanotube Arrays for Enhanced Thermal Interfaces to Thermoelectric Modules," *Proceedings of the 10th International Energy Conversion Engineering Conference*, Atlanta, 2012, Also submitted to the AIAA Journal of Thermophysics and Heat Transfer.

7. Liang, Daxin; Yang, Haoran, Finefrock, Scott W.; Wu, Yue* Flexible Nanocrystal-coated glass fibers for high-performance thermoelectric energy harvesting. Nano Letters, 2012, 12, 2140, highlighted by Chemical & Engineering News and National Public Radio.

8. Yang, Haoran; Jauregui, Luis A.; Zhang, Genqiang; Chen, Yong P.; Wu, Yue* Nontoxic and Abundant Copper Zinc Tin Sulfide Nanocrystals for Potential High-Temperature Thermoelectric Energy Harvesting. Nano Letters, 2012, 12, 540.

9. Qiu, Bo; Bao, Hua; Zhang, Gengqiang; Wu, Yue; Ruan, Xiulin, Molecular dynamics simulations of lattice thermal conductivity and spectral phonon mean free path of PbTe: Bulk and nanostructures Computational Materials Science, 2012, 53, 278.

10. Zhang, Genqiang; Kirk, Benjamin; Jauregui, Luis A.; Yang, Haoran; Xu, Xianfan; Chen, Yong P.; Wu, Yue* Rational Synthesis of Ultrathin n-type Bi2Te3 Nanowires with Enhanced Thermoelectric Properties. Nano Letters, 2012, 12, 56.

11. Gautam, Yadav G.; Susoreny, Joseph A.; Zhang, Genqiang; Yang, Haoran; Wu, Yue* Nanostructure-based thermoelectric conversion: an insight into the feasibility and sustainability for large-scale deployment. Selected as feature article, Nanoscale, 2011, 3, 3555.

12. Gautam, Yadav G.; Zhang, Genqiang; Qiu, Bo; Susoreny, Joseph A.; Ruan, Xiulin; Wu, Yue* Self-templated synthesis and thermal conductivity investigation for ultrathin perovskite oxide nanowires. Nanoscale, 2011, 3, 4078.

13. High mobility and high thermoelectric power factor in epitaxial ScN films deposited by reactive magnetron sputtering onto MgO(001) substrate: Polina Burmistrova, Bivas Saha,, Timothy D. Sands, et al. (Under preparation).

14. Electronic and Optical Properties of ScN and Mn-doped ScN Thin Films Deposited by DC-Magnetron Sputtering. Bivas Saha, G. V. Naik, V. Drachev, A. Boltasseva, and Timothy D. Sands. (Under preparation).

15. Growth, Characterization and Optoelectronic properties of Mn-doped ScN. Electronic Materials Conference, Penn. State University, July 2012.

V.7 Automotive Thermoelectric Modules with Scalable Thermo- and Electro-Mechanical Interfaces

Kenneth Goodson
Stanford University

Thermoelectric generators (TEGs) have been proposed for use in automobiles and other combustion systems to generate electricity from waste heat in exhaust streams. Components to be addressed include:

- Evaluation of novel nanostructured interface options that can accommodate large fluctuations in thermomechanical strain while maintaining thermal and electrical contact.
- Synthesis and measurement of efficient and stable high-temperature p- and n-type thermoelectric (TE) materials, which can be reliably attached to heat sinks and electrodes.
- Development of practical metrology and metrics relevant for system development, which also can be used to assess durability during thermal cycling of TEGs.

Approach/Accomplishments

At the conclusion of Fiscal Year (FY) 2011 and FY 2012, the Stanford-USF-Bosch team produced 12 archival papers and four in conference proceedings. A unique experimental apparatus for high-temperature infrared imaging of thermoelectric modules (during thermal cycling) supports a hot side temperature exceeding 600°C while maintaining a cold side at ambient temperatures using chilled water cooling. Breakthrough thermal properties were reported for carbon nanotube thermal interface materials bonded to metallized surfaces using reactive metal bonding layers, along with low elastic modulus data making them promising for thermal cycling reliability. We demonstrated a corresponding thermal boundary resistance associated with bonding as low as ~30 K-mm^2/W and proved that the bond is stable with high temperature thermal cycling. In addition, we reported the first in situ degradation data under thermal cycling for figure of merit (ZT) and its component properties for commercial modules – along with infrared imaging – to assess the role of interfaces in the reliability of thermoelectrics. The reduction in electrical conductivity with thermal cycling was found to be the primary degradation mechanism.

Our efforts focus on investigating the fundamental properties and optimizing the TE properties of p-type $CoSb_3$-based skutterudites as well as filled ternary skutterudites that are isoelectronic to this binary composition. We have successfully synthesized partially-filled p-type skutterudites with ZT = 0.85 at 500ºC. In addition, we are investigating ternary skutterudites. These form by substitution at the anion site by elements from groups 14 and 16 (e.g. $CoGe_{1.5}S_{1.5}$),[5] or by isoelectronic substitution at the cation site by a pair of elements from groups 8 and 10 (e.g. $Fe_{0.5}Ni_{0.5}Sb_3$). We performed computational screening of metals for low resistance electrical contacts to skutterudites and half-Heusler alloys. Schottky barrier heights at the interfaces between metals and TE materials are computed using the Mott-Schottky model and employing the density functional theory with GW corrections in order to better estimate band gaps. We have also computed the electronic transport coefficients of n- and p-type half-Heuslers by solving the Boltzmann transport equation for electrons under the constant relaxation time approximation. We are thus able to quantitatively predict effects of composition changes on the electronic transport and influence of carrier concentration on thermopower.

Status

During FY 2013 we will utilize this novel infrared thermometry experimental setup to perform measurements of TE materials and nanostructured interfaces under high temperature operating conditions. This experimental setup will also be used to conduct thermal cycling of the materials and interfaces with in situ measurements of thermoelectric properties and contact resistances. Candidate nanostructured thermal interface materials will be explored that are synthesized via metal electrodeposition through removable templates, such as vertically-aligned metal nanowires.

Structural studies carried out on ternary skutterudite materials prepared by anion substitution, such as $CoSn_{1.5}S_{1.5}$ and $CoGe_{1.5}Te_{1.5}$, suggest that these compounds crystallize in a modification (Rhombohedral, *R*-3) of the skutterudite structure (Cubic, *Im*-3). We are in the process of investigating the transport properties of these novel skutterudite compositions as well as half-Heusler alloys. Through simulation, we will focus on computing the electronic relaxation time and on solving the Boltzmann transport equation for phonons from first principles. We will address the question of the relevance

and accuracy of the Mott-Schottky model for interfaces between metals and heavily-doped semiconductors, as this issue that is not well explored.

Journal Articles

1. Barako, M. Park, W., Marconnet, A.M., Asheghi, M., and Goodson, K.E., "Thermal Cycling, Mechanical Degradation, and the Effective Figure of Merit of a Thermoelectric Module." J. Electronic Materials, Accepted. (2012)

2. Dong, Y., Puneet, P., Tritt, T.M., Martin, J., and Nolas, G.S., "High temperature thermoelectric properties of p-type skutterudites BaxYbyCo4-zFezSb12", J. Appl. Phys. 112 (2012) 083718.

3. Dong, Y., Wei, K., and Nolas, G.S., "Transport properties of partially filled skutterudite derivatives Ce0.13Co4Ge6Se6 and Yb0.14Co4Ge6Se6", to be submitted.

4. Gao, Y., Kodama, T., Won, Y., Dogbe, S., Pan, L., and Goodson, K.E., 2012, "Impact of Nanotube Density and Alignment on the Elastic Modulus near the Top and Base Surfaces of Aligned Multi-Walled Carbon Nanotube Films," Carbon, Vol. 50, pp. 3789-3798.

5. Gao, Y., Marconnet, A.M., Xiang, R., Maruyama, S., and K.E. Goodson. "Heat Capacity, Thermal Conductivity, and Interface Resistance Extraction for Single Walled Carbon Nanotube Films using Frequency-Domain Thermoreflectance." Components, Packaging and Manufacturing Technology, IEEE Transactions on. Under Review.

6. LeBlanc, S. and Goodson, K.E., "System and Material Parameter Effects on Thermoelectric Power Generation in Three Combustion Systems," Energy Conversion and Management. (submitted and under review)

7. LeBlanc, S., Phadke, S., Kodama, T., Salleo, A., and Goodson, K.E., 2012, "Electrothermal Phenomena in Zinc Oxide Nanowires and Contacts," Applied Physics Letters, Vol. 100, 163105.

8. Marconnet, A.M., Panzer, M.A., and Goodson, K.E., "Thermal Conduction Phenomena in Carbon Nanotubes and Related Nanostructured Materials," Reviews of Modern Physics, invited and under review.

9. Marconnet, A.M., Yamamoto, N., Panzer, M.A., Wardle, B.K., and Goodson, K.E, "Thermal Conduction in Aligned Carbon Nanotube-Polymer Nanocomposites with High Packing Density", ACS Nano, p. 4818, vol. 5, (2011).

10. Volja, D., Kozinsky, B., Li, A., Wee, D., Marzari, N., and Fornari, M., "Electronic, vibrational, and transport properties of pnictogen-substituted ternary skutterudites," Phys. Rev. B85, 245211 (2012).

11. Wee, D., Kozinsky, B., Pavan, B., and Fornari, M., "Quasi-harmonic vibrational properties of TiNiSn from ab initio phonons," J. of Electron Mat. J. 41, 977 (2012).

12. Won, Y., Gao, Y., Panzer, M.A., Dogbe, S., Pan, L., Kenny, T.W., and Goodson, K.E., 2012, "Mechanical Characterization of Aligned Multi-Wall Carbon Nanotube Films," Carbon, Vol. 50, pp 347-355.

Conference Proceedings

1. Barako, M.T., Gao, Y., Marconnet, A.M., Asheghi, M., Goodson, K.E. "Solder-Bonded Carbon Nanotube Thermal Interface Materials." IEEE Intersociety Conference on Thermal and Thermomechanical Phenomena in Electronic Systems (ITHERM) 2012, May 30 – June 1, San Diego, CA.

2. Barako, M.T., Park, W., Marconnet, A.M., Asheghi, M., and Goodson, K.E. "A Reliability Study with Infrared Imaging of Thermoelectric Modules under Thermal Cycling". IEEE Intersociety Conference on Thermal and Thermomechanical Phenomena in Electronic Systems (ITHERM) 2012, May 30 – June 1, San Diego, CA.

3. Marconnet, A.M., Motoyama, M., Barako, M.T., Gao, Y., Pozder, S., Fowler, B., Ramakrishna, K., Mortland, G., Asheghi, M., Goodson, K.E., "Nanoscale Conformable Coatings for Enhanced Thermal Conduction of Carbon Nanotube Films," IEEE Intersociety Conference on Thermal and Thermomechanical Phenomena in Electronic Systems (ITHERM) 2012, May 30 – June 1, San Dego, CA.

4. Park, W., Barako, M.T., Marconnet, A.M., Asheghi, M., and Goodson, K.E. "Effect of Thermal Cycling on Commercial Thermoelectric Modules". IEEE Intersociety Conference on Thermal and Thermomechanical Phenomena in Electronic Systems (ITHERM) 2012, May 30 - June 1, San Diego, CA.

V.8 NSF/DOE Thermoelectrics Partnership: Integrated Design and Manufacturing of Cost-Effective and Industrial-Scalable TEG for Vehicle Applications

Lei Zuo (Primary Contact), Jon Longin, Sanjay Sampath
Stony Brook University

Qiang Li
Brookhaven National Laboratory

Overall Objectives

- Development of a scalable high-throughput, non-equilibrium synthesis process for high figure of merit (ZT) thermoelectric (TE) materials from abundant low-cost feedstock by using thermal spray technology.
- Development of an integrated manufacturing process to fabricate TE structures directly onto exhaust pipe components with enhanced performance and durability.

Approach

- Various thermal spray methods and conditions were used to find optimal spray parameters of Mg_2Si.
- X-ray diffraction (XRD) and scanning electron microscope analyses were used to analysis thermal sprayed coating structure.
- Thermal conductivity, electrical conductivity and Seebeck coefficient were measured to analysis sample TE properties.
- Three-dimensional fabrication of a TE module being developed to demonstrate the ability to make all functional components of the TE device by thermal spray.
- Parametric study of laser cutting parameters was done to determine optimal condition to micromachining of the Mg_2Si coatings.

Accomplishments

- High-velocity low-temperature atmospheric plasma spray (APS) using SG100 internal power injection gun produced almost the same XRD as the original feedstock powder, and with very dense microstructure. The SG100 internal power injection significantly reduces oxidation of Mg_2Si compared with other APS samples.
- Vacuum plasma spray (VPS) with different power levels has been explored for Mg_2Si, and XRD results show 21 kW deposition with the substrate temperature cooled has the minimum MgO and Si peaks.
- The thermal conductivity, electrical conductivity and Seebeck coefficient of the sprayed Mg_2Si have been characterized. Results show (1) both VPS thermal spray method and APS with internal power injection can reduce thermal conductivity, likely due to enhanced phonon scattering. (2) APS with internal power injection achieved good electrical conductivity. (3) VPS with proper power level setting and substrate temperature control achieved similar Seebeck coefficient compared with either hot press or spark plasma sintering.
- Filled skutterudite material has been successfully sprayed by APS method, and microstructure shows dense structure and good mechanical bonding. Annealing is expected to be required to enhance performance.
- A three-dimensional TE module is been fabricated, which includes the insulation layer, conducting layer and TE material layer. Standard thermocouple materials are being used as surrogates for the Mg_2Si material to demonstrate device operation.
- A cylindrical-geometry three-dimensional TE module has been designed, and the insulation layer and conducting layer have been sprayed using APS method and conformal masks. Results show good mechanical bonding and thermal expansion match.

Status of the project

- More APS runs of Mg_2Si with internal power injection are being conducted to verify the repeatability of the spray method on Mg_2Si TE material. The thermal, electrical conductivity as well as Seebeck coefficient will be characterized as well.
- Annealling of the VPS samples (21 kW, with substrate temperature control) will be done to enhance the microstructure by reduce the boundary layers.
- Thicker filled-skutterudite samples will be sprayed and annealed to form the correct TE phase.

- Iron disilicide (Fe_2Si) will be sprayed to make the three-dimensional TE module to demonstrate the manufacturing process with thermal spray and laser cutting using an actual TE material.
- Thermal sprayed TE properties modeling using effective medium theory, percolation theory and Millman's theorem will be investigated to gain better understanding of thermal sprayed material properties.

FY 2012 Publications

1. "Fabrication of Thermoelectric Devices Using Thermal Spray: Application to Vehicle Exhaust Systems to Improve Fuel Economy", Jon P. Longtin, Lei Zuo, David Hwang, Gaosheng Fu, Mahder Tewolde, Yikai Chen and Sanjay Sampath, *Journal of Thermal Spray Technology*, accepted.

2. "Thermoelectric Properties of Magnesium Silicide Produced using VPS and APS Thermal Sprays", Gaosheng Fu, Lei Zuo, Jon Longtin, Yikai Chen and Sanjay Sampath, 2012 MRS Fall Meeting & Exhibit, Boston - November 25–30, 2012.

3. "Fabrication of Thermoelectric Devices For Vehicle Exhaust Applications Using Thermal Spray and Laser Processing", M. Tewolde, J. Longtin, L. Zuo, D. Hwang, and S. Sampath, ASME 2012 Summer Heat Transfer Conference - HT2012, July 8–12, 2012.

4. "Thermoelectric properties of magnesium silicide prepared by thermal spray", B. Zhang, L. Zuo, et al, ASME 2012 Summer Heat Transfer Conference - HT2012, July 8–12, 2012.

5. "Review of Waste Energy Resource in Vehicle Exhaust Heat", G. Fu, L. Zuo, and J.Longtin, ASME 2012 Summer Heat Transfer Conference - HT2012, July 8–12, 2012.

6. "Heat Transfer Modeling and Geometry Optimization of TEG for Automobile Applications", G. Fu, L. Zuo, J. Longtin, S. Sampath, B. Zhang, ASME 2012 Summer Heat Transfer Conference - HT2012, July 8–12, 2012.

V.9 NSF/DOE Thermoelectrics Partnership: Inorganic-Organic Hybrid Thermoelectrics

Sreeram Vaddiraju
Texas A&M University

Overall Objectives

- Synthesis of inorganic nanowires and quantum wires of both $CoSb_3$ and InSb, and organic conducting polymer thin films, and assembling them into inorganic-organic hybrid thermoelectric cells with sizes ranging from a few mm^2 to a few cm^2, using conjugated linker molecules to tether the nanowires to each other or to conducting polymer thin films.
- Systematically studying the effect of inorganic nanowire size and organic conducting polymer thin film chemistry and thickness on their individual thermoelectric performance, and also on their performance when used in unison as 'molecular wired' inorganic-organic hybrids, in the temperature range of 300-1,100 K.
- Determine the type of the metal required for assembling individual thermoelectric devices into thermoelectric modules without lowering their performance, i.e., finding metals that have very low contact resistance with individual thermoelectric cells.

Approach

Figure of merit, *ZT*, of thermoelectric materials can be enhanced by synthesizing materials in single-crystalline nanowire format with diameters in the sub-10 nm regime. Fabrication of thermoelectric modules using these nanowires requires strategies for their large-scale synthesis and assembly. The approach employed in this work involves the use of self-catalysis for the synthesis of nanowire powders devoid of any unintentional contaminants or dopants. Additionally, layer-by-layer decomposition, an exclusive nanoscale phenomenon, served as the approach uniformly decomposing nanowires all along their lengths and reducing nanowire powders into quantum wire powders (with diameters ≤10 nm). The approach used for the large-scale assembly of nanowires powders in an interface-engineered manner simply involves binding nanowires together using conjugated linkers.

Accomplishments

- Accomplished the large-scale synthesis of both unfunctionalized and conjugated organic molecule functionalized Zn_3P_2 nanowire powder using self-catalysis. Experimental bottlenecks preventing the large-scale synthesis of nanowire powders have been resolved. Vapor transport of phosphorus onto zinc foils was employed for the self-catalytic synthesis of Zn_3P_2 nanowires. Currently, surfaces of foils with areas as large as 240-480 cm^2 can be completely converted into Zn_3P_2 nanowires in the PI's laboratory. In other words, 0.5-1 gram of Zn_3P_2 nanowire powder can be produced in an experimental run lasting 2 hours. Similar quantities of surface functionalized Zn_3P_2 nanowires (useful for the fabrication of inorganic-organic hybrids) can also be produced using in situ functionalization.
- Evaluated the thermoelectric performance of pellets obtained by hot pressing Zn_3P_2 nanowire powders. For this purpose, hot uniaxial pressing of nanowire powders into 12-mm diameter, 2-mm thick pellets was performed. Uniaxial pressing did not alter the morphology of the nanowires, even though densities as high as 98% of the theoretical densities have been achieved in the pellets. Thermoelectric performance of Zn_3P_2 pellets was observed to be better than that reported for spark plasma sintered Zn_3P_2 spherical particle powders. For instance, nanowire morphology resulted in a 30% reduction in the thermal conductivity of Zn_3P_2, compared to bulk Zn_3P_2.
- Evaluated the thermoelectric performance of poly(3,4-ethylenedioxythiophene) (PEDOT) films of various thicknesses. The thermoelectric performance of PEDOT films was observed to be very low, irrespective of the film thickness. Seebeck coefficients of conducting polymer thin films of PEDOT ranged from 15-35 μV/K irrespective of the film thickness. As-obtained conducting polymer thin films do not exhibit good thermoelectric performance. It was decided that stand-alone conducting polymer films are not ideal for thermoelectrics fabrication.
- Accomplished the small-scale synthesis of phase-pure $CoSb_3$ nanowires (i.e., devoid of any contaminant $CoSb_2$ and CoSb phases) and phase-pure InSb nanowires (i.e., devoid of any indium oxide contaminant). Mass production of $CoSb_3$ and InSb nanowire powders is currently underway.

Publications*

1. Brockway, L., Pendyala, C., Jasinski, J., Sunkara, M.K., & Vaddiraju, S. (2011). A Postsynthesis Decomposition Strategy for Group III-Nitride Quantum Wires. *Crystal Growth & Design, 11*(10), 4559-4564.

**Manuscripts in preparation have not been included*

V.10 Integration of Advanced Materials, Interfaces, and Heat Transfer Augmentation Methods for Affordable and Durable Thermoelectric Devices

Y. Sungtaek Ju (PI), Bruce Dunn (co-PI)
University of California, Los Angeles

Objective

One of the project tasks is focused on synthesizing nano-composites whose coefficients of thermal expansion (CTE) can be tailored to match those of thermoelectric (TE) materials being developed for vehicle exhaust waste heat harvesting, in particular silicides and other low-cost TE materials. These nanocomposites will be used as electrical contacts/interconnects in TE modules. We are also developing liquid-based flexible thermal interfaces to further improve the thermomechanical and mechanical reliability of TE modules.

Approach

We prepare nanocomposite materials where nano-fillers that exhibit negative thermal expansion (e.g. zirconium tungstate, ZrW_2O_8) are dispersed within a metal matrix. The nanofillers are prepared by the sol-gel method. The composites are prepared by hot pressing a pellet composed of ZrW_2O_8 and metal powders. For flexible interfaces, we develop a numerical model based on the surface energy minimization algorithm to predict and design the mechanical behavior of capillary confined liquid elements. Approaches to minimize the impact of oxidation and material loss, such sacrificial rings, are experimentally tested to validate their effectiveness.

Results

Our high-resolution scanning electron microscopy (SEM), CTE, and conductivity measurements showed that pores remaining in nano-composites are detrimental to achieving desired properties. We found that, to minimize open pores, metal particles have to be of nanometer size. We have synthesized Cu nanoparticles by using a direct and economic approach where a copper salt (copper sulfate, $CuSO_4$) is dissolved in water and Cu^{2+} ions are reduced to metallic Cu NPs using a strong reducing agent. Sintered pellets of pure Cu and a series of Cu-ZrW_2O_8 compositions with up to 50 wt% (74 vol%) oxide have been prepared. There is reasonable agreement between the measured thermal expansion coefficient and the expected values. SEM analyses show a homogeneous dispersion of zirconium tungstate particles within a polycrystalline copper matrix. The density of the materials, however, is still about 85-90% of the theoretical density, suggesting that further improvement is necessary.

We also successfully developed a numerical model for the mechanical characteristics of capillary confined liquid elements and experimentally confirmed its validity. The relationships between the morphology (mechanical deformation) of liquid elements and corresponding capillary forces have been established to enable physics-based design of flexible interfaces.

Future Work

Measurements of the thermal and electrical conductivities of the nanocomposites are currently under way. Efforts to improve the processing conditions and starting materials will also continue. We are also planning to carry out hot pressing experiments in which the Cu-ZrW_2O_8 composite will be bonded directly to Mg_2Si thermoelectric elements. Design, fabrication, and experimental characterization of flexible interfaces and oxidation-mitigation structures will also be carried out.

Publication/Presentations

1. "Metal-Matrix Nanocomposites with Tailored Coefficients of Thermal Expansion for Improved Thermomechanical Reliability," J.E. Trujillo, J.W. Kim, E.H. Lan, S. Sharratt, Y.S. Ju, and B. Dunn, Journal of Electronic Materials, Vol. 41, No. 6, 2012, 1020-1023.

2. "Combining Positive and Negative Thermal Expansion Materials to Tailor the Coefficient of Thermal Expansion in Metal/Ceramic Composites," Joy E. Trujillo, Jong W. Kim, Esther Lan, Y.S. Ju, and Bruce Dunn, Materials Science & Technology 2012 Conference & Exhibition October 7–11, 2012 – Pittsburgh, Pennsylvania.

V.11 High Performance Thermoelectric System Based on Zintl Phase Materials with Embedded Nanoparticles

Ali Shakouri (Primary Contact), Zhixi Bian
University of California, Santa Cruz
Baskin School of Engineering
1156 High Street
Santa Cruz, CA 95064

Susan M. Kauzlarich (UC Davis)
University of California, Davis
Chemistry Department
One Shields Ave
Davis, CA 95616

NSF Manager: Sumanta Acharya

DOE Technology Development Manager: John Fairbanks

NETL Project Manager: Carl Morande

Overall Objectives

- Develop novel thermoelectric (TE) materials based on abundant and non-toxic Zintl phase magnesium silicide alloys.
- Demonstrate that with the use of embedded nanoparticles of appropriate concentration (0.01-5%) and diameter (2-15 nm), thermal conductivity will be reduced by scattering of mid to long wavelength phonons.
- Optimize the TE power factor and figure of merit by band engineering and electron filtering using embedded nanoparticles.

Fiscal Year (FY) 2012 Objectives

- Synthesis of n-type $Mg_{2-x}Yb_xSi$, $Mg_2Si_xGe_{1-x}$ with embedded Si, Ge nanoparticles and $(Mg_2Si)_{1-x}/(Mg_2Sn)_x$.
- Structural and TE characterizations.
- TE transport modeling.
- Optimization of both thermal conductivity and TE power factor by modifying the alloy composition, nanoparticle sizes and concentrations.

Accomplishments

- Low temperature synthesis and spark plasma sintering (SPS) of n-type Mg_2Si w/embedded Si nanoparticles (2011).
- Characterization and transport modeling (2011).
- Developed SPS processing of Mg_2Si nanocomposites (2011).
- Developed an understanding of electron scattering in Mg_2Si nanocomposites (2012).
- Optimized $Mg_2Si_{0.4}Sn_{0.6}$ with and without embedded nanoparticle scattering at different electron concentrations and temperatures (2012).
- Low temperature synthesis and SPS of n-type $Mg_{2-x-}Yb_xSi$ with embedded Yb_3Si_5 nanoparticles (2012).
- Low temperature synthesis and SPS of n-type $Mg_2Si_{1-x}Sn_x$ with embedded Si and Mg_2Si nanoparticles (2012).

Future Directions

- Low temperature synthesis and SPS of p-type Mg_2Si with embedded nanoparticles.
- Characterization and transport modeling.

Introduction

We are developing novel TE materials based on abundant and non-toxic Zintl phase magnesium silicide alloys. We have demonstrated a synthetic method that naturally provides embedded nanoparticles within a magnesium silicide alloy matrix, providing uniform mixing with minimal aggregation. With the use of embedded nanoparticles of appropriate concentration (0.01-5%) and diameter (2-15 nm), thermal conductivity will be reduced by scattering of mid to long wavelength phonons. Controlling the heterostructure band offset and the potential barrier of nanoparticles with respect to matrix, power factor will be increased by selective scattering of hot carriers. Preliminary transport calculations show that figure of merit (ZT) >1.8 at 800 K could be achieved.

Approach

Mg_2Si can be synthesized with MgH_2 and Si powders as starting materials [1]. By changing the ratio of the

starting materials, a proper amount of Si nanoparticles can be easily be incorporated into the matrix. N-type dopants are also homogeneously mixed with the starting materials in a ball mill to tune the carrier concentration. Either a flow furnace and SPS combination or SPS processing were employed to achieve the doped nanocomposite product in the form of fully dense pellets for transport properties characterizations. In order to obtain Mg_2Si containing Yb_3Si_5 nanocomposites, YbH_2 was employed along with MgH_2 and Si. Bi was used for adjusting the carrier concentration. In contrast to previously described Mg_2Si/xSi nanocomposite samples [1], the Yb-containing samples were ball milled for a significantly shorter amount of time. Powders were reacted and densified using SPS. Ge-containing Mg_2Si composites were synthesized similar as described above utilizing reaction of MgH_2 with SiGe alloy or Si with Ge nanoparticles prepared by a solution method developed in this group [1]. Powders were reacted and sintered using SPS. Ge nanoparticles with narrow size distribution and average size of 10 nm were produced by solution microwave-assisted method [2]. X-ray diffraction, microprobe and TE properties were measured on three dense pellets of Mg_2Si with 2% of Ge nanoparticles, $Mg_2Si_{0.8}Ge_{0.2}$ and $Mg_{1.95}Si_{0.8}Ge_{0.2}$. A robust and accurate high temperature TE system is built to characterize the Seebeck coefficient and the electrical conductivity of nanocomposites simultaneously in a large temperature range. We also develop a multiband Boltzmann transport model including nanoparticle scattering to explain the Seebeck and electrical conductivity measurement results and provide a guideline for material optimization.

Results

TE transport modeling: Based on Boltzmann transport theory and band engineering via alloying, we calculated the TE transport properties of bulk $Mg_2Si_{0.4}Sn_{0.6}$ and compared the results with published experiment data by other research groups. As seen in Figure 1, the theoretical results matched with experiments very well. Further, it could be shown that the TE power factor could be increased by utilizing increased band degeneracy.

There are opportunities in reducing the thermal conductivity and increasing TE power factor further by embedding nanoparticles which can contribute a lot of electrons to the hosting $Mg_2Si_{0.4}Sn_{0.6}$ matrix. Figure 2 shows the effects of Silicon nanoparticle inclusions on the lattice thermal conductivity of Mg_2Si and Mg_2SiSn. In Figure 3, it is also shown that the TE power factor can be greatly increased by embedding nanoparticles. In Figure 4, it shows the thermoelectric power factor enhancement is stronger at lower temperatures because

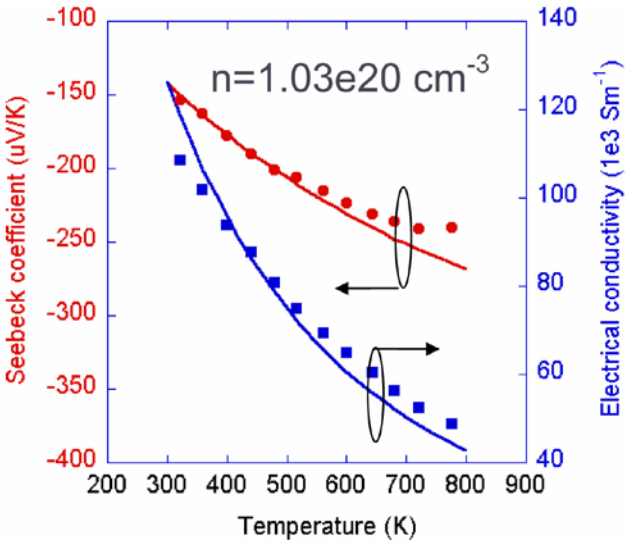

FIGURE 1. Comparison of Seebeck coefficient and electrical conductivity between theoretical calculations and published experiment data.

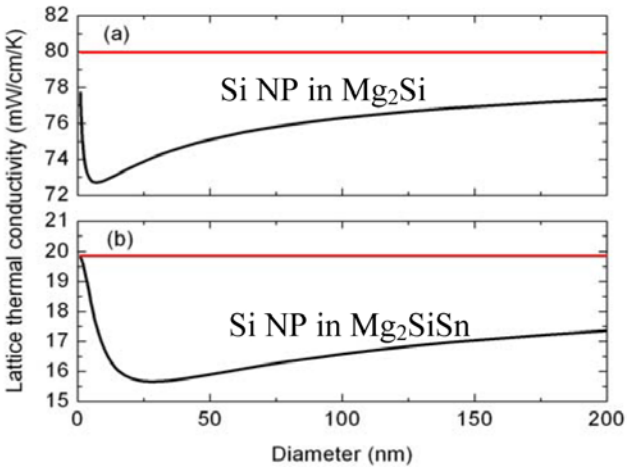

FIGURE 2. The lattice thermal conductivity of Mg_2Si and Mg_2SiSn with embedded Si nanoparticles.

at higher temperatures the electron phonon scattering is dominant and the effects of nanoparticles become relatively weaker.

Summary of theoretical results: In the second year, we theoretically studied the TE transport in $Mg_2Si_xSn_{1-x}$ solid solutions. There are two benefits in adding Sn: first, the lattice thermal conductivity can be greatly reduced due to phonon alloy scattering; second, the conduction band degeneracy can be increased so as to increase the TE power by band engineering through alloying. Our theoretical calculations could fit with published experiment data very well for bulk $Mg_2Si_{0.4}Sn_{0.6}$. We also studied the effects of nanoparticles embedded in $Mg_2Si_{0.4}Sn_{0.6}$ matrix on TE and thermal transport.

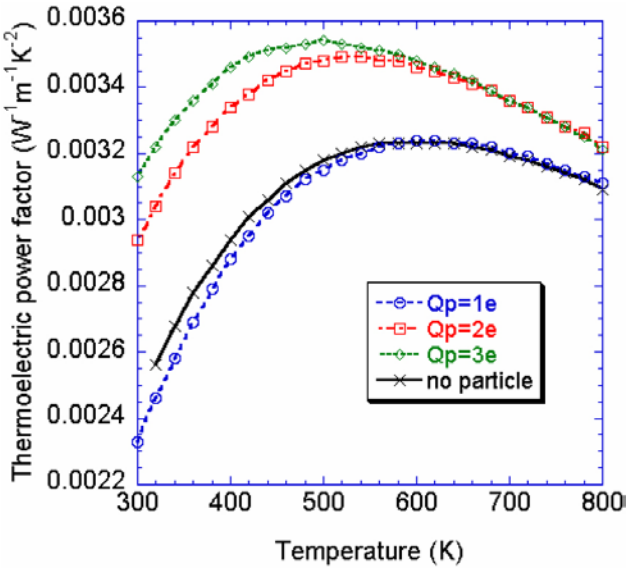

FIGURE 3. The TE power factor of $Mg_2Si_{0.4}Sn_{0.6}$ with and without nanoparticles of different electron doping capacities.

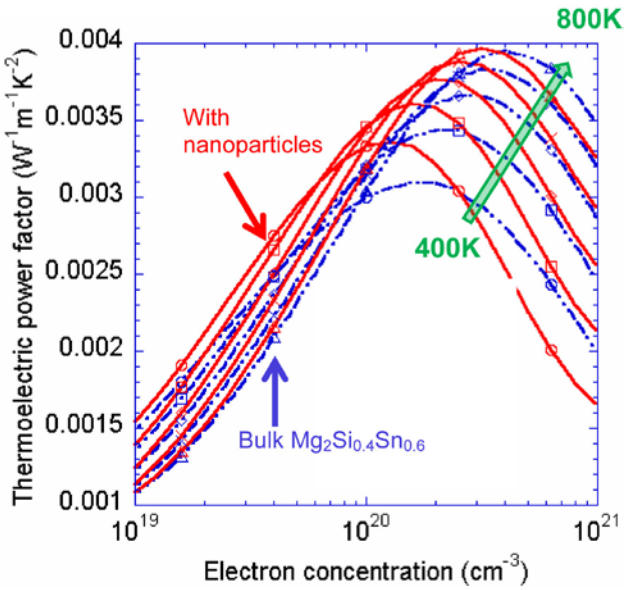

FIGURE 4. Comparison of TE power factors of $Mg_2Si_{0.4}Sn_{0.6}$ with and without nanoparticles at different electron concentrations and temperatures.

Yb-doped Mg_2Si: Nanocomposites of $Mg_{2-x}Yb_xSi$ with Yb_3Si_5 nano-inclusions were prepared. Fragments of the pressed pellets were used for electron microprobe analysis (EMPA), some were ground into powders and used for powder X-ray diffraction as well as high angle annular dark field scanning transmission electron microscopy (HAADF-STEM) investigations. Powder X-ray diffraction indicates the formation of Mg_2Si and Yb_3Si_5 after the reaction and densification of the

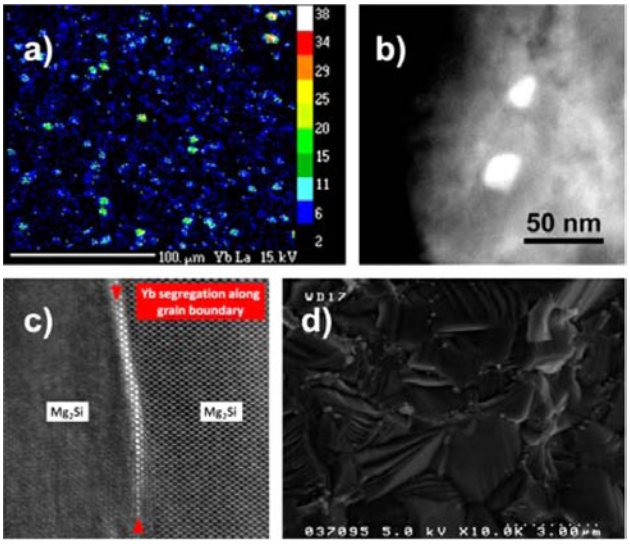

FIGURE 5. a) EMPA X-ray maps of the Yb distribution in a 1.0% doped sample. b) HAADF-STEM image of Yb_3Si_5 inclusions in a Mg_2Si matrix with a size of about 30–70 nm. c) HAADF-STEM image of the grain boundary showing Yb-doping onto the Mg-site in between to Mg_2Si grains. d) Scanning electron microscope image of the methanol-etched fracture face of a Mg_2Si pellet showing large well connected grains.

material. EMPA shows that the Yb_3Si_5 inclusions are well distributed over the whole specimen and are not clustered (Figure 5a). HAADF-STEM analysis of the $Mg_{2-x}Yb_xSi$ with Yb_3Si_5 nanocomposite reveals that the Yb_3Si_5 inclusions have a size of about 50 nm (Figure 5b). The presence of Yb has been proven furthermore by energy-dispersive spectroscopy. Additional Yb could be found at the grain boundaries of these samples and also located at the magnesium site (Figure 5c). The presence of Yb can be understood as an isovalent doping of Yb^{2+} onto the Mg^{2+} positions in the crystal structure. Scanning electron microscope investigations of the fracture faces of the pellets indicate a well sintered material with large grains (Figure 5d).

Transport properties have been measured so far on different specimen only so no concluding result and figure-of-merit will be given. The thermal conductivity drops with increasing Yb content suggesting that Yb-doping onto the Mg^{2+} sites as well as the Yb_3Si_5 inclusions are effectively scattering the heat carrying phonons. Co-doping of Bi decreases the thermal conductivity even further since another heavy element is added to the system. For electrical transport and Seebeck these samples show an electrical resistivity characteristic for a heavily doped semiconductor. For the Mg_2Si/xSi nanocomposite samples [1] the electrical resistivity showed impurity scattering at temperature between room temperature and 700ºC. We now attribute this to interfaces derived from the crystallite size, defects, and interfaces that were introduced from long ball-milling

times used in the processing. The electrical resistivity and Seebeck data of the $Mg_{2-x}Yb_xSi$ with Yb_3Si_5 samples are of the same order of magnitude as seen in other examples in the literature (Figure 6).

Ge-containing Mg_2Si composites: Thermal conductivity of Mg_2Si can be reduced due to the additional interfaces and phonon scattering centers introduced by Si nanoinclusions [1]. This approach can be further extended to Ge nanoparticles. The composites Mg_2Si with embedded Ge nanoparticles were prepared by two approaches. In one, Ge nanoparticles were produced by solution assisted method [1]. In the other, Ge was ball milled together with Si in order to obtain the alloy of $Si_{1-x}Ge_x$ powder. Nanocomposites of Mg_2Si with different amount of Ge were successfully synthesized utilizing reaction of MgH_2 with Si/Ge and densified by means of SPS. EMPA showed that in the case of composites prepared via reaction of MgH_2 and SiGe alloy, Ge substitutes Si in either Mg_2Si or bulk Si, e.g. leading to the $Mg_2Si_{1-x}Ge_x$ and/or Si_xGe_{1-x} phases. In the case of composites with Ge nanoparticles prepared by solution, Ge is incorporated into the Mg_2Si matrix leaving extra Si as inclusions (Figure 7).

The addition of Ge, either in the form of nanoparticles prepared by solution or by alloying of Si with Ge, leads to the drastic lowering of thermal conductivity (Figure 8). Phonon scattering is the primary mechanism leading to the low values of thermal conductivity. However, the samples are poor electrical conductors with associated high values of electrical resistivity, which hampers their TE performance. Further optimization of the electrical properties of the Mg_2Si/Ge composites by introducing different concentrations of dopants, such as Bi or Sb is currently in progress.

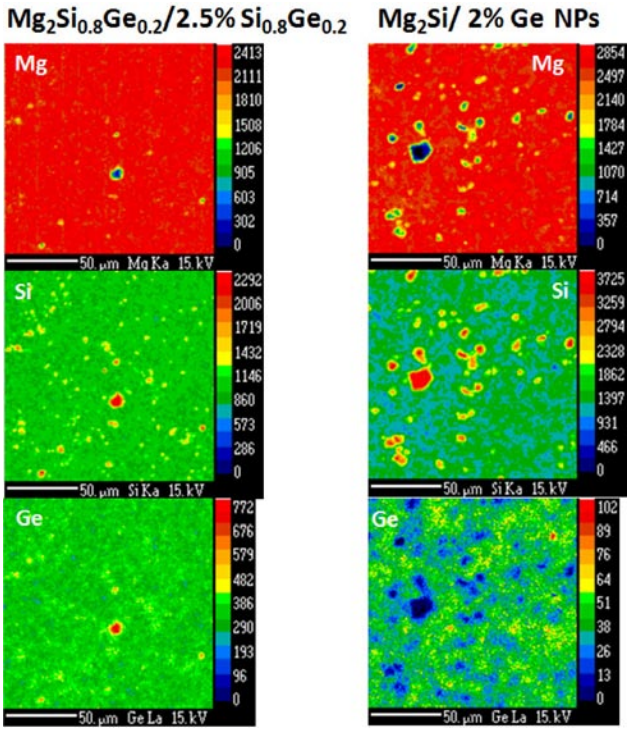

FIGURE 7. EMPA X-ray maps showing Mg, Si and Ge distribution in Mg_2Si/2.5% $Si_{0.8}Ge_{0.2}$ sample (left) and Mg_2Si/2% Ge nanoparticles (right).

$(Mg_2Si)_{1-x}/(Mg_2Sn)_x$ composite materials: In order to make $(Mg_2Si)_{1-x}/(Mg_2Sn)_x$ composite materials with various ratios of Si to Sn a two step method was developed giving quick access to a variety of stoichiometric ratios. Mg_2Sn was prepared by a classic solid state reaction using the elements and reacting them in a Ta tube. Large quantities of polycrystalline phase pure Mg_2Sn can be obtained by this method. In

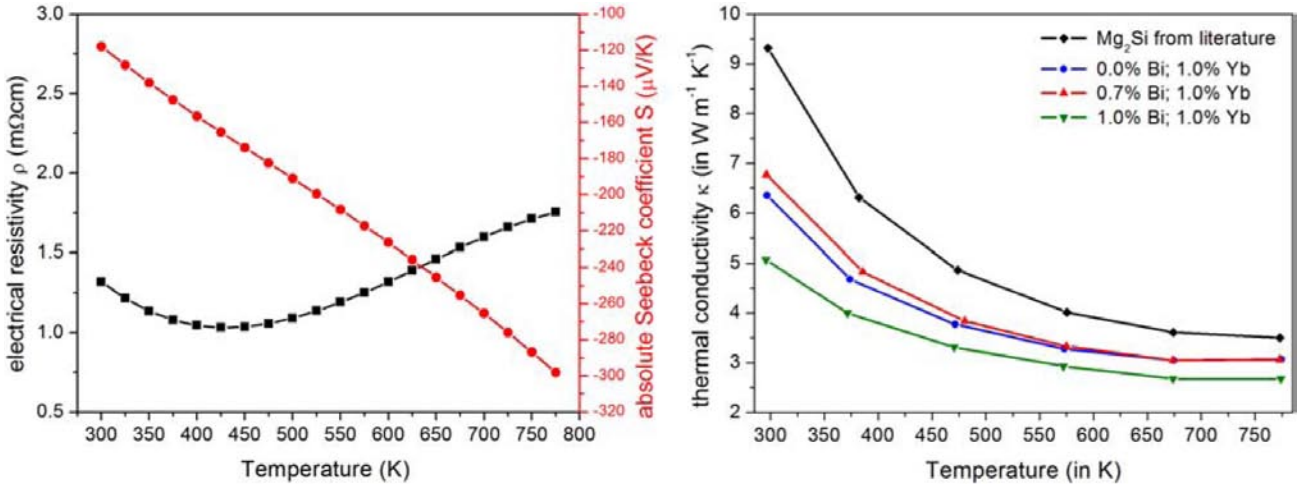

FIGURE 6. Electrical resistivity (left, black) and Seebeck coefficient (left, red) of a 1.0% Bi doped sample of Mg_2Si. Thermal conductivity of 1.0% Yb doped Mg_2Si co-doped with different amounts of Bi and compared with the literature value (Mg_2Si from the literature) is from Tani and Kido [3].

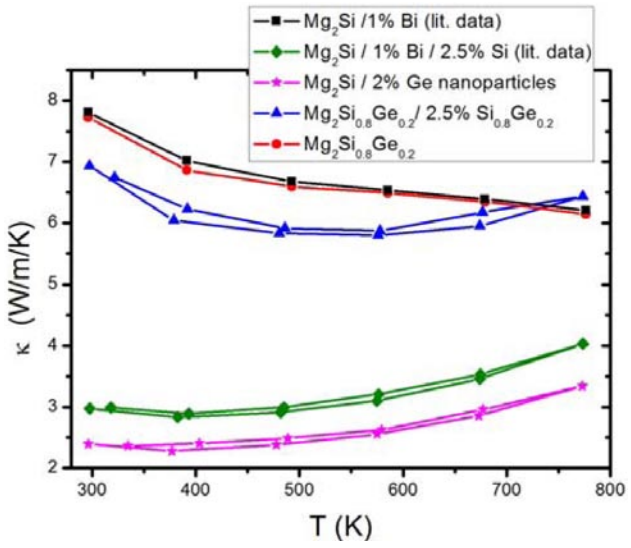

FIGURE 8. Thermal conductivity for Ge-containing Mg_2Si samples in comparison with literature data (Mg_2Si/1% Bi is from Tani and Kido and Mg_2Si/1%Bi/2.5%Si is from Yi et al).

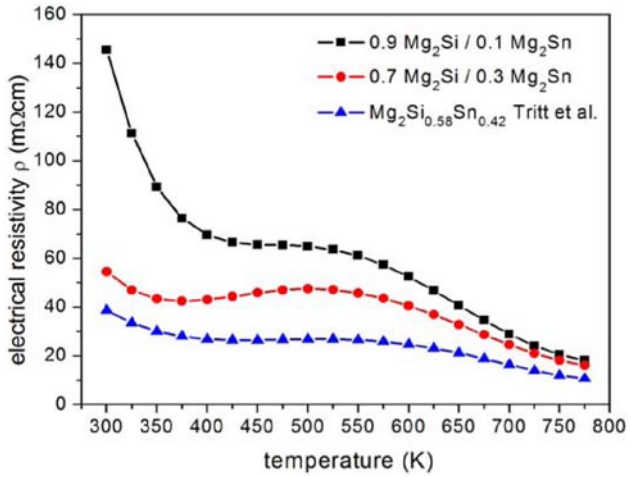

FIGURE 9. Electrical resistivity of two Mg_2Si/Mg_2Sn composite samples compared to a literature sample. The trend shows that the resistivity decreases with increasing Sn content.

a second step MgH_2, Si and Mg_2Sn were mixed using a ball mill, after which the material was reacted and sintered *via* SPS at 700°C. Powder X-ray diffraction indicates that the sample consists of two phases: Mg_2Si and Mg_2Sn with significantly shifted lattice parameters suggesting some solid solution phase products. X-ray maps obtained by EMPA show a distribution of Sn over the whole sample with local maxima of Si. Electrical transport properties were measured on two samples with a nominal composition of $(Mg_2Si)_{0.9}(Mg_2Sn)_{0.1}$ and $(Mg_2Si)_{0.7}(Mg_2Sn)_{0.3}$. Compared to literature those samples fit the trend of decreasing electrical resistivity with increasing Sn content (Figure 9).

Conclusions

We have shown that nanoinclusions provide a significant lowering of the thermal conductivity. We have shown that long ball-mill processing of starting materials is not necessary for high quality nanocomposites. Yb can both isovalent substitute for Mg and provides Yb_3Si_5 inclusions. We have shown that Ge nanoparticles provide a larger effect than simple alloying of Mg_2Si. We have shown that $(Mg_2Si)_{1-x}/(Mg_2Sn)_x$ transport properties can be modified by x. We have identified the optimum carrier concentration for highest power factor in $Mg_2Si_{0.4}Sn_{0.6}$ alloy with and without embedded nanoparticles with 1 nm nanoparticles with a band offset of 0.1 eV, improvements in power factor at room temperature by ~10% are possible.

References

1. Yi, T.; Chen, S.; Li, S.; Yang, H.; Bux, S.; Bian, Z.; Katcho, N.A.; Shakouri, A.; Mingo, N.; Fleurial, J.-P.; Browning, N.D.; Kauzlarich, S. M., *J. Mater. Chem.* 2012, *Advance Article.*

2. Muthuswamy, E.; Iskandar, A.S.; Amador, M.M.; Kauzlarich, S.M., *Chem. Mater.* ASAP.

3. Tani, J.-i.; Kido, H., *Physica B* 2005, *364* (1-4), 218-224.

FY 2012 Publications/Presentations

1. Tanghong Yi, Shaoping Chen, Shawn Li, Hao Yang, Sabah Bux, Zhixi Bian, Nebil A. Katcho, Ali Shakouri, Natalio Mingo, Jean-Pierre Fleurial, Nigel D. Browning and Susan M. Kauzlarich. Synthesis and characterization of Mg_2Si/Si nanocomposites prepared from MgH_2 and silicon, and their thermoelectric properties. *Journal of Materials Chemistry*, (2012), **22**, 24805-24813.

2. Susan M. Kauzlarich, Oliver Janka and Tanghong Yi, Synthesis and characterization of Mg_2Si/Si nanocomposites for thermoelectric enhancement, Presented at the ACS Spring Meeting 2012, San Diego, CA, March 25–29, 2012.

3. Oliver Janka, Sabah K. Bux, Susan M. Kauzlarich, Thermoelectric properties of Yb-doped Mg_2Si, Presented at the ACS Spring Meeting 2012, San Diego, CA, March 25–29, 2012.

4. Ali Shakouri, Zhixi Bian and Susan Kauzlarich, "High performance Zintl phase TE materials with embedded nanoparticles," Thermoelectrics Applications Workshop III, Baltimore, MD; March 2012.

5. Susan M. Kauzlarich, High performance Zintl phase TE materials with embedded nanoparticles. Invited Speaker for the local section, MRS Chapter seminar, March 19, 2012.

6. Ali Shakouri, "Nanostructured materials for thermoelectric conversion," Invited talk, SPIE (International Society for Optics and Photonics) Defense, Security + Sensing, Baltimore, MD; April 2012.

7. Ali Shakouri, "Nanostructured thermoelectric materials for waste heat recovery," Invited talk, Symposium on Nanomaterials for Energy, Purdue University; April 2012.

8. Zhixi Bian, Ali Shakouri, Tanghong Yi, Susan Kauzlarich, Sabah Bux, Jean-Pierre Fleurial, Thermoelectric transport in nanostructured $Mg_2Si_xSn_{1-x}$, The 31st International Conference on Thermoelectrics, Aalborg, Denmark, July 2012.

9. Oliver Janka, Susan M. Kauzlarich, Thermoelectric properties of Yb-doped Mg_2Si, Presented at the 16. Vortragstagung Fachgruppe Festkörperchemie und Materialforschung 2012, Darmstadt, Germany, September 17–19, 2012.

10. Oliver Janka, Sabah K. Bux, Zhixi Bian, Ali Shakouri, Susan M. Kauzlarich, Enhancing the Thermoelectric Properties of Mg2Si using Rare Earth Dopants, Presented at the Materials Research Society Meeting Fall 2012, Boston, MA, November 25–30, 2012.

11. Julia V. Zaikina, Elayaraja Muthuswamy, Tanghong Yi, Susan M. Kauzlarich, Synthesis and characterization of Mg2Si/Ge nanocomposites for thermoelectric applications, Presented at the Summer school on Inorganic Materials for Energy Conversion and Storage, Santa Barbara, CA, August 19 – September 1, 2012.

V.12 An Integrated Approach Towards Efficient, Scalable, and Low-Cost Thermoelectric Waste Heat Recovery Devices for Vehicles

Scott Huxtable (Primary Contact),
Srinath Ekkad, Shashank Priya
Virginia Tech

Andrew Miner
Romny Scientific

The objective of our work is to make scientific and technical advances that will aid in enabling widespread deployment of thermoelectric devices to generate useful electric power from waste heat in vehicle exhaust. This work will help improve vehicle efficiency and also reduce harmful emissions. Our approach is to focus on making practical, industry relevant, improvements in thermoelectric materials, heat sinks, thermal management, interfaces, and durability.

On the materials side, we are examining several abundant low-cost materials that we form into nanostructured bulk elements using techniques that are inexpensive, repeatable, rapid, and scalable for large volume production. We have created n-type $Mg_2Si_xSn_y$ elements with figure of merit (ZT) values up to 0.8 at 300°C and complementary p-type elements with ZT up to 0.2 at 300°C (work ongoing) using a scalable isostatic pressing process. These n-type materials are a factor of 20 better than PbTe in terms of ZT/$. Our interface work with these same materials has shown that we can make robust electrical contact and adhesion between interconnect materials (e.g. Cu and Fe) and $Mg_2Si_xSn_y$ that withstands high temperature thermal cycles. We have also created $ZnAl_2O_4$ composites using solid-state reaction methods with nanoinclusions that reduce thermal conductivity by a factor of three compared with ZnO. We found that the grain size and electrical conductivity were strong functions of sintering temperature which allows for careful tuning and optimizing of thermal and electrical properties.

We have made significant advances with respect to our heat exchangers on both the exhaust and coolant side. On the liquid side we have designed, fabricated, and tested heat exchangers that use impinging jets that provide excellent heat transfer with limited pressure drop penalty. We have found that the heat exchangers with impinging liquid jets provide temperatures 10-20°C lower than for geometries tested with standard guided flow. On the exhaust side, we explored a variety of pin-fin configurations and found that simple pin-fins with length <15% of the channel height can increase heat transfer rates by a factor of two on the exhaust-side heat exchanger, while limiting pressure drop to <2 psi. In order to fully examine the heat exchangers and to verify our computational models for thermal management and power output, we have recently created a scaled down test rig that includes the hot gas flow, a coolant loop, both heat exchangers, and thermoelectric elements all integrated in an exhaust system.

In the upcoming year we will work to improve our p-type Mg-Silicide material and to optimize the sintering temperature and time of the ZnO system in order to maximize ZT. For our established Mg-Silicide materials, we are subjecting the materials and interfaces to long-term thermal cycling and reliability studies. On the thermal management and heat exchanger side, we are using our experimentally verified computational fluid dynamics models to design improved second-generation heat sinks, and we using our laboratory test rig to quantitatively examine the performance of each component on the overall thermoelectric generator system.

Publications

1. Y. Zhao, Y. Yan, A. Kumar, H. Wang, W.D. Porter, and S. Priya, "Thermal conductivity of self-assembled nano-structured ZnO bulk ceramics," Journal of Applied Physics, Vol. 112, p. 034313, 2012.

2. J. Pandit, M. Dove, S.V. Ekkad, S.T. Huxtable, "Heat Exchanger Design for Waste Heat Recovery from Automobile Exhaust Using Thermoelectric Generators," 50th AIAA Aerospace Sciences Meeting including the New Horizons Forum and Aerospace Exposition, January 9–12, 2012, Nashville, Tennessee, Paper No: 2012-1011, Chapter DOI: 10.2514/6, 2012.

3. J. Pandit, M. Dove, S.V. Ekkad, and S.T. Huxtable, "Effect of Variation in Channel Height on Heat Transfer Performance of 3-Dimensional Partial Pin-Fins, Paper No: ISHT8-08-15, Proceedings of the 8th International Symposium on Heat Transfer, ISHT-8, Beijing, China, October 21–24, 2012.

4. M. Dove, J. Pandit, S.V. Ekkad, and S.T. Huxtable, "Experimental Validation Of Temperature Distributions Across A Heat Exchanger For A Thermoelectric Generator," Paper No: IMECE2012-88282, ASME International Mechanical Engineering Congress and Exposition, Houston TX, November 9th – 15th, 2012.

5. J. Pandit, M. Dove, S.V. Ekkad, and S.T. Huxtable, "Effect Of Partial 3-Dimensional Pin Fin Geometry For Heat Transfer Enhancement In High Aspect Ratio Channels, Paper No: IMECE2012-88251, ASME International Mechanical Engineering Congress and Exposition, Houston TX, November 9th – 15th, 2012.

6. Y. Zhao, A. Kumar , Y. Yan , H. Wang, and S. Priya, "Probing the chemical defects induced variation in electrical resistivity in nano-structured assembled ZnO bulk ceramics," Journal of Applied Physics, submitted and under review.

V.13 NSF/DOE Thermoelectric Partnership: High-Performance Thermoelectric Devices Based on Abundant Silicide Materials for Vehicle Waste Heat Recovery Report

Li Shi (Primary Contact), John Goodenough, Matthew J. Hall, Jianshi Zhou
University of Texas at Austin

Song Jin
University of Wisconsin-Madison

Objectives

- Increase the figure of merit (*ZT*) of earth-abundant and low-cost magnesium and manganese silicides (Mg_2Si and $MnSi_{1.73}$, or HMS) to the level found in state-of-the-art thermoelectric (TE) materials that contain scarce and expensive elements.
- To enhance thermal management performance for silicide TEs installed on a diesel engine exhaust.

Approaches

- Synthesis of bulk and nanostructured silicides: a) preparation of nanopowders by ball-milling and consolidation by spark plasma sintering, b) solid-state phase immiscibility to produce nanostructured silicide composites, and c) design and synthesis of silicide nanostructures by chemical vapor deposition.
- Develop computational models to: a) improve heat exchanger design and TE placement of spatially varied TE properties and b) optimize the design of TE elements to be manufactured.
- High temperature cycling to investigate changes in grain size and doping on TE performance of silicides.
- Investigate the phonon dispersion of HMS single-crystal by inelastic neutron scattering measurement.
- Reduce contact resistance by proposing a system of suitable interface materials to improve thermomechanical compliance.
- Build a heat exchanger and test silicide TE devices using a 6.7-liter Cummins diesel engine.

Accomplishments

Mg_2Si-Based Compounds

- We have developed a scalable method of synthesizing Mg_2Si-Mg_2Sn-Mg_2Ge ternary solid solutions.
- Carrier concentration tuning by varying both Mg self-doping and Sb doping.
- ZT of 1.2 at 800 K was obtained for Sb-doped $Mg_2Si_{0.4}Sn_{0.4}Ge_{0.2}$. This result indicates Mg_2Si-Mg_2Sn-Mg_2Ge solid solutions have the potential of achieving desirable ZT at high temperature.

HMS bulk materials

- HMS samples with different grain sizes and porosities have been prepared by the cold-pressing method. The effects of the grain size and porosity on the TE properties have been systematically investigated.
- Doping HMS with Ge and Al increased the power factor and reduce the lattice thermal conductivity, improving ZT to 0.65 at 820 K, which is 40% higher than that of undoped HMS.
- Phonon dispersion of HMS measured by neutron scattering revealed the broadening of the transverse acoustic phonon branch along the *c*-axis, which helps to explain the much lower thermal conductivity along the *c*-axis of HMS.

Bulk Nanostructured HMS

- We have developed a matrix encapsulation method to successfully generate HMS – Cu_3Si nanocomposites. Fully embedded nanostructures between 2-20 nm and larger Cu_3Si lamellae 100 nm – 20 μm in size are observed by microscopy. Preliminary thermal analysis suggests thermal conductivity is reduced.
- Using chemical vapor deposition, a facile approach to generate high yields of silicide nanowires has been developed. Si nanowire arrays can be fully converted into single-crystalline HMS in the presence of Mn vapor.

Modeling and Device Testing

- A finite difference model for thermal performance of a heat exchanger and TE device model has been

created and optimized for steady-state operation. They have been combined for a full-scale model.

- A flat plate-straight fin heat exchanger was built and tested for thermal performance under various loading on a 6.7-liter Cummins diesel engine. Surrogate materials with similar materials properties and resistance to heat flow as TE materials were used.

Status

Research is being carried out to further increase the ZT of both p-type HMS and n-type Mg_2Si-Mg_2Sn-Mg_2Ge ternary solid solutions, and use them to fabricate TE devices for engine test.

Journal Articles and Conference Proceedings

1. C. Baker, P. Vuppuluri, L. Shi, M.J. Hall, "Model of Heat Exchangers for Waste Heat Recovery from Diesel Engine Exhaust for Thermoelectric Power Generation," Journal of Electronic Materials 41, 1290-1297 (2012).

2. X. Chen, A. Weathers, A.L. Moore, J.S. Zhou, L. Shi, "Thermoelectric Properties of Cold-Pressed Higher Manganese Silicides for Waste Heat Recovery," Journal of Electronic Materials 41, 1564-1572 (2012).

VI. Acronyms, Abbreviations and Definitions

η_g	Gross indicated thermal efficiency
γ	Ratio of specific heats (c_p/c_v)
κ	Thermal conductivity
λ	Stoichiometric ratio; air/fuel equivalence ratio
φ	Fuel/air equivalence ratio
σ	Electrical conductivity
µs	Micro-second
°C	Degrees Celsius
°CA	Degrees crank angle, 0° = TDC
°F	Degrees Fahrenheit
ΔP	Pressure change
ΔT	Delta (change in) temperature
0-D	Zero-dimensional
1-D, 1D	One-dimensional
2-D, 2D	Two-dimensional
3-D, 3D	Three-dimensional
T_{90}	90% volume recovered temperature
ABDC	After bottom-dead center
AC	Alternating current
AC	Air conditioning
ACES	Advanced Collaborative Emissions Study
A/F, AFR	Air/fuel ratio
Ag	Silver
AGM	Absorbed glass mat
AHRR	Apparent heat release rate
a.k.a.	Also known as
Al	Aluminum
Al_2O_3	Aluminum oxide
ALE	Arbitrary Lagrangian-Eulerian
ANL	Argonne National Laboratory
ANR	NH_3/NOx ratio
API	American Petroleum Institute
APS	Atmospheric plasma spray
APU	Auxiliary power unit
ASC	Ammonia slip catalyst
ASI	After start of injection
ASME	American Society of Mechanical Engineers
atdc, ATDC, aTDC	After top-dead center
atm	Atmosphere
a.u.	Arbitrary units
Au	Gold
Avg.	Average
B	Boron
B10	Blend of 10% biodiesel and 90% diesel fuel
Ba	Barium
$BaAl_2O_4$	Barium aluminate
$Ba(NO_3)_2$	Barium nitrate
BaO	Barium oxide
bar	unit of pressure (14.5 psi or 100 kPa)
BBDC	Before bottom-dead center
BDC	Bottom-dead center
BES	Basic Energy Sciences
BET	Named after Brunauer, Emmett and Teller, this method for determining the surface area of a solid involves monitoring the adsorption of nitrogen gas onto the solid at low temperature and, from the isotherm generated, deriving the volume of gas required to form one monolayer adsorbed on the surface. This volume, which corresponds to a known number of moles of gas, is converted into a surface area though knowledge of area occupied by each molecule of adsorbate.
bhp-hr	Brake horsepower hour
BiTe	Bismuth telluride
BMEP	Brake mean effective pressure
Bsfc, BSFC	Brake specific fuel consumption
bsNOx, BSNOx	Brake specific NOx emissions
BTDC, btdc	Before top-dead center
BTE	Brake thermal efficiency
C_2H_4	Ethene
C_2H_6	Ethane
C_3H_6	Propylene
ca.	About, approximately
CA	Crank angle
CA50	Crank angle at which 50% of the combustion heat release has occurred
CAC	Charge air cooler
CAD	Crank angle degrees, computer-aided design
CAE	Computer-aided engineering
cc	Cubic centimeter
CCD	Charge-coupled device
CDC	Conventional diesel combustion
CDI	Compression direct injection
CDPF	Catalyzed diesel particulate filter
Ce	Cerium

CeO_2	Cerium oxide
CFD	Computational fluid dynamics
CH_4	Methane
CHA	Chabhazite zeolite
CI	Compression ignition
CIDI	Compression ignition direct injection
CLC	Chemical looping combustion
CLCC	Closed-loop combustion control
CLEERS	Cross-Cut Lean Exhaust Emissions Reduction Simulations
cm	Centimeter
cm^3	Cubic centimeters
CMOS	Complementary metal oxide semiconductor
CN	Cetane number
CNT	Carbon nanotube
CNG	Compressed natural gas
CO	Carbon monoxide
CO_2	Carbon dioxide
COP	Coefficient of performance
COV	Coefficient of variation (variance)
cP	Centipoise
CPF	Catalyzed particulate filter
cpsi	Cells per square inch
CPU	Central processing unit
Cr	Chromium
CR	Compression ratio
CRADA	Cooperative Research and Development Agreement
CRC	Coordinating Research Council
CRF	Combustion Research Facility
CSI	Convergent Science, Inc.
CTC	Cummins Technical Center
CTE	Coefficient of thermal expansion
Cu	Copper
CVD	Chemical vapor deposition
DADS	Direct ammonia delivery system
DBI	Diffused back-illumination
DC, dc	Direct current; dynamic capacity
DCN	Derived cetane number
deg	Degrees
D-EGR	Dedicated exhaust gas recirculation
°CA	Degrees crank angle, 0° = TDC
ΔT	Delta (change in) temperature
DFT	Density function theory
DI	Direct injection, direct-injected
DMP	Diesel micro pilot
DOC	Diesel oxidation catalyst
DOE	U.S. Department of Energy
DOHC	Double overhead camshaft
dP	Differential pressure
DPF	Diesel particulate filter
DRIFTS	Diffuse reflectance infrared Fourier-transform spectroscopy
DSC	Differential scanning calorimeter
E10	10% ethanol, 90% gasoline fuel blend
E15	15% ethanol, 85% gasoline fuel blend
E20	20% ethanol, 80% gasoline fuel blend
E85	85% ethanol, 15% gasoline fuel blend
ECM	Electronic (engine) control module
ECN	Engine Combustion Network
ECU	Electronic (engine) control unit
EDS	Energy-dispersive spectroscopy
EDX	Energy dispersive X-ray
EELS	Electron energy loss spectroscopy
EERE	Energy Efficiency and Renewable Energy
EEVO	Early exhaust valve opening
EGR	Exhaust gas recirculation
EHT	Equivalent homogenous temperature
ELOC	Extended-lift-off combustion
EMPA	Electron microprobe analysis
EOI	End of injection
EPA	U.S. Environmental Protection Agency
EPR	Electron paramagnetic resonance
ERC	Engine Research Center
ESL	ElectroScience Inc.
et al.	Et Alii: and others
EV	Exhaust valve
EVC	Exhaust valve closing
EVO	Exhaust valve opening
EVVT	Electrical variable valve timing
EXAFS	Extended X-ray absorption fine structure
Fe	Iron
FE	Fuel economy
FEA	Finite-element analysis
FEM	Finite-element method
FFVA	Fully flexible valve actuation
FMEA	Failure mode and effects analysis
FMEP, fmep	Friction mean effective pressure
FPEG	Free-piston electric generator
FSN	Filter smoke number
FTIR	Fourier transform infrared
ft-lb	Foot-pound
FTP	Federal Test Procedure
FY	Fiscal year
g, G	Gram

g/bhp-hr	Grams per brake horsepower-hour
GC	Gas chromatography
GC-FID	Gas chromatograph combined with a flame ionization detector
GC-MS	Gas chromatography – mass spectrometry
GDCI, GDICI	Gasoline direct-injection compression ignition
GDI	Gasoline direct injection
Ge	Germanium
g/hphr	Grams per horsepower-hour
GHSV	Gas hourly space velocity
gIMEP	Gross indicated mean effective pressure
GM	General Motors
g/mi	Grams per mile
GPF	Gasoline particulate filter
GPU	Graphical processing unit
GTDI	Gasoline turbocharged direct injection
GTI	Gas Technology Institute
H_2	Diatomic (molecular) hydrogen
H_2CO	Formaldehyde
H_2O	Water
H_2O_2	Hydrogen peroxide
HAADF STEM	High angle annular dark field scanning transmission electron microscopy
HC	Hydrocarbons
HCCI	Homogeneous charge compression ignition
HD	Heavy-duty
He	Helium
HECC	High-efficiency clean combustion
HEI	Health Effects Institute
HEV	Hybrid electric vehicle
HHV	Higher heating value
HIL	Hardware-in-the-loop
hp	Horsepower
HPC	High-performance computing
HPL	High pressure loop
HPLB	High-pressure, lean-burn
hr	Hour
HR	Heat release
HRR	Heat release rate
HRTEM	High-resolution transmission electron microscopy (microscope)
HVA	Hydraulic valve actuation
HVAC	Heating, ventilation and air conditioning
HWFET	Highway Fuel Economy Test
Hz	Hertz
IARC	International Agency for Research on Cancer
IC	Internal combustion
ICCD	Intensified charged-coupled device
ICE	Internal combustion engine
ID	Internal diameter
IMEP	Indicated mean-effective pressure
$IMEP_g$	Indicated mean effective pressure, gross
$IMEP_{net}$	Indicated mean effective pressure, net
IR	Infrared
ISFC	Indicated specific fuel consumption
ISX	Cummins Inc. 15-liter displacement, inline, 6-cylinder heavy duty diesel engine
ITE	Indicated thermal efficiency
IV	Intake valve
IVC	Intake valve closing
IVO	Intake valve opening
J	Joule
k	thousand
K	Kelvin, potassium
kg	Kilogram
kHz	Kilohertz
KIVA	Combustion analysis software developed by Los Alamos National Laboratory
KIVA-CMFZ	KIVA Coherent Flamelet Multi-Zone
kJ	Kilojoules
kJ/L	Kilojoules per liter
kJ/m^3	Kilojoules per cubic meter
KMC	Kinetic Monte Carlo
kPa	Kilopascal
kW	Kilowatt
L	Liter
La	Lanthanum
LANL	Los Alamos National Laboratory
lb ft	Pound foot
lb/min	Pounds per minute
lbs	Pounds
lbs/sec	Pounds per second
LD	Light-duty
LDB	Lean downsize boost
LDT	Light-duty truck
LED	Light-emitting diode
LES	Large eddy simulation
LHV	Lower heating value
LIF	Laser-induced fluorescence
LII	Laser-induced incandescence
LLNL	Lawrence Livermore National Laboratory

LMO	$LaMnO_3$
LNT	Lean-NOx trap
LOL	Lift-off length
LP	Low pressure
LPL	Low-pressure loop
LRRI	Lovelace Respiratory Research Institute
LSC	$La_{1-x}Sr_xO_{3-\delta}$
LSCO	$(La,Sr)CoO_3$
LSMO	$(La,Sr)MnO_3$
LTC	Low-temperature combustion
m^2	Square meters
m^2/gm	Square meters per gram
m^3	Cubic meters
mA	Milliamps
MAP	Manifold air pressure
mbar	Millibar
MBT	Minimum (spark advance) for best torque; Maximum brake torque
MCE	Multi-cylinder engine
MD	Medium-duty
MER	Molar expansion ratio
Mg	Magnesium
mg/cm^2	Milligrams per square centimeter
mg/mi	Milligram per mile
mg/mm^2	Micrograms per square millimeter
mg/scf	Milligrams per standard cubic foot
mi	Mile
µs	Micro-second
min	Minute
MIR	Mid-infrared
MIT	Massachusetts Institute of Technology
MPRR	Maximum pressure rate rise
µm	Micrometer
mm	Millimeter
mmols	Micro-moles
Mn	Manganese
Mo	Molybdenum
mol	Mole
mol/s	Moles per second
MPa	Megapascals
mpg	Miles per gallon
mph	Miles per hour
MPICH	Portable Implementation of MPI
MPT	MAHLE Powertrain
ms	Millisecond
MS	Mass spectrometry
MSU	Michigan State University
MTU	Michigan Technological University
MWASP	Microwave-assisted spark plug
MZ	Multizone
N_2	Diatomic nitrogen
N_2O	Nitrous oxide
N_2O_3	Nitrogen trioxide
Na	Sodium
NETL	National Energy Technology Laboratory
NH_3	Ammonia
nm	Nanometer
Nm	Newton meter
NMEP	Net mean effective pressure
NMHC	Non-methane hydrocarbon
NO	Nitric oxide
NO_2	Nitrogen dioxide
NOx, NO_X	Oxides of nitrogen
NRE	NOx reduction efficiency
ns	Nanosecond
NSC	NOx storage capacity
NSR	NOx storage and reduction
NTC	Negative temperature coefficient
NTE	Negative thermal expansion
NVH	Noise, vibration, and harshness
NVO	Negative valve overlap
O_2	Diatomic (molecular) oxygen
O_3	Ozone
OBD	On-board diagnostics
OCC	Output covariance constraint
OD	Outside diameter
ODE	Ordinary differential equation
OEM	Original equipment manufacturer
OH	Hydroxyl
OH PLIF	Planar laser-induced fluorescence of OH
ORC	Organic Rankine cycle
ORNL	Oak Ridge National Laboratory
OSC	Oxygen storage capacity
P	Pressure
PAH	Polycyclic aromatic hydrocarbon
PCCI	Premixed charge compression ignition
PCI	Premixed compression ignition
PCS	Predictor-corrector split
PDF	Probability density function
PDI	Port direction injection
PEDOT	poly(3,4-ethylenedioxythiophene)
PFI	port fuel injected, port fuel injection
PFS	Partial fuel stratification
P-G	Petrov-Galerkin
PGM	Platinum-grade metal, platinum group metal

P_{in}	Intake pressure
PLII	Planar laser-induced incandescence
PLIF	Planar laser-induced fluorescence
PM	Particulate matter; premixed
PME20	Palm-oil methyl ester 20% + ULSD 80% blend
PMP	Particle Measurement Program
PNA	Passive NOx adsorber
PNNL	Pacific Northwest National Laboratory
ppb	Parts per billion
PPC	Partially premixed combustion
PPCI	Partially premixed compression ignition
ppi	Pores per square inch
ppm	Parts per million
PRF	Primary reference fuel
PRF80	PRF mixture with an octane number of 80 (i.e., 80% iso-octane and 20% n-heptane)
PRR	Pressure rise rate
PSAT	Powertrain Systems Analysis Toolkit
psi	Pounds per square inch
psig	Pounds per square inch gauge
Pt	Platinum
PTO	$PbTiO_3$
PV	Pressure-volume
PVT	Pressure-volume-temperature
Q	Heat
Q1, Q2, Q3, Q4	First, second, third and fourth quarters
R&D	Research and development
RCCI	Reactivity-controlled compression ignition
RCF	Rapid compression facility
RCM	Rapid compression machine
Re	Reynolds number; radius of gyration
RF	Radio frequency
Rh	Rhodium
RI	Ringing intensity
RON	Research octane number
RPM, rpm	Revolutions per minute
S	Seebeck coefficient
S	Sulfur
SA	Spark assist(ed)
SACI	Spark-assisted compression ignition
SAE International	Technical association formerly known as the Society of Automotive Engineers
SA-HCCI	Spark-assisted homogeneous charge compression ignition
sccm	Standard cubic centimeters
SCE	Single-cylinder engine
SCF/min	Standard cubic feet per minute
SCR	Selective catalytic reduction
SCRF	Selective catalytic reduction on filter; integrated DPF and SCR technologies
sec	Second
SEM	Scanning electron microscopy
Si	Silicon
SI	Spark ignition, spark-ignited
SIDI	Spark ignition direct injection
SFC	Specific fuel consumption
SKU	Skutterudite
SLPM	Standard liters per minute
SME	Soy methyl ester
SME20	Soy methyl ester 20% + ULSD 80% blend
SMPS	Scanning mobility particle sizer
SNL	Sandia National Laboratories
SO_2	Sulfur dioxide
SOC	Start of combustion; soluble organic compound
SOI	Start of injection
SOF	Soluble organic fraction
SO_x	Oxides of sulfur
SpaciMS	Spatially resolved capillary inlet mass spectrometer
SPS	Spark plasma sintering
Sr	Strontium
SRM	Stochastic reactor model
SU	Stanford University
SULEV	Super Ultra-Low Emissions Vehicle
SUV	Sport utility vehicle
SwRI®	Southwest Research Institute®
T	Temperature
T_{90}	90% volume recovered temperature
TAP	Temporal analysis of products
TC	Turbocompound; total capacity
TCR	Thermochemical recuperation
TDC	Top-dead center
TDL	Tunable diode laser
TE	Thermoelectric
T-E	Thermal efficiency, gross indicated
TED	Thermoelectric device
TEG	Thermoelectric generator
TEM	Transmission electron spectroscopy; thermoelectric module
TGA	Thermal gravimetric analysis (analyzer)
THC	Total hydrocarbon
TIM	Thermal interface material

T_{in}	Intake temperature
TJI	MAHLE Powertrain's Turbulent Jet Ignition
TPD	Temperature-programmed desorption
TPO	Temperature-programmed oxidation
TPR	Temperature-programmed reduction or reaction
TPRX	Temperature-programmed reaction
TS	Thermal stratification
T_{wall}	Temperature, wall
TWC	Three-way catalyst
UC	Unused capacity
UCB	University of California, Berkeley
UDDS	Urban Dynamometer Driving Schedule
UEGO	Universal exhaust gas oxygen
UHCs	Unburned hydrocarbons
ULSD	Ultra-low sulfur diesel
UM	University of Michigan
US06	Supplemental Federal Test Procedure (SFTP) drive cycle
USSET	U.S. Supplemental Emission Testing
UV	Ultraviolet
UW	University of Wisconsin
UW-ERC	University of Wisconsin Engine Research Center
UWS	Urea-water solution
V	Volt
VAC	Volts, alternating current
VCR	Variable compression ratio
VDC	Volts – direct current
VEM	Vehicle Energy Model
VES	Vehicle Energy Simulator
VGC	Variable geometry compressor
VGT	Variable geometry turbocharger
VNT	Variable nozzle turbine
VOCs	Volatile organic compounds
VOIS	Variable output ignition system
VPS	Vacuum plasma spray
VTCE	Virtual Thermal Comfort Engineering
VVA	Variable valve actuation
VVT	Variable valve timing
W	Watt
WGS	Water-gas shift
WHR	Waste heat recovery
wt%	Weight percent
WTT	Well-to-tank
XAFS	X-ray aborption fine structure
XPS	X-ray photoelectron spectroscopy
XRD	X-ray diffraction
Y	Yttrium
yr	Year
YSZ	Ytrria-stabilized zirconia
Zn	Zinc
Zr	Zirconium
zT	Dimensionless thermoelectric figure of merit; equal to: (electrical conductivity) (Seebeck coefficient)^2(temperature)/ (thermal conductivity)
ZTO	Zn_2SnO_4

VII. Index of Primary Contacts

DOE/EE-0872 February 2013
Printed with a renewable-source ink on paper containing
at least 50% wastepaper, including 10% post consumer waste.

U.S. DEPARTMENT OF ENERGY | Energy Efficiency & Renewable Energy

For more information
eere.energy.gov